1995

Reservoir sedimentation modelling

Mehdi Ghomeshi
University of Wollongong

RESERVOIR SEDIMENTATION MODELLING

A thesis submitted in fulfilment of the
requirement for the award of the degree
Doctor of Philosophy

from

UNIVERSITY OF WOLLONGONG

by

Mehdi Ghomeshi, B.Sc., M.Sc.

Department of Civil and Mining Engineering

1995

IN THE NAME OF GOD

AFFIRMATION

I hereby certify that the work presented in this thesis has been carried out in the Department of Civil and Mining Engineering of the University of Wollongong and has not been submitted for any other degree.

.....

Mehdi Ghomeshi

Volume I

ACKNOWLEDGMENT

I would first and foremost like to sincerely thank my supervisor, Associate Professor Muttucumaru Sivakumar; his guidance and assistance throughout the period of my work is greatly appreciated.

This work was carried out in the Department of Civil and Mining Engineering, and the provision of experimental facilities greatly expedited my work.

The Ministry of Culture and Higher Education, Islamic Republic of Iran supported this study for three and half years. Khozestan Water and Power Authority provided the Dez River and Reservoir data for this study; the support of both is gratefully acknowledged.

During the experimental work, I have benefited from the cooperation and suggestions of many of my colleagues including Dr. M. Magareh and Dr. S. Boromand-Nasab, former Ph.D. students in this department, and Mr. F Sharify a current Ph.D. student. I would like to thank all of them.

I thank Mr. S. Shirzad who provide some of the geometric data of Dez Reservoir, Mr. Christopher D. Stevens and the staff of the Learning Development Centre of Wollongong University for improving my thesis writing and structure, and my colleague Mr. M. Chinnaiyan and Dr. J. Hematian for checking the linguistic aspects of my thesis.

Finally, I would like to express my deepest thanks and love to my Family: to my Wife, Batool, for her forbearance and understanding in difficulties resulting from my study, as well as her assistance in typing parts of this thesis and her encouragement, and to my children Mohammad, Zahra, and Hossein for their patience. I am proud of all of them.

I would like to dedicate this work to both my Wife and my Mother for their love and sacrifices over the years.

ABSTRACT

The purpose of this study is to consider sediment deposition in large reservoirs with high suspended sediment inflows. A characterising feature of this kind of reservoir is the existence of turbidity currents due to density differences between inflow and ambient waters of the reservoir. Therefore, two major parts can be found in this study: firstly, experiments and analysis of the experiments on gravity currents, and secondly the development of a computer model for reservoir sedimentation modelling.

Some experiments were conducted using a laboratory flume to consider different aspects of gravity currents including: the development of the head of gravity currents, the body of subcritical gravity currents, and deposition due to the head and the body of turbidity currents. The analyses of the measured velocities, concentrations and the sizes of sediment particles have been presented. By using the data collected from this study and other available data a new coefficient for the equation of the head of gravity currents was proposed with the help of a statistical package. Sediment transport by the head of gravity currents is discussed. Based on the calculated water entrainment and using other available water entrainment data, an equation for the water entrainment coefficient was proposed. A new equation for sediment entrainment over an erodible bed was presented by using the available data from other investigators.

A new procedure for the prediction of sediment processes in reservoirs was developed recognising the fact that turbidity currents affect long-term sedimentation, particularly when suspended sediment concentration is relatively high. Based on this a new computer program, DEPO, for the prediction of sediment processes in reservoirs was developed by incorporating the effects of turbidity currents on long term sedimentation. Although the model is theoretically one-dimensional, some options exist for the distribution of sediment deposited on the bed or for sediment scoured from the bed. This makes the model a pseudo two dimensional model.

To verify the proposed model, four different turbidity currents were run in the laboratory flume. The computations performed by DEPO for: the water elevation, the height of the turbidity current and the amount of the deposited material on the bed, showed excellent agreement with the measured values. The proposed model was also tested by application

to a prototype situation, Dez Reservoir (a large reservoir in the south-west of Iran). Test results showed the capabilities of the model as a practical tool for the prediction of long term reservoir sedimentation. The DEPO model was tested using Dez Reservoir to consider the effects of alternative bottom gates on deposited sediment. By using the alternative bottom gates the amount and the pattern of sediment deposited in the reservoir were affected significantly. The height of the sediment deposited in the reservoir was reduced, particularly in the region from the dam wall to 20 km upstream of the dam. The estimated volume of deposited sediment was reduced by about 55 percent and the trap efficiency was reduced to 0.46. The model was also utilised to predict the future volume and bed elevation of Dez Reservoir after 60 years of operation.

The results showed the capabilities of the model for predicting long term reservoir sedimentation, for the management of reservoirs, for considering the effects of the bottom gate on reservoir life, and for controlling turbidity currents in reservoirs.

Table of Contents

Volume I

List of Figures

List of Tables

List of Symbols

a = weight factor

A = cross section area of flow

A_* = coefficient

A_d = mean absolute deviation of the discrepancy ratio

A_0 = water surface area of the original reservoir basin at height h_0

A_p = a dimensionless relative area at relative distance p above the stream bed

A_s = surface area exposed to scour

A_{sp} = cross section area of suspended sediment

A^y_x = the rate of change of A with respect to x when y is held constant

b = the weight factor

b_1 = parameter defined by log (M_c)

b_2 = parameter defined by log (A_d)

B = width of the flow

B_0 = initial buoyancy flux

c = sediment concentration

c_0 = initial volumetric concentration

c_{ae} = near-bed concentration in equilibrium condition

c_{aep} = predicted near bed sediment concentration

c_{aeo} = observed near bed sediment concentration

c_{ai} = near-bed volumetric concentration of sediment in the ith size range

c_{aie} = the value of c_{ai} at equilibrium state

c_{av} = the average volumetric sediment concentration within a control volume

c_b = layer-averaged concentration

c_d = dimensionless concentration, i.e ratio of the mass of the particular size-class particles to the total mass of the elemental volume

c_f = concentration at the end of time period

c'_p = suspended concentration in the longitudinal direction at a section

c_L = total volumetric concentration of suspended sediment at a given point

c_s = concentration at beginning of time period

c_{sa} = average sediment concentration in the cross section on a volume basis

c_t = total sediment concentration in parts per million by weight

C = the capacity of the reservoir in acre-feet in Brown's method

C' = Chézy- coefficient related to grains

C_0 = initial volume of reservoir

C_c = constant coefficient

C_{ce} = loss coefficient for contraction or expansion

C_D = drag coefficient or bed friction coefficient

C_r =the design capacity of the reservoir

C_s =volume of the channel

C_u = dimensionless constants which are determined by the type of reservoir

C_v = constant coefficient

d = coefficients of sediment transport capacity

d_{50} = median diameter of bed material (m)

dh_1 = the value of change in each coordinate point in a given cross section

dh_{tw} = the value of change in the thalweg of the cross section

$d\rho_0$ =density difference between inflow and ambient water

D = water depth or flow depth

D_{50} = median size of sediment particles (50%)

D_{90} = a size of sediment particle that 90% of grain particles is less than this size

D_a = arithmetic mean diameter of the particles

D_e = minimum water depth for negligible sediment transport

D_g = geometric mean size of the material

D_i = mean size of the sediment particle range

D_L = the size of fraction, L

D_S = median size of particles

D_* = non-dimensional particle parameter

e = represents the departure from a straight line of the plot of V_s/C_0 versus t at V_s/C_0 approximately equals to 0.6

e_b = bed load transport efficiency

e_s = suspended load transport efficiency

E = number of channels

E_m = active-layer thickness

E_s = sediment entrainment

E_{si} = sediment entrainment function for non uniform sediment

E_w = water entrainment coefficient of the gravity current

E_{w0} = initial water entrainment coefficient of the gravity current

f = bed friction coefficient

f_{ave} = a parameter in Runge-Kutta numerical method

f_i = the function evaluated at the point x

$f_{i'}$ = the function evaluated at some intermediate points

f_t = total friction coefficient

F = $c_L{}'w'$ is Reynolds sediment flux

F_b = body force

F_p = densimetric Froude number at plunge point

g = acceleration due to gravity

g' = is effective gravitational acceleration ($=\Delta g$)

g_0' = is the initial effective gravitational acceleration

g'_f = the actual effective gravitational acceleration inside the head

h = gravity current thickness

h_0 = depth of sediment at dam wall

h_1 = total water depth at the head of the gravity current

h_4 = bottom region depth of head

$\overline{h}$ = the mean depth of the reservoir

h_a = thickness of the active layer

h_{ce} = energy loss due to contractions and expansions

h_e = total energy loss

h_f = friction loss

h_n = distance of the nose of gravity current from the bed

h_p = plunge depth

h_r = variable depth measured from original zero elevation

H = maximum reservoir depth at dam wall measured from original zero elevation

H_1 = the region from the bed to the maximum velocity flow in the profile of vlocity

H_2 = the region from the maximum velocity point to the edge of the flow in the profile of vlocity

H_f = height of the gravity current head

i = dimensionless constants which are determined by the type of reservoir

I = the volume of annual water inflow

j = dimensionless constants which are determined by the type of reservoir

k = coefficient of sediment transport capacity

k_c = diffusion coefficient for the sediment particles in the lateral direction

k_s = hydraulic roughness

k_x = the diffusion coefficient in x direction

k_y = the diffusion coefficient in y direction

K = constant dependent on the size analysis of the sediment

K_1 = loading-law coefficient

L = distance between two cross sections

m = slope of V_s/C_0 versus t on log-log paper

M = the reciprocal of the slope of the line obtained by plotting the reservoir depth as ordinate against reservoir capacity as abscissa on log-log paper

M_1 = erosion rate for particle scour

M_e = mean of the discrepancy ratio

n, n_s = Manning coefficients

n_o = number of data points

N = number of particle size fraction

p = relative distance

p_0 = bed-sediment porosity

p_c = percentages of clay in the incoming sediment

p_i = percentage weight corresponding to the size D_i

p_m = percentages of silt in the incoming sediment

p_s = percentages of sand in the incoming sediment

P = the wetted perimeter

P_d = probability of particles sticking to the bed and not being re-entrained by the flow

P_i = percentage of the size fraction

q = water discharge per unit width of flow

q_0 = initial flow discharge per unit width

q_b = unit bed load transport rate

q_{bv} = measured unit-width volumetric bed load transport rate

q^*_{bv} = equilibrium value of q_{bv}

q_d = suspended sediment diffusion flux

q_{dE} = sediment transfer between channels (units of weight per unit time)

q_L = lateral inflow into stream

q_{LE} = lateral flow between channels

q_s = suspended load in dry weight per unit of channel width

q_{sd} = lateral discharge of sediment

q_t = lateral discharge of sediment-laden water

q_w = lateral discharge of water

Q = water discharge

Q_0 = initial flow rate

Q_c = the erosion rate per unit area per unit time

Q_f = the floc erosion rate

Q_S = suspended sediment discharge in tonne per day

Q_{sd} = sediment discharge

r = coefficients of sediment transport capacity

r_0 = ratio of the near-bed concentration to layer-averaged concentration

R = submerged specific gravity of the sediment

R^2 = the coefficient of determination

R_b = hydraulic radius

R_{e0} = initial Reynolds numbers

R_i = bulk Richardson number

R_{i0} = initial Richardson number

R_p = particle Reynolds number

R_{pi} = particle Reynolds number of ith fraction

R_{p50} = particle Reynolds number of median size

R_b' = hydraulic radius with respect to the grains

s = the curvilinear coordinate along discharge centerline measured from the upstream entrance

S = slope of the bed

S_e = energy slope

S' = energy slope due to grain resistance

S_* = mean sediment concentration during flood season (kg/m^3)

S_1 = density deficiency coefficient, ranging from 0.2 to 0.3 (Ellison and Turner 1959)

S_2 = density deficiency coefficient, ranging from 0.6 to 0.9 (Ellison and Turner 1959)

S_{af} = active-layer floor 'source'

S_f = the slope of the energy grade line (friction slope)

S_{qs} = suspended load 'source'

S_t = the topset slope of delta

t = time

t_1, t_2, t_3 = time in the distance of x_1, x_2 and x_3 respectively

t_* = time when $V_s = C_0$ (reservoir full with sediment)

t_s = duration of spill over period in seconds

T = temperature in Celsius degree

T_0 = transport stage parameter

TE = trap efficiency of reservoir

u = average local velocity

$u(x,z)$ = local component of the flow velocity in the x direction

u_* = bed shear velocity

u' = fluctuating (instantaneous value minus mean value) or turbulent components of longitudinal velocity

u_*' = bed shear velocity due to grain friction

$u_{*,cr}$ = critical bed-shear velocity according to shields curve

U = current averaged velocity

U_0 = initial current velocity

U_f = velocity of the head of gravity current

U_s = mean velocity of solid

v_s = fall velocity of sediment particles

$\overline{v}_s$ = mean fall velocity of sediment particles

v_{si} = fall velocity associated with the size D_i

V = average velocity of flow

V_0 = volume of sediment accumulated under depth h_0

V_{ds} = average velocity at the downstream section

V_L = velocity component of the lateral flow in the x-direction

V_q = velocity of the lateral inflow in the direction of the main flow

V_s = total volume of sediment deposition

$w(x,z)$ = local component of the flow velocity in the z direction

w' = fluctuating (instantaneous value minus mean value) or turbulent components of transverse velocity

W = area of the watershed in square miles in brown method

W_c = coefficients of clay

W_m = coefficients of silt

W_s = coefficients of sand

WS = water surface elevation at the current section

WS_{ds} = water surface elevation at the downstream section

x = longitudinal direction

x_1, x_2, x_3 = distance of the points 1,2 and 3 from inlet gate

y = longitudinal direction

y_b = the bed elevation

y_d = water depth above the coordinate point

y_i, y_{i+1} = hydraulic parameters

y_{tw} = water depth above the thalweg of the cross section

z = vertical distance from the bed

Z = sediment entrainment variable

Z_c = critical value of Z found to be equal to five (Akiyama and Fukushima, 1985)

Z_e = the stage or water surface elevation

Z_{eff} = effective sediment entrainment variable for non-uniform sediment

Z_f = upper limit for Z (= 13.2 Akiyama and Fukushima, 1985)

Z_m = sediment entrainment variable for non-uniform sediment

Z_u = sediment entrainment variable with respect to grain friction

α = bed slope

α_2 = an empirical constant

α_d = coefficient of dynamic solid friction

α_{ds} = velocity distribution coefficients for flow at the downstream section

α_p = the position of the intermediate points

α_s = ratio of interfacial to bed shear stress

α_v = velocity distribution coefficients for flow at the current section

β = the position of the intermediate points

β_a = active-layer size fraction

β_b = coefficient

β_m = momentum correction factor for velocity distribution

δ = average local fractional density

Δ = current averaged fractional density

Δ_0 = initial fractional density

Δy_0 = a parameter in the Runge-Kutta method

Δy_1 = a parameter in the Runge-Kutta method

Δy_2 = a parameter in the Runge-Kutta method

Δy_3 = a parameter in the Runge-Kutta method

Δx = distance

γ = initial unit weight of sediment deposited

γ_1 = unit weight of sediment deposited in the end of first year

γ_{At} = average unit weight of sediment deposited after t years of compaction

γ_d = dilution coefficient

γ_{dE} = specific weight of the sediment deposits at the Eth stream

γ_s = unit weight of sediment materials

γ_{SE} = specific weight of the transported sediment particles

γ_t = unit weight of sediment deposited after t years of compaction

γ_w = unit weight of water

λ = a constant value to fit the non-uniform measured data to the uniform equation

λ_b = a parameter in the Engelund and Fredsoe's sediment entrainment equation

λ_L = porosity of sediment of fraction, L

ν = kinematic viscosity of the water

ρ = density of the fluid

$d\rho_0$ = density difference between inflow and ambient water

ρ_s = density of the sediment particles

ρ_w = density of water

τ = Reynolds stress

τ_b = bed shear stress

τ_d = critical shear stress under which deposition occurs

τ_s = critical bed shear stress above which erosion occurs

ϕ = a parameter in the Karaushev's trap efficiency equation

ψ = volumetric sediment discharge per unit width

ψ_e = volumetric sediment discharge in equilibrium state

ψ_i = volumetric sediment discharge in the point of i

ψ_{i+1} = volumetric sediment discharge in the point of i+1

θ' = a parameter in the Engelund and Fredsoe's sediment entrainment equation

Chapter One

AN INTRODUCTION TO RESERVOIR SEDIMENTATION

1.1 Introduction

Although more than two thirds of the earth's surface is covered by water, less than 3 percent of that is fresh water. A large amount of fresh water is unusable as it is trapped in various forms such as polar ice, icecaps and in the atmosphere. Therefore, only about 0.003 percent of the world's water is available for human consumption.

Following the rapid population growth and development of the world in the last century, the demand for water has increased very rapidly. As a result, most of the rivers have been exploited and only a few rivers are still flowing in their natural condition. The supply of sufficient water for urban, industrial and agricultural activities, flood control and supply of electricity requires large reservoirs to store fresh water in the flood seasons.

In general, reservoirs are formed by constructing different types of dams on natural streams. The benefits and costs of a reservoir are evaluated before constructing a dam. Finding an appropriate place for construction of a dam is very important and depends on the reservoir volume. Therefore, comprehensive geological and geomorphological information is needed for this purpose. One of the most important characteristics of a reservoir is its useful life time. This is the period of time over which the reservoir performs its functions. This life of a multi-purpose reservoir is usually more than 100 years.

1.2 Reservoirs and Sediment Deposition

Controlling the excess water in a region by constructing a hydraulic structure disturbs the natural equilibrium of a stream. The velocity of water flow is reduced and a large volume of sediment is usually deposited in the reservoir basin. These sediment deposits have many effects on the reservoir, as well as on the downstream and upstream parts of the reservoir. These effects are of great concern to water resource engineers. In planning and designing a reservoir, it is very important for the engineer to have a good idea of the sediment deposit distribution in the reservoir during its life time. This is crucial for the prediction of sedimentation and the incorporation of its effects into design measures, or reservoir management.

In the 50's and before that, when some large reservoirs came into operation, it was thought that depositing sediments first filled the deepest part of the reservoir and then got distributed to the other parts. Based on this assumption, a storage space was usually considered for sediment accumulation in the reservoir. As reservoirs were resurveyed, it was realised that the sediment deposition process within the reservoir was very complex and a number of factors such as water and sediment inflow, sediment specification, shape of the reservoir, operation mode and turbidity current affected the pattern of sediment distribution. As a result, the above processes should be taken into account in the analysis of sediment deposition in reservoirs.

It is important to note that not only the amount of sediment deposition in the reservoir but also the location of sediment accumulation are key factors in the design and management of such projects. Many attempts have been made to study the sediment-flow interactions in reservoirs over the last 50 years. A number of researchers tried to find a general method for predicting the phenomenon of sediment deposition in reservoirs. They examined numerous factors which affect the sediment processes, but they were hampered by a lack of information about some of these factors. To avoid a complicated, difficult solution, particularly in a time when high speed computers were not available, the attempts were mostly confined to simple empirical methods. The empirical methods were based on general trends of measured sediment depositions in reservoirs. Generally, the application of empirical methods are simple and do not need

large amount of data for prediction of sediment deposition. Also, these methods do not cover all aspects and all conditions because they are based on one or more observations. Generalising from such a model to all cases is not appropriate. Mathematical methods, on the other hand, are based on the solution of a number of equations which govern and represent the behaviour of the sediment processes. The mathematical methods always utilise computer programs and they always need geometric data from selected sections of the reservoir as well as data on the hydraulics and hydrologic boundary elements. In comparison with the empirical methods, the mathematical methods are more reliable. The major deficiencies of the latter methods are that large amount of data are needed and often the computer program needs to be calibrated to fit with the particular data measured from sediment deposition surveys.

1.3 Statement of the Problem

Deposition in the reservoirs has a tremendous influence on the surrounding environment and is quite difficult to analyse. Sediment deposition in a reservoir affects not only the reservoir itself but also the upstream and downstream parts of the reservoir.

The first problem is the influence of a decrease in reservoir volume on the performance of the reservoir. Important functions of the reservoir which may be affected by sediment deposition are:

- water yield
- loss of flood-control
- impairment of navigability
- entrainment of sediment through hydropower equipment
- blockage of gates
- determination of water quality

The effect on the upstream part is another problem. Sediment deposition in the deltaic region increases flooding in the upstream region. This condition is shown schematically in Figure 1.1.

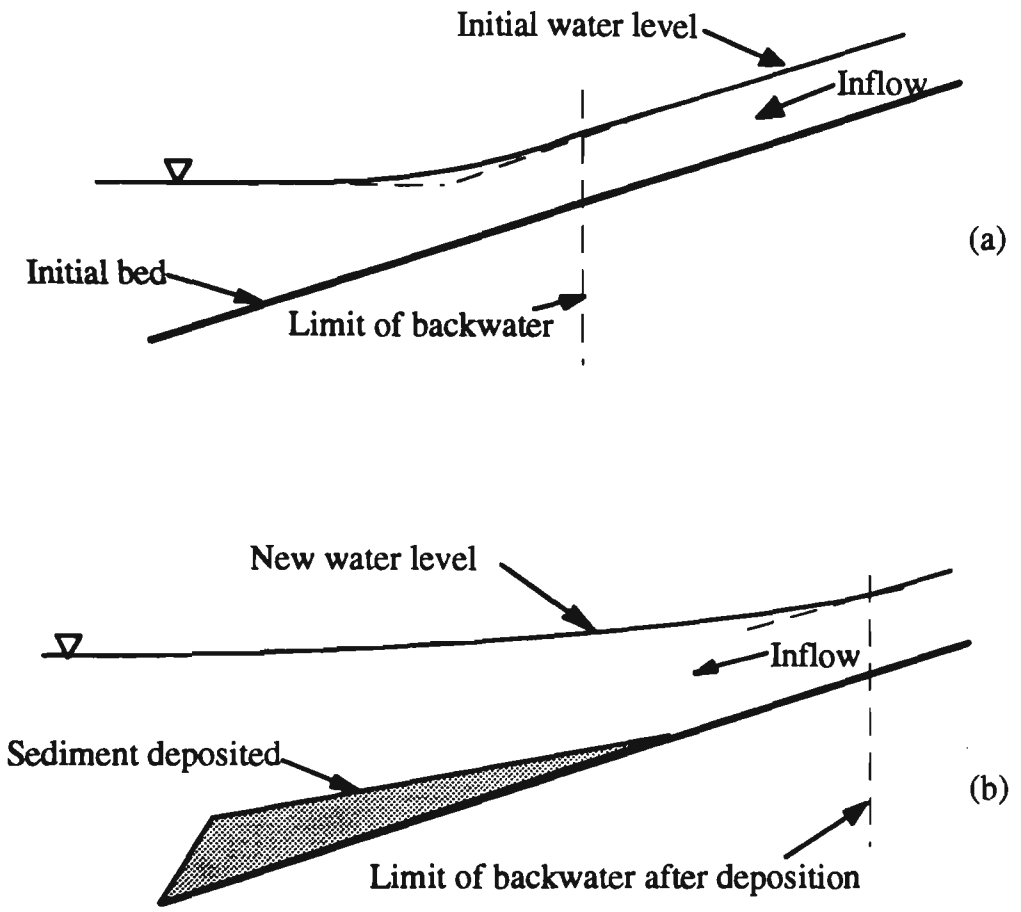

Figure 1.1 Effect of sediment deposition on upstream of the reservoir.

The other significant problem occurs on the downstream part of the reservoir. The lack of sediment in the water outflow from the reservoir causes scouring by the water and the water entrains bed material downstream of the dam wall. This case is shown in Figure 1.2.

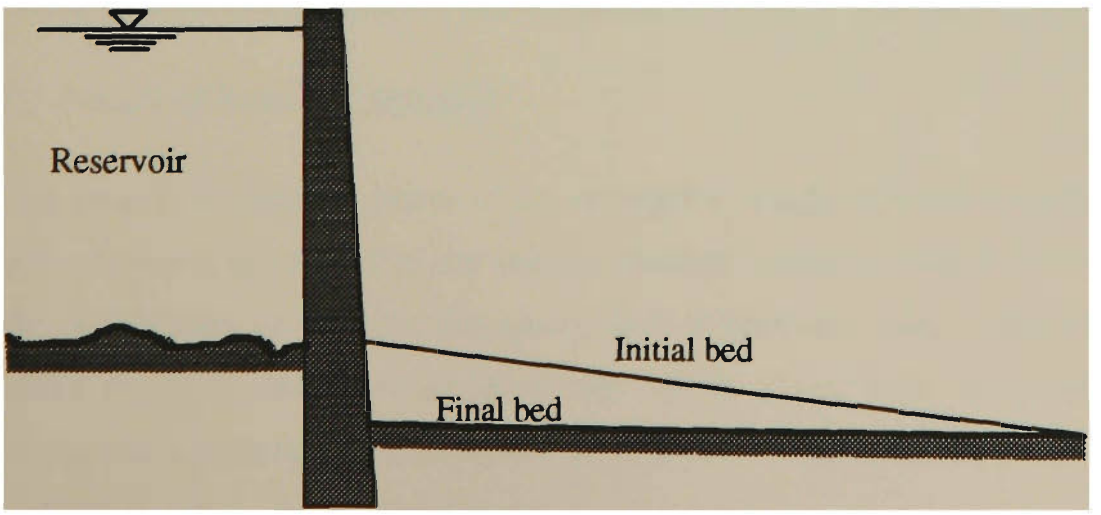

Figure 1.2 River bed degradation.

Some additional environmental concerns are reported due to sedimentation such as effects on the water quality, aquatic life (Fan and Springer, 1990), nutrient supply downstream, and recreation. In some cases these problems are of great concern for engineers, and sometimes they are very expensive to repair or there may be irreversible damage.

1.4 Factors Affecting Reservoir Deposition

Recognising factors which may affect sediment deposition in the reservoir is the first step towards understanding, controlling and modelling this phenomenon. There are many interrelated factors contributing to the sediment deposition process. They can be summarised as follows:

A) Quantity of Sediment Discharge

The amount of sediment discharge is one of the most important factors in reservoir sedimentation. Factors such as run-off yield in the basin, vegetation cover in the basin, and geometry and paedology of the basin may significantly affect the sediment discharge.

B) Trap Efficiency

The ratio of the sediment retained in the reservoir to the total inflow of river sediment is called "the trap efficiency" of the reservoir. The capacity of the reservoir, water and sediment inflow, sediment specification, shape of the reservoir, operation duration curve and density current are factors which affect the trap efficiency of the reservoir.

C) Density of Sediment Deposited

The amount of sediment inflow to the reservoir is usually reported in terms of weight. For converting this weight to the volume which the sediment occupies in the reservoir, the bulk density of sediment deposition plays a significant role. Some factors which affect the bulk density of sediment are: depth of sediment deposition, sediment characteristics, chemical characteristics of cohesive sediment, variation of the pool level and the age of the deposited sediment.

D) Turbidity Current

When water with high suspended sediment flows into the clear ambient water of a reservoir, the difference between the two densities will create two different layers in the reservoir. This phenomenon has a significant effect on the pattern of sediment deposition in some large reservoirs. Consideration of the effects due to this phenomenon is the subject of the present research. Figure 1.3 shows a schematic view of such a current.

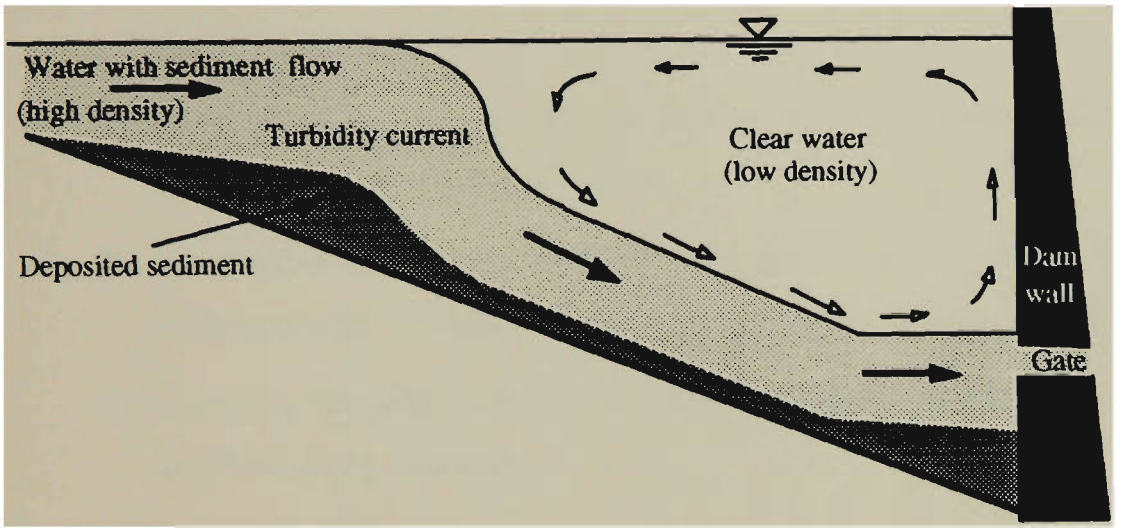

Figure 1.3 Turbidity current in a reservoir.

There are some other factors that can effects reservoir deposition such as wind and thermal stratification. These factors are not significant in compare with the above mentioned factors.

1.5 Objectives of the Research

Consideration of the effect of turbidity current in reservoirs, particularly in large reservoirs with high suspended sediment inflow, and its effects on the sedimentation process is the objective of the current study. The prediction of long term reservoir sedimentation will result in an error if turbidity current effects are ignored. Furthermore, mathematical models in which the turbidity current is taken into account should consider other factors such as water level, the non-equilibrium transportation of sand particles, scour and deposition of cohesive sediment particles, the effect of flocculation on fall velocity of fine sediments and the unit weight of the deposited sediments.

Based on these concepts, the objectives of the present study are:

I. to review literature on reservoir sedimentation methods, theoretical aspects of sediment transport and depositional processes in watercourses and turbidity current.

II. to study some aspects of the head of the gravity current, including its velocity of the head and its sediment transport and deposition processes, through laboratory experiments.

III. to study the steady state gravity current, water entrainment and sediment transport and depositional processes.

IV. to develop a new mathematical model for predicting the sediment depositional processes in reservoirs which takes into account the turbidity current effects.

V. to test and verify the proposed model through laboratory experiments and field data from a large reservoir

VI. to test the applicability of the new model in controlling turbidity current and estimating the effects on the sediment deposition in reservoirs.

1.6 Contributions made in the Research

The main aim of this investigation was to consider the effects of turbidity currents on the sediment transport and depositional processes in reservoirs. Gravity current experiments were conducted in a laboratory flume. A new equation for the prediction of the velocity of the gravity current is proposed. The sediment transport by the head and the body of the turbidity current are compared and the role of the head of the current on the sediment transport and deposition processes is discussed. A new equation for water entrainment coefficient is introduced based on the results of the experiments in this study and some available laboratory and field data from literature. Furthermore, an equation based on the available data is presented for sediment entrainment of the turbidity current.

The equations of flow and sediment were linked with those of the turbidity current and a new computer program called "DEPO" has been developed. DEPO is the first sedimentation model that can handle the effects of turbidity currents on the sediment

transport and depositional processes in reservoirs. The model was tested using data collected from the laboratory experiments. It has been shown that the model including the turbidity current effects provides a very accurate prediction of the sedimentation processes. Furthermore, the new model, DEPO, was applied to Dez Reservoir, one of the largest reservoirs in Iran. The estimated data with and without consideration of the turbidity current are compared with measured data from the reservoir. The results show a remarkable improvement in prediction when the turbidity current is included in the sedimentation processes. Finally, the model was run to predict the sedimentation in Dez Reservoir when a bottom gate is installed to release some of the floodwater as an alternative to it being released through the existing gates. In the case of using a bottom gate, the model predicted that a significant reduction of sediment deposited in the reservoir can be achieved. One of the most significant advantages of the proposed model - that can be used in reservoir management - is to predict the occurrence, movement and sedimentation of the turbidity current. Thus, the reservoir manager can estimate the effects of the storage or release of each discharge on future sedimentation and arrive at an optimum decision. This model can also estimate the distribution of bed gradation in the surface layer of the material deposited.

1.7 Scope of the Research

In accordance with the objectives outlined in section 1.5, this thesis includes nine chapters.

The first chapter describes the main aim of the research, the impact of reservoir sedimentation on the environment and factors affecting reservoir sedimentation.

Chapter two is a literature review of investigations related to the subject. Important research on reservoir sedimentation factors are reviewed. The existing methods for predicting reservoir sedimentation and the advantages and disadvantages of each method are discussed.

In Chapter three, the theoretical aspects of sediment process computation have been described. The sand and cohesive sediment transport functions are presented. The

concepts of active layer and armour layer are described and the turbidity current characteristics and its behaviour in a large reservoir have been studied.

Chapter four describes the experimental equipment and procedures. All experimental apparatus and the measurement equipment are described. The experiments and the methods of collecting data are described.

In Chapter five the results of the experiments on the head of the gravity currents are presented. A summary of the collected data is shown and the results related to the flow and sediment aspects of the head are obtained. A new equation has been proposed for the velocity of the head.

In Chapter six the results of the experiments on the sub-critical gravity currents (the body) are presented. The initial conditions and a summary of the collected data are shown. The results related to the flow and sediment aspects of the head are obtained. Based on the calculated data from this study and the available data in water and sediment entrainment of the turbidity current, new equations are presented.

Chapter seven describes the governing equations for modelling sediment deposition with consideration of the turbidity current effects. All details of the new computer model, "DEPO", including turbidity current effects are explained. The theoretical basis, numerical technique and data requirements are described.

In Chapter eight, the new model is verified with experimental and actual reservoir data. The details of experimental results are discussed and compared with model results. The model is then applied to Dez Reservoir, a large reservoir in Iran, based on the actual data obtained. Also the data of Dez Reservoir are used for running the HEC-6 model entitled "Scour and Deposition in Rivers and Reservoirs" and the results are compared with the results obtained from the new model "DEPO".

A summary of the major conclusions from this research together with some suggestions for future studies are presented in Chapter 9.

The structure of the nine chapters is shown in Figure 1.4.

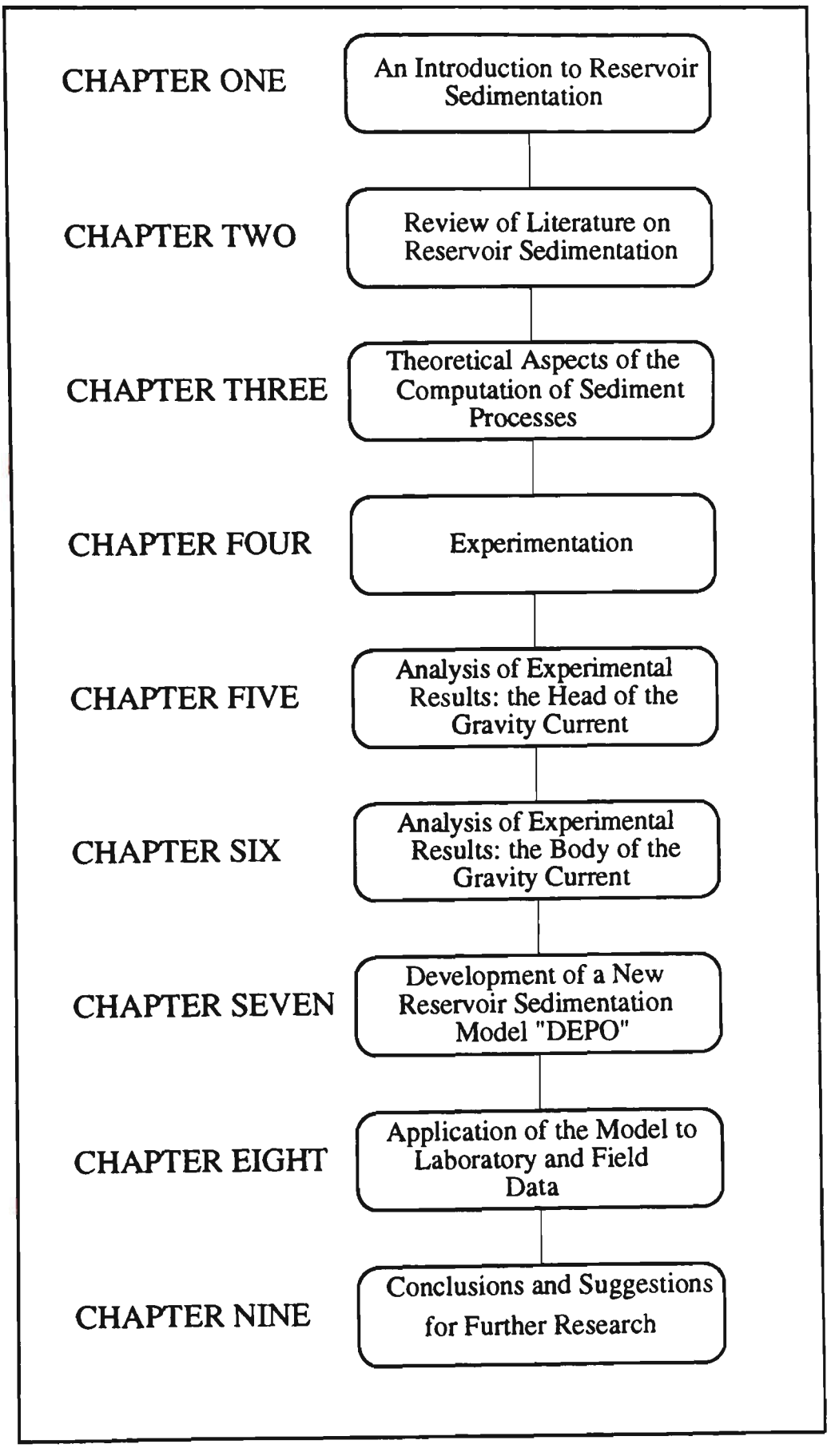

Figure 1.4 The structure of the chapters.

Chapter Two

REVIEW OF LITERATURE ON RESERVOIR SEDIMENTATION

2.1 Introduction

Prediction of sediment deposition is always needed in the planning, design and operation stages of reservoir systems. Researchers in this area have examined numerous parameters which affect the sediment processes. Modelling of this phenomenon requires knowledge of the principles of open channel hydraulics, hydrology, geomorphology and structural features.

In this chapter the methods of trap efficiency and the existing methods to predict reservoir sedimentation are presented and discussed.

2.2 Trap Efficiency

The ratio of the quantity of deposited sediment to the total sediment inflow is called trap efficiency. This parameter is mostly used in empirical methods of reservoir sedimentation. It is not used in mathematical methods of reservoir sedimentation, because it can be calculated directly from a comparison of the sediment discharge into and out of the reservoir. The methods formulated to predict trap efficiency are very simple for predicting the quantity of sediment deposited in, or passed through, the reservoir without deposition. These methods are empirical and based on measured data from different reservoirs. Although most of the sediment and reservoir characteristics

affect the value of trap efficiency, only some of them are used in the trap efficiency formulae.

Brown (1944) related trap efficiency to the ratio of capacity of the reservoir and the area of the watershed. He used data from 34 actual reservoirs and provided a graph as shown in Figure 2.1 for calculating the trap efficiency. He defined the ratio of C/W, where C is the capacity of the reservoir in acre-feet and W is the area of the catchment in square miles.

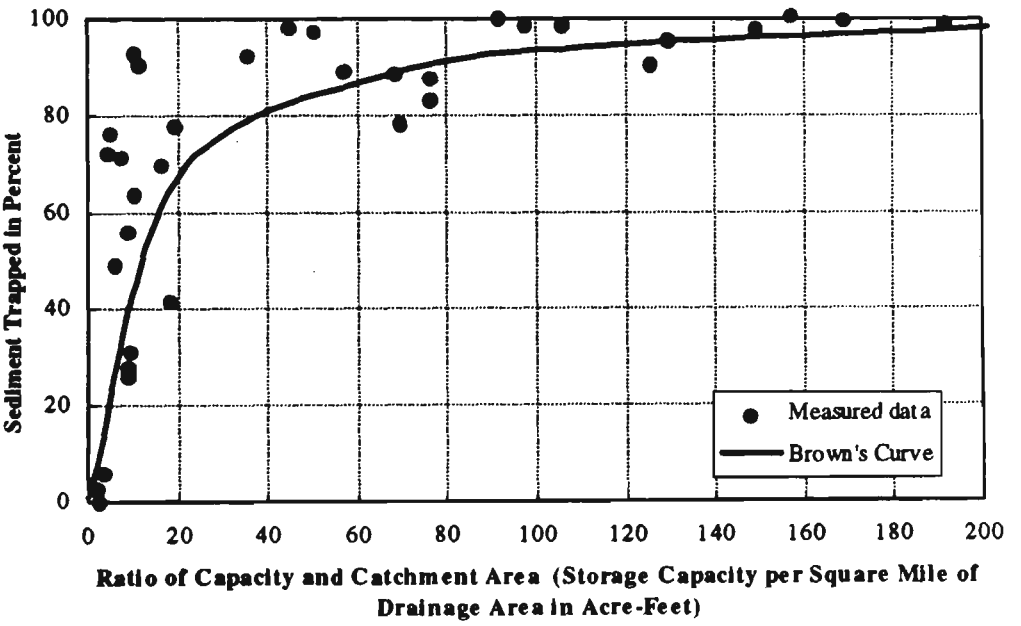

Figure 2.1 Reservoir trap efficiency [after Brown, 1944].

Churchill (1948) correlated the trap efficiency with a sedimentation index based on Tennessee Valley Authority reservoirs. The sedimentation index is equal to the ratio of the retention period to the mean velocity of the flow through the reservoir. The Churchill curve is shown in Figure 2.2. Terms used in Figure 2.2 are defined as follows:

Capacity = capacity of the reservoir in the mean operating pool for the period of the analyses (ft^3).

Inflow = average daily inflow rate during the study period (ft^3/sec).

Retention time = capacity divided by average inflow rate ($ft^3/ft^3/sec$).

Length = reservoir length at mean operating pool level (ft).

Velocity = mean velocity, which is arrived at by dividing the inflow by the average cross sectional area in square feet. The average cross sectional area can be determined by dividing capacity by the length (ft/sec).

Sedimentation index = retention time divided by velocity (sec^2/ft).

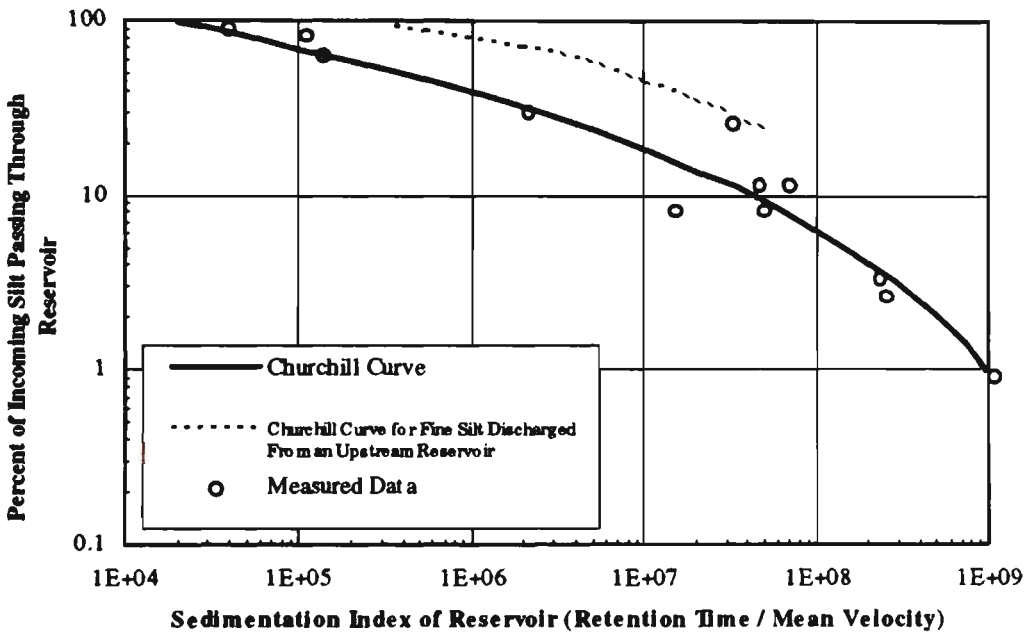

Figure 2.2 Reservoir trap efficiency [after Churchill, 1948].

Brune (1953) developed a relationship between the trap efficiency and the reservoir capacity-inflow (C_r/I) ratio where C_r is the capacity of the reservoir (m^3) and I is the volume of annual water inflow (m^3). The curves resulting from this method is depicted in Figure 2.3.

Karaushev (1966) developed an equation for trap efficiency in small reservoirs as:

$$TE = 1 - \left[1 - (C_r/I)\right] \exp\left[\frac{-\phi (C_r/I)}{1 - (C_r/I)}\right] \qquad (2.1)$$

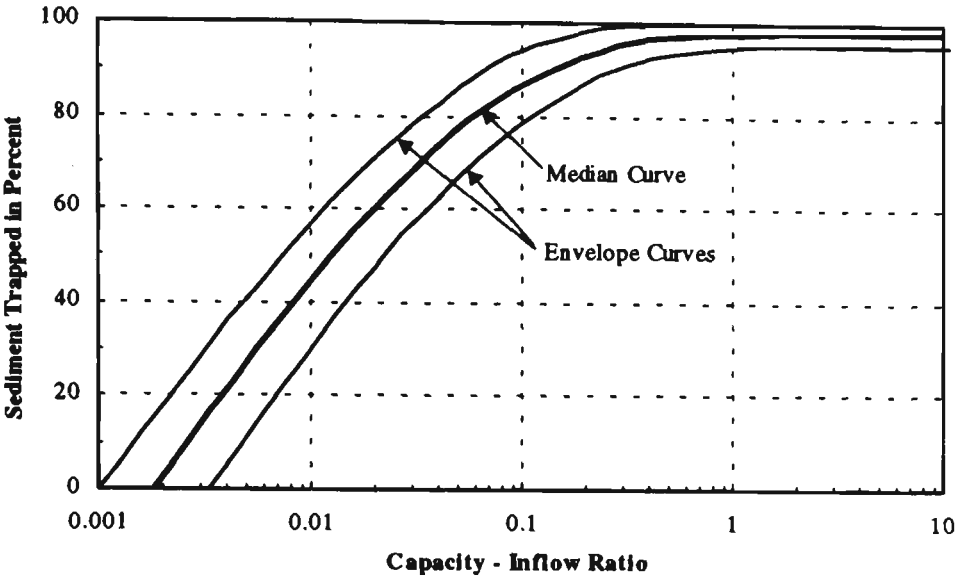

Figure 2.3 Reservoir trap efficiency [after Brune, 1953].

where

TE = trap efficiency

$\phi = \dfrac{\bar{v}_s t_s}{\bar{h}_r}$

$\bar{v}_s$ = mean fall velocity of the transported sediment (m/s)

t_s = duration of spill over period (s)

$\bar{h}_r$ = the mean depth of the reservoir (m).

Bube and Trimble (1986) revised the Churchill curves based on measured data from some of the US reservoirs. Figure 2.4 shows a revision of the Churchill curves conducted by Bube and Trimble. For the sedimentation index less than 10^5 the revised curve shows a considerable difference compared with the curves presented by Churchill (1948). For the other ranges there is no significant difference.

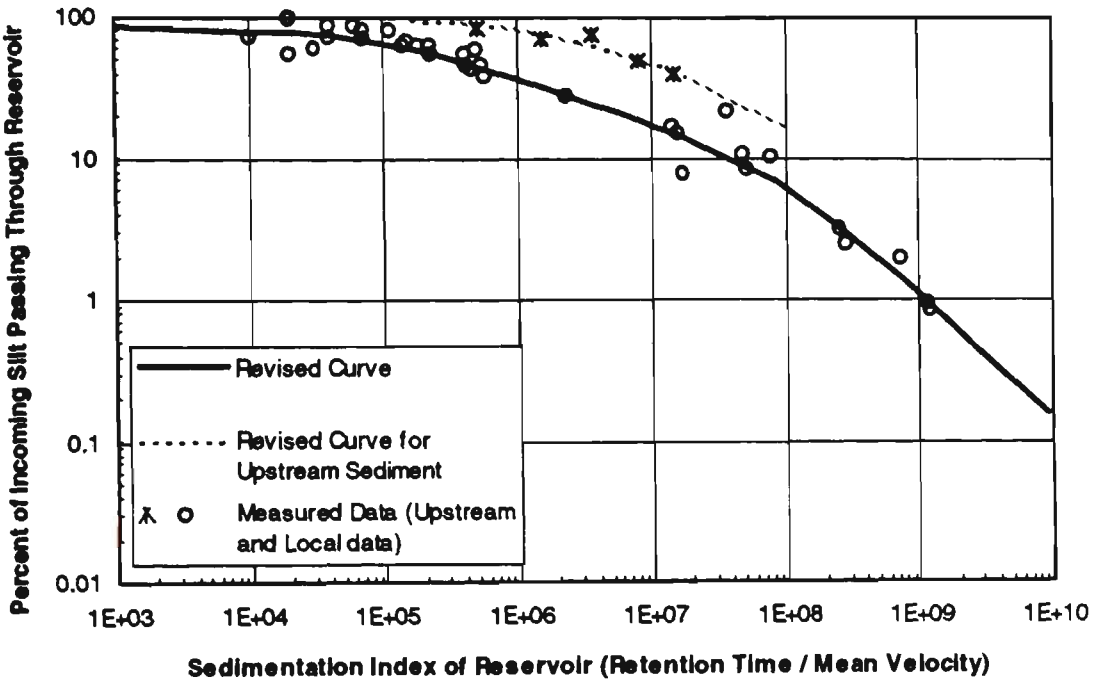

Figure 2.4 Reservoir trap efficiency, revision of the Churchill Curves [after Bube and Trimble, 1986].

Based on some actual reservoirs and laboratory data, Skryl'nikov (1989) related the trap efficiency to the ratio of the volume of the channel C_s in which the flow transports the design amount of sediments of a given fractional composition and with the design capacity of the reservoir C_r. He divided the trap efficiency values into two stages. The trap efficiency in the first stage is a constant and equal to one (TE=1). The ratio of $C_s/C_r = 0.12$ is an index for transition from the first to the second stage. According to this criterion, if the initial storage capacity of the reservoir,

$$C_r > 8.33\, C_s \qquad (2.2)$$

then the siltation will occur at first stage, and if,

$$C_r \leq 8.33\, C_s \qquad (2.3)$$

then the siltation will occur at the second stage. In the second stage the trap efficiency will be calculated as follows:

$$TE = 0.041\left[(C_s/C_r)^{-1.5} - (C_s/C_r)\right] \qquad (2.4)$$

Generally, the methods outlined above for calculating trap efficiency are very simple and basically determine the volume of sediment deposition without regard to the sediment distribution. Most empirical methods for distributing sediment in reservoirs also need to determine the volume of deposition by using the trap efficiency of the reservoir. The equations of trap efficiency are empirical and are obtained based on field or laboratory data. Significant differences may be obtained using different equations. Therefore, equations of trap efficiency should be qualified, based on their initial conditions, before using them in a particular case.

2.3 Reservoir Sedimentation Prediction Methods

Study on reservoir sedimentation began in the 1950's when the first reservoirs were resurveyed. Many efforts, were made to describe the sediment deposition processes in reservoirs. The first attempts were empirical and were based on few actual observations.

The first important attempt to construct a mathematical method for sediment deposition for field situations was developed in 1968 by Bonham-Carter and Sutherland. They used jet theory to simulate sediment deposition at a river mouth discharging into the sea. In 1974 Merrill used diffusion equations for modelling reservoir sedimentation. Subsequently many investigators have used sediment transport equations to model sediment processes in rivers and reservoirs. This category of methods was developed with the aid of high speed computers and the development of knowledge occurred on various aspects of sediment deposition and scour in the reservoir.

2.3.1 Empirical Methods

Empirical methods are based on observations and field measurements made on existing reservoirs. The capability of these methods are limited to a few features only, which may be important in the preliminary evaluation of reservoir planning. Investigators in this area tried to establish a general trend for sediment deposition in reservoirs based on the

measured data from some existing reservoirs. Some of the important methods are mentioned briefly.

Cristofano (1953) presented the "Area Increment Method" for predicting the distribution of sediment in a reservoir. This method assumes that the deposition follows a constant pattern, and deposition could be approximated by reducing a fixed amount of reservoir area at each elevation. The application of this method in a reservoir needs Equation 2.5 to be solved in an iterative manner to balance the calculated and expected sediment deposition volume.

$$V_s = \sum_h A_0 \left(h_r - h_0\right) + V_0 \qquad (2.5)$$
$$H \geq h_r \geq h_0$$

where V_s is total volume of sediment; A_0 is water surface area of the original reservoir basin at height h_0; H is maximum reservoir depth at dam wall measured from original zero elevation; h_0 is assumed as the depth of sediment at dam wall; V_0 is volume of sediment accumulated under depth h_0; and h_r is variable depth measured from original zero elevation. The sediment distribution under this method is very simple and it is schematically shown in Figure 2.5.

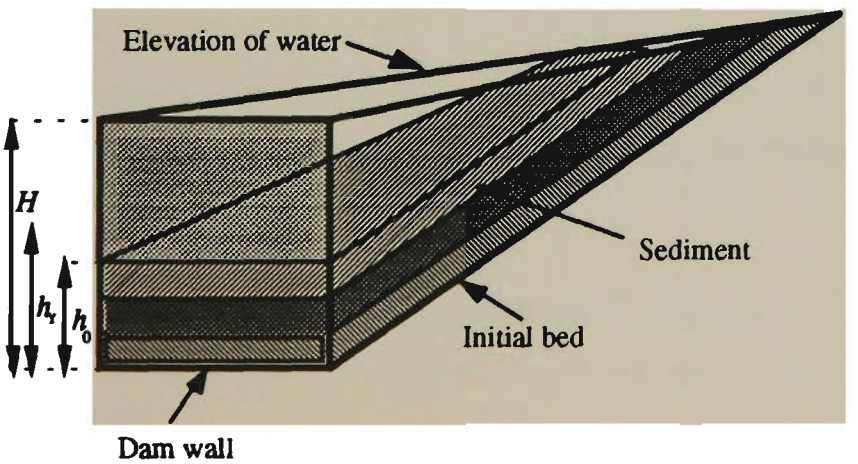

Figure 2.5 Sediment distribution by the area-increment method (Cristofano, 1953).

Borland and Miller, in 1958, presented the well known "Empirical Area-Reduction Method". This prediction method for probable sediment distribution is accomplished through two main steps: (1) Classify the reservoir using 4 basic standard type curves which were developed from actual resurvey data. (2) Make a trial and error type computation using the average area or prismoidal formulae until the computed capacity

equals the predetermined capacity. The resurvey data from 30 reservoirs has been used to develop four standard type curves of percentages of sediment deposit versus reservoir depth percentages. The general classification of reservoirs is shown in Table 2.1.

Table 2.1 Standard reservoir type for using Empirical Area-Reduction Method

M*	Reservoir type	Standard classification
1.0-1.5	Gorge	IV
1.5-2.5	Hill	III
2.5-3.5	Flood Plain-Foothill Lake	II
3.5-4.5	Lake	I

* M is the reciprocal of the slope of the line obtained by plotting the reservoir depth (m) as ordinate against reservoir capacity (m^3) as abscissa on log-log paper.

The dimensionless relative area for each standard type of reservoirs is expressed by Equation 2.6.

$$A_p = C_u \; p^i \; (1-p)^j \qquad (2.6)$$

where A_p represents a dimensionless relative area at relative distance p above the stream-bed. C_u, i and j are dimensionless constants which are determined by the type of reservoir as given in Table 2.2

Table 2.2 Dimensionless coefficients C_u, m and n.

Type	C_u	i	j
I	3.4170	1.5	0.2
II	2.3240	0.5	0.4
III	15.882	1.1	2.3
IV	4.2324	0.1	2.5

The rest of the procedure would be mathematical calculation. The schematic distribution of sediment deposition is shown in Figure 2.6.

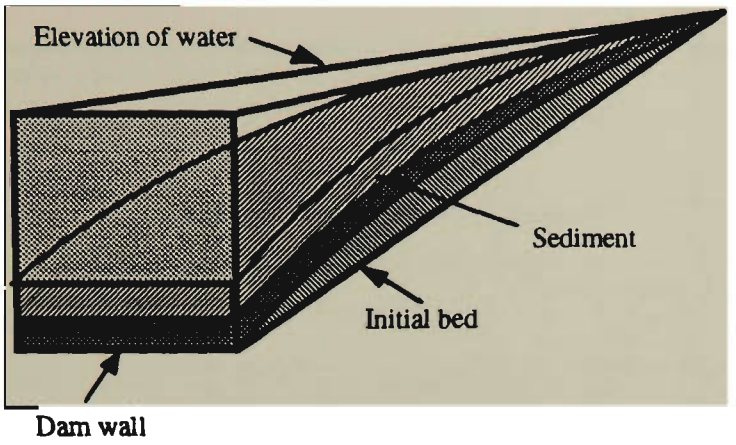

Figure 2.6 Sediment distribution pattern in Empirical Area-Reduction Method.

Hobbs' in 1969 presented a method, called the "Pool-Elevation Duration Method". According to this method, a part of the total sediment deposition will be deposited above the pool-elevation that will be exceeded only 5 percent of the time. The remainder of the sediment will be distributed below the pool level. Distribution of the sediment deposition in this method requires a pool-elevation-duration analysis and sediment size distribution to estimate the amount of deposition above and below the pool level. The percentage of the total sediment deposits above the water level can be determined from Figure 2.7 which is based on the data from 11 reservoirs. Figure 2.8 is used for distribution of the rest of the sediment throughout the reservoir.

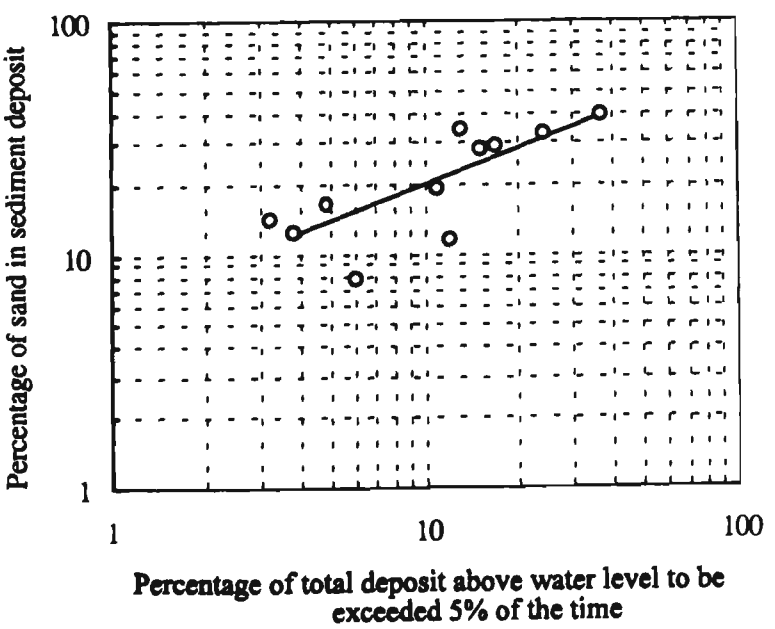

Figure 2.7 Percentage of sediment to be deposited above 5 per cent pool elevation level [Hobbs, 1969].

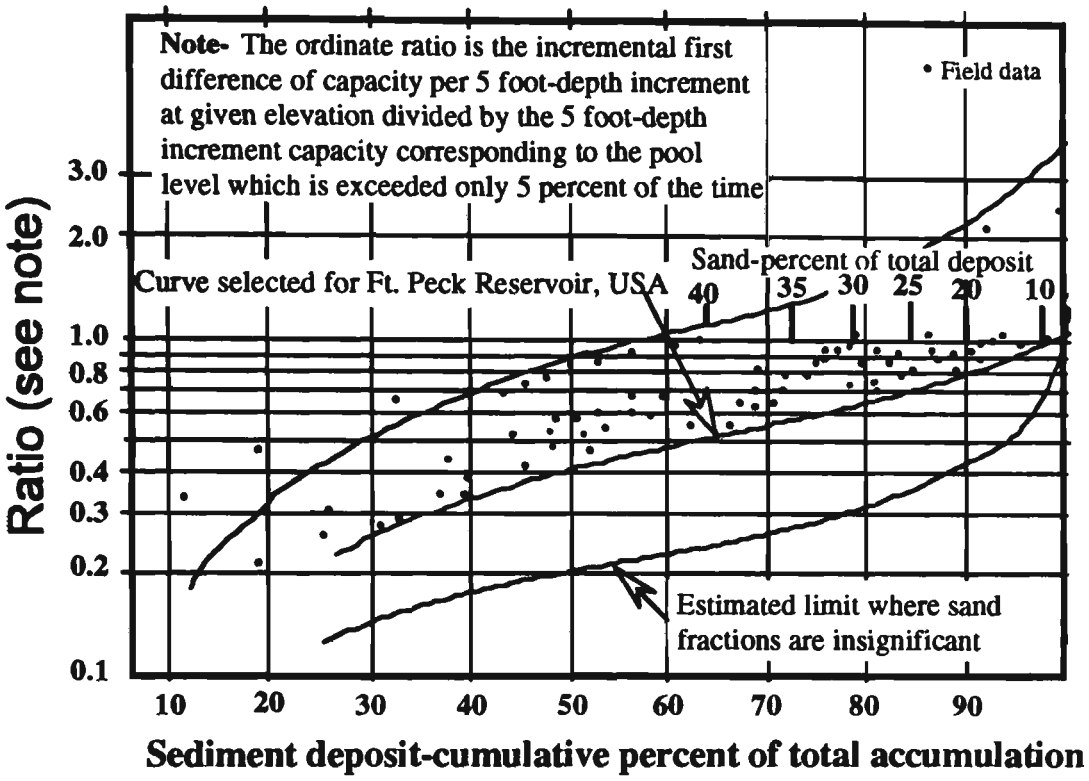

Figure 2.8 Sediment distribution in large reservoirs (Hobbs, 1969).

Borland in 1971 proposed a method for calculating the slopes of the sediment deposited in a typical delta (Figure 2.9). He assumed that all the sediment is deposited in a typical delta. Based on the results obtained from 31 American reservoirs, he found a ratio between the topset slope of the delta and the original river bed slope. According to the measured data, the ratio was between a 1.0 (curve 1) and a 0.2 (curve 3). The ratio of 0.5 (curve 2) was proposed by Borland for design purposes. The frontset slope is calculated by multiplying the topset slope by a constant factor equal to 6.5. The relationship between the original river bed slope and topset slope is shown in Figure 2.10.

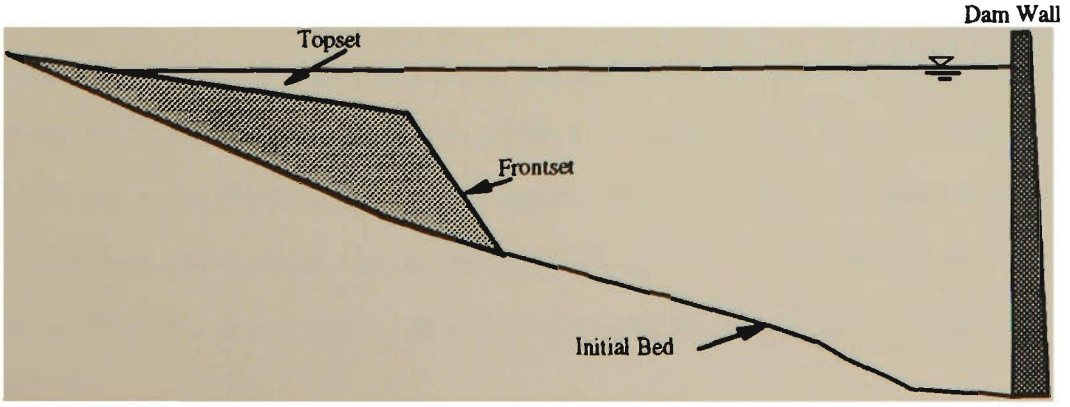

Figure 2.9 Typical delta in a reservoir.

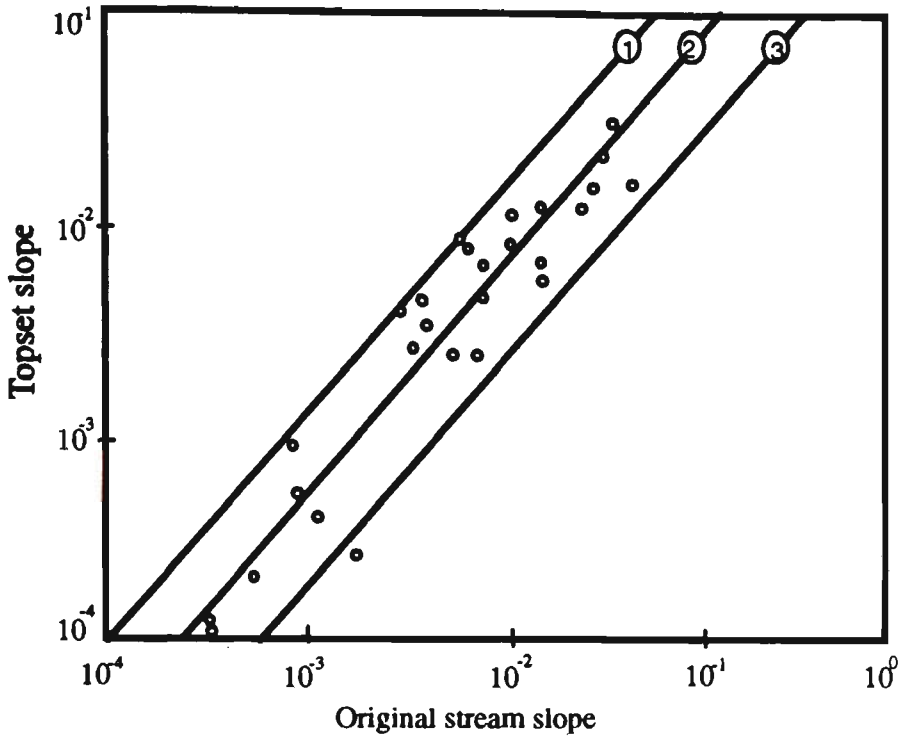

Figure 2.10 Relationship between original stream slope and topset slope [after Borland, 1971].

Szechowycz and Qureshi (1973) took into account the delta formation and progressed to calculate the rate of storage depletion and estimate the useful life of Mangla Reservoir in Pakistan. They used the available methods to calculate the volume of sediment deposition in the reservoir. Available data was used to calculate the mean annual suspended sediment load and the bed load was assumed to be 10% of the estimated suspended load. They also used Lane and Koelzer's (1943) formula for estimating the specific weight of sediment deposition, assuming that deltas were formed only by deposition of the bed material load. They also assumed that all particles in bed load plus all sand particles and 25% of silt particles in suspended load, will form the bed material load. The rest of the sediment including 75% of the silt, and all the clay particles were deposited in the lower reaches of the reservoir or passed through the reservoir. Based on previous assumptions and considering annual fluctuations of the water level, median size of the bed material load, channel width and depth of the dominant discharge, they calculated the delta deposition. The amount of trapped fine sediment was determined using the lower curve from the Brune method (1953). The pattern of fine sediment deposition was not determined. A schematic description of their method is shown in Figure 2.11.

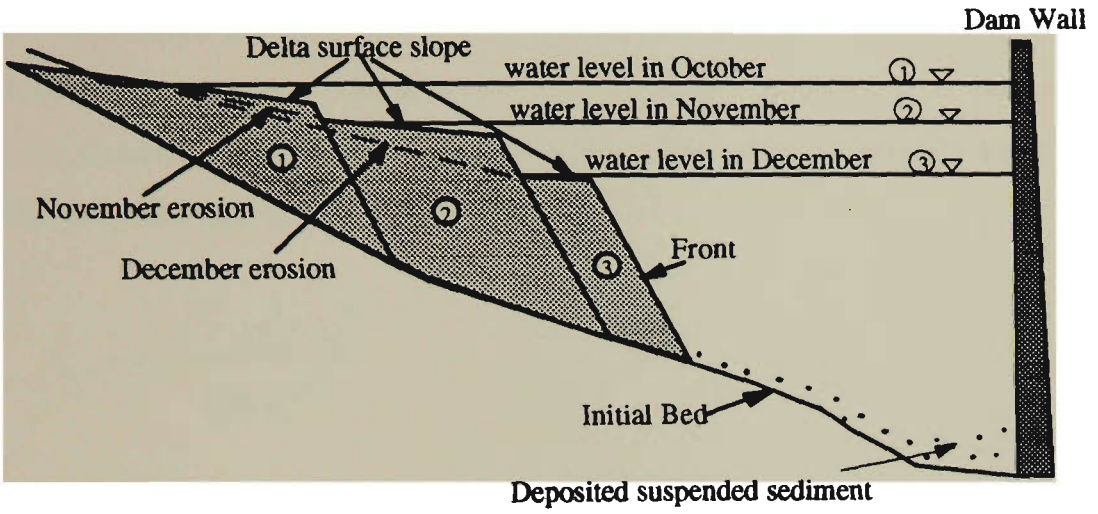

Figure 2.11 Schematic description of delta formation [Szechowycz and Qureshi, 1973].

Garde et al. in 1978 (Simons et al, 1982) developed a scheme for predicting progressive delta formation. They estimated the progressive loss of capacity using Equation 2.7.

$$\frac{V_S}{C_0} = \frac{(t/t_*)^m}{\left[1+(t/t_*)^{m/e}\right]^e} \qquad (2.7)$$

where

C_0 = initial volume of reservoir (m^3)

V_S = volume of sediment deposited in t years (m^3)

t = time in years since reservoir operation began

m, n = constants for a given reservoir,

t_* = time in years when $V_s = C_0$ (reservoir full with sediment)

m = slope of V_s/C_0 versus t on log-log paper

e = represents the departure from a straight line of the plot of V_s/C_0 versus t at V_s/C_0 approximately equals to 0.6. Based on the analysis of reservoirs that were completely filled, n is approximately equals to 0.25.

When the constants are established in Equation 2.7, the distribution of the sediment in the reservoir can be predicted with the aid of empirical relationships between geometric variables.

Chien in 1982 (cited in Annandale 1987) presented an empirical equation to estimate the delta formations based on Chinese reservoirs. He used Equation 2.8 to estimate topset slope, and frontset slope by multiplying the topset slope with the constant value equal to 1.6. The proposed equation is as follows:

$$S_t = A_* \frac{S_*^{5/6} D_{50}^{5/3} d_{50}^{1/3}}{(Q/B)^{1/2}} \qquad (2.8)$$

where

S_t = the topset slope of delta

A_* = a coefficient ranging between 1.21×10^4 and 1.68×10^4 for various Chinese reservoirs

S_* = mean sediment concentration during flood season (kg/m^3)

D_{50} = median diameter of bed material in suspension (m)

d_{50} = median diameter of bed material (m)

Q = mean discharge during flood season (m^3/s)

B = width of the flow (m)

In addition to these methods, Menne and Kriel (1959), Croley et al. (1978) and Pemberton (1978, cited in Annandale 1987) presented reservoir sedimentation methods that are similar to the methods described in this section.

2.3.2 Discussion on Empirical Methods of Reservoir Sedimentation

The empirical methods of reservoir sedimentation can be classified into two major groups. Some of them such as the Area Increment Method, Empirical Area-Reduction Method, Menne and Kriel Method, and the Pool-Elevation Duration Method assume that the sedimentation in a reservoir follows a relatively constant pattern. The methods described by Borland, Szechowycz and Qureshi, Garde et al, and Chien assume that the bulk of sediment is deposited in a typical delta and, based on this assumption, they attempted to formulate the slopes of delta formation.

Generally, empirical methods do not cover all aspects and conditions of reservoir sedimentation. These methods are based on one or more observations and generalising the model for all cases is not appropriate. There are glaring differences among the deposition pattern results from these methods. These have been schematically illustrated in Figures 2.5, 2.6 and 2.10. This causes difficulty in selecting a method that is suitable for each reservoir. Dividing reservoirs into a few categories or applying a specific equation for the deltaic sediment deposition without a precise analysis of the hydraulic and sediment process in actual geometric conditions provides a very low approximation. Although empirical methods are not very reliable in comparison with mathematical methods, some of them (eg. "Empirical Area-Reduction Method" by Borland and Miller, 1958) are still utilised for reservoirs sediment analysis. The simplicity of the methods and less data requirement for analysis are reasons for employing empirical methods in some cases.

2.3.3 Mathematical Methods

Mathematical models are based on mathematical solutions for all phenomena affecting sediment transportation, distribution, deposition and scour. These models often require repeated calculations of a number of equations by computer. From a theoretical point of view, three different concepts can be found in the mathematical methods; "Jet Theory", "Diffusion Theory", and the methods using sediment transport theory. Apart from Bonham-Carter and Sutherland (1968) (using the "Jet Theory"), and Merrill (1974) (using the "Diffusion Theory") methods, the other mathematical methods are based on sediment transport theories and are solved using the continuity of sediment, continuity of water flow, dynamic equation, and sediment transport equation. Some of the analytical methods are briefly mentioned as follows:

Bonham-Carter and Sutherland (1968) presented the "Jet Theory" method for predicting delta deposition in a river mouth discharging into the sea. They used plane jets theory to predict sediment deposition. A rectangular open channel flow is assumed for the river and the situation is compared with a jet discharging from a slot. The streamwise velocity is predicted by different equations in three parts of jet zones as shown in Figure 2.12.

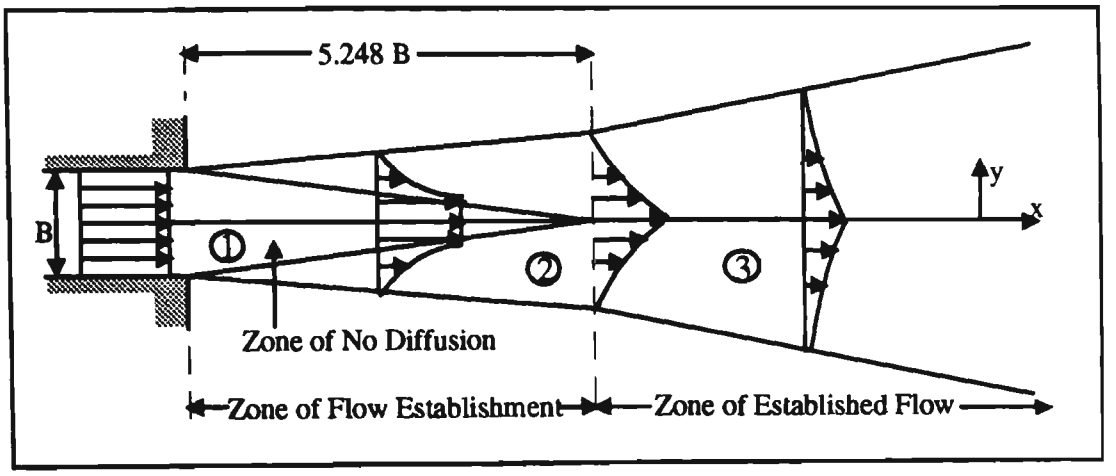

Figure 2.12 Structure of velocity field in Jet Theory.

To calculate the sediment deposition, the river mouth is divided into a number of cells by means of a vertical grid as shown in Figure 2.13. All sediment which passes through a grid river-mouth cell are assumed to follow the same path as would a nominal particle that had the coordinates of the cell center at x = 0.

This model can be used for an expanded connection between river and reservoir where the width of channel will be abruptly expanded. Also, the model can be used for coarse particles but could not apply when fine particles are present in significant amount in the flow. No records of using this model for the prediction of sediment deposition in actual reservoirs have been reported.

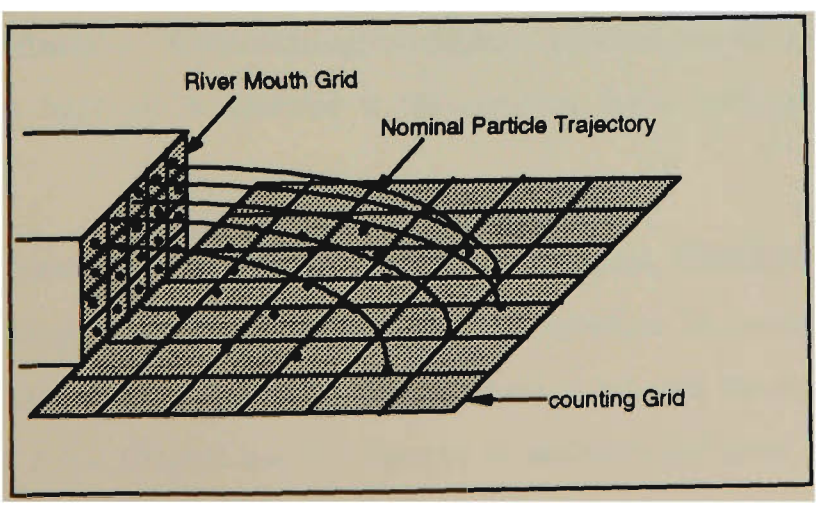

Figure 2.13 Orientation of computational grids at river mouth and nominal particle trajectories.

Merrill (1974), used "Diffusion Theory" to predict deposition in reservoirs. He modelled the process by a two-dimensional diffusion equation as:

$$\frac{\partial c}{\partial t} = k_x \frac{\partial^2 c}{\partial x^2} + k_y \frac{\partial^2 c}{\partial y^2} \qquad (2.9)$$

where

c = the sediment concentration

x, y = the longitudinal and lateral directions, respectively

t = time

k_x, k_y = the diffusion coefficient in x and y direction, respectively.

The reservoir is divided into two-dimensional cells to solve Equation 2.9 by finite-difference numerical method. A volume of sediment, for the period of analysis, is diffused by an iterative manner until a predetermined trap efficiency is achieved. At this time it is assumed that all sediment in suspension settles to a location below its present position and the additional thickness is added to the previous elevation of the cells.

The important problem of this method is that the value of diffusion coefficients is not known and the output of the model is significantly affected with values of the coefficients. Furthermore the large particles (sand and large silt) obviously not diffuse and cannot model with Equation 2.9. The diffusion coefficients used in this model are the same for all fractions. Consolidation of different particles are not considered. The elevation of the reservoir is assumed to be constant for a long period (ten years minimum).

There are some models (eg: FLUVIAL, HEC-6, CARICHAR, CHARIMA, FCM) which use sediment transport theories for simulating sedimentation in rivers and reservoirs. The models procedure in general compare the difference between the sediment transport capabilities of a given channel and the amount of sediment fed from upstream of the channel. The difference between these quantities show the amount of scour or deposition in the channel. These models are generally based on the equations of continuity and motion for water and sediments over a mobile bed. The bed elevation is

evaluated by relating the sediment transport capacity to local flow and bed characteristics. Generally these methods are realistic for prediction of sediment-flow interaction in natural streams.

A one-dimensional solution has been widely used for the prediction of the sedimentation process in rivers and reservoirs since the 1970s. The applicability and accuracy of models depends on the recognition of physical foundation and numerical techniques employed.

A complete model of reservoir sedimentation would require the mathematical solution of three-dimensional water flow and sediment transport models. This is still not possible at this stage of knowledge of computational hydraulics and it is also believed that the three-dimensional model is not necessary for most conditions. For most practical purposes, however, one-dimensional models provide a satisfactory answer and most of the work on this area relates to such cases.

Chang and Richards (1971) developed a model to determine the sensitivity of the method of characteristics. Three basic equations describing the unsteady flow in alluvial channels are derived from the equation of continuity for sediment, the equation of continuity for water, and the equation of motion of sediment-laden water as follows:

continuity of sediment

$$\frac{\partial Q_{sd}}{\partial x} + (1 - p_o)\frac{\partial A_{sp}}{\partial t} - q_{sd} = 0 \qquad (2.10)$$

continuity of water

$$\frac{\partial Q}{\partial x} + \frac{\partial A}{\partial t} + p_o \frac{\partial A_{sp}}{\partial t} - q_t = 0 \qquad (2.11)$$

momentum equation

$$\frac{\partial Q}{\partial t} + \frac{\partial (VQ)}{\partial x} + g A \frac{\partial (D + y_b)}{\partial x} + g A S_e = 0 \qquad (2.12)$$

where

Q_{sd} = sediment discharge

A_{sp} = cross section area of suspended sediment

Q = water discharge

A = cross section area of flow

x = the distance along channel

t = time

V = mean velocity of water

g = gravitational acceleration

D = flow depth

y_b = the bed elevation

S_e = energy slope

p_o = bed-sediment porosity

q_{sd} = lateral discharge of sediment

q_w = lateral discharge of water

q_t = lateral discharge of sediment-laden water

The definition sketch is shown in Figure 2.14.

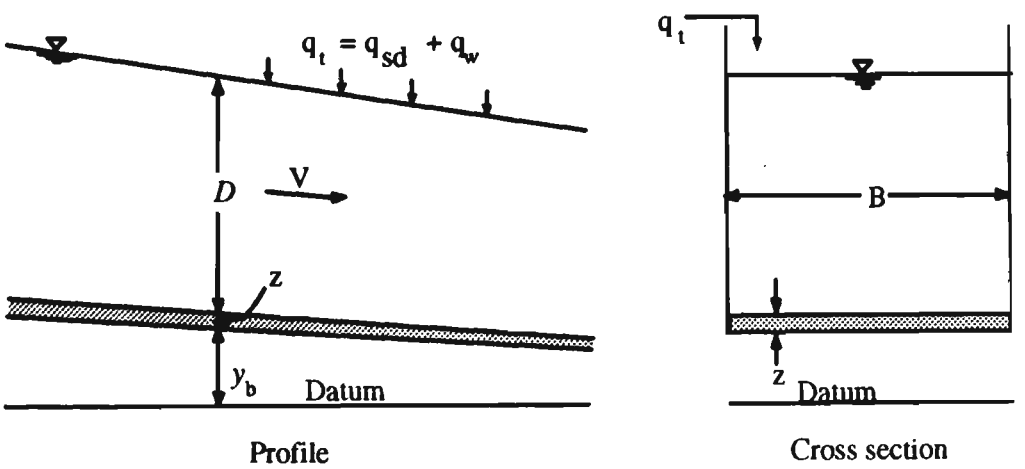

Figure 2.14 Definition sketch of an alluvial channel.

The total concentration of sediment per unit width is expressed by Chang and Richards in terms of V and D as:

$$c = \frac{k}{g\, v_s} V^d D^r \qquad (2.13)$$

where

c = concentration of sediment

k, d, r = coefficients of sediment transport capacity

v_s = average fall velocity of sediment

The model was applied only to a hypothetical reservoir and no prediction has been reported for actual reservoir.

Yücel and Graf (1973) developed a computer model for simulating sediment deposition in a rectangular reservoir which has a unit width. The procedure was based on first calculating the water elevation using the "standard step method" (Henderson, 1966) and then route sediment from upstream. Three bed load equations; Schoklitsch, Meyer-Peter and Müller (1948), and Einstein (1942) were used in the model.

The model was applied only to a hypothetical reservoir rectangular cross-section for comparison. The different patterns of sediment deposition in a delta region obtained using Schoklitsch, Meyer-Peter and Müller, and Einstein bed load equations are shown in Figure 2.15.

The model was developed for comparison of the three above mentioned bed load equations and no actual prediction is reported. The prediction of sediment deposition in actual cases using this model requires many modifications.

Asada (1973) presented a model for mountain rivers and reservoirs based on his own sediment transport equation. The procedure is similar to the above methods. At first backwater profiles for initial bed slope is calculated using non-uniform steady equations. After that, the amount of bed deformation, dz, during time interval, dt, is calculated using the sediment transport equation and equation of continuity of sediment. Finally, the grading curves of bed materials after dt in each reach are calculated based on the difference of sediment discharges for each grain size and the amount of grain size which is distributed in the sub-surface layer. These procedures can be repeated for calculation of the bed elevation at an optional time.

He used the model for Shingo regulating pondage and upstream of the Shingo pondage in the Agano river (in Japan) and fairly good results between prediction and measured bed elevation were reported. In Figure 2.16 the result of the sediment bed profile calculation in the Shingo pondage is shown. The poundage is mainly fed by the Agano

River and the location of a tributary (Tadami River) entry into the poundage is also shown in Figure 2.15.

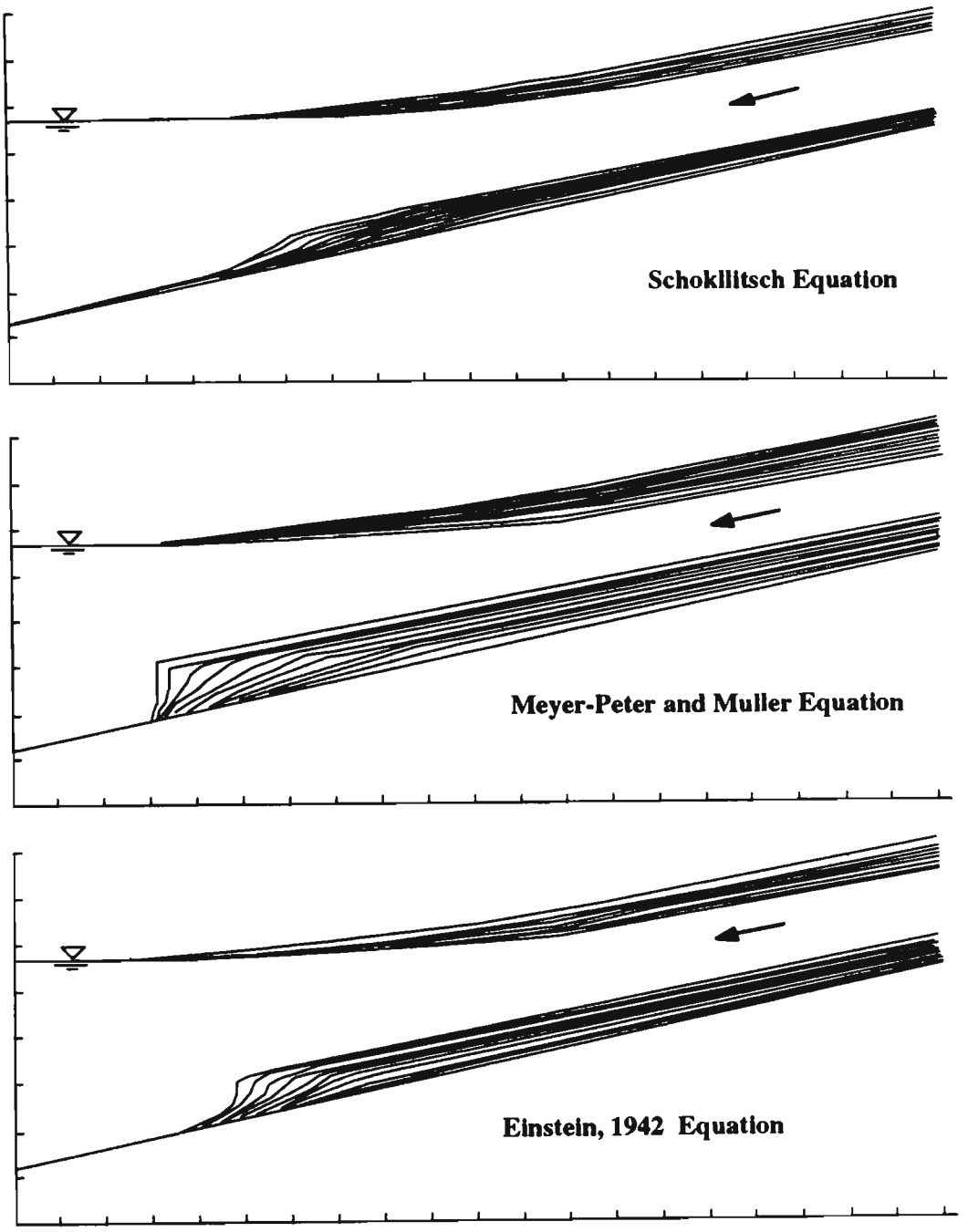

Figure 2.15 Prediction of sediment distribution patterns obtained using different bed load equations [after Yücel and Graf, 1973].

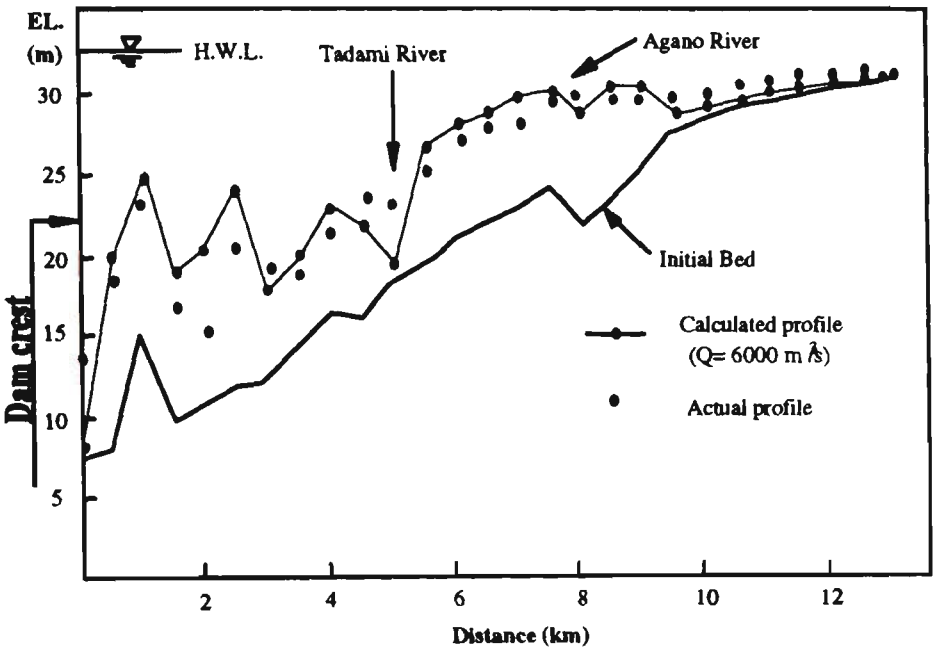

Figure 2.16 Calculated and measured bed profiles for Shingo regulating pondage (Asada, 1973)

The main problem in using this model is the unique sediment transport equation used for mountain river. The sediment transport equation has empirical coefficients that should be determined for each grain size based on the data of deposited sediment in a reservoir or river bed deformation. The cohesive sediment processes are also not considered.

Lopez (1978) presented a model using both sediment transport and jet theory to predict reservoir sedimentation. The model considers the reservoir as a set of multiple channels and uses a compound stream model approach together with a two-dimensional jet theory to route the flow of water and sediment through the system.

A reservoir is divided into three zones; the river, transition and reservoir zones. Discharge in the river zone is considered as a one-dimensional flow. Continuity and momentum equations for water flow and the sediment continuity equation are used for analysing water and sediment in this zone. In the transition zone, a simplified model for the velocity distribution of a two-dimensional submerged jet is proposed. The flow in the reservoir zone is divided into a number of imaginary canals and flow in each imaginary canal is considered to be one-dimensional. In Figure 2.17 the river and reservoir system simulated by this model is shown schematically.

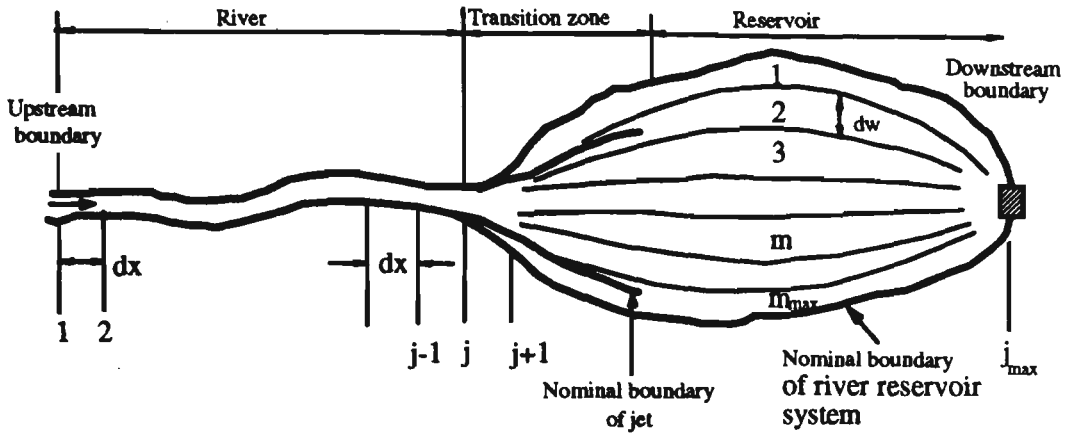

a) Plan view

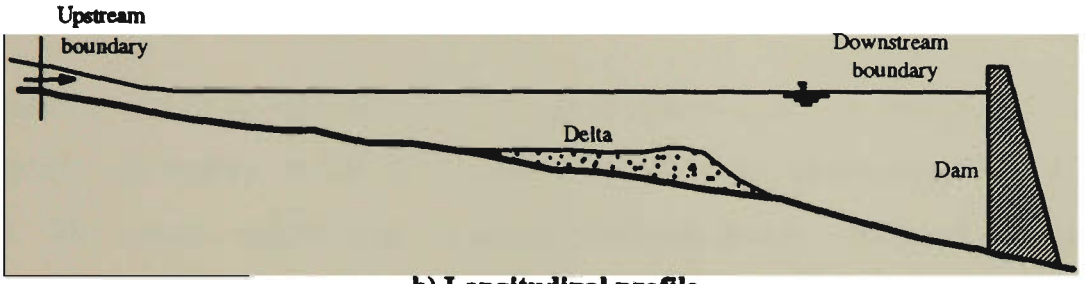

b) Longitudinal profile

Figure 2.17 The river-reservoir system simulated by the Lopez Model [after Lopez, 1978].

In the model the gradually varied, unsteady flow and momentum equations for flow are expressed as:

$$\frac{\partial Q}{\partial x}+\frac{\partial A}{\partial t}-q_L=0 \qquad (2.14)$$

$$\frac{\partial(\beta_m Q V)}{\partial x}+\frac{\partial Q}{\partial t}+g A\frac{\partial D}{\partial x}=g A(S-S_f)+q_L V_L \qquad (2.15)$$

where

q_L = lateral inflow into stream

β_m = momentum correction factor for velocity distribution

S = bed slope

S_f = friction slope

V_L = velocity component of the lateral flow in the x-direction

The implicit scheme of finite differences is employed to solve the above equations.

The sediment continuity equation is expressed as:

$$\frac{\partial Q_{sd}}{\partial x} + (1 - p_o)\frac{\partial A_{sp}}{\partial t} + \frac{\partial A c_{sa}}{\partial t} - q_{Sd} = 0 \qquad (2.16)$$

where

Q_{sd} = total sediment load in units of volume per unit time

c_{sa} = average sediment concentration in the cross section on a volume basis

p_o = bed-sediment porosity

The total flow at a cross section is divided into imaginary canals by multiplying the total flow by the conveyance of the sub-channel divided by the conveyance of the entire channel. The specific weight of the deposited sediment is also considered instead of p_o which varies according to sediment gradation. Then the sediment continuity equation for each individual canal becomes:

$$\frac{\partial Q_{sdE}}{\partial x} + \gamma_{dE}\frac{\partial A_{spE}}{\partial t} + \gamma_{SE}\frac{\partial (Ac_{sa})_E}{\partial t} - q_{dE} + q_{d(E-1)} = 0 \quad (2.17)$$

for $E = 1,2.....E_{max}$

where

E = number of channels

Q_{sd} = total sediment load in units of weight per unit time

γ_{dE} = specific weight of the sediment deposits at the Eth stream

γ_{SE} = specific weight of the transported sediment particles

q_{dE} , $q_{d(E-1)}$ = sediment transfer between channels (units of weight per unit time)

The q_{dE} and $q_{d(E-1)}$ are terms that can be evaluated by first solving the continuity equation for flow between channels q_{LE} and then substituting them into the following equation.

$$q_{dE} = c'_p\, q_{LE} + k_c\, D\frac{\partial c'_p}{\partial y} \qquad (2.18)$$

where

q_{LE} = lateral flow between channels

c'_p = suspended concentration in the longitudinal direction at a section

k_c = diffusion coefficient for the sediment particles in the lateral direction

D = average flow depth

$\frac{\partial c'_p}{\partial y}$ = suspended sediment concentration gradient in the lateral direction

The sediment transport equation is express as:

$$Q_{sd} = k V^d \qquad (2.19)$$

k and d are two parameters which can be obtained by calibration from field data.

Problems associated with the use of this method are as follows:

1. the model can be applied to predict the distribution of sediment in small reservoirs in which the effect of turbidity currents may be neglected;
2. the sediment processes of cohesive grains are not considered;
3. the method relates to reservoir systems with merely expanded channels; and,
4. running the model requires many parameters and coefficients. Therefore, the calibration of the model becomes very difficult.

The FLUVIAL model (different versions) has been developed for water and sediment routing in rivers by Chang (1982, 1984, 1988). This model is the only one which can handle bank scour. The model uses unsteady equations for water flow and substitutes conservation of momentum for conservation of energy to derive the water flow equations. The model has five major components: water routing, sediment routing, changes in channel width, changes in channel-bed profile, and changes in geometry due to curvature effect. The continuity and momentum equations in the longitudinal direction, are derived as:

$$\frac{\partial A}{\partial t}+\frac{\partial Q}{\partial s}-q_l=0 \qquad (2.20)$$

$$\frac{1}{A}\frac{\partial Q}{\partial t}+g\frac{\partial Z_e}{\partial s}+\frac{1}{A}\frac{\partial}{\partial s}\left(\frac{Q^2}{A}\right)+gS-\frac{Q}{A^2}q_l=0 \qquad (2.21)$$

where

s = the curvilinear coordinate along discharge centerline measured from the upstream entrance

Z_e = the stage or water surface elevation

In this model the transverse energy gradient, and the mean flow curvature, due to secondary current in curved channel are also employed.

The sediment routing component for this model has four features:

1. computation of sediment transport capacity using DuBoys (bed load, Vanoni 1975) and Graf (1971) suspended load formula for the physical conditions
2. determination of actual sediment discharge by making corrections for availability, sorting, and diffusion
3. upstream conditions for sediment inflow
4. numerical solution of the continuity equation for sediment.

These features are evaluated at each time step, and the value of change in cross-sectional area (dA_b) obtained are used in determining the changes in channel configuration.

The changes in width of channel is calculated. The direction of width adjustment is determined following the stream power approach, and the rate of change is based on bank erodibility and sediment transport functions. After the banks are adjusted, the remaining dA_b is applied to the bed. The changes in bed topography due to curvature is also considered in this model.

The model can not handle the cohesive sediment process and also the effects of turbidity current on sediment processes is not considered.

The US Army Corps of Engineers released several versions of HEC-6, (ver. 1, 1977, ver. 4.1, 1986, 1993) a one dimensional mathematical model, for simulating scour and deposition in the river and reservoirs. This model is popularly used for the prediction of sediment transport, because it is developed and supported by the Corps of Engineers and is widely distributed (Dawdy and Vanoni, 1986). The latest versions has the capability to model scour and deposition of sand, silt and clay (MacArthur et al. 1990).

In HEC-6 the flow and sediment are routed in two phases. First, the water is routed from downstream to upstream by using the backwater "standard step method" (Henderson, 1966); then, the sediment is routed from upstream to downstream. The sediment processes and bed evaluation of this model has the following procedures.

1. computation of non-cohesive sediment transport capacity using different optional equations for the physical conditions of the section;
2. determination of actual sediment discharge by making corrections for availability of each grain size based on calculating active and sub-surface layers, existing of clay particles, and effect of armour layer;
3. solving the continuity equation for sediment with actual sediment discharge of the section and the upstream sediment discharge;
4. applying the same procedures for cohesive sediment processes by using krone (1962) for deposition and Parthenaides (1965) for erosion, and then calculating the rate of cohesive sediment deposition or scour (only in version 4.1, 1993); and,
5. calculating the bed deformation based on accumulated sediment deposited or scour, bulk unit weight of sediment, and geometry of the section.

The rate of scour and deposition distributes uniformly across the active portion of the channel which is set by the user. In the new version of the model eleven sediment transport equations are available as: Toffaleti's (1969), Madden's (1963), Yang's (1973), DuBoys' (Vanoni 1975), Ackers and White (1973), Colby (1964), Toffaleti and Schoklitch (1934) combination, Meyer-Peter and Müller (1948), Toffaleti and Meyer-Peter and Müller combination, Madden's (1985, unpublished) modification of Laursen's (1958) relationship, and Copeland's (1990) modification of Laursen's relationship. The

armouring process is used in the model. An equilibrium depth is defined by combining Manning's equation, a form of the Strickler equation and Einstein's bed load equation. The equilibrium depth for a given grain size and unit discharge is defined as the depth for which no transport of bed material of that size occurs. The depth of scour required to produce a volume of a particular grain size sufficient to completely cover the bed to a thickness of one grain diameter is used to determine the required depth of scour to fully develop an armour layer, at which point all bed material movement ceases. The one-grain layer criterion is derived from Gessler (1971).

Problems associated with the use of this model are as follows:

1. the model can be applied to predict the distribution of sediment in rivers and small reservoirs in which the effect of turbidity current can be neglected; and,

2. the user should specify the active portion of each cross section. The pattern of sediment deposition and scour is highly sensitive with this parameter and it is very difficult to determine.

HEC-2SR is a version of HEC-2 with sediment routing added (National Research Council, 1983). The model uses a combination of the Meyer-Peter and Müller bed load equation (1948), and the Einstein's suspended load equation (1950). It also includes bed armouring algorithms. Shields' criterion is used to determine a non-moving size, and a layer, which is two-grain diameters thick (based on the smallest non-moving particle), armours the bed. The model distributes scour and fill proportionally relative to the conveyance in the cross section.

The effects of turbidity current is not considered in this model. Therefore, the model can be used in rivers and in only small reservoirs. Also, the process of cohesive sediment is not considered.

Rahuel et al. (1989) presented a coupled simulation of unsteady water and sediment movement in mobile-bed alluvial rivers called CARICHAR. The basic equations describing the unsteady flow (the same as Equations 2.10, 2.11 and 2.12) were solved in

a coupled, implicit manner using a finite difference scheme. Two equations are adopted to determine the bed load transport:

1. Meyer-Peter and Müller's (1948) sediment bed load equation as a bed load predictor
2. Bell and Sutherland's (1983) loading law equation to take into account the spatial bed load delay compared to its equilibrium value as:

$$q_{bv} = \left[1 + \left(\frac{q_{bv1}}{q^*_{bv1}} - 1\right) e^{-K_1(x-x_1)}\right] q^*_{bv} \qquad (2.22)$$

where

q_{bv} = measured unit-width volumetric bed load transport rate

q^*_{bv} = equilibrium value of q_{bv}

K_1 = loading-law coefficient

x = distance

index 1 = the upstream limit of the reach being considered.

A particular concept for active layer and armouring is defined and used in this model. The equation proposed by Borah et al. (1982) is employed for calculating thickness of the active layer. The model is used in a hypothetical reservoir to show the processes of the model and the affects of considering the loading law equation on predicting sediment processes. The model can be used for predicting of water level and sediment processes in rivers, but the suspended load and cohesive sediments were not considered in the prediction of sediment transport. Using the model for reservoirs is limited to small ones because the turbidity current is not considered.

Holly et al. (1990) presented a model called CHARIMA for simulating the unsteady water and sediment movement in multiple connected networks of mobile-bed channels. The equations of unsteady water and sediment movement (the same as Equations 2.10 to 2.12) are solved in Preissmann's finite-difference scheme. Four total-load predictors are available in the model and hydraulic sorting and bed armouring procedures are considered. The model is used in three natural river systems (A river reach of Missouri

River, Cho-Shui River in western Taiwan, and Susitna River in Alaska) and the prediction results were in good agreement with measured data. The cohesive sediment process and the effects of turbidity currents are not considered.

Correia et al. (1992) presented a coupled one dimensional model for rivers called FCM. The governing equations for mass and momentum balance of sediment-water mixture under unsteady flow conditions in natural rivers with irregular geometry, are considered as follows:

$$\frac{\partial Q}{\partial x} + P\left(\frac{\partial y_b}{\partial t}\right) + B\left(\frac{\partial D}{\partial t}\right) = q_t \qquad (2.23)$$

$$\frac{\partial Q}{\partial t} + 2\frac{Q}{A}\left(\frac{\partial Q}{\partial x}\right) - B\frac{Q^2}{A^2}\left(\frac{\partial D}{\partial x}\right) - \frac{Q^2}{A^2}A_x^y + gA\left(\frac{\partial D}{\partial x}\right) = gA(S - S_f) + q_t\left(V_q - \frac{Q}{A}\right) \qquad (2.24)$$

$$\frac{\partial Q_s}{\partial x} + P\left(\frac{\partial y_b}{\partial t}\right)p + Bc_{av}\left(\frac{\partial D}{\partial t}\right) + A\left(\frac{\partial c_{av}}{\partial t}\right) = q_{sd} \qquad (2.25)$$

where

P = the wetted perimeter

B = the top width of the channel

A^y_x = the rate of change of A with respect to x when y is held constant

S = the slope of the bed

S_f = the slope of the energy grade line

V_q = the velocity of the lateral inflow in the direction of the main flow

c_{av} = the average volumetric sediment concentration within a control volume

these equations are solved in coupled, one-dimensional manner using the Preissmann four-point linear implicit scheme with weighting factors for space and time coordinates. The bed load equations of Ackers and White (1973), Brownlie (1983), van Rijn (1984a, 1984b), Graf (1971), Schoklitsch (1934), Smart and Jaeggi (1983), and Meyer-Peter and Müller (1948) are available in the model and also the process of bed armouring is

simulated. The model is tested in a hypothetical reservoir to demonstrate the original features of the model. This model can not handle the cohesive sediment process and turbidity currents.

Spasojevic and Holly (1990) presented a two dimensional model, MOBED2, for simulating mobile-bed processes. The governing equations for fluid flow, sediment transport, and bed evolution were as:

mass-conservation equation (continuity) for fluid flow:

$$\nabla \cdot \vec{V} = 0 \tag{2.26}$$

momentum-conservation equation for fluid flow:

$$\frac{\partial \vec{V}}{\partial t} + (\vec{V} \cdot \nabla)\vec{V} = \frac{1}{\rho}\vec{F}_b - \frac{1}{\rho}\nabla p + \frac{1}{\rho}\nabla \cdot \tau_b \tag{2.27}$$

mass-conservation equation for one size class of suspended sediment:

$$\frac{\partial c_d}{\partial t} + \nabla \cdot (c_d \vec{V}) = -\frac{1}{\rho}\nabla \cdot \vec{q}_d \tag{2.28}$$

mass-conservation for one size class of active-layer sediment:

$$\rho_s (1 - p_o)\frac{\partial (\beta_a E_m)}{\partial t} + \nabla \cdot \vec{q}_b + S_{qs} - S_{af} = 0 \tag{2.29}$$

global mass-conservation equation for bed sediment:

$$\rho_s (1 - p_o)\frac{\partial y_b}{\partial t} + \sum(\nabla \cdot \vec{q}_b + S_{qs}) = 0 \tag{2.30}$$

where

$\vec{V}$ = velocity vector

ρ = density of the fluid

$\vec{F}_b$ = body force

c_d = dimensionless concentration, i.e. ratio of the mass of the particular size-class particles to the total mass of the elemental volume

$\vec{q}_d$ = suspended sediment diffusion flux

$\vec{q}_b$ = bed load flux

E_m = active-layer thickness

β_a = active-layer size fraction

S_{qs} = suspended load 'source'

S_{af} = active-layer floor 'source'

y_b = the bed elevation

ρ_s = density of the sediment particles

Several numerical solutions are employed to solve the equations. The model was run for a simulation period of 8 days for Coralville Reservoir, which is located on the Iowa River near Iowa City. The output results of the model are demonstrated. Comparison between the measured and predicted values were not reported.

Many assumptions have been made to solve the procedures system of equations used in MOBED2. The model is applicable to the so-called "shallow" watercourses where the depth is much less than the other two dimensions. The generalisation and the procedures of this model is still under development (Holly, 1992: personal communication).

2.3.4 Discussion on Mathematical Methods

Amongst the mathematical methods, the jet theory method and diffusion theory method have some limitations. The jet theory method can be used for very large particle sizes settled down in the mouth of the river and reservoir or estuary. It doesn't have the ability to take into account the small size sediments and even the transport rate of large particles in the process. The diffusion theory may be used for very fine sediment processes but it can not handle the large sediment size particles.

Methods based on the sediment transport theory are comparatively more reliable for simulating the stream deformation due to sedimentation processes. That is why many valuable investigations have been carried out to develop and completing this kind of mathematical methods over the last two decades. In recent years, most attempts are focused to couple the sediment and flow phases, and also to analyses the problem as a two dimensional model.

Although some of the mathematical methods are reliable enough to predict the sediment process in a watercourse, their uses in deep reservoirs are limited. This limitation is due to the existence of the turbidity current in deep reservoirs. It should be emphasised here that although in some cases, ignoring the effects of the turbidity current on long term sediment process does not cause significant error, in the case of high suspended sediment discharge, the difference may be remarkable and can not be ignored.

2.4 Summary

In this chapter the existing reservoir sedimentation methods were briefly reviewed and some comments were also made considering the available theories. The methods to find the trap efficiency of reservoirs including, Brown (1944), Churchill (1948), Brune (1953), Karaushev (1966), Bube and Trimble (1986, revised the Churchill curves), and Skrylnikov (1989) were presented. The existing reservoir sedimentation methods were divided into empirical and mathematical categories. The empirical methods presented included the "Area Increment Method" (Cristofano, 1953), the "Empirical Area-Reduction Method" (Borland and Miller, 1958), the "Pool-Elevation Duration Method" (Hobbs, 1969), Borland (1971), Szechowycz and Qureshi (1973), Garde et al. (1978, Simons et al. 1982), and Chien (1982, cited in Annandale 1987). The advantages and disadvantages of these methods were presented. Generally, these methods do not cover all aspects of reservoir sedimentation. These methods are based on one or more field observations. Therefore, generalising the model for all cases is not appropriate. There are glaring differences among the deposition pattern results from these methods. This causes difficulty in selecting a method that is suitable for a specific reservoir. Dividing reservoirs into a few categories (that is proposed in some of these methods) or applying

a specific equation for the deltaic sediment deposition without a precise analysis of the hydraulic and sediment processes in actual geometric conditions provides a very low approximation. However, in some cases the simplicity and less data requirement for analysis are the advantages of using these methods. The theoretical aspects of the mathematical methods category included the "Jet Theory" (Bonham-Carter and Suthreland, 1968), the "Diffusion Theory" (Merrill, 1974), Chang and Richards (1971), Yücel and Graf (1973), Asada (1973), Lopez (1978), the FLUVIAL (Chang, 1982, 1984), the HEC-6 (US Army Corps of Engineers, 1977), the HEC-2SR (National Research Council, 1983), the CARICHAR (Rahuel et al., 1989), the CHARIMA (Holly et al., 1990), the FCM (Correia et al., 1992), and the MOBED2 (Spasojevic and Holly, 1990). The capabilities and limitations of each model were discussed. In the existing mathematical models only the new version of HEC-6 (version 4.1) can simulate the cohesive sediment process. In all the mathematical models described, the main limitation is the fact that they can be used only in rivers and small reservoirs in which the effect of turbidity currents can be neglected. In the case of a deep reservoir, in which the depth is enough for establishment of turbidity current, the error in using an existing mathematical model would be remarkable.

Chapter Three

THEORETICAL ASPECTS OF THE COMPUTATION OF SEDIMENT PROCESSES

3.1 Introduction

Sediment transport computations in watercourses are needed to simulate the channel morphological processes. Prediction of aggradation and degradation of channels needs adequate understanding of several concepts: coarse sediment transport; fine or cohesive sediment transport; unit weight of sediment deposited; turbidity current; active-layer thickness and armour layer. These factors affect the sediment processes which need accurate evaluation. However, the processes involved are very complicated. Hence the evaluation of sediment processes can be made only by considering the most significant parameters that control the processes under investigation and by neglecting description of less relevant aspects (Silvio, 1992). In this chapter, the factors affecting the sediment processes in the rivers and reservoirs will be described briefly. Also the derivation of turbidity current equations that especially apply to the sediment processes in reservoirs are presented.

3.2 Sediment Transport

Sediment transport formulae provide an estimation of the rate of discharge of sediment in terms of the sediment and the hydraulic properties of the flow. These formulae can be divided into suspended and bed load transport. Much of the research in the early decades of this century dealt with the development of relations for transport of bed load by streams (Vanoni, 1984). Bed load relations are used when the bed sediment is coarse

and moves on or near the bed and negligible amounts move in suspension. Since, both suspended and bed load depend on almost the same parameters, they may be considered in terms of total sediment discharge, as proposed by some investigators (Laursen, 1958; Engelund and Hansen, 1967; Yang, 1973 and 1979, and Graf, 1971). Total load transport equations give the entire sediment discharge of bed material. However, total load relations usually do not give the discharge of the silt and clay (D_g<62μm), which usually move in suspension as "wash load." A number of equations which have been developed to explain sediment transport rates under equilibrium conditions. Most of them are empirical, in which the coefficients are determined by fitting the equations to usually laboratory data. Some of the important equations are:

- Meyer-Peter and Müller, 1948, for bed load
- Einstein, 1950, for bed and suspended load
- Laursen, 1958, for total load
- Bagnold, 1966, for bed and suspended load
- Engelund and Hansen, 1967, for total load
- Toffaleti, 1969, for bed and suspended load
- Graf, 1971, for total load
- Bishop et al., 1965, Total load
- Ackers and White, 1973 for total load
- Yang, 1973, 1979, for total (sand transport)
- Yang, 1984, for total (gravel transport)
- van Rijn, 1984, for bed and suspended load
- Wiuff, 1985, for suspended load
- Samaga et al., 1986, for bed and suspended load
- Celik and Rodi, 1984, for suspended load
- Habibi and Sivakumar, 1993 for suspended and 1994, for bed load

For each of the above equations, the conditions used for their calibration were different. Before using each of the equations for a particular river or reservoir, it should be made sure that the existing conditions in the river or reservoir and the conditions used for calibrating that equation are similar. An evaluation of the utility of different sediment transport equations is not an objective of the current study. Here, three of these

equation were selected and presented in detail. The Meyer-Peter and Müller's theory was selected because it is one of the most popular procedures for the calculation of sediment transport and is one which is still being used widely. The Bagnold theory was selected because it was the first theory which employs the energy concept for sediment transport calculation. The Yang theory is presented because it utilises the stream power concept and is widely used.

3.2.1 Meyer-Peter and Müller Equation

Meyer-Peter and Müller in 1948, using their own measured data, developed an empirical equation for the prediction of bed load transported in open channels. The equation can be written as:

$$q_b^{2/3} = 250 q^{2/3} S - 42.5 D_s \qquad (3.1)$$

where

q_b = unit bed load transport rate in kg/s.m

q = water discharge per unit width in $m^3/s.m$

S = slope of the bed

D_s = size of bed materials in metres.

Since the Equation 3.1 was limited to relatively coarse uniform material, Meyer-Peter and Müller conducted experiments on non-uniform and smaller grains to develop the following equation for non-uniform sediments:

$$(n_s/n)^{3/2} R_b S/(R D_a) = 0.047 + 0.25 \rho^{1/3} (q_b/\gamma_s)^{2/3} \Big/ \left[(\gamma_s - \gamma_w)^{1/3} D_a\right] \qquad (3.2)$$

$$n = \frac{1}{V} R_b^{2/3} S^{1/3} \qquad (3.3)$$

$$n_s = \frac{1}{V} R_b^{2/3} S'^{1/2} \qquad (3.4)$$

where

R_b = hydraulic radius

D_a = arithmetic mean diameter of the particles

R = submerged specific gravity of the sediment particles $(= \frac{\rho_s - \rho}{\rho})$

ρ = density of water

γ_s = unit weight of sediment materials

γ_w = unit weight of flow

n, n_s = Manning coefficients

V = average velocity of flow

S' = energy slope due to grain resistance.

3.2.2 Bagnold's Sediment Transport Equation

Bagnold (1966) derives an expression for suspended and bed load based on the work rate. Based on his approach, the proposed equation for suspended load is given as:

$$q_s = \frac{1}{R}(1 - e_b) e_s \tau_b V \frac{U_s}{v_s} \qquad (3.5)$$

and for bed load transport the equation is given as:

$$q_b = \frac{1}{R} \tau_b V \frac{e_b}{\tan \alpha_d} \qquad (3.6)$$

where

q_s = suspended load in dry weight per unit of channel width

ρ_s = density of the sediment particles

e_b = bed load transport efficiency

e_s = suspended load transport efficiency

τ_b = bed shear stress

V = mean velocity of water

U_s = mean velocity of solids

v_s = mean fall velocity of solids

α_d = coefficient of dynamic solid friction.

For the total load, the equation can be written as:

$$q_t = q_s + q_b \tag{3.7}$$

3.2.3 Yang's Sediment Transport Equation

Yang (1972, 1973, 1976) has proposed a stream power equation which can be utilised for estimating total bed material concentrations in sand bed rivers. Based on this theory, the relevant equations for sediment concentration is given as:

$$\log c_t = I + J \log\left(\frac{VS}{v_s}\right) \tag{3.8}$$

$$I = 5.165 - 0.153 \log\left(\frac{v_s D_s}{\nu}\right) - 0.297 \log\left(\frac{u_*}{v_s}\right) \tag{3.9}$$

$$J = 1.78 - 0.36 \log\left(\frac{v_s D_s}{\nu}\right) - 0.48 \log\left(\frac{u_*}{v_s}\right) \tag{3.10}$$

where

c_t = total sediment concentration in parts per million by weight

D_s = median sieve diameter of bed material

u_* = shear velocity

ν = kinematic viscosity of water.

3.3 Cohesive Sediment: Deposition and Scour

To study the non cohesive sediment a particle can be characterised with known parameters such as, diameter, density and shape. But the properties of cohesive particles depend on the sediment characteristics (mineralogical composition, organic content, etc) and water properties (temperature and chemical composition). The interactions between these properties are complex and the determination of the physico-chemical properties of cohesive particles is needed. Therefore, study of cohesive sediment is very difficult.

Cohesive sediments are composed principally of clay and silt minerals that are eroded from watershed soils. The active part, that is, the clay minerals, consist of small particles typically less than two microns that have negative surface charges (Peterson, 1988). Krone (1962) for the first time conducted valuable experiments on deposition rates of cohesive materials. Base on laboratory studies he presented an empirical equation for deposition rates of cohesive materials (at concentrations less than 300 *mg/L*) as follows:

$$\frac{c_f}{c_s} = e^{(-k't)} \qquad (3.11)$$

$$k' = \frac{v_s P_d}{D} \qquad (3.12)$$

where

c_f = concentration at the end of the time period

c_s = concentration at beginning of the time period

t = time = reach length/ flow velocity

v_s = fall velocity of sediment particles

P_d = probability of particles sticking to the bed and not being re-entrained by the flow. $P_d = 1 - (\tau_b/\tau_d)$ when $\tau_b < \tau_d$ and $P_d = 0$ when $\tau_b \geq \tau_d$

D = water depth

τ_b = bed shear stress

τ_d = critical shear stress under which deposition occurs. This value should be determined by laboratory testing on the particles.

The erosion rate of cohesive sediment, based on work by Parthenaides (1965), can be found by the following equation:

$$Q_c = M_1\left(\frac{\tau_b}{\tau_s} - 1\right) \qquad (3.13)$$

$$Q_c = 0 \quad \text{when} \quad \tau_b < \tau_s$$

where

Q_c^* = the erosion rate per unit area per unit time

M_1 = erosion rate for particle scour

τ_s = critical bed shear stress above which erosion occurs

For computation processes Equation 3.13 can be written as:

$$c_f = \frac{M_1 A_s}{Q\gamma_w}\left(\frac{\tau_b}{\tau_s} - 1\right) + c_s \qquad (3.14)$$

where

A_s = surface area exposed to scour

Q = water discharge

γ_w = unit weight of water.

In this equation τ_s should be determined with laboratory testing on specific sediment particles. M_1 is dependent on the specific sediment particles and water properties, and can be obtained with laboratory testing.

The same equation for cohesive sediment scour has been reported by Cormault (1971). He determined the constant M_1 for Gironde Estuary as equal to 0.00002 (g/cm^2.s).

Parchure and Mehta (1985) found the rate of surface erosion as:

$$Q_c = Q_f \exp\left[\alpha_2 (\tau_b - \tau_s)^{1/2}\right] \qquad (3.15)$$

where

α_2 = an empirical constant

Q_f = the floc erosion rate

τ_s, α_2, and Q_f are depend on physico-chemical properties of particles and water and should be determined with experimental tests.

3.4 Active-Layer Thickness and Armouring

When particles are scoured from the bed, the exchange between bed and flow takes place in a thin layer at the bed surface. This layer is called the "active layer" and below this the bed material remains undisturbed and is called the "inactive layer". The materials existing in an active layer may be scoured away by the flow and large particles existing in this layer establish an armour coat on the inactive layer to prevent any scour from the bed. The scour can not remove the material under the armour coat until a high flow removes this coat. A new active layer can be defined after the armour coat is removed. In deposition processes several active layers may be formed. In Figure 3.1 a schematic presentation of the layers is shown.

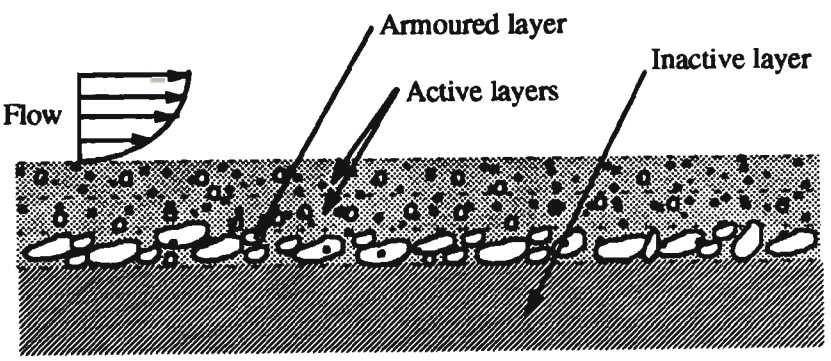

Figure 3.1 Schematic of layers in bed processes.

Several algorithms are presented to define the active layer thickness. These equations can be used in the computation of the bed processes. Borah et al. (1982) presented an equation for active layer thickness as:

$$h_a = \frac{100}{\sum_{i=L}^{N} P_i} \frac{D_L}{1-\lambda_L} \qquad (3.16)$$

where

h_a = thickness of the active layer

P_i = the percentage of the fraction i

D_L = the size of fraction, L

λ_L = the porosity of fraction, L

N = number of particle size fraction

Fraction L is the smallest sized (d_L) material which the flow cannot transport.

Another algorithm to define and to calculate the bed layers is presented in HEC-6 sedimentation computer program. This method is based on defining two layers in the active layer; the cover layer and the sub-surface layer. The cover layer is a thin layer of bed material at the bed surface which is continually mixed by the flow. As the bed progresses towards an equilibrium condition in which deposition and resuspension of each size class is balanced, the slow moving thin cover layer becomes coarser and serves as a shield, regulating the entrainment of finer particles below. If the cover layer is replenished by deposition from the water column, it will remain as a shield constraining the entrainment of finer material from below. This shielding began to occur when as little as 40% of the bed surface was covered. There are two components of the active layer; a cover layer that is retained from the previous time step and a sub-surface layer that is created at the beginning of the time step from the inactive layer. The sub-surface layer material is returned to the inactive layer at the end of the time step. The cover layer from the previous time step is limited to an arbitrary maximum thickness of 0.6 m. If the previous cover layer thickness is 0.6 m or greater, the new cover layer is assigned a thickness of 0.06 m. The residual material is mixed with the inactive layer. The armouring process is applied by using the equilibrium depth which is calculated by combining Manning's, Strickler's, and Einstein's equations as follows:

$$D_e = \left[\frac{q}{10.21 D_i^{1/3}} \right]^{6/7} \qquad (3.17)$$

where

D_e = the minimum water depth for negligible sediment transport (ie, equilibrium depth) for grain size D_i

q = water discharge per unit width of flow.

The initial thickness of the sub-surface layer is calculated from D_e. The maximum thickness of the sub-surface layer, however, is constrained by an estimated maximum scour that could occur during the exchange increment. The estimated maximum scour is

calculated from the hydraulics, inactive bed gradation, and selected transport function. This constraint will almost always override the thickness calculated using equilibrium depth. A minimum thickness of two times the largest grain size in transport is also imposed.

3.5 Unit Weight of Sediment Deposition

Generally, the sediment inflow to the reservoir is estimated in terms of weight per time, eg tonnes per day, and must be converted to a volume equivalent. The density of the fine sediment is subject to compaction during the sediment deposition process. This means that the average unit weight of sediment deposition will increase with time. Therefore, two different unit weights are defined: namely an initial unit weight and an average unit weight with time. There are several factors influencing the initial unit weight such as sediment texture, reservoir operation, chemical properties of the sediment, vegetation in the reservoir and slope of the reservoir bed. The size of sediment particles and the reservoir operation system are probably the most influential.

Lara and Pemberton (1965) developed a method for estimating the initial unit weight based on analyses of 1316 samples. They used two parameters in their equation; the particles size in three classification as clay, silt and sand, and a reservoir operation scheme. Table 3.1 shows the proposed reservoir operation schemes.

Table 3.1 Classification of reservoirs based on their operation [after Lara and Pemberton, 1965].

Type	Reservoir operation
1	Sediment always submerged or nearly submerged.
2	Normally moderate to considerable reservoir drawdown.
3	Reservoir normally empty.
4	River bed sediments.

The equation for unit weight of the sediment is presented as:

$$\gamma = 16.02\left(W_c\ p_c + W_m\ p_m + W_s\ p_s\right) \qquad (3.18)$$

where

γ = initial unit weight (kg/m^3).

p_c, p_m, p_s, = percentages of clay, silt, and sand, respectively in the incoming sediment (%).

W_c, W_m, W_s = coefficients of clay, silt and sand, respectively, which can be obtained from Table 3.2.

Table 3.2 Values of coefficients of clay, silt and sand [after Lara and Pemberton, 1965].

Reservoir type	W_c	W_m	W_s
1	26	70	97
2	35	71	97
3	40	72	97
4	60	73	97

As the sediment remains in the reservoir, the unit weight increases with time. Lane and Koelzer (1943) proposed the following equation for calculating unit weight with time.

$$\gamma_t = \gamma_1 + K \log_{10} t \qquad (3.19)$$

where

γ_t = unit weight after T years of compaction (kg/m^3)

γ_1 = the initial unit weight considered at the end of first year (kg/m^3)

K = constant dependent on the size analysis of the sediment

t = time (year)

The values of γ_1 and K can be obtained from Table 3.3.

Table 3.3 Values of γ_1 and K of Equation 3.19 [after Lane and Koelzer, 1943].

Reservoir operation	*Sediment material*					
	Sand		**Silt**		**Clay**	
	γ_1 kg/m^3	*K*	γ_1 kg/m^3	*K*	γ_1 kg/m^3	*K*
(a) Sediment always submerged or nearly submerged	1489.86	0	1041.30	91.31	480.60	256.32
(b) Normally a moderate reservoir drawdown	1489.86	0	1185.48	43.25	736.92	171.41
(c) Normally considerable reservoir drawdown	1489.86	0	1265.58	16.02	961.20	96.12
(d) Normally empty	1489.86	0	1313.64	0	1249.56	0

In Figure 3.2 the variations of unit weight of sediment materials over 100 years are shown using Equation 3.19 and reservoir operation (a) from Table 3.3.

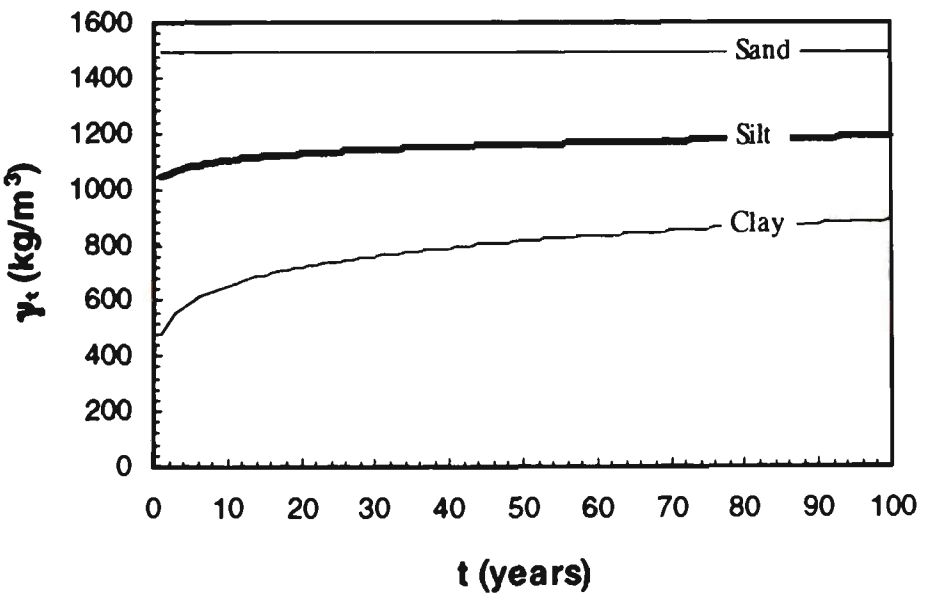

Figure 3.2 Variation of unit weight with time based on Lane and Koelzer's equation and reservoir operation (a) from Table 2.3.

Miller (1953) developed an approximation of the integral of the Lane and Koelzer (1943) formula for determining the average unit weight (γ_{At}) of all sediment deposited in t years of operation as follows:

$$\gamma_{At} = \gamma_1 + 0.434\, K\left[\frac{t}{t-1}\ln(t) - 1\right] \qquad (3.20)$$

where

γ_{At} = average unit weight after t years of compaction (kg/m^3)

γ_1 = the initial unit weight considered at the end of first year (kg/m^3)

K = constant dependent on the size analysis of the sediment

t = time (year)

The usage of Lara and Pemberton (1965) and Lane and Koelzer (1943) equations for estimating the initial unit weight of deposited sediment is tested in Dez Reservoir in Iran. It has been shown by (Bina et al, 1993) that the calculation using Lara and Pemberton equation is better than Lane and Koelzer equation for the application in Dez Reservoir.

3.6 Turbidity Current

Turbidity currents are defined as gravity currents or density currents. When water with density ($\rho_w+d\rho_0$) flows into a water body which has a density (ρ_w), a density current occurs. The nature of the density current depends on the condition of the ambient water and the density difference.

A density difference may occur because of one or several of the following conditions:

1) Temperature difference

2) Difference in dissolved substance concentration

3) Difference in concentration of suspended particles

In a continuously fed gravity current where the density difference is due to the temperature or to the presence of dissolved substance, the buoyancy flux is conserved throughout the current, and it is referred to as a "conservative gravity current". A

turbidity current on a mobile bed, however may change its buoyancy flux either by eroding or by depositing sediment. Thus, it is referred to as a "non-conservative gravity current" where the settling velocity of the suspended particles constitutes an additional parameter. In contrast to the conservative gravity current, the non-conservative gravity current seem to have received relatively little attention. This is perhaps due to the difficulties inherent in its study which partly comes from the fact that the presence of the transported sediment generates and maintains the turbidity current (Altinakar, 1990). In fluvial hydraulics, turbidity currents are encountered if a sediment-laden discharge enters into a reservoir, where, during the passage, it unloads the granular material (Graf, 1983). In this situation four sections can be recognised in the turbidity currents: plunge point, plunge region, body and head as shown in Figure 3.3.

One of the greatest difficulties in the study of gravity current is the lack of field data. Monitoring the data of the gravity current is a very difficult task; particularly from the body of currents. In many cases the equipment used for this purpose have been reported as being damages by the currents. Hebbert et al. (1979) recorded the movement of a conservative density current (saline) in Wellington Reservoir in Western Australia. The results of their study for six days (Julian date 76198, 76222, 76228, 76230, 76231, and 76232) are presented in Figure 3.4. The isopycnals have been plotted for a midstream longitudinal section of the reservoir.

3.6.1 Plunge point

When a turbidity current flows into a reservoir or lake, a plunging flow will occur. Some investigators studied the depth of the plunge point. Their studies are mainly based on laboratory tests and some field observations. These investigations can be expressed in a general form with a unknown value of F_p as follows:

$$h_p = \left(\frac{1}{F_p^2}\right)\left(\frac{q^2}{\Delta g}\right)^{1/3} \qquad (3.21)$$

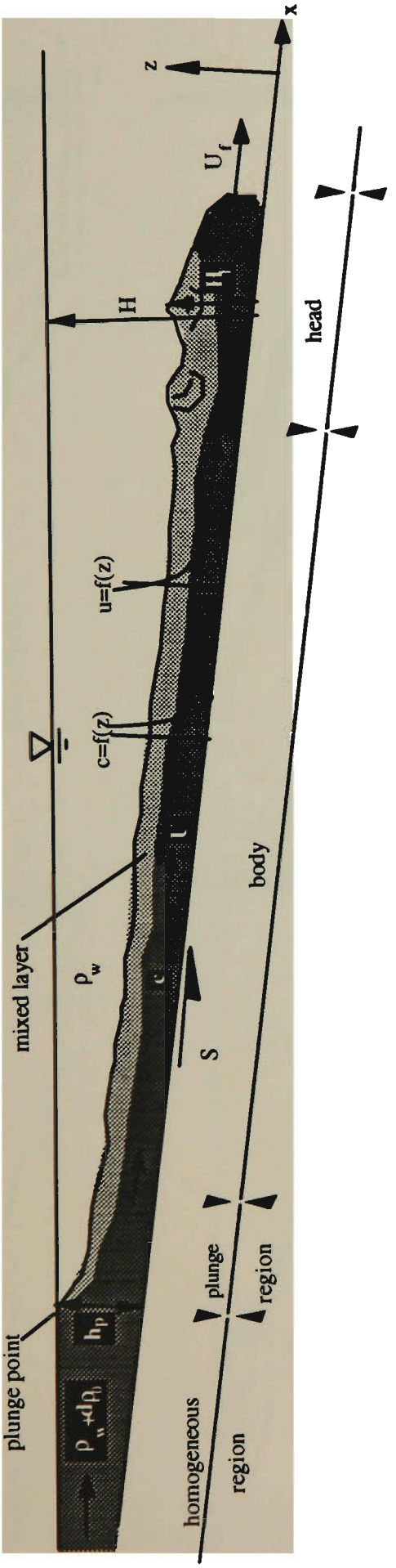

Figure 3.3 A typical turbidity current

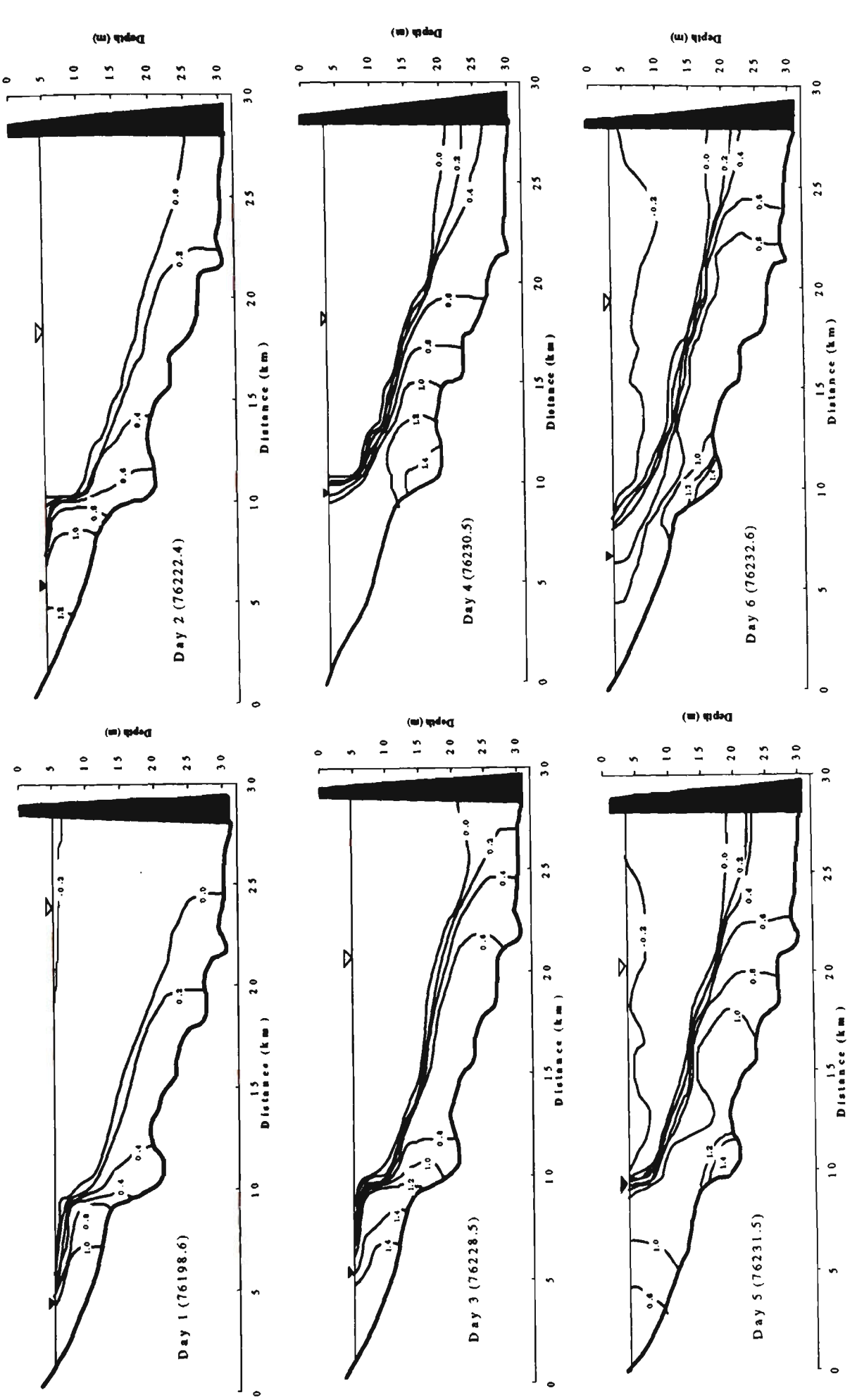

Figure 3.4 Isopycnal sections of a density current in Wellington Reservoir (numbers on lines refer to density minus 1000, in kg/m^3) (after Hebbert et al., 1979)

where:

h_p = plunge depth (L)

F_p = densimetric Froude number at plunge point

q = inflow per unit span (L^2T^{-1})

Δ = relative density difference between inflow ($\rho_w+d\rho_0$) and ambient water (ρ_w), ($=d\rho_0/\rho_w$)

The following are specific equations proposed by different investigators for the plunge point depth;

Singh and Shah (1971)

$$h_p = 1.85 + 1.3\left(\frac{q^2}{\Delta g}\right)^{1/3} \qquad (3.22)$$

Wunderlich and Elder (1973)

$$h_p = \left(\frac{1}{0.5}\right)^{2/3}\left(\frac{q^2}{\Delta g}\right)^{1/3} \qquad (3.23)$$

Savage and Brimberg (1975)

$$h_p = \left\{\frac{2.05}{(1+\alpha)}\left(\frac{S}{f}\right)^{0.478}\right\}^{-2/3}\left(\frac{q^2}{\Delta g}\right)^{1/3} \qquad (3.24)$$

Hebbert et al. (1979) for Wellington Reservoir

$$h_p = 1.16\left(\frac{Q^2}{\Delta g}\right)^{1/5} \qquad (3.25)$$

Jain (1981)

$$h_p = 1.6\left(\frac{\alpha_s}{1+\alpha_s}\right)^{0.126}\left(\frac{8S}{f_t}\right)^{0.008}\left(\frac{q^2}{\Delta g}\right)^{1/3} \qquad (3.26)$$

Akiyama and Stefan (1984)

(a) mild slope ($S < \frac{1}{150}$)

$$h_p = \frac{1}{2}\left\{\frac{(2+\gamma_d)}{2} + \left(\frac{S_2 S}{f_t}\right) + \sqrt{\left[\frac{(2+\gamma_d)}{2} + \frac{S_2 S}{f_t}\right]^2 - \frac{4}{1+\gamma_d}\left(\frac{S_2 S}{f_t}\right)}\right\}\left(\frac{f_t}{S S_2}\right)^{1/3}\left(\frac{q^2}{\Delta g}\right)^{1/3} \quad (3.27)$$

(b) steep slope ($S > \frac{1}{150}$)

$$h_p = \frac{1}{2}\left\{\frac{(2+\gamma_d)}{2} + S_1 + \sqrt{\left[\frac{(2+\gamma_d)}{2} + S_1\right]^2 - \frac{4 S_1}{(1+\gamma_d)}}\right\}\left(\frac{1}{S_1}\right)^{1/3}\left(\frac{q^2}{\Delta g}\right)^{1/3} \quad (3.28)$$

where:

f	= bed friction coefficient
S	= bed slope
γ_d	= dilution coefficient
f_t	= total friction coefficient (it is assumed approximately equal to 0.02)
S_1, S_2	= coefficients (S_1 = 0.2~0.3; and S_2 = 0.6~0.9; Ellison and Turner, 1959)
α_s	= ratio of interfacial to bed shear stress
Q	= water discharge of Wellington Reservoir

3.6.2 Turbidity Current Head

Turbidity currents always develop a head in ambient water. The head of a turbidity current has a velocity of U_f and can be calculated by a simple Chezy-type relationship (Turner, 1973) such as:

$$U_f = C_c \sqrt{g'_f H_f} \quad (3.29)$$

where g'_f is the actual effective gravitational acceleration inside the head and is calculated using the following equation

$$g'_f = \frac{g\left(\rho_s - \rho_w\right)}{\rho_w} \qquad (3.30)$$

and:

C_c = constant coefficient

H_f = height of the current head

ρ_s = density of the sediment particles

According to Middleton (1966a) and Turner (1973), the C_c coefficient can be taken as 0.75. For small slope bed $S \leq 3\%$ and $\sqrt{g'_0 H_f} <\sim 20$ (g'_0 is the initial effective gravitational acceleration) Altinakar et al (1990) suggested a smaller friction coefficient C_c =0.63 based on their experimental and Denton et al. (1981) data.

3.6.3 Under Flow Region

The buoyancy flux of the turbidity current may change either by eroding or by depositing sediment during passage through the reservoir. The focus of this section is to demonstrate how the effect of a turbidity current can be formulated in a quantitative form.

As the turbidity current is characterised by various parameters such as concentration of sediment, discharge of water, slope of bed, and upstream and downstream conditions particular analysis is required to develop equations which can express the effect of individual parameters on the turbidity current. The important part of the turbidity current in reservoir sedimentation analysis is the body of current in a steady continuous situation. Ellison and Turner (1959) presented a set of equations for the "conservative gravity current". Following them Plapp and Mitchell (1960), Chu et al. (1979), Luthi (1981), Akiyama and Fukushima (1985), Fukushima et al. (1985), Parker et al. (1986) and Garcia (1990) used almost the same analysis for deriving equations for a steady state turbidity current.

Figure 3.5 shows the situation of a turbidity current which is used to derive the equations. The cross section is assumed to be a wide rectangular shape. The slender-flow or boundary approximations are taken into account for a two-dimensional turbidity

current. Variations in the lateral (y) direction are ignored. The submerged specific gravity of the sediment is denoted by $R = \left(\frac{\rho_s}{\rho_w} - 1 \right)$, where ρ_s and ρ_w are densities of the sediment and water, respectively. The local components of the flow velocity are $u(x,z)$ and $w(x,z)$ in the x and z directions respectively. Variation in the lateral direction is neglected. It is assumed that $u \gg w$, $\partial/\partial z \gg \partial/\partial x$, the slope, S, is constant and small, and the turbidity current is fully turbulent with all viscous terms being negligible.

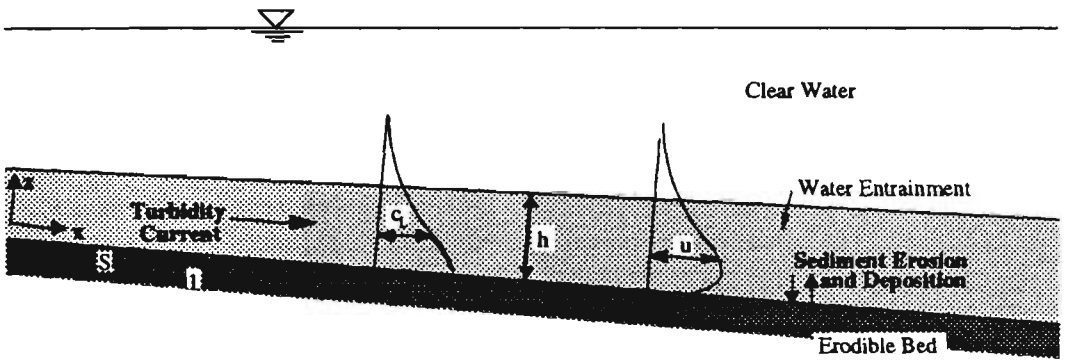

Figure 3.5 A turbidity current flowing through a quiescent clear water.

Under these constraints, the equation of mean fluid mass balance can be presented as:

$$\frac{\partial u}{\partial x} + \frac{\partial w}{\partial z} = 0 \qquad (3.31)$$

and the mean momentum balance in the x and z directions as:

$$\frac{\partial u^2}{\partial x} + \frac{\partial uw}{\partial z} = \frac{1}{\rho_w}\frac{\partial p}{\partial x} + gRc_L S + \frac{1}{\rho_w}\frac{\partial \tau}{\partial z} \qquad (3.32)$$

$$0 = -\frac{1}{\rho_w}\frac{\partial p}{\partial z} + gRc_L \qquad (3.33)$$

where $\tau = -\rho_w \overline{u'w'}$ is Reynolds stress. u' and w' denote the fluctuating (instantaneous value minus mean value) or turbulent components of longitudinal and transverse velocity respectively, c_L is local volumetric concentration of suspended sediment, and p is hydrostatic pressure.

The mean sediment mass balance for the material is then expressed by Equation 3.34.

$$\frac{\partial uc_L}{\partial x}+\frac{\partial wc_L}{\partial z}=-\frac{\partial}{\partial z}\left(F-v_s c_L\right) \qquad (3.34)$$

where $F=\overline{c_L' w'}$ is Reynolds sediment flux and v_s is the fall velocity of the sediment.

The upward component of the mean momentum balance (Equation 3.33) can be reduced to

$$p=\rho g R\int_z^{\infty} c_L dz \qquad (3.35)$$

which corresponds to the extra component of the hydrostatic pressure due to the weight of the sediment. The downslope component of mean momentum balance (Equation 3.32) is reduced to

$$\frac{\partial u^2}{\partial x}+\frac{\partial uw}{\partial z}=-gR\frac{\partial}{\partial x}\int_z^{\infty} c_L\, dz+gR c_L S+\frac{1}{\rho}\frac{\partial \tau}{\partial z} \qquad (3.36)$$

After integrating Equation 3.36 over the vertical direction, and considering similarity assumptions, including , similarity of local velocity and excess density profiles, and "top hat" assumption (Turner, 1973), Equation 3.31, Equation 3.34, and Equation 3.36 are transformed to Equation 3.37 to Equation 3.39, respectively.

$$\frac{dUh}{dx}=E_w U \qquad (3.37)$$

$$\frac{dUch}{dx}=v_s\left(E_s-r_0 c\right) \qquad (3.38)$$

$$\frac{dU^2 h}{dx}=gRchS-\frac{1}{2}gR\frac{dch^2}{dx}-C_D U^2 \qquad (3.39)$$

where

c = average sediment concentration

h = current thickness

U = current averaged velocity

E_w = water entrainment coefficient

E_s = dimensionless sediment entrainment coefficient

r_0 = ratio of the near-bed concentration c_b to layer-averaged concentration c. The experiments carried out by Parker et al (1987) indicated that r_0 was almost a constant, equal to 2.0 for a wide range of dimensionless shear velocities.

C_D = bed friction coefficient ($=\frac{u_*^2}{U^2}$). Values of constant C_D for a turbidity current may vary between 0.002 and 0.05 (Garcia, 1985). The lower values correspond to observations in reservoirs and the higher values are associated with laboratory experiments.

u_* = bed shear velocity

The Richardson number is an important parameter governing the behaviour of stratified slender flows, defined as follows:

$$R_i = \frac{gRch}{U^2} \tag{3.40}$$

The volumetric sediment discharge per unit width is denoted as ψ and is expressed as:

$$\psi = chU \tag{3.41}$$

As the down-channel buoyancy transport is $gR\psi$, Equation 3.40 can be written as:

$$R_i = \frac{gR\psi}{U^3} \tag{3.42}$$

Parameter ψ_e which shows the volumetric sediment discharge in equilibrium state is defined as,

$$\psi_e = \frac{E_s hU}{r_0} \tag{3.43}$$

Finally, Equation 3.37, to Equation 3.39, can be cast in the following forms:

$$\frac{h}{U}\frac{dU}{dx} = E_w - \frac{dh}{dx} \tag{3.44}$$

$$\frac{dh}{dx} = \frac{-R_i S + C_D + \left(2 - \frac{R_i}{2}\right)E_w + \frac{R_i}{2} r_0 \frac{v_s}{U}\left(\frac{\psi_e}{\psi} - 1\right)}{(1 - R_i)} \tag{3.45}$$

$$\frac{h}{\psi}\frac{d\psi}{dx} = r_0 \frac{v_s}{U}\left(\frac{\psi_e}{\psi} - 1\right) \qquad (3.46)$$

A comprehensive explanation on the preceding equations has been presented by Parker et al. (1986) and Garcia (1990).

3.7 Summary

In this chapter several concepts related to sediment process computation in natural beds were presented. Computation of sediment deposition and scour in reservoirs and rivers requires the understanding of the concepts and solution of the equations related to coarse sediment transport, cohesive sediment transport, active-layer thickness, armour layer, unit weight of sediment deposited and turbidity current. The literature was reviewed to find the available methods for calculating the above-mentioned concepts. The important sediment transport equations (suspended load and bed load) were listed and three of them (The Meyer-Peter and Müller's theory, Bagnold theory, and Yang theory) were presented in detail. The available theories to estimate the deposition rate and scour rate of cohesive sediment were explained. The actual sediment transport of each hydraulic condition depends on the composition of the active layer and the establishment of the armour layer. Therefore, two available theories about the thickness of the active layer and the establishment of the armour layer were presented. The equations to estimate the initial unit weight of deposited sediment and average unit weight with time were described. Also, the turbidity current definition and the available equations to estimate plunge point, velocity of the head, and body of the steady state turbidity currents were presented in detail.

Chapter Four

EXPERIMENTATION

4.1 Introduction

The study on behaviour of gravity currents in the field and the laboratory began in the 1960s. In pervious studies, the motion of the head of density currents (saline) have received more attention and some valuable experiments have been reported. However, study on the body of gravity currents, especially turbidity currents that are created by density differences due to solid material, have received little attention. Due to the exchange of material between the bed and the turbidity current, the study of this kind of gravity currents is very complicated. It should be noted that turbidity currents occur in many reservoirs and these are known as the phenomena responsible for siltation near dam walls in large reservoirs and causes deterioration in water quality for water supply purposes. Understanding of the sediment processes in the head and the body of the turbidity currents needs more investigation. In this study the experimental works are focused on the subcritical gravity currents.

4.2 Experimental Apparatus

The experiments were conducted in a flume 43 cm wide, 55 cm deep and 4.1 m long. The slope of the flume bed was constant and equal to 0.00635 (0.36 degrees). The bed and the sides of flume was made from acrylic sheet (plexiglass). The flume was equipped with several apparatus to prepare the dense fluid and to control the steady state of the turbidity current during the experiments. The flume and the associated equipment are shown schematically in Figure 4.1. They consist of the following parts:

- Two tanks with a capacity of 570 litres each, one for preparing dense fluid and the other for storing clear water.
- A mixer to mix the dense fluid in the tank and prevent deposition of particles in the mixing tank.
- A pump for pumping the water from the mixing tank to the head tank.
- A head tank to supply constant fluid head during the experiments.
- An orifice flow meter for measuring the flow rate into the flume.
- A valve for controlling the water rate to the flume.
- A gate at the entrance of the flume for controlling the initial depth of the turbidity current.
- A fibre optic turbidity probe for measuring the concentration of sediment
- A fibre optic Laser Doppler Velocimeter system for measuring the velocity.
- A laser particle sizer for analysing particle size distribution of samples
- Two thermometers to measure the temperatures in the mixing tank and the flume.

The dense fluid was prepared in the mixing tank by either mixing sediment and water or dissolving salt in water. All of the measuring instruments were prepared properly and the flume was filled with clear water before starting the experiments. Then the dense fluid was pumped up to the constant head tank. The dense water was delivered from the head tank to the flume with a system of hoses, valves and an orifice flow meter (the connection of the head tank and the flume is shown in Figure 4.2). The initial depth of the current was created by the entrance gate. The current was driven into the flume and then it flowed downstream of the flume. The current was piped to the drain system by pipes and a valve. During the experiments uncontaminated water was supplied to the flume from a separate tank (ranging from 0.2 L/s to 0.35 L/s) to replace the water entrained by the underflow current and to keep the elevation of water at a constant level.

This apparatus and the components can be used to do experiments on gravity currents and to measure the flow in detail.

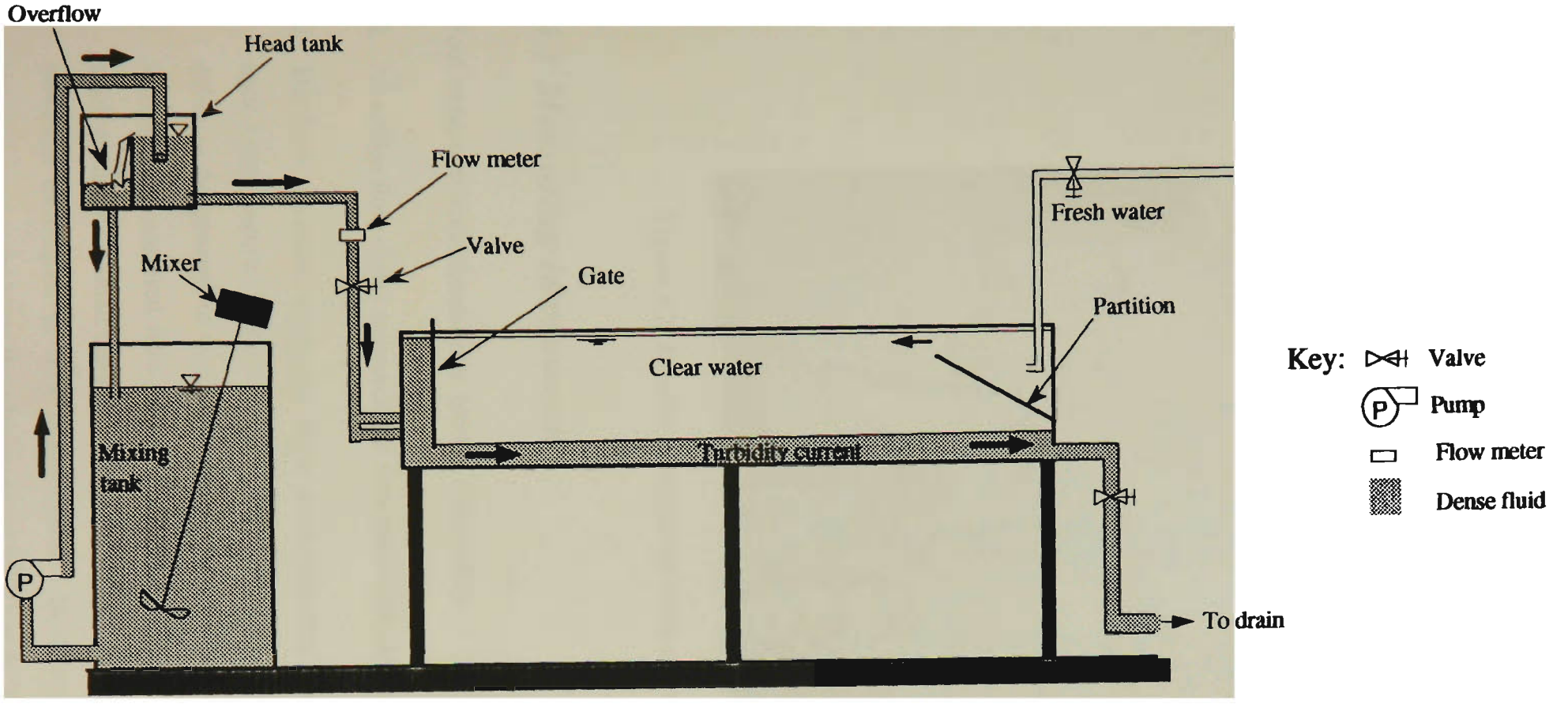

Figure 4.1 Schematic diagram of experimental facility at the University of Wollongong.

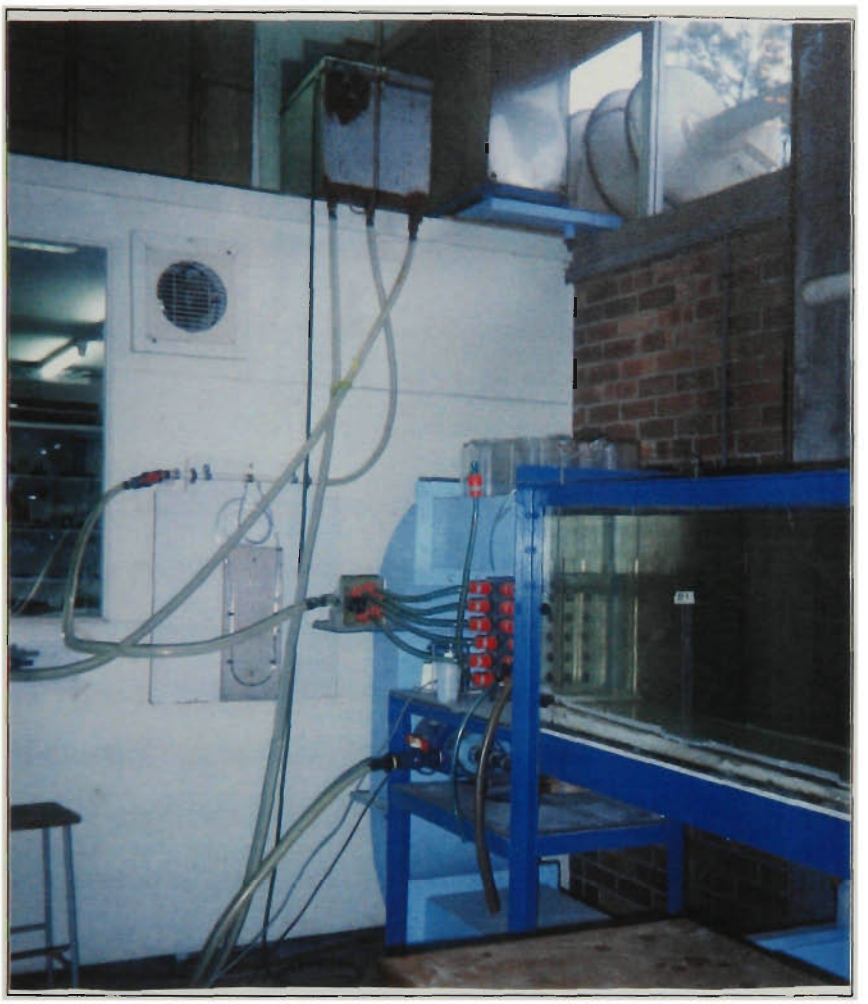

Figure 4.2 Experimental facility (inlet arrangement).

4.3 Measuring Instruments

Four important instruments were used to collect data:

1. An orifice flow meter measured the flow rate to the flume.

2. The flow velocities within the flume were measured using a two dimensional fibre optic Laser Doppler Velocimeter system (LDV) from TSI Incorporated. Using LDV refers to the process of measuring the motion of a fluid by measuring the frequency shift of light scattered from objects in the fluid. These "objects" are usually either small particles or small bubbles in the fluid. LDV is fast becoming one of the most powerful techniques in flow measurement. In comparison with the other flow measurement techniques the advantages of LDV are as follows :

    - no flow disturbance

- no "in situ" calibration needed
- very large velocity range
- accurate measurement of very slow flow and flow reversals
- close to a point measurement
- precise separation of velocity components

Existence of sediment particles does not affect the flow measurement if the concentration is not high enough to prevent the beam passing through the fluid. In applications where the sediment concentration prevents the beam from passing through the fluid, the measurement of velocity with LDV is not possible. The main parts of any LDV are the laser source, the optical transmitter/receiver and the electronic signal processor. The LDV used for these experiments had two components. The laser source was an argon-ion laser and it generates green (514.5 nm), blue (488 nm), and violet (476.5 nm) colours. Two of these colours (green and blue) are used to measure two components of the velocity vector. The transmitting optic was a 9201 Colorburst and it separated the beam output from the laser source. The optical receiver was a 9230 Multicolor Receiver. The signal processor was an IFA 750 Automatic Burst Correlator with FIND Software for data analysis and display of the data. The beams were focused to the measurement point by a 83 mm diameter 9253 fibre optic probe which had a focal length of 350 mm. The LDV system components and the relationship between them are shown in Figure 4.3.

In Figures 4.4 and 4.5, the LDV system components and the actual TSI LDV system are shown respectively. The range of velocities recorded in the experiments were between -7.5 $^{mm}/_{s}$ and 41.5 $^{mm}/_{s}$.

3. A fibre optic turbidity probe (Analite Portable Nephelometer from McVAN Instruments) was used to measure the sediment concentration with uniform particles along the flume. This turbidity probe could measure turbidity between 0.1 to 1999 NTU in two ranges (one from 0.1 to 199.9 and the other from 2 to 1999).

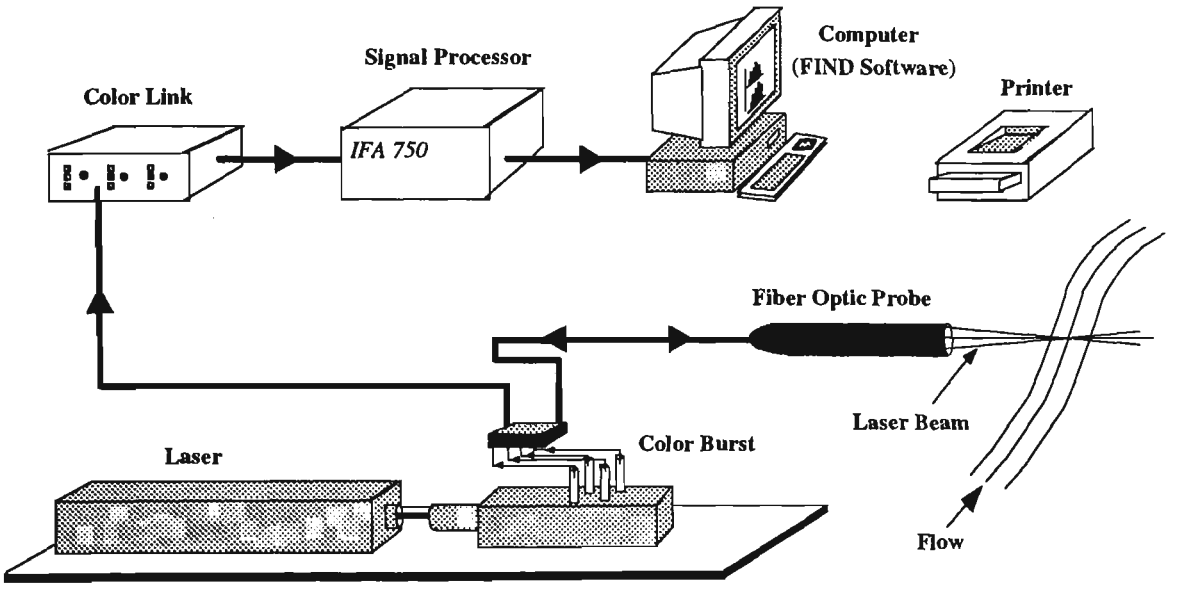

Figure 4.3 Relationship between LDV system components.

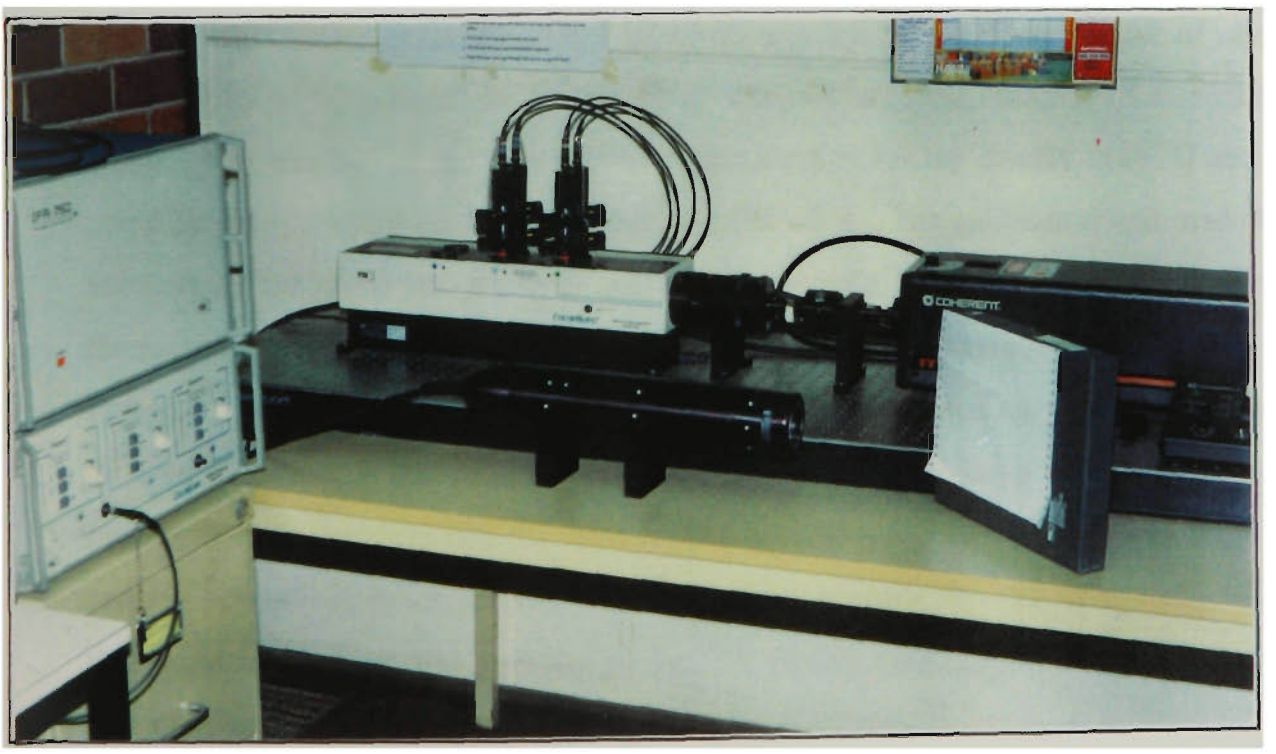

Figure 4.4 Two component Laser Doppler Velocimeter system.

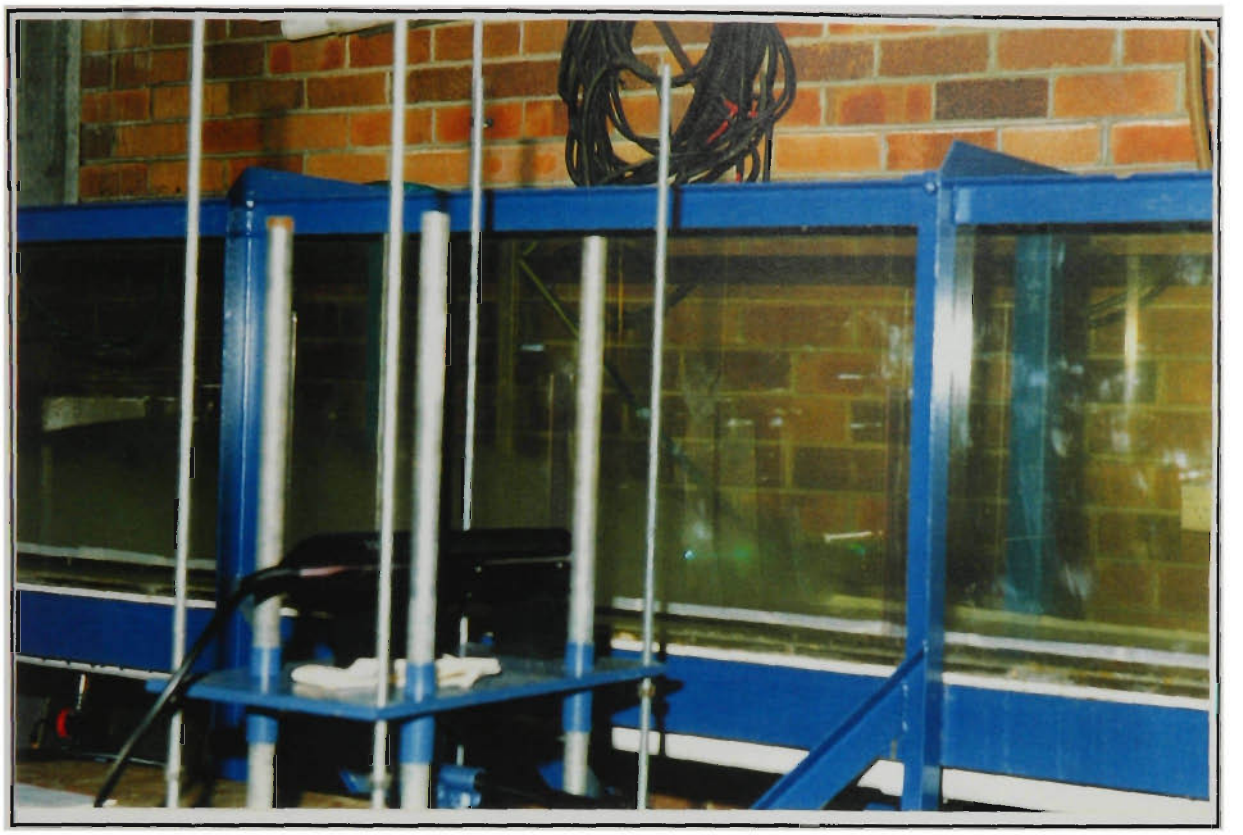

Figure 4.5 Laser probe in operation.

The accuracy of the high sensitive range (range from 0.1 to 199.9) was ± 0.1 NTU and for the other range (range from 2 to 1999) was ± 1 NTU. The principle of using the turbidity probe is based on the scattering of light due to the presence of suspended solids. The output voltage was related to the reading on the display in NTU and it could be calibrated for each particle size concentration. The calibration was made by submerging the probe into a known sediment concentration suspension and recording the associated signal. The turbidity probe and a typical calibration curve are shown in Figure 4.6 and Figure 4.7 respectively. The turbidity probe was also used to measure differences in density due to salt water. This was done by adding a certain amount of potassium permanganate into the mixing tank. A sample of the solution was used to prepare several reference samples of known salt concentration. These samples were then used to calibrate the turbidity probe. A typical calibration curve of turbidity meter for saline currents is shown in Figure 4.8.

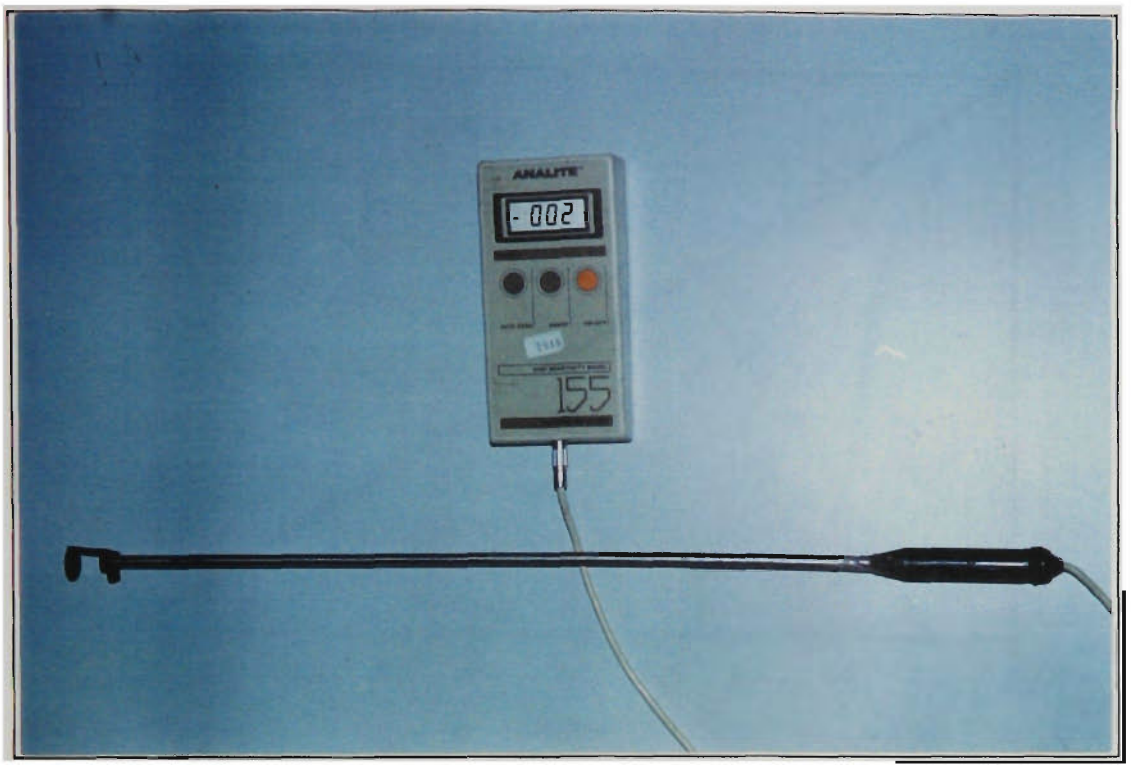

Figure 4.6 The Analite Fibre Optic turbidity probe.

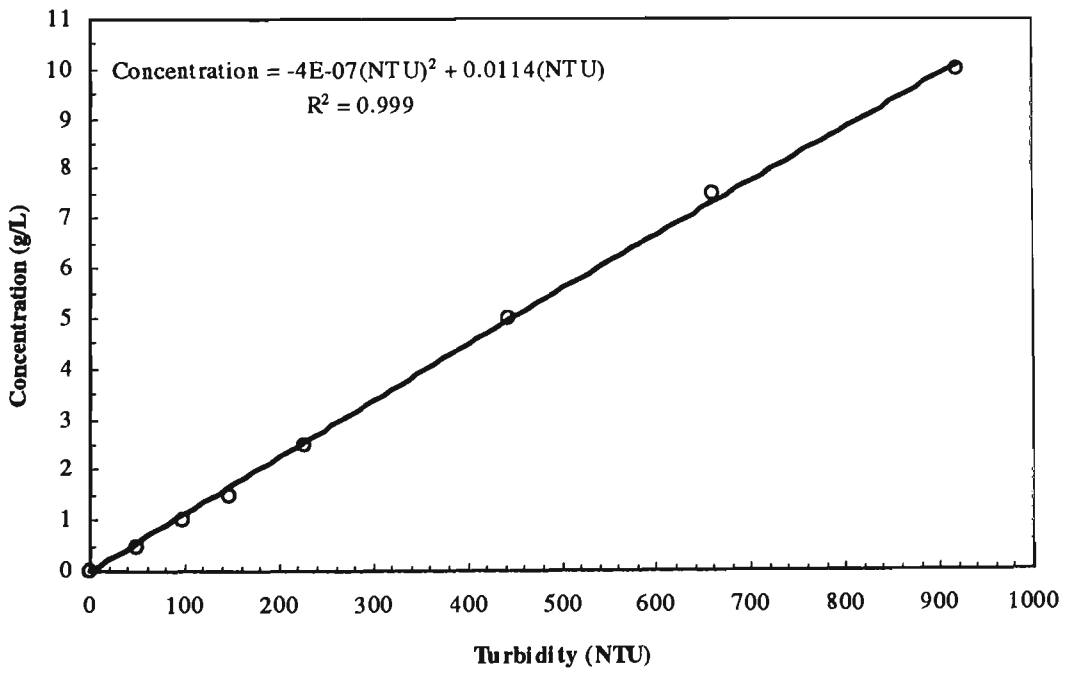

Figure 4.7 The calibration curve of the turbidity probe for the solid material.

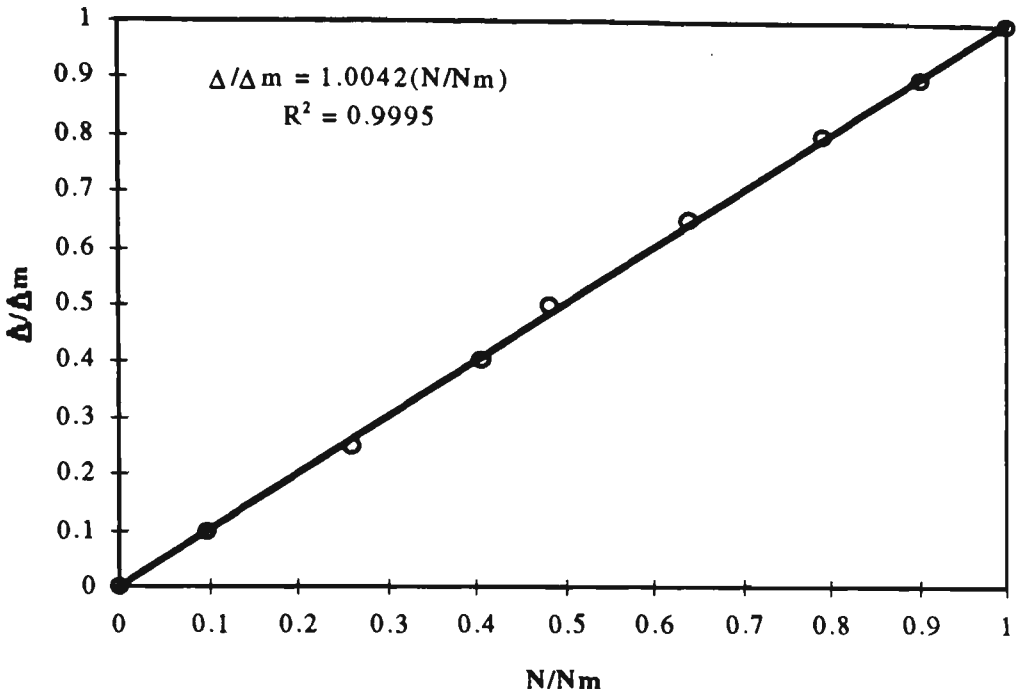

Figure 4.8 Typical calibration curve of the turbidity probe for the saline water. N_m is initial turbidity of fluid (in the mixing tank), N is turbidity of fluid (in the flume), Δ_m is initial fractional density of fluid (in the mixing tank), and Δ is fractional density of fluid (in the flume).

4. A laser particle sizer with the range of 0.5 μm to 564 μm was used for analysing the particles of samples collected from different part of experimental works. The particle sizer are all based on the principle of laser ensemble light scattering. They fall into the category of non imaging optical systems due to the fact that sizing is accomplished without forming an image of the particle onto a detector. The particle sizer used in this study (model 2600 of Malvern Company) used optical method, called conventional Fourier Optics. The light from low power Helium-Neon laser is used to form a collimated and monochromatic beam of light, 9 mm in diameter. This beam of light is known as the analyser beam and any particles present within it will scatter this laser light. The light scattered by the particles and the unscattered remainder falling onto a receiver lens, also known as the range lens. This operates as a Fourier transform lens forming the far field diffraction pattern of the scattered light at its focal plane. An annular sector, gathers the scattered light over a range of solid angles of scatter. A schematic diagram of the laser particle sizer is shown in Figure 4.9. The measurement accuracy of this equipment is ± 4% of volume median diameter (measured by an approved technique using a diffraction reference reticule).

A photograph of the Laser Particle Sizer is presented in Figure 4.10. The range measured in this study was between 1 and 150 μm.

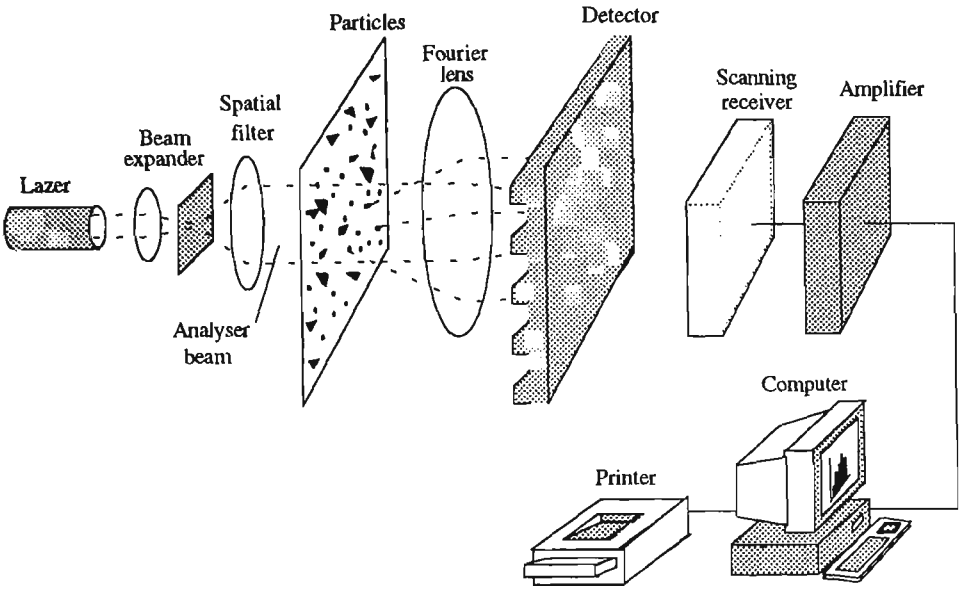

Figure 4.9 Schematic diagram of laser particle sizer.

Figure 4.10 Model 2600 of Malvern laser particle sizer.

4.4 Sediment Materials

The material used was filter aids (amorphous silica) from Olin Chemicals. The geometric mean size of the material (D_g) was 36.25 μm. The specific gravity of particles was 2.33 and the apparent bulk density was 2330 kg/m^3.

The fall velocity of the sediment particles are calculated from the equation developed by Dietrich (1982) which is applied successfully for natural particles ranging from 14 μm to 67 mm. The equation is given as:

$$v_s = \left(g R \nu W_*\right)^{1/3} \tag{4.1}$$

where

$$\log(W_*) = -3.7617 + 1.92944\log(D_*) - 0.09815\left(\log(D_*)\right)^2 - 0.00575\left(\log(D_*)\right)^3 + 0.00056\left(\log(D_*)\right)^4 \tag{4.2}$$

and

$$D_* = \frac{g R D_g^3}{\nu^2} \tag{4.3}$$

v_s = fall velocity

R = submerged specific gravity of the sediment

ν = kinematic viscosity of the water

D_g = geometric mean size of the sediment

g = acceleration due to gravity

The sediment size distribution curve is determined by using a Malvern model 2600 Laser Particle Sizer. A small amount of sediment particles is suspended in water and this liquid is taken to the laser particle sizer to obtain the size distribution curve. The size distribution curve of the material is shown in Figure 4.11.

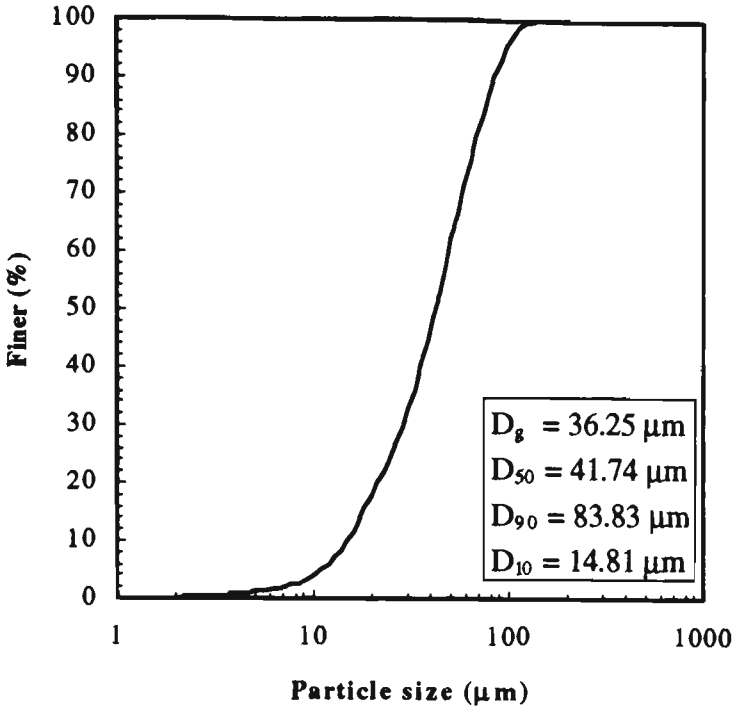

Figure 4.11 Typical sediment particle size distribution.

4.5 Details of Experimental Work

A sediment material with geometric size equal to 36.25 μm was used. The inlet current thickness (h_0) was set equal to 40 mm for all experiments. The current reached the normal depth after a short distance. The buoyancy discharge per unit width and the inlet Richardson number was varied by changing the sediment concentration and fluid discharge. For each part of experimental work several different Richardson numbers greater than 1 were tried. The conservative current was created by dissolving ordinary salt in water. In experiments related to the head of saline density currents, some potassium permanganate (almost 10 mg/L) was also added to be used as a criterion for measuring the concentration and to make the current visible so that the height and the velocity of the head can be measured. The outflow water drained directly to the drainage system. A pipe was installed at the end of the flume to add clear water (ranging from 0.2 L/s to 0.35 L/s) to the flume to replace the entrainment rate of clear water by the current.

Nine points along the flume, with a distance of 0.5 m between each of them, were chosen as the data collection stations. The location of the stations are shown in Figure 4.12. The first 50 cm of the flume and 50 cm from the end part of the flume were not

monitored as the current was not in a normal condition in these zones. In the remaining parts of the flume, the data were measured along the flume. The turbidity probe was attached to a vernier gauge and mounted above the flume. The turbidity probe could be moved along the flume and the vernier gauge could be moved up and down. The LDV was installed on a traverse near the side of the flume. The traverse could be moved vertically with the accuracy of ±1 mm. These facilities allowed access to all points of the flume to measure the velocity and concentration. In Figure 4.13 the position of the LDV and turbidity probe are shown in the profile of the flume.

Five sampling taps were installed along the flume, one at the entrance, one near the outlet and three inside the flume (in stations 2, 4 and 6) each with one meter intervals. These taps were used to collect water samples from the head and from the body of turbidity current for particle size analyses. Also, the first and the last point were used for calculating inflow and outflow sediment concentration from the flume. In Figure 4.14 these sampler are shown schematically.

In the turbidity current experiments conducted in this study, due to settling coarse particles in the mixing tank and the head tank, the sediment concentrations in the mixing tank and at the flow entrance to the flume were different. Therefore, the sediment

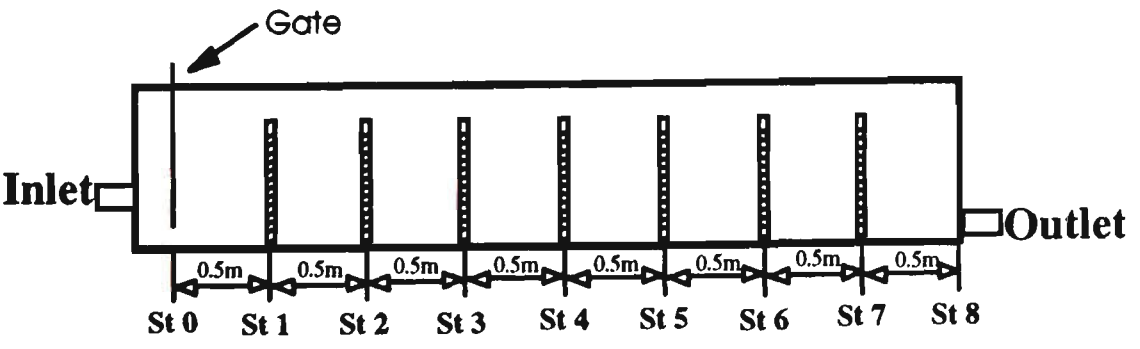

Figure 4.12 Location of sampling stations.

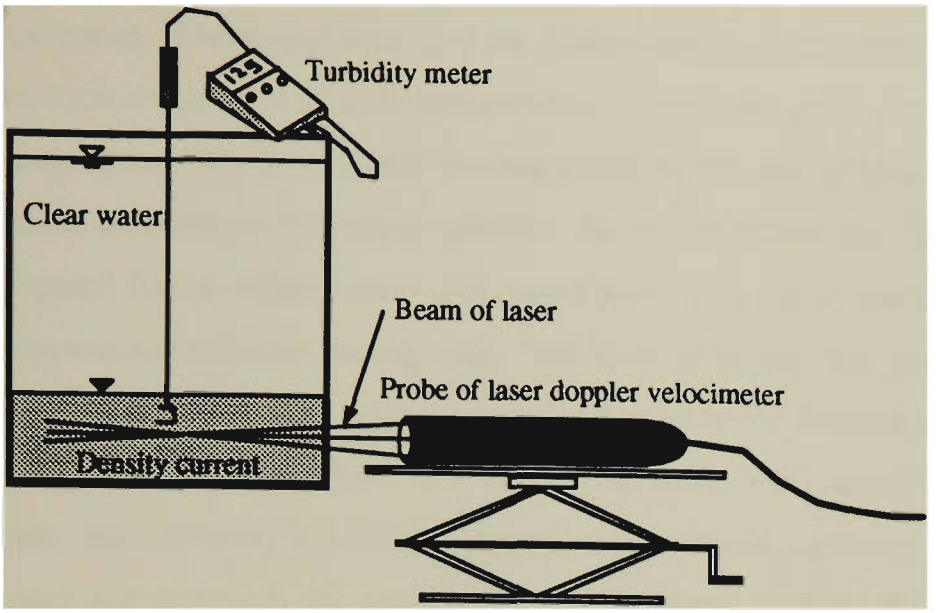

Figure 4.13 Position of the LDV and turbidity probe in profile of the flume.

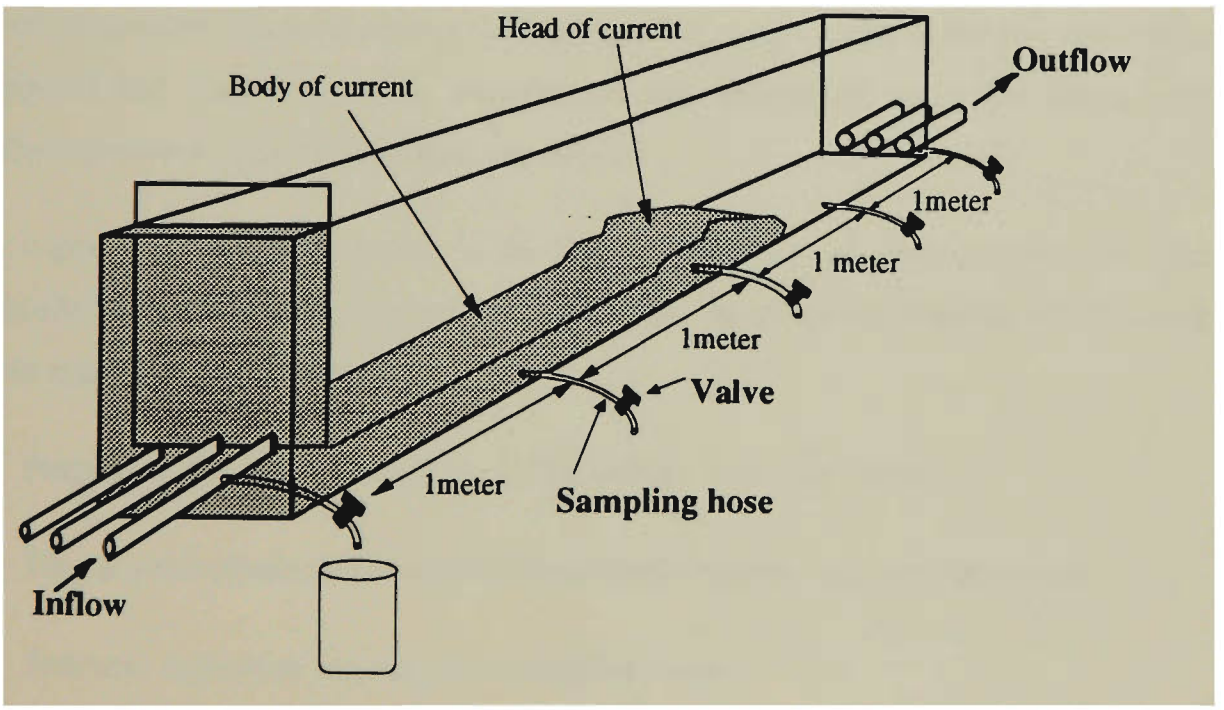

Figure 4.14 Schematic of stations and water sampling locations.

concentrations and sizes calculated from inlet point were used for analyses of the experimental results instead of the concentrations and sizes in the mixing tank.

4.6 Experimental Procedure

The measuring instruments were checked before each experiment and the mixing tank and flume were thoroughly cleaned to remove deposited sediment particles from

previous experiment. The mixing tanks and the flume were then filled from potable tap water. Then a known amount of sediment particles (range from 1000 g to 7000 g) or table salt (range from 1500 g to 10000 g) were added to the mixing tank to generate turbidity current or conservative density current. In this procedure, the desired dense fluid was prepared for the experiments. The mixer pump was run to mix the fluid and prevent sedimentation within the mixing tank. The dense fluid was then pumped to the head tank to be fed to the flume. Inflow rate was adjusted to the determined discharge with the aid of the valve and the orifice flow meter. The outflow was adjusted more than the inflow rate (approximately 0.4 L/s) to prevent any backwater in the current. Clear water was also supplied from the surface pipe to the flume to keep the water at a constant level. The temperatures were measured from the flume and the mixing tank to ensure that there was no significant difference between the temperature of the two layers to create another source of density differences. The temperatures of the two fluids were collected and controlled. The experiments was abandoned when the temperature differences were equal or more than one degree.

66 experiments were conducted in the flume. Only five of these experiments were cancelled because of large temperature differences. In all the experiments, the following three conditions were evaluated:

1. Progress of the head of turbidity current and saline density current

2. The progress of subcritical conservative density current and turbidity current

3. Sediment deposition resulting from turbidity current.

4.6.1 Data Collection: Head of Gravity Current

35 experiments were conducted to study the head of gravity current. 17 of them were non conservative turbidity currents that were established by mixing the sediment particles in water. The dense fluids were prepared in the mixing tank by mixing certain amounts of sediment material (range from 2300 g to 6000 g) or salt (range from 1500 g to 9000 g) and clear water (almost 570 litre). The flume was filled with the clear water and the inlet gate opening was set on 40 mm. The fluid was pumped to the head tank and was

fed by gravity to the flume. The height of the turbidity current head and the time were collected along the flume at 0.5 m intervals. Two samples were collected from each sampling tape, one from the head of the current and one from the body. These samples were collected in plastic bottles and used for particle sizing analyses. The profiles of particle concentration of the current head were collected by using the turbidity probe in the center-line of the flume at stations 2, 4, and 6. The turbidity meter was moved to each measurement station before the current reached that station in order to prevent the disturbance of the current by the meter. Two one litre samples were collected from the first and last sampler points respectively. These samples were dried in an oven and weighed to calculate the inflow and outflow particle concentration. No fresh water was added to the flume for these experiments and the outlet gate was closed until the current was reached to the end of the flume.

18 of the experiments were conservative saline density currents. The procedure used was similar to that used in the experiments related to non conservative turbidity currents. This type of current could be considered to have a zero settling velocity. Several different buoyancy of saline density current were conducted in the flume. The conservative dense fluid was also mixed with some permanganate (almost 10 mg/L) to be used as a criterion for measuring the concentration, and the turbidity probe was calibrated by making several reference fluids from the fluid of the mixing tank. The velocity and the height of the current were collected inside the flume and the profile of the density of the current was collected using the turbidity probe. The flow parameters of the runs and a summary of the data collected are presented in chapter five. The raw data are presented in Appendix I.

4.6.2 Data Collection: Subcritical Conservative Density Current and Turbidity Current

For conducting experiments on conservative density currents, the dense fluid was prepared in the mixing tank by dissolving a certain amount of salt (3000 g to 10000 g) with fresh water (almost 570 litre). The flume was filled with clear water. The tap water was opened in the flume and the outlet gate was opened. The tap water was adjusted to keep water level constant (almost 0.5 m from the bed). Two mercury thermometers

were used to collect the temperatures of the two fluids. The collected temperatures were controlled to make sure the differences were less than one Celsius degree.

After starting the experiments no data was collected until the current reached the end of the flume and a steady condition was achieved. When a steady condition of current was achieved, data were collected at several vertical points at station 2 (1 meter distance from inlet gate) and at station 6 (3 meters distance from inlet gate).

Ten different currents of dense fluid were selected for this experiment. The density differences between fresh water and dense fluid were calculated by weighing the same volume of water and dense water with a sensitive weighing machine. In each station, the local velocities were measured at the center-line of the flume and at some vertical points ranging from 10 mm above the bed up to a few centimetres above the density current, all at 5 mm intervals. The turbidity measurements were also made at the center-line of the flume and at selected vertical points from 10 mm above the bed up to a few centimetres above the density current using 10 mm intervals. The measuring instruments were moved to station 2 and were located at the first vertical point to collect the data. The collection of data was then continued for the other vertical points and at other station. The flow parameters of the conservative density current experiments and a summary of the data collected are presented in chapter six. The raw data are presented in Appendix I.

The same procedure was used for the experiments related to the turbidity current. Ten different currents of dense fluid were selected for this experiment. The determined sediment particles were weighed with a sensitive (0.01 g) weighing machine (range from 1000 g to 5000 g) and mixed with water in the mixing tank (almost 570 litre). The locations of the measurement points were the same as those for the subcritical saline density current experiments. Unfortunately in this part of the experiment, the profile of the velocity could not be collected properly because the LDV could not collect the velocity from the center-line of the flume. This was because of the existence of a large amount of fine particles in the turbidity current scattering the laser beams before the measurement point. The measurement point (from center-line of the flume) was changed to find a point at which the velocity could be recorded by the LDV. This point was found to be almost 50 mm from the wall of the flume. The effects of the wall on the

local velocity at this point was too large to ignore. Therefore, the collected velocities were not used for analysing the data and the analyses of the velocity profiles are limited to the data collected from the saline density current. The flow parameters of the runs and a summary of the data collected are presented in chapter six. The raw data are presented in Appendix I.

4.6.3 Data Collection: Sediment Deposition Results from Turbidity Current

In this part of the experiments, sediment deposition results from turbidity current is considered. The flume was assumed as a laboratory reservoir and the dense fluids were gravity fed into the flume. The inlet gate was set at 40 mm and four different turbidity currents were run. The steady state turbidity currents were established in the flume and kept for more than half an hour. Water samples (500 ml) were collected from inflow and outflow for calculating the inflow and outflow concentration and particle size distribution. The turbidity current height were measured along the flume. After each run, the water was pounded in the flume and 8 samples were collected from the bed of flume to calculate the amounts of the sediment deposition along the flume. Bed samples were collected every 50 cm along the center-line of the flume. A plexiglass tube with 38.046 cm^2 in area was used to collect the bed samples. The tube were fixed on the bed and the sediments inside of the tube were collected on a glass beaker by the aids of a vacuum sampler. These samples were dried and weighed later to determined the amount of sediment deposited. Further samples were collected from the same place for sediment analyses. In Figure 4.15, a schematic sketch of the sample points and the tube are shown. The flow parameters of the runs and a summary of the data collected are presented in chapter eight. The raw data are presented in Appendix I.

4.7 Summary

In this chapter the experimental apparatus and the measurement equipment were presented. The flume and related parts, and the location and methods of collecting data were described. The flume was rectangular in cross section with 43 cm wide, 55 cm deep and 4.1 m long. The slope of the flume bed was constant and equal to 0.00635.

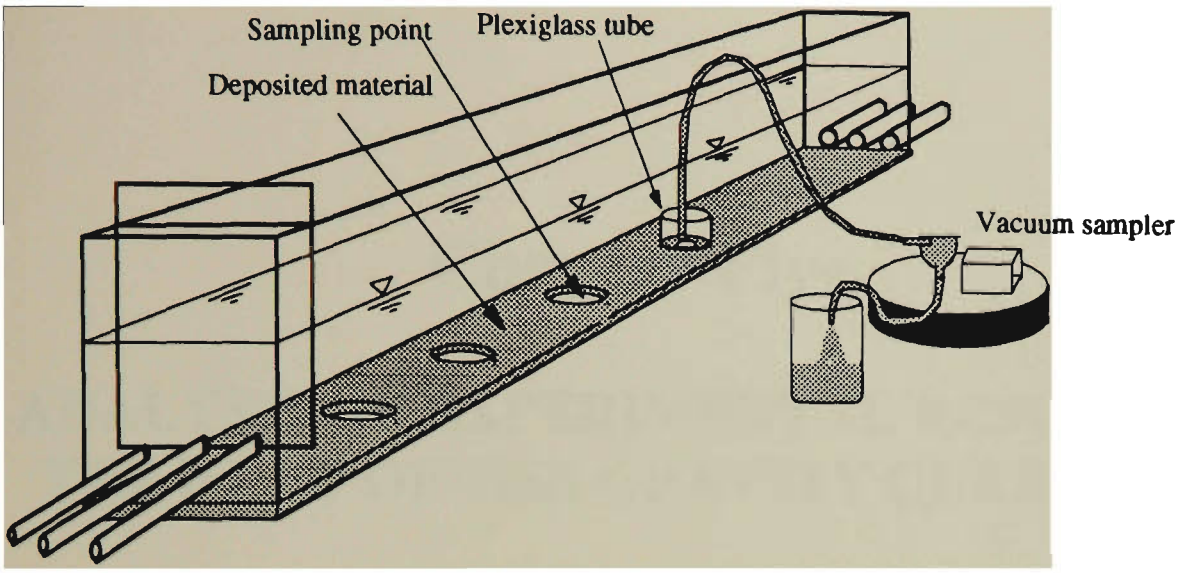

Figure 4.15 Schematic of collection of deposited materials.

The flume was equipped with several apparatus to prepare the dense fluid and to control all details of the experiments. The mechanics of the measuring instruments used to collect data, including the fiber optic Laser Doppler Velocimeter system, the fibre optic turbidity probe with accuracy of ± 0.1 NTU and the laser particle sizer with accuracy of ± 4% of volume median diameter, were presented. Usage of highly accurate equipment such as the fiber optic Laser Doppler Velocimeter to measure very low velocities including flow reversal was one of the advantages of the present study. The inflow to the flume was measured by means of a standard orifice meter and it has been found that this simple measuring technique was adequate for this purpose. The sediment material used was diatomaceous earth (swimming pool filter aids) with the geometric mean size equal to 36.25 μm and specific gravity equal to 2.33. Finally, the experimental procedures were presented in detail. All together fifty nine experiments were conducted. 35 experiments were conducted to study the head of gravity current including head of non conservative turbidity currents (by mixing sediment particles in water) and conservative saline density currents (by mixing salt in water). 20 experiments were conducted to study the subcritical conservative density current and turbidity current. 4 experiments (experiments 1, 2, 4, and 6) were conducted to study the sediment deposition results from turbidity current.

Chapter Five

ANALYSIS OF EXPERIMENTAL RESULTS: THE HEAD OF THE GRAVITY CURRENT

5.1 Introduction

The edge of a gravity current forms a typical frontal zone that is often called the head of the gravity current. The pressure gradient arising from the density difference between two fluids forms the shape of the head. The head usually has a foremost point which is raised above the bed. The motion of the head has been studied mainly in the experiments of Middleton (1966a) and in the theoretical work of Benjamin (1968). The velocity of the head is expressed by the densimetric Froude number called 'Keulegan's formula' (Middleton, 1966a) as follows:

$$U_f = C_c\sqrt{g'H_f} \qquad (5.1)$$

where g' is effective gravitational acceleration ($=\Delta g$), U_f is the velocity of the head, Δ is the relative density difference between two fluids, g is acceleration due to gravity, H_f is the thickness of the head, and C_c is a constant equal to the value of the Froude number. The parameters are shown schematically in Figure 5.1. The coefficient C_c can be taken as 0.7 according to Keulegan (1958, cited in Middleton, 1966a) for flow Reynolds numbers greater than 10^3. Middleton (1966a) found that $C_c = 0.75$, for slopes up to 4%. Altinakar et al. (1990) suggested that $C_c = 0.63$ for small slopes. Using Equation 5.1 is easy, but the disadvantage in doing so is that it combines the two major dependent variables, H_f and U_f. To overcome this problem Britter and Linden (1980) and Denton (1981) preferred to explain the head velocity with initial parameters of the current as:

$$U_f = C_v (g' q_0)^{1/3} \qquad (5.2)$$

where C_v is a coefficient and q_0 is discharge of the fluid in unit width. The coefficient can be taken as $C_v = 1.5 \pm 0.2$ for bed slopes between 5° and 90° according to Britter and Linden (1980) and $C_v = 1.06$ for small slopes according to Denton (1981).

From a sediment transport point of view no studies have been found in the literature relating to the head of the gravity current. In this chapter the data collected from the heads of both conservative saline density currents and non conservative turbidity currents are analysed.

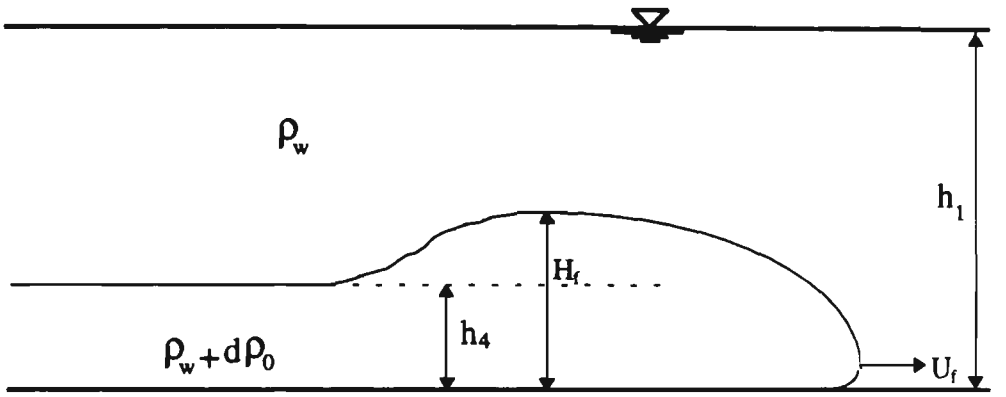

Figure 5.1 Diagram of the head of turbidity current.

5.2 Experimental Conditions

Thirty five sets of experiment were conducted in this part of the study. 17 of them (experiments 8 to 24) were non conservative turbidity currents that were established by mixing the sediment particles in water and 18 of the experiments (27 to 44) were conservative saline density currents that were established by mixing table salt in water. The raw data for all thirty five experiments are given in Appendix I. For all the experiments, the inlet current thickness was set at 40 mm with the help of a sluice gate, the height of clear water in the flume was kept at 500 mm, and the currents were in sub-critical condition. The range of parameters in the experiments are presented in Tables 5.1 and 5.2. In these tables Q_0 is the inlet flow rate, c_0 is the inlet volumetric concentration, Δ_0 is the inlet fractional density (= Rc_0 for sediment, $R = (\rho_s/\rho_w) - 1$, ρ_s and ρ_w are densities of the sediment and water, respectively.). B_0 is the inlet buoyancy

flux $B_0 = g\ \Delta_0\ q_0$ (q_0 is inlet discharge per unit width), and R_{i0} is the inlet Richardson number $R_{i0} = B_0/U_0^3$. The selected range was limited by the size of the experimental flume and by the need to keep the current in a subcritical condition that mostly occurs in reservoirs.

Table 5.1 Range of parameters related to the turbidity current head experiments.

Non-conservative turbidity current		
Parameter	**Minimum**	**Maximum**
C_0	0.001716	0.004292
Q_0 (L/s)	0.095	0.275
U_0 (mm/s)	5.52	16.00
Δ_0	0.002283	0.005708
B_0 (m^3/s^3)	4.4E-6	22.8E-6
R_{i0}	3	35
T (°C)	19	22

Table 5.2 Range of parameters related to the saline density current head experiments.

Conservative saline density current		
Parameter	Minimum	Maximum
Q_0 (L/s)	0.110	0.290
U_0 (mm/s)	6.395	16.86
Δ_0	0.001906	0.01114
B_0 (m^3/s^3)	7.61E-6	65.97 E-6
R_{i0}	2	88
T (°C)	21	25

One type of sediment materials was used during the turbidity current head experiments. The size distribution curve of the material was shown in Chapter 4. The slope of the flume was kept constant and equal to 0.00635. This slope was chosen to make sure that the currents always stay in a sub-critical condition. In all the experiments, the inlet Reynolds numbers were between 220 and 675. The parameters of all the experiments are presented in Tables 5.3 and 5.4. The parameters used in the tables are described as follows:

T = Temperature in degree Celsius

q_0 = Input discharge per unit width

B_0 = Initial buoyancy flux (= g $\Delta_0 q_0$)

x = Distance from the inlet gate

Δ = fractional density at a given section

H_f = Height of the head of gravity current

U_f = Velocity of the head

D_g = Mean geometric size of the particles at a section

Geometric mean size D_g is defined as:

$$\log D_g = \frac{1}{100} \sum p_i \log D_i \qquad (5.3)$$

in which p_i is the percentage weight corresponding to the size D_i.

In Figure 5.2 the measurement points to find U_f and H_f in the location of x = 1.0 m are shown schematically. The error in determination of H_f is probably ±5%. This is due to existing large eddies in the upper layer of the fluid of the head which disturbs the boundary of the two fluids. The average velocities of the head in each measurement point were measured by reading the time (with a digital chronometer) of reaching the front of head between the points 0.5m before and 0.5m after the measurement point. The error in determination of U_f should be less than ±2.5%. It is important that the fractional density is measured locally rather than at the inlet or in the mixing tank because inlet mixing and interfacial entrainment can cause substantial dilution of the current.

Therefore, the layer-averaged density fraction of the head (Δ) was determined by using the density fraction (for saline density current) or sediment concentration (for turbidity current) profiles measured along the center-line of the head and calculating the mean value with integration. The error in determination of Δ should be less than ±2.5%.

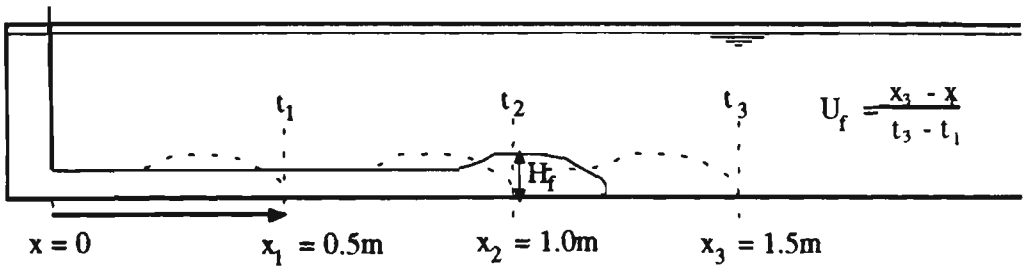

Figure 5.2 Schematic diagram showing the relationship between H_f, U_f, and x.

5.3 Development of a Typical Gravity Current Head

As the current entered the flume the front of the head was established within the first 50 cm of the flume. A mixing region then develops in the lee side of the front. The head of the current rapidly reached an equilibrium value. It also advanced on the bed of the flume without significant changes in the shape, height and velocity. The interaction between dense fluid and fresh water created a very complex pattern of flow inside and around the head. The height of the current had a remarkable reduction in height immediately behind the head. This part of the current had uniform pattern of flow and continuously follows the head. It is called the body of the gravity current. The shape of the heads were almost the same for both turbidity and saline density currents. A typical shape of the gravity current head is shown in Figure 5.3. It was observed that in the turbidity current experiments using sediment particles, the average concentration of the sediment were changed with the distance due to settling of sediments. A thin layer of deposited sediments was observed on bed when the flume was emptied. Two photographs showing the development of a sediment type turbidity current and a salt type density current heads are shown in Figure 5.4 and Figure 5.5 respectively.

Table 5.3 Experimental parameters related to the head for all turbidity current.

Exp. No.	Type	T (° C)	q_0 (m^2/s)	B_0 (m^3/s^3)	x (m)	Δ	H_t (mm)	U_t (mm/s)	D_g (mm)
					1	0.000584	140	17.9	27.91
8	Solid	20.0	0.000640	22.83E-6	2	0.000584	140	23.8	25.11
					3	0.000613	150	25.0	25.88
					1	0.000270	110	15.8	22.93
9	Solid	21.0	0.000349	9.65E-6	2	0.000309	110	14.1	22.87
					3	0.000281	115	16.1	21.46
					1	0.000190	100	12.0	24.34
10	Solid	21.0	0.000221	5.11E-6	2	0.000209	100	13.3	19.77
					3	0.000130	90	10.3	18.03
					1	0.000475	110	16.7	28.72
11	Solid	21.0	0.000430	12.38E-6	2	0.000524	110	19.2	23.67
					3	0.000391	115	16.1	21.04
					1	0.000234	160	11.8	32.92
12	Solid	19.0	0.000407	8.77E-6	2	0.000266	160	13.3	25.84
					3	0.000241	160	11.1	26.24
					1	0.000173	145	15.4	30.63
13	Solid	21.0	0.000530	10.89E-6	2	0.000250	150	17.0	27.35
					3	0.000237	150	15.2	25.23
					1	0.000184	110	12.5	28.60
14	Solid	21.0	0.000340	4.40E-6	2	0.000215	105	13.0	24.09
					3	0.000170	110	10.8	21.53
					1	0.000196	100	8.7	26.05
15	Solid	21.0	0.000256	4.54E-6	2	0.000169	120	8.3	21.58
					3	0.000174	80	5.2	19.73
					1	0.000249	80	10.2	25.13
16	Solid	22.0	0.000256	6.01E-6	2	0.000309	80	11.2	23.93
					3	0.000193	75	8.9	22.88
					1	0.000512	120	18.9	32.07
17	Solid	20.0	0.000605	10.54E-6	2	0.000480	120	19.2	26.68
					3	0.000384	125	16.7	24.49
					1	0.000283	130	13.3	26.66
18	Solid	21.0	0.000442	6.76E-6	2	0.000217	130	14.7	23.84
					3	0.000258	130	13.7	22.45
					1	0.000563	110	20.0	28.06
20	Solid	22.0	0.000523	19.21E-6	2	0.000602	100	23.8	24.05
					3	0.000596	105	18.5	24.05
					1	0.000464	110	18.2	26.35
21	Solid	22.0	0.000453	14.74E-6	2	0.000499	110	21.3	24.77
					3	0.000489	110	17.9	23.11
					1	0.000501	90	15.4	25.70
22	Solid	22.0	0.000360	14.07E-6	2	0.000360	90	18.2	23.55
					3	0.000290	95	16.7	21.66
					1	0.000358	80	13.5	24.69
23	Solid	22.0	0.000233	7.01E-6	2	0.000410	75	13.5	21.14
					3	0.000265	75	12.5	21.43
					1	0.000565	105	16.1	26.74
24	Solid	19.0	0.000337	15.15E-6	2	0.000548	105	18.2	23.96
					3	0.000531	105	16.4	21.10

Table 5.4 Experimental parameters related to the head for all saline gravity current.

Exp. No.	Type	T (° C)	q_0 (m^2/s)	B_0 (m^3/s^3)	x (m)	Δ	H_f (mm)	U_f (mm/s)
					1	0.002262	60	19.2
27	Salt	23.0	0.000279	29.87E-6	2	0.000827	70	23.8
					3	0.002466	70	23.2
					1	0.002403	90	25.0
28	Salt	23.5	0.000291	31.12E-6	2	0.002844	90	30.3
					3	0.003249	90	3.03
					1	0.002398	75	28.6
29	Salt	23.0	0.000616	65.97E-6	2	0.003160	95	34.5
					3	0.003268	95	34.5
					1	0.002667	70	20.8
30	Salt	22.0	0.000326	35.58E-6	2	-	85	30.3
					3	0.002432	85	27.8
					1	0.002992	95	35.7
31	Salt	22.0	0.000453	49.56E-6	2	-	95	38.5
					3	0.003115	95	37.0
					1	0.00288	110	34.5
32	Salt	22.0	0.000593	64.81E-6	2	-	120	40.0
					3	0.002979	120	38.5
					1	0.001883	120	24.4
33	Salt	21.0	0.000302	20.24E-6	2	-	105	27.0
					3	-	105	23.8
					1	0.001198	120	25.0
34	Salt	22.0	0.000488	32.69E-6	2	0.001442	120	33.3
					3	0.001644	115	30.3
					1	0.001615	135	27.8
35	Salt	22.0	0.000593	39.69E-6	2	-	135	32.3
					3	0.001545	135	32.3
					1	0.000765	85	25.0
36	Salt	25.0	0.000256	17.12E-6	2	0.001730	85	27.8
					3	0.001581	85	25.6
					1	0.000996	130	25.6
37	Salt	22.0	0.000442	26.34E-6	2	0.001025	130	28.6
					3	0.001121	125	27.0
					1	0.000913	140	25.0
38	Salt	22.0	0.000558	33.27E-6	2	0.000579	140	34.5
					3	0.001011	140	29.4
					1	0.001534	150	27.0
39	Salt	22.0	0.000674	40.20E-6	2	-	155	32.3
					3	0.001675	150	32.3
					1	0.002149	130	19.2
40	Salt	22.0	0.000349	13.44E-6	2	0.001780	140	23.8
					3	0.001110	135	22.2
					1	0.000439	145	23.3
41	Salt	22.0	0.000542	20.88E-6	2	0.001532	145	28.6
					3	0.001671	150	27.0
					1	0.000599	240	18.9
42	Salt	22.0	0.000674	12.61E-6	2	0.000535	210	19.2
					3	0.000577	210	18.5
					1	0.000217	210	20.8
43	Salt	23.0	0.000553	10.35E-6	2	0.000787	200	22.7
					3	0.000779	180	21.3
					1	0.000418	190	14.7
44	Salt	22.0	0.000407	7.61E-6	2	0.000735	190	14.9
					3	0.000679	190	14.9

- indicates measurement not taken.

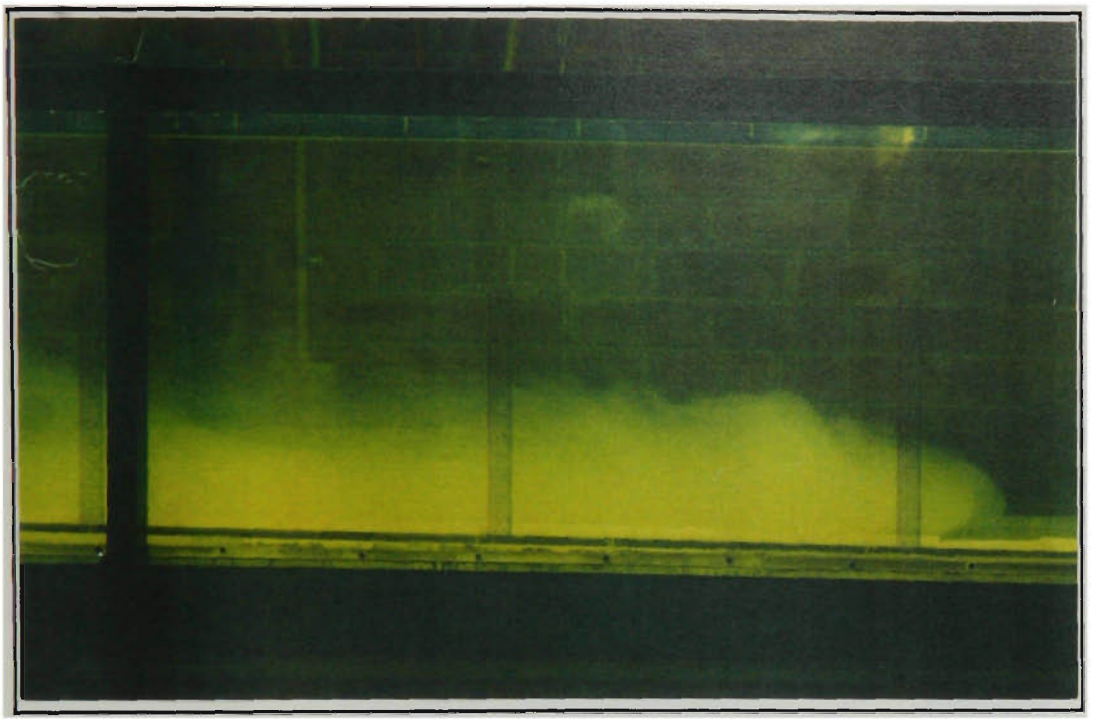

Figure 5.3 Typical shape of the head of a gravity current.

The photographs show a side view of the head movement along the flume taken at right angles to the flume.

As can be seen the head develops to a certain height after a small distance. The nose is raised above the bed (h_n) and vortex structures are observed in the head. The billows are formed at the front. It was found that they had the properties of Kelvin-Helmholtz billows (Simpson, 1986). This type of billow is associated with instability formed at the interface between two fluids. The ambient water is entrained into the head by the billows and the vortices. Due to friction at the stationary bed, the lowest streamlines in the flow relative to the head returns towards the rear and this causes the front nose of the head to raise above the bed. A schematic diagram of a two-dimensional flow pattern of such a gravity current head is shown in Figure 5.6.

In some experiments, as the gravity current advanced, some parts of the upper layer of the head ran out of the head into ambient water, and this caused the cancellation of the experiments (ie experiment no. 19). This separation layer was found especially in the sediment type of current. By controlling and checking the various parameters it was found that this separation was due to temperature differences between the current and the ambient water (2 °C or more). This shows the sensitivity of the currents and the effect of different sources of currents on each other.

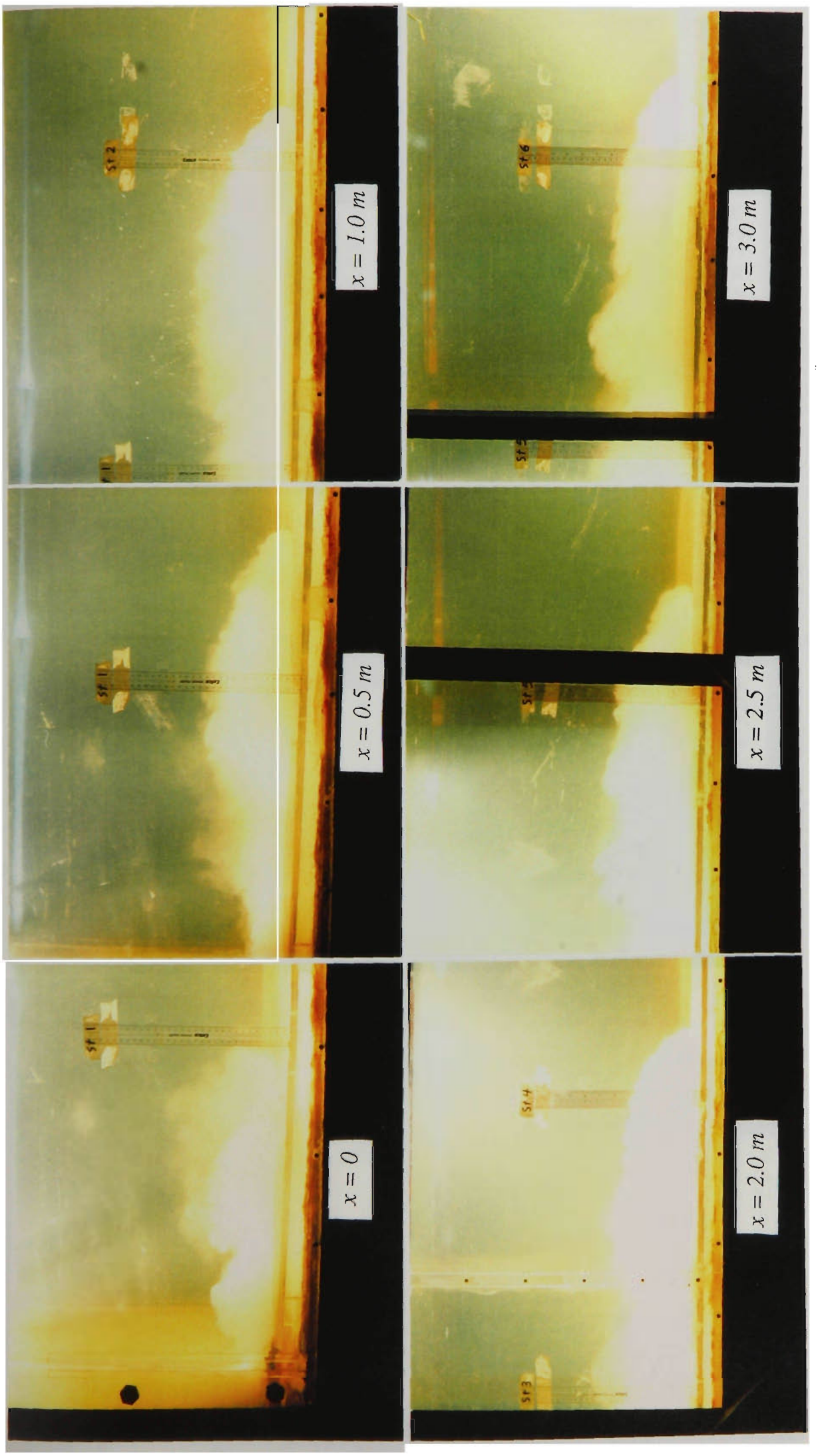

Figure 5.2 The advance of a typical turbidity current. $q_0 = 7.7$ cm^2/s, fractional density, $\Delta_0 = 0.0033$, $T = 24°$ C, $h_0 = 4$ cm.

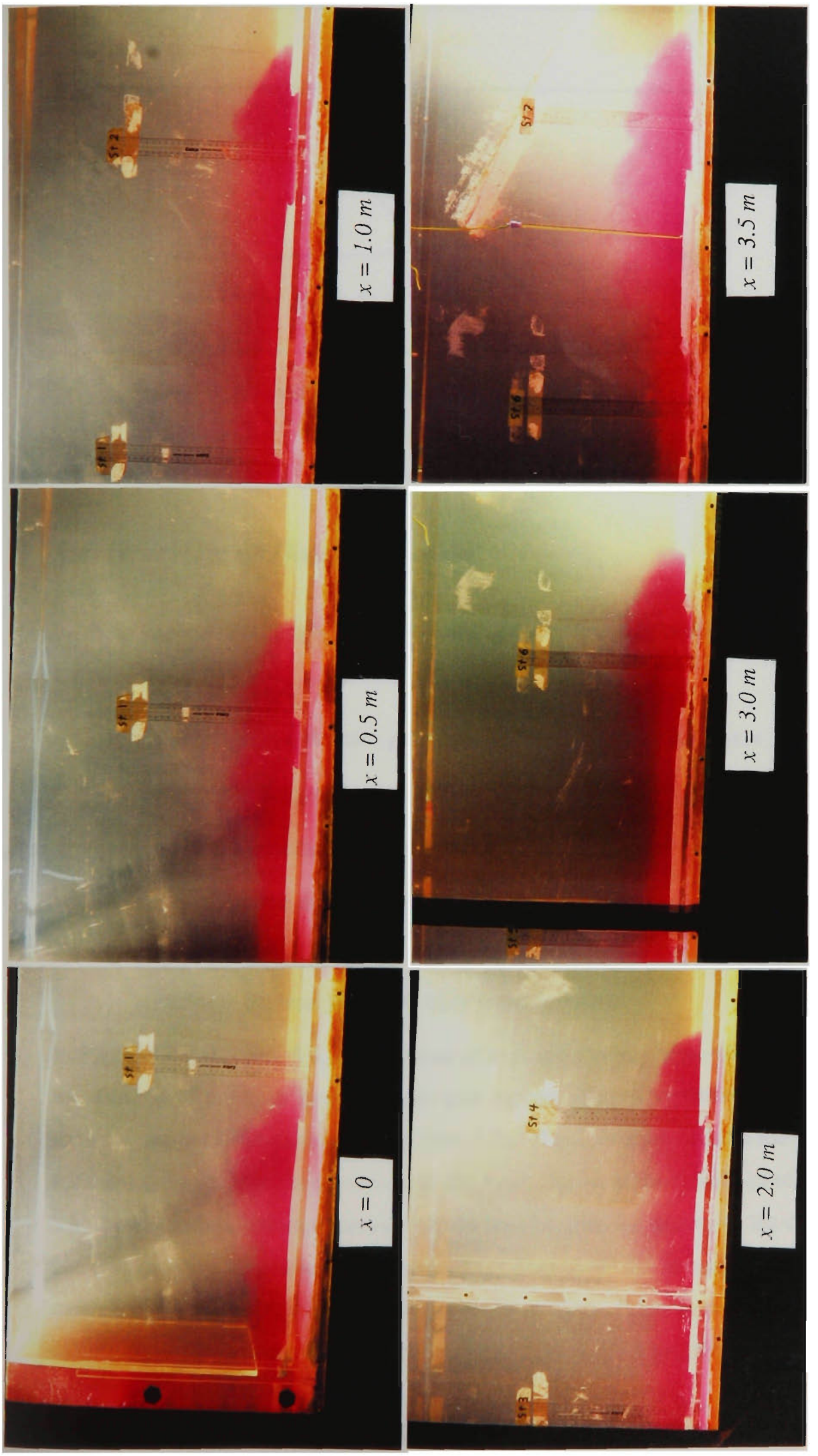

Figure 5.3 The advance of a typical saline density current. $q_0 = 6.28$ cm²/s, fractional density, Δ_0, = 0.00505, $T = 23.5°$ C, $h_0 = 4$ cm.

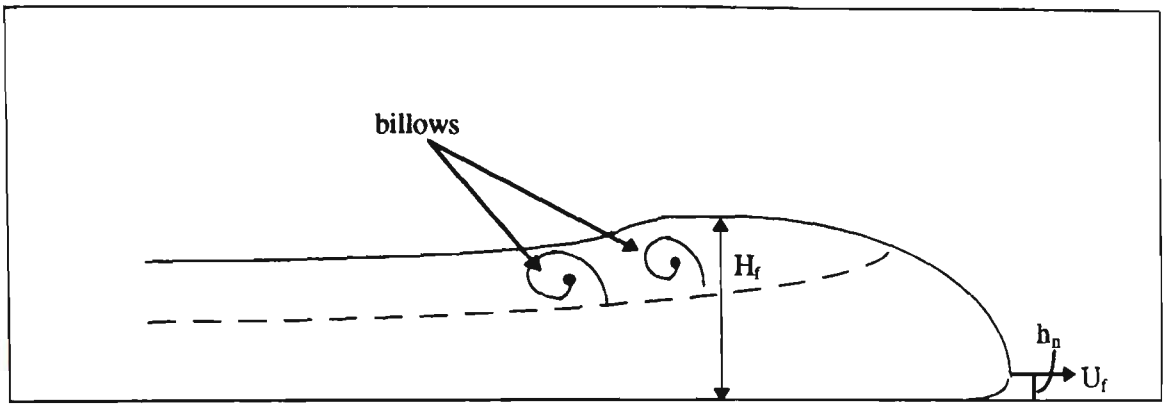

Figure 5.6 Schematic of the flow pattern at the head of a gravity current.

5.4 Overview of Data Collection

In these experiments, apart from the initial parameters, five other parameters were collected as follows:

- the distance from the inlet gate based on the name of the stations, x
- the height of the gravity current head, H_f
- time from beginning of the experiment
- the profile of the density fraction, Δ
- also in the sediment type of gravity current, the distribution curve of sediment particles in the head and in the body were measured.

In Figure 5.7 and Figure 5.8, the advances of both types of heads are shown by plotting the distance of the head from the inlet gate against time. A variation can be seen in turbidity current head experiments (Figure 5.7). This variation reflects the effects of sediment deposition on the movement of the head. In the saline density current (Figure 5.8) however, no significant variation can be seen because the density of the current did not change along the flume. The slopes of the lines show the average velocities. The mean head velocity, U_f, was found for three parts of the flume in each experiment by calculating dx/dt between 0.5m to 1.5m, 1.5m to 2.5m and 2.5 to 3.5m.

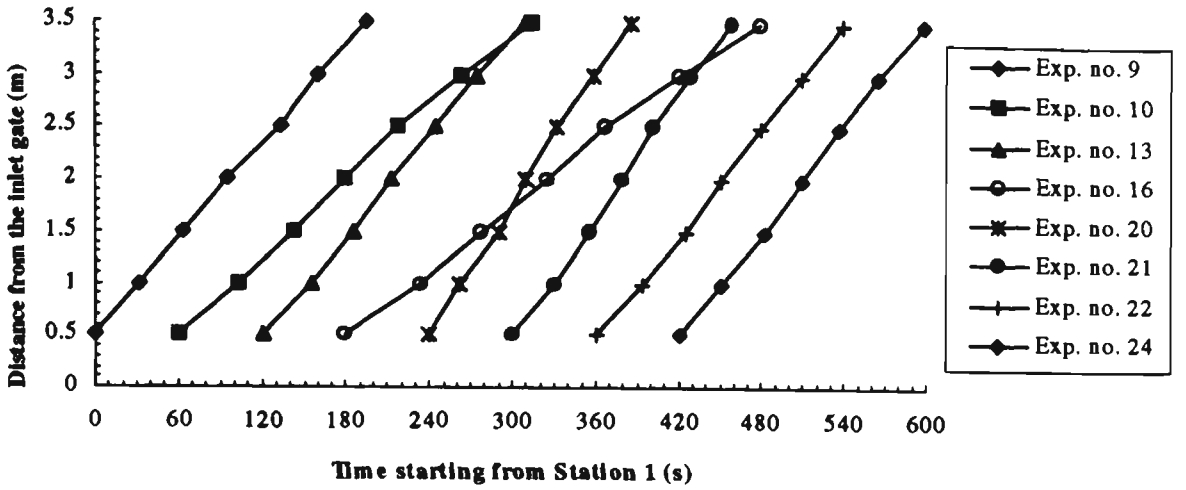

Figure 5.7 Advance of the head along the flume for selected turbidity current runs.

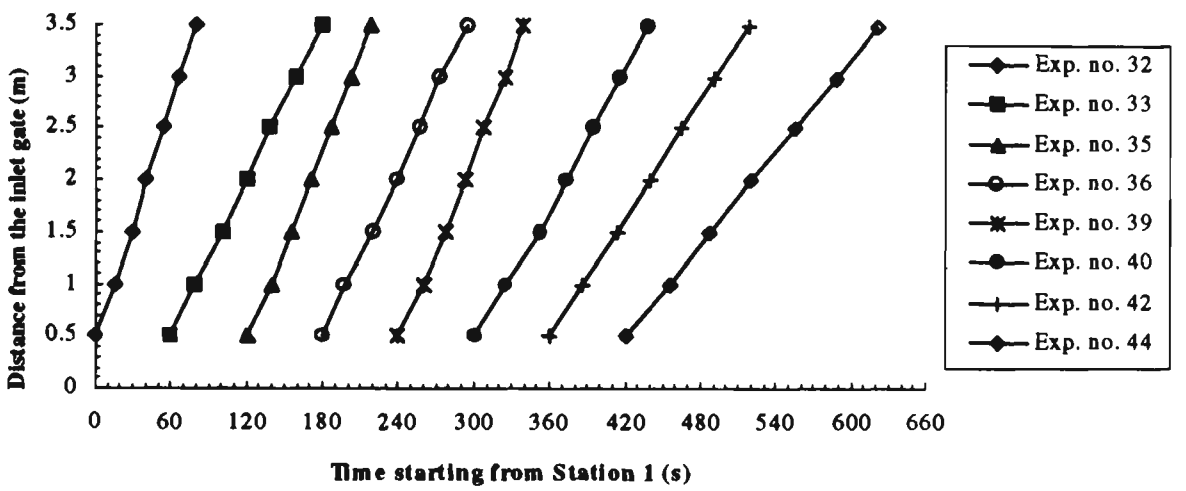

Figure 5.8 Advance of the head along the flume for selected saline current runs.

In Figure 5.9 and Figure 5.10, the height of the head H_f, is plotted against distance for selected turbidity and saline current runs respectively. As can be seen in most of the experiments, the heights of the currents are not stable in the first meter from the entrance and the 0.5 m from the end of the flume, and between that points, the heights are almost stable. In Figure 5.11 and Figure 5.12 the velocity of the head is plotted against distance for selected turbidity and saline current runs, respectively. The averages of the velocities at two consecutive points are used to calculate the velocity of the head at each measurement station (Station 2, Station 4 and Station 6). For experiments 13 and 16 (related to the turbidity current) and experiments 42 and 44 (saline density current) the best fit linear lines are shown by the broken lines. In Figure 5.13 the geometric mean size of the particles presented in the head are plotted against the distance for selected

turbidity current runs. As can be seen, in all experiments runs, the geometric mean size reduces with distance and this is one of the effects of deposition of particles along the flume by the head of turbidity current. The sudden decrease in the value of D_g in the first part of the flume shows the deposition of large particles in the entrance gate. After this point the reduction continues almost linearly along the flume and reflects the gradual deposition of sediment particles from the head.

Although the existing vortices in the head of the gravity current created mixing in the dense fluid, a distinguishable profile of height versus fractional density in the head of the gravity currents is observed. The profiles of fractional density of the head for selected turbidity and saline density currents are shown respectively in Figures 5.14 and 5.15. As can be seen the variations of fractional density in the profiles of the head for turbidity currents (Figure 5.14) are relatively high in comparison with the saline density currents (Figure 5.15). This difference is related to the effect of the particles' fall velocity existing in the turbidity current. The high reduction of fractional density in upper layers of both figures is probably related to the mixing of clear water with dense fluid (see Figure 5.23).

5.5 *Velocity of Head*

In Figures 5.11 and 5.12, the variations of the average head velocity with distance are shown. In these figures some small fluctuations in the average velocity of the head are seen. These variations may be related to the existing billows and instability at the interface between the two fluids. The lines that were fitted in the velocity data of the experiments show a slight difference between the velocity of the turbidity and the saline density currents. The velocity of the turbidity current shows a small deceleration as in Figure 5.11. Similar results were reported by Altinakar et al., 1990. Because the velocity of the head is proportional to the fractional density, the reduction of velocity found in the turbidity current experiments is related to the reduction of the fractional density due to the settling of particles from the current.

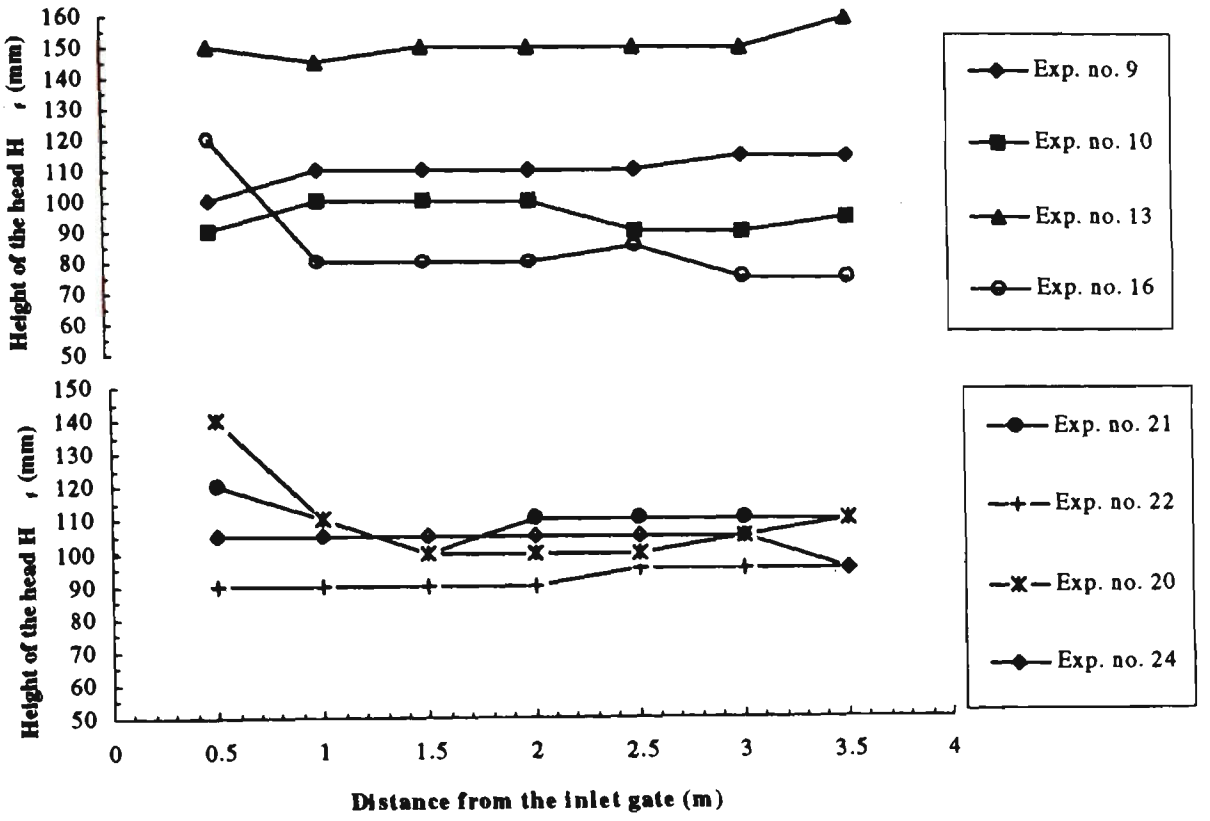

Figure 5.9 Height of the head with distance for selected turbidity current runs.

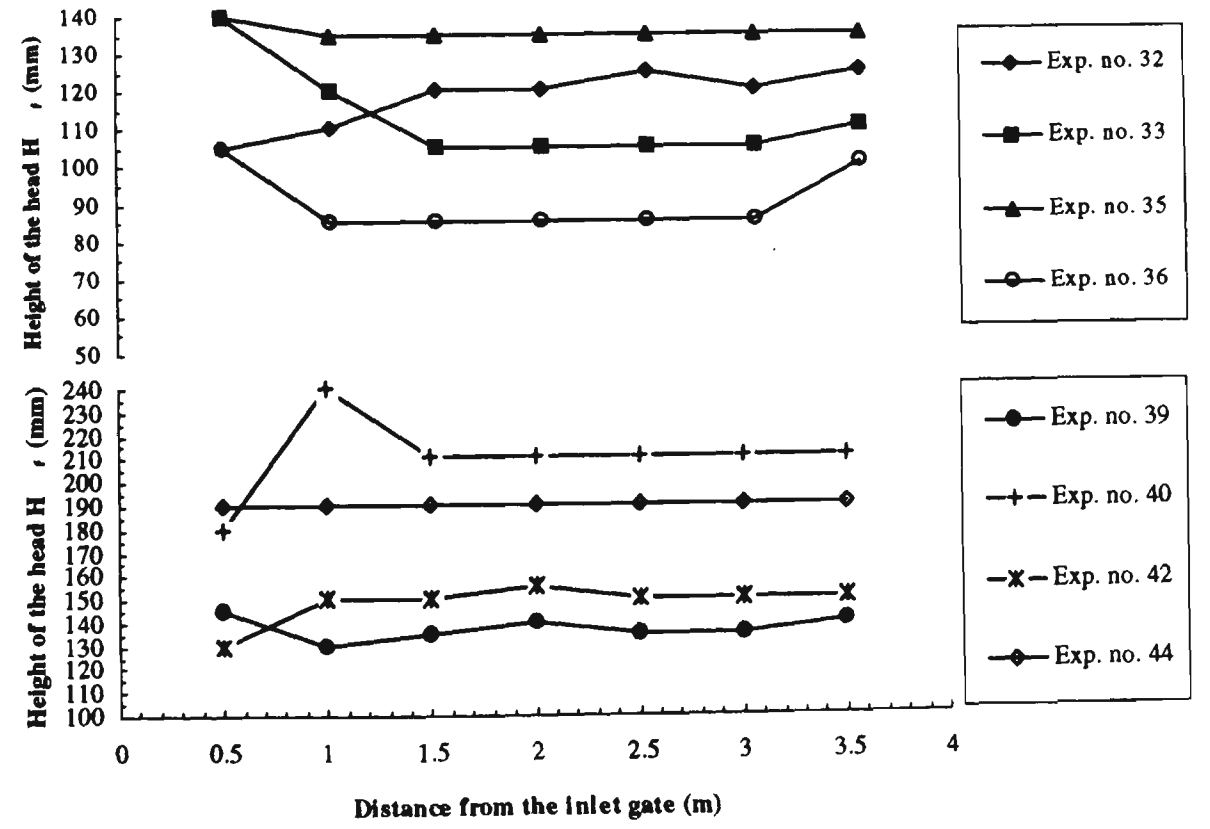

Figure 5.10 Height of the head with distance for selected saline gravity current runs.

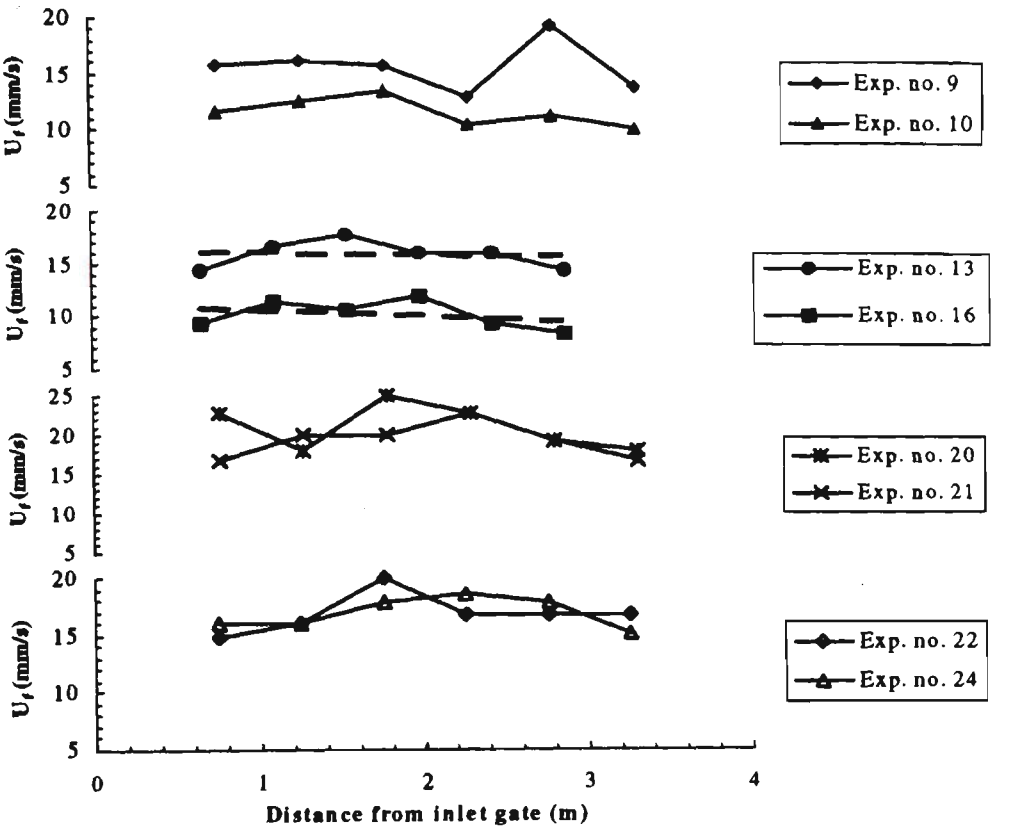

Figure 5.11 Velocity of the head against the distance for selected turbidity current runs.

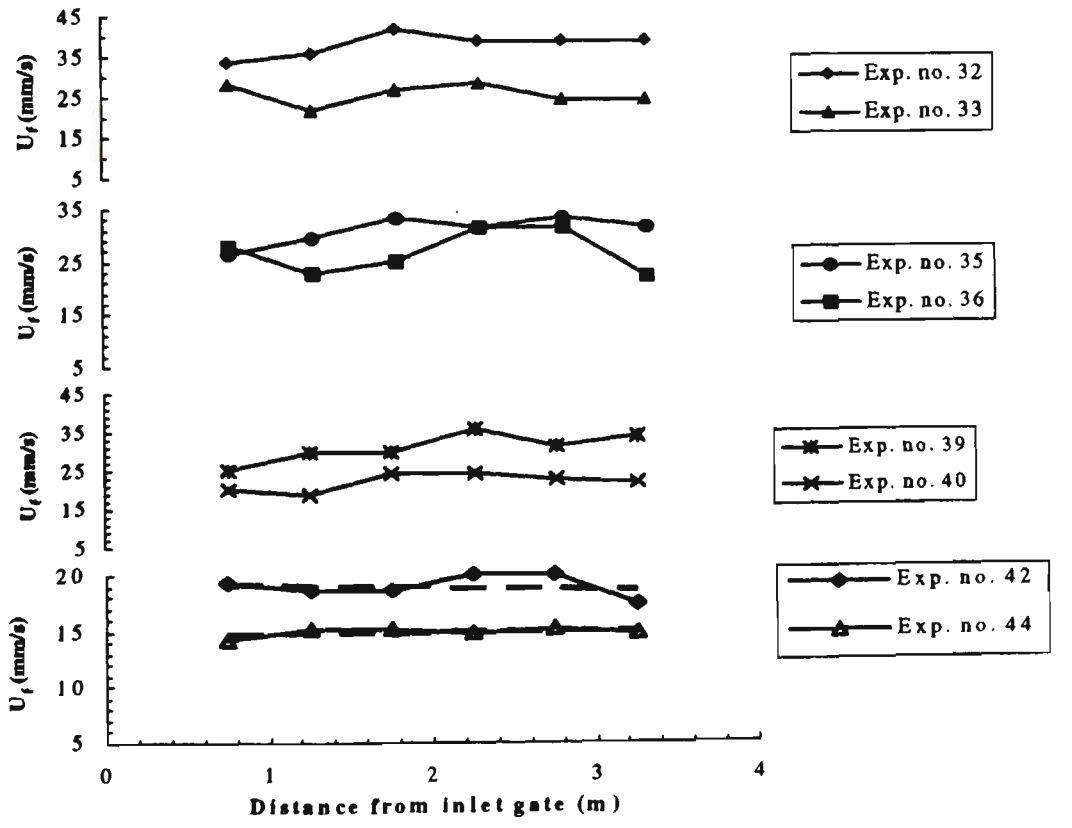

Figure 5.12 Velocity of the head against the distance for selected saline gravity current runs.

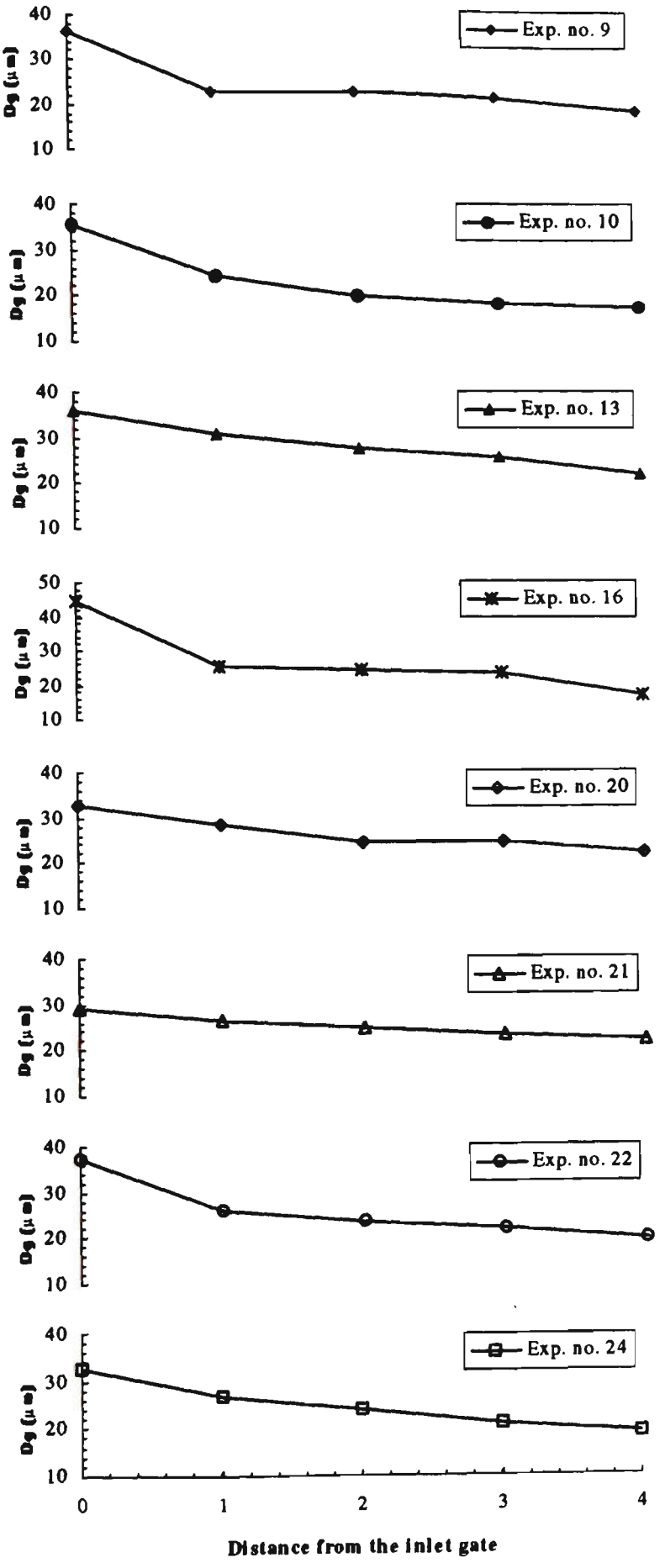

Figure 5.13 Geometric mean size of particles in the head as a function of distance for selected turbidity current runs.

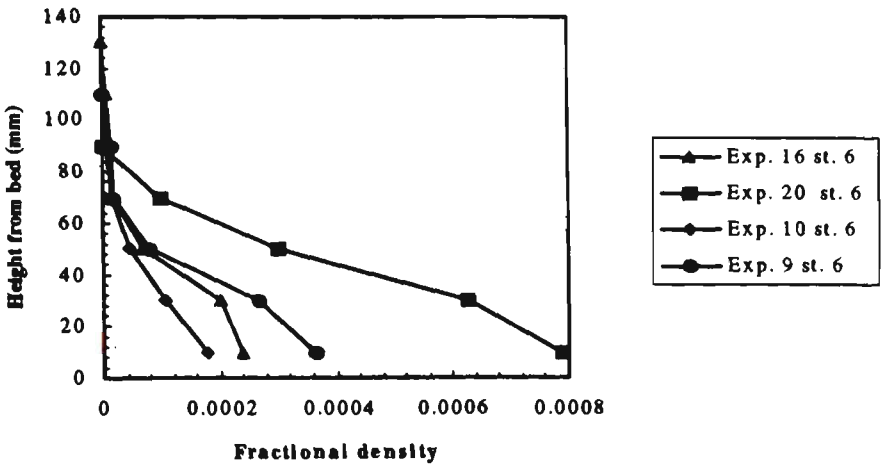

Figure 5.14 Fractional density profile in the head of selected turbidity current experiments at station 6.

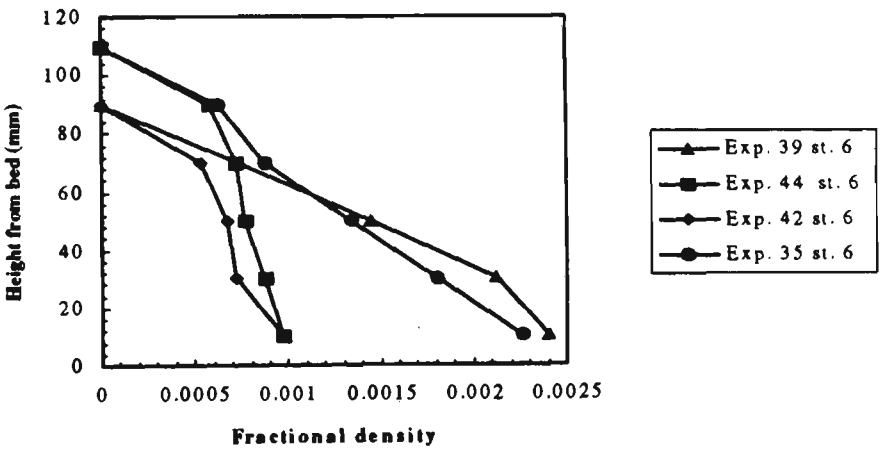

Figure 5.15 Fractional density profile in the head of selected saline density current experiments at station 6.

For analysing the velocity of the head, the data presented in Tables 5.3 and 5.4 were used. It should be noted that for each measurement point in the flume, the layer-averaged density fraction of the head (Δ) was used for analysis. This was done by using the density fraction (for saline density current) or sediment concentration (for turbidity current) profiles measured along the center-line of the head.

The velocity of the head U_f is often calculated by Equation 5.1. The data obtained from the present study, turbidity current data of Middleton (1966b), turbidity and saline density current data of Altinakar et al. (1990), saline density current data of Denton et al. (1981), and the data obtained by Wright (1979, cited in Bühler et al., 1991) were used to find the accuracy of Equation 5.1. The data were analysed with the statistical package, SPSS. The results of the data analysis significantly agreed with the combination of the

equation and also the value of power, 0.5, for the variable ($\Delta g H_f$). The coefficient of determination of this analysis was quite high (98 percent). The coefficient, C_c, was determined using the above data analysis. In Figure 5.16 the head velocity, U_f, is plotted against $\sqrt{g'H_f}$, for the data of the present study. The best linear correlation between this data point can be expressed by Equation 5.1 with $C_c = 0.65$. The solid line plotted in Figure 5.16 corresponds to this correlation line. In Figure 5.17, the data of the present experiments as well as those by Middleton (1966b, turbidity current using plastic beads), Altinakar et al. (1990, saline density current and turbidity current using quartz fluor), Denton et al. (1981), and Wright (1979, cited in Bühler et al. 1991, saline density current) are plotted. These data are presented in Appendix A. The best linear correlation for this set of data was obtained when $C_c = 0.72$. As can be seen in Figure 5.17, the data collected in the present study are located in the lower part of the figure and the lower value of C_c is due to an increased influence of the bottom drag on small slopes (Altinakar et al., 1990). From Figure 5.17, it can be seen that the solid line related to $C_c = 0.72$ covered all of the data points with a very high coefficient of determination (98%). Hence it is recommended that this value of 0.72 may be used in future. Then the equation for the velocity of the gravity current can be written as:

$$U_f = 0.72\sqrt{g'H_f} \qquad (5.4)$$

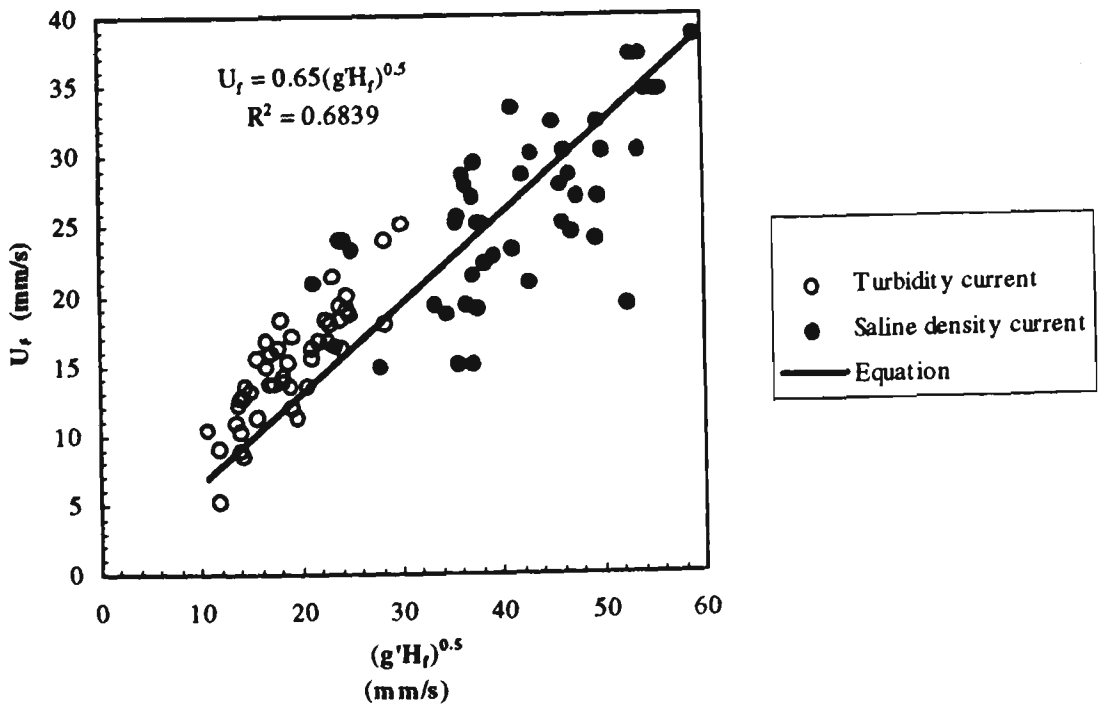

Figure 5.16 Head velocity U_f, against $\sqrt{g'H_f}$, (data of present study).

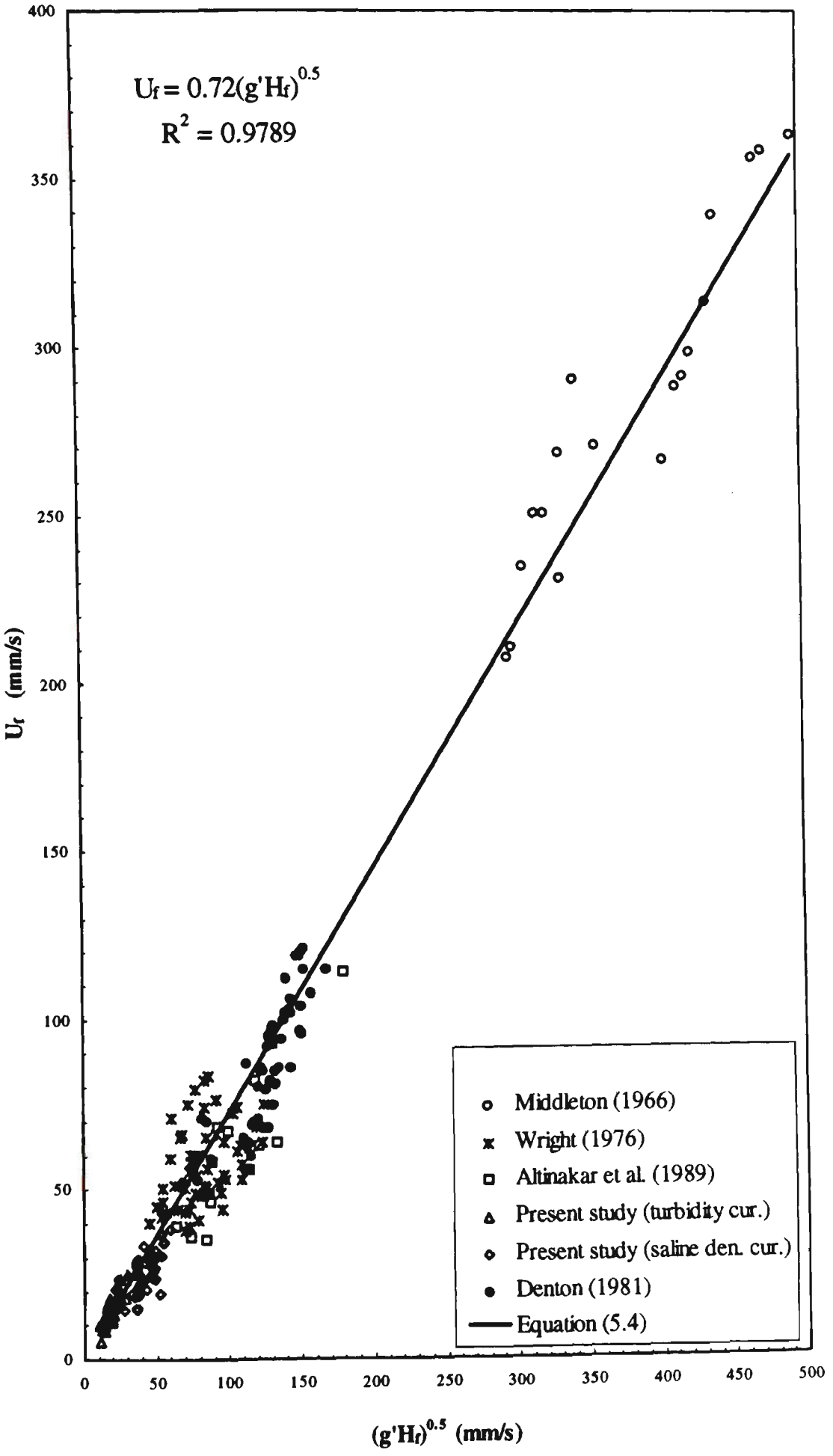

Figure 5.17 Head velocity U_f, against $\sqrt{g'H_f}$, (all data).

Based on saline density current experiments in six different slopes, Middleton (1966b) reported that C_c varied with slope. The averages of C_c which Middleton calculated for different slopes are summarised in Table 5.5.

Table 5.5 The average values of the coefficient, C_c for different slopes (calculated from Middleton, 1966a experiments)

Slope	C_c
0.0025	0.67
0.005	0.7
0.01	0.719
0.02	0.76
0.03	0.85
0.04	0.8

Using these values and the value obtained from the present study (slope = 0.00635, C_c = 0.65) and Denton et al. (1981) (slope = 0.015, C_c = 0.68) a statistical analysis of this data shows a relation between the slope and the coefficient C_c as:

$$C_c = 1 \times S^{0.08} \qquad (5.5)$$

The data and the values obtained from Equation 5.5 are shown in Figure 5.18

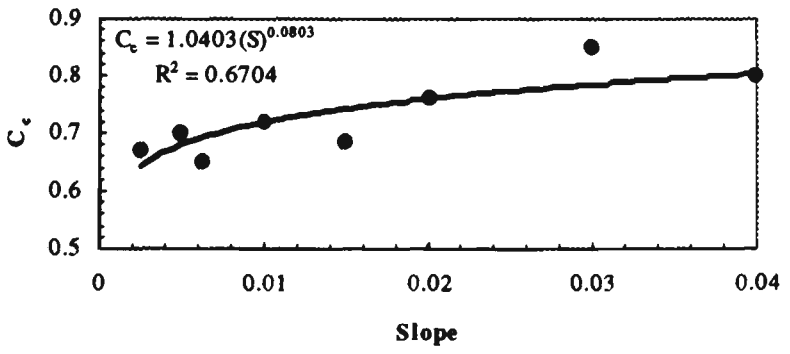

Figure 5.18 Variation of the coefficient C_c with the slope.

As a result, for slopes less than 0.04, the equation of the velocity of the head can be proposed as:

$$U_f = S^{0.08}\sqrt{g'H_f} \qquad \text{for } 0 < S \le 0.04 \qquad (5.6)$$

5.5.1 Height of Head

It has been already pointed out that for using Equation 5.1, in order to calculate U_f, H_f needs to be measured. This is one of the disadvantage of using Equation 5.1. Therefore, to overcome this problem a criterion to calculate the height of the head is needed.

As indicated before, due to existing large eddies in the upper layer of the fluid of the head, the error of reading the height of the head is large and probably of the order of ±5%. Therefore, developing an equation for estimating the height of the head is difficult. However, an attempt is made to explain the height of the head as a function of initial parameters.

$$H_f = f(q_0, g, \Delta) \tag{5.7}$$

From dimensional analysis, it can be shown that,

$$H_f = f\left(\sqrt[3]{\frac{q_0^2}{g}}, \Delta\right) \tag{5.8}$$

The measured data of the present study (Tables 5.3 and 5.4), as well as data from Altinakar et al. (1990) and Denton et al. (1981) have been used to find the best fit relationship between the non-dimensional parameters in Equation 5.8. The final equation is expressed as:

$$H_f = 2.2\left(\frac{q_0^2}{\Delta g}\right)^{1/3} \qquad \text{for } 0 < S \leq 0.04 \tag{5.9}$$

The measured data and the proposed equation (5.9) are shown in Figure 5.19

5.5.2 Comparison of the Present Equations with Denton's Approach

Equations 5.6 and 5.9 respectively can be used to calculate the velocity and height in the turbidity current when no information is available. To compare usage of Equations 5.6 and 5.9 (for predicting velocity of the head) with the Denton equation, both methods are used to predict head velocity. The measured data of Denton et al. (1981) Altinakar et al.

(1990) and the present study are used. The results are almost same and are shown in Figure 5.20 and 5.21.

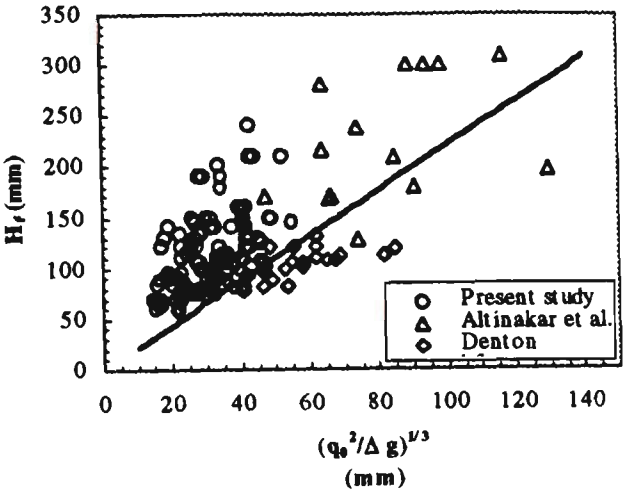

Figure 5.19 Height of the head of gravity current, H_f, against $\left(\frac{q_0^2}{\Delta g}\right)^{1/3}$.

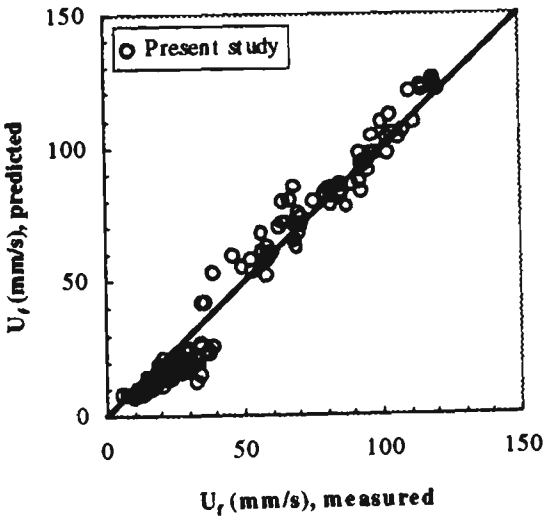

Figure 5.20 Comparison of the measured and predicted velocity of the head with Equations 5.6 and 5.9.

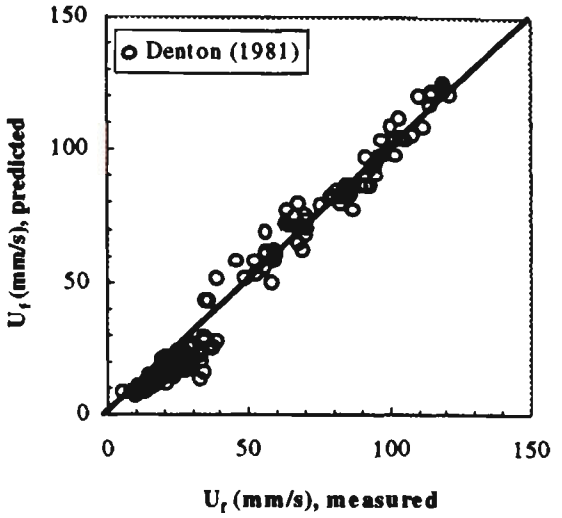

Figure 5.21 Comparison of the measured and predicted velocity of the head with Denton equation (1981) (Equation 5.2).

5.5.3 Velocity of the Head by Simpson and Britter's Approach

Simpson and Britter (1979) used a Froude number based approach to express to velocity of head, U_f and h_4 (bottom region depth of head, see Figure 5.1). They found that this Froude number varied with the fraction of the current depth over total depth. The data of the present study is shown in Figure 5.22. The unbroken line shows the regression line through the measurement points. It appears that the densimetric Froude number is inversely dependant on h_4/h_1.

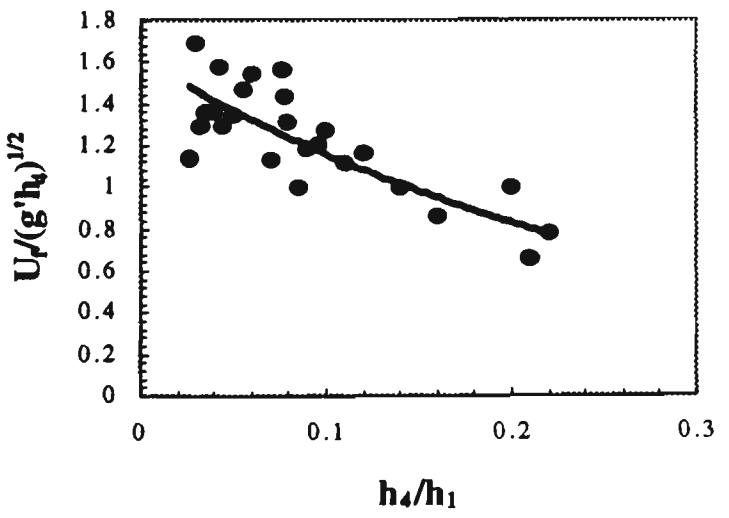

Figure 5.22 Variation of Froude number with the fraction of the current depth over total depth.

5.6 Sediment Transport in the Head of the Turbidity Current

It is very difficult to model the processes of sediment transport by the head of gravity currents. This difficulty can be related to the existence of secondary flows inside the head. In Figure 5.23, a pattern of the flow in a head is shown schematically.

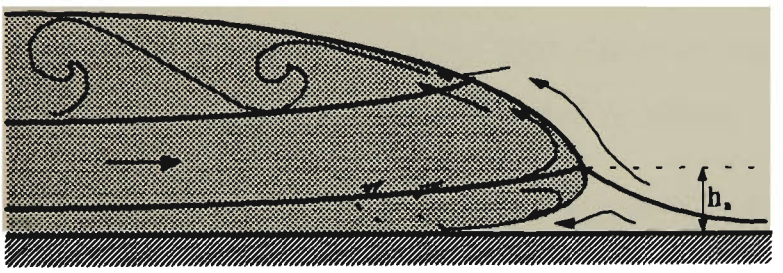

Figure 5.23 The nature of the flow related to the front of a gravity current. The mean two dimensional flow is shown (after Simpson 1987).

In the present study, the information were obtained with reference to sediment transport: the characteristic of the head, the average and profile of the sediment concentration in three stations along the flume, the size distribution curve of the particles from the head and the body of the current and the initial condition of the runs. Although this information is useful in finding some unknown characteristics of the head of the currents, the limitation of the experiments (using one slope and one solid with a mean size of 36.25 μm) and the unavailability of any other data prevented the finding of a relationship between the hydraulic phenomena and sediment transport of the head.

The samples collected from the head and the body of the current at different locations were analysed with the laser particle sizer. In Figure 5.24, typical particle size distribution curves in the head and in the body of the turbidity current, of two section of the flume, are shown. These curves are used to calculate the geometric mean size of the particles. A summary of the geometric mean size of the sediment particles, calculated from particle size distribution curves, is presented in Table 5.6. It can be seen that in all

experiments, the geometric mean size of the particles, D_g, gradually decreases with distance for both the head and the body of the current. This indicates that settling of particles take place both within the head and body of the current. Also, D_g of the head is always greater than D_g of the body for all the locations after the inlet gate, and for all the experiments. Probably this is due to the difference of flow patterns in the head and the body of the current. The variation of D_g in the head and the body of the turbidity current are plotted in Figure 5.25 for selected experiments. In Figure 5.26 the concentration of the particles in the head of turbidity current are plotted against the distance for four of the experiments. A high reduction of the concentration can be seen in the first part of the flume and this reduction of concentration continues slightly for the rest of the flume. The settling of a considerable amount of the large grain size at the entrance gate is the reason for this reduction in concentration in the first part of the flume.

The results obtained from Table 5.6, Figure 5.25 and Figure 5.26 are summarised as follows:

1. The hypothesis that "sediment is not deposited from the head itself, but that deposition begins to take place some distance behind the head (Middleton 1966b, 1967)" may not be applicable for all conditions. The results of data analysis seen in Figures 5.25 and 5.26, show that the head of the turbidity current had some deposition on the bed.

2. Although the average velocity of the head is always lower than that of the body (because the height of the head is greater than the body of the current), the sediment transport potential of the head is much higher than that of the body of the turbidity current. This can be found from Table 5.6 and Figure 5.25 in which the head always transported larger particles in comparison with the body. Existence of vortices in the head increases the potential of sediment transport of the head (see the flow pattern of the head in Figure 5.26). Existence of high turbulence in the head may be another reason (value of turbulence can be measured with the LDV, but due to high sediment concentration and fast movement of the head it was not measured). Therefore, in nature, sometime the head of the current has high potential erosion and has the capability to decrease the bed strength due to the existence of the cohesive sediment in the composition of the bed. Alternatively, it may disperse the consolidated layer of

the bed or destroy the armour layer. Finally, the separated particles are available to be swept up with the head itself or the body of the current. A sketch of this mechanism is shown in Figure 5.27.

3. The sediment transport equations of open channels cannot be used for estimating sediment transport potential of the head of a gravity current. These equations may be used for estimating potential sediment transport of the body of the gravity current.

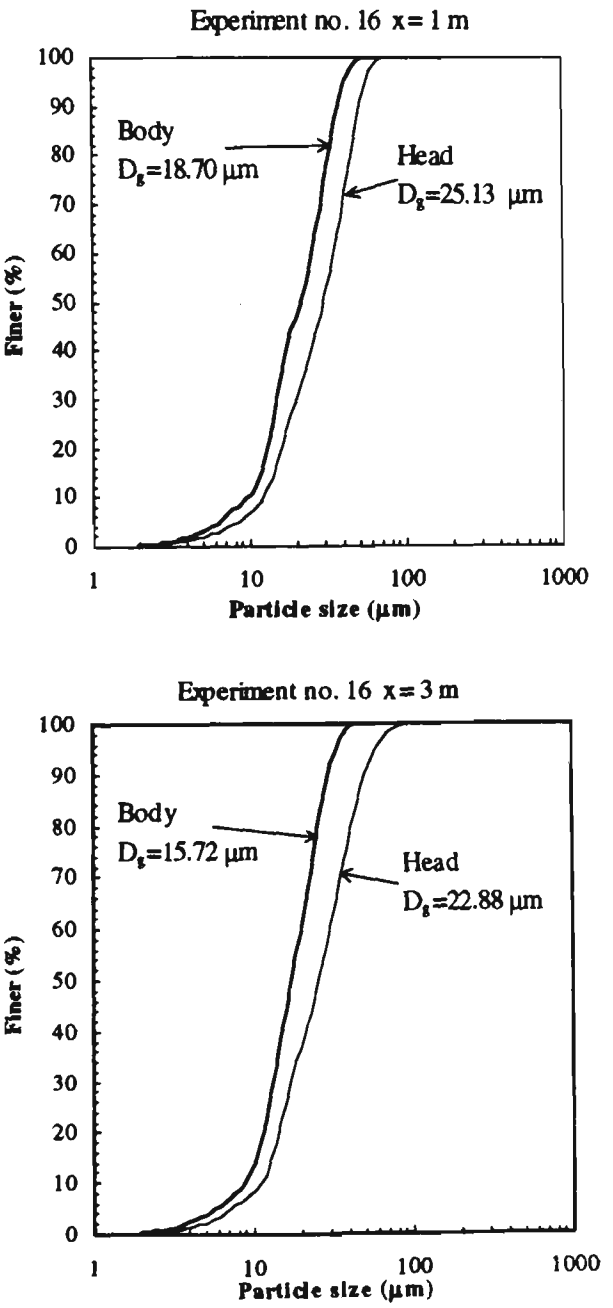

Figure 5.24 Particle size distribution curves in the head and the body of the turbidity current at two sections of the flume. (data from experiment no. 16)

Table 5.6 Geometric mean size of the particles transported in the head and the body of turbidity current runs and the location of the samples.

Experiment No.	Position	Dg (μm)	
		Dg Body	Dg Head
8	Inflow	32.00	32.00
	St 2	25.07	27.91
	St 4	22.99	25.11
	St 6	21.25	25.88
9	Inflow	36.29	36.29
	St 2	20.76	22.93
	St 4	19.82	22.87
	St 6	18.98	21.46
10	Inflow	35.45	35.45
	St 2	19.43	24.34
	St 4	16.50	19.77
	St 6	16.44	18.03
11	Inflow	34.16	34.16
	St 2	22.48	28.72
	St 4	19.66	23.67
	St 6	18.57	21.04
12	Inflow	50.05	50.05
	St 2	24.46	32.92
	St 4	21.39	25.84
	St 6	20.52	26.24
13	Inflow	35.98	35.98
	St 2	24.59	30.63
	St 4	22.31	27.35
	St 6	20.47	25.23
14	Inflow	37.08	37.08
	St 2	22.12	28.60
	St 4	20.48	24.09
	St 6	18.32	21.53
15	Inflow	39.02	39.02
	St 2	20.42	26.05
	St 4	18.19	21.58
	St 6	15.45	19.73
16	Inflow	44.67	44.67
	St 2	18.70	25.13
	St 4	16.93	23.93
	St 6	15.72	22.88
17	Inflow	30.99	30.99
	St 2	23.51	32.07
	St 4	22.52	26.68
	St 6	20.81	24.49
18	Inflow	25.34	25.34
	St 2	21.36	26.66
	St 4	19.89	23.84
	St 6	18.70	22.45
19	Inflow	32.07	32.07
	St 2	19.74	24.57
	St 4	17.74	20.22
	St 6	15.83	17.77
20	Inflow	32.71	32.71
	St 2	23.60	28.06
	St 4	21.15	24.05
	St 6	19.69	24.05
21	Inflow	29.02	29.02
	St 2	23.35	26.35
	St 4	20.86	24.77
	St 6	19.29	23.11
22	Inflow	37.10	37.10
	St 2	20.89	25.70
	St 4	19.38	23.55
	St 6	17.81	21.66
23	Inflow	35.10	35.10
	St 2	20.37	24.69
	St 4	17.62	21.14
	St 6	16.16	21.43
24	Inflow	32.79	32.79
	St 2	19.68	26.74
	St 4	21.44	23.96
	St 6	18.05	21.10

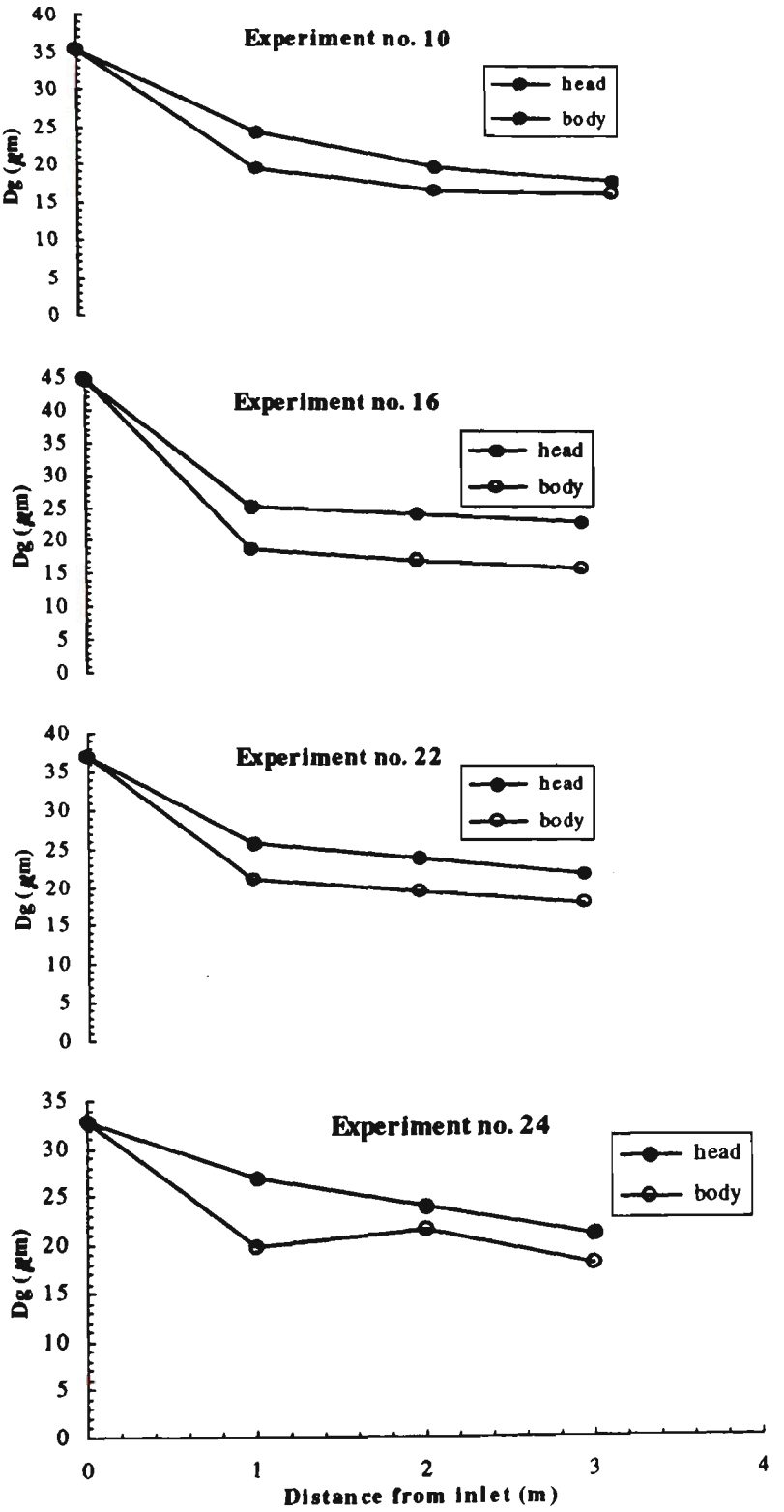

Figure 5.25 The geometric mean size of the particles against the distance for the head and the body of the turbidity current.

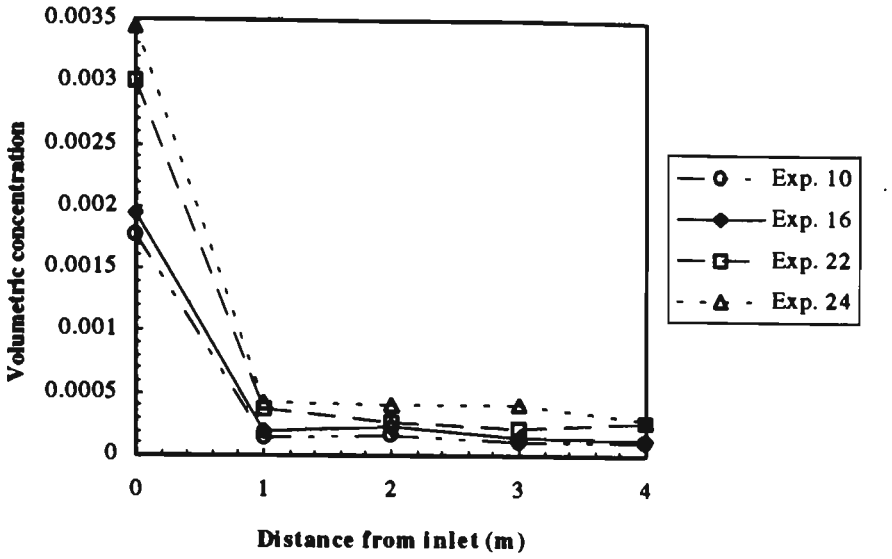

Figure 5.26 Average concentration in the head of the turbidity current against the distance.

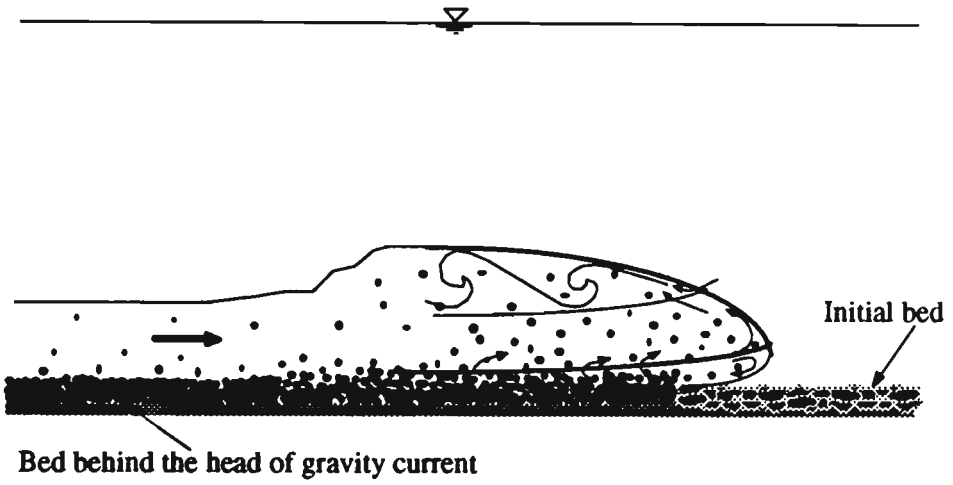

Figure 5.27 Effect of the head of the gravity current on a natural bed.

5.7 Summary

In this chapter the data collected from the head of both turbidity and saline density currents were analysed and discussed. Two aspects of the head including the velocity and the sediment transport have been considered. Critical analysis of the head velocities along the flume showed a small deceleration in the turbidity current experiments. This reduction of velocity was related to the reduction of the fractional density due to the settling of particles from the current. Although the existing vortices in the head of the

gravity current makes the dense fluid almost uniform, it has been shown that a profile for fractional density can be distinguished in the head.

The data collected from the present study and the data obtained from laboratory experiments by Middleton (1966a), Wright (1976, as reported by Bühler et al. 1991), Denton et al. (1981), and Altinakar et al. (1990) were used to find the coefficient of the velocity equation. The SPSS statistical package was used to find the best fitting line through the data. A value equal to 0.72 was obtained for the coefficient, C_c. Therefore Equation 5.1 was proposed as:

$$U_f = 0.72\sqrt{g'H_f} \qquad (5.4)$$

The coefficient, C_c, calculated by Middleton (1966a) for different slopes and the C_c calculated from the experiments of the present study were analysed and a relationship was proposed for C_c as a function of slope as:

$$U_f = S^{0.08}\sqrt{g'H_f} \qquad \text{for } 0 < S \leq 0.04 \qquad (5.6)$$

The measured data of the present study, Altinakar et al. (1990) and Denton et al. (1981) are used to find a relationship between the parameters of the height of the head of the gravity current. Finally, the equation for predicting the height of the head of the gravity current is proposed as:

$$H_f = 2.2\left(q_0^2/\Delta g\right)^{1/3} \qquad \text{for } 0 < S \leq 0.04 \qquad (5.9)$$

The data from the turbidity current experiments, including concentration and mean particle size, shows that some sediment deposition occurs from the head of the current. Hence the hypothesis that "sediment is not deposited from the head itself, but that deposition begins to take place some distance behind the head" (Middleton, 1966a), may be correct in some conditions, but can not be applicable for all conditions. Although the average velocity of the head is always lower than that of the body, it was found that the sediment transport capacity of the head is much higher than that of the body of the turbidity current. Therefore, in nature the head of the current plays a very important role in destroying consolidated layers and prepares separated particles to be swept up with the head itself or by the body of the current. Finally, it was emphasised that the sediment

transport equations of open channels cannot be used for estimating the sediment transport potential of the head of a gravity current.

Chapter Six

ANALYSIS OF EXPERIMENTAL RESULTS: THE BODY OF THE GRAVITY CURRENT

6.1 Introduction

There are certain parameters in the equations of the gravity current (the body) that need to be determined only by experimental test. The velocity and the fractional density profiles, water entrainment and sediment entrainment are the parameters that could not be determined theoretically. The focus of this chapter is to analyse the data collected from the body of saline density and turbidity currents. The data obtained by other investigators are also utilised to complete this study.

6.2 Experimental Conditions

A total of 19 experiments were conducted in this part of the study, 9 of which (experiments 47 to 55) were conservative saline density current experiments, and 10 of which (experiments 56 to 66) were concerned with non-conservative turbidity currents. The raw data for these set of experiment are given in Appendix I. Experiment 57 was cancelled because the temperature difference between the ambient and dense fluids was higher than 1° C. For all the experiments, the inlet current thickness was set at 40 mm with the help of a sluice gate. The range of parameters in the experiments are summarised in Tables 6.1 and 6.2. The range selected for each parameter was limited by the size of the experimental flume.

Table 6.1 Range of parameters used in experiments of the saline density current.

Conservative saline density current		
Parameter	Minimum	Maximum
Q_0 (m^3/s)	0.000110	0.000265
U_0 (mm/s)	6.40	15.41
Δ_0	0.00349	0.01119
B_0 (m^3/s^3)	13.54E-6	67.65E-6
R_{i0}	7.7	55.1
T (°C)	22.0	23.0

Table 6.2 Range of parameters used in experiments of the turbidity current.

Non-conservative turbidity current		
Parameter	Minimum	Maximum
Q_0 (m^3/s)	0.000140	0.000265
U_0 (mm/s)	8.14	15.41
C_0	0.000925	0.00293
Δ_0	0.00123	0.0039
B_0 (m^3/s^3)	5.69E-6	22.18E-6
R_{i0}	2.58	17.5
T (°C)	22.0	24.0

In all the experiments the inlet Reynolds numbers $R_{e0} = U_0 h_0 / \nu$ were greater than 255. Typical shapes of saline and turbidity currents are shown in Figures 6.1 and 6.2 respectively. The inlet parameters of all the experiments are presented in Table 6.3. In this table Δ_0 is the fractional density at the inlet of the flume and R_{i0} is the inlet bulk Richardson number.

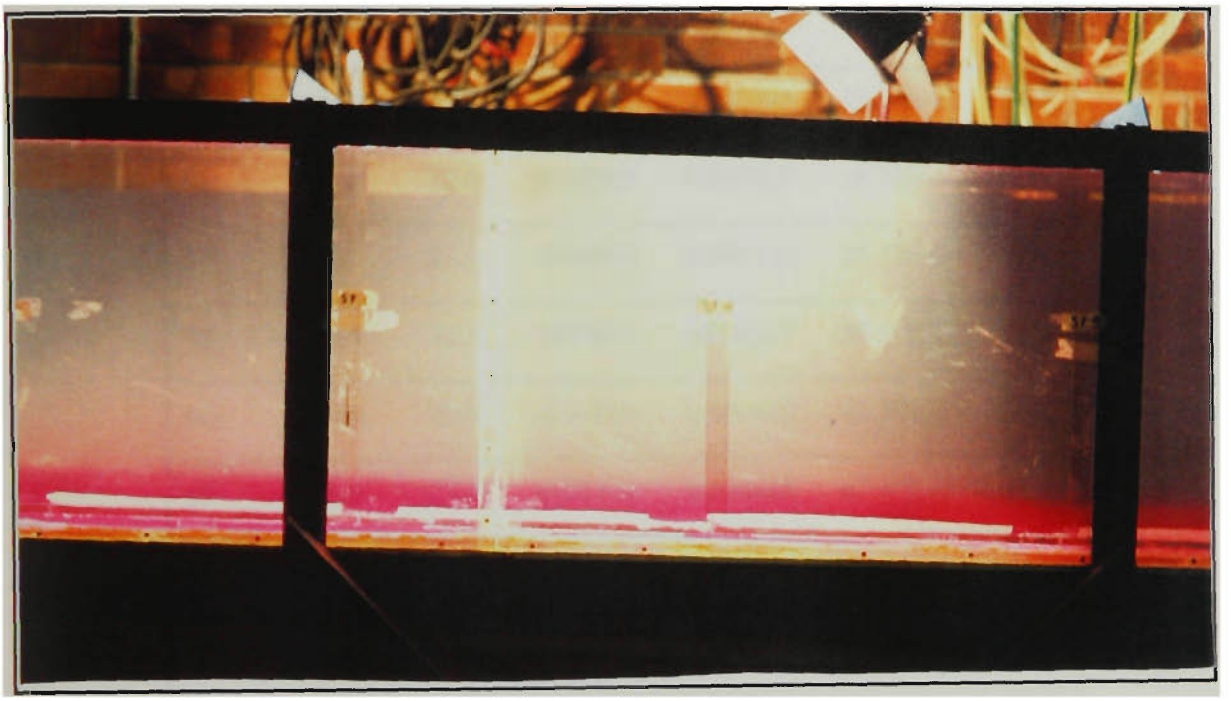

Figure 6.1 Typical shape of the subcritical saline density current.

Figure 6.2 Typical shape of the subcritical turbidity current.

Table 6.3 Experimental parameters related to all turbidity and saline gravity currents.

Exp. No.	Type	T (° C)	Δ_0	q_0 (m^2/s)	B_0 (m^3/s^3)	R_{i0}
47	Salt	23.0	0.00774	0.000337	25.60E-6	42.7
48	Salt	23.0	0.00774	0.000500	37.96E-6	19.4
49	Salt	23.0	0.00574	0.000256	14.40E-6	55.1
50	Salt	22.0	0.00349	0.000395	13.54E-6	14.0
51	Salt	22.0	0.00349	0.000535	18.31E-6	7.7
52	Salt	22.5	0.00894	0.000337	29.57E-6	49.4
53	Salt	22.5	0.00894	0.000581	50.99E-6	16.6
54	Salt	22.5	0.01119	0.000442	48.50E-6	36.0
55	Salt	22.5	0.01119	0.000616	67.65E-6	18.5
56	Solid	22.0	0.00123	0.000535	6.45E-6	2.7
58	Solid	22.5	0.00164	0.000353	5.69E-6	8.3
59	Solid	22.5	0.00156	0.000616	9.42E-6	2.6
60	Solid	22.0	0.00214	0.000605	12.67E-6	3.7
61	Solid	23.0	0.00185	0.000326	5.92E-6	11.0
62	Solid	23.5	0.00223	0.000488	10.69E-6	5.9
63	Solid	23.2	0.00264	0.000337	9.75E-6	16.3
64	Solid	24.0	0.00264	0.000581	15.04E-6	4.9
65	Solid	23.0	0.00386	0.000372	14.08E-6	17.5
66	Solid	23.5	0.00389	0.000581	22.18E-6	7.2

In the experiments, relating to the body of the gravity currents apart from the initial parameters (initial density fraction, initial discharge of dense fluid, initial value of

Richardson number, and temperature), four other parameters were collected. They are as follows:

- the velocity profile of the current at two measurement points (stations 2 and 6)
- the observed height of the gravity current
- the profile of the density fraction, Δ, at two stations (stations 2 and 6)
- the size distribution curve of grain particles transported by the turbidity current.

6.3 Profiles of Velocity and Fractional Density

During each run, two vertical velocity profiles and two vertical excess fractional densities were measured along the center-line of the flume. Measurement of local mean velocity for currents with very low local velocities (from very small negative velocity to less than 35 $^{mm}/_{s}$) is not possible with existing micropropellers. Therefore, an accurate and non-intensive measuring method such as the LDV for measuring the local mean velocity is inevitable. In Figure 6.3, local mean velocities at two measuring points are plotted as a function of height from the bed for three typical runs. It can be seen that the minimum velocity occurs along the interface of the two layers of fluids (dense water and ambient water). Most of the time small negative values were shown in the interface layer and again a small positive local velocity was shown above the interface. This velocity pattern in upper layer shows the circulation in ambient water due to movement of gravity current. Comparison of the velocity profiles of the two measurement locations shows a growing rate in the height of the turbidity current along the flume. This is due to water entrainment from ambient water and, as a result a growing rate of the discharge of the dense fluid. Based on the data from experiment 47, the velocity patterns and the heights of two fluids are shown in Figure 6.4. In the velocity profile, the location of the maximum velocity divides the flowing layer into two subregions. The region from the bed to the maximum velocity will be referred to as the inner or wall region (H_1) and the region from the maximum velocity point to the edge of the flow as the outer or free mixing region (H_2).

In Figure 6.5, the measured excess fractional density for three of the experiments are shown. The excess fractional density is seen to decrease gradually in a vertical direction. The differences between the excess fractional density at station 2 (x = 1 m) and at station 6 (x = 3 m) reflect the growing height of the current between these two stations.

In Figure 6.6, the dimensionless velocity profile for all of the saline density current experiments are plotted. Figure 6.7 and Figure 6.8 show the excess fractional density profiles for both the saline density and turbidity current. The measured values collected from the first measurement point (Station 2) are used in these three figures. The parameters used are defined as follows:

z = vertical distance from the bed

h = current thickness

u = average local velocity

U = current averaged velocity

δ = average local fractional density

Δ = current averaged fractional density

From Figures 6.6, 6.7 and 6.8 the similarity of the local velocity and excess density profiles can be evaluated. It can be seen for Figure 6.6 that the velocity profile collapse together when the ratio of local velocity to mean velocity is plotted against local height to mean height of turbidity current. This collapse is very good in outer layer of the flow ($z/h > 0.3$). For the inner layer, large deviation is seen and for collapse to occur variables other than mean velocity and height may have to used. The collapse shown in excess density profile in Figure 6.7 and 6.8 are not as good as the velocity profile particularly in the middle region. . This variation is found to be due to the equipment used to collect the turbidity of the current. The turbidity meter used to collect the fractional density gives the average turbidity in 20 mm vertical longitudinal sections. Hence in the middle region, the turbidity readings are affected by the probe being submerged in both the clear water and turbidity current. Therefore, in the thin layer of the turbidity current it showed high variation when a part of the deflector cone is located in the interface between two fluids.

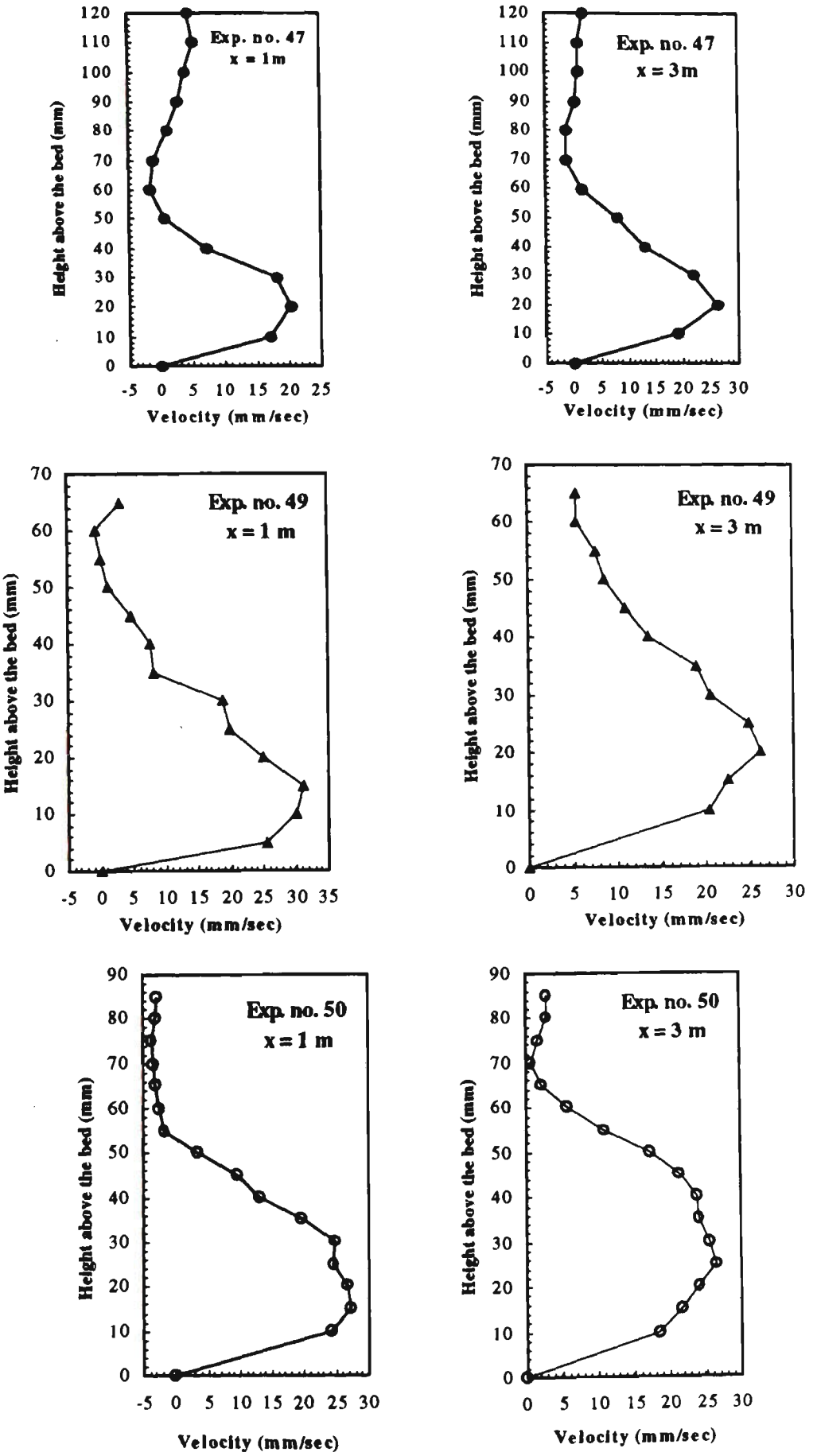

Figure 6.3 Local velocity profiles at locations x = 1 m and 3 m. Data related to experiments 47, 49, and 50.

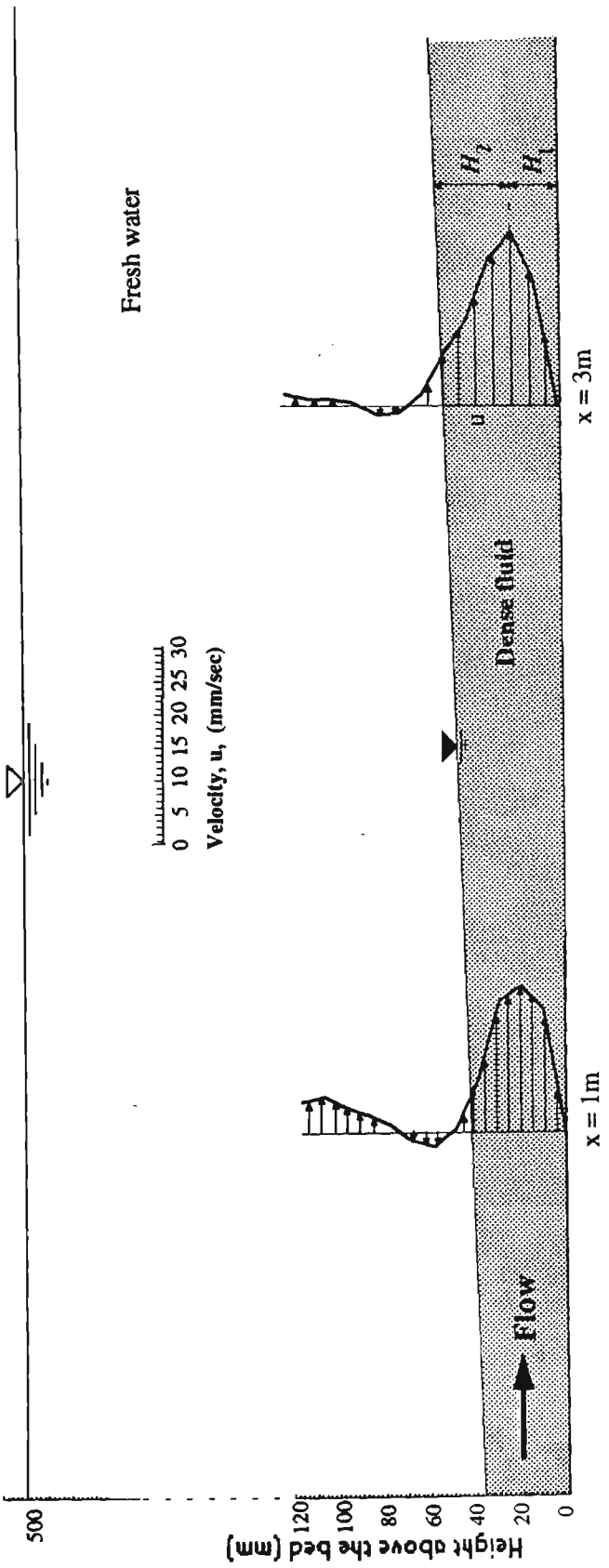

Figure 6.4 Height of density current flow in ambient fresh water and local velocity pattern of two layers. (All data is related to experiment 47).

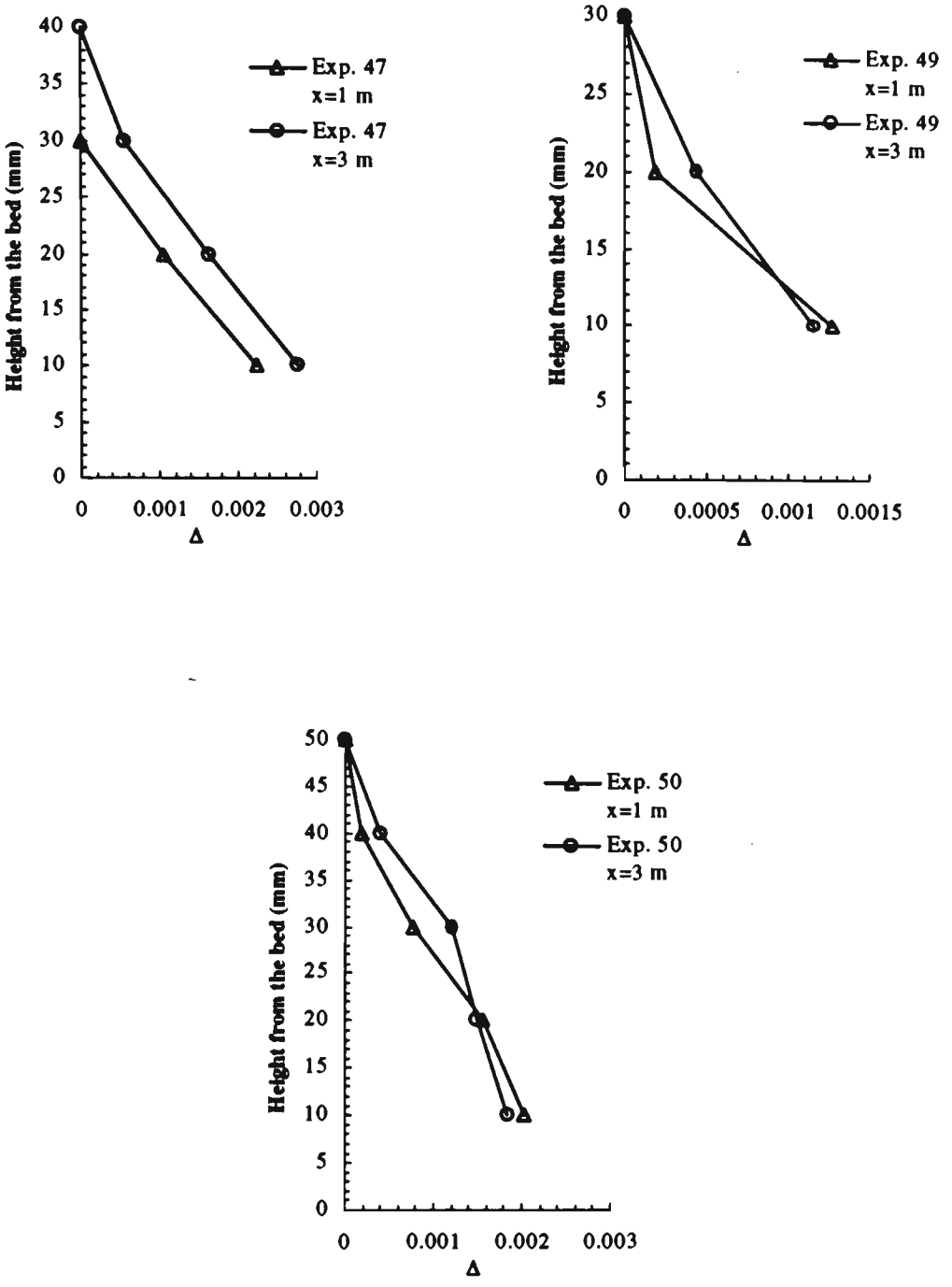

Figure 6.5 Local excess fractional density Profiles at locations x = 1 m and x = 3 m. (Data related to experiments 47, 49, and 50.)

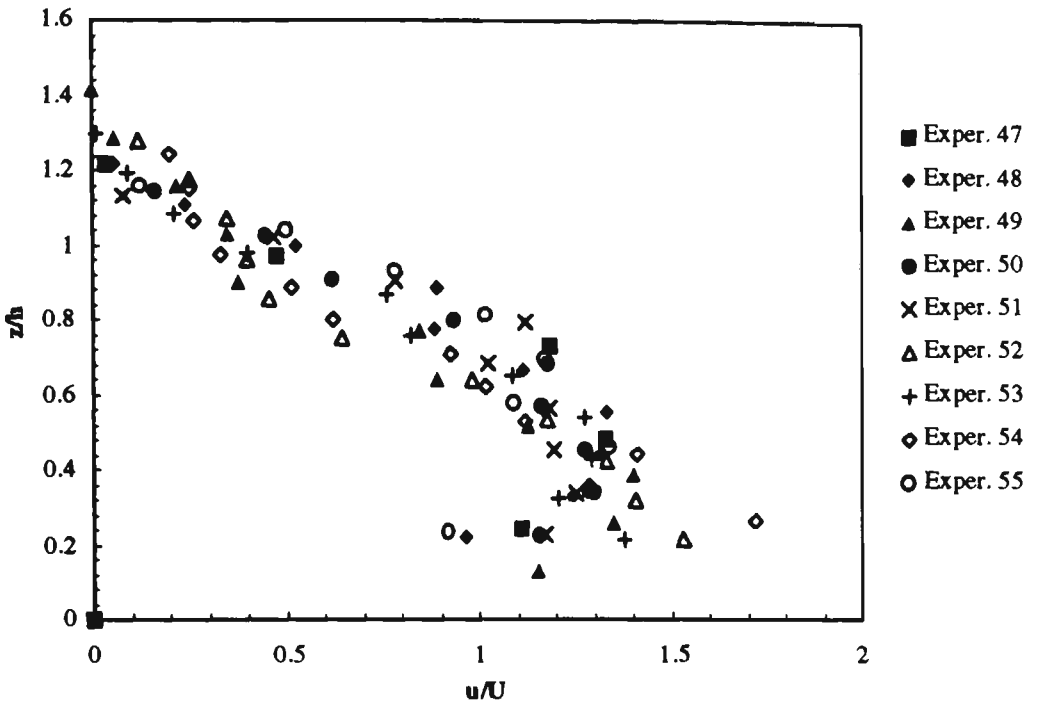

Figure 6.6 Dimensionless velocity profile

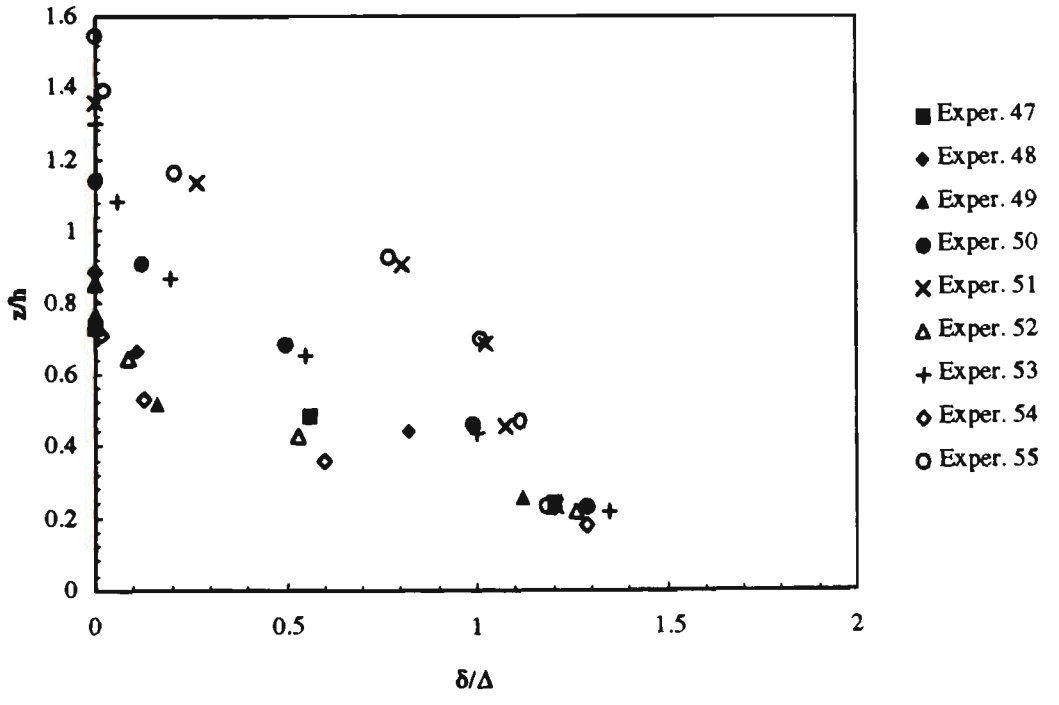

Figure 6.7 Dimensionless excess fractional density for saline density current.

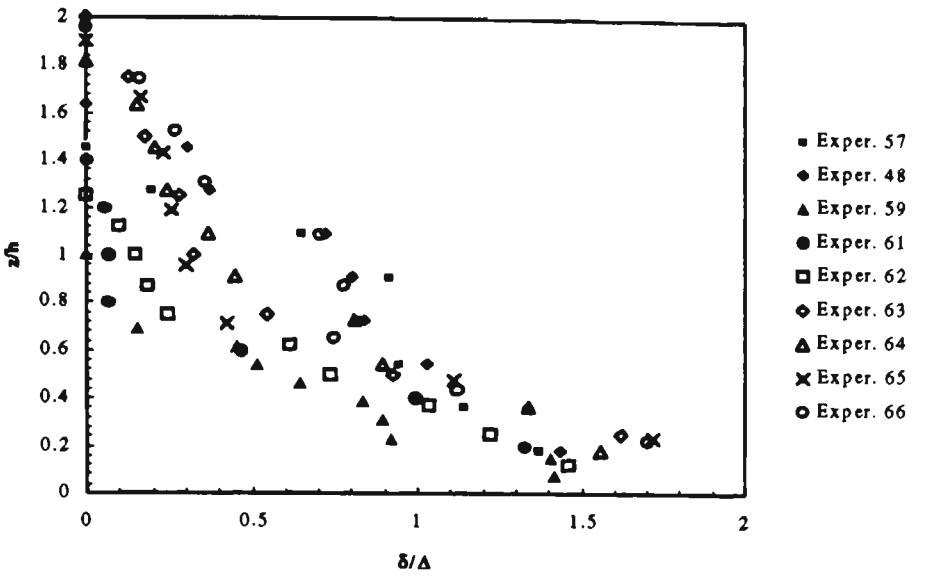

Figure 6.8 Dimensionless excess fractional density for turbidity current.

6.4 Grain Size in Turbidity Current Experiments

During each experiment related to turbidity currents, five water samples were collected from the dense fluid and their particle size distributions were determined. These samples were collected from inlet and outlet points, and from three points inside the flume at one meter intervals. The particle size distribution curves were then used to calculate the geometric mean size of the particles. During these experiments some particles were deposited from the suspension and a layer of deposited material was observed after each experimental run. Measurements of the amount of, and the characteristics of, the deposited material were considered separately and are discussed in chapter 8.

In Table 6.4, the geometric mean sizes (Dg) of the suspended material of the turbidity current experiments are summarised. Figure 6.9 shows a typical plot of Dg against distance from inlet. It can be seen that the geometric mean sizes of the particles sharply decrease between the inlet and the first measurement point. This is due to the settling of large particles coming from the head tank at the entrance gate. In the other part of the flume, the decrease in the mean sizes continued slowly in the downstream direction. This reduction is due to further deposition of some large grain sizes present in the body of the current. In Figure 6.10, the size distribution curves of the suspended material are shown for a typical run. In this figure the reduction of the large grain sizes with increasing distance is clearly indicated.

Table 6.4 Geometric mean size of the suspension particles in five measurement points for all turbidity current experiments.

	Geometric mean size, Dg, (μm)				
	x = 0	x = 1 m	x = 2 m	x = 3 m	x = 4 m
Exp. 57	30.9	22.3	18.7	17.9	17.7
Exp. 58	37.7	23.2	19.6	17.3	18.0
Exp. 59	29.0	23.7	20.1	18.8	18.9
Exp. 60	31.8	22.2	20.7	19.4	18.8
Exp. 61	32.8	21.5	19.2	18.1	16.9
Exp. 62	37.1	24.2	21.2	17.9	18.6
Exp. 63	38.5	21.2	18.8	17.8	17.3
Exp. 64	30.6	22.7	20.6	19.6	21.4
Exp. 65	33.7	22.0	19.9	15.7	15.6
Exp. 66	32.8	22.3	21.9	18.7	19.3

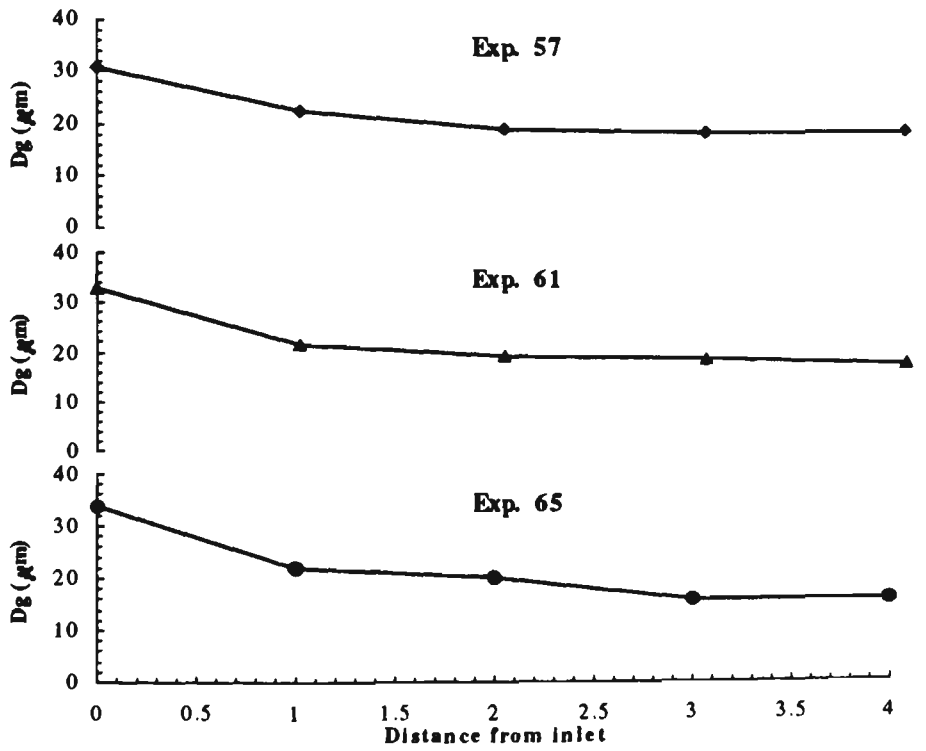

Figure 6.9 Variation of geometric mean size of suspension with the distance for three typical experiments.

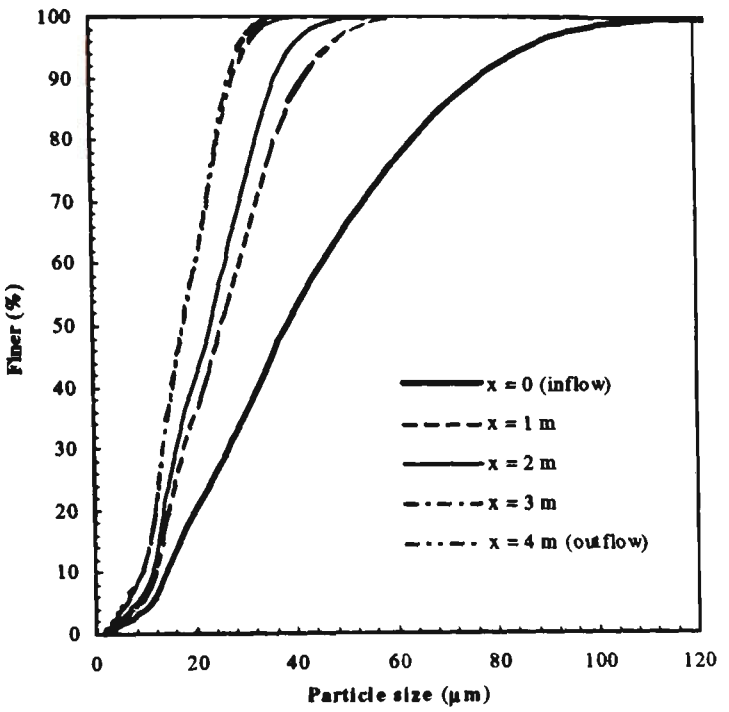

Figure 6.10 Typical variation size distribution curves of the suspended material with the distance. (Data related to experiment 65.)

6.5 Water Entrainment

The water entrainment coefficient of the gravity current, E_w, is known to be a function of the bulk Richardson number, R_i ,

$$E_w = f(R_i) \tag{6.1}$$

This parameter has been taken into account as an important parameter of the turbidity equations by several investigators. The following are some equations suggested for this purpose.

Ashida and Egashira (1977):

$$E_w = \frac{0.0015}{R_i} \tag{6.2}$$

Fukushima et al. (1985) and Parker et al. (1986):

$$E_w = \frac{0.00153}{0.0204 + R_i} \tag{6.3}$$

Parker et al. (1987):

$$E_w = \frac{0.075}{\left(1+718R_i^{2.4}\right)^{0.5}} \qquad (6.4)$$

Chikita and Okumura (1990) for Katsurazawa Reservoir in Japan:

$$E_w = 0.0087\exp\left(-0.106/R_i\right) \qquad (6.5)$$

During the course of the present research, the water entrainment coefficient was calculated by using the velocity profile data of the saline density current experiments. The layer-averaged velocity, U, and the current thickness, h, were calculated at stations 2 and 6 (1 m and 3 m from entrance gate) with the aid of the following equations:

$$U = \frac{\int_0^\infty u^2 dz}{\int_0^\infty u dz} \qquad (6.6)$$

$$h = \frac{\left[\int_0^\infty u dz\right]^2}{\int_0^\infty u^2 dz} \qquad (6.7)$$

The water entrainment coefficient can be calculated from Equation 3.37 as:

$$\frac{dUh}{dx} = E_w U \qquad (6.8)$$

With the aid of Equations 6.6 to 6.8, the water entrainment coefficients were calculated. The calculated water entrainment coefficients are presented in Table 6.5. In this table R_i is the average Richardson number at two stations.

Table 6.5 Measured water entrainment.

Exp. no.	R_i	E_w
47	3.5	0.00793
48	2.4	0.00661
49	0.8	0.00253
50	1.5	0.00575
51	1.2	0.00746
54	4.2	0.00138
55	3.7	0.00103

Based on the measured data from the present study and the available data in the literature related to the conservative density currents and turbidity currents (Ellison and Turner, 1959; Lofquist, 1960; Ashida and Egashira, 1975; Fukuoka and Fukushima, 1980; Alavian, 1986; Parker et al., 1987; Stacey and Bowen, 1988; Chikita and Okumura, (1990) and Garcia, (1990), a new equation for water entrainment coefficient E_w was developed. The above mentioned data are presented in Appendix B.

In order to determine the relationship between the water entrainment and the slope of bed, the data were plotted in the form of Figure 6.11. In this figure the horizontal axis shows the slope of bed and the vertical axis shows water entrainment. The simple regression analysis on the data resulted in a coefficient of determination $R^2 = 0.925$. This showed that E_w has a linear relationship with S as expressed in Equation 6.9:

$$E_w = 0.00295 + 0.00094S \qquad (6.9)$$

For the gravity currents, the relationship between the water entrainment coefficient and the Richardson number is preferable. In Figure 6.12, all the data are plotted as a function of the Richardson number, R_i. The linear regression line with a good coefficient of determination $R^2 = 0.858$ is given as follows:

$$E_w = \frac{0.0024}{R_i^{1.06}} \qquad (6.10)$$

If a value of 0.075 for a neutral jet is accepted as the maximum value of the water entrainment coefficient (Ellison and Turner, 1959), then the Equation 6.10 can be written in a form as follows:

$$E_w = \frac{0.075}{\left(1 + 30517\, R_i^{3.18}\right)^{1/3}} \qquad (6.11)$$

Equation 6.11 is compared with the available data in Figure 6.13. Figure 6.14 presents a comprehensive comparison of Equation 6.11 and other equations with the measured data. Among the previous equations proposed by other researchers only that of Parker et al. (1987) is close to Equation 6.11. The equation of Chikita and Okumura is far away from the measured data.

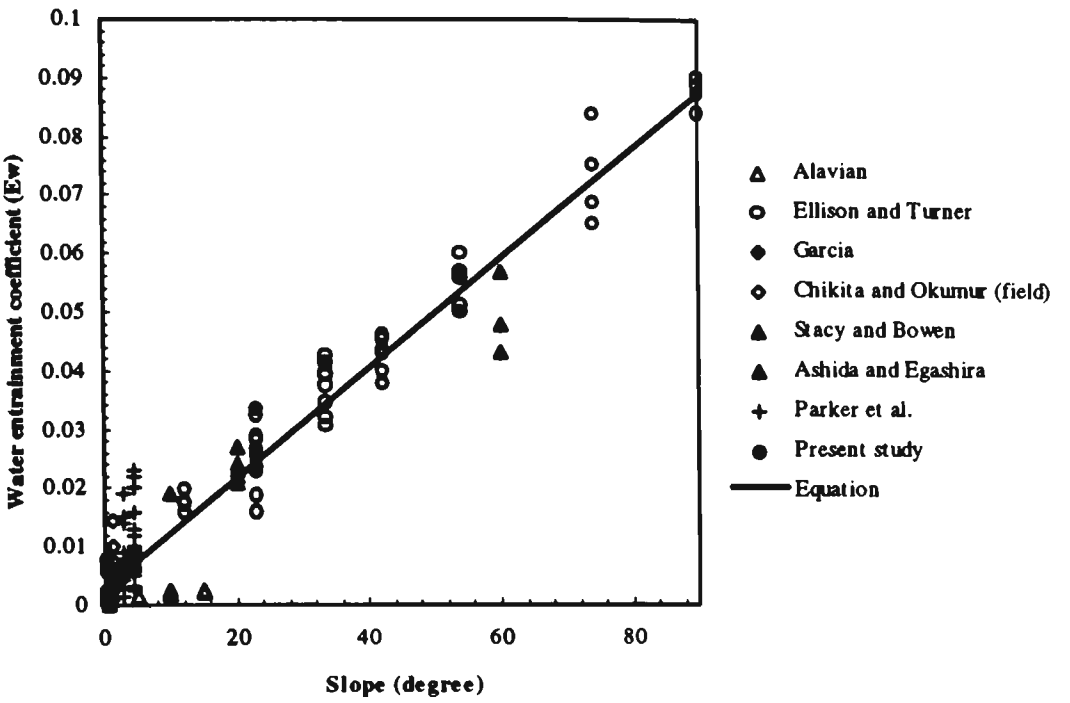

Figure 6.11 Water entrainment data as a function of slope.

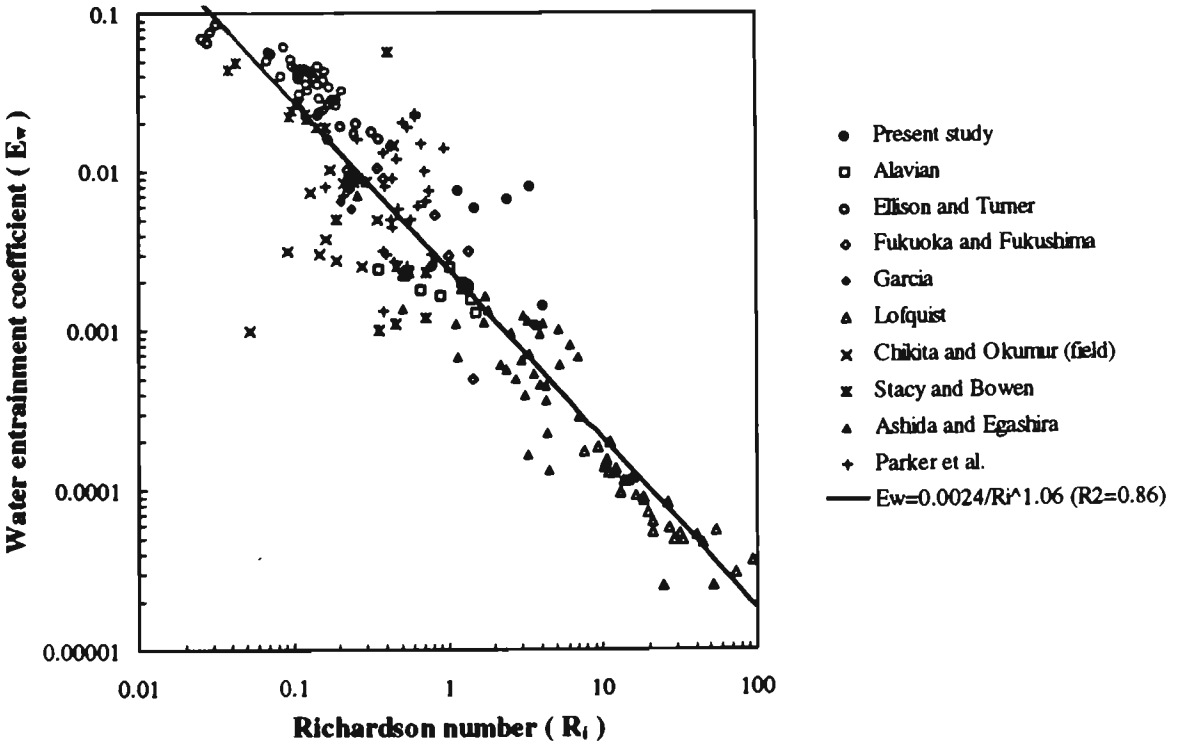

Figure 6.12 Water entrainment data as a function of the Richardson number.

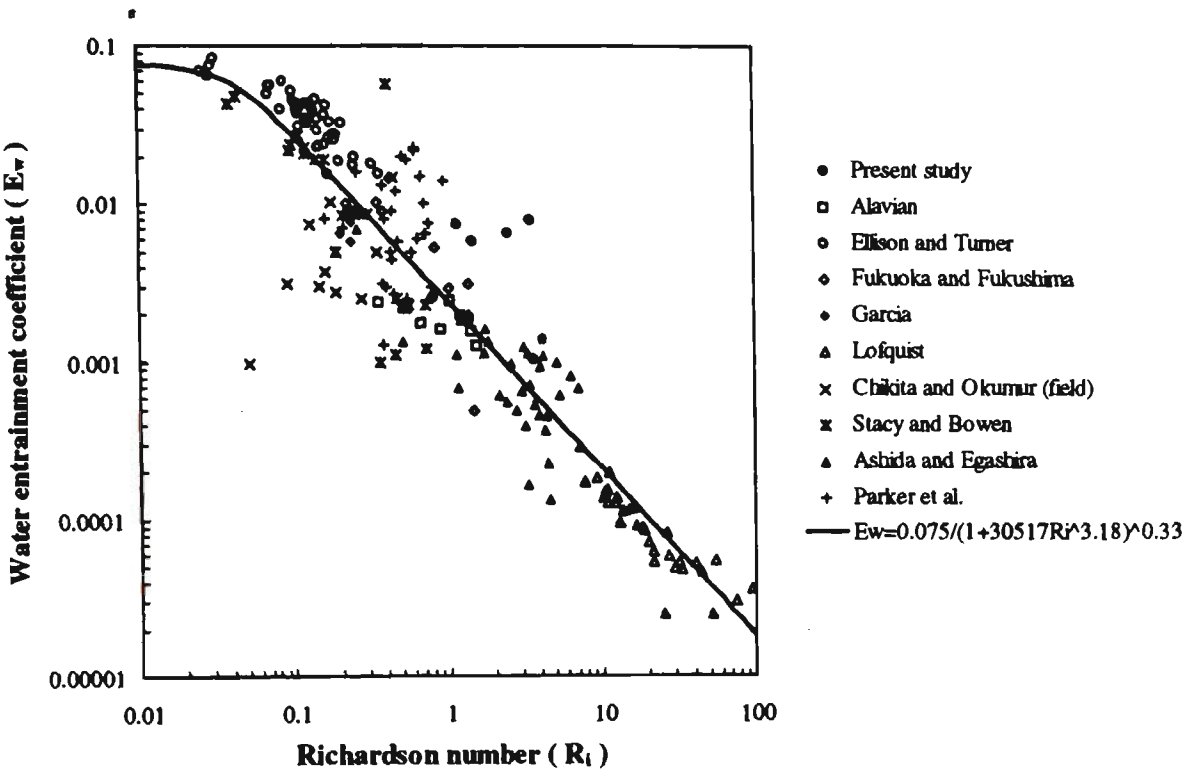

Figure 6.13 Comparison of water entrainment data with Equation 6.11.

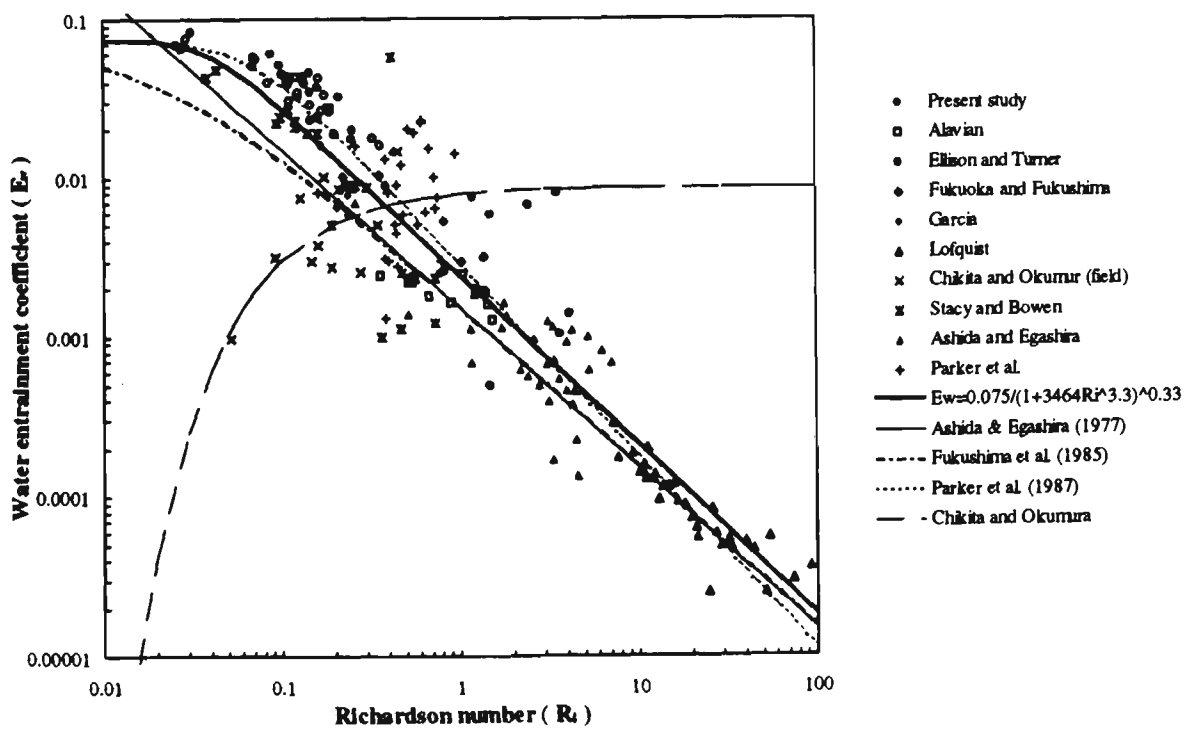

Figure 6.14 Comparison of different water entrainment formulae with the measured data.

6.6 Sediment Entrainment

The function of sediment entrainment is the same for both open channel flow and for the turbidity current. The sediment entrainment is defined as the amount of sediment concentration near the bed. There are different concepts defined for the point at which the near bed concentration is measured. For example, Einstein (1950) and Engelund and Fredsoe (1976) used a distance twice the mean diameter of the representative sediment above the bed, D_s. van Rijn (1984) used a distance equal to half of the bed-form height, and Celik and Rodi (1984), Itakura and Kishi (1980), Akiyama and Fukushima (1985), Akiyama and Stefan (1985) and Garcia and Parker (1993) used the value equal to 0.05D where D is the depth of the water. Use of value of 0.05D appear most popular in recent research because of the simplicity of the calculation and its consistency with experimental work.

Many investigators proposed various equations to include the near bed concentration in the calculation of suspended sediment in an open channel flow.

6.6.1 Equations for Sediment Entrainment

The sediment entrainment, E_s, is determined as being equal to the near-bed concentration c_a at a distance "a" above the bed for an equilibrium condition, c_{ae}.

$$E_s = c_{ae} \tag{6.12}$$

Engelund and Fredsoe (1976) presented an equation for the value c_{ae} at a distance $2D_s$ as:

$$c_{ae} = \frac{0.65}{(1+\lambda_b^{-1})^3} \tag{6.13}$$

where

$$\lambda_b = \left[\frac{\theta' - 0.06 - \beta_b \cdot p \cdot \pi/6}{0.027 \cdot (R+1) \cdot \theta'}\right]^{0.5} \tag{6.14}$$

$$\theta' = u_*'^2 / (g \cdot R \cdot D_s) \tag{6.15}$$

$$p = \left[1 + \left(\frac{\beta_b \cdot \pi/6}{\theta' - 0.06}\right)^4\right]^{-0.25} \qquad (6.16)$$

$$u_*' = (g \cdot R_b' \cdot S)^{0.5} \qquad (6.17)$$

$$R_b' = \frac{U^2}{g \cdot S}\left[6 + 2.5\ln(R_b'/k_s)\right]^{-2} \qquad (6.18)$$

R = specific gravity of a submerged particle, [= (ρ_s/ρ_w)-1]

g = gravitational acceleration

D_s = size of sediment particles

u_*' = bed shear velocity due to grain friction

k_s = hydraulic roughness (= 2 D_s)

R_b' = hydraulic radius with respect to the grains

S = slope of the bed

β_b = coefficient equal to 0.51 (Engelund and Fredsoe, 1976) and it was later modified to 1.0 (Engelund and Fredsoe, 1982)

U = mean flow velocity

van Rijn (1984) proposed an equation for c_{ae} as:

$$c_{ae} = 0.015\frac{D_s}{a}\frac{T_0^{1.5}}{D_*^{0.3}} \qquad (6.19)$$

where

$$D_* = D_s\left[\frac{g \cdot R}{\nu^2}\right]^{1/3} \qquad (6.20)$$

$$T_0 = \frac{u_*'^2 - u_{*,cr}^2}{u_{*,cr}^2} \qquad (6.21)$$

$$u_*' = (g^{0.5}/C')U \qquad (6.22)$$

$$C' = 18 \cdot \log(12R_b/3D_{90}) \qquad (6.23)$$

D_* = non-dimensional particle parameter

ν = kinematic viscosity of water

T_0 = transport stage parameter

u'_* = bed shear velocity due to grain friction

$u_{*,cr}$ = critical bed-shear velocity according to shields curve

C' = Chézy- coefficient related to grains

R_b = hydraulic radius

a = assumed to be equal to half the bed-form height

D_{90} = a size of sediment particle that 90% of grain particles is less than this size

Based on the analysis carried out by Parker and Anderson (1977), the most general dimensionless relationship for water-sediment flow is expressed as follows:

$$E_s = f\left(\frac{u_*}{v_s}, \frac{D}{D_s}, R_p, R\right) \qquad (6.24)$$

where the particle Reynolds number, R_p, is calculated using Equation 6.25.

$$R_p = \frac{(R g D_s)^{0.5} D_s}{\nu} \qquad (6.25)$$

where

ρ_s = density of the sediment

ρ_w = density of the clear water

u_* = bed shear velocity ($= \tau / \rho_w$, and τ is the bed shear stress)

v_s = fall velocity of sediment particles

D = depth of the water

Under most conditions the sediment particle has a specific gravity of about 2.65, thus the submerged specific gravity of particles (R) is a constant value equal to 1.65 and can be eliminated from Equation 6.24. Akiyama and Fukushima (1985) and Garcia and Parker (1991) showed that the measured data did not confirm the clear dependency between D/D_s (the relative roughness) and E_s. Therefore, Equation 6.24 is simplified as:

$$E_s = f\left(\frac{u_*}{v_s}, R_p\right) \qquad (6.26)$$

and finally the sediment entrainment variable is chosen (by Akiyama and Fukushima, 1985, Parker et al., 1987, and Garcia and Parker, 1991) as:

$$Z = \frac{u_*}{v_s} R_p^n \qquad (6.27)$$

Based on this approach and taking a = 0.05*D*, Akiyama and Fukushima (1985) and Akiyama and Stefan (1985) used the data for uniform sediment to determine the following relationship for E_s.

$$E_s = \begin{cases} 0, & for \quad Z < Z_c, \\ 3\times 10^{-12} Z^{10}\left(1-\frac{Z_c}{Z}\right), & for \quad Z_c < Z < Z_f \\ 0.3, & for \quad Z > Z_f \end{cases} \qquad (6.28)$$

where

$$Z = \frac{u_*}{v_s} R_p^{0.5} \qquad (6.29)$$

For a non-uniform sediment grain size, they used Z_m instead of Z as:

$$E_{si} = 3.0\times 10^{-12} Z_m^{10}\left(1-\frac{Z_c}{Z_m}\right) \qquad (6.30)$$

$$E_{si} = \frac{c_{aei}}{p_i} \qquad (6.31)$$

$$Z_m = \frac{u_*}{v_{si}} R_{p50}^{0.5}\left[\frac{D_i}{D_{50}}\right]^{1.4} \qquad (6.32)$$

where

Z_c = critical value of Z found to be equal to five (Akiyama and Fukushima, 1985)

Z_f = upper limit for Z (= 13.2, Akiyama and Fukushima, 1985)

i = is an index for a specific range of the sediment particles

50 = is an index for mean size of sediment particles

p_i = size fraction

c_{ae} = near-bed concentration in equilibrium condition

Parker et al. (1987) fitted the following equation for data obtained with uniform sediments as:

$$E_s = \frac{3\times10^{-11}Z^7}{1+(1\times10^{-10}Z^7)} \qquad (6.33)$$

where:

$$Z = \frac{u_*}{v_s} R_p^{0.75} \qquad (6.34)$$

Another Equation was proposed by Garcia and Parker (1991) as:

$$E_s = \frac{1.3\times10^{-7}Z_u^5}{\left(1+4.33\times10^{-7}Z_u^5\right)} \qquad (6.35)$$

where:

$$Z_u = \frac{u_*'}{v_s} R_p^{0.6} \qquad (6.36)$$

and u_*' is the bed shear velocity due to grain friction.

He also presented a sediment entrainment function for a non-uniform sediment as follows:

$$E_{si} = \frac{1.3\times10^{-7}Z_{eff}^5}{(1+4.33\times10^{-7}Z_{eff}^5)} \qquad (6.37)$$

where

$$Z_{eff} = \lambda Z_m \qquad (6.38)$$

and

$$Z_m = \frac{u_*'}{v_{si}} R_{pi}^{0.6}\left[\frac{D_i}{D_{50}}\right]^{0.2} \qquad (6.39)$$

λ is a constant value used to fit the non-uniform measured data to the uniform equation. The constant λ was determined to be equal to 0.802 for Niobrara River in USA.

6.6.2 The New Proposed Equation for Sediment Entrainment

Based on the Parker and Anderson (1977) analysis, Equation 6.26 was obtained. The available measured data from Vanoni (1941), Vanoni and Nomicos (1959), Onishi et al, (1976), Coleman (1969), Coleman (1981), Straub et al., Einstein and Chien, (cited in Akiyama and Stefan, 1987), Ismail, Ashida and Michiue, Ashida and Okabe, Barton and Lin, Kalinske and Pien, and Lyn (cited in Garcia, 1990) were employed to find a relationship between the sediment entrainment and its variation. The laboratory data of the sediment entrainment of uniform sediment were collected. The data used for this purpose are summarised in Appendix C. Multiple regressions analysis from the statistical package, SPSS, was used to calculate the relationship between the data and the variables of Equation 6.27. The result was quite different from the above mentioned equations. The best fitting equation to the data was found to be:

$$E_s = 3.3\times 10^{-7} Z^4 \qquad (6.40)$$

$$Z = \frac{u_*}{v_s} R_p^{0.65} \qquad (6.41)$$

The coefficient of determination, R^2, was 58.9%. In Figure 6.15 the measured data are plotted against Z together with the proposed equation.

In Figures 6.16 to 6.21, the predicted sediment entrainment values using different equations, are plotted against the available measured values. These figures can be used to compare the accuracy of the newly proposed equation with the existing equations. In Figure 6.16 (equation of Engelund and Fredsoe) the c_{ae} at a=0.05D is obtained by extrapolating from the calculated c_{ae} at a= $2D_s$, with the aid of the Rouse distribution as:

$$c_{ae}\Big|_{a=0.05D} = c_{ae}\Big|_{a=2D_s}\left[\frac{D-0.05D}{0.05D}\frac{2D_s}{D-2D_s}\right]^{\left(v_s/0.4u_*\right)} \qquad (6.42)$$

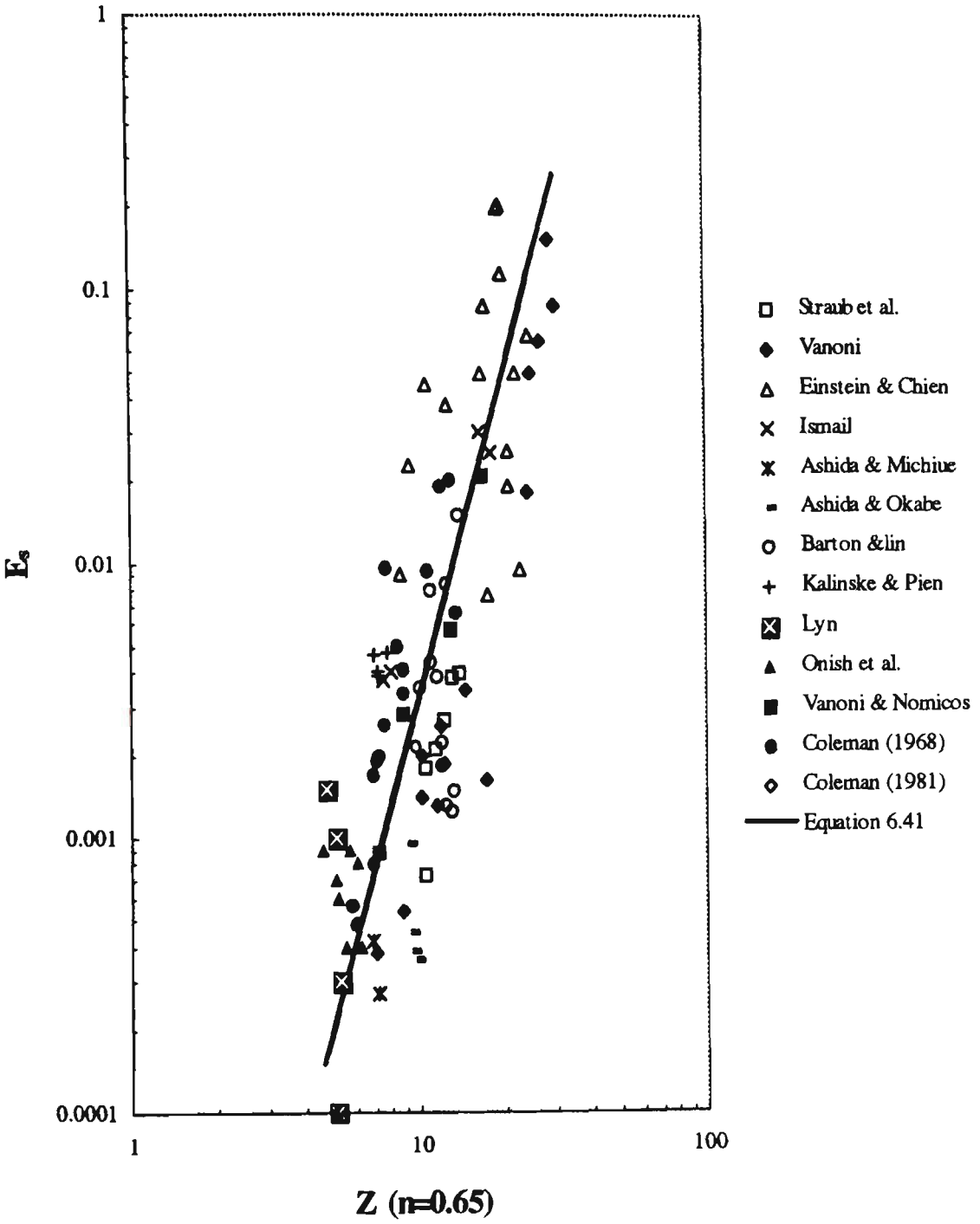

Figure 6.15 Measured sediment entrainment data and the proposed equation.

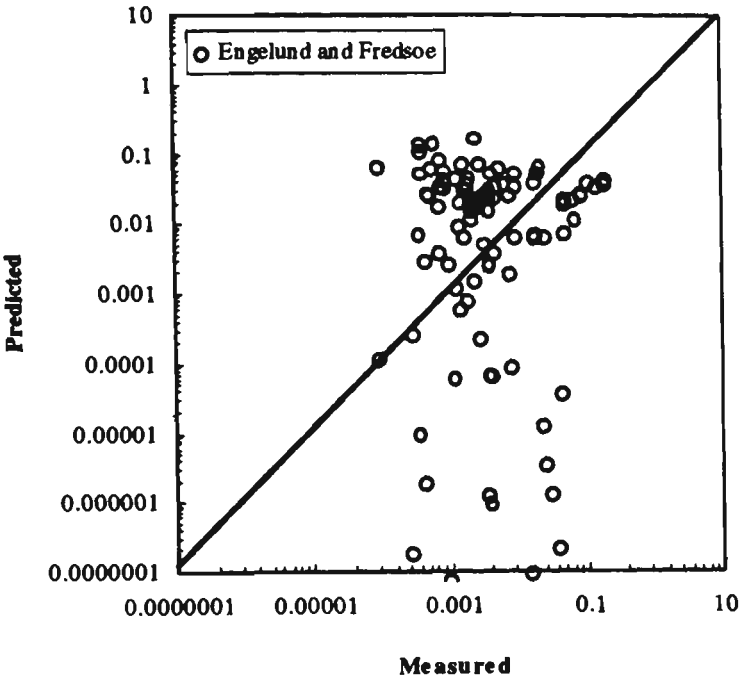

Figure 6.16 Predicted values of E_s, obtained from the Engelund and Fredsoe equation against the measured values.

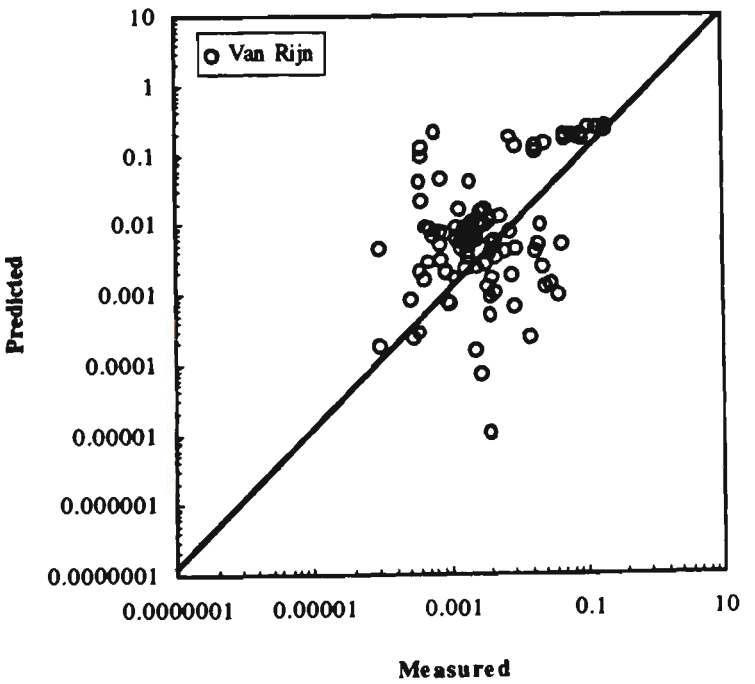

Figure 6.17 Predicted values of E_s, obtained from the van Rijn equation against the measured values.

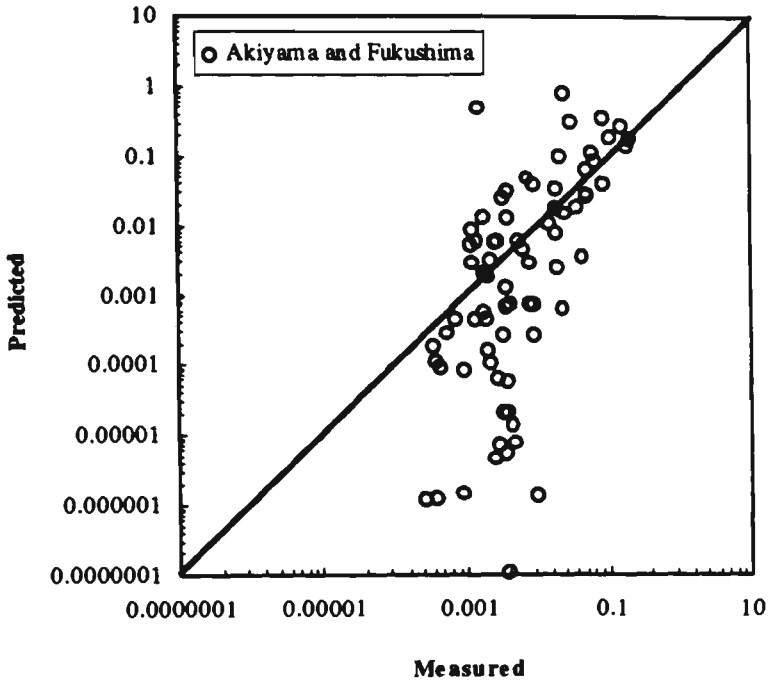

Figure 6.18 Predicted values of E_s, obtained from the Akiyama and Fukushima equation against the measured values.

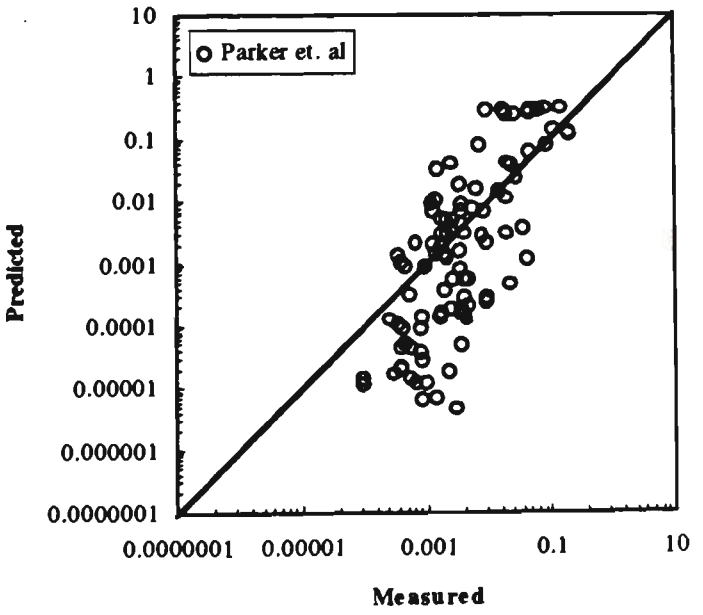

Figure 6.19 Predicted values of E_s, obtained from the Parker et al. equation against the measured values.

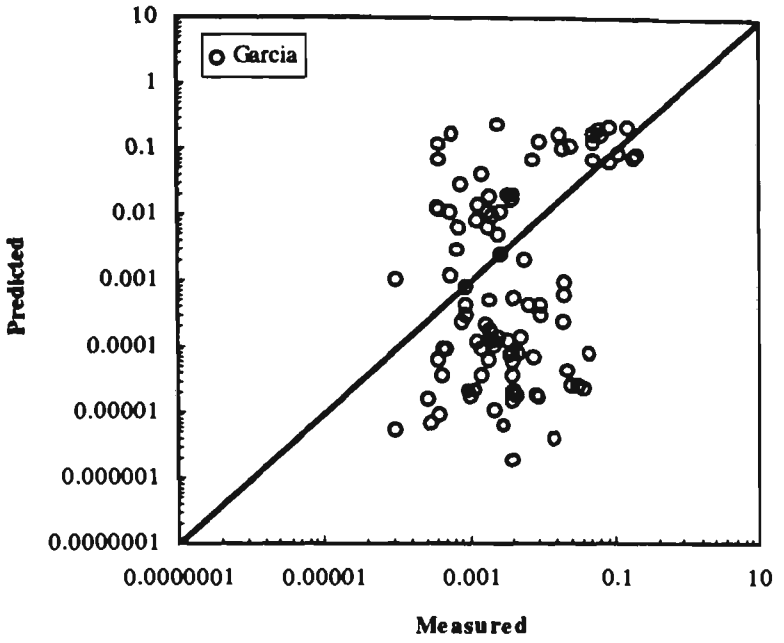

Figure 6.20 Predicted values of E_s, obtained from the Garcia equation against the measured values.

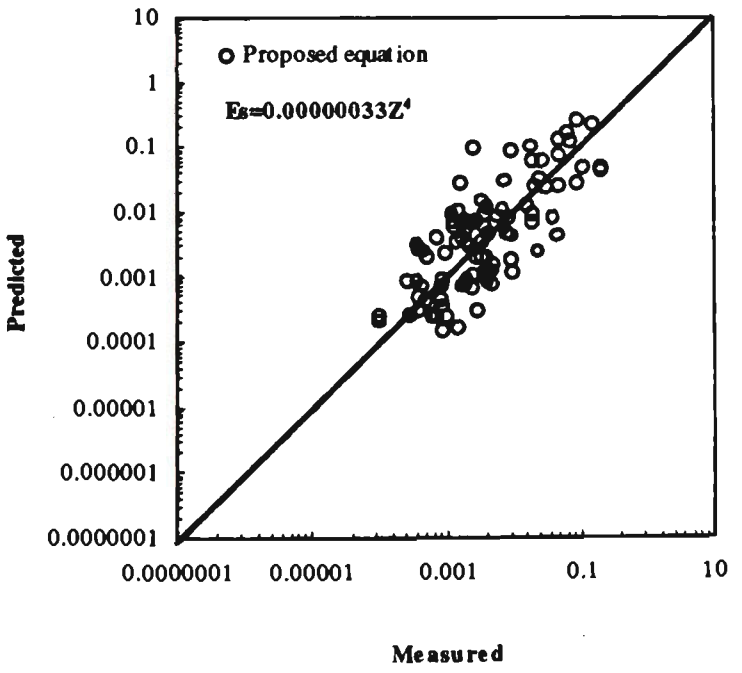

Figure 6.21 Predicted values of E_s, obtained from the proposed equation against the measured values.

The mean of the discrepancy ratio, M_e, and the mean absolute deviation of the discrepancy ratio, A_d, are employed to show the performance of each equation as:

$$M_e = 10^{b_1} \qquad (6.43)$$

$$A_d = 10^{b_2} \tag{6.44}$$

$$b_1 = \frac{1}{n_0}\sum_{i=1}^{n_0}\log(c_{aep}/c_{aeo}) \tag{6.45}$$

$$b_2 = \frac{1}{n_0}\sum_{i=1}^{n_0}\left|\log(c_{aep}/c_{aeo}) - b_1\right| \tag{6.46}$$

where

c_{aep} = predicted near bed sediment concentration

c_{aeo} = observed near bed sediment concentration

n_o = number of data points

The perfect agreement is indicated by M_e =1 and A_d =1. These estimators are calculated for a number of predictor equations and are presented in Table 6.6.

Table 6.6 The value of M_e, A_d, obtained using various formulae with the measured data.

Formula	M_e	A_d
Engelund and Fredsoe	0.76	25.94
van Rijn	1.86	4.45
Akiyama and Fukushima	0.41	7.37
Parker et al.	0.40	6.24
Garcia	0.24	16.86
Present study	1.04	2.89

It can be clearly seen from Table 6.6 that the equations of this study and van Rijn show a very good agreement with the measured data in comparison with the others.

In Figure 6.22 the data of sediment entrainment obtained by Parker et al. (1987) and Garcia and Parker (1993) from turbidity current experiments are presented as a function of the proposed Z. In this figure the unbroken line shows the proposed equation. It can be seen that the data results from turbidity current experiments are in good agreement with Equation 6.40.

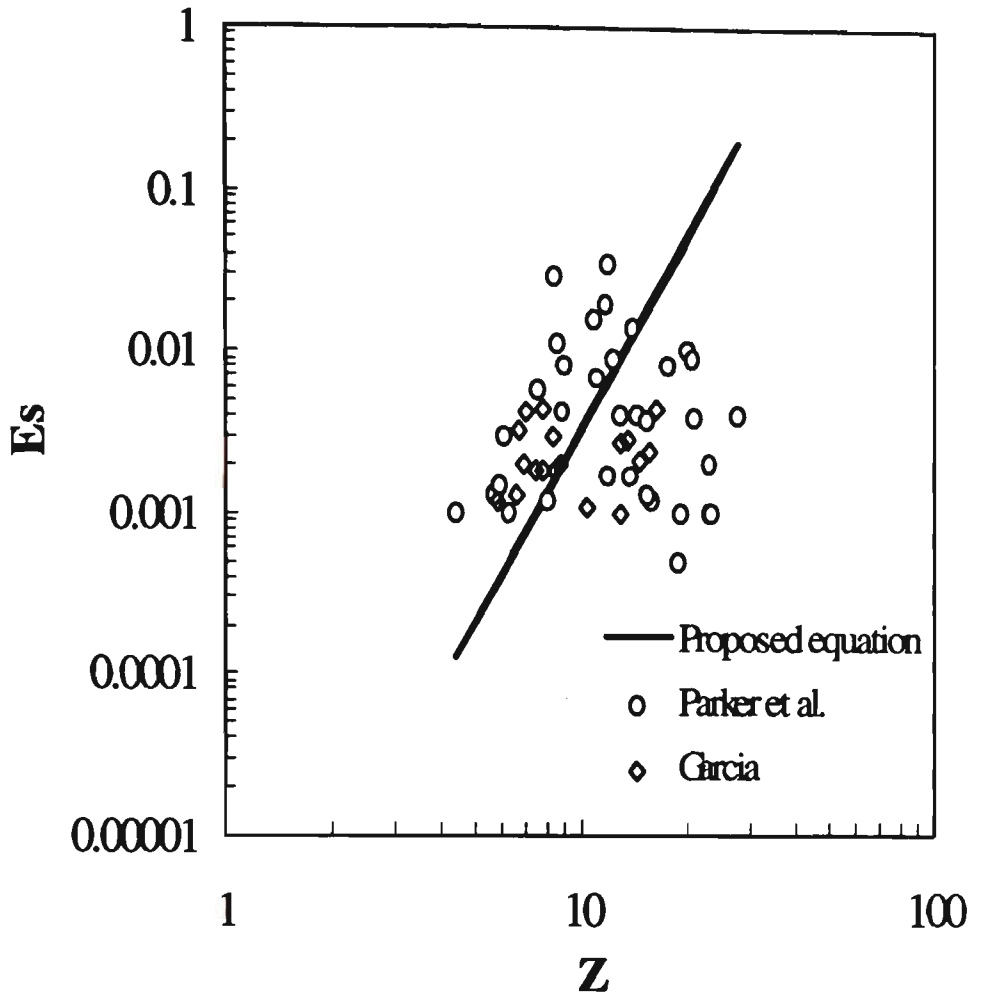

Figure 6.22 Sediment entrainment data obtained from turbidity current experiments as a function of the proposed Z.

Equation 6.40 does not show any limitation, even at very high sediment concentration. Engelund and Fredsoe (1976) showed upper limitation of the near bed concentration. They suggested that the near bed concentration should not exceed a value of 0.3. Therefore, to include this value, Equation 6.40 can be written as:

$$E_s = \frac{3.3\times10^{-7} Z^4}{1+1.1\times10^{-6} Z^4} \qquad (6.47)$$

In a river, the sediment particles are a mixture of different sized grains. If the material is divided into N size ranges and each size fraction is denoted by p_i, the mass conservation equation gives a sediment entrainment rate for the ith size particle as follows:

$$E_{si} = \frac{c_{aie}}{p_i} \qquad (6.48)$$

and Equation 6.24 can be further generalised to the following form:

$$E_{si} = f(\frac{u_*}{v_{si}}, \frac{D}{D_{50}}, R_{p50}, P_i, \frac{D_i}{D_{50}}) \qquad (6.49)$$

where:

c_{aie} = the value of c_{ai} at equilibrium state

D_i = the mean size of the sediment particle range

D_{50} = the mean size of the mix particles.

The application of the newly developed Equation 6.40 is extended for a mixed sediment as follows:

$$Z_m = \frac{u_*}{v_{si}} R_{p50}^{0.65} \left[\frac{D_i}{D_{50}}\right]^m \qquad (6.50)$$

The field data collected by Colby and Hembree (1955) from the Niobrara River in USA and by Nordin and Dempster (1963) from the Bernallio and Socorro in USA, are used to calculate the value of m in Equation 6.49. For this set of the measured data m was found to be equal to 0.5. It means the equation can be written for non-uniform particles as follows:

$$Z_m = \frac{u_*}{v_{si}} R_{p50}^{0.65} \left[\frac{D_i}{D_{50}}\right]^{0.5} \qquad (6.51)$$

$$E_{si} = \frac{3.3\times10^{-7} Z_m^4}{1+1.1\times10^{-6} Z_m^4} \qquad (6.52)$$

The measured data for non-uniform sediments together with the measured data for uniform sediments and the proposed equation are plotted in Figure 6.23. As can be seen, the proposed equation is in good agreement with all measured data. The non-uniform sediment data show a small disagreement when E_{si} is in the range of 0.0001 to 0.002.

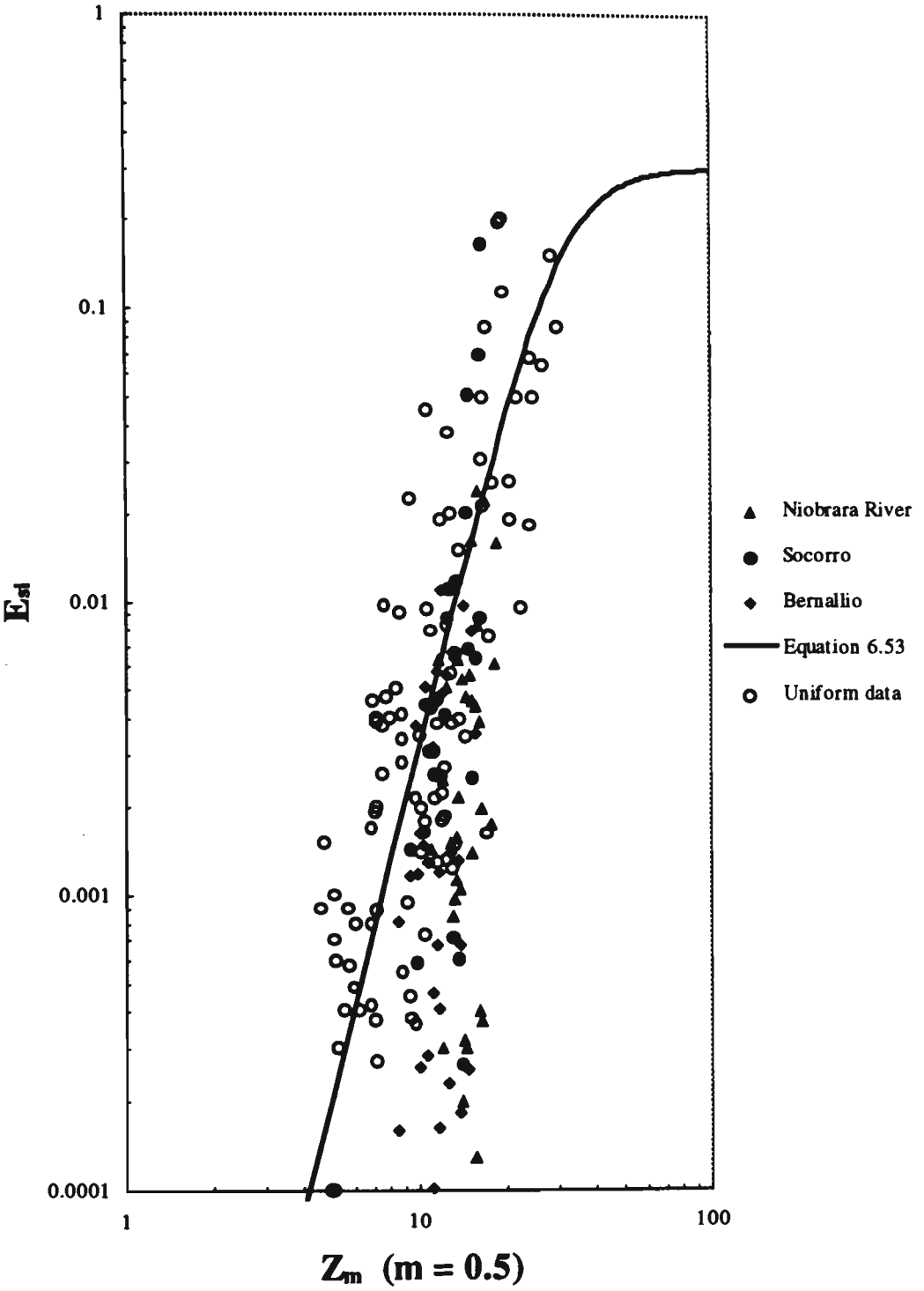

Figure 6.23 The measured uniform and non-uniform data together with the proposed equation.

6.7 Summary

In this chapter the data collected from the steady state of the gravity current were analysed and discussed. The profiles of the local velocity and the excess fractional density were shown and the accuracy of the similarity assumption were considered. The results showed good similarity for the velocity profile . The profiles of the excess fractional density showed a large variation in the profiles. Analysing the grain size in the body of the turbidity current revealed a significant reduction of mean grain size with distance. This reduction was due to deposition of some of the large particles in the bed. The value of the water entrainment coefficient was calculated by analysing the velocity profiles at two sequence measurement points. A new water entrainment coefficient, E_w, was found based on the data of the present study and on other available data. The measured data of the uniform sediment entrainment over an erodible bed from other investigators were employed to find a new formula and to test the existing formulations. It was shown that the proposed sediment entrainment equation is in good agreement with the available data in comparison with existing equations.

Chapter Seven

DEVELOPMENT OF A NEW RESERVOIR SEDIMENTATION MODEL "DEPO"

7.1 Introduction

A number of computer programs are available for predicting flow and sediment interaction in streams and reservoirs. Although they are used for predicting sedimentation in the reservoirs, application of them for analysis of sediment in large reservoirs is limited particularly when the suspended sediment discharge is relatively high. Ignorance of the effects of turbidity currents that occur in such reservoirs is the limitation of using the available programs for accurate prediction of long term sedimentation.

During the course of this research, a new computer program, DEPO, is developed. The program can predict long term sedimentation in large reservoirs taking into account the effects of turbidity current. Furthermore, this program can be used to predict sediment processes and bed evaluation of rivers and reservoirs.

DEPO is a one-dimensional sedimentation program for modelling sediment processes and bed evaluation in a reservoir. DEPO can also be used for one dimensional analysis of fluvial streams. Furthermore, the program can be used as a powerful tool to analyse the establishment and transportation of turbidity currents in reservoirs during flood events. It can be used to evaluate the effects of storing or releasing turbidity currents on the reservoir bed. The model is particularly recommended for prediction of sedimentation processes in large reservoirs with relatively high suspended sediment concentration. Subcritical flows and turbidity currents, which are generally dominant in the man-made reservoirs in the steady condition, are considered in the model.

The computer program "DEPO" is written in FORTRAN-77L. It consist of one main program with 9 subroutines and functions. It uses the conventional memory of the computer and accepts data for up to 100 cross sections. The flow chart of the model and other details are shown later in section 7.3.

All input data are sent to the program from an input file and the results are written in an output file. The input data requirements are described in section 7.8. The output file contains the important results including a summary of input data, elevation of water surface and turbidity current surface, final geometry of sections, final reservoir thalweg elevation and final bed composition of cross sections.

7.2 Water Surface Level

The one dimensional energy equation was applied to estimate the water elevation in the channel. Standard Step Method (Henderson 1966) was used to solve the energy equation. For each discharge, the computation starts from the downstream section and continues towards the upstream section. Based on this method, the relationship between each section and the last downstream section is expressed as:

$$WS + \frac{\alpha_v V^2}{2g} = WS_{ds} + \frac{\alpha_{ds} V_{ds}^2}{2g} + h_e \qquad (7.1)$$

where

WS, WS_{ds} = water surface elevation at the current section and downstream section

α_v , α_{ds} = velocity distribution coefficients for flow at the current and downstream sections respectively (in the computer program it was assumed to be a constant equal to 1.15)

V, V_{ds} = average velocities at the current and downstream sections respectively

g = acceleration due to gravity

h_e = total energy loss.

In a natural stream, the main part of the total energy loss is due to friction, contractions and expansions. Based on the average flow parameters at each section, the friction loss (h_f) can be calculated from Manning's Equation as:

$$Q = \frac{A}{n} R_b^{2/3} S^{1/2} \qquad (7.2)$$

When $S = \frac{h_f}{L}$ is replaced in Equation 7.2 and the equation is solved for h_f, then the following equation can be obtained:

$$h_f = \frac{Q^2}{\left[\frac{A R_b^{2/3}}{n L^{1/2}}\right]^2} \qquad (7.3)$$

where

Q = water discharge

A = cross section area of flow

n = Manning's coefficient

R_b = hydraulic radius

S = slope of the bed

L = distance between two cross sections.

In the computer program, the average values of A and R_b from the upstream and downstream sections are used to calculate Equation 7.3.

Losses due to contractions or expansions can be calculated from the following equation:

$$h_{ce} = C_{ce} \left| \frac{\alpha_v V^2}{2g} - \frac{\alpha_{ds} V_{ds}^2}{2g} \right| \qquad (7.4)$$

where h_{ce} is energy loss due to contractions and expansions and C_{ce} is loss coefficient for contraction or expansion .

The computation begins by assuming an initial value of water surface elevation (usually equal to the water surface elevation in previous section) and computes the water surface by using Equation 7.1. The process will continue until the assumed and computed values are within an allowable error (less than 0.000001×depth of flow at the thalweg of section). The critical depth will be calculated in each section based on the specific

energy curve to make sure the flow is subcritical (flow depth in the section is greater than critical depth). In the case where a supercritical condition is detected in a section (flow depth in the section is less than critical depth), the appropriate hydraulic parameters are determined based on the normal supercritical flow.

7.3 Plunge Point of Turbidity Current

Plunge point is a location in a reservoir or lake where the dense fluid goes under ambient water. This point is very important to locate in order to determine where the turbidity current will commence. The available equations to calculate this point are described in section 3.6.1 of Chapter three. The equations of Akiyama and Stefan (1984) (Equations 3.27 and 3.28) are employed in the computer program.

7.4 Surface Level of Turbidity Current

The set of turbidity current equations (Equations 3.44 to 3.46 of Chapter three) should be solved for subcritical conditions for the segment located between the plunge point and the downstream section (close to the dam wall). These equations are a combination of depth and sediment concentration parameters of the turbidity current. It means that the depth of current is dependant on the sediment concentration of the current. In the case of a supercritical condition, both turbidity current depth and sediment concentration are solved from upstream. However, in the case of a subcritical condition, the depth of current should be solved from downstream and sediment concentration should be solved from upstream and this, therefore, makes it difficult to solve mathematically. To over this problem, the elevation of the downstream boundary of the current (close to the dam wall) should be determined (actual measurement or assume an elevation based on the elevation of the outlet gates). For the sediment concentration of the downstream boundary, the information of the upstream boundary can be applied. The strategy that can be employed for this condition is a trial and error method. The numerical solution starts with the assumption of a value for sediment concentration in the downstream boundary condition. Then the value of the upstream boundary gained from the numerical solution is compared with the value of the boundary that has already been determined (in the plunge point calculation). If the difference between both values of the plunge point sediment concentrations is within the acceptable range (less than one percent of the value of sediment concentration at the plunge point calculation), then the depths of turbidity

current estimated in cross sections will be used to calculate hydraulic parameters and sediment processes. In the case when the difference is not acceptable, a new assumption will be made for the concentration of the downstream boundary. This process will be continued until an agreement is reached between the two calculated sediment concentrations in the upstream boundary. The concept of equilibrium sediment entrainment can be applied for the first assumption of sediment concentration of the downstream boundary.

One of the major contribution of the present study is the development of a new solution method for the sediment process in the reservoirs with consideration of the turbidity currents. For solving the turbidity current equations, a numerical scheme is to be employed. The Runge-Kutta method is employed for this purpose. The Runge-Kutta numerical solution is a kind of a finite-difference scheme and it is the most popular method for obtaining numerical solutions to differential equations. The method is very easy to code and is very stable and accurate. It is also self-starting, and the step size can easily be adjusted in the middle of calculation in order to accommodate a function which is rapidly changing. The method is based on the basic Euler Method. The slope that is used in the linear extrapolation is taken to be a weighted average of the slope at the left end of the interval and some intermediate points. To solve a differential equation as $y' = f(x, y)$, (f is known function of x and y) the algorithm can be written as follows;

$$y_{i+1} = y_i + f_{ave}\,\Delta x \qquad (7.5)$$

where y_{i+1} is a hydraulic parameter at the next nodal point, y_i is the same hydraulic parameter at the previous nodal point which is known, Δx is distance interval, and f_{ave} is determined by the following equation:

$$f_{ave} = a\,f_i + b\,f_{i'} \qquad (7.6)$$

where

a, b = weighting factors

f_i = the function evaluated at the point x_i

$f_{i'}$ = the function evaluated at some intermediate points defined as follows:

$$f_{i'} = f\left(x_i + \alpha_p\,\Delta x,\ y_i + \beta\ f_i\,\Delta x\right) \qquad (7.7)$$

parameters α_p and β specify the position of the intermediate points.

Four unknown parameters α_p, β, a and b are written as two following forms:

$$a = 0 \qquad b = 1 \qquad \alpha_p = \beta = 1/2$$

and

$$a = b = 1/2 \qquad \alpha_p = \beta = 1$$

Both of the above parameters are known as second-order Runge-Kutta procedures, meaning that the accumulated truncation error is proportional to $(\Delta x)^2$ in either methods.

By including more sampling points in the interval, the basic Runge-Kutta Method (Benjamin, 1992) can be improved to a procedure that has an accumulated truncation error proportional to $(\Delta x)^4$ that is a fourth-order method. This algorithm and the parameters are expressed as follows:

$$y_{i+1} = y_i + \tfrac{1}{6}[\Delta y_0 + 2\Delta y_1 + 2\Delta y_2 + \Delta y_3] \qquad (7.8)$$

where:

$$\Delta y_0 = f(x_i, y_i)\Delta x$$
$$\Delta y_1 = f\left(x_i + \tfrac{1}{2}\Delta x, y_i + \tfrac{1}{2}\Delta y_0\right)\Delta x$$
$$\Delta y_2 = f\left(x_i + \tfrac{1}{2}\Delta x, y_i + \tfrac{1}{2}\Delta y_1\right)\Delta x$$
$$\Delta y_3 = f(x_{i+1}, y_i + \Delta y_2)\Delta x$$

The above algorithm is used to solve the system of partial differential equations for turbidity currents (Equations 3.42 to 3.46) as:

$$h_{i+1} = h_i - \frac{\Delta x}{6}(h_0 + 2h_1 + 2h_2 + h_3)$$
$$U_{i+1} = U_i - \frac{\Delta x}{6}(U_0 + 2U_1 + 2U_2 + U_3)$$
$$\psi_{i+1} = \psi_i - \frac{\Delta x}{6}(\psi_0 + 2\psi_1 + 2\psi_2 + \psi_3)$$

$$R_{i0} = \frac{g R \psi_i}{U_i^3}$$

$$E_{w0} = \frac{0.075}{(1 + 30517\, R_{i0}^{3.18})^{1/3}}$$

$$E_{s0} = \frac{3.3\times10^{-7} Z_0^4}{1+1.1\times10^{-6} Z_0^4} \qquad Z_0 = \frac{U_i\, C_D}{v_s} R_p^{0.65}$$

$$\Psi_{e0} = \frac{E_{s0} h_i\, U_i}{r_0}$$

$$h_0 = \frac{-R_{i0}S + C_D + \left(2 - \frac{R_{i0}}{2}\right)E_{w0} + \frac{R_{i0}}{2} r_0 \frac{v_s}{U_i}\left(\frac{\Psi_{e0}}{\Psi_i} - 1\right)}{\left(1 - R_{i0}\right)}$$

$$U_0 = \left(\frac{U_i}{h_i}\right)\left(E_{w0} - h_0\right)$$

$$\Psi_0 = \frac{\Psi_i}{h_i} r_0 \frac{v_s}{U_i}\left(\frac{\Psi_{e0}}{\Psi_i} - 1\right)$$

$$R_{i1} = \frac{g\, R\left(\Psi_i + \Delta x \frac{\Psi_0}{2}\right)}{\left(U_i + \Delta x \frac{U_0}{2}\right)^3}$$

$$E_{w1} = \frac{0.075}{(1+30517\, R_{i1}^{3.18})^{1/3}}$$

$$E_{s1} = \frac{3.3\times10^{-7} Z_1^4}{1+1.1\times10^{-6} Z_1^4} \qquad Z_1 = \frac{\left(U_i + \Delta x \frac{U_0}{2}\right) C_D}{v_s} R_p^{0.65}$$

$$\Psi_{e1} = \frac{E_{s1}\left(h_i + \Delta x \frac{h_0}{2}\right)\left(U_i + \Delta x \frac{U_0}{2}\right)}{r_0}$$

$$h_1 = \frac{-R_{i1}S + C_D + \left(2 - \frac{R_{i1}}{2}\right)E_{w1} + \frac{R_{i1}}{2} r_0 \frac{v_s}{\left(U_i + \Delta x \frac{U_0}{2}\right)}\left(\frac{\Psi_{e1}}{\Psi_i + \Delta x \frac{\Psi_0}{2}} - 1\right)}{\left(1 - R_{i1}\right)}$$

$$U_1 = \left(\frac{U_i + \Delta x \frac{U_0}{2}}{h_i + \Delta x \frac{h_0}{2}}\right)\left(E_{w1} - h_1\right)$$

$$\psi_1 = \left(\frac{\psi_i + \Delta x \frac{\psi_0}{2}}{h_i + \Delta x \frac{h_0}{2}}\right)\left(\frac{r_0 v_s}{U_i + \Delta x \frac{U_0}{2}}\right)\left(\frac{\psi_{e1}}{\psi_i + \Delta x \frac{\psi_0}{2}} - 1\right)$$

$$R_{i2} = \frac{g R\left(\psi_i + \Delta x \frac{\psi_1}{2}\right)}{\left(U_i + \Delta x \frac{U_1}{2}\right)^3}$$

$$E_{w2} = \frac{0.075}{(1 + 30517 R_{i2}^{3.18})^{1/3}}$$

$$E_{s2} = \frac{3.3\times10^{-7} Z_2^4}{1 + 1.1\times10^{-6} Z_2^4} \qquad Z_2 = \frac{\left(U_i + \Delta x \frac{U_1}{2}\right) C_D}{v_s} R_p^{0.65}$$

$$\psi_{e2} = \frac{E_{s2}\left(h_i + \Delta x \frac{h_1}{2}\right)\left(U_i + \Delta x \frac{U_1}{2}\right)}{r_0}$$

$$h_2 = \frac{-R_{i2} S + C_D + \left(2 - \frac{R_{i2}}{2}\right) E_{w2} + \frac{R_{i2}}{2} r_0 \frac{v_s}{\left(U_i + \Delta x \frac{U_1}{2}\right)}\left(\frac{\psi_{e2}}{\psi_i + \Delta x \frac{\psi_1}{2}} - 1\right)}{(1 - R_{i2})}$$

$$U_2 = \left(\frac{U_i + \Delta x \frac{U_1}{2}}{h_i + \Delta x \frac{h_1}{2}}\right)(E_{w2} - h_2)$$

$$\psi_2 = \left(\frac{\psi_i + \Delta x \frac{\psi_1}{2}}{h_i + \Delta x \frac{h_1}{2}}\right)\left(\frac{r_0 v_s}{U_i + \Delta x \frac{U_1}{2}}\right)\left(\frac{\psi_{e2}}{\psi_i + \Delta x \frac{\psi_1}{2}} - 1\right)$$

$$R_{i3} = \frac{g\,R\left(\psi_i + \Delta x \frac{\psi_2}{2}\right)}{\left(U_i + \Delta x \frac{U_2}{2}\right)^3}$$

$$E_{w3} = \frac{0.075}{(1 + 30517\,R_{i3}^{3.18})^{1/3}}$$

$$E_{s3} = \frac{3.3\times10^{-7} Z_3^4}{1 + 1.1\times10^{-6} Z_3^4} \qquad Z_3 = \frac{\left(U_i + \Delta x \frac{U_2}{2}\right) C_D}{v_s} R_p^{0.65}$$

$$\psi_{e3} = \frac{E_{s3}\left(h_i + \Delta x \frac{h_2}{2}\right)\left(U_i + \Delta x \frac{U_2}{2}\right)}{r_0}$$

$$h_3 = \frac{-R_{i3}S + C_D + \left(2 - \frac{R_{i3}}{2}\right)E_{w3} + \frac{R_{i3}}{2} r_0 \frac{v_s}{\left(U_i + \Delta x \frac{U_2}{2}\right)}\left(\frac{\psi_{e3}}{\psi_i + \Delta x \frac{\psi_2}{2}} - 1\right)}{(1 - R_{i3})}$$

$$U_3 = \left(\frac{U_i + \Delta x \frac{U_2}{2}}{h_i + \Delta x \frac{h_2}{2}}\right)(E_{w3} - h_3)$$

$$\psi_3 = \left(\frac{\psi_i + \Delta x \frac{\psi_2}{2}}{h_i + \Delta x \frac{h_2}{2}}\right)\left(\frac{r_0\, v_s}{U_i + \Delta x \frac{U_2}{2}}\right)\left(\frac{\psi_{e3}}{\psi_i + \Delta x \frac{\psi_2}{2}} - 1\right)$$

7.5 Sediment Processes

Sediment processes are analysed based on the following procedure:

- calculate sediment transport capacity from one of the appropriate sediment transport equations,

- calculate actual sediment transport for every sediment size fraction based on size distribution of bed materials, change in composition of bed materials during time step and duration of flow passing the control volume. All of the concepts described in Chapter three have been used.

- calculate the value of change in the bed level using mass-conservation equation, unit weight of sediment deposition or scour, and choose an option for sediment distribution in the sections.

The processes are calculated by following the above procedure over each time step and the control volume is defined around a main computation section. There are seven methods available to calculate the capacity transport of sand particles. The Exner Equation (continuity equation of sediment material), which is expressed in a finite difference algorithm, is used to calculate the bed level after each time step.

Quantification of cohesive sediment transport is required for the study of sediment processes in the reservoir. Cohesive sediment particles, including clay and silt size particles are analysed. The deposition rate is calculated by the Krone's Formulation (1962), and the scour rate is calculated using Cormault Method (1971). These equations are presented in Chapter three.

In DEPO, the volume of sediment deposition or scour in each section is estimated based on the methods described in Chapter three (using the approach of HEC-6 for predicting active-layer thickness and armouring, and the Miller equation for predicting unit weight of sediment deposition). Meanwhile the form of bed change can be defined manually. Two options are available in the program: flat distribution and ratio distribution. In flat form, which is more likely in deep reservoirs, the bed change will occur from the bottom of the cross section in an even manner across the section. It means that the deposition or scour will fill or empty the section from the bottom depending on the volume of deposition or scour in horizontal layers. It affects some parts of the bed between the bottom of a given section and the water elevation. An example of this form of bed change is shown in Figure 7.1.

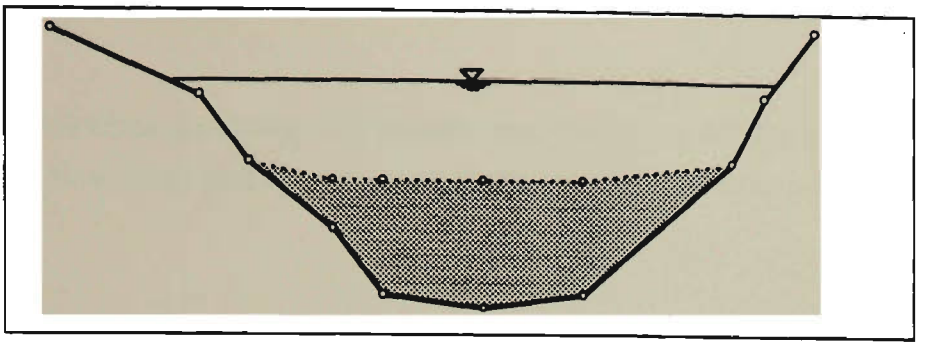

Figure 7.1 Flat distribution of sediment deposition in the DEPO model.

In ratio distribution, the bed change will affect all the points in a given section. Scour and fill is distributed proportionally relative to the conveyance in the cross section. The value of change in each point is dependent on the following equation:

$$dh_1 = dh_{tw}\left(\frac{y_d}{y_{tw}}\right)^{(1+p)} \qquad (7.9)$$

where

dh_1 = the value of change in each coordinate point in a given cross section

dh_{tw} = the value of change in the thalweg of the cross section

y_d = the water depth above the coordinate point

y_{tw} = the water depth above the thalweg of the cross section

p = a power based on the user's choice.

The value of m will define the relationship between the two coordinate points (each coordinate point and thalweg point) and its value is between 0 and 1. Two examples of this form of bed change with different m values are shown in Figure 7.2.

The computation of sediment distribution in each section starts with assuming a value of change for the thalweg point, and continues to calculate the bed change at other coordinate points. The computed and estimated area of sediment in each cross section are compared. The process is continued in an iterative manner until the difference between the two values are within the allowable range (0.2 m^2).

7.6 Computational Processes

This section describes the computer process and functions of the various parts in the program. The flow chart and the structure of the program are summarised in Figures 7.3 and 7.4.

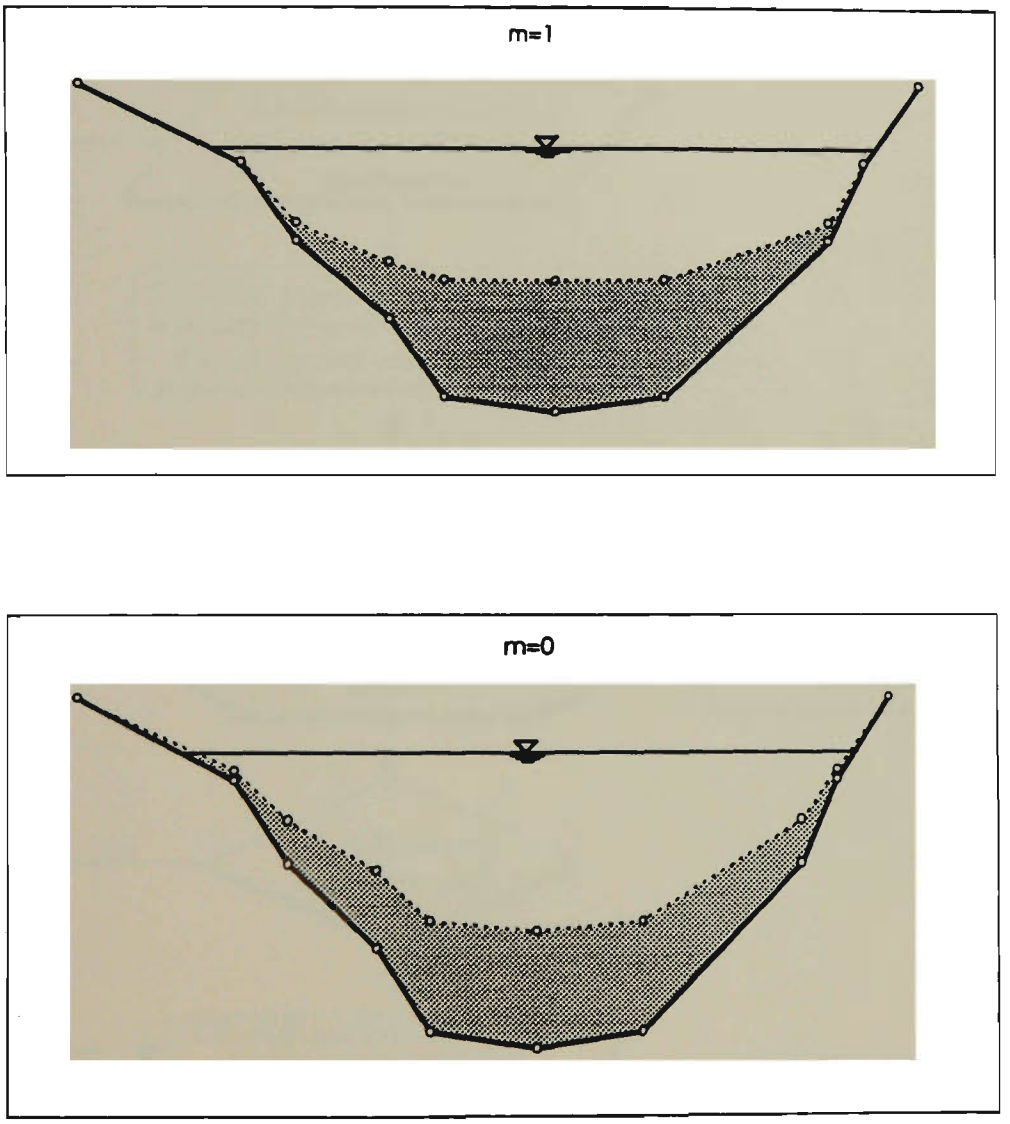

Figure 7.2 Ratio distribution of sediment deposition in the DEPO model.

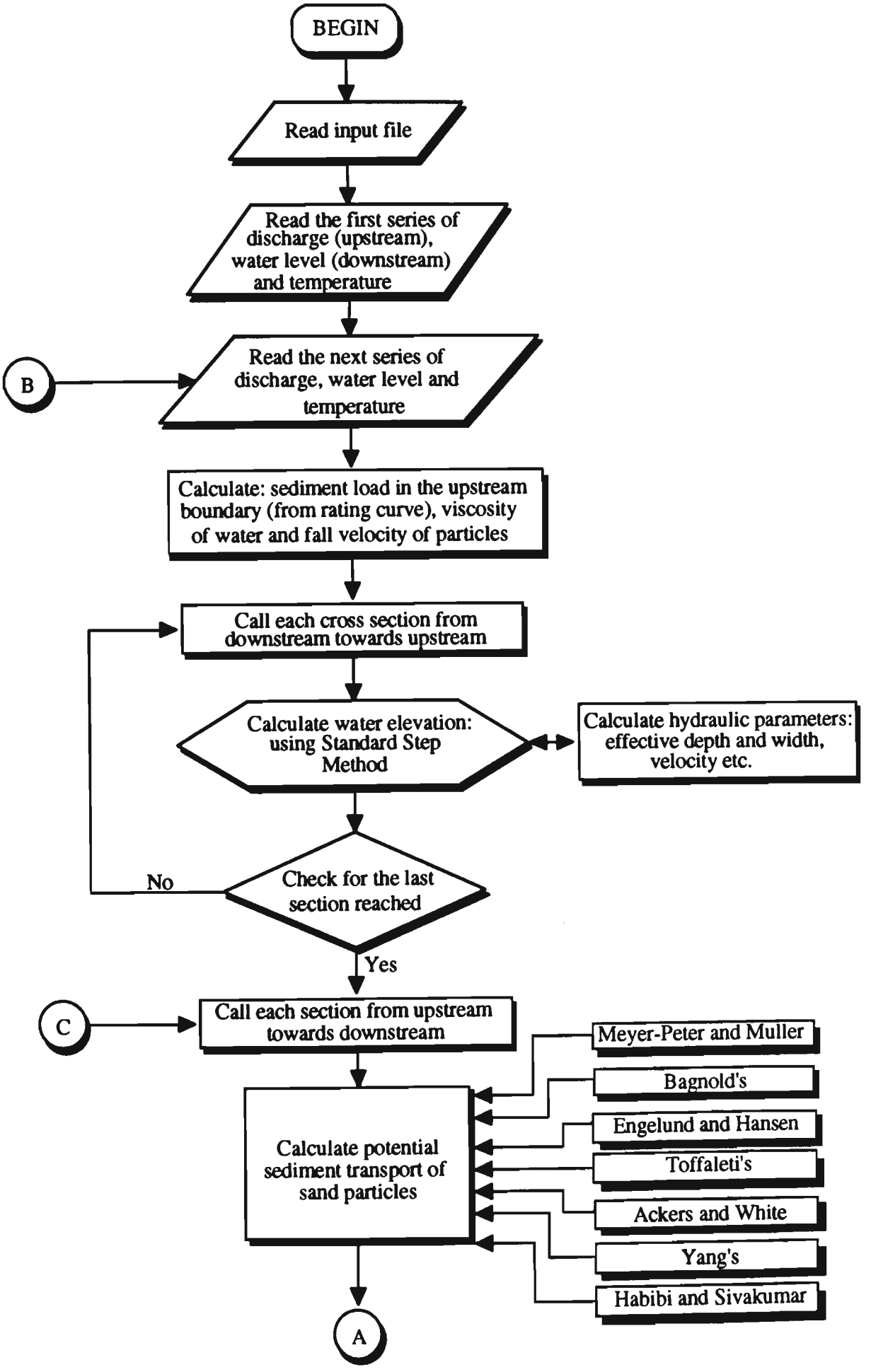

Figure 7.3 Flow chart of the new computer program DEPO.

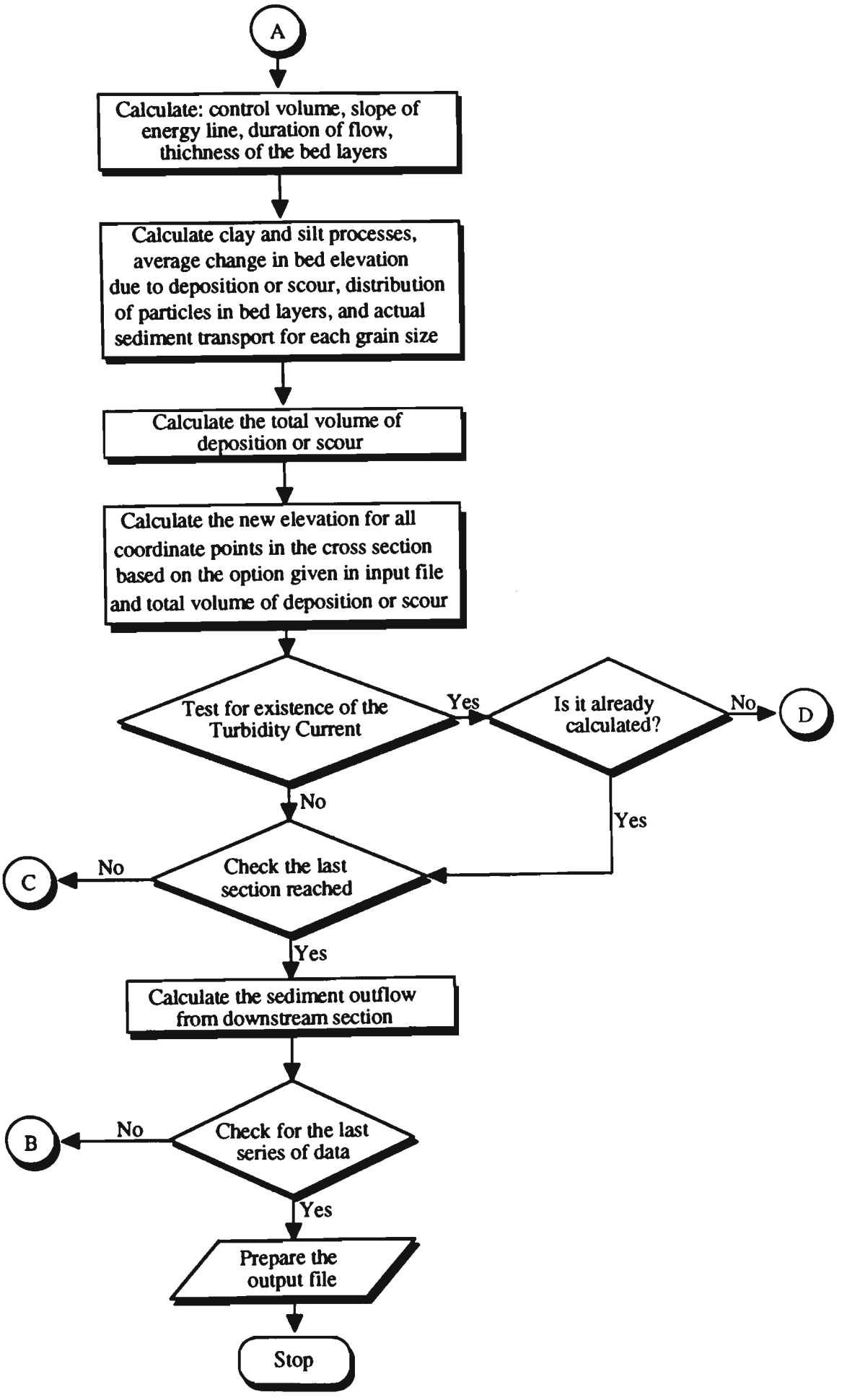

Figure 7.3 Flow chart of the new computer program DEPO (continued).

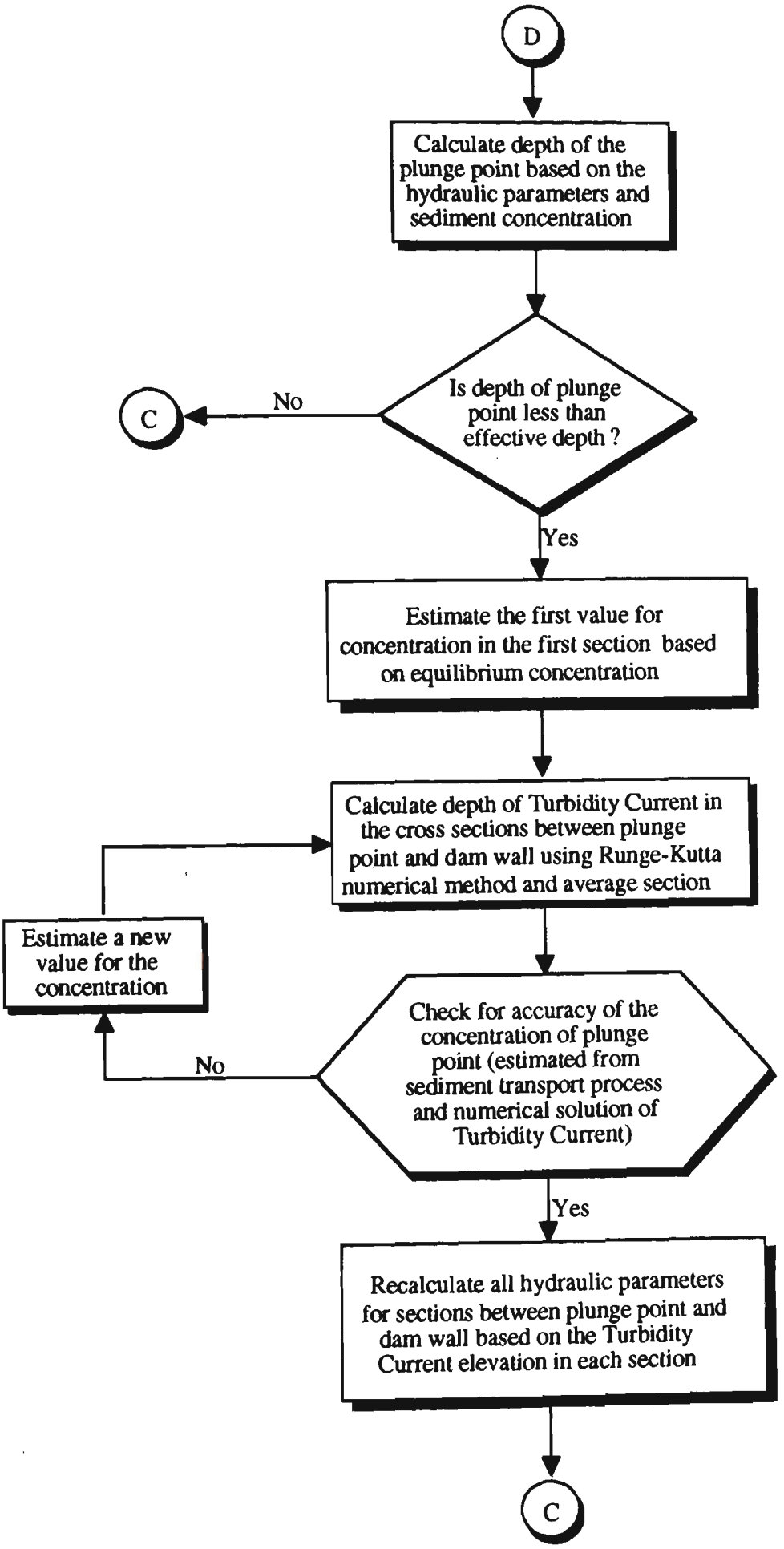

Figure 7.3 Flow chart of the new computer program DEPO (continued).

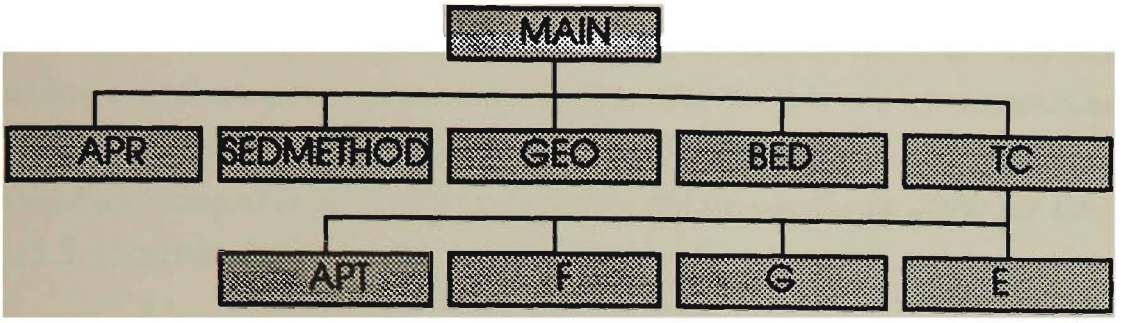

Figure 7.4 Major parts of the new program, DEPO.

The MAIN program manages the input data, output file, and controls all subroutines. In addition, some of the processes including sediment discharge from the upstream boundary, water elevation, depth of plunge point of the turbidity current, trap efficiency and total volume of sediment deposition or scour are carried out in the MAIN. The input data are tested for any possible errors which may occur in the sequential arrangement of input data. There would be a message in the output file and on the screen if there is any error in the input data. After checking the input data, a main loop will start to run and the hydrological data will be considered group by group. The sediment discharge entering into the segment for each grain size particles will be calculated based on the flow discharge and "power interpolation" among input sediment-flow discharge data. Subsequently, the fall velocity of each grain size will be calculated. The water elevation in the downstream boundary, flow discharge and geometry of sections are used to calculate water elevations and hydraulic parameters in all the sections employing the APR subroutine. SEDMETHOD and GEO subroutines calculate the capacity of sediment transport, the volume of deposition or scour and the composition of bed material in each section. The change in the geometry of sections are calculated in the BED subroutine. The establishment of the turbidity current is checked and if turbidity currents occur the TC subroutine and its components (APT, F, G, and E) are called to handle the new situation. The iteration is continued for other hydrological data and finally the output file is prepared by the MAIN. The source code of the computer program is presented in Appendix D.

The program consists of five subroutines. Each subroutine is designed to calculate a part of the computational process as described in the following sections.

7.6.1 APR Subroutine

The APR subroutine is designed to calculate the hydraulic parameters. Based on the water level and section geometry sent to the subroutine, the hydraulic parameters

consisting of area, wetted perimeter, effective depth, effective width, water surface width and thalweg elevation are calculated and returned to MAIN. Calculations are based on the geometrical solution of some subsections defined between elevation of water and two consecutive coordinate points of the cross section. For the first and last subsections, the location of the intersection between the water surface and bed is calculated and it is considered as a temporary point. The subsections and the coordinate points are shown in Figure 7.5 schematically.

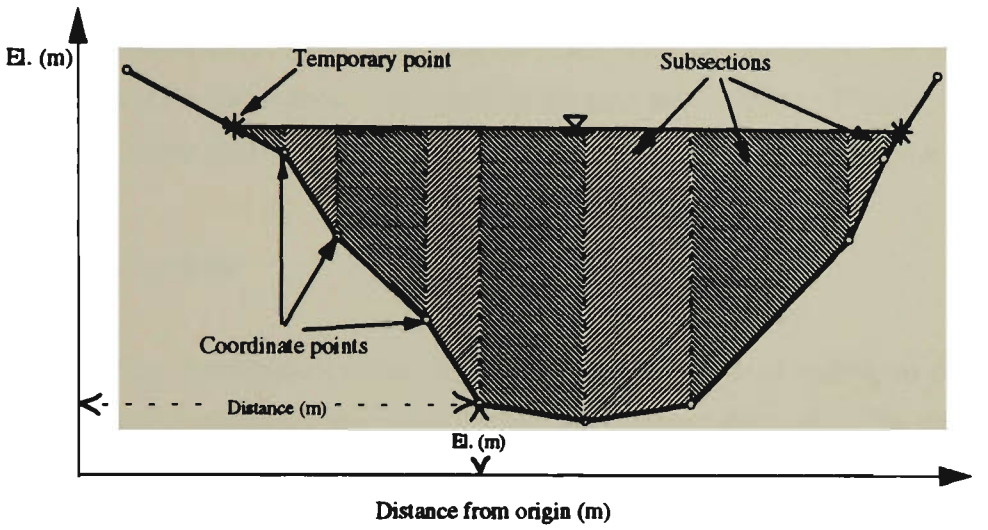

Figure 7.5 Schematic of subsections, coordinate points and temporary points.

7.6.2 SEDMETHOD Subroutine

The SEDMETHOD subroutine serves to estimate the sediment transport capacity. Based on the hydraulic parameters of each cross section, characteristics of sediment particles and the sediment transport method (that the user has specified in the input file), the sediment transport is calculated. Although some of the methods available in the subroutine estimate the bed load and suspended load separately, only total load is returned to the MAIN. The methods available for estimating sediment transport are as follows:

1. Meyer-Peter and Müller (1948) for bed load (suitable for the streams in which suspended load is not significant)
2. Bagnold (1966) for bed load and suspended load
3. Engelund and Hansen (1967) for total load
4. Toffaleti (1969) for bed load and suspended load
5. Ackers and White (1973) for total load

6. Yang (1973) for total load

7. Habibi and Sivakumar, 1993 for suspended load and 1994, for bed load

7.6.3 GEO Subroutine

The GEO subroutine is programmed to estimate the actual sediment transport. The capacity of sediment transport, bed material composition, depth of bed layers, and other control volume characteristics is analysed to estimate the actual sediment transport. Transport of cohesive sediments is estimated in this subroutine. Finally, the average change in the bed layer and bed composition is estimated and sent to the MAIN program.

7.6.4 BED Subroutine

The BED subroutine is considered for distributing the volume of sediment deposition or scour in the bed and estimating the new shape of the cross section. The data including the water level, average change of the bed, geometry of the section and the option chosen for distribution form come from the MAIN (based on the user choice), and the new elevation of the coordinate point is sent back to the MAIN.

7.6.5 TC Subroutine

The TC subroutine estimates the turbidity current characteristics detected in the MAIN. It uses APT subroutine and three functions named F, G and E for this propose. The hydraulic parameters, geometry of cross sections, sediment characteristic and boundary conditions are taken from the subroutine and the new hydraulic parameters are sent to the MAIN. The F, G and E functions are parts of the Runge-Kutta numerical solution, and the APT subroutine calculates the hydraulic parameters of sections based on the effective depth of turbidity currents.

7.7 Numerical Solution

The water surface elevation, sediment transport, bed level, bed material, and turbidity current establishment and transportation are always elements of a complex system resulting in a complicated process. A small change in one of the elements, such as bed elevation, will affect all or some of the other elements directly. However, in the numerical solution for prediction of long term reservoir sedimentation, it is quite

acceptable to solve equations independently in relatively small time steps. Turbidity current depth is directly related to the flow and suspended sediment concentration, and separation between flow and sediment concentration is considered impossible. In supercritical conditions of turbidity current, the solution technique is not very difficult because the upstream is used as the control section for both the flow and sediment. But for subcritical turbidity current conditions, a particular numerical technique is required because, while the flow is controlled from downstream, the sediment concentration is controlled from upstream.

The solution technique for sedimentation processes in a reservoir needs to solve all of the equations (flow, sediment, and turbidity current equations) in an iterative manner for several time steps. At each time step, the flow and sediment are routed in two phases. First, the flow equations are solved to determine water elevation and hydraulic parameters in each section - based on the bed surface elevation from the previous time step. It is routed from downstream to upstream. The sediment is then routed from upstream to downstream. Meanwhile, for each section, a control volume is defined and then input and output volume of sediment are compared to calculate the volume of deposition or scour. The new bed elevation and bed material composition are obtained from sediment analysis within the control volume.

Based on the calculated hydraulic parameters, each section is tested to see whether the plunge point of the turbidity current has occurred. If the turbidity current has not occurred, then the process is repeated for the next section. In the case where the turbidity current plunge point occurs in a section, the analysis of sediment processes is changed to a new mode. The turbidity current equations will be solved for all of the sections between the plunge point and the downstream section to estimate the elevation of the turbidity current surface. Then a set of new hydraulic parameters is defined for these sections. Based on the new hydraulic parameters, the sediment processes will be analysed from the plunge point towards the downstream section.

The geometry of sections and the composition of bed material obtained at the end of each time steps are basic parameters for running the next time step. It is assumed that changes in the bed level and bed composition are reasonably small during each time step, although the changes may be significant over several time steps.

7.8 Input Data Requirements

An input data file is required in order to apply this model to a specific reservoir or river. The input data includes geometrical, sediment discharge and characteristics, bed material characteristics and hydrological data. The input file is written in free format and in the order which is shown in Appendix E.

The geometry of sections and the other dependent parameters should be written from the downstream boundary towards the upstream boundary, respectively. The sections will be defined by coordinate points and they will be written from the left hand side towards the right hand side of the channel respectively.

The sediment characteristics consisting of specific gravity and initial unit weight are defined for clay, silt and sand fractions. The sediment compaction coefficient and the critical bed shear stress for cohesive sediment deposition are defined for clay and silt fractions. The grain shape factor and sediment transport method are defined for the sand fraction. The upstream boundary element for sediment discharge should be defined for the program. At least two points of the flow-sediment correlation curve are needed in the input data. A flow-sediment correlation curve can be calculated from an analysis of historical flow and sediment discharge data or estimated using the sediment transport method. However, some points (up to 10) of the flow-sediment discharge curve should be defined in the input data.

The bed characteristics are defined as a fraction of every grain size in each section. The bed material characteristics can be defined from one to several cross sections. If it is defined in one or some cross sections, the program will calculate the bed gradation in the other cross sections based on the existing data of the nearest upstream and downstream cross sections and by using linear interpolation.

The user indicates his or her desire to consider the turbidity current in the sediment processes, or not, by writing "Y" or "N". Also, the distribution form of sediment deposition or scour in the cross sections must be given in the input data. Following the above, the hydrological data including water discharge, water surface elevation, flow duration, water temperature and turbidity current elevation are defined. These data can be repeated as many times as the user chooses. The number of hydrological data will determine the running time of the program and, therefore, it co-determines the running time for each set of data. In Figure 7.6 a shortened example of the input file with description is presented, however a complete file is presented in Appendix F.

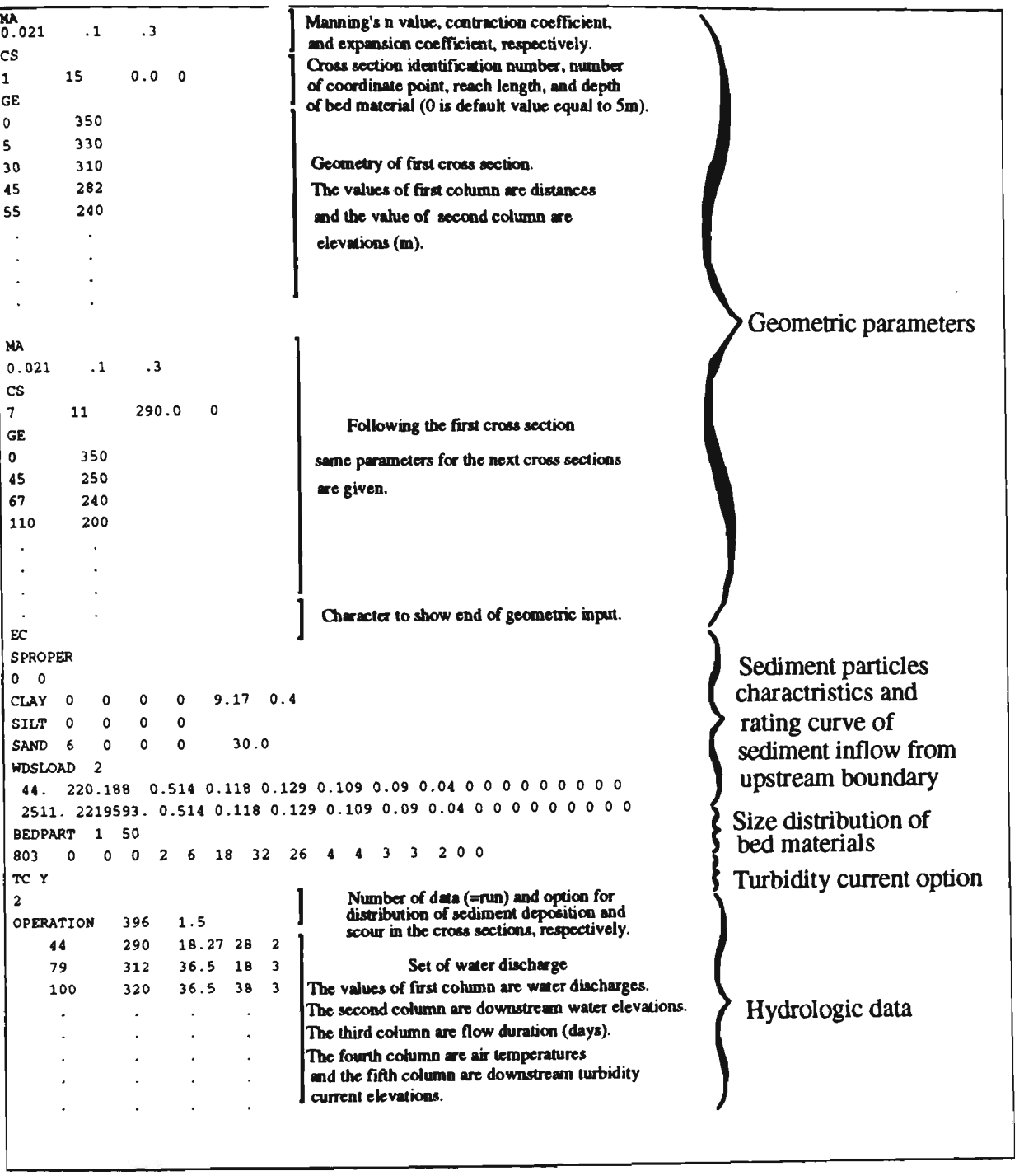

Figure 7.6 An example of the input file of DEPO program.

7.9 Output File

The output file consists of the following information.

- A summary of the input data
- The new geometry of the all cross sections.
- The volume of the inflow sediment and outflow.

- The trap efficiency of the reservoir for the sand, silt, and clay particles
- The initial and new elevation of the bed in the thalweg of the reservoir
- The new bed composition at all of the cross sections.

In Figure 7.7, a shortened example of the output file with description is presented and a complete file is presented in Appendix F.

7.10 Summary

A new model for predicting reservoir sedimentation taking into account the effects of turbidity currents has been developed. The computation processes and numerical solutions employed for modeling have been determined. A feature of the model computation has been shown in a flowchart. All parts of the computer program and their functions have been given briefly. The data will be given to the program via an input file. The input data required for running the computer program and the format have been given. All the results from the computations will be written in an output file. The information from an output file, with an example, are presented. In general, it can be said that the major difference between the proposed computer code and the other available models is in the employment of turbidity current concepts as a function that effects long term sedimentation processes in reservoirs. Seven optional methods are available in the model for predicting the capacity of sediment transport in rivers and reservoirs. Based on the calculated capacity of sediment transport, size distribution of bed materials, active layer thickness, and the possibility of the establishment of an armour layer, the actual sediment transport will be calculated by the program. Transport of cohesive particles are also considered in the prediction of sediment processes. The amount of the sediment deposition or scour in each control volume will be calculated based on the amount of sediment inflow to the control volume and outflow from the control volume.

```
Cross section number=      1.00000
Number of coordinate points=      15
Manning,s n=    0.210000E-01Contraction coefficient=    0.100000
Expansion coefficient=    0.300000     Reach length=    0.000000
points DISTANCE & ELEVATION respectively
       0.000    350.000
       5.000    330.000
      30.000    310.000
      45.000    282.000
         .          .
         .          .
         .          .
Cross section number=      7.00000
Number of coordinate points=      11
Manning,s n=    0.210000E-01Contraction coefficient=    0.100000
Expansion coefficient=    0.300000     Reach length=     290.000
points DISTANCE & ELEVATION respectively
       0.000    350.000
      45.000    250.000
      67.000    240.000
         .          .
         .          .
Specific gravity of water=     1.00000
Acceleration due to gravity=     9.81000
Properties of CLAY particles
Specific gravity=     2.65000     Shear threshold= 0.100000
Initial unit weight= 481.000
Compaction coefficient=     256.000
Properties of SILT particles
Specific gravity= 2.65000
Initial unit weight= 1041.00
Compaction coefficient=     91.3000
Properties of SAND particles
Specific gravity= 2.65000     Initial unit weight= 1490.00
Grain shape factor=    0.667000
Parameter for calculating equilibrium bed=     30.0000
YANG Transport capacity method
**********************************************************************
*          Final Results of Sedimentation Modelling                  *
**********************************************************************
Cross section number       1.00000
points DISTANCE,INITIAL ELEVATION AND FINAL ELEVATION
           0.00       350.00              350.00
          45.00       250.00              250.00
          67.00       240.00              240.00
         110.00       200.00              200.00
         130.00       190.00              193.85
         140.00       180.00              193.85
         155.00       180.00              193.85
         175.00       250.00              250.00
         210.00       250.00              250.00
         230.00       300.00              300.00
         242.00       350.00              350.00
 Cross section number       3.00000
 points DISTANCE,INITIAL ELEVATION AND FINAL ELEVATION
           0.00       350.00              350.00
             .          .                   .
             .          .                   .
```

Geometric data according to input file

Sediment characteristic according to input file

Initial and final coordinate points of the cross sections

Figure 7.7 An example of the output file of DEPO program.

Total Days	Total Sediment Inflow		
	SAND & GRAVEL (in m3)	SILT (in m3)	CLAY (in m3)
7299.96	0.53E+07	0.79E+08	0.15E+09

Total Sediment Outflow		
SAND & GRAVEL (in m3)	SILT (in m3)	CLAY (in m3)
0.14E-05	0.39E+08	0.86E+08

Trap Efficiency of Reservoir			
SAND & GRAVEL	SILT	CLAY	TOTAL
1.0000	0.5101	0.4110	0.4588

Amount of sediment inflow to the reservoir and outflow from the reservoir and trap efficiency of the reservoir

SECTION NO.	DISCHARGE (m3/s)	WS ELE (m)	DISTANCE FROM DAM(m)	INITIAL TALWAGE ELE.(m)	FINAL TALWAGE ELE.(m)
803.00	52.00	336.07	60303.90	309.00	334.63
793.00	52.00	335.95	59903.90	309.00	335.61
780.00	52.00	335.61	59313.90	308.00	335.36
770.00	52.00	335.11	58593.90	308.00	334.89
755.00	52.00	333.26	57633.90	305.00	333.08
.	.	.	.	.	.
.	.	.	.	.	.
.	.	.	.	.	.
.	.	.	.	.	.
.	.	.	.	.	.
.	.	.	.	.	.

Elevation of water after last run, initial and final elevation of cross sections talwage

PERCENTAGE OF EACH PARTICLE SIZE IN COVER LAYER

CROSS SECTION	RLENTO	CLAY(%)	SILT(%)	SAND(%)
1.00000	0.000000	89.0480	10.9513	0.000000
7.00000	290.000	87.8824	12.1174	0.000000
3.00000	1170.00	85.7781	14.2220	0.000000
18.0000	1490.00	79.3638	20.6362	0.000000
124.000	3140.00	59.3534	40.6466	0.000000
.	.	.	.	.
.	.	.	.	.
.	.	.	.	.
.	.	.	.	.
.	.	.	.	.

Final size distribution in cover layer of the bed in all cross sections

Figure 7.7 An example of the output file of DEPO program (continued).

An optional parameter is available in the program for the user to control the distribution of the sediment deposition or scour in the cross sections. Consideration of the effects of turbidity currents on sediment processes is an option in the DEPO model. Therefore, the model is applicable to rivers in addition to reservoirs.

Chapter Eight

APPLICATION OF THE MODEL TO LABORATORY AND FIELD DATA

8.1 Introduction

In order to validate all the procedures and to demonstrate the capabilities of the new model, the model is evaluated with the following two tests:

1. laboratory experiment
2. actual reservoir

A laboratory experiment is a suitable method to find the accuracy of the procedures of the model or to compare the results of two or more solutions. Availability of the complete details of experiments and the possibility to create and control different conditions are the principal advantages of laboratory experiments. Also, the capabilities of a model on a smaller scale can be tested.

Eventually each computer model should be used in an actual watercourse, and so, testing the model in an actual reservoir and comparing the output results with the measured data is very important. On the other hand, actual channels are characterised by irregularity in all aspects. Irregular inlet and outlet discharge of the flow, irregular shape and composition of the bed, irregular bed slope etc., make the prototype case very complicated to model accurately. In this chapter the new model, DEPO, is verified using data from four laboratory experiments and Dez Reservoir. Dez Reservoir is the largest reservoir in the south-west of Iran.

8.2 Experiments on Depositional Turbidity Current

Four turbidity current experiments were conducted in this part of the study (experiments 1, 2, 4, and 6). The turbidity currents were established by mixing the sediment particles in water. The inlet current thickness was set at 40 mm with the help of a sluice gate. The duration's of the experiments were adjusted with the volume of the dense fluid in the mixing tank. The initial parameters in the experiments are presented in Table 8.1. In this table t is the duration of the experiment.

Table 8.1 The initial parameters of the depositional turbidity experiments.

Exp. No.	h_0 (mm)	T (° C)	q_0 (mm^2/s)	Δ_0	t (s)	R_{e0}
1	40	20.0	3.256E-4	0.00243	4080	326
2	40	19.5	1.86E-4	0.0034	5520	186
4	40	19.0	4.07E-4	0.0047	2220	407
6	40	19.2	4.419E-4	0.00538	2460	442

The mean geometric sizes (D_g) of the deposited particles were calculated from the distribution curve of the grains for each of the measurement stations. In Figure 8.1, the mean geometric sizes of the deposited particles are plotted against distance from the inlet gate. In this figure, as expected a progressive shift towards the finer grain size can be distinguished as the distance increases from inlet gate.

8.2.1 Verification of the Model with the Laboratory Experiments

To verify the model with laboratory experiments, some parts of the program including the acceptable errors were changed to adjust them for the smaller scale of the laboratory flume and for the experimental conditions (For example: calculating sediment inflow from rating curve was changed to merely accepting a value from the input file; calculation of the depth of the plunge point was changed to reflect the existing depth of

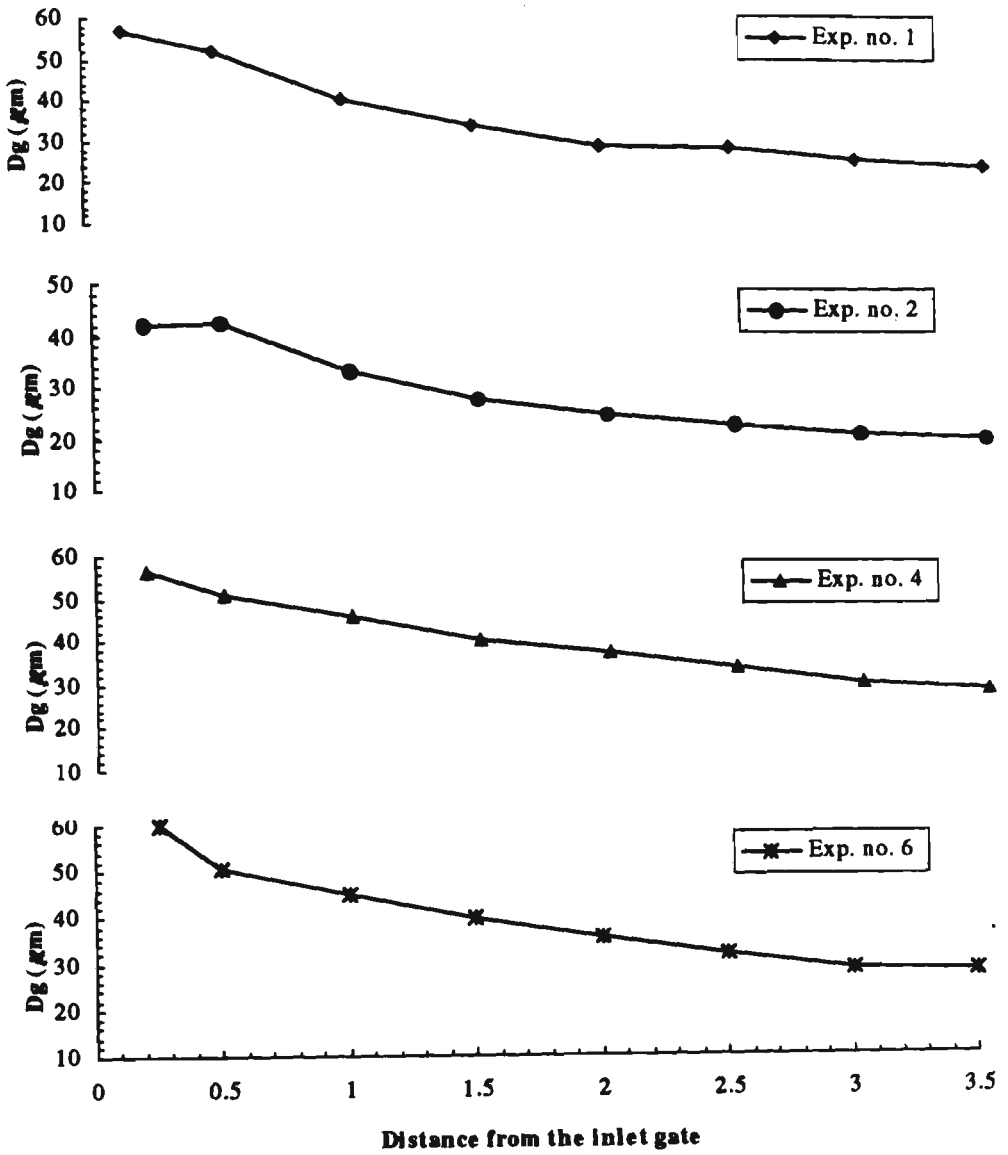

Figure 8.1 Variation in the mean size of the deposited particles with distance from the gate.

the turbidity current at the entrance gate which was 40 mm; the minimum acceptance height of deposited material in each run was changed from 1×10^{-5} m to 1×10^{-10} m; to find the correct value of the new bed elevation, minimum change of computing elevation of the cross sections was changed from 0.005 m to 0.0001 m).

The geometry of the flume at all measurement stations and the slope of the flume were arranged in the input file as the geometric data. Manning's Roughness Coefficient was chosen to be 0.01 according to the material of the bed and the sides of the flume. The percentage of each grain size was calculated from the sediment distribution curve of the inflow particles. Yang's Stream Power equation was chosen for calculating the transport

of particles larger than 62 μm. The inflow discharge, the duration, the elevation of water at the downstream section, the elevation of the turbidity current at the downstream section, and the temperature of the flow were used in the input file based on the measured values. The flat distribution (Figure 7.1) was chosen for distributing sediment deposition on the bed. The model was run for each data set of the experiments. The output results of the model are compared with the measured ones in the following sections.

8.2.1.1 Water Elevation and Turbidity Current Height

The results of the water elevation and the turbidity current height computations performed by the model showed excellent agreement with the measured values. In Figure 8.2, the measured and the estimated water elevation and turbidity current height are plotted against distance for experiment 1, 2, 4 and 6. These results confirm the validation of the numerical solution of the hight of turbidity current.

8.2.1.2 Amount of Sediment Deposition

In Figure 8.3, the measured and estimated amount of sediment deposited in the bed of the flume are presented for all experiments. The amounts of deposited material are presented in kg/m^2 to show both the values in a bigger scale. In this figure, the unbroken lines show the measured value and the broken lines show the estimated value. Comparison of the results show very good agreement between the computed and measured deposited material. The observational error between the two values is very low and can be ignored. This part of the results confirm that the DEPO model can be used for the computation of sediment process in an actual reservoir.

8.2.1.3 Size Gradation of Deposited Sediment

In the output of the model, composition of the bed in the cover layer will be divided into three classes: particles larger than 62 μm; particles between 4 and 62 μm; and particles less than 4 μm. Therefore, the bed material distribution curve at each of the measurement locations were divided in these three classes and are plotted in column format in Figure 8.4. In this figure, the results predicted by the model are also shown.

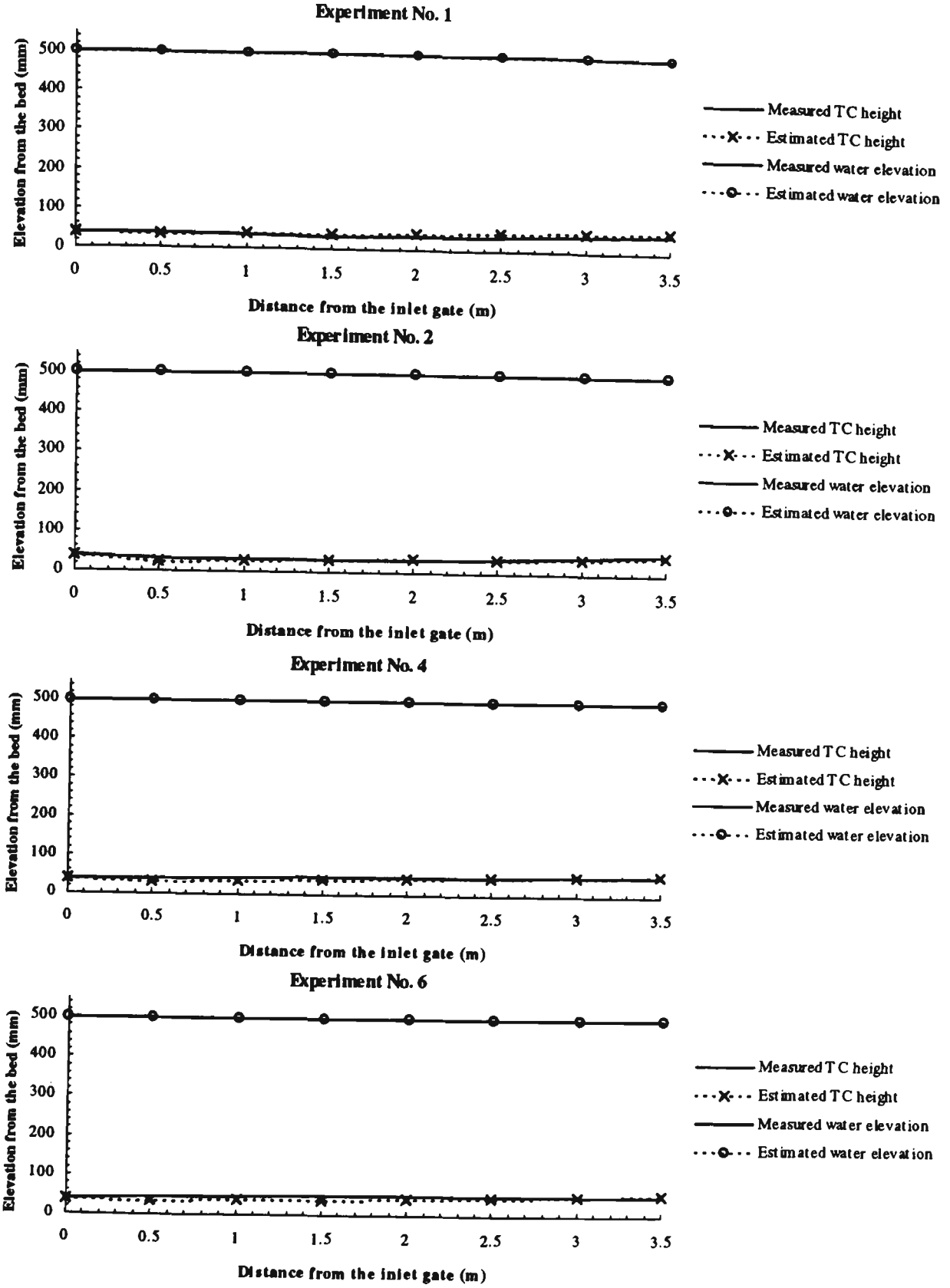

Figure 8.2 Measured and estimated water elevation and height of turbidity current.

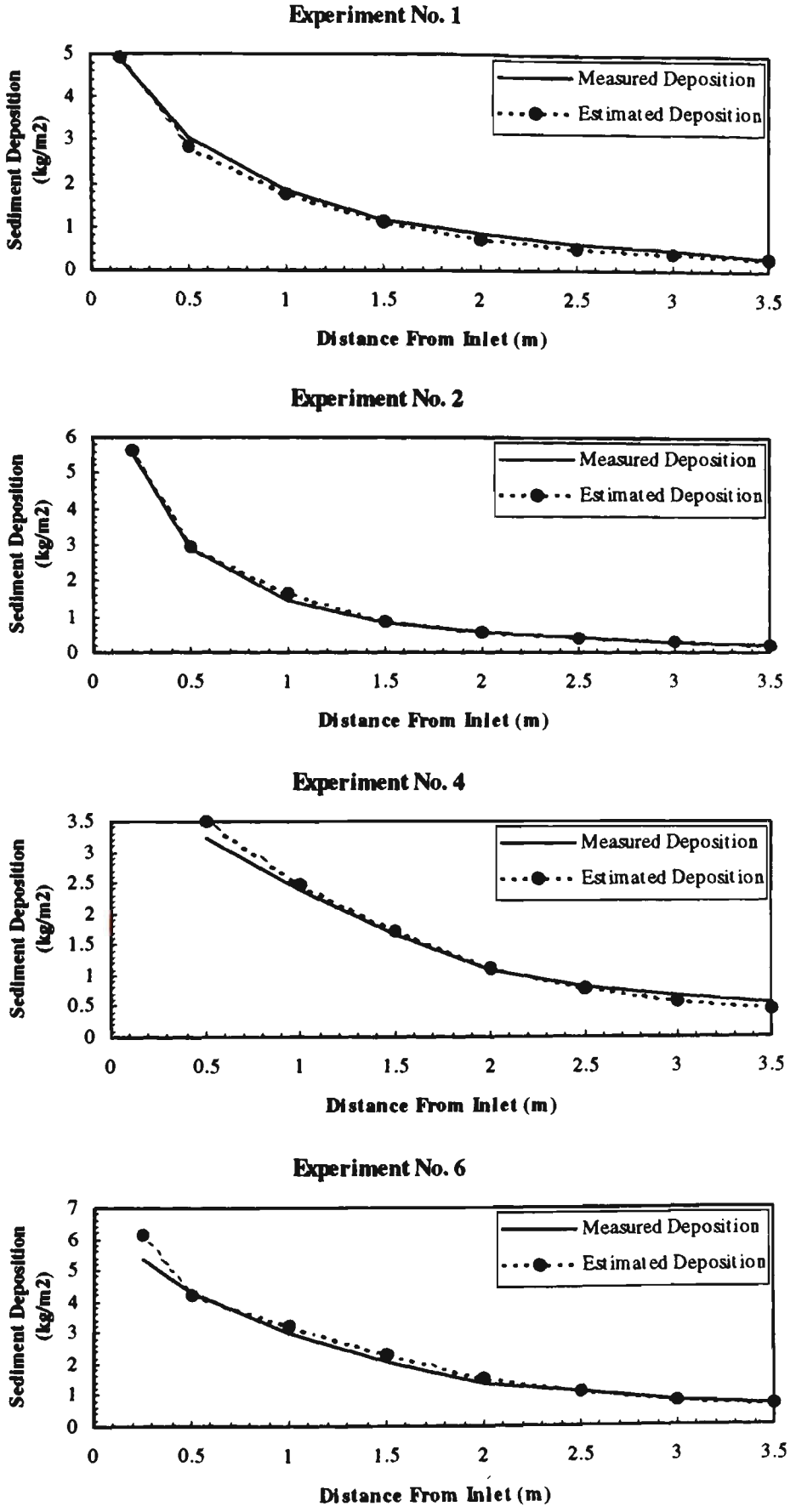

Figure 8.3 Measured and estimated amount of sediment deposited in the bed of the flume.

Comparison of both the measured and the estimated values shows a disagreement between the predicted and the measured values of size particles larger than 62 μm. The measured composition of the deposited particles shows that significant amounts of particles larger than 62 μm are deposited in the first measurement location and it gradually reduces in the other locations. In some of the experiments, the particles larger than 62 μm can be found even 3 metres away from the inlet gate. But the output of the model does not show any of this size particles in the above mentioned locations and based on these results, the particles larger than 62 μm should be deposited before the first measurement location. For sizes less than 4 μm the predicted and measured values show relatively good agreement in all experiments. Further consideration of the results obtained from the experiments of the head of the turbidity current shows that this disagreement is related to the effects of the head. In Figure 8.5 and Figure 8.6, the result from two sets of experiments of the head that have initial parameters similar to experiments 1 and 2 are shown. The largest grain size available in the head and body of the two turbidity currents can be seen in these figures. The broken line shows the particle size equal to 62 μm. As can be seen in both of the figures, that particles larger than 62 μm have not been found in the body of the currents after the inlet gate. On the other hand, in both experiments, the sand size particles have been found in the head of the current some distance after the inlet gate. In Figure 8.5, the particles larger than 62 μm have been found up to 3 metres away from inlet gate and, consequently, this size of particles was slowly lost as these particles settled down. This finding is in complete agreement with the results of deposited materials shown in the Figure 8.5 (Exp. no. 1). In Figure 8.6, the same finding can be found for experiment 2.

In summary, it is confirmed that the head of the turbidity current itself has different effects on the sedimentation processes. These effects are more pronounced specially when the duration of the current becomes small. Also, the disagreement observed in the grain sizes of the deposited material is related to the effect of the head of current that could not be considered in the model.

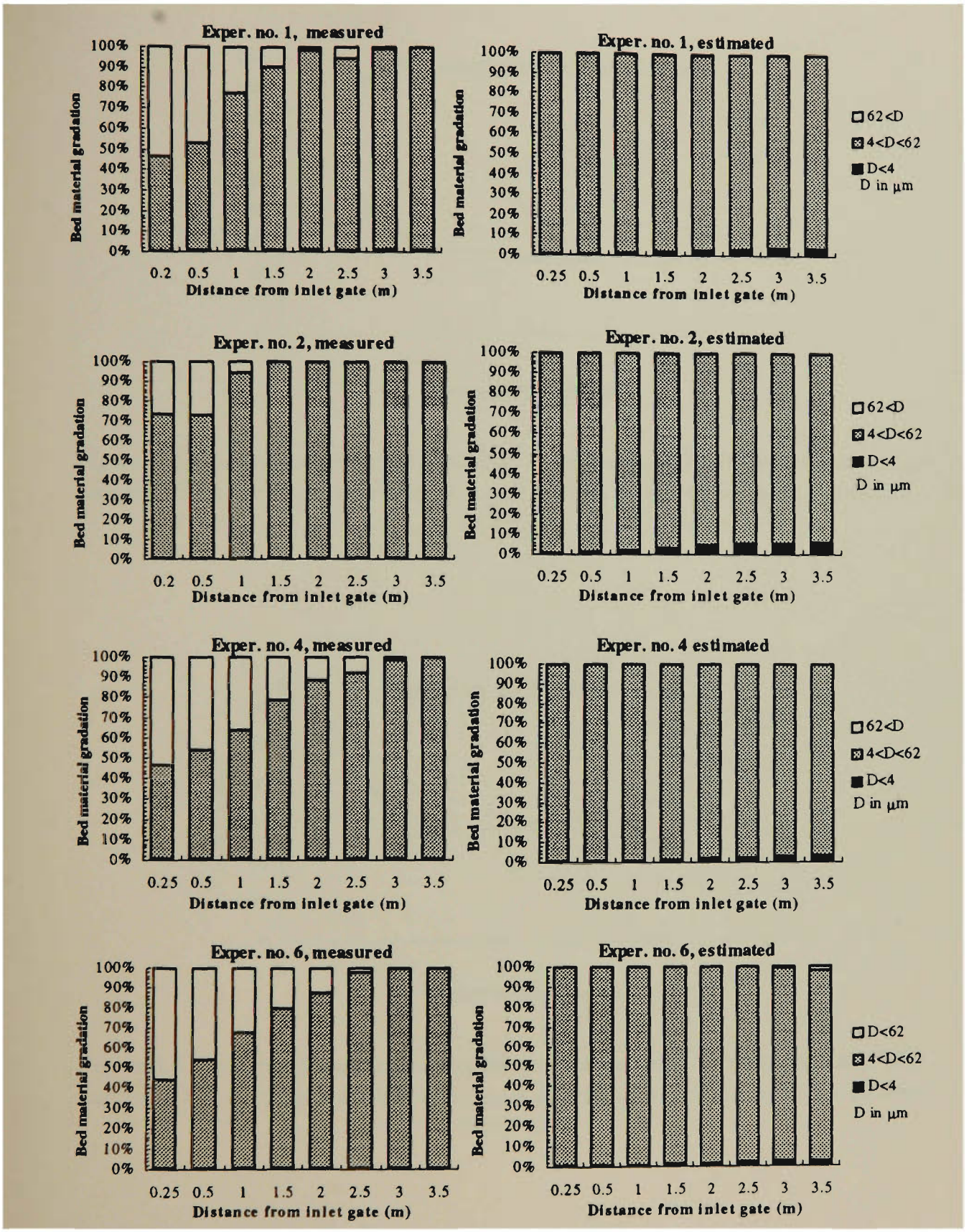

Figure 8.4 Measured and estimated material composition in the bed of flume.

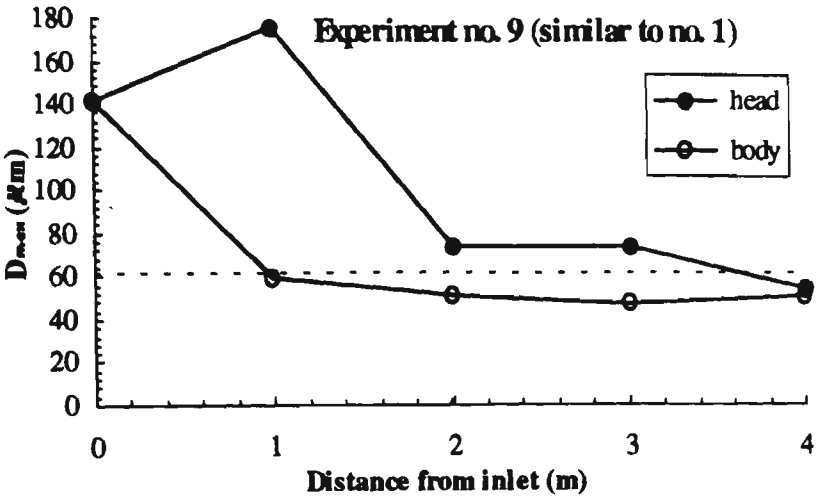

Figure 8.5 The largest grain size available in the head and the body of the turbidity current. Data are from experiment 9. Δ_0 = 0.00282, q_0 = 3.49E-4 m^2/s, h_0=40 mm, T=21°C.

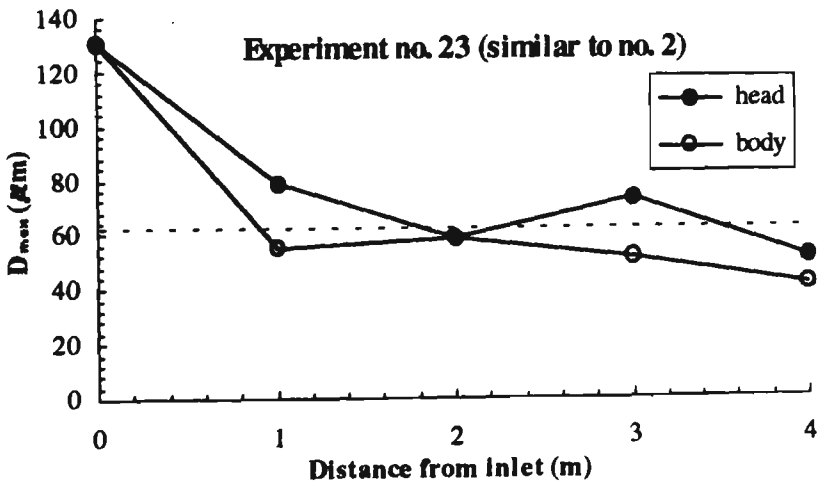

Figure 8.6 The largest grain size available in the head and the body of the turbidity current. Data are from experiment 23. Δ_0 = 0.0031, q_0 = 2.32E-4 m^2/s, h_0=40 mm, T=22°C.

8.3 Dez Reservoir Sedimentation Model

In a semi-arid country like Iran, with a long dry period in the summer and high probability of flood in winter and spring, the role and performance of reservoirs are crucial. The supply of sufficient water for urban, industrial and agricultural activities, flood control and supply of electricity requires large reservoirs to store fresh water

during flood seasons. While collecting and capturing water during floods, a large volume of sediment is transported into and deposited in reservoirs affecting the life-time of the reservoirs. Thus, a precise evaluation of sediment distribution and a reliable prediction of future sedimentation in a reservoir is very important, and must be estimated before the construction of the dam and also during the reservoir operation.

8.3.1 General Description of the Reservoir

Dez Dam is the highest dam in Iran. It is located in the south west of Iran. This double curvature arched dam is 203 meters high and is constructed on the Dez River. Its average annual discharge is 229 cubic meters per second. The location of the reservoir in relation to its catchment is shown in Figure 8.7. The reservoir came into operation in 1962.

The length of the reservoir is 60 km and the surface area is about 63 km^2. Figure 8.8 shows the plan view of the reservoir (the cross sections used for computation are also shown in this figure). Its capacity in full supply is 3330 million cubic meters and it provides flood protection, hydro-electric power and water storage for irrigation of 125,000 ha of agricultural lands in dry season as reported by K.W.P.A. (1971a). Two monitoring stations named Tale-Zang and Dast-Mashon are located upstream of the reservoir entrance and downstream of the dam, respectively.

Outflow from the reservoir takes place from three different levels:

- Three irrigation gates are located at an elevation of 222.7m of dam wall and the maximum discharge through each gate is 60 cubic meters per second.
- Two turbine tunnels each 10 m in diameter, are located at an elevation of 275m near dam wall and the maximum discharge through each tunnel is 240 cubic meters per second.
- Two tunnels are located at an elevation of 335m for bypassing flood and the maximum discharge through each one is 3000 cubic meters per second.

The section of the dam wall showing the important elevation are shown in Figures 8.9 and 8.10.

The reservoir watershed has an area of 17365 km^2 and has an average slope of 12.1%. The catchment is located between 48° 10′ and 50° 21′ E longitude and between 31° 34′ and 34° 7′ N latitude. It is a young catchment from the geological point of view. Therefore, many parts of the catchment have very high slopes. High slopes and other human activities in the catchment are reasons for high erosion in the basin. The river and branches are also geologically new and have strongly eroded beds. The bed slope and elevation of the river, and its branches with downstream distances, are shown in Figure 8.11.

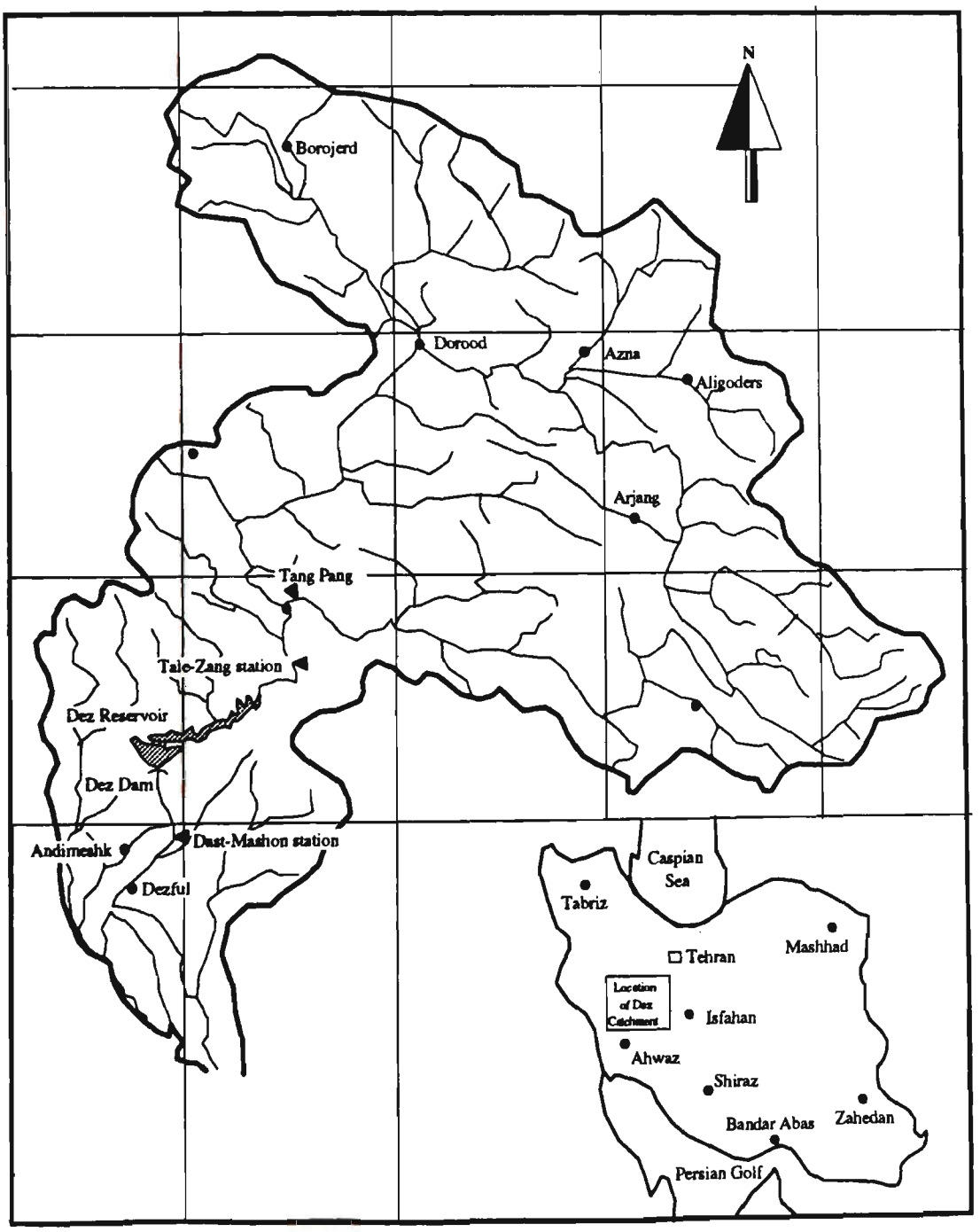

Figure 8.7 Dez Reservoir and its catchment.

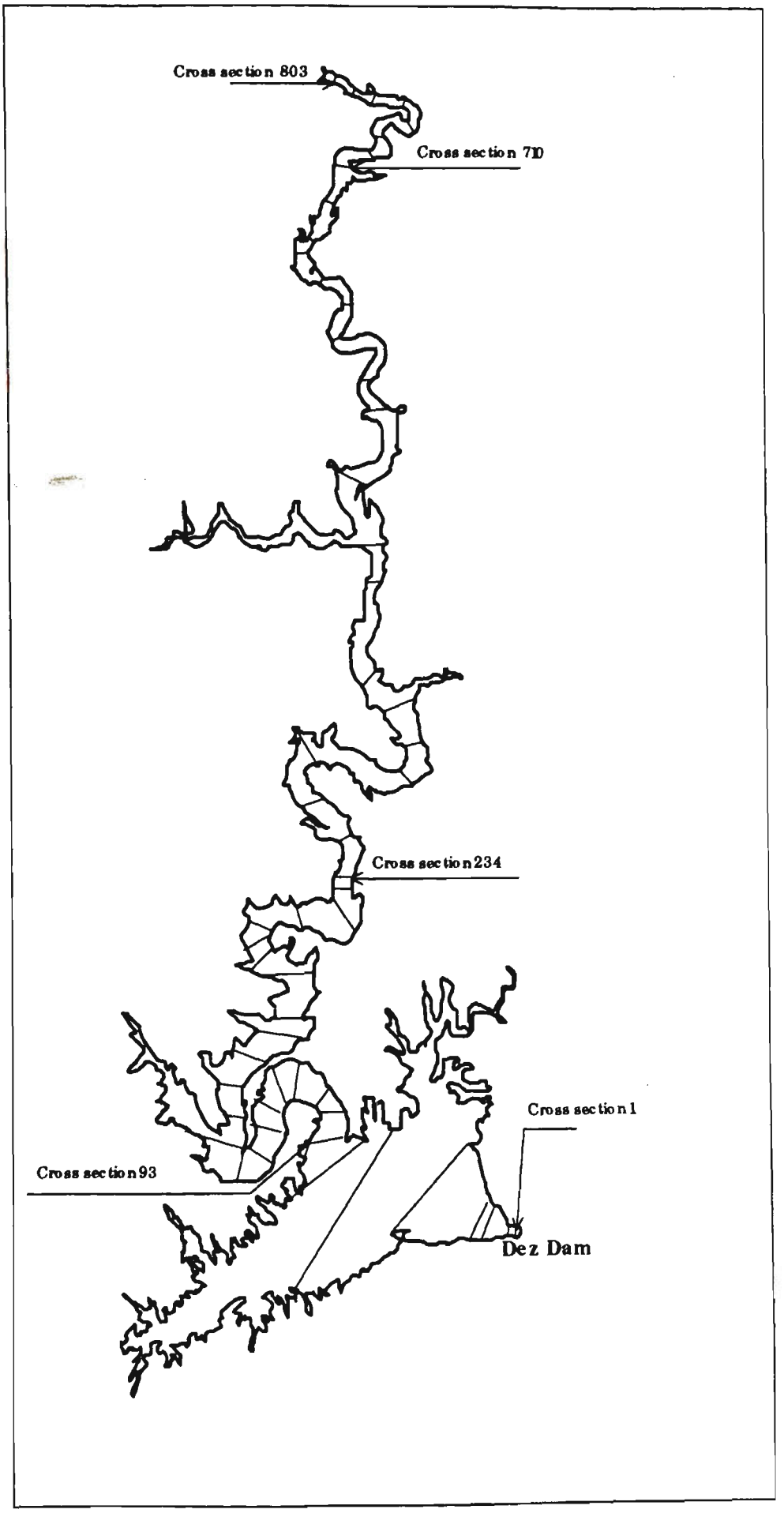

Figure 8.8 Plan view of Dez Reservoir.

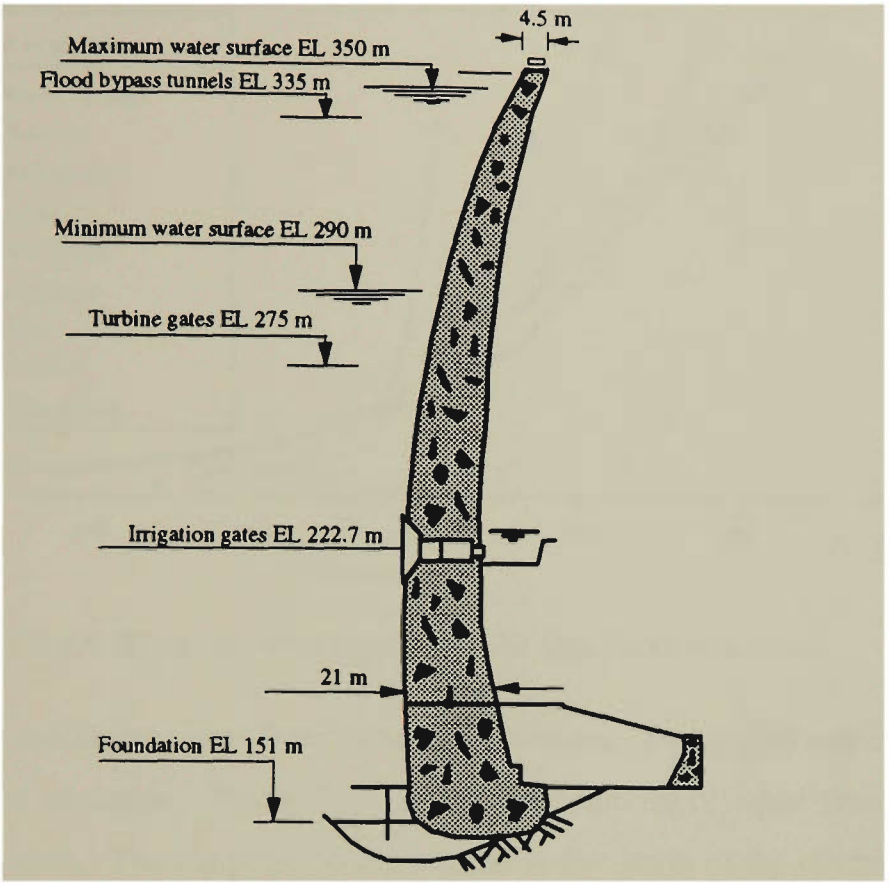

Figure 8.9 Dez Dam cross-section and important elevations (Khozestan Water and Power Authority, 1983).

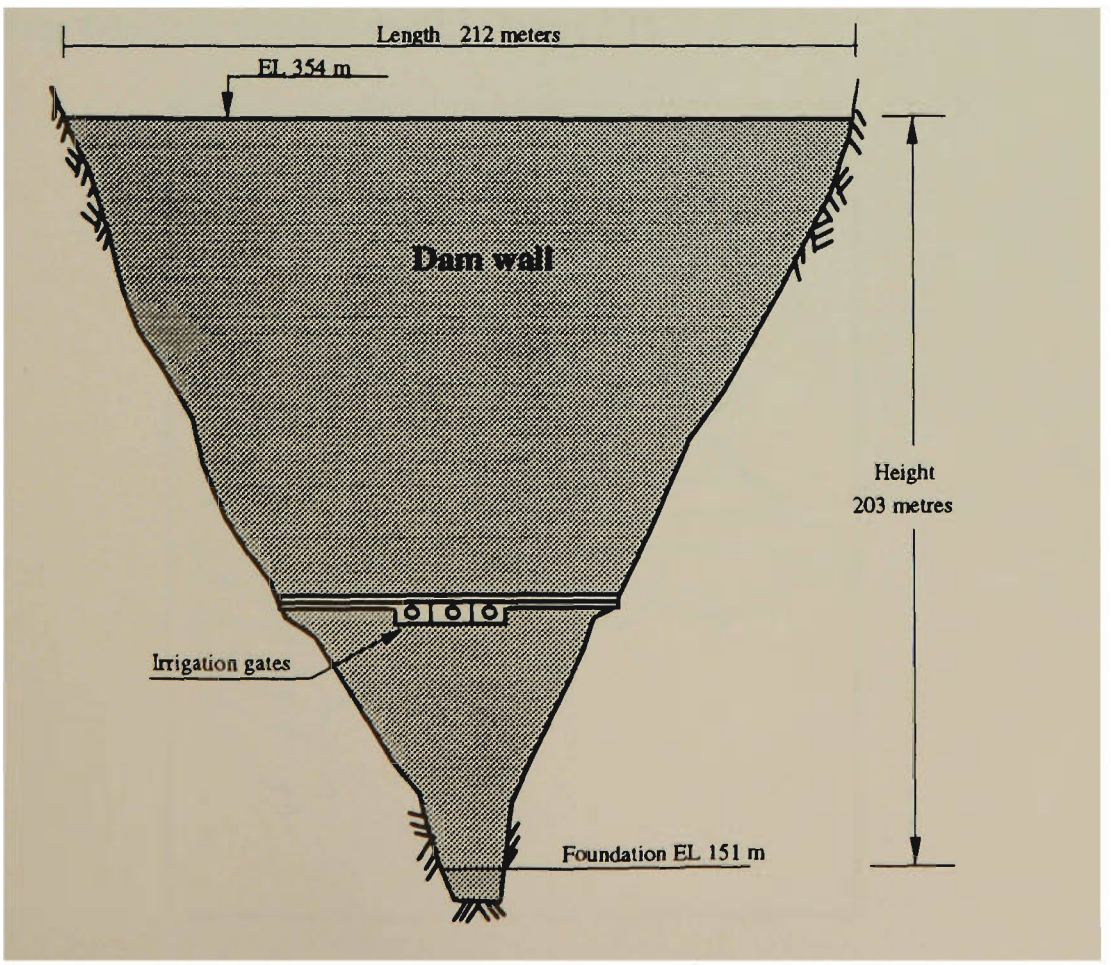

Figure 8.10 View of Dez Dam from downstream.

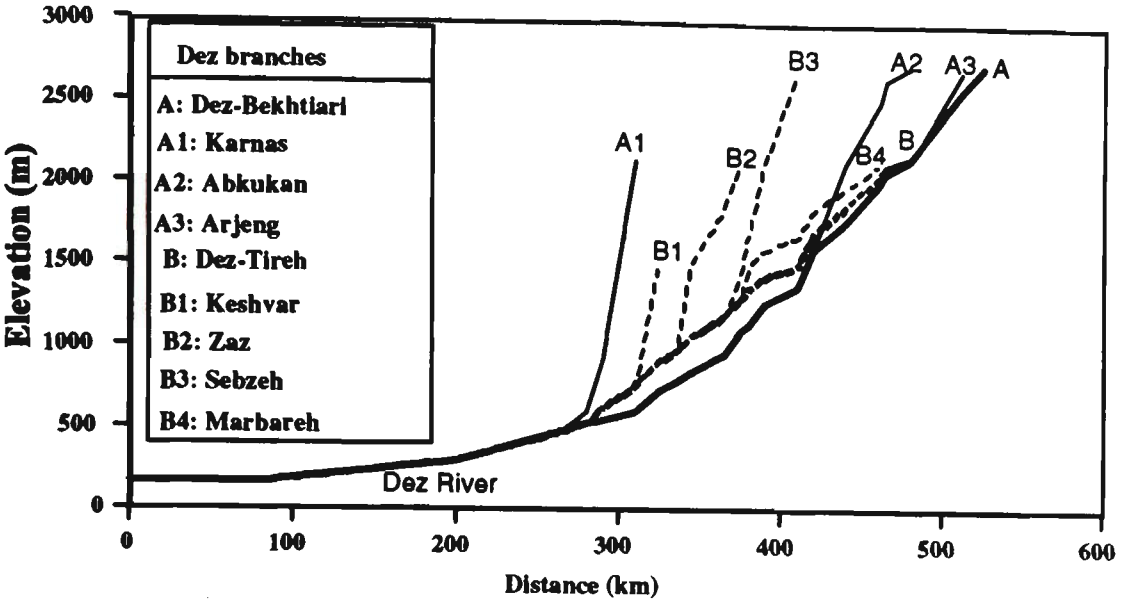

Figure 8.11 Slope and the elevation of the Dez River branches.

The climate in the catchment varies from location to location. The rainfall rate increases with the catchment elevation. Figure 8.12 shows the contours of equal precipitation depth in the catchment. The temperature and rainfall in two parts of the catchment are shown in Figure 8.13. Most of the rainfall occurs between November and May and about seventy percent of the runoff flows during these months. Monthly average river inflow in the Tale-Zang station is shown in Figure 8.14.

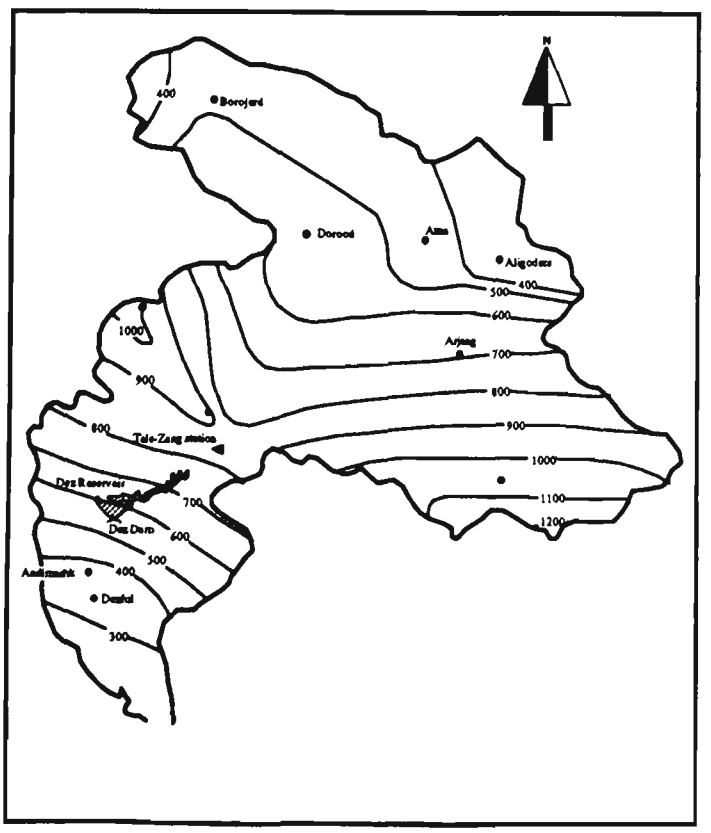

Figure 8.12 Isohyets map of annual precipitation in Dez Catchment.

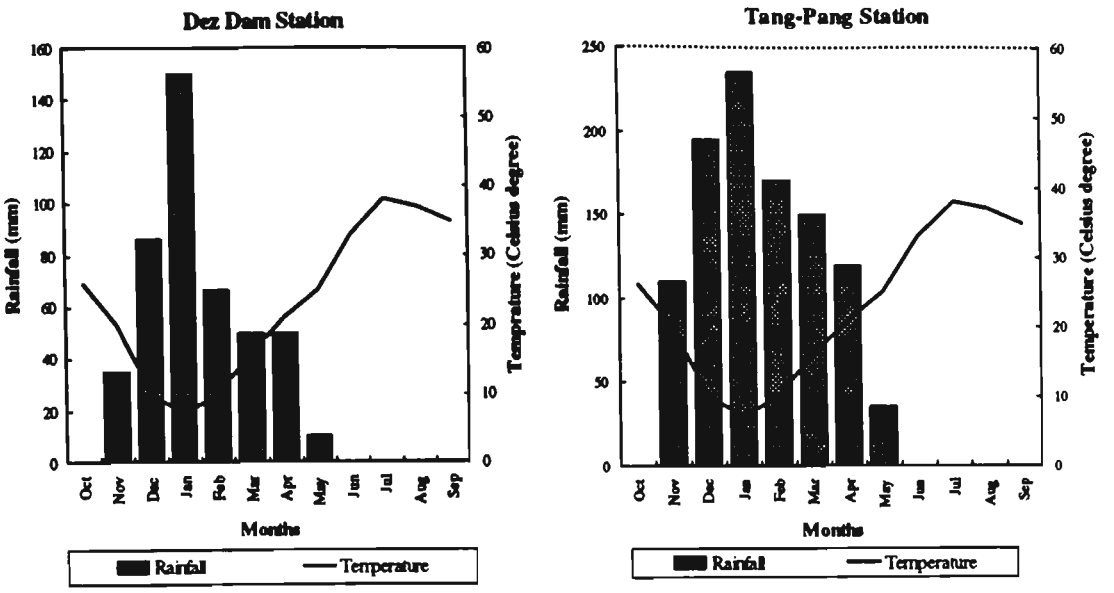

Figure 8.13 Temperature and rainfall in two parts of the Dez catchment.

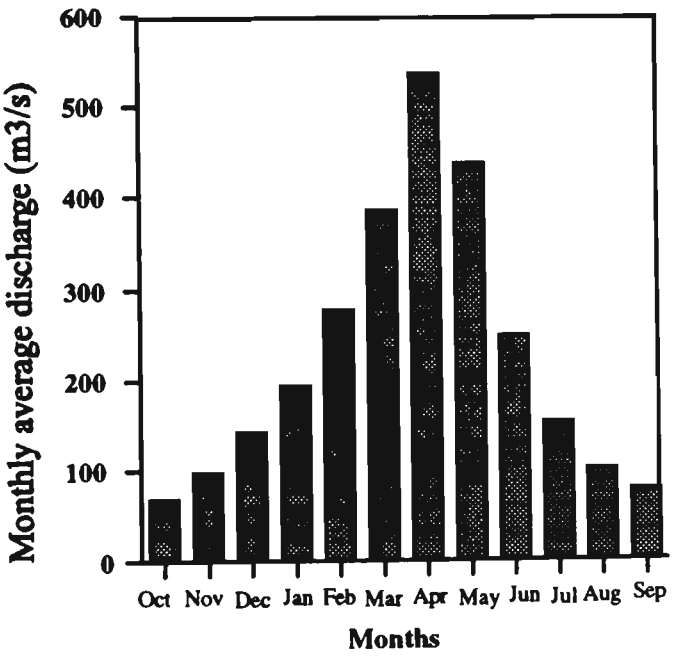

Figure 8.14 Twenty years average monthly discharge of Dez Reservoir (1957 to 1977).

8.3.2 Initial Data For Computation

The hydraulical and hydrological data for the Dez Reservoir were collected mainly from Tale-Zang and Dast-Mashon stations. The Dez reservoir resurveyed in 1981 and the results are available. The following data have been compiled for the Dez Reservoir.

1. Average daily river discharge from the Tale-Zang station based on thirty years (1955 - 1985) measured data (Figure 8.15, Ghomeshi, 1988)

2. Eighteen years (1969 - 1986) average sediment concentration data from the Tale-Zang monitoring station (Ghomeshi, 1988)
3. Average gradation curve of sediment inflow from Tale-Zang monitoring station (T.M.A.B., 1986)
4. Ten years (1977 - 1987) stream bed grain size from river in the Tale-Zang monitoring station (Ghomeshi, 1988)
5. Average daily discharge from the Dast-Mashon station based on ten years (1975 - 1985) river data (Ghomeshi, 1988)
6. Fourteen years (1974 - 1987) sediment concentration data from the Dast-Mashon station (Ghomeshi, 1988)
7. The results of reservoir resurvey in 1981 (T.M.A.B., 1986)
8. Monthly temperature at the reservoir (T.M.A.B., 1986)
9. Average Manning's n value from the Tale-Zang monitoring station
10. Monthly average water elevation near dam wall (1989 to 1992) as shown in Figure 8.16 (Khozestan Water and Power Authority, 1992)

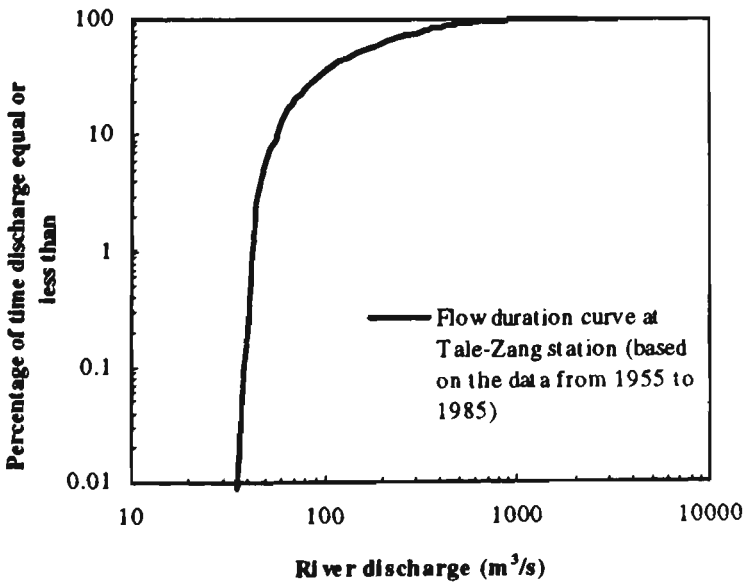

Figure 8.15 Flow duration curve of Dez River at Tale-Zang station.

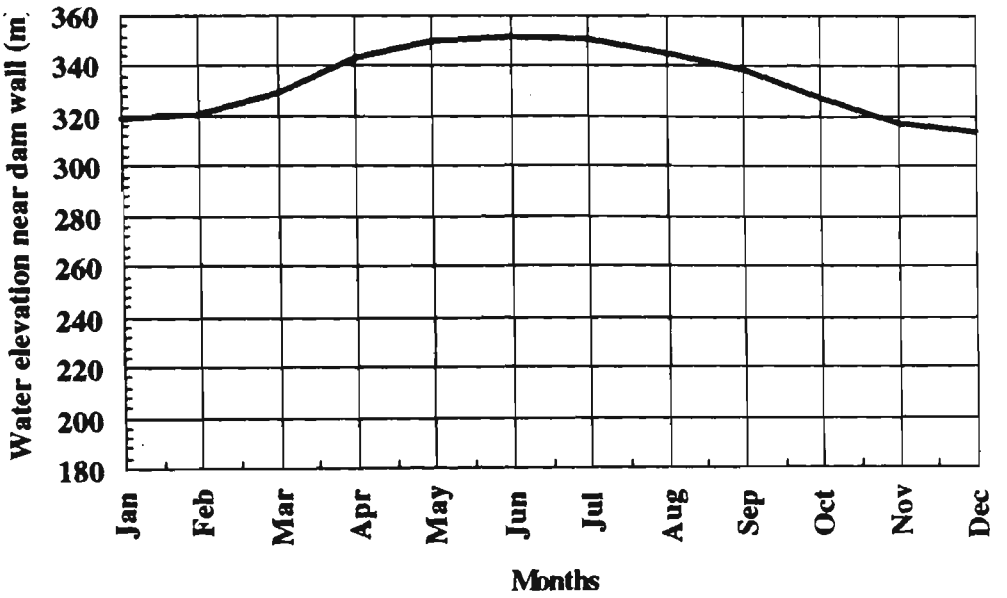

Figure 8.16 Monthly average water elevation near dam wall in Dez Reservoir. (show period 89-92)

8.3.3 Sediment

The suspended sediment rating curve for the inflow sediment is drawn by using 237 sediment concentration samples over seventeen years (1970 to 1987) with the help of the statistical package "SAS". The measured data are presented in Appendix G. The result of the statistical analysis is given by the following equation.

$$Q_s = 0.0329(Q)^{2.2796} \qquad (8.1)$$

where

Q_S = suspended sediment discharge in tonnes per day.

Q = flow discharge in cubic meters per second.

The suspended sediment rating curve and Equation 8.1 are shown in Figure 8.17. The average materials gradation curve of sediment inflow is shown in Figure 8.18. The bed materials gradation curve has been determined from analyses of ten years data of the bed particle size distribution at the Tale-Zang station and is shown in Figure 8.19. This information is used as initial bed characteristics of the other cross sections in the reservoir. As can be seen, the gradation curve of bed materials is very different from the gradation curve of sediment materials transported by the flow. This significant difference

is perhaps due to the dominance of the wash load in the suspended load of the stream. It should be noted that in Dez River the suspended load is almost 90% of the total load (Ghomeshi, 1988)

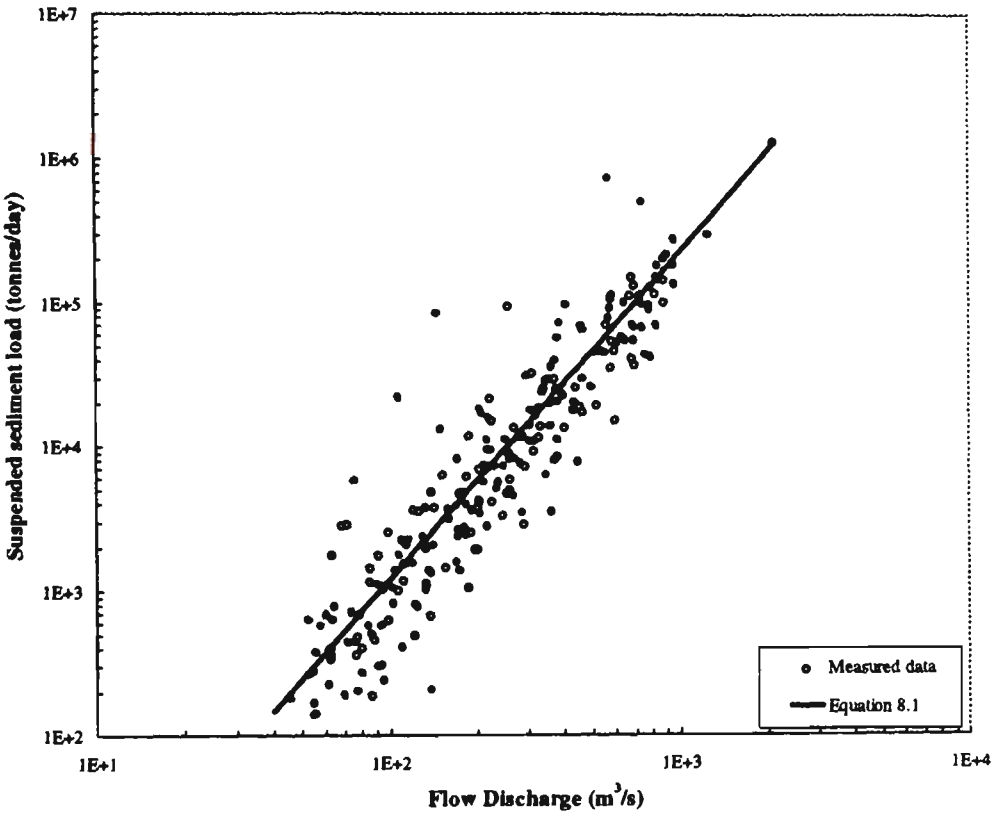

Figure 8.17 Suspended sediment rating curve of the Tale-Zang monitoring station.

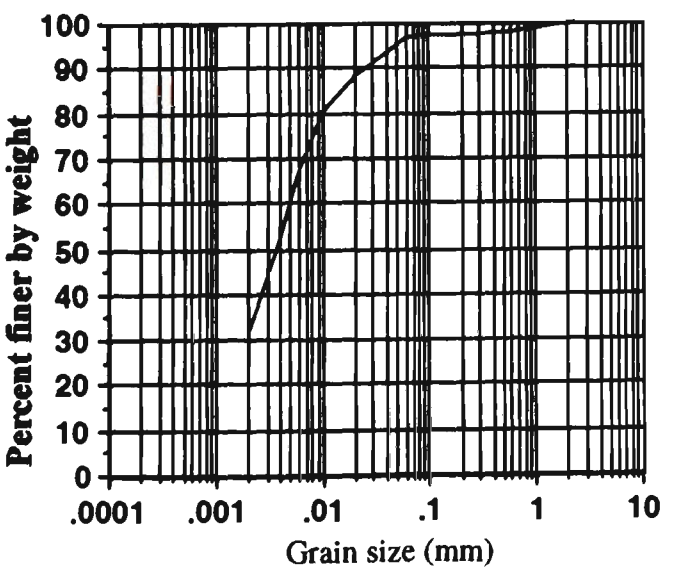

Figure 8.18 Gradation curve of sediment inflow to Dez Reservoir.

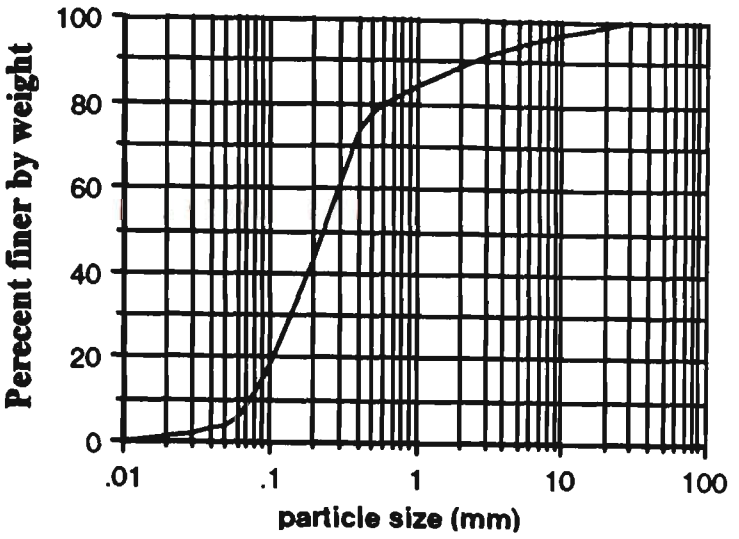

Figure 8.19 Gradation curve of Dez River bed-material at the Tale-Zang station.

8.3.4 Water Flow and Turbidity Current Computations

The computer model "DEPO" was run using 57 reservoir cross sections. The location of the cross sections are shown in Figure 8.8 and the node points can be found in the first part of Appendix F. All the data needed for this purpose, including node points of cross sections and sediment and hydrologic data, were collected and arranged in an input data file. Sediment particles were divided into six classes including clay, very fine silt, fine silt, medium silt, coarse silt and sand particles (Table 8.2). Yang's stream power equation was chosen as a sediment transport formula because it is reliable to use for natural stream (Habibi and Sivakumar, 1993).

Table 8.2 Classification of sediment and percent of each class in sediment inflow

Classification	Grain size (mm)	Percent of each class presented in sediment inflow at Tale-Zang Station
Clay	Less than 0.004	52.5
Very fine silt	0.004-0.008	19.5
Fine silt	0.008-0.016	12
Medium silt	0.016-0.031	5.35
Coarse silt	0.031-0.0625	7.65
Sand	0.0625-2.0	3

The downstream elevation of turbidity currents are assumed to be equal to 300 m (the elevation between two main outlet; turbine tunnels and overflow tunnels). It seems this elevation is a good assumption for upper elevation of turbidity current in the absence of any measured data is in the cause when no.

In reservoirs usually the water elevation near the dam wall is measured. In Dez Reservoir, except for the data on the boundary condition required for running the model, the other flow data inside the boundary were not available to compare the computed and measured values. The computed elevation and velocity are ideal to test the numerical procedures of the water and turbidity current computations.

The annual water inflow to the reservoir was divided into eighteen categories between 2510 m^3/s (with a duration of 3.6 hours in a year), and 44 m^3/s (with a duration of 18.27 days in a year). These categories and their corresponding downstream water elevations and air temperatures are shown in Table 8.3.

Table 8.3 The classified water inflow to Dez Reservoir for running the "DEPO" model with corresponding downstream elevations, durations and air temperatures.

Water inflow (m^3/s)	Downstream water elevation (m)	Duration (Days)	Temperature (° C)
44	290	18.27	28
79	312	36.5	18
100	320	36.5	38
170	289	36.5	10
295	329	36.5	18
405	350	36.5	30
770	343.2	10.95	25
1100	335	3.65	25
2300	335	0.18	25
2510	335	0.15	25
2000	335	0.4	25
1700	335	1.1	25
1310	335	1.8	25
570	343.2	18.25	25
220	320	36.5	38
128	321	36.5	10
62	299	36.5	32
52	290	18.25	28

In Figure 8.20, the predicted elevation of clear water and turbidity current depth along the reservoir resulting from three different initial conditions are shown. In this figure it can be seen that in the high flow the estimated depth for turbidity current is very close to the water elevation and affects the whole reservoir. In low flow the depth of turbidity current is low and follow near the bed of the reservoir.

8.3.5 Bed Level Computation and Comparison with Measured Data

The "DEPO" model was run in order to predict bed elevation after 20 years of operation. The average annual inflow was divided into eighteen categories for each year (Table 8.3) and was continued for 20 years . The initial bed gradation of all the cross sections was considered as the same as the bed gradation in the Tale-Zang Station. The flat distribution option (as shown in Figure 7.1) was chosen for calculating the distribution of the sediment deposition in each section. This was because the reservoir is a deep reservoir and also the results of resurvey have shown this kind of sediment distribution on the reservoir bed.

The program was run, without using the turbidity current effects, and different sediment transport equations were used. The results of using the available sediment transport equations are shown in Figure 8.21. These figures can be used for comparing the applicability of different sediment transport equations to Dez Reservoir.

The sudden reduction in prediction of the bed close to the dam wall, which appears in all cases (Figure 8.21), is related to the reservoir cross sections at that location which are very narrow and, therefore, the prediction coincides with the hydraulic condition at those cross sections. Measurement of some sediment deposition in that part of the reservoir may be related to the effects of the dam wall. The mean of the discrepancy ratio, M_c, and the mean absolute deviation of the discrepancy ratio, A_d, are used to show the performance of each equation. These estimators are introduced in Chapter 6. These estimators were calculated for the above-mentioned methods and are presented in Table 8.4.

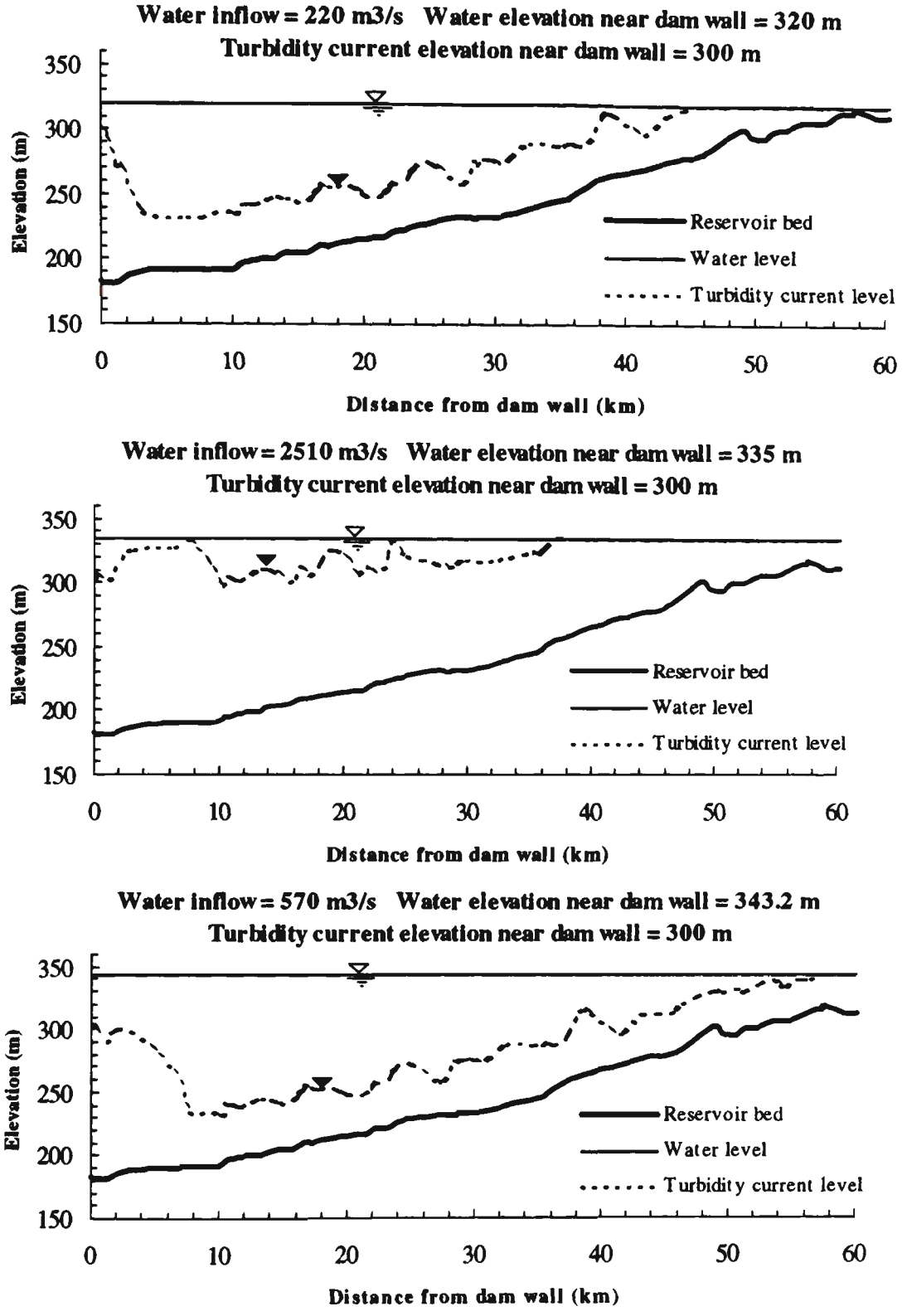

Figure 8.20 The estimated water level and turbidity current depth along the Dez Reservoir using the "DEPO" model.

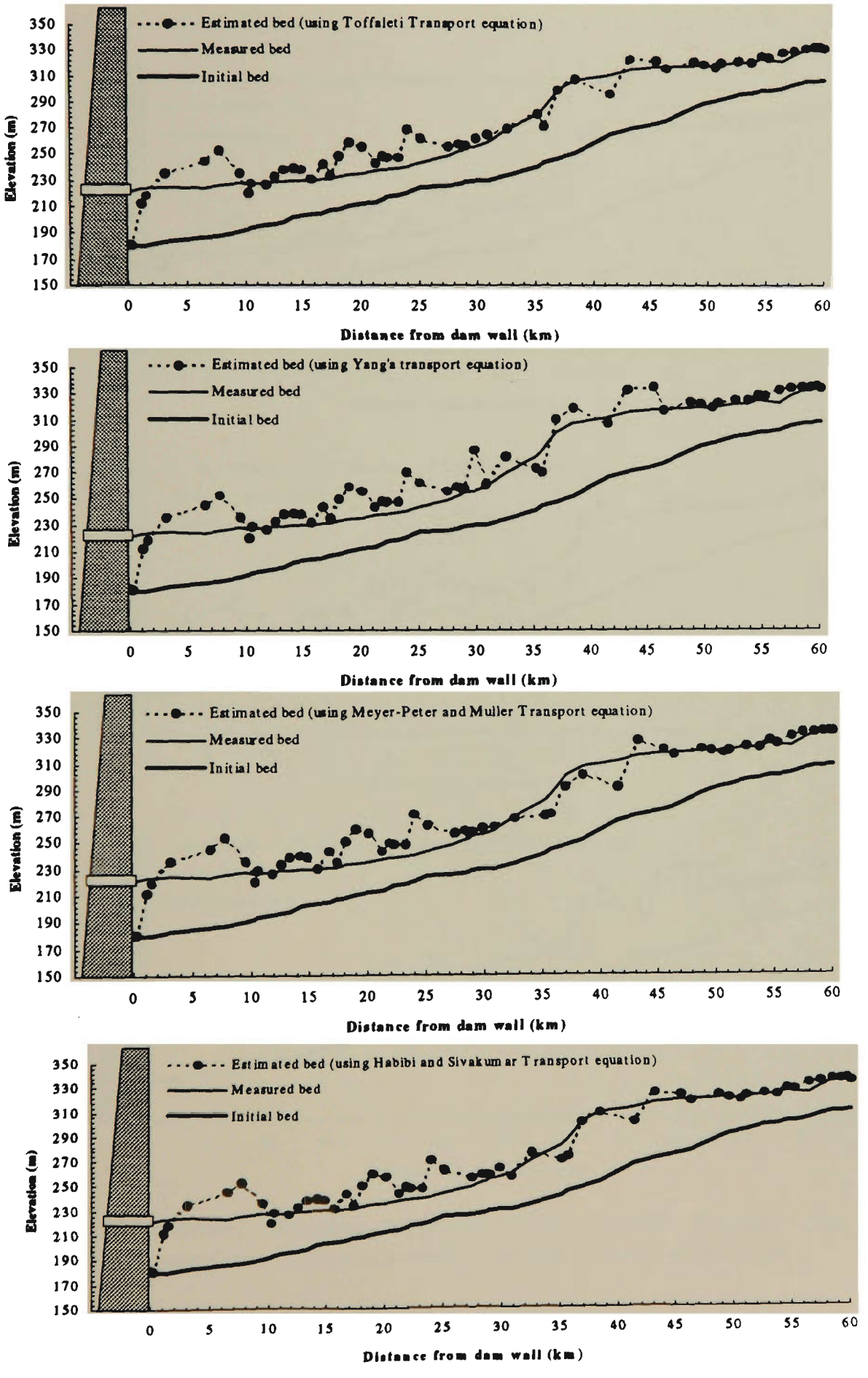

Figure 8.21 Measured and estimated bed level of Dez Reservoir after 20 years operation. Effects of turbidity currents were not considered.

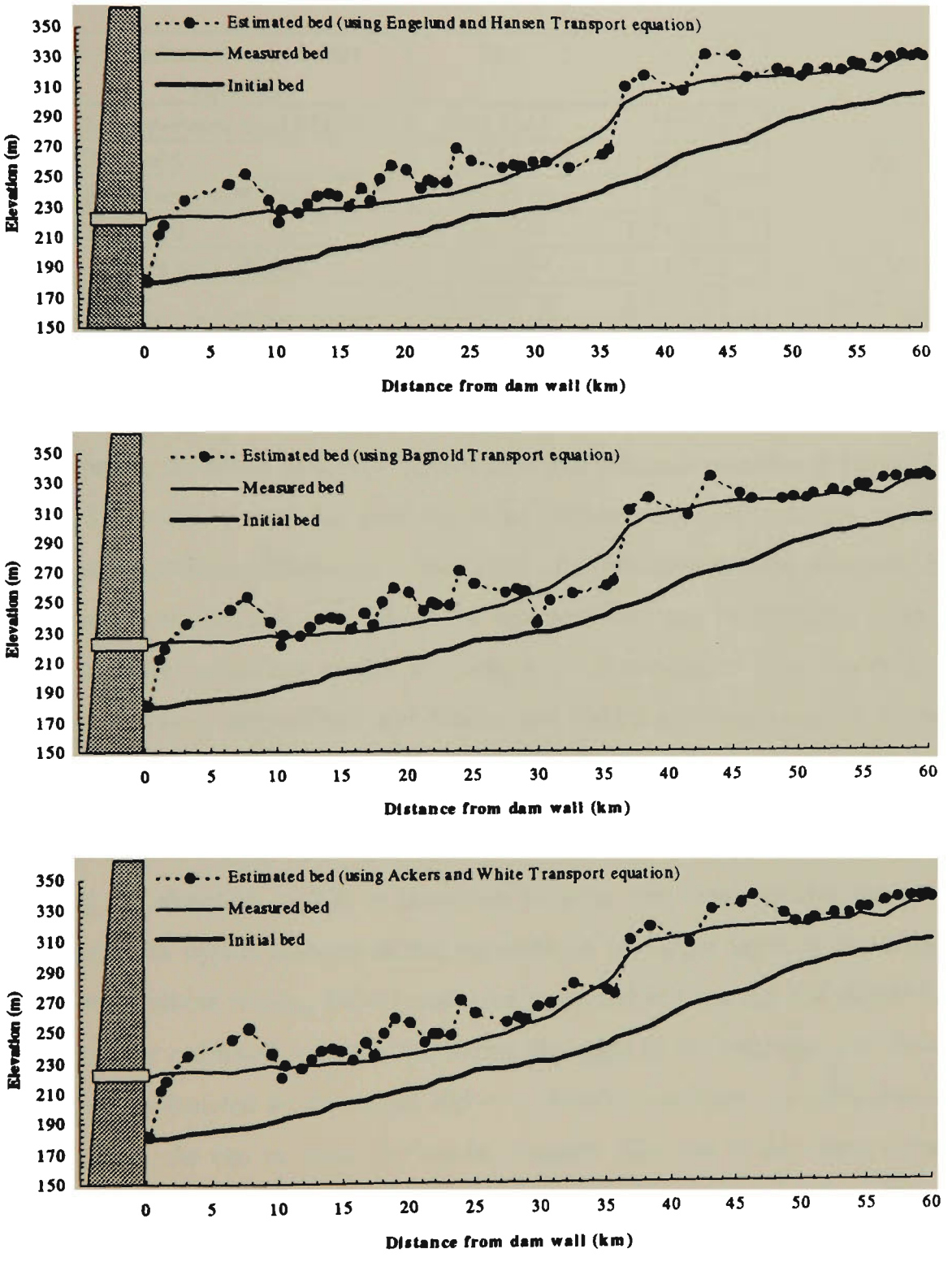

Figure 8.21 (continued) Measured and estimated bed level of Dez Reservoir after 20 years operation. Effects of turbidity currents were not considered.

Table 8.4 The values of M_e and A_d obtained using different equations to evaluate bed level in Dez Reservoir with the measured data.

Sediment transport equation	M_e	A_d
Meyer-Peter and Müller	1.011561	1.035843
Bagnold	1.012344	1.03868
Engelund and Hansen	1.014976	1.03868
Toffaleti	1.01174	1.032517
Ackers and White	1.020384	1.032756
Yang	1.019371	1.035305
Habibi and Sivakumar	1.012382	1.033723

From comparing the result of using different sediment transport equation in Figure 8.21 and Table 8.4, it can be seen that generally using different sediment transport equations does not show significant differences in prediction of sedimentation in the reservoir. This may be due to the fact that only 3% of the sediment load can be predicted using the sediment transport equations shown in Table 8.2. However, in Dez Reservoir the methods of Toffaleti, Meyer-Peter and Müller, and Habibi and Sivakumar have shown better results.

The option of existence of turbidity currents was run with the aid of initial data and by considering the elevation of 300 m (elevation between two main outlets; the turbine tunnels and flood bypass tunnels) as the elevation of the upper layer of the turbidity current. The results of running DEPO model are presented in Table 8.5 and Figure 8.22. In Table 8.5, the estimated volume of sediment deposited in the reservoir, and also the trap efficiency calculated by the model and two empirical methods are compared with measured value. As can be seen, the results obtained from the model using turbidity current effects match the measured values showing the importance of including this effect in large reservoirs.. In this table, the estimated volume and trap efficiency by DEPO model can be compared with the estimated value obtained from the methods of Churchill (1948) and Brune (1953). As can be seen, the trap efficiency estimated by the DEPO model is very close to the measured one, while the Churchill and Brune methods have shown a value larger than the measured.

Table 8.5 Sediment volume and trap efficiency measured and estimated with different methods after 20 years.

Method	**Sediment volume accumulation (m^3)**	**Trap efficiency**
Measured (1981)	200000000	0.85
DEPO model estimate, considering turbidity current effects	202900000	0.86
DEPO model estimate, without considering turbidity currents effects	217336680	0.93
Brune Method	217899000	0.93
Churchill Method	234300000	1.0

In Figure 8.22, the measured and estimated sediment deposition profile after 20 years and the initial bed of the reservoir are shown together. This figure can be compared with the case of not considering turbidity current effects presented in Figure 8.21. The mean of the discrepancy ratio, M_e, and the mean absolute deviation of the discrepancy ratio, A_d, are also calculated to evaluate the prediction method as:

$M_e = 1.001714$

$A_d = 1.026489$

By comparing both these values and the parameters in Figure 8.22 with the cases not considering turbidity currents, it can be seen that the estimated profile is significantly improved by incorporating the effect of turbidity current. In Figure 8.23, the measured and estimated sediment deposition are shown in selected cross sections of the reservoir. The location of these cross sections can be found Figure 8.8.. As can be seen from these four cross sections, except cross section number 1 (see page 194 for the explanation of the problems in predicting in this cross-section) the predicted bed level are very close to the measured bed.

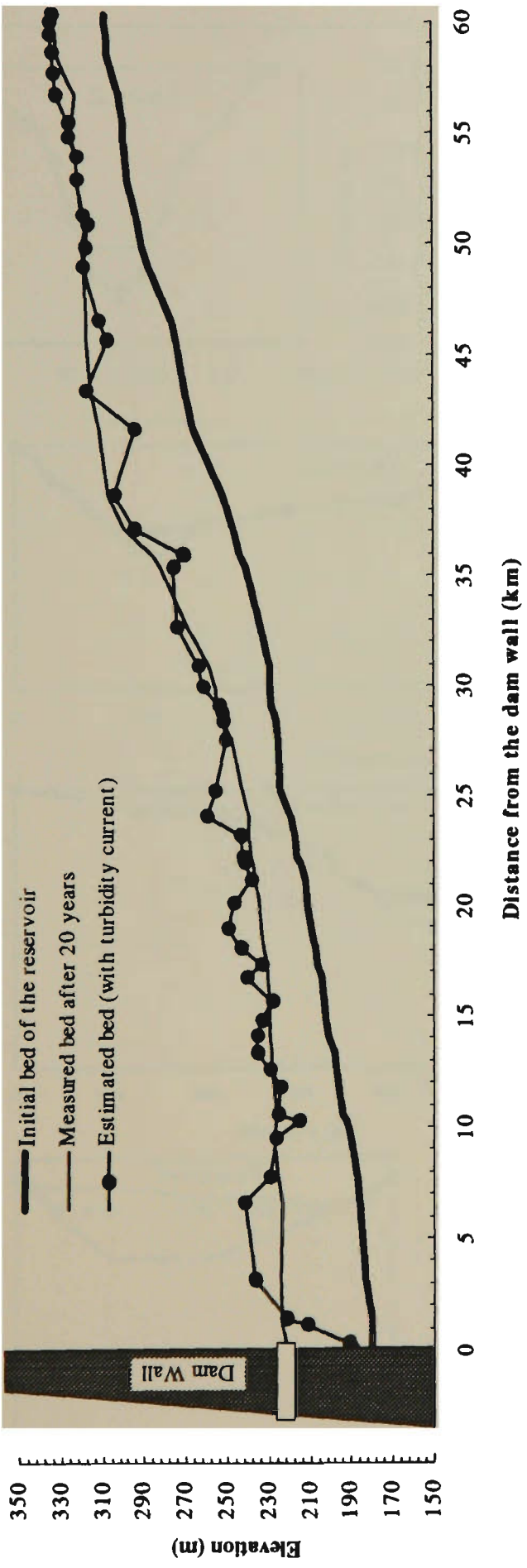

Figure 8.22 Profile of estimated and measured sediment deposition in Dez Reservoir thalweg corrected for the effect of turbidity currents.

199

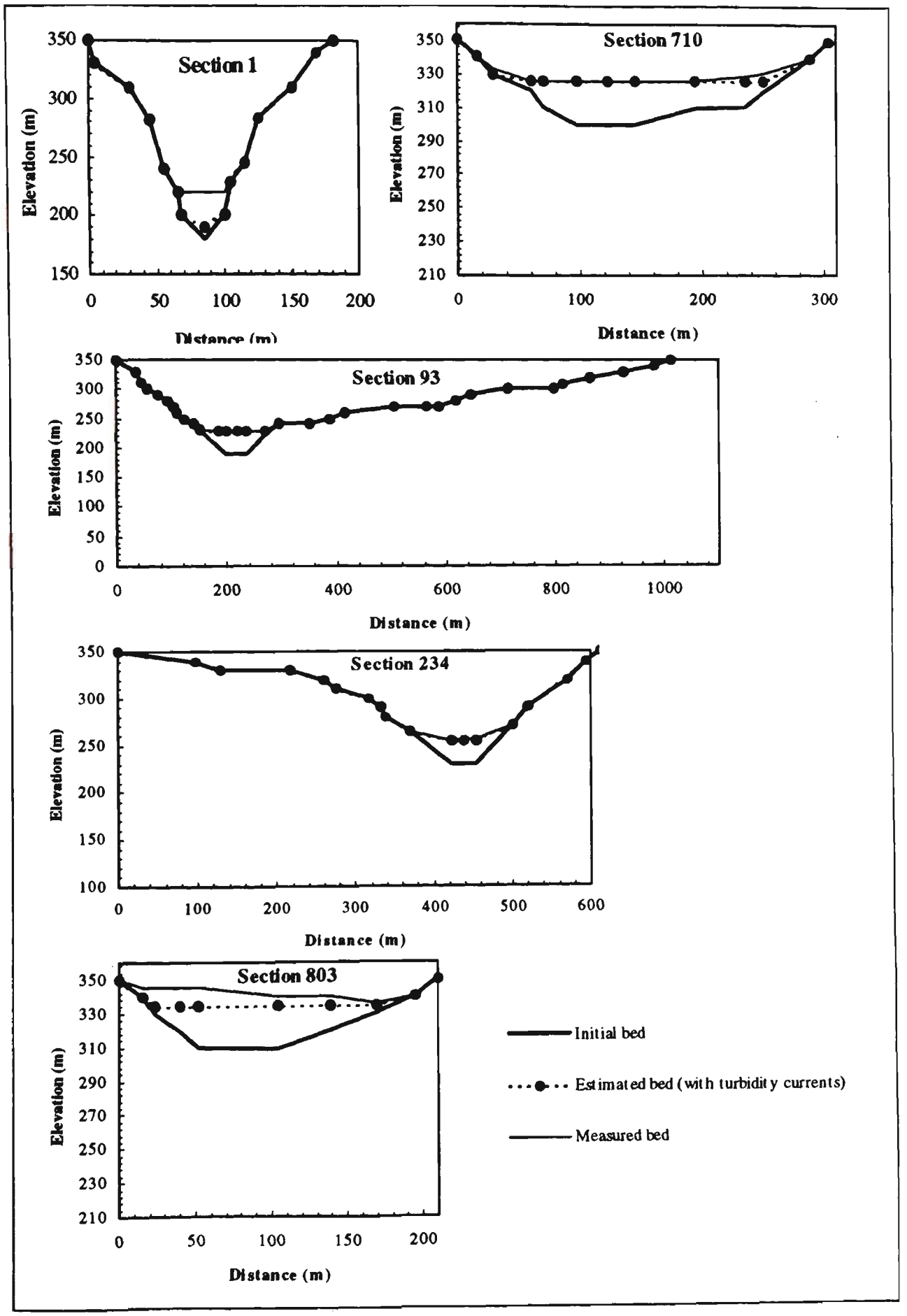

Figure 8.23 Sediment deposition measured and estimated by DEPO in five cross sections of Dez Reservoir.

8.3.6 Computed and Measured Bed Material Composition

In reservoirs, the composition of material in the surface layer of the bed will be changed significantly due to the deposition processes. The average bed material will progressively change to finer material during the operation period. In the input data, the average bed material composition at Tale-Zang Station (near the entrance of the reservoir) was assumed to be the initial bed composition for all cross sections of the reservoir (Figure 8.24). In Dez Reservoir, data on the measured bed material composition in the surface layer after 20 years of operation was available and they are shown in Figure 8.25. The bed material composition in the active layer of the bed after 20 years of operation was calculated by the DEPO model and it is shown in Figure 8.26. From the comparison of the measured and predicted bed material compositions, it can found that in the segment between the dam wall (distance = 0) and the cross section number 420 (distance = 45572 m), the model did not predict any sand particles in the active layer and is in agreement with the measured data. The differences between silt and clay fractions in all cross sections are less than 10%. The model predicted sand particles in the active layer in the cross sections between cross section number 420 (distance = 45572 m) and cross section 803 (distance = 60304 m). However, the measurement only showed the sand particles between cross sections number 755 (distance = 57634 m) and cross section 803 (distance = 60304 m). Generally, these errors are acceptable in such complicated processes.

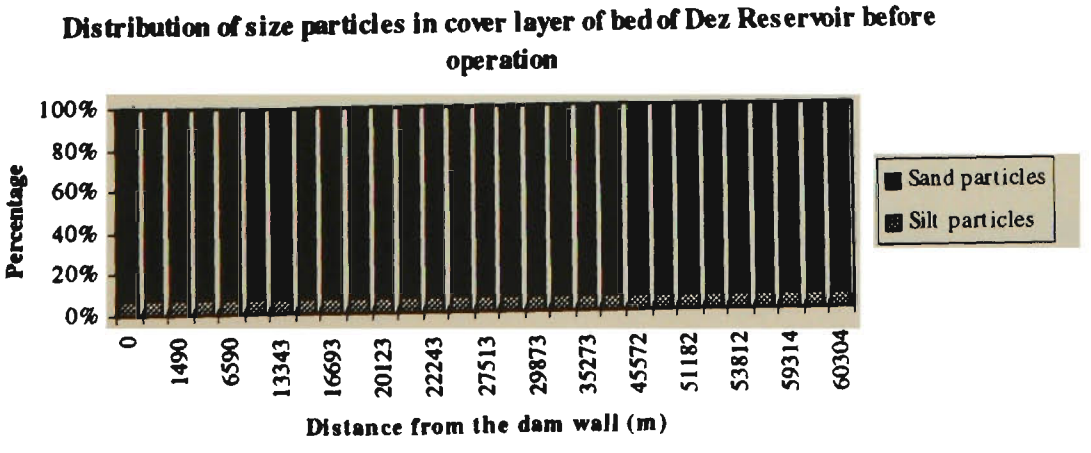

Figure 8.24 Bed material composition in cover layer of bed of Dez Reservoir before commissioning (it assumed same as bed material at Tale-Zang Station).

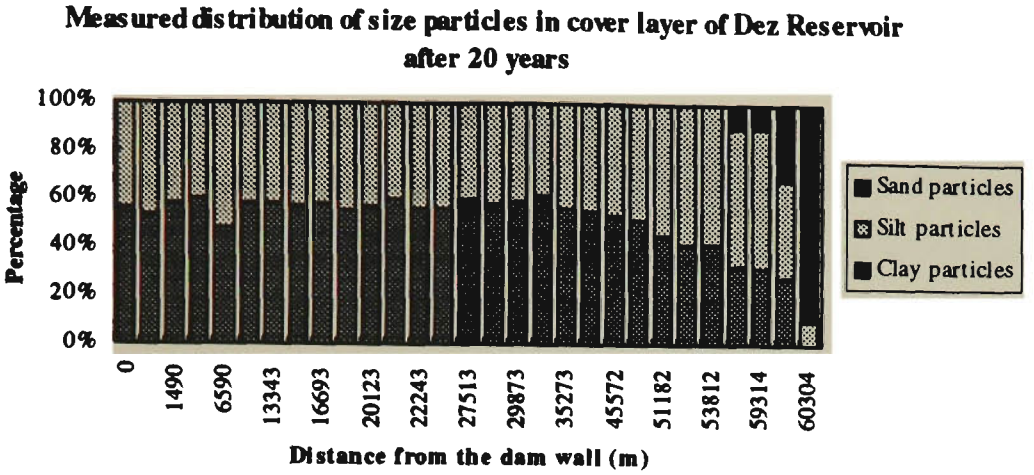

Figure 8.25 Measured bed material composition in the surface layer of Dez Reservoir after 20 years of operation

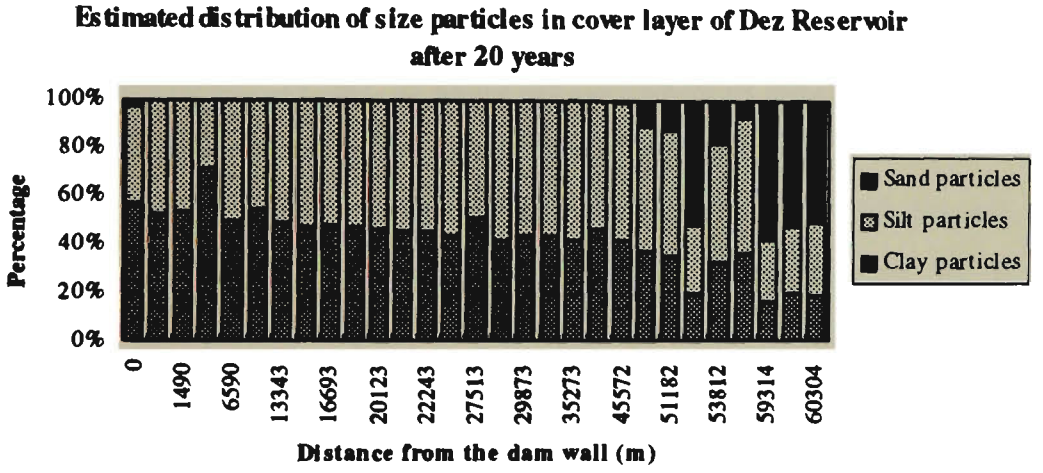

Figure 8.26 Estimated bed material composition in the surface layer of Dez Reservoir after 20 years of operation by the DEPO model.

8.3.7 Considering Alternative Bottom Gates in the Reservoir

One of the advantages of the DEPO model is its ability to model the turbidity current under different conditions and to predict the sedimentation processes related to each turbidity current condition. The downstream boundary condition of a turbidity current is highly related to outlet gates, particularly the gates used for bypassing floods. In Dez Reservoir, two tunnels are located at an elevation of 335m for releasing floods. The program was run for a case if such gates are installed at the bottom (EL 195 m), near the bed of the reservoir. This will enable the excess water to be bypassed during floods from

bottom layers of water instead of from the existing condition where excess water is bypassed from the elevation of 335m and above. It was assumed that all floods with discharge of more than 570 m^3/sec are subject to release from the reservoir (these occur approximately on 36 days during the average annual floods) and the other discharges can be kept in the reservoir. The results of running the model with these assumptions are presented in Table 8.6 and Figure 8.27.

Table 8.6 Summary of the model results in the case of alternative bottom gate.

Total sediment inflow (m^3)	Total sediment outflow (m^3)	Total sediment accumulated (m^3)	Trap efficiency
234300000	125000000	109300000	0.46

It can be seen from Figure 8.27 that, by using the alternative of bottom gates, the amount and the pattern of sediment deposited in the reservoir has been significantly affected, and the estimated volume of sediment deposition is reduced by about 55 percent. This comparison supports the installation of bottom gates in such reservoirs and is highly recommended for the future operation of the reservoir. Such methods are common to large reservoir in China. For example, in the Three Gorges Dam Project under construction, it is proposed to drain turbid water so that even after 100 years of operation, the reduction in volume of reservoir is 10-15%.

8.3.8 Using DEPO Model for Predicting the Future of Dez Reservoir

The DEPO model was utilised to predict the future volume and bed elevation of Dez Reservoir. All input data were the same as outlined in Section 8.3.5. The effects of turbidity currents were considered in the prediction. The program was run to predict the reservoir bed level and volume of sediment deposition after 60 years of operation assuming that the existing operational practice and with alternative bottom gate. The results are presented in Table 8.7 and Figures 8.28 and 8.29. In Figures 8.30 and 8.31 three dimensional view of Dez Reservoir depths before operation and predicted depths by DEPO model after 60 years operation are shown.

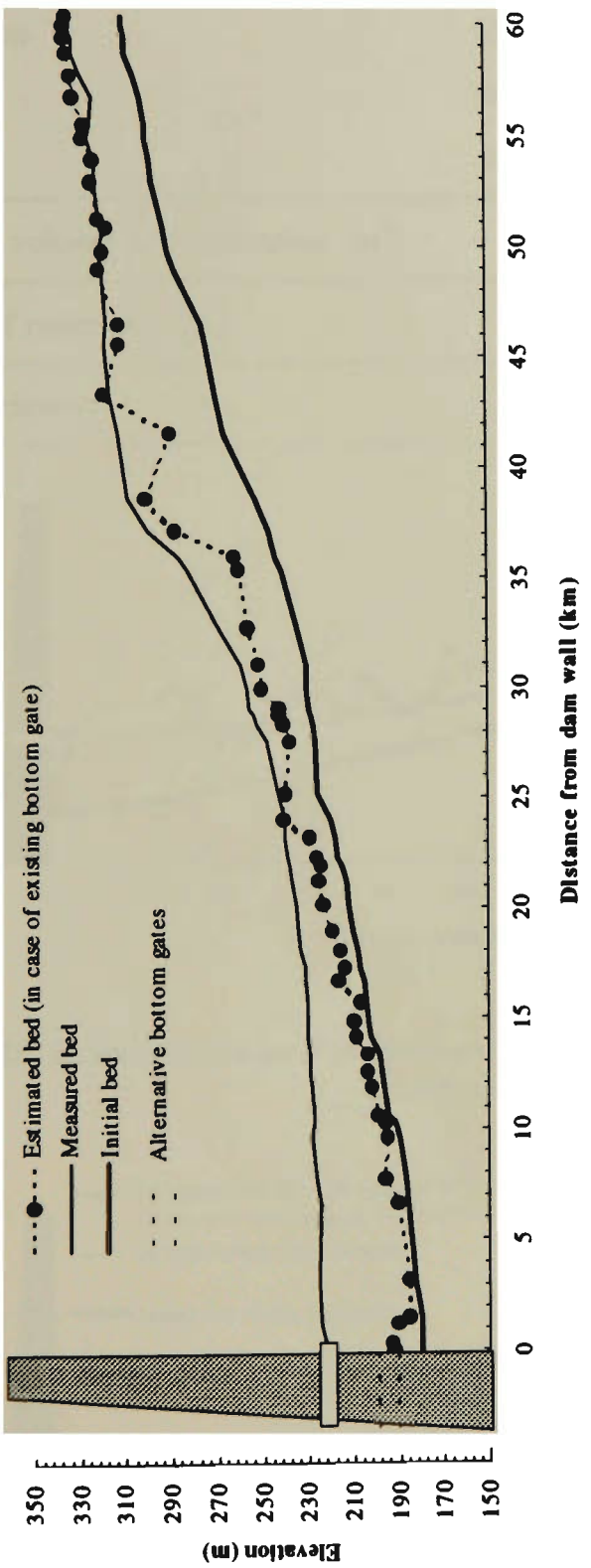

Figure 8.27 Estimated bed level in Dez Reservoir after 20 years operation in case of existing bottom gates to bypass the high floods.

Table 8.7 Volume of sediment deposition and volume of Dez Reservoir after 60 years operation estimated by DEPO model.

Parameters	Estimated after 60 years according to existing condition	Estimated after 60 years with alternative bottom gate
Sediment volume accumulation (m^3)	569000000	321986000
Volume of reservoir (m^3)	2761000000	3008014000
Trap efficiency	0.92	0.52

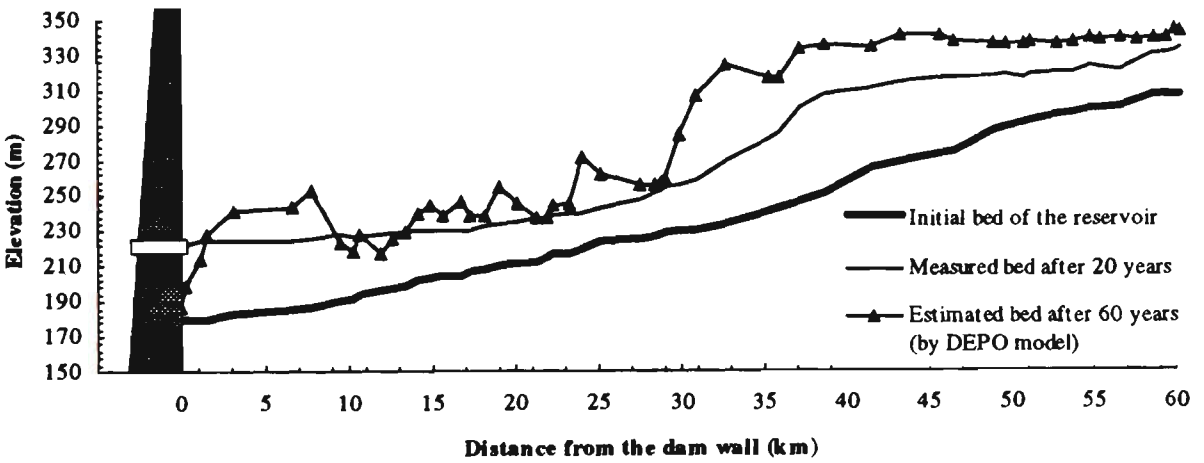

Figure 8.28 Estimated bed level in Dez Reservoir after 60 years operation (existing condition).

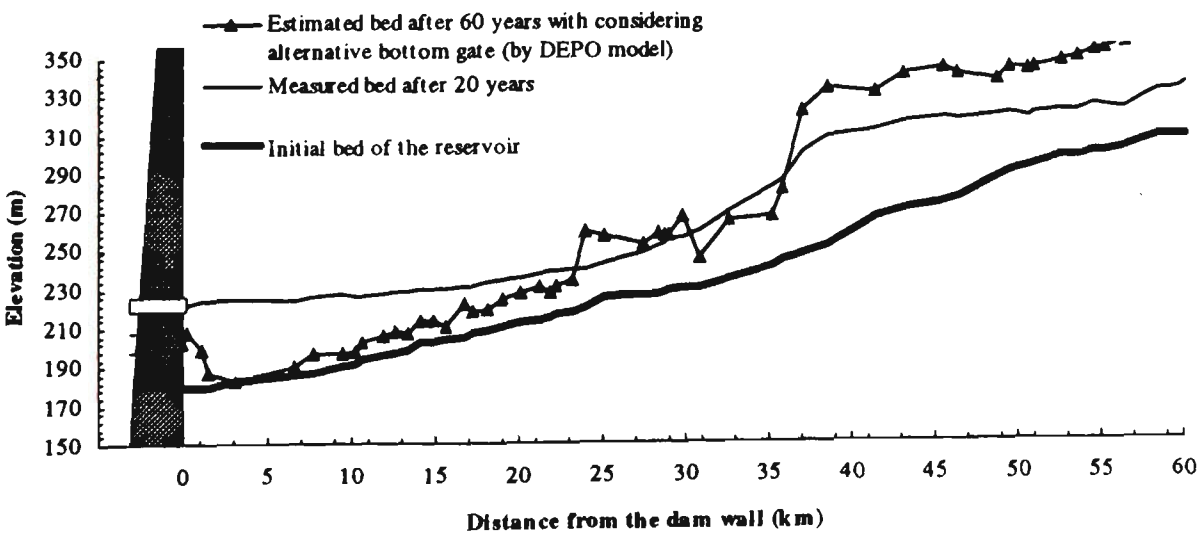

Figure 8.29 Estimated bed level in Dez Reservoir after 60 years operation (with alternative bottom gate).

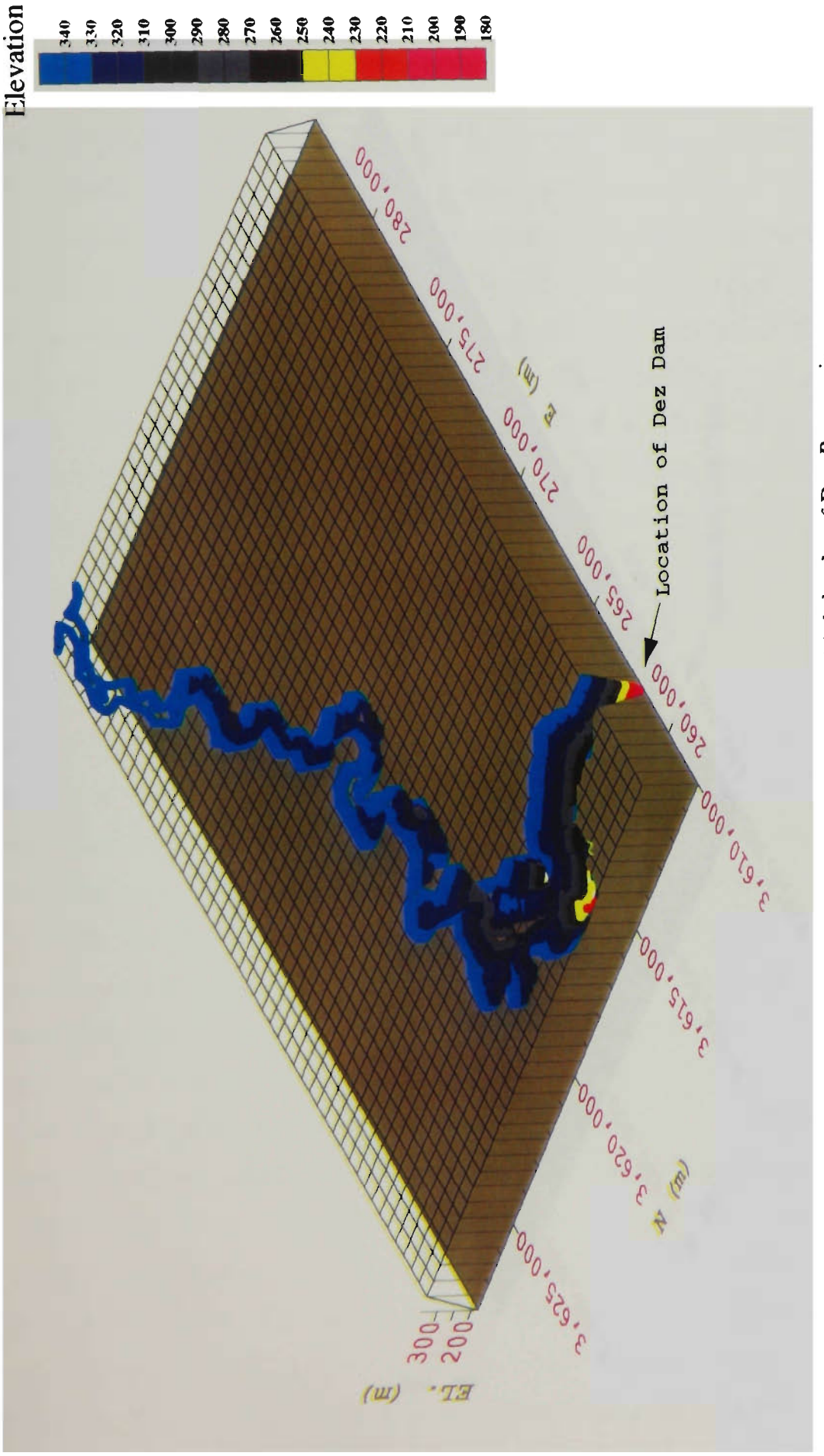

Figure 8.30 Three dimensional view of initial depths of Dez Reservoir.

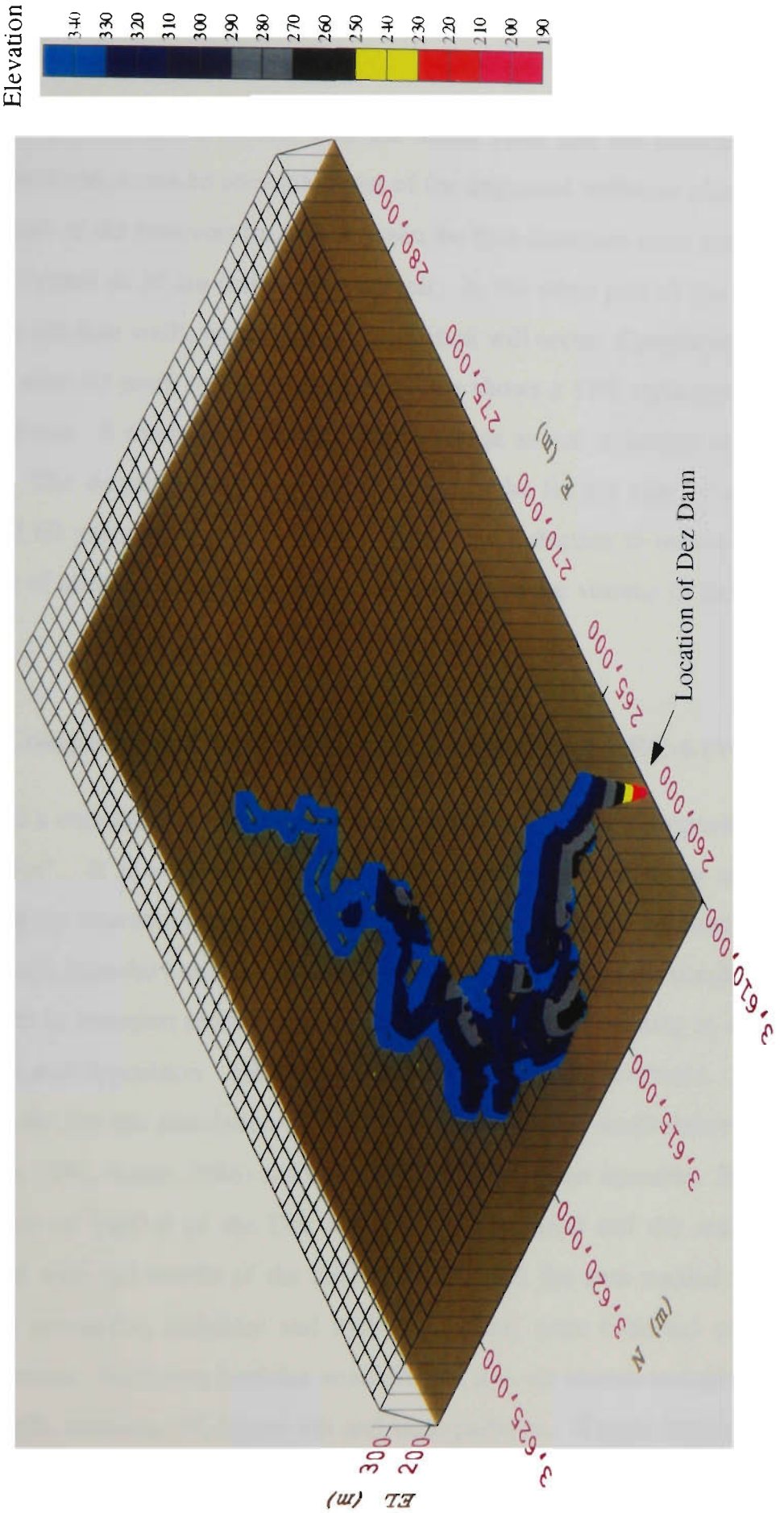

Figure 8.31 Three dimensional view of Dez Reservoir depths after 60 years operation predicted by DEPO model.

From comparison of the results with the initial value and the measured value after 20 years operation, it can be seen that most of the deposited sediment after 1981 will mainly fill the part of the reservoir located between the first upstream cross section and the cross section located at 30 km inside the reservoir. In the other part of the reservoir (first 30 km from the dam wall), no significant deposition will occur. Comparison of the reservoir volume after 60 years with the original volume shows a 17% reduction in the volume of the reservoir. It means that the estimated average annual reduction of Dez Reservoir is 0.28%. The output results from running the model for the case of alternative bottom gate and 60 years of operation show a significant reduction in sediment deposition. In the case of alternative bottom gate, the reduction in the volume of the reservoir will be 9.7%.

8.3.9 Comparison of the Results with the Results of HEC-6 (Ver. 4.1)

HEC-6 is a one-dimensional computer code entitled "Scour and Deposition in Rivers and Reservoirs". It is a simulation program designed to analyse scour and deposition by modeling the interaction between the water-sediment mixture, sediment material forming the stream's boundary and the hydraulics of flow. This program simulates the ability of the stream to transport sediment, and considers the function relating to sand, silt and clay transport and deposition. HEC-6 cannot simulate turbidity currents. It has been used successfully for the simulation of natural river beds and small reservoirs (Stoker and Williams, 1991, Amar, 1986) and it is used by the US water agencies. In this section, the application of HEC-6 to the Dez Reservoir is discussed and the results obtained are compared with the results of the DEPO model. All the data needed for this purpose, including geometric, sediment and hydrologic data, were collected and arranged in a certain format. Sediment particles were divided into six classes including clay, very fine silt, fine silt, medium silt, coarse silt and sand particles. Yang's stream power equation was chosen as a sediment transport formula and the model is run for 20 years after operation. The results from the model were calibrated by comparing these with the 1981 resurvey results. Calibration was carried out several times. All the input and output details were considered to find the optimum results in calibration. The results are

summarised in Table 8.8, Figures 8.32 and 8.33, and can be compared with the results obtained from DEPO model. The predicted volume of sediment deposited in the reservoir and trap efficiency calculated by HEC-6 are very close to the results obtained from the proposed model, without considering the effects of turbidity currents and with small differences with the measured values. However, the results obtained from the DEPO model with the effects of turbidity currents are very close to the measured values. From comparison, the estimated of bed elevation (Figure 8.32) and the distribution pattern of deposited sediment in cross sections (Figure 8.33) with the measured data, it can be seen that using HEC-6 for Dez Reservoir (or in general for large reservoirs) does not give reliable results. In prediction of sediment processes by the HEC-6, the user should specify a part of each cross section as the movable part of the cross section and sediment deposition and scour will occur in this part. Determining this part in watercourses is very difficult or may be impossible. This point is one of the deficiencies of using HEC-6, especially in reservoirs. The prediction of the distribution of sediment deposition and scour in cross sections using HEC-6 also do not coincide with actual measurements.

Table 8.8 Sediment deposition volume and trap efficiency measured and estimated by HEC-6 and DEPO after 20 years operation of the reservoir.

Parameters	**Estimated**		**Measured**
	DEPO	HEC-6	**(1981)**
Sediment volume accumulation (m^3)	202900000	217950720	200000000
Trap efficiency	0.86	0.93	0.85

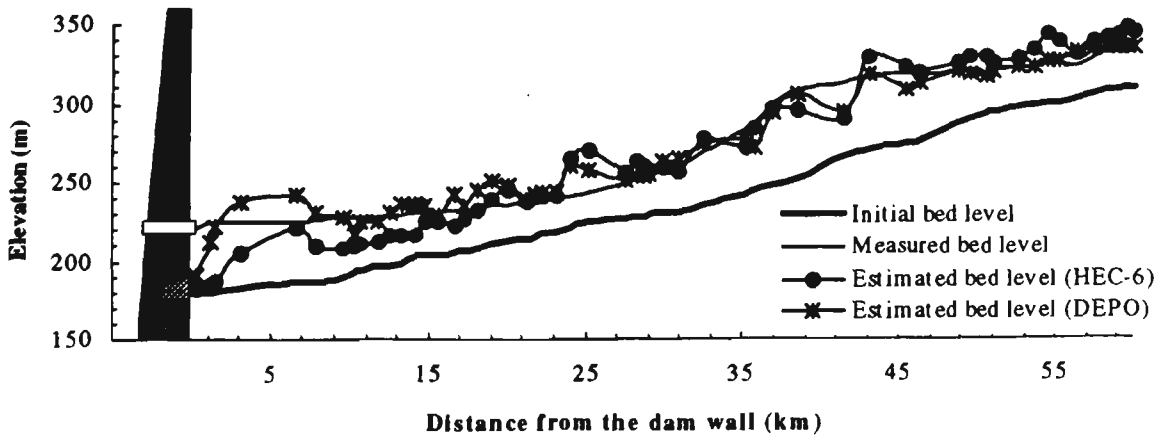

Figure 8.32 Profile of sediment deposition measured and estimated by HEC-6 in Dez Reservoir

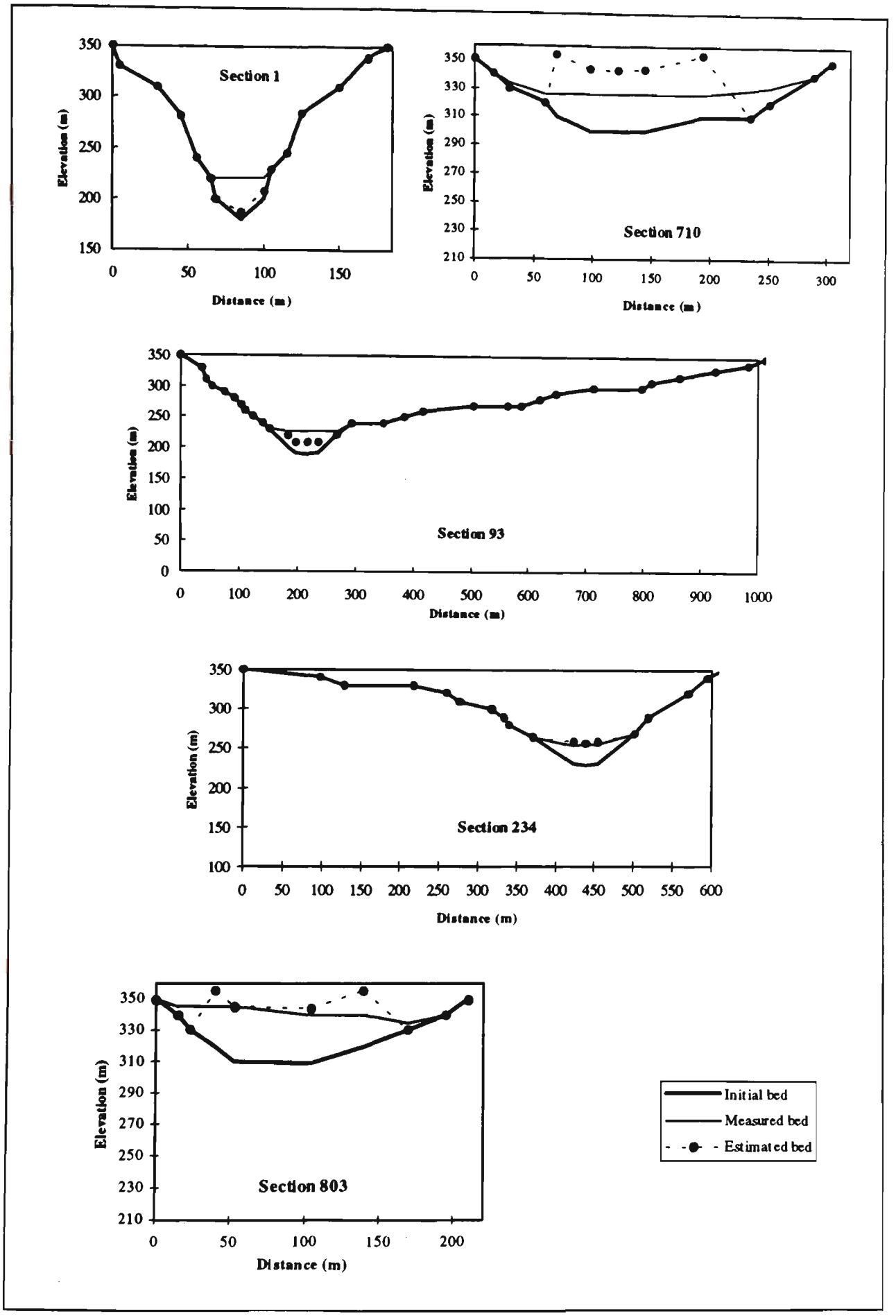

Figure 8.33 Sediment deposition measured and estimated by HEC-6 at five cross sections of Dez Reservoir.

8.4 Summary

In this chapter, the proposed "DEPO" model has been verified by testing with the laboratory experiments and data obtained from Dez Reservoir. The data of four different turbidity current experiments were considered. Based on the boundary conditions of each of the experiments, the model was run and the output results were compared with the measured data. The results are summarised as follows:

- The computations of the water elevation and the height of the turbidity current predicted by the model showed excellent agreement with the measured values.

- Comparison of the results show very good agreement between the computed and measured amount of deposited material. The observational error between the two values was very low and can be ignored. The accuracy of the equipment and measurement parameters is presented in Appendix H.

- Comparison of both the measured and the estimated bed composition values shows a disagreement between the predicted and the measured values of particles size larger than 62 μm. Further consideration of the results obtained from the experiments of the head of the turbidity current shows that this disagreement is related to the effects of the head that could not be considered in the model. These effects are more pronounced especially when the duration of the current becomes small.

The DEPO model was run for Dez Reservoir and comparing these results with the measured data shows the validity of the model to predict the sediment processes in very large reservoirs. The results of running the DEPO model to Dez Reservoir can be summarised as follows:

- Running the model without using the turbidity current effects and with different sediment transport equations showed no significant differences between the available sediment transport equations.

- Comparison of the estimated sediment accumulation in the reservoir and the trap efficiency with the measured values showed exact agreement. The estimated trap efficiency also was compared with the results obtained from two well known

empirical methods of Churchill (1948) and Brune (1953). The estimated trap efficiency obtained from the model was in excellent agreement with measured value in comparison with the other two empirical methods.

- The bed profile of the reservoir was predicted by the model (including the effects of turbidity currents) and compared with the measured value. The estimated profile had relatively good agreement with the measured profile. Comparison between the estimated sediment deposition profile and the case without considering turbidity current and HEC-6 were presented. The comparison showed that the estimated profile is significantly improved by using the DEPO model which incorporates turbidity current effects.

- The bed material composition in the active layer of the bed after 20 years of operation was calculated by the program and it was compared with the measured value. The result confirmed the reliability of the model in the prediction of bed material composition.

- The downstream boundary condition of a turbidity current is highly related to outlet gates, particularly the gates used for bypassing floods. The model was run in the reservoir with the assumption that there is an alternative bottom gate for bypassing the high flood. It is shown that using the alternative of bottom gates, the amount and the pattern of sediment deposited in the reservoir can be changed significantly. The estimated volume of sediment deposition is reduced by about 55 percent. It appears that the DEPO model can be successfully used for prediction of reservoir sedimentation and can be used as a tool in the design of large reservoirs to predict reservoir sediment deposition and associated problems.

Chapter Nine

CONCLUSIONS AND SUGGESTIONS FOR FURTHER RESEARCH

9.1 Conclusions

The major conclusions of this study can be divided into two parts. Firstly, the experiments and the analysis of the experiments on gravity currents in laboratory and field, and secondly, the development of the computer model DEPO for reservoir sedimentation modelling and its application to Dez Reservoir.

At first, literature is reviewed to find the available river and reservoir sedimentation methods as it is required for all research study. Different valuable models are available for predicting bed elevation and sediment processes in rivers and reservoirs. The existing models have not considered the turbidity currents as a parameter that affect long term reservoir sedimentation. In the second part of this study the literature is reviewed to find the theoretical aspects of the computation of sediment processes in streams. The available equations in this regards are presented in Chapter 3.

9.1.1 Experimental Results

The laboratory experiments were conducted on a flume 4 m in length, 43 cm in width and 50 cm in height. The slope of the bed of the flume was constant and equal to 0.00635 (0.36 degrees). In order to measure the velocity and sediment parameters accurately, Laser Doppler Velocimetry and Laser Particles Size equipment were used respectively. Experiments on two types of gravity currents, 1) saline density current and

2) turbidity current with solid materials, were conducted. In all of the experiments the following three conditions were evaluated:

1. Progress of the head of turbidity current and saline density current
2. The progress of subcritical conservative density current and turbidity current
3. Sediment deposition resulting from turbidity current.

The analysis of the measured parameters are presented in chapters 5, 6 and 8.

Thirty five sets of experiments were conducted to study the head of gravity currents. Seventeen of them were of non conservative turbidity currents that were established by mixing the sediment particles in water. Eighteen of the experiments were conservative saline density currents that were established by mixing table salt in water. From the analysis of the experiments of this study and the available laboratory data on the head of gravity current an equation is proposed for the head of gravity current as:

$$U_f = 0.72\sqrt{g'H_f}$$

Analysis of the slopes of the data on head of gravity currents showed a relationship between the densimetric Froude number (constant value in the above mentioned equation) and the slope as:

$$C_c = 1 \times S^{0.08}$$

With this relationship the equation of velocity of the head is presented as:

$$U_f = S^{0.08}\sqrt{g'H_f} \quad \text{for} \quad 0 < S \leq 0.04$$

The height of the head of gravity currents are analysed based on the available data. The result showed a relationship between the height of gravity currents and the initial parameters of the flow as:

$$H_f = 2.2\left(q_0^2/\Delta g\right)^{1/3}$$

Comparison of the geometric mean size of the sediment in the head along the flume has shown that the head of the turbidity current may have some deposition on the bed. It has been shown that the sediment transport capacity by the head is much higher than what can be transported by the body of the current. Hence the sediment transport equations of open channels cannot be applied to predict sediment transport of the head of gravity currents.

Nineteen experiments were conducted to study the subcritical gravity currents (the body), nine of which were conservative saline density current experiments, and ten of which were concerned with non-conservative turbidity currents. The data obtained from these experiments are presented in Chapter Six. The profiles of the velocity are measured with a fibre optic Laser Doppler Velocimeter system. The measured velocity profiles from the steady state saline density currents (body of the current) showed good similarity of profiles between different subcritical currents. The water entrainment coefficient was calculated by analysing the velocity profiles at two sequence measurement points. Based on the calculated water entrainment, and using the other available water entrainment data, an equation for the water entrainment coefficient was proposed as a function of Richardson number (R_i) as:

$$E_w = \frac{0.075}{\left(1 + 30517\, R_i^{3.18}\right)^{1/3}}$$

Sediment entrainment by turbidity currents has not been measured in this study. The available sediment entrainment in laboratory open channels and field are employed to analyse and to test the accuracy of the existing equations. Based on laboratory data (uniform particles), a new equation for sediment entrainment over an erodible bed was proposed as:

$$Z = \frac{u_*}{v_s} R_p^{0.65}$$

$$E_s = \frac{3.3 \times 10^{-7} Z^4}{1 + 1.1 \times 10^{-6} Z^4}$$

For non-uniform sediment data, Equation 6.42 can be used when Z is changed to Z_m as:

$$Z_m = \frac{u_*}{v_{si}} R_{p50}^{0.65} \left[\frac{D_i}{D_{50}} \right]^{0.5}$$

9.1.2 Computer Model Results

A new computer program, DEPO, for the prediction of sediment processes in reservoirs was developed by incorporating the effects of turbidity currents on long term sedimentation. Although the model is theoretically one dimensional, some options exist for the distribution of sediment deposited and scoured on cross sections. A user can choose a distribution form of deposition and scour in the cross sections from flat layer to proportional water depths in a variety of options. This makes the model a pseudo two dimensional model. The major assumptions introduced in the development of DEPO are:

- The flow is assumed to be in steady at each computation time step. This means an unsteady hydrograph of the flow should be divided in to some steady parts.
- Changes in bed elevation and composition of the material on the bed during one computational time step are assumed to be not significantly influence the flow elevation and velocity.
- The effects of the turbidity current head in sedimentation are not considered.
- To find the turbidity current height in different sections of the reservoir the average hydraulics parameters of the sections were used.
- The height of the downstream boundary of the turbidity current is available.

To verify and to test the proposed model, both laboratory experiments and an actual reservoir were considered. Four different turbidity currents were run in the laboratory flume and the required hydraulic and sediment data was collected. Based on the boundary conditions of the experiments the DEPO model was run and the output results were compared with the measured data. The computations performed by DEPO for the water elevation, the height of the turbidity current and the amount of the deposited material on the bed, showed excellent agreement with the measured values. Comparison between the measured and the estimated bed composition values shows a disagreement

between the predicted and the measured values of particles size greater than 62 μm. Further consideration of the results obtained from the experiments of the head of the turbidity current showed that this disagreement is related to the effects of the head that is not considered in the model. This is due to the lack of information about sediment transport by the head of turbidity currents.

The DEPO model was also successfully run for Dez Reservoir, a large reservoir in the south-west of Iran. All raw measured data of the Dez River over a 30 year period was collected and summarised to prepare the input data required for running the model. The major conclusion from running the DEPO model for Dez Reservoir is summarised as follows:

- Running the model without the effect of turbidity current but using different sediment transport equations showed no significant differences between the available sediment transport equations in Dez Reservoir and in term of sediment deposition predictions. However the methods of Toffaleti, Meyer-Peter and Müller, and Habibi and Sivakumar have shown better results.

- Comparison of the estimated sediment accumulation in the reservoir and the trap efficiency with the measured values showed excellent agreement. The estimated trap efficiency also was compared with the results obtained from two well known empirical methods of Churchill (1948) and Brune (1953), and also with HEC-6. The estimated trap efficiency obtained from the model showed excellent prediction compared to the well known empirical methods and the well known computer model "HEC-6". This was primarily due to consideration of the effects of turbidity currents in the DEPO model.

- The bed profile of the reservoir was predicted by the DEPO model with turbidity current effects and it was compared with the measured value. The estimated profile showed good agreement with the measured profile. The same data is used to evaluate the bed elevation by the HEC-6 computer program. Comparisons between the estimated sediment deposition profile with and without the effect of turbidity current using DEPO and HEC-6 were presented. The comparisons showed that the

estimated profiles are significantly improved by using the DEPO model with turbidity current effects.

- The bed material composition in the active layer of the bed after 20 years of operation was calculated by the program and it was compared with the measured value. The result confirmed the reliability of the model in the prediction of bed material composition.

- The DEPO model is used to predict the future bed elevation of Dez Reservoir after 60 years operation (year 2022). A summary of the output file is shown in Table 8.7, Figure 8.28 and Appendix I. The results showed that most of the deposition of sediment after year of 1981 will mainly fill the part of the reservoir located between first upstream cross section and the cross section located at 30 km inside the reservoir. In the other part of the reservoir (first 30 km from the dam wall) no significant deposition will occur. Comparison of the reservoir volume after 60 years with the original volume shows a 17% reduction in the volume of the reservoir. This means the annual average reduction of Dez Reservoir volume is about 0.28%. Also, the model is run to predict the effects of the alternative bottom gate after 60 years operation. The results are presented in Table 8.7 and Figure 8.29 and it showed significant reduction in sediment deposition in Dez Reservoir.

One of the capabilities of the model is to handle different conditions of sub-critical turbidity currents. This ability can be used to examine different modes of operation of reservoirs and to examine the effect of alternative locations of outlet gates on long-term reservoir sedimentation. This model was tested in the Dez Reservoir to consider the effects of alternative bottom gate on deposited sediment when floods with more than 570 m^3/sec (on average, these occur approximately on 36 days during the annual floods) released from the reservoir. It was found that by using the alternative of bottom gates the amount and the pattern of sediment deposited in the reservoir have been affected significantly. The height of the sediment deposited in the reservoir was reduced significantly, particularly in the region from the dam wall and up to 20 km upstream the dam in the reservoir. The estimated volume of sediment deposition was reduced by about 55 percent and the trap efficiency was reduced to 0.46.

It is envisaged that the proposed model could be used for:

- Prediction of river sediment processes and bed evaluation.
- Prediction of the loss of storage capacity and of the pattern of deposited sediment in reservoirs.
- Prediction of the effects of location and operation of the opening gates may conserve a part of the storage capacity normally destroyed by deposition.
- Prediction and management of the reservoir's water quality (that is, turbidity).
- Prediction of the development of gravity currents in natural watercourses.
- Controlling the height of mud water in reservoirs to avoid wear on hydraulic machinery by sediment.

9.2 Recommendations for Further Research

- The results of the experiments of this study on the head of turbidity current have shown that the sediment transport in the head of current is higher than the body. Therefore, the sediment transport equations for open channels cannot be used for estimating the capacity of sediment transport by the head of gravity currents. No study on this topic is found in literature. Therefore, some more experimental and theoretical studies are needed to find an equation for this purpose. It is recommended that further experiments should be conducted with different size of particles and with different slopes.
- For analysing sediment sizes in the body and the head, it is recommended to get the samples from different vertical locations rather than at one point.
- Measuring the turbulence level in the body and the head of turbidity current will help to recognise the sediment transport by the head and the body of the turbidity current.
- In this study, the velocity and sediment concentration have been measured using Eulerian concept. However new equipment are coming in the market (such as

Particle Image Velocimeter etc.) which uses the Lagrangian concept of fluid flow. These techniques can be employed to improve the accuracy of measurement.

- Development of the new model "DEPO" is based on several assumptions, presented in this chapter. Any attempt to reduce the assumptions would increase the accuracy of the model. Particularly, solution of unsteady water and turbidity current, rather than the steady state assumed in this model, is recommended. It should be noted that the theoretical solution of unsteady turbidity current is still not available.

- The proposed model was used on Dez Reservoir by assuming that the turbidity current height near the dam wall is known. Although the applied assumptions were chosen on the basis of existing outlet gates, using this model in a reservoir with some real measured data on the existing turbidity current would be preferable when comparing the model prediction results with the measured ones.

REFERENCES

Ackers, P., and White, W. R., 1973. "Sediment Transport: New Approach and Analysis," *Journal of Hydraulic Engineering*, Vol. 99, No. HY11, pp. 2041-2060.

Akiyama, J., and Fukushima, Y., 1985. "Entrainment of Noncohesive Sediment into Suspension," *External Memorandum*, No. 195, St. Anthony Falls Hydraulic Laboratory, University of Minnesota.

Akiyama, J., and Stefan, H. G., 1984. "Plunging Flow into a Reservoir: Theory," *Journal of Hydraulic Engineering*, Vol. 110, No. 4, pp. 484-499.

Akiyama, J., and Stefan, H. G., 1985. "Turbidity Current with Erosion and Deposition," *Journal of Hydraulic Engineering*, Vol. 111, No. 12, pp. 1473-1496.

Akiyama, J., and Stefan, H. G., 1987. "Gravity Current in Lakes, Reservoirs and Coastal Regions: Two-Layer Stratified Flow Analysis," *Project Report*, No. 253, St. Anthony Falls Hydraulic Laboratory, University of Minnesota.

Alavian, V., 1986. "Behaviour of Density Currents on an Incline," *Journal of Hydraulic Engineering*, Vol. 112, No. 1, pp. 27-42.

Altinakar, S., Graf, W. H., and Hopfinger, E. J., 1990. "Weakly Depositing Turbidity Current on a Small Slope," *Journal of Hydraulic Research*, Vol. 28, No. 1, pp. 55-80.

Amar, A. C., 1986. "Hansen Dam Sediment Modeling Study, Impact of Water Supply vs. Flood Control Operational Modes on Sediment Deposition in the Reservoir Area," *Water Forum 86*, pp. 1435-1443.

Annandale, G. W., 1987. "Developments in Water Science 29: Reservoir Sedimentation," Elsevier Science Publishers B. V., Amsterdam, The Netherlands.

Asada, H., 1973. "Prediction of Sediment Bed Profile in Reservoir and River Bed Deformation: A Practical Method and Some Examples of Calculation," *Transaction of the Eleventh International Congress on Large Dams*, Q40-R26 Paper, pp. 381-402.

Ashida, K., and Egashira, S., 1975. "Basic Study on Turbidity Currents," *Proceedings JSCE*, No. 237, pp. 37-50.

Ashida, K., and Egashira, S., 1977. "Hydraulic Characteristics of Thermocline in Reservoirs," *Proceedings, 17th congress of the International Association for Hydraulic Research*, Vol. 2, pp. 33-40.

Bagnold, R. A., 1966. "An approach to the Sediment Transport Problem from General Physics," *US Geological Survey Professional Paper* 422-J, pp. 37.

Bell, R. G., and Sutherland, A. J., 1983. "Non-Equilibrium Bedload Transport by Steady Flow." *Journal of Hydraulic Engineering*, Vol. 109, No. 3, pp. 351-367.

Benjamin, F. P., 1992. "An Introduction to Applied Numerical Analysis," PWS-Kent Publishing Company, Boston.

Benjamin, T. B., 1968. "Gravity Currents and Related Phenomena," *Journal of Fluid Mechanics*, Vol. 31, Part 2, pp. 209-248.

Bina, M., Ghomeshi, M., and Shokrollahi, A., 1993. "Initial Unit Weight of Reservoir Deposited Sediment," *Environmental Management Geo-Water and Engineering Aspects*, Proceeding of the International Conference on Environmental Management, Wollongong, NSW, Australia, Feb. 1993, pp. 527-531.

Bishop, A. A., Simons, D. B., and Richardson, E. E., 1965. "Total Bed Transport," *Journal of Hydraulic Engineering*, Vol. 91, No. HY2, pp. 175-191.

Bonham-Carter, G. F., and Sutherland, A. J., 1968. "Mathematical Model and Fortran IV Program for Computer Simulation of Deltaic Sedimentation," *Kansas Geological Survey Computer Program*, The University of Kansas, Lawrence, pp. 1-56.

Borah, D. K., Alonso, C. V., and Prasad, S. N., 1982. "Routing Graded Sediments in Streams: Formulations," *Journal of the Hydraulics Division*, Vol. 108, No. HY12, pp. 1486-1503.

Borland, M., 1971. "Reservoir Sedimentation," *River Mechanics*, edited and published by H. W. Shen, Colorado State University, Fort Collins, Colorado.

Borland, W. M., and Miller, C. R., 1958. "Distribution of Sediment in Large Reservoirs," *Journal of the Hydraulics Division*, Vol. 84, No. HY2, pp. 1587-1-1587-18.

Britter, R. E., and Linden, P. F., 1980. "The Motion of the Front of a Gravity Current Travelling Down an Incline," *Journal of Fluid Mechanics*, Vol. 99, Part 3, pp. 531-543.

Brown, C. B., 1944. "Discussion of 'Sedimentation in Reservoirs,' by B. J. Witzig," *Transactions, ASCE*, Vol. 109, Paper No. 2227, pp. 1080-1086.

Brownlie, W. R., 1983. "Flow Depth in Sand-Bed Channels," *Journal of Hydraulic Engineering*, Vol. 109, No. 7, pp. 959-990.

Brune, G. H., 1953. "Trap Efficiency of Reservoirs," *Am. Geophysical Union Trans.*, Vol. 34, No. 3, pp. 407-418.

Bube, K. P., and Trimble, S. W., 1986. "Revision of the Churchill Reservoir Trap Efficiency Curves Using Smoothing Splines," *Water Resources Bulletin*, Vol. 22, No. 2, pp. 305-309.

Bühler, J., Wright, S. J., and Kim, Y., 1991. "Gravity Currents Advancing into a Coflowing Fluid," *Journal of Hydraulic Research*, Vol. 29, No. 2, pp. 243-257.

Celik, I., and Rodi, W., 1984. "A Deposition Entrainment Model for Suspended Sediment Transport," SFB 210/T/6, November, Universitat Karlsruhe.

Chang, F. F. M., and Richards, D. L., 1971. "Deposition of Sediment in Transient Flow," *Journal of the Hydraulics Division*, Vol. 97, No. HY6, pp. 837-849.

Chang, H. H., 1982. "Mathematical Model for Erodible Channels," *Journal of the Hydraulics Division*, Vol. 108, No. HY5, pp. 837-849.

Chang, H. H., 1984. "Modeling of River Channel Changes," *Journal of Hydraulic Engineering*, Vol. 110, No. 2, pp. 157-172.

Chang, H. H., 1988. "Fluvial Processes in River Engineering," By John Wiley & Sons, New York.

Chikita, K., and Okumura, Y., 1990. "Dynamics of Turbidity Currents Measured in Katsurazawa Reservoir, Hokkaido, Japan," *Journal of Hydrology*, Vol. 117, pp. 323-338.

Chu, F. H., Pilkey, W. D., and Pilkey, O. H., 1979. "An Analytical Study of Turbidity Current Steady Flow," *Marine Geology*, Vol. 33, pp. 205-220.

Churchill, M. A., 1948, "Discussion of 'Analysis and Use of Reservoir Sedimentation Data,' by L. C. Gottschalk," Federal Interagency Sedimentation Conf., Denver, Colorado, 1947, Proc., pp. 139-140.*

Colby, B. R., 1964. "Discharge of Sands and Mean-Velocity Relationships in Sand-Bed Streams," *US Geological Survey Professional Paper*, 462-A, 47 pp.

Colby, B. R., and Hembree, C. H., 1955, "Computations of Total Sediment Discharge Niobrara River near Nebraska," *Water Supply Paper 57*, U.S. Geological Survey, Washington, D. C. *

Coleman, N. L., 1969. "A New Examination of Sediment Suspension in Open Channels," *Journal of Hydraulic Research*, Vol. 7, No. 1, pp. 67-82.

Coleman, N. L., 1981. "Velocity Profiles with Suspended Sediment," *Journal of Hydraulic Research*, Vol. 19, No. 3, pp. 211-229.

Copeland, R. R., 1990. "Waimea Sedimentation Study, Kauai, Hawaii," Numerical Model Investigation, Technical Report HL 90-3, USACE, Waterways Experiment Station, Vicksburg, MS. *

Cormault, P., 1971. "Experimental Determination of the Solid Flow Rate of Erosion of Fine Cohesive Sediments," *IAHR, 14th Congress*, Paris, pp. 9-16.

Correia, L. R. P., Krishnappan, B. G., and Graf, W. H., 1992. "Fully Coupled Unsteady Mobile Boundary Flow Model," *Journal of Hydraulic Engineering*, Vol. 118, No. 3, pp. 476-493.

Cristofano, E. A., 1953, "Area Increment Method for Distributing Sediment in a Reservoir," U.S. Bureau of Reclamation, Albuquerque, New Mexico. *

Croley, T. E., Raja Rao, K. N., and Karim, F., 1978. "Reservoir Sedimentation Model with Continuing Distribution, Compaction, and Sediment Slump," *IIHR Report,* No. 198, Iowa Institute of Hydraulic Research, The University of Iowa.

Dawdy, D. R., and Vanoni, V. A., 1986. "Modeling Alluvial Channels," *Water Resources Research*, Vol. 22, No. 9, pp. 71S-81S.

Denton, R. A., Faust, K. M., and Plate, E. J., 1981. "Aspects of Stratified Flow in Man-Made Reservoirs," *Mitt. Heft 20*, Institut Wasserbau III, Universität Karlsruhe.

Dietrich, W. E., 1982. "Settling Velocity of Natural Particles," *Water Resources Research*, Vol. 18, No. 6, pp. 1615-1626.

Einstein, H. A., 1942, "Formulae for the Transportation of Bed Load," *Transactions, ASCE*, Vol. 107.

Einstein, H. A.,1950, "The Bed Load Function for Sediment Transportation in Open Channels," *Technical Bulletin 1026*, U.S. Department of Agriculture, Soil Conservation Service, Washington, D. C. *

Ellison, T. H., and Turner, J. S., 1959. "Turbulent Entrainment in Stratified Flows," *Journal of Fluid Mechanics*, Vol. 6, pp. 423-448.

Engelund, F. and Hansen, E., 1967, "A monograph on Sediment Transport in Alluvial Streams," Teknisk Vorlag, Copenhagen.

Engelund, F., and Fredsoe, J., 1976. "A Sediment Transport Model for Straight Alluvial Channels," *Nordic Hydrology*, Vol. 7, pp. 293-306.

Engelund, F., and Fredsoe, J., 1982. "Hydraulic Theory of Alluvial Rivers," *Advances in Hydroscience*, Vol. 13, pp. 187-215.

Fan, S. S., and Springer, F. E., 1990. "Major Sedimentation Issues and Ongoing Investigations at the Federal Energy Regulatory Commission," *Hydraulic Engineering*: Proceedings of the 1990 National Conference on Hydraulic Engineering, ASCE, pp. 1015-1020.

Fukuoka, S., and Fukushima, Y., 1980. "Mechanics of Gravity Currents Advancing into a Stratified Reservoir," *Proceedings, JSCE*, No. 293, pp. 65-77. (in Japanese)

Fukushima, Y., Parker, G., and Pantin, H. M., 1985. "Prediction of Ignitive Turbidity Currents in Scripps Submarine Canyon," *Marine Geology*, 67, pp. 55-81.

Garcia, M. H., 1985. "Experimental Study of Turbidity Currents," *M. S. Thesis*, Department of Civil and Mineral Engineering , University of Minnesota, 138 p. *

Garcia, M. H., 1990. "Depositing and Eroding Sediment-Driven Flows: Turbidity Currents," *Ph.D. Thesis*, University of Minnesota, St. Anthony Falls Hydraulic Laboratory.

Garcia, M. H., and Parker, G., 1991. "Entrainment of Bed Sediment into Suspension," *Journal of Hydraulic Engineering*, Vol. 117, No. 4, pp. 414-435.

Garcia, M. H., and Parker, G., 1993. "Experiments on the Entrainment of Sediment into Suspension by a Dense Bottom Current," *Journal of Geophysical Research*, Vol. 98, No. C3, pp. 4793-4807.

Garde, R. G., and Ranga Raju, K. G., 1977. "Mechanics of Sediment Transportation and Alluvial Stream Problems," Wiley Eastern Limited, New Delhi.

Gessler, J., 1971. "Beginning and Ceasing of Sediment Motion," *River Mechanics*, edited and published by H. W. Shen, Fort Collins, Colorado, USA, pp. 7-1-7-22.

Ghomeshi, M., 1988. "Sediment Deposition in Dez Reservoir," *M. S. Thesis*, University of Shahid Chamran, Ahwaz, IRAN, (in Persian).

Graf, E. H., 1983. "The Behaviour of Silt-Laden Currents," *Water Power and Dam Construction*, September, pp. 33-38.

Graf, W. H., 1971. "Hydraulics of Sediment Transport," McGraw-Hill Book Company, New York.

Habibi, M., and Sivakumar, M., 1993. "Tests on a new method of suspended load estimation," *Environmental Management, Geo-Water Engineering Aspects*, Proceeding of the International Conference on Environmental Management, Wollongong, NSW, Australia, Feb. 1993, pp. 553-558.

Habibi, M., and Sivakumar, M., 1994. "New Formulation for Estimation of Bed Load Transport," *International Conference on Hydraulics in Civil Engineering*, University of Queensland, Brisbane, Australia, pp. 81-86.

Hebbert, B., Imberger, J., Loh, I., and Patterson, J., 1979. "Collie River Underflow into the Wellington Reservoir," *Journal of the Hydraulical Division*, Vol. 105, No. HY5, pp. 533-545.

Henderson, F. M., 1966. "Open Channel Flow," The Macmillan Company 1966.

Hobbs, B. L., 1969, "Forecasting Distribution of Sediment Deposites in Large Reservoirs," *Engineer Technical Letter*, No. 1110-2-64, O.C.E.*

Holly, F. M., and Rahuel, J. L., 1990. "New Numerical/Physical Framework for Mobile-Bed Modelling," *Journal of Hydraulic Research*, Vol. 28, No. 4, pp. 401-416.

Holly, F. M., Yang, J. C., Schwarz, P., Schaefer, J., Hsu, S. H., and Einhellig, R., 1990. "Numerical Simulation of Unsteady Water and Sediment Movement in Mobile-Bed Channels," *IIHR Report,* No. 343, Iowa Institute of Hydraulic Research, The University of Iowa.

Itakura, T., and Kishi, T., 1980. "Open Channel Flow with Suspended Sediments," *Journal of the Hydraulics Division*, Vol. 106, No. HY8, pp. 1325-1343.

Jain, S. C., 1981. "Plunging Phenomena in Reservoirs," *Proceedings of Symposium on Surface Water Impoundment's*, Minneapolis, Minnesota, June, 1980, ASCE, pp. 1249-1257.

Karaushev, A. V., 1966. "Silting of Small Reservoirs and Ponds-Theory and Calculation Method," *American Geophysical Union*, Soviet Hydrology, Selected Papers, No. 1, pp. 35-46.

Khozestan Water and Power Authority, 1971. "Dez River Watershed Stabilisation Program," *K. W. P. A.*, Ahwaz, Iran.

Khozestan Water and Power Authority, 1971. "Long-Term Operation and Capabilities of Dez Dam and Reservoir on the Dez River in Khuzestan," *Resource Investigation Project*, K. W. P. A., Ahwaz, Iran.

Khozestan Water and Power Authority, 1983. "A Summary about Dez Dam and the Installations," *Khozestan Water and Power Authority.* (in Persian)

Khozestan Water and Power Authority., 1992. "Normal Water Elevation of Dez Reservoir," *K. W. P. A.*, Ahwaz, Iran.

Krone, R. B., 1962. "Flume Studies of the Transport of Sediment in Estuarine Shoaling Processes," *Tech. Rep.* Hydraulic Engineering Lab., University of California, Berkeley, 1963.

Lane, E. W., and Koelzer, V. A., 1943. "Density of Sediments Deposited in Reservoirs," *Report* No. 9 of a Study of Methods Used in Measurement and Analysis of Sediment Loads in Streams, St. Paul, US Eng. Dist. Sub-Office Hydraulic Lab., University of Iowa City, Iowa.

Lara, J. M., and Pemberton, E. L., 1965. "Initial Unit Weight of Deposited Sediments," *Proc. of the Federal Inter-Agency Sedimentation Conference* 1963, Miscellaneous Publication No. 970, US Department of Agriculture, Agricultural Research Service pp. 818-845.

Laursen, E. M., 1958. "The Total Sediment Load of Sreams," *Journal of Hydraulic Engineering*, Vol. 84, pp. 1-36.

Lofquist, K., 1960. "Flow and Stress Near an Interface Between Stratified Liquids," *The Physics of Fluids*, Vol. 3, No. 2, pp. 158-175.

Lopez, J. L., 1978. "Mathematical Modeling of Sediment Deposition in Reservoirs," *Hydrology Papers*, Colorado State University No. 95.

Luthi, S., 1981. "Experiments on Non-Channelized Turbidity Currents and Their Deposits," *Marine Geology*, Vol. 40, M59-M68.

MacArthur, R. C., Williams, D. T., and Thomas, W. A., 1990. "Status and New Capabilities of Computer Program HEC-6: Scour and Deposition in Rivers and Reservoirs," *Hydraulic Engineering*, Proceedings of the 1990 National Conference, pp. 475-480.

Madden, E. B., 1963. "Channel Design for Modified Sediment Regime Conditions on the Arkansas River," Paper No. 39, Proceedings of the Federal Interagency Sedimentation Conference, Miscellaneous Publication No. 970, Agricultural Research Service, U.S. Government Printing Office, pp. 335-352.*

Menne, T.C., and Kriel, J. P., 1959. "Determination of Sediment Load in River and the Deposition of Sediment in Storage Reservoirs," *Division of Hydrological Research*, Department of Water Affairs, Republic of South Africa.

Merrill, W. M., 1974, "Reservoir Sedimentation: A Computer Simulation," The Kansas Water Resources Institute, University of Kansas.*

Meyer-Peter, E., and Müller, R., 1948, "Formulas for Bed-Load Transport," *Proceedings, 3rd Meeting of Intern. Assoc. Hydraulic Res.*, Stockholm, pp. 39-64.*

Middleton, G. V., 1966a. "Experiments on Density and Turbidity Currents, I. Motion of the Head," *Canadian Journal of Earth Sciences*, Vol. 3, pp. 523-546.

Middleton, G. V., 1966b. "Experiments on Density and Turbidity Currents: II. Uniform Flow of Density Currents," *Canadian Journal of Earth Sciences*, Vol. 3, pp. 627-637.

Middleton, G. V., 1967. "Experiments on Density and Turbidity Currents: III. Deposition of Sediment," *Canadian Journal of Earth Sciences*, Vol. 4, pp. 475-505.

Miller, C. R., 1953, "Determination of the Unit Weight of Sediment for Use in Sediment Volume Computations," Bureau of Reclamation, Denver, Colorado.*

National Research Council, 1983. "Advisory Board on the Built Environment, An Evaluation of Flood-Level Prediction Using Alluvial-River Models," *Technical Report*, Comm. on Hydrodyn. Comput. Models for Flood Insurance Stud., Washington, D.C. (HEC-2SR) *

Nordin, C. F., Jr., and Dempster, G. R., 1963. "Vertical Distribution of Velocity and Suspended Sediment Middle Rio Grande New Mexico," *US. Geological Survey*, Professional Paper 462-B.

Onishi, Y., Jain, S. C., and Kennedy, J. F., 1976. "Effects of Meandering in Alluvial Streams," *Journal of Hydraulics Division*, Vol. 102, No. HY7, pp. 899-917.

Parchure, T. M., and Mehta, A. J., 1985. "Erosion of Soft Cohesive Sediment Deposits," *Journal of Hydraulic Engineering*, Vol. 111, No. 10, pp. 1308-1326.

Parker, G., and Anderson, A. G., 1977. "Basic Principles of River Hydraulics," *Journal of Hydraulic Engineering*, ASCE, Vol. 103, No. HY9, pp. 1077-1087.

Parker, G., Fukushima, Y., and Pantin, H. M., 1986. "Self-Accelerating Turbidity Currents," *Journal of Fluid Mechanics*, Vol. 171, pp. 145-181.

Parker, G., Garcia, M., Fukushima, Y., and Yu, W., 1987. "Experiments on Turbidity Currents over an Erodible Bed," *Journal of Hydraulic Research*, Vol. 25, No. 1, pp. 123-147.

Partheniades, E., 1965. "Erosion and Deposition of Cohesive Soils," *Journal of Hydraulics Division*, Vol. 91, No. HY1, pp. 105-139.

Peterson, M. S., 1988. "Summary of Sedimentation Panel Discussion," *50th Anniversary of the Hydraulics Division*, 1938-1988, Edited by Adnan M. Alsaffar, pp. 1-19.

Plapp, J. E., and Mitchell, J. P., 1960. "A Hydrodynamic Theory of Turbidity Currents," *Journal of Geophys. Res.*, Vol. 65, No. 3, pp. 983-992.

Rahuel, J. L., Holly, F. M., Chollet, J. P., Belleudy, P. J., and Yang, G., 1989. "Modeling of Riverbed Evolution for Bedload Sediment Mixtures," *Journal of Hydraulic Engineering*, Vol. 115, No. 11, pp. 1521-1542.

Samaga, R. B., Ranga Raju, G. K., and Garde, J. R., 1986a. "Concentration Distribution of Sediment Mixtures in Open Channel Flow," *Journal of Hydraulic Engineering*, Vol. 112, No. 11, pp. 1003-1018.

Samaga, R. B., Ranga Raju, G. K., and Garde, J. R., 1986b. "Concentration Distribution of Sediment Mixtures in Open Channel Flow," *Journal of Hydraulic Engineering*, Vol. 112, No. 11, pp. 1019-1035.

Savage, S. B., and Brimberg, J., 1975. "Analysis of Plunging Phenomena in Water Reservoirs," *Journal of Hydraulic Research*, Vol. 13, No. 2, pp. 187-204.

Schoklitsch, A., 1934, "Geschiebetrieb und die Geschiebefracht," Wasserkraft and Wasserwirtsch, Jgg. 39, Heft 4.*

Silvio, G. D., 1992. "Modelling Sediment Transport under Different Hydrological and Morphological Circumstances," *Dynamics of Gravel-Bed Rivers*, 1992, Edited by P. Billi, R. D. Hey, C. R. Thorne and P. Tacconi, pp 363-371.

Simons, D. B., Li., R. M., & Associates, 1982. "Engineering Analysis of Fluvial Systems," Fort Collins, Colorado 80522, USA.

Simpson, J. E., 1986. "Mixing at the Front of a Gravity Current," *Acta Mechanica*, Vol. 63, pp. 245-253.

Simpson, J. E., 1987. "Gravity Currents: In the Environment and the Laboratory," Ellis Horwood series in Environmental Science, John Wiley & sons, New York, USA.

Simpson, J. E., and Britter R. E., 1979. "The Dynamics of the Head of a Gravity Current Advancing over a Horizontal Surface," *Journal of Fluid Mechanics*, Vol. 94, Part 3, pp. 477-496.

Singh, B., and Shah, C. R , 1971. "Plunging Phenomenon of Density Currents in Reservoirs," *LaHouille Blanche*, Vol. 26, No. 1, pp. 59-64.

Skryl'nikov, V. A., 1989. "Calculation of Reservoir Siltation," *Hydrotechnical Construction*, Vol. 22, No. 8, pp. 481-486.

Smart, G. M., and Jaeggi, M., 1983. "Sediment Transport on Steep Slopes," Mitt. 64, Versuchsanstalt für Wasserbau, Hydrologie und Glaziologie, ETH, Zürich.*

Spasojevic, M., and Holly, F. M., 1990. "MOBED2 - Numerical Simulation of Two-Dimensional Mobile-Bed Processes," *IIHR Report* No. 344, Iowa Institute of Hydraulic Research, The University of Iowa.

Stacey, M. W., and Bowen, A. J., 1988. "The Vertical Structure of Turbidity Currents and a Necessary Condition for Self-Maintenance," *Journal of Geophysical Research*, Vol. 93, No. C4, pp. 3543-3553.

Stoker, B. A., and Williams, D. T., 1991. "Sediment Modeling of Dam Removal Alternatives, Elwha River, Washington," *Hydraulic Engineering*, Proceedings of the 1991 National Conference, pp. 674-679.

Szechowycz, R. W., and Qureshi, M. M., 1973. "Sedimentation in Mangla Reservoir," *Journal of the Hydraulics Division*, Vol. 99, No. HY9, pp. 1551-1572.

T. M. A. B., 1986. "Sediment Deposition in Dez Reservoir," T. M. A. B. Company, Sediment Study Section, No. 89. (in Persian)

Toffaleti, F. B., 1969. "Definitive Computations of Sand Discharge in Rivers," *Journal of the Hydraulics Division*, Vol. 95, No. HY1, January, pp. 225-246.

Turner, J. S., 1973. "Buoyancy Effects in Fluids," Cambridge Univ. Press.

US Army Corps of Engineers, 1977. "HEC-6, Scour and Deposition in Rivers and Reservoirs, User's Manual," US Army Corps of Engineers, Hydrologic Engineering Center.

US Army Corps of Engineers, 1993. "HEC-6, Scour and Deposition in Rivers and Reservoirs, User's Manual," US Army Corps of Engineers, Hydrologic Engineering Center.

van Rijn, L. C., 1984a. "Sediment Transport, Part I: Bed Load Transport," *Journal of Hydraulic Engineering*, Vol. 110, No. 10, pp. 1431-1456.

van Rijn, L. C., 1984b. "Sediment Transport, Part II: Suspended Load Transport," *Journal of Hydraulic Engineering*, Vol. 110, No. 11, pp. 1613-1641.

van Rijn, L. C., 1984c. "Sediment Transport, Part III: Bed Forms and Alluvial Roughness," *Journal of Hydraulic Engineering*, Vol. 110, No. 12, pp. 1733-1754.

Vanoni, V. A., 1941. "Some Experiments on the Transportation of Suspended Load," *Transactions,* American geophsical Union, Vol. 22, pp. 608-628.*

Vanoni, V. A., Editor 1975. "Sedimentation Engineering," American Society of Civil Engineers.

Vanoni, V. A., 1984. "Fifty Years of Sedimentation," *Journal of Hydraulic Engineering*, Vol. 110, No. 8, pp. 1021-1057.

Vanoni, V. A., and Nomicos, G. N., 1959. "Resistance Properties of Sediment-Laden Streams," *Transactions*, ASCE, Paper No. 3055, pp. 1140-1175.

Wiuff, R., 1985. "Transport of Suspended Materials in Open Submerged Streams," *Journal of Hydraulic Engineering*, Vol. 111, No. 5, pp. 774-792.

Wunderlich, W. O., and Elder, R. A., 1973. "Mechanics of Flow Through Man-Made Lakes," *Man-Made Lakes: Their Problem and Environmental Effects*, W. C. Ackermann, G. F. White, and E. B. Worthington, eds., American Geophysical Union, Washington, DC, pp. 300-310.

Yang, C. T., 1972. "Unit Stream Power and Sediment Transport," *Journal of the Hydraulics Division*, Vol. 98, No. HY10, pp. 1805-1827.

Yang, C. T., 1973. "Incipient Motion and Sediment Transport," *Journal of the Hydraulics Division*, Vol. 99, No. HY10, pp. 1679-1704.

Yang, C. T., 1976. "Unit Stream Power Equation for Total Load," *Journal of Hydrology*, Vol. 40, No. 1/2, pp. 123-138.

Yang, C. T., 1979. "Minimum Unit Stream Power and Fluvial Hydraulics," *Journal of the Hydraulics Division*, Vol. 102, No. HY7, pp. 919-934.

Yang, C. T., 1984. "Unit Stream Power Equation for Gravel," *Journal of Hydraulic Engineering*, Vol. 110, No. 12, pp. 1783-1797.

Yücel, O. and Graf, W. H., 1973. "Bed Load Deposition and Delta Formation: A Mathematical Model," Lehigh University, Fritz Engineering Laboratory, Report No. 384.1.

RESERVOIR SEDIMENTATION MODELLING

A thesis submitted in fulfilment of the
requirement for the award of the degree
Doctor of Philosophy

from

UNIVERSITY OF WOLLONGONG

by

Mehdi Ghomeshi, B.Sc., M.Sc.

Department of Civil and Mining Engineering

1995

Volume II

Table of Content

Volume II

	H_t (mm)	U_t (mm/s)	g' (mm/s^2)
Wright (1976, cited in Bühler et al. 1990)	187	49	48
	184	75	84
	94	48	72
	127	54	74
	44	43	72
	72	43	67
	108	44	39
	71	46	42
	109	46	50
	120	49	50
	137	74	50
	91	66	50
	148	83	50
	172	66	49
	177	64	53
	177	44	51
	113	58	49
	110	60	57
	117	60	50
	104	60	52
	141	56	52
	77	51	51
	107	75	48
	90	65	50
	135	65	53
	73	71	51
	69	59	52
	57	50	52
	133	50	53
	139	51	50

	H_t (mm)	U_t (mm/s)	g' (mm/s^2)
Wright (1976, cited in Bühler et al. 1990)	123	79	48
	144	82	48
	99	53	120
	93	61	120
	93	74	120
	119	68	120
	109	62	120
	126	64	121
	99	57	120
	98	63	119
	69	76	121
	87	72	120
Denton (1981)	63	56	195.219
	61	64	208.953
	58	65	206.991
	73	80	197.181
	72	86	206.01
	72	85	206.01
	79	85	193.257
	82	98	206.01
	77	92	206.01
	89	100	212.877
	82	97	204.048
	-	120	206.991
	-	110	205.029
	72	71	201.105
	68	70	202.086
	87	86	-
	95	86	214.839
	78	85	-

	H_f (mm)	U_f (mm/s)	g´ (mm/s²)
Wright (1976, cited in Bühler et al. 1990)	187	49	48
	184	75	84
	94	48	72
	127	54	74
	44	43	72
	72	43	67
	108	44	39
	71	46	42
	109	46	50
	120	49	50
	137	74	50
	91	66	50
	148	83	50
	172	66	49
	177	64	53
	177	44	51
	113	58	49
	110	60	57
	117	60	50
	104	60	52
	141	56	52
	77	51	51
	107	75	48
	90	65	50
	135	65	53
	73	71	51
	69	59	52
	57	50	52
	133	50	53
	139	51	50

	H_f (mm)	U_f (mm/s)	g´ (mm/s²)
Wright (1976, cited in Bühler et al. 1990)	123	79	48
	144	82	48
	99	53	120
	93	61	120
	93	74	120
	119	68	120
	109	62	120
	126	64	121
	99	57	120
	98	63	119
	69	76	121
	87	72	120
Denton (1981)	63	56	195.219
	61	64	208.953
	58	65	206.991
	73	80	197.181
	72	86	206.01
	72	85	206.01
	79	85	193.257
	82	98	206.01
	77	92	206.01
	89	100	212.877
	82	97	204.048
	-	120	206.991
	-	110	205.029
	72	71	201.105
	68	70	202.086
	87	86	-
	95	86	214.839
	78	85	-

	H_f (mm)	U_f (mm/s)	g' (mm/s^2)		H_f (mm)	U_f (mm/s)	g' (mm/s^2)
	82	85	214.839		92	94	185.409
	92	85	186.39		-	94	186.39
	88	82	186.39		102	-	192.276
	97	102	209.934		106	103	190.314
	96	102	201.105		107	119	206.01
	102	106	201.105		113	120	198.162
	110	115	210.915		89	86	202.086
	110	121	209.934		-	92	189.333
	66	56	197.181		-	89	187.371
	70	60	187.371		-	84	183.447
	80	68	201.105		82	93	202.086
Denton	75	68	202.086	**Denton**	-	95	202.086
(1981)	86	81	204.048	**(1981)**	99	112	198.162
	89	-	179.523		107	119	202.086
	108	97	206.01		109	53	55.917
	109	96	206.01		-	56	60.822
	107	104	208.953		-	59	55.917
	122	108	202.086		82	52	55.917
	122	-	212.877		-	60	60.822
	131	115	212.877		105	59	56.898
	-	68	167.751		121	59	62.784
	89	69	150.093		-	70	58.86
	76	87	164.808		113	71	57.879
	79	79	199.143		119	70	58.86
	97	75	175.599				
	92	95	177.561				
	97	94	193.257				

APPENDIX B

WATER ENTRAINMENT OF GRAVITY CURRENTS

	R_i	E_w	*Slope* (°)
Alavian (1986)	0.8983	0.00161	5
	1.4269	0.00156	5
	1.5229	0.00126	5
	0.6733	0.00177	10
	1.0331	0.00246	10
	1.226	0.00197	10
	0.3574	0.00241	15
	0.5461	0.00231	15
Ellison and Turner (1959)	0.2461	0.0174	12
	0.2524	0.0199	12
	0.3229	0.0178	12
	0.3594	0.0158	12
	0.1464	0.0288	23
	0.1744	0.0335	23
	0.1453	0.0227	23
	0.1482	0.0234	23
	0.1593	0.0239	23
	0.1712	0.0265	23
	0.1817	0.028	23
	0.1906	0.028	23
	0.1884	0.0257	23
	0.2096	0.0323	23
	0.1684	0.0158	23
	0.2012	0.0188	23
	0.1326	0.0414	33.5
	0.1111	0.0397	33.5
	0.1367	0.0391	33.5
	0.1632	0.0423	33.5
	0.1594	0.0374	33.5
	0.1454	0.0346	33.5
	0.1232	0.0347	33.5
	0.1258	0.0321	33.5
	0.1112	0.0307	33.5
	0.1011	0.0455	42
	0.0848	0.0398	42
	0.1058	0.0432	42
	0.112	0.0434	42
	0.121	0.0432	42
	0.132	0.0428	42
	0.144	0.0459	42
	0.1076	0.0399	42
	0.1082	0.0378	42
	0.0874	0.06	54
	0.0706	0.0569	54
	0.0699	0.056	54
	0.0726	0.0558	54

	R_i	E_w	*Slope* (°)
Ellison and Turner (1959)	0.0688	0.05	54
	0.0986	0.051	54
	0.0315	0.0839	74
	0.0295	0.075	74
	0.0257	0.0686	74
	0.0282	0.0651	74
	0	0.0904	90
	0	0.0888	90
	0	0.0874	90
	0	0.0842	90
Fukuoka and Fukushima (1980)	1.4448	0.00049	0
	1.3708	0.00181	0
	1.3695	0.00194	0
	1.0181	0.00291	0
	1.3600	0.00312	0
	0.8162	0.00527	0
	0.3830	0.00896	0
	0.3495	0.01033	0
	0.2210	0.01014	0
	0.4252	0.01462	0
Garcia (1990)	0.2035	0.00643	4.6
	0.2356	0.00583	4.6
	0.2347	0.00769	4.6
	0.2263	0.00928	4.6
Lofquist (1960)	7.0871	2.88E-04	0
	7.63366	1.73E-04	0
	9.21912	1.84E-04	0
	11.1302	1.99E-04	0
	10.6826	1.56E-04	0
	10.3395	1.47E-04	0
Lofquist (1960)	10.11973	1.39E-04	0
	10.83545	1.26E-04	0
	12.23529	1.37E-04	0
	11.97707	1.28E-04	0
	13.56364	1.13E-04	0
	13.00345	9.60E-05	0
	14.66213	1.15E-04	0
	15.67135	1.18E-04	0
	16.4441	9.20E-05	0
	18.18835	8.90E-05	0
	18.40706	8.50E-05	0
	19.72477	7.20E-05	0
	26.01843	8.20E-05	0
	21.13002	6.30E-05	0
	21.18109	5.40E-05	0
	27.04222	5.80E-05	0
	28.9781	4.90E-05	0
	31.65065	5.30E-05	0
	32.76924	4.80E-05	0
	40.01237	5.20E-05	0
	44.32071	4.60E-05	0
	54.02138	5.50E-05	0
	24.76172	2.50E-05	0
	51.68812	2.50E-05	0
	73.64291	3.00E-05	0
	92.82916	3.60E-05	0
Chikita and Okumura (1990)	0.0517	0.000976	1.4
	0.1276	0.00742	1.4
	0.277	0.00251	1.4
	0.1736	0.0102	1.4

	R_i	E_w	*Slope* (°)		R_i	E_w	*Slope* (°)
Chikita and Okumura (1990)	0.1479	0.00297	1.4	**Stacey and Bowen (1988)**	0.12	0.023	20
	0.4444	0.0145	1.4		0.12	0.021	20
	0.346	0.00498	1.4		0.098	0.024	20
	0.189	0.00274	1.4		0.41	0.057	60
	0.0918	0.00314	1.4		0.038	0.043	60
	0.16	0.00376	1.4		0.043	0.048	60
Stacey and Bowen (1988)	0.46	0.0011	0.29	**Ashida and Egashira (1975)**	1.14	0.0011	0.6
	0.36	0.001	0.29		2.57	0.000958	0.6
	0.72	0.0012	0.29		3.03	0.000651	0.6
	0.56	0.0023	0.57		3.58	0.000534	0.6
	0.51	0.0022	0.57		3.91	0.000458	0.6
	0.53	0.0022	0.57		4.27	0.000365	0.6
	0.47	0.0025	0.57		1.2	0.00182	0.6
	0.52	0.0022	0.57		3.29	0.00114	0.6
	0.51	0.0023	0.57		3.96	0.00093	0.6
	0.72	0.0023	0.57		5.29	0.000608	0.6
	0.19	0.005	2.29		0.75	0.00249	0.6
	0.24	0.009	4		1.76	0.00161	0.6
	0.26	0.009	4		3.35	0.000707	0.6
	0.21	0.0084	4		4.34	0.000449	0.6
	0.23	0.009	4		4.45	0.000223	0.6
	0.25	0.0086	4		4.55	0.000132	0.6
	0.3	0.0086	4		0.26	0.00698	0.6
	0.14	0.019	9.87		1.82	0.00134	0.6
	0.16	0.019	9.87		3.07	0.00123	0.6
	0.11	0.027	20		4.16	0.00109	0.6
	0.094	0.022	20		5.13	0.000995	0.6

	R_i	E_w	*Slope* (°)
Ashida and Egashira (1975)	6.17	0.000808	0.6
	6.97	0.000676	0.6
	0.51	0.00136	0.6
	1.16	0.000679	0.6
	1.7	0.00112	0.6
	2.16	0.000609	0.6
	2.38	0.000561	0.6
	2.76	0.000491	0.6
	3.15	0.000387	0.6
	3.29	0.000165	0.6
Parker et al. (1987)	0.58	0.005	2.86
	0.4	0.003	2.86
	0.21	0.007	2.86
	0.75	0.0075	2.86
	0.25	0.009	2.86
	0.64	0.006	2.86
	0.67	0.015	2.86
	0.78	0.003	2.86
	0.72	0.0064	2.86
	0.44	0.0044	2.86
	0.38	0.0013	2.86
	0.39	0.008	2.86
	0.16	0.008	2.86
	0.55	0.019	2.86
	0.94	0.014	2.86
	0.61	0.023	4.6
	0.55	0.0025	4.6
	0.61	0.022	4.6
	0.38	0.0031	4.6
	0.47	0.012	4.6
Parker et al. (1987)	0.43	0.005	4.6
	0.51	0.02	4.6
	0.45	0.0027	4.6
	0.48	0.0058	4.6
	0.71	0.01	4.6
	0.38	0.013	4.6
	0.44	0.009	4.6
	0.26	0.016	4.6

SEDIMENT ENTRAINMENT FUNCTION

1) Laboratory Data

	u_* (mm/s)	u'_* (mm/s)	v_s (mm/s)	R_p	E_s	u_*/v_s	D_g (mm)	U (mm/s)	Slope	D (mm)
Straub,	36.1	33.51	16.0	10.60	0.00072	2.256	0.16	622	0.00235	74.7
Anderson	37.2	34.58	15.0	9.07	0.00178	2.480	0.16	640	0.00256	72.5
and Flammer,	38.6	35.58	13.0	7.80	0.00211	2.969	0.16	655	0.00282	70.7
1958 (cited in	41.8	36.25	12.0	6.92	0.00269	3.483	0.16	658	0.00324	70.4
Akiyama and	40.9	37.09	10.4	6.30	0.00384	3.933	0.16	677	0.00326	68.6
Stefan, 1987)	43.2	37.77	9.40	5.39	0.00397	4.596	0.16	683	0.00362	68.0
Vanoni and	36.0	21.69	9.45	0.254	0.00570	3.809	0.105	374.9	0.00250	86.6
Nomicos	30.8	31.29	9.45	0.297	0.00940	3.259	0.105	615.7	0.00200	74.4
(1959)	31.7	34.33	9.45	0.287	0.00940	3.354	0.105	688.8	0.00206	78.3
	35.4	35.36	18.9	0.344	0.00260	45.974	0.161	694.9	0.00258	77.7
Vanoni	63.4	53.62	18.0	8.84	0.00343	3.522	0.16	1113	0.00250	164.0
(1941)	45.1	53.62	17.6	8.24	0.00198	2.562	0.16	1113	0.00250	83.5
	44.8	50.22	17.6	8.34	0.00140	2.545	0.16	1113	0.00125	163.7
	31.7	50.22	17.3	7.93	0.00037	1.832	0.16	1113	0.00125	82.0

239

	u_* (mm/s)	u'_* (mm/s)	v_s (mm/s)	R_p	E_s	u_*/v_s	D_g (mm)	U (mm/s)	Slope	D (mm)
Vanoni	41.5	35.54	8.4	3.98	0.00185	4.940	0.10	768.0	0.00125	140.8
(1941)	29.7	35.54	8.4	4.00	0.00054	3.536	0.10	768.0	0.00125	71.9
	58.8	47.22	8.7	4.17	0.00161	6.759	0.10	1005.8	0.00250	140.8
	41.5	34.95	8.4	3.69	0.00129	4.940	0.10	691.9	0.00250	71.3
	46.9	35.99	2.4	5.82	0.00255	3.782	0.13	691.9	0.00250	89.9
Einstein and	114.2	121.91	149.0	196.0	0.0181	0.766	1.30	1870	0.0139	138.1
Chien, 1955	128.5	135.64	149.0	175.0	0.0491	0.862	1.30	2040	0.0194	119.5
(cited in	132.7	138.92	149.0	184.0	0.0642	0.891	1.30	2080	0.0209	116.4
Akiyama and	142.3	142.07	149.0	199.0	0.0867	0.955	1.30	2100	0.0236	115.2
Stefan, 1987)	145.2	147.53	149.0	180.0	0.1510	0.974	1.30	2180	0.0255	108.5
	118.2	118.57	125.0	132.0	0.0094	0.946	0.94	1890	0.0143	142.3
	117.8	118.57	125.0	115.0	0.0189	0.943	0.94	1890	0.0143	141.4
	116.4	119.05	125.0	116.0	0.0257	0.931	0.94	1900	0.0143	138.7
	118.0	122.12	125.0	124.0	0.0491	0.944	0.94	1950	0.0150	134.1
	126.8	126.64	125.0	133.0	0.0679	1.014	0.94	2000	0.0173	128.3
	105.8	103.88	41.1	18.6	0.0075	2.574	0.27	1930	0.0131	133.2
	100.5	103.10	41.1	18.8	0.0491	2.445	0.27	1930	0.0122	131.9
	104.3	101.76	41.1	18.8	0.0868	2.538	0.27	1890	0.0126	133.2
	121.6	112.27	41.1	18.3	0.1130	2.959	0.27	2050	0.0174	124.1
	120.4	110.64	41.1	17.6	0.1960	2.929	0.27	2020	0.0169	124.1
	124.5	113.52	41.1	17.2	0.2000	3.029	0.27	2060	0.0186	119.2
Onishi,	38.40	22.37	33.2	9.93	0.0001	1.156	0.25	368.8	0.00154	102.1
Jain, and	42.37	28.82	30.1	7.38	0.0010	1.404	0.25	495.3	0.00193	100.9
Kennedy	37.79	32.26	31.4	8.20	0.0015	1.204	0.25	585.2	0.00165	96.3
(1976)	40.54	24.08	32.6	9.24	0.0003	1.243	0.25	402.3	0.00163	107.6
	41.45	25.69	31.1	7.97	0.0007	1.333	0.25	429.8	0.00184	100.3
	49.99	25.51	31.1	7.97	0.0004	1.608	0.25	405.4	0.00254	81.4

	u_* (cm/s)	u'_* (mm/s)	v_s (mm/s)	R_p	E_s	u_*/v_s	D_g (mm)	U (mm/s)	Slope	D (mm)
Onishi,	48.768	30.26	31.1	7.97	0.0008	1.569	0.11	1075.6	0.00256	75.0
Jain and	44.196	24.63	31.1	7.97	0.0004	1.422	0.21	1063.1	0.00267	77.1
Kennedy	42.976	22.80	32.0	8.79	0.0004	1.343	0.42	1069.3	0.00256	75.6
(1976)	40.538	27.06	32.0	8.79	0.0006	1.266	0.16	626.0	0.00146	122.5
	38.404	23.71	32.6	9.24	0.0001	1.178	0.16	638.0	0.00122	133.2
	35.661	20.12	32.3	9.05	0.0009	1.104	0.17	400.0	0.00109	127.1
	43.890	29.55	32.3	9.05	0.0009	1.358	0.17	354.0	0.00156	135.3
Ismail, 1951	30.2	27.96	8.14	3.62	0.0090	3.710	0.18	423.7	0.00277	41.5
(cited in Garcia,	33.4	37.96	8.78	3.94	0.0226	3.804	0.18	432.8	0.00415	35.0
1990)	39.0	47.13	8.47	3.62	0.0450	4.604	0.18	487.7	0.00591	34.1
	44.7	56.37	8.67	3.90	0.0377	5.156	0.18	533.4	0.00827	32.0
	59.2	66.40	8.96	4.02	0.0302	6.607	0.18	734.6	0.01150	34.8
	63.9	77.49	8.83	3.98	0.0253	7.237	0.18	786.4	0.01487	36.6
Coleman	37.2	31.34	17.5	8.84	0.0028	2.126	0.18	792.5	0.00160	121.9
(1968)	54.0	41.21	17.5	8.84	0.0057	3.086	0.18	816.9	0.00308	121.9
	70.0	50.94	17.5	8.84	0.0210	4.000	0.18	835.1	0.00517	121.9
	30.5	26.54	17.5	8.84	0.0009	1.743	0.18	865.6	0.00085	182.9
	37.0	31.05	17.5	8.84	0.0041	2.114	0.18	911.3	0.00120	182.9
	45.1	39.02	17.5	8.84	0.0094	2.577	0.18	914.4	0.00180	182.9
	28.9	26.04	17.5	8.84	0.0008	1.651	0.18	981.4	0.00067	243.8
	31.8	30.72	17.5	8.84	0.0026	1.817	0.18	1097.3	0.00085	243.8
	33.0	35.49	28.0	14.92	0.0017	1.179	0.18	867.5	0.00144	121.9
	64.8	43.21	28.0	14.92	0.0066	2.314	0.18	993.7	0.00420	121.9
	61.8	52.15	28.0	14.92	0.0200	2.207	0.15	628.0	0.00420	121.9
	28.0	26.61	28.0	14.92	0.0006	1.000	0.19	636.0	0.00075	182.9
	42.4	28.55	28.0	14.92	0.0034	1.514	0.24	692.0	0.00135	182.9
	40.0	40.40	28.0	14.92	0.0050	1.429	0.19	646.0	0.00156	182.9
	28.6	26.72	28.0	14.92	0.0005	1.021	0.21	533.4	0.00065	243.8
	33.8	28.59	28.0	14.92	0.0019	1.207	0.21	563.9	0.00082	243.8

	u_* (mm/s)	u'_* (mm/s)	v_s (mm/s)	R_p	E_s	u_*/v_s	D_g (mm)	U (mm/s)	Slope	D (mm)
Coleman	39.1	49.27	90.0	4.72	0.01890	4.344	0.11	1075.6	0.0020	170.0
(1981)	39.6	51.92	28.0	13.36	0.00961	1.414	0.21	1063.1	0.0020	172.0
	41.1	56.50	60.0	36.82	0.00199	0.685	0.42	1069.3	0.0022	171.0
Ashida and	36.9	35.68	18.0	8.14	0.00400	2.050	0.16	626.0	0.0040	42.0
Michiue (1964)	34.3	34.11	18.0	8.14	0.00377	1.906	0.16	638.0	0.0023	70.5
*										
Ashida and	32.7	24.70	18.5	8.50	0.00027	1.768	0.17	400.0	0.0031	46.0
Okabe (1982) *	31.3	22.51	18.5	8.50	0.00042	1.692	0.17	354.0	0.0031	41.0
Barton and	39.5	23.27	20.0	10.62	0.00094	1.975	0.18	423.7	0.00116	146.3
Lin (1955) *	40.4	22.81	20.0	10.62	0.00038	2.020	0.18	432.8	0.00082	222.5
	42.0	24.49	20.0	10.62	0.00036	2.100	0.18	487.7	0.00065	420.6
	39.7	26.15	20.0	10.62	0.00045	1.985	0.18	533.4	0.00061	313.9
	43.3	36.17	20.0	10.62	0.00350	2.165	0.18	734.6	0.00121	182.9
	46.9	38.33	20.0	10.62	0.00792	2.345	0.18	786.4	0.00125	210.3
	49.5	38.54	20.0	10.62	0.00380	2.475	0.18	792.5	0.00124	237.7
	52.9	40.39	20.0	10.62	0.00130	2.645	0.18	816.9	0.00156	210.3
	51.4	41.36	20.0	10.62	0.00181	2.570	0.18	835.1	0.00166	185.9
	55.7	42.98	20.0	10.62	0.00123	2.785	0.18	865.6	0.00183	198.1
	59.5	44.47	20.0	10.62	0.01500	2.975	0.18	911.3	0.00170	231.6
	56.4	44.51	20.0	10.62	0.00147	2.820	0.18	914.4	0.00167	228.6
	47.1	46.93	20.0	10.62	0.00430	2.355	0.18	981.4	0.00160	170.7
	53.0	52.72	20.0	10.62	0.00830	2.650	0.18	1097.3	0.00210	161.5
Kalinske and	41.6	42.22	20.0	10.62	0.00213	2.080	0.18	867.5	0.00150	158.5
Pien (1943) *	58.3	51.94	20.0	8.83	0.00221	2.915	0.18	993.7	0.00400	189.0
Lyn (1986) *	33.5	33.67	16.0	7.45	0.00470	2.094	0.15	628.0	0.00244	64.5
	34.0	34.98	23.0	10.78	0.00460	1.478	0.19	636.0	0.00251	65.1
	37.2	39.02	31.0	15.41	0.00390	1.200	0.24	692.0	0.00296	65.4
	35.2	36.03	23.0	10.75	0.00400	1.530	0.19	646.0	0.00295	57.2

* cited in Garcia, 1990

2) Field Data

	E_s/p	R_p	D_g (mm)	v_s (mm/s)	u_*/v_s	D_i/D_{50}
Middle	0.00959	3.4	0.09	6.5	12.246	0.276
Rio Grande	0.00666	3.0	0.09	6.5	12.046	0.276
Data:	0.00574	3.2	0.09	6.5	9.938	0.294
near	0.01090	3.4	0.09	6.5	11.723	0.210
Bernalillo,	0.00354	3.4	0.09	6.5	12.000	0.340
	0.00320	3.0	0.09	6.5	9.338	0.340
Nordin and	0.00377	3.1	0.09	6.5	9.477	0.240
Dempster	0.00437	3.1	0.09	6.5	9.662	0.304
(1963)	0.00484	3.0	0.09	6.5	10.969	0.285
	0.00513	3.3	0.09	6.5	9.000	0.285
	0.00786	3.9	0.09	6.5	10.923	0.327
	0.00561	3.9	0.09	6.5	9.569	0.285
	0.00643	3.4	0.09	6.5	10.923	0.294
	0.00138	9.7	0.18	20.3	3.921	0.553
	0.00067	8.6	0.18	20.3	3.857	0.536
	0.00147	9.1	0.18	20.3	3.182	0.590
	0.00128	9.7	0.18	20.3	3.754	0.421
	0.00067	9.6	0.18	20.3	3.842	0.681
	0.00161	8.6	0.18	20.3	2.990	0.681
	0.00081	8.7	0.18	20.3	3.034	0.473
	0.00117	8.7	0.18	20.3	3.094	0.610
	0.00129	8.6	0.18	20.3	3.512	0.571
	0.00116	9.3	0.18	20.3	2.882	0.571
	0.00130	11.1	0.18	20.3	3.498	0.656
	0.00046	11.1	0.18	20.3	3.064	0.571
	0.00120	9.6	0.18	20.3	3.498	0.590
	0.00018	27.5	0.35	52.0	1.528	1.110
	6.10E-05	24.3	0.35	52.0	1.503	1.070
	0.00010	25.7	0.35	52.0	1.240	1.180
	0.00016	27.5	0.35	52.0	1.463	0.843
	4.40E-05	27.1	0.35	52.0	1.497	1.360
	0.00016	24.3	0.35	52.0	1.165	0.843
	4.20E-05	24.6	0.35	52.0	1.182	0.956
	0.00029	24.6	0.35	52.0	1.205	1.220
	0.00041	24.3	0.35	52.0	1.369	1.140
	0.00026	26.4	0.35	52.0	1.123	1.140
	0.00026	31.5	0.35	52.0	1.363	1.310
	4.40E-05	31.5	0.35	52.0	1.194	1.140
	0.00023	27.1	0.35	52.0	1.363	1.180

	E_s/p	R_p	D_g (mm)	v_s (mm/s)	u_*/v_s	D_i/D_{50}
Middle	0.00466	2.7	0.09	6.5	8.354	0.519
Rio Grande	0.00447	2.9	0.09	6.5	7.323	0.519
Data:	0.00312	3.3	0.09	6.5	6.738	0.551
near Socorro,	0.00692	3.5	0.09	6.5	9.985	0.420
	0.00873	3.3	0.09	6.5	8.292	0.465
Nordin and	0.01170	3.2	0.09	6.5	8.492	0.552
Dempster	0.00251	3.5	0.09	6.5	8.723	0.589
(1963)	0.01110	3.6	0.09	6.5	8.015	0.465
	0.06930	3.5	0.09	6.5	11.816	0.367
	0.16500	3.6	0.09	6.5	12.000	0.353
	0.00165	7.8	0.18	20.3	2.675	1.040
	0.00143	8.1	0.18	20.3	2.345	1.040
	0.00058	9.3	0.18	20.3	2.158	1.110
	0.00071	9.8	0.18	20.3	3.197	0.842
	0.00259	9.5	0.18	20.3	2.655	0.932
	0.00413	9.2	0.18	20.3	2.719	1.110
	0.00061	10.0	0.18	20.3	2.793	1.180
	0.00311	10.2	0.18	20.3	2.567	0.932
	0.02030	9.8	0.18	20.3	3.783	0.738
	0.05120	10.3	0.18	20.3	3.842	0.708
	0.00027	27.8	0.35	52.0	1.246	1.680
	0.00644	27.8	0.35	52.0	1.474	1.480
	0.00879	29.2	0.35	52.0	1.497	1.420
Niobrara	0.00510	2.2	0.09	6.5	13.415	0.304
River:	0.01110	2.2	0.09	6.5	14.292	0.304
	0.00630	2.2	0.09	6.5	14.708	0.304
Colby and	0.00460	2.2	0.09	6.5	16.308	0.304
Hembree	0.00440	2.2	0.09	6.5	16.923	0.304
(1955)	0.00610	2.9	0.09	6.5	16.923	0.285
	0.01590	2.9	0.09	6.5	17.231	0.285
	0.02210	2.9	0.09	6.5	15.846	0.285
	0.02400	2.9	0.09	6.5	14.923	0.285
	0.01620	2.9	0.09	6.5	14.154	0.285
	0.00830	3.0	0.09	6.5	13.692	0.315
	0.00390	3.0	0.09	6.5	14.000	0.315
	0.00470	3.0	0.09	6.5	12.615	0.315
	0.00140	3.0	0.09	6.5	13.231	0.315
	0.00144	6.2	0.18	20.3	4.296	0.610
	0.00634	6.2	0.18	20.3	4.576	0.610
	0.00248	6.2	0.18	20.3	4.709	0.610
	0.00112	6.2	0.18	20.3	5.222	0.610
	0.00104	6.2	0.18	20.3	5.419	0.610
	0.00040	8.1	0.18	20.3	5.419	0.571
	0.00196	8.1	0.18	20.3	5.517	0.571
	0.00559	8.1	0.18	20.3	5.074	0.571
	0.00541	8.1	0.18	20.3	4.778	0.571
	0.00157	8.1	0.18	20.3	4.532	0.571
	0.00032	8.6	0.18	20.3	4.384	0.632

	E_s/p	R_p	D_g (mm)	v_s (mm/s)	u_*/v_s	D_i/D_{50}
Niobrara	0.0003	8.6	0.18	20.3	4.482759	0.632
River:	0.00084	8.6	0.18	20.3	4.039409	0.632
(continue)	0.00217	8.6	0.18	20.3	4.236453	0.632
	0.0003	17.6	0.35	52	1.673704	1.221
Colby and	0.00149	17.6	0.35	52	1.783109	1.221
Hembree	0.00096	17.6	0.35	52	1.834933	1.221
(1955)	0.0003	17.6	0.35	52	2.034549	1.221
	0.00174	22.9	0.35	52	2.149712	1.142
	0.00037	22.9	0.35	52	1.976967	1.142
	6.40E-05	24.3	0.35	52	1.708253	1.264
	0.00013	24.3	0.35	52	1.746641	1.264
	0.0002	24.3	0.35	52	1.573896	1.264

APPENDIX D.

SOURCE LISTING OF "DEPO" MODEL

```
1.  PROGRAM SEDIMENTATION
2.  ************************************************************************
3.  *  This program calculates sediment processes (deposition and scour)  *
4.  *  in reservoirs and rivers. The significant difference between this  *
5.  *  model and the others, is the effect of Turbidity Currents as a     *
6.  *  part of sedimentation in reservoirs. All the data needed for this  *
7.  *  program is called from one input file. All the output is           *
8.  *  written to one output file. The program will the ask user to       *
9.  *  specify the input and output files.                                *
10. *  This model was developed by Mehdi Ghomeshi as a part of PhD study  *
11. *  under the supervision of Prof. M. Sivakumar, in the Department of  *
12. *  Civil and Mining Engineering, University of Wollongong, Australia. *
13. ************************************************************************
14. C    DIST is distance of each node point of a cross section from the origin (m).
15. C    ELEV is elevation of each node point of the cross section (m).
16. C    CDNUMBER is the cross section identification number.
17. C    ANMAN is Manning's n value for the cross section.
18. C    CONCO is contraction coefficient.
19. C    EXPANCO is expansion coefficient.
20. C    RLENGTH is reach length each cross section and the downstream cross section.
21. C    QWATER is water discharge (in water and sediment rating curve).
22. C    QSEDI is total sediment load in tonness per day (in water and
23. C    sediment rating curve).
24. C    QGS is the fraction for each grain size(in water and sediment rating curve).
25. C    ELETAL is elevation of thalweg point of the cross section.
26. C    IPOINT is number of coordinate points used in the cross section.
27. C    AREA is area of the cross section.
28. C    WPR is wetted perimeter
29. C    HRAD is hydraulic radius of the cross section
30. C    VLCITY is average velocity of water in the cross section.
31. C    COK is conveyance, from Manning's formula
32. C    EFD is effective depth of water in the cross section.
33. C    EFW is effective width of water in the cross section.
34. C    WSELE is water surface elevation.
35. C    WWS is width of water surface
36. C    AMGS is the mean grain size of each sediment size class.
37. C    QSP is sediment transport capacity  of each grain size.
38. C    PRSP is percentage of particle in the bed
39. C    TCSP is actual sediment transport for each grain size.
40. C    VS is fall velocity of a particle.
```

```
41. C     PCSP is percent of each grain size in cover layer
42. C     DBM is depth of sediment in bed of section.
43. C     DCCL is cover layer thickness.
44. C ELEVN is the elevation of each node point of the cross section after each run (m).
45. C ELETALN is the elevation of thalweg point of the cross section after each run (m).
46. C     RLENTO is length of each cross section from frist downstream section.
47. C     TCELE is elevation of turbidity current in the cross section
48. C
49. C
50.       DIMENSION DIST(100,100),ELEV(100,100),CSNUMBER(100),ANMAN(100)
51.      &,CONCO(100),EXPANCO(100),RLENGTH(101),QWATER(10),QSEDI(10),
52.      &QGS(15,10),ELETAL(100),IPOINT(100),AREA(100),
53.      &WPR(100),HRAD(100),VLCITY(100),COK(100),EFD(100),EFW(100)
54.      &,WSELE(100),WWS(100),AMGS(15),QSP(15),PRSP(15,100),TCSP(15,101),
55.      &VS(15),PCSP(15,100),DBM(100),DCCL(100),ELEVN(100,100),
56.      &ELETALN(100),RLENTO(100),TCELE(100)
57.       DOUBLE PRECISION HF,H00,HE,VK,CDBM,TCSP
58.       character*12 infile
59.       character*12 output1
60.       character*2  MANNING
61.       character*2  CROSS
62.       character*2  GEOMETRY
63.       character*7  SPROPER
64.       character*4  CLAY
65.       character*4  SILT
66.       character*4  SAND
67.       character*7  WDSLOAD
68.       character*9  OPERATION
69.       character*7  BEDPART
70.       CHARACTER*1  TUCU
71.       CHARACTER*2  TURBIDITY
72. 223   FORMAT(2X,6F10.3)
73.       WRITE(*,*)'  '
74.       WRITE(*,*)'  '
75.       WRITE(*,*)'          ********************************************
76.      &************'
77.       WRITE(*,*)'          *               UNIVERSITY OF WOLLONGONG
78.      &           *'
79.       WRITE(*,*)'          *
80.      &           *'
81.       WRITE(*,*)'          *       *****        *******    ****
82.      &***        *'
83.       WRITE(*,*)'          *       ***  ***     *******    ******     **
84.      &   **      *'
85.       WRITE(*,*)'          *       ***   ***    **         **   **   ***
86.      &   ***     *'
87.       WRITE(*,*)'          *       ***    ***   *******    *******   ***
88.      &   ***     *'
```

```
89.       WRITE(*,*)'          *       ***   ***    **         ****      ***
90.      &   ***     *'
91.       WRITE(*,*)'          *       ***  ***     *******    **         **
92.      &   **      *'
93.       WRITE(*,*)'          *       *****        *******    **
94.      &***        *'
95.       WRITE(*,*)'          *
96.      &           *'
97.       WRITE(*,*)'          *  DEPO, the program for simulating sediment
98.      &deposition *'
99.       WRITE(*,*)'          *  and scour in reservoirs and rivers.
100.     &           *'
101.      WRITE(*,*)'          *                    By: M. GHOMESHI
102.     &           *'
103.      WRITE(*,*)'          ********************************************
104.     &************'
105.      WRITE(*,*)'  '
106.      WRITE(*,*)'  '
107.224   FORMAT(6F5.3)
108.      WRITE(*,*) 'Please type input filename  '
109.      READ(*,'(a12)')infile
110.      OPEN(5,file=infile,status='old')
111.      WRITE(*,*) 'Please type output filename  '
112.      READ(*,'(a12)')output1
113.      OPEN(2,file=output1,status='unknown')
114.      WRITE(*,*) 'Please wait the program is running'
115.C     Reading geometric data and writing in output
116.      DO 210 L=1,100
117.      READ(5,*) MANNING
118.      IF (MANNING.EQ.'MA') GO TO 238
119.      IF (MANNING.EQ.'EC') GO TO 240
120.      IF (L.EQ.1)THEN
121.      WRITE(*,*) 'The program expected MA series data in first cross
122.     & section, but it was not found'
123.      WRITE(2,*) 'The program expected MA series data in first cross
124.     & section, but it was not found'
125.      GO TO 299
126.      ELSE
127.      WRITE(*,*) 'The program expected MA series data after',
128.     &CSNUMBER(L-1), 'cross section, but it was not found'
129.      WRITE(2,*) 'The program expected MA series data after',
130.     &CSNUMBER(L-1), 'cross section, but it was not found'
131.      GO TO 299
132.      ENDIF
133.238   READ (5,*)ANMAN(L),CONCO(L),EXPANCO(L)
134.      IF(ANMAN(L).EQ.0) ANMAN(L)=ANMAN(L-1)
135.      IF(CONCO(L).EQ.0) CONCO(L)=CONCO(L-1)
136.      IF(EXPANCO(L).EQ.0) EXPANCO(L)=EXPANCO(L-1)
```

```
137.      READ(5,*)CROSS
138.      IF (CROSS.EQ.'CS') GO TO 230
139.      IF (L.EQ.1)THEN
140.      WRITE(*,*) 'The program expected CS series data in first cross
141.     & section, but it was not found'
142.      WRITE(2,*) 'The program expected CS series data in first cross
143.     & section, but it was not found'
144.      GO TO 299
145.      ELSE
146.      WRITE(*,*) 'The program expected CS series data after ',
147.     &CSNUMBER(L-1),'cross section, but it was not found'
148.      WRITE(2,*) 'The program expected CS series data after ',
149.     &CSNUMBER(L-1),'cross section, but it was not found'
150.      GO TO 299
151.      ENDIF
152.230   READ (5,*)CSNUMBER(L),IPOINT(L),RLENGTH(L),DBM(L)
153.C     DBM is height of erodible bed in the section
154.      IF (DBM(L).EQ.0) DBM(L)=5.0
155.C     DCCL Is cover layer thickness. Initialy equal to 0.06m and maximum is
156.C     0.6m. When it exceeds from 0.6 it changes to 0.06 again and the residual
157.C     will mix with the inactive layer
158.      DCCL(L)=0.06
159.      IF (DBM(L).LT.0.06) DCCL(L)=DBM(L)
160.      NN=IPOINT(L)
161.      WRITE(2,*)'Cross section number= ',CSNUMBER(L)
162.      IF (NN.EQ.0)THEN
163.      IPOINT(L)=IPOINT(L-1)
164.      ENDIF
165.      WRITE(2,*)'Number of coordinate points=',IPOINT(L)
166.      WRITE(2,*)'Manning,s n=',ANMAN(L),  'Contraction coefficient='
167.     &,conco(L)
168.      WRITE(2,*)'Expansion coefficient=',EXPANCO(L), 'Reach length='
169.     &,RLENGTH(L)
170.      WRITE(2,*) 'points DISTANCE & ELEVATION respectively'
171.      IF (NN.EQ.0)THEN
172.      DO 232 K=1,IPOINT(L)
173.      ELEV(L,K)=ELEV(L-1,K)
174.      ELEVN(L,K)=ELEV(L,K)
175.      DIST(L,K)=DIST(L-1,K)
176.      WRITE(2,223) DIST(L,K),ELEV(L,K)
177.232   CONTINUE
178.      GO TO 210
179.      ENDIF
180.      READ(5,*)GEOMETRY
181.      IF (GEOMETRY.EQ.'GE') GO TO 235
182.      WRITE(*,*) 'The program expected GE series data in',CSNUMBER(L),'
183.     &cross section, but it was not found'
184.      WRITE(2,*) 'The program expected GE series data in',CSNUMBER(L),'
```

```
185.      &cross section, but it was not found'
186.       GO TO 299
187.235    ELETAL(L)=100000.
188.       DO 200 K=1,NN
189.       READ (5,*)DIST(L,K),ELEV(L,K)
190.       ELEVN(L,K)=ELEV(L,K)
191.       WRITE(2,223)DIST(L,K),ELEV(L,K)
192.       IF (ELETAL(L).LT.ELEV(L,K)) GO TO 200
193.C      ELETAL is elevation of talwage
194.       ELETAL(L)=ELEV(L,K)
195.       ELETALN(L)=ELETAL(L)
196.200    CONTINUE
197.       NUMCS=L
198.210    CONTINUE
199.C
200.C      Reading sediment data and writing output
201.C
202.240    READ (5,*)SPROPER
203.       IF (SPROPER.EQ.'SPROPER') GO TO 245
204.       WRITE(*,*) 'The program expected SPROPER  series data but it was
205.      & not found'
206.       WRITE(2,*) 'The program expected SPROPER  series data but it was
207.      & not found'
208.       GO TO 299
209.245    READ (5,*)SGW, ACG
210.       IF(SGW.EQ.0)SGW=1.0
211.       IF(ACG.EQ.0)ACG=9.81
212.C
213.       READ (5,*)CLAY,SGCP,UWCP,CCCP,TCD,TCS,AM1
214.       IF(SGCP.EQ.0) SGCP=2.65
215.       IF(UWCP.EQ.0)UWCP=481.
216.c  initial unit wieght for clay particle when the sediment is always under water
217.       IF(CCCP.EQ.0) CCCP=256.
218.       IF (TCD.EQ.0) TCD=0.06
219.       READ (5,*)SILT,SGSP,UWSP,CCSP
220.       IF(SGSP.EQ.0)SGSP=2.65
221.       IF(UWSP.EQ.0) UWSP=1041.
222.       IF(CCSP.EQ.0) CCSP=91.3
223.       READ (5,*)SAND,ITCM,SGSA,UWSA,GSF,PEBE
224.       IF(SGSA.EQ.0) SGSA=2.65
225.       IF(UWSA.EQ.0) UWSA=1490.
226.       IF(GSF.EQ.0) GSF=0.667
227.       IF(PEBE.EQ.0) PEBE=30.
228.       AMGS(1)=0.003
229.       AMGS(2)=0.005
230.       AMGS(3)=0.011
231.       AMGS(4)=0.022
232.       AMGS(5)=0.044
```

```
233.      AMGS(6)=0.088
234.      AMGS(7)=0.177
235.      AMGS(8)=0.354
236.      AMGS(9)=0.707
237.      AMGS(10)=1.414
238.      AMGS(11)=2.828
239.      AMGS(12)=5.657
240.      AMGS(13)=11.31
241.      AMGS(14)=22.63
242.      AMGS(15)=45.26
243.      READ (5,*)WDSLOAD,IQNUM
244.      WRITE(2,*)'Specific gravity of water=',SGW
245.      WRITE(2,*)'Acceleration due to gravity=',ACG
246.      WRITE(2,*)'Properties of CLAY particles'
247.      WRITE(2,*)'Specific gravity=',SGCP,
248.      WRITE(2,*)'fully compacted Unit weight=',UWCC,      'Initial unit
249.     &weight=',UWCP
250.      WRITE(2,*)'Compaction coefficient=',CCCP
251.      WRITE(2,*)'Properties of SILT particles'
252.      WRITE(2,*)'Specific gravity=',SGSP,
253.      WRITE(2,*)'fully compacted Unit weight=',UWCS,      'Initial unit
254.     &weight=',UWSP
255.      WRITE(2,*)'Compaction coefficient=',CCSP
256.      WRITE(2,*)'Properties of SAND particles'
257.      WRITE(2,*)'Specific gravity=',SGSA,     'Initial unit weight=',UWSA
258.      WRITE(2,*)'Grain shape factor=',GSF
259.      WRITE(2,*)'Parameter for calculating equilibrium bed=',PEBE
260.      IF (ITCM.EQ.1)THEN
261.      WRITE(2,*) 'MEYER-PETER AND MULLER Transport capacity method'
262.      ELSEIF (ITCM.EQ.2)THEN
263.      WRITE(2,*) 'BAGNOLD Transport capacity method'
264.      ELSEIF (ITCM.EQ.3)THEN
265.      WRITE(2,*) 'ENGELUND AND HANSEN Transport capacity method'
266.      ELSEIF (ITCM.EQ.4)THEN
267.      WRITE(2,*) 'TOFFALETI Transport capacity method'
268.      ELSEIF (ITCM.EQ.5)THEN
269.      WRITE(2,*) 'ACKERS AND WHITE Transport capacity method'
270.      ELSEIF (ITCM.EQ.6)THEN
271.      WRITE(2,*) 'YANG Transport capacity method'
272.      ELSEIF (ITCM.EQ.7)THEN
273.      WRITE(2,*) 'HABIBI and SIVAKOMAR Transport capacity method'
274.      ELSE
275.      WRITE(2,*) 'Unknown value is entered for sediment capacity method'
276.      GO TO 299
277.      ENDIF
278.283   DO 284 MN=1,IQNUM
279.
280.      READ (5,*)QWATER(MN),QSEDI(MN),QGS(1,MN),QGS(2,MN),QGS(3,MN),
```

```
281.      &QGS(4,MN),QGS(5,MN),QGS(6,MN),QGS(7,MN),QGS(8,MN),QGS(9,MN),
282.      &QGS(10,MN),QGS(11,MN),QGS(12,MN),QGS(13,MN),QGS(14,MN),QGS(15,MN)
283.284    CONTINUE
284.       READ (5,*)BEDPART,NUMBCS,NISS
285.       READ (5,*)CSEC,PRSP(1,1),PRSP(2,1),PRSP(3,1),PRSP(4,1),PRSP(5,1),
286.      &PRSP(6,1),PRSP(7,1),PRSP(8,1),PRSP(9,1),PRSP(10,1),PRSP(11,1),
287.      &PRSP(12,1),PRSP(13,1),PRSP(14,1),PRSP(15,1)
288.       DO 285 MM=2,NUMCS
289.       IF (CSEC.EQ.CSNUMBER(MM-1) .AND. NUMBCS.GT.1)GO TO 287
290.       DO 575 MMV=1,15
291.       PRSP(MMV,MM)=PRSP(MMV,MM-1)
292.575    CONTINUE
293.285    CONTINUE
294.       GO TO 291
295.287    DO 510 IMN=2,NUMBCS
296.       READ (5,*)CSEC,PRCLAY1,PRVFSI1,PRFSI1,PRMSI1,PRCSI1,
297.      &PRVFSA1,PRFSA1,PRMSA1,PRCSA1,PRVCSA1,PRVFGR1,PRFGR1
298.      &,PRMGR1,PRCGR1,PRVCGR1
299.       TOTALL=0
300.       DO 295 MNN=MM,NUMCS
301.       IF (CSEC.EQ.CSNUMBER(MNN))GO TO 297
302.       TOTALL=TOTALL+RLENGTH(MNN)
303.295    CONTINUE
304.297    PRSP(1,MNN)=PRCLAY1
305.       PRSP(2,MNN)=PRVFSI1
306.       PRSP(3,MNN)=PRFSI1
307.       PRSP(4,MNN)=PRMSI1
308.       PRSP(5,MNN)=PRCSI1
309.       PRSP(6,MNN)=PRVFSA1
310.       PRSP(7,MNN)=PRFSA1
311.       PRSP(8,MNN)=PRMSA1
312.       PRSP(9,MNN)=PRCSA1
313.       PRSP(10,MNN)=PRVCSA1
314.       PRSP(11,MNN)=PRVFGR1
315.       PRSP(12,MNN)=PRFGR1
316.       PRSP(13,MNN)=PRMGR1
317.       PRSP(14,MNN)=PRCGR1
318.       PRSP(15,MNN)=PRVCGR1
319.       IF (MM.EQ.MNN)GO TO 510
320.       TRLEN=0
321.       DO 293 MMM=MM,MNN-1
322.       TRLEN=TRLEN+RLENGTH(MMM)
323.       DO 518 MBM=1,15
324.       PRSP(MBM,MMM)=(PRSP(MBM,MNN)-PRSP(MBM,MM-1))*(TRLEN/TOTALL)+
325.      &PRSP(MBM,MM-1)
326.518    CONTINUE
327.293    CONTINUE
328.       MM=MNN
```

```
329.510   CONTINUE
330.      IF (MM.EQ.NUMCS)GO TO 291
331.      DO 501 JMM=MM+1,NUMCS
332.      DO 502 JBM=1,15
333.      PRSP(JBM,JMM)=PRSP(JBM,MM)
334.502   CONTINUE
335.501   CONTINUE
336.291   DO 505 JMN=1,NUMCS
337.      DO 583 NS=1,15
338.C     PCSP is percent of each grain size in cover layer
339.      PCSP(NS,JMN)=PRSP(NS,JMN)
340.583   CONTINUE
341.505   CONTINUE
342.      READ (5,*)TURBIDITY,TUCU
343.      IF (TUCU.EQ.'Y')THEN
344.      READ (5,*)MSO
345.      ENDIF
346.      READ (5,*)OPERATION,NUMQ,COM
347.      DAYS=365
348.      AMCLAY=0
349.      AMSILT=0
350.      AMSAND=0
351.      DMCLAY=0
352.      DMSILT=0
353.      DMSAND=0
354.      DO 555 NT=1,NUMQ
355.      WRITE (*,*)'Run=',NT
356.      IF (TUCU.EQ.'Y')THEN
357.      READ (5,*)QW,WSEL,DUR,TEM,TCELEI
358.      TCELE(1)=TCELEI
359.      ELSE
360.      READ (5,*)QW,WSEL,DUR,TEM
361.      ENDIF
362.      DAYS=DAYS+DUR
363.      IYEAR=DAYS/365
364.C     In the following do loop the program will find the amount of sediment
365.C     that enters from upstream of the segment. It is simulated from input
366.C     sediment-discharge relationship and power interpolation between sequnce
367.C     points.
368.       DO 551 IE=1,IQNUM
369.       IF (QW.LT.QWATER(IE))THEN
370.         IF (IE.EQ.1)THEN
371.         SED1=((ALOG10(QSEDI(2))-ALOG10(QSEDI(1)))/(ALOG10(QWATER(2)
372.     &     )-ALOG10(QWATER(1))))*(ALOG10(QW)-ALOG10(QWATER(1)))+ALOG10
373.     &     (QSEDI(1))
374.         QSED1=10.**SED1
375.         DO 631 NU=1,15
376.         TCSP(NU,NUMCS+1)=QGS(NU,1)*QSED1/86.4
```

```
377.631        CONTINUE
378.           GO TO 633
379.           ENDIF
380.         SED1=((ALOG10(QSEDI(IE))-ALOG10(QSEDI(IE-1)))/(ALOG10(QWATER(IE)
381.      &  )-ALOG10(QWATER(IE-1))))*(ALOG10(QW)-ALOG10(QWATER(IE-1)))+
382.      &  ALOG10(QSEDI(IE-1))
383.         QSED1=10.**SED1
384.         QCO=(QSEDI(IE)-QSED1)/(QSEDI(IE)-QSEDI(IE-1))
385.           DO 635 NR=1,15
386.           TCSP(NR,NUMCS+1)=(QGS(NR,IE)-QCO*(QGS(NR,IE)-QGS(NR,IE-1)))*
387.      &     QSED1/86.4
388.635        CONTINUE
389.         GO TO 633
390.         ENDIF
391.551      CONTINUE
392.       SED1=((ALOG10(QSEDI(IE))-ALOG10(QSEDI(IE-1)))/(ALOG10(QWATER(IE)
393.      &)-ALOG10(QWATER(IE-1))))*(ALOG10(QW)-ALOG10(QWATER(IE-1)))+
394.      &ALOG10(QSEDI(IE-1))
395.       QSED1=10.**SED1
396.       DO 636 NW=1,15
397.       TCSP(NW,NUMCS+1)=QGS(NW,IQNUM)*QSED1/86.4
398.636    CONTINUE
399.C
400.C      Calculation of VK (Kinematic Viscosity) in m2/s. (Equation was written for
401.C      temp. between 4 degrees and 66 degrees Celsius)
402.633    VK=-4.3196E-12*TEM**3.+7.4219E-10*TEM**2.-5.0076E-8*TEM+1.7502E-6
403.C
404.C      AMCLAY is accumulated clay entering the segment from upstream in kg.
405.       AMCLAY=AMCLAY+TCSP(1,NUMCS+1)*DUR*86400.
406.C      ACCLAY is accumlated clay entering in cubic meters
407.       IF (IYEAR.GT.1)THEN
408.       ACCLAY=AMCLAY/(UWCP+CCCP*0.434*((IYEAR/(IYEAR-1))*LOG(IYEAR)-1))
409.       ELSE
410.       ACCLAY=AMCLAY/UWCP
411.       ENDIF
412.C      AMSILT is accumulated silt entering the segment from upstream in kg.
413.       AMSILT=AMSILT+(TCSP(2,NUMCS+1)+TCSP(3,NUMCS+1)+TCSP(4,NUMCS+1)
414.      &+TCSP(5,NUMCS+1))*DUR*86400.
415.C      ACSILT is accumlated silt entering in cubic meters
416.       IF (IYEAR.GT.1)THEN
417.       ACSILT=AMSILT/(UWSP+CCSP*0.434*((IYEAR/(IYEAR-1))*LOG(IYEAR)-1))
418.       ELSE
419.       ACSILT=AMSILT/UWSP
420.       ENDIF
421.C      AMSAND is accumulated sand entering in segment from upstream in kg.
422.       AMSAND=AMSAND+(TCSP(6,NUMCS+1)+TCSP(7,NUMCS+1)+TCSP(8,NUMCS+1)
423.      &+TCSP(9,NUMCS+1)+TCSP(10,NUMCS+1)+TCSP(11,NUMCS+1)+TCSP(12,NUMCS+
424.      &1)+TCSP(13,NUMCS+1)+TCSP(14,NUMCS+1)+TCSP(15,NUMCS+1))*DUR*86400.
```

```
425.C     ACSAND is accumlated sand entering in cubic meters
426.      ACSAND=AMSAND/UWSA
427.      DO 90 I=1,15
428.      D50G=AMGS(I)/1000.0
429.      DELTA=(SGSA/SGW)-1.0
430.C     DELTA is the submerged specific gravity of the sediment, RP is the
431.C     particle Reynolds number
432.      RP=(D50G*(DELTA*ACG*D50G)**0.5)/VK
433.C     Estimation of sediment fall velocity, VS, (Dietrich, 1984)
434.      ARP=RP**2.
435.      ADS=ALOG10(ARP)
436.      AOW=-3.7617+1.92944*ADS-0.09815*ADS**2.-0.00575*ADS**3.+0.00056
437.     &*ADS**4.
438.      W=10.**AOW
439.      VS(I)=(ACG*DELTA*VK*W)**(1./3.)
440.90    CONTINUE
441.
442.C     Water surface profile calculations using standard step method.
443.C     Calculation of hydraulic and geometric characteristic for first
444.C     cross section. WSELE(I)=water surface elevation in ith cross section.
445.C     AREA(I)=area of ith cross section. WPR(I)=wetted perimeter.
446.C     HRAD(I)=hydraulic radius. COK(I)=conveyance, from Manning's formula.
447.C     VLCITY(I)=velocity in ith cross section. EFD(I)=effective depth.
448.C     EFW(I)=effective width. ELETAL(I)=talwage elevation of ith cross section.
449.C     WWS(I)=width of water surface.
450.      IP=IPOINT(1)
451.
452.      CALL APR(1,DIST,ELEVN,IP,WSEL,AREAA,WPRR,EFDD,EFWW,WWSS,ELETALL)
453.      AREA(1)=AREAA
454.      WPR(1)=WPRR
455.      HRAD(1)=AREAA/WPRR
456.      COK(1)=(1./ANMAN(1))*AREA(1)*HRAD(1)**(2./3.)
457.      VLCITY(1)=QW/AREAA
458.      EFD(1)=EFDD
459.      EFW(1)=EFWW
460.      ELETALN(1)=ELETALL
461.      WWS(1)=WWSS
462.      WSELE(1)=WSEL
463.C     Calculation of hydraulic and geometric characteristic for the other
464.C     sections. HF=friction losses. DVE=difference of energy of velocity
465.C     between two sections. H00=losses due to contractions or expansions.
466.C     HE=total losses. WSELEA=assumed water elevation. The first trial is
467.C     equal to water elevation of previous section. The second trial is
468.C     equal to WSELEA2=WSELEA1+0.9*DY1 (DY1=difference between computed and
469.C     assumed water elevation). The third trial is equal to intersection
470.C     of trial 1 and 2 assumed elevation line with trial 1 and 2 computed
471.C     elevation line. This process continues until the assumed and computed
472.C     values are within the acceptable error. Maximum number of trails is 100.
```

```
473.        DO 388 LM=2,NUMCS
474.C       WSELEA1 is first trial to find water elevation in the cross section.
475.C       It is equal to the previous water surface elevation.
476.        WSELEA1=WSELE(LM-1)
477.        ELETALL=100000.
478.        DO 329 ICC=1,IPOINT(LM)
479.        IF (ELETALL.LT.ELEVN(LM,ICC)) GO TO 329
480.        ELETALL=ELEVN(LM,ICC)
481.329     CONTINUE
482.C       If the previous water surface elevation is less than talwage elevation
483.C       +1 meter, the first trial will start from talwage elevation+1
484.        IF (WSELEA1.LE.(ELETALL+1.0)) WSELEA1=ELETALL+1.0
485.        DO 315 MI=1,100
486.        IP=IPOINT(LM)
487.        CALL APR(LM,DIST,ELEVN,IP,WSELEA1,AREAA,WPRR,EFDD,EFWW,WWSS,ELETAL
488.       &L)
489.        AREA(LM)=AREAA
490.        WPR(LM)=WPRR
491.        HRAD(LM)=AREAA/WPRR
492.        COK(LM)=(1./ANMAN(LM))*AREA(LM)*HRAD(LM)**(2./3.)
493.        VLCITY(LM)=QW/AREAA
494.        EFD(LM)=EFDD
495.        EFW(LM)=EFWW
496.        ELETALN(LM)=ELETALL
497.        WWS(LM)=WWSS
498.        WSELE(LM)=WSELEA1
499.        IF (WSELEA1.LE.(ELETALN(LM)+0.30)) GO TO 367
500.C       HF is friction loss
501.        HF=RLENGTH(LM)*(QW/((1./ANMAN(LM))*((AREA(LM)+AREA(LM-1))/2.)*((
502.       &HRAD(LM)+HRAD(LM-1))/2.)**(2./3.)))**2.
503.C       DVE is difference between kinematic energy for calculating energy losses
504.C       due to contraction and expansion
505.        DVE=(1.15*VLCITY(LM)**2./(2.*ACG))-(1.15*VLCITY(LM-1)**2./(2.*ACG)
506.       &)
507.        IF (DVE.LT.0)THEN
508.        CL=CONCO(LM)
509.        GO TO 311
510.        ELSE
511.        CL=EXPANCO(LM)
512.        ENDIF
513.C       H00 is energy losses due to contraction or expansion
514.311     H00=CL*ABS(DVE)
515.C       HE is total energy losses
516.        HE=HF+H00
517.C       WSELEC1 is first computed water elevation related to first trial.
518.        WSELEC1=-DVE+WSELE(LM-1)+HE
519.        DY1=WSELEC1-WSELEA1
520.        YTAL=WSELEA1-ELETALN(LM)
```

```
C     If the assumed water elevation value and the computed value are within
C     the allowable error, the process will stopped. Otherwise the second
C     trial (WSELEA2) will be started.
      IF (ABS(DY1).LT.(0.000001*YTAL) .OR. ABS(DY1).LT.0.0001) GO TO 313
      WSELEA2=WSELEA1+0.9*DY1
      IF (WSELEA2.LE.(ELETALN(LM)+0.3)) WSELEA2=ELETALN(LM)+0.3
      CALL APR(LM,DIST,ELEVN,IP,WSELEA2,AREAA,WPRR,EFDD,EFWW,WWSS,ELETAL
     &L)
      AREA(LM)=AREAA
      WPR(LM)=WPRR
      HRAD(LM)=AREAA/WPRR
      COK(LM)=(1./ANMAN(LM))*AREA(LM)*HRAD(LM)**(2./3.)
      VLCITY(LM)=QW/AREAA
      EFD(LM)=EFDD
      EFW(LM)=EFWW
      ELETALN(LM)=ELETALL
      WWS(LM)=WWSS
      WSELE(LM)=WSELEA2
      IF (WSELEA2.LE.(ELETALN(LM)+0.3)) GO TO 367
      HF=RLENGTH(LM)*(QW/((1./ANMAN(LM))*((AREA(LM)+AREA(LM-1))/2.)*((
     &HRAD(LM)+HRAD(LM-1))/2.)**(2./3.)))**2.
      DVE=(1.15*VLCITY(LM)**2./(2.*ACG))-(1.15*VLCITY(LM-1)**2./(2.*ACG)
     &)
      IF (DVE.LT.0)THEN
      CL=CONCO(LM)
      ELSE
      CL=EXPANCO(LM)
      ENDIF
      H00=CL*ABS(DVE)
      HE=HF+H00
      WSELEC2=-DVE+WSELE(LM-1)+HE
      DY2=WSELEC2-WSELEA2
      YTAL=WSELEA2-ELETALN(LM)
      IF (ABS(DY2).LT.(0.000001*YTAL) .OR. ABS(DY2).LT.0.0001)GO TO 313
C     If the second assumed water elevation value and the computed value are
C     within the allowable error, the process will stoped. Otherwise the
C     third trial (WSELEA1) will be started and this process continue untill
C     untill the allowable error is achived.
      IF(ABS(DY2).GE.ABS(DY1))THEN
      WSELEA1= WSELEA2+0.9*DY2
      ELSE
      WSELEA1=(WSELEA1*(WSELEC2-WSELEC1)-WSELEC1*(WSELEA2-WSELEA1))/
     &(WSELEC2-WSELEC1+WSELEA1-WSELEA2)
      ENDIF
      IF(WSELEA1.LE.(ELETALN(LM)+0.3))THEN
      WSELEA1=ELETALN(LM)+0.3
      ENDIF
315   CONTINUE
```

```
569.C     Velocity distribution factor, ALPHA=1.15
570.C     To determine if the water elevation remains above critical depth,
571.C     the following procces will be carried out.
572.C     CRSF=the critical section factor. COSF=computed section factor.
573.C     SENER=specific energy.
574.C     If CRSF is less than COSF, subcritical flow exists and computation
575.C     continues. Otherwise, critical depth is calculated by tracing the
576.C     specific energy curve. If the water elevation is equal or less than
577.C     critical depth, the program computes the critical depth to
578.C     calculate hydraulic and geometric charactristics of section.
579.313   CRSF=QW/SQRT(ACG/1.15)
580.      COSF=AREA(LM)*SQRT(AREA(LM)/WWS(LM))
581.      IF (CRSF.LT.COSF) GO TO 388
582.C     In the following process critical depth (CRDEPTH) will be obtained by
583.C     obtaining depth of flow in minimum specific energy
584.367   SENER=EFD(LM)+VLCITY(LM)**2./(2.*ACG)
585.      WSELE1=WSELE(LM)+0.01
586.      CALL APR(LM,DIST,ELEVN,IP,WSELE1,AREAA,WPRR,EFDD,EFWW,WWSS,ELETALL
587.     &)
588.      SENER1=EFDD+QW**2./(2.*ACG*AREAA**2.)
589.      IF (SENER1.GT.SENER) THEN
590.      COIN=-0.01
591.      ELSEIF(ABS(SENER1-SENER).LT.1.E-4)THEN
592.      CRELE=WSELE1
593.      GO TO 292
594.      ELSE
595.      COIN=0.01
596.      ENDIF
597.      SENER2=SENER1
598.      SENER22=SENER2
599.      WSELE11=WSELE1
600.      DO 290 JI=1,20000
601.      WSELE1=WSELE1+COIN
602.      CALL APR(LM,DIST,ELEVN,IP,WSELE1,AREAA,WPRR,EFDD,EFWW,WWSS,ELETALL
603.     &)
604.      SENER=EFDD+QW**2./(2.*ACG*AREAA**2.)
605.      IF (SENER.GT.SENER2) GO TO 296
606.      SENER2=SENER
607.290   CONTINUE
608.      IF (COIN.GT.0)THEN
609.      COIN=-0.0001
610.      ELSE
611.      COIN=0.0001
612.      ENDIF
613.      DO 259 JIJ=1,2000
614.      WSELE11=WSELE11+COIN
615.      CALL APR(LM,DIST,ELEVN,IP,WSELE11,AREAA,WPRR,EFDD,EFWW,WWSS,ELETAL
616.     &L)
```

```
617.       SENER=EFDD+QW**2./(2.*ACG*AREAA**2.)
618.       IF (SENER.GT.SENER22)THEN
619.       WSELE1=WSELE11
620.       GO TO 296
621.       ENDIF
622.       SENER22=SENER
623.259    CONTINUE
624.       GO TO 388
625.296    CRELE=WSELE1-COIN
626.       IF(WSELE(LM).GT.CRELE.AND.WSELE(LM).gt.(ELETALN(LM)+0.3))GO TO 388
627.292    WSELE(LM)=CRELE
628.       CALL APR(LM,DIST,ELEVN,IP,CRELE,AREAA,WPRR,EFDD,EFWW,WWSS,ELETALL)
629.       AREA(LM)=AREAA
630.       WPR(LM)=WPRR
631.       HRAD(LM)=AREAA/WPRR
632.       COK(LM)=(1./ANMAN(LM))*AREA(LM)*HRAD(LM)**(2./3.)
633.       VLCITY(LM)=QW/AREAA
634.       EFD(LM)=EFDD
635.       EFW(LM)=EFWW
636.       ELETALN(LM)=ELETALL
637.       WWS(LM)=WWSS
638.       S=(ELETALN(LM)-ELETALN(LM-1))/RLENGTH(LM)
639.       IF (S.LT.1.E-6) S=1.E-6
640.       Q=COK(LM)*SQRT(S)
641.       IF (Q.GT.(QW+0.005*QW)) GO TO 337
642.       GO TO 388
643.337    WSELE4=WSELE(LM)
644.       DO 302 JIC=1,20000
645.       WSELE4=WSELE4-0.01
646.       IF(WSELE4.LT.0)WSELE4=WSELE4+0.01-0.001
647.       CALL APR(LM,DIST,ELEVN,IP,WSELE4,AREAA,WPRR,EFDD,EFWW,WWSS,ELETAL
648.      &L)
649.       AREA(LM)=AREAA
650.       WPR(LM)=WPRR
651.       HRAD(LM)=AREAA/WPRR
652.       COK(LM)=(1./ANMAN(LM))*AREA(LM)*HRAD(LM)**(2./3.)
653.       VLCITY(LM)=QW/AREAA
654.       EFD(LM)=EFDD
655.       EFW(LM)=EFWW
656.       WWS(LM)=WWSS
657.       Q=COK(LM)*SQRT(S)
658.       IF (Q.LT.(QW+0.005*QW)) GO TO 388
659.302    CONTINUE
660.       GO TO 388
661.C      WRITE(2,*)'Flow is supercritical in cross section',CSNUMBER(LM)
662.388    CONTINUE
663.       RLEN=0
664.       DO 22 LKG=1,NUMCS
```

```
665.        IF (LKG.GE.2) TCELE(LKG)=WSELE(LKG)
666.        RLENTO(LKG)=RLEN+RLENGTH(LKG)
667.        RLEN=RLENTO(LKG)
668.22      CONTINUE
669.C       SMEAN is mean slope of segment.
670.        SMEAN=(ELETALN(NUMCS)-ELETALN(1))/RLENTO(NUMCS)
671.        ICONTR=0
672.        DO 400 LI=1,NUMCS
673.        NIS=NISS
674.        LII=NUMCS+1-LI
675.        VLCITYY=VLCITY(LII)
676.        EFDD=EFD(LII)
677.        HRADD=HRAD(LII)
678.        ANMANN=ANMAN(LII)
679.        EFWW=EFW(LII)
680.        WSELLL=WSELE(LII)
681.C       Hydraulic parameters are converted into representative values for
682.C       simulating sediment transport capacity in each section if it is desired.
683.C       Potential transport of sand particles will be calculated in SEDMETHOD
684.C       subroutine. Seven methods are avilable for this purpose .
685.        CALL SEDMETHOD(ITCM,SGSA,SGW,VLCITYY,EFDD,HRADD,ANMANN,
686.       &AMGS,ACG,EFWW,VK,VS,TEM,QW,QSP)
687.C       TCSP is actual transport for each size in Kg/Sec
688.        DO 544 NBN=6,15
689.        TCSP(NBN,LII)=PCSP(NBN,LII)*QSP(NBN)/100.
690.544     CONTINUE
691.C       Method for finding the largest grain size in transport.
692.        BGS=AMGS(5)/1000.
693.        DO 556 JT=6,15
694.        IF (TCSP(JT,LII).NE.0)THEN
695.C       BGS is the largest grain size in transport.
696.        BGS=AMGS(JT)/1000.
697.        ENDIF
698.556     CONTINUE
699.        RLENGTH1=(RLENGTH(LII+1)+RLENGTH(LII))/2.
700.C       Continuity equation for sediment material (the Exner equation).
701.C       TIN is the initial number for recalculation of particle size
702.C       exchange in the bed
703.        TIN=DUR*86400*VLCITY(LII)/RLENGTH1
704.        IF (NIS.EQ.0)NIS=TIN
705.        IF (NIS.GT.TIN)NIS=TIN
706.        DTT=RLENGTH1/VLCITY(LII)
707.        AMSCO=0
708.        DO 578 LB=6,15
709.        IF (TCSP(LB,LII+1).LT.TCSP(LB,LII))THEN
710.        DTC=(TCSP(LB,LII+1)-TCSP(LB,LII))
711.        IF(ABS(DTC).LT.1E-10) DTC=0
712.C       AMSCO is maximum scour
```

```
713.        AMSCO=AMSCO-DTT*DTC/(EFW(LII)*UWSA*RLENGTH1)
714.        ENDIF
715.578     CONTINUE
716.C       EQ is water discharge per unit width of flow obtained by
717.C       combining Einstein's and Manning and Strickler equations.
718.C       DE is equilibrium depth for specific grain size
719.        DE=((QW/EFW(LII))/(29.3*SQRT((SGSA-SGW)/SGW)*(AMGS(6)/1000.)**(1./
720.       &3.)/SQRT(PEBE)))**(6./7.)
721.C       DSSL is sub-surface layer thickness
722.        DSSL=DE-EFD(LII)-DCCL(LII)
723.        IF (DSSL.GT.(AMSCO-DCCL(LII)))THEN
724.        DSSL=AMSCO-DCCL(LII)
725.        ENDIF
726.C       The minimum thickness of sub-surface layer is twice the
727.C       largest grain size in transport.
728.        IF (DSSL.LT.(2.*BGS))THEN
729.        DSSL=2.*BGS
730.        ENDIF
731.C       DIAL is inactive layer thickness
732.        DIAL=DBM(LII)-DCCL(LII)-DSSL
733.        IF (DIAL.LE.0)THEN
734.        DIAL=0
735.        DSSL=DBM(LII)-DCCL(LII)
736.        IF(DSSL.LT.0)THEN
737.        DSSL=0
738.        DCCL(LII)=DBM(LII)
739.        ENDIF
740.        ENDIF
741.        S=((VLCITYY*ANMANN)/HRADD**(2./3.))**2.
742.        DCL=DCCL(LII)
743.C       The value of change in each layer, transport capacity and characteristic
744.C       of the bed will be simulated in GEO subroutine
745.        CALL GEO(RLENGTH1,PCSP,LII,DTT,TCSP,VS,EFDD,SGW,ACG,NIS,
746.       &QW,TCD,HRADD,S,IYEAR,EFWW,UWCP,CCCP,UWSP,CCSP,UWSA,DCL,DSSL,
747.       &DIAL,AMGS,PRSP,T0,TCS,AM1)
748.        DCCL(LII)=DCL
749.C       DBCH is the change in bed cross section in meter
750.        DBC=DIAL+DCL+DSSL-DBM(LII)
751.        IF (ABS(DBC).LT.1E-15) DBC=0
752.        DBCH=DBC*TIN
753.        IP=IPOINT(LII)
754.C       COM=1.5
755.        IF (ABS(DBCH).LT.1E-8)GO TO 528
756.         IF(DBCH.LT.0)THEN
757.         IF(DBM(LII).LT.ABS(DBCH))DBCH=DBM(LII)
758.         ENDIF
759.         DBM(LII)=DBM(LII)+DBCH
760.         IF (DBM(LII).LT.0) DBM(LII)=0
```

```
761.       CALL BED(LII,DIST,EFWW,WSELLL,IP,DBCH,COM,ELEVN,ELEV,ELETALN)
762.528    IF (TUCU.EQ.'Y' .AND. ICONTR.EQ.0)THEN
763.C      Plunge point calculation from Akiyama and Stefan 1984
764.C      E0 is relative density difference between inflow and ambient water
765.       IF (TCELE(1).GE.WSELE(1))GO TO 400
766.       E0=(TCSP(1,LII)*(1.-SGW/SGCP)+(TCSP(2,LII)+TCSP(3,LII)+TCSP(4,LII)
767.      &+TCSP(5,LII))*(1.-SGW/SGSP)+(TCSP(6,LII)+TCSP(7,LII)+TCSP(8,LII)+
768.      &TCSP(9,LII)+TCSP(10,LII)+TCSP(11,LII)+TCSP(12,LII)+TCSP(13,LII)+
769.      &TCSP(14,LII)+TCSP(15,LII))*(1.-SGW/SGSA))/(1000.*QW)
770.       IF (E0.LT.1.E-15)GO TO 400
771.       Q0=QW/EFW(LII)
772.C      FT is total friction factor
773.       FT=0.02
774.C      S1 and S2 are coefficients
775.       S1=0.25
776.       S2=0.75
777.C      DC is dilution coefficient
778.       DC=0.
779.       SC=Ft*S1/S2
780.       IF (SMEAN.LT.SC) THEN
781.C      HP is plunge depth and HTC is the underflow depth downstream of
782.C      the plunge point
783.       HP=(1/2.0)*((2.+DC)/2.0+(S2*SMEAN/FT)+(((2.+DC)/2.0+(S2*SMEAN/FT))
784.      &**2.0-4.*(S2*SMEAN/FT/(1+DC)))**0.5)*(FT/(SMEAN*S2))**(1/3.)*(Q0**
785.      &2./(E0*ACG))**(1/3.0)
786.       HTC=(FT*Q0**2./(SMEAN*S2*E0*ACG))**(1./3.)*(1.+DC)
787.       ELSE
788.       HP=(1/2.)*(((2.+DC)/2.+S1)+(((2.+DC)/2.+S1)**2.
789.      &-4.*S1/(1+DC))**0.5)*(1./S1)**(1/3.)*(Q0**2./(E0*ACG))**(1./3.0)
790.       HTC=(Q0**2./(S1*E0*ACG))**(1./3.0)*(1.0+DC)
791.       ENDIF
792.C      CN is concentration of sediment in plunge point.
793.       CN=TCSP(1,LII)/(QW*1000.*SGCP)+(TCSP(2,LII)+TCSP(3,LII)+TCSP(4,LII
794.      &)+TCSP(5,LII))/(QW*1000.*SGSP)+(TCSP(6,LII)+TCSP(7,LII)+TCSP(8,LII
795.      &)+TCSP(9,LII)+TCSP(10,LII)+TCSP(11,LII)+TCSP(12,LII)+TCSP(13,LII)+
796.      &TCSP(14,LII)+TCSP(15,LII))/(QW*1000.*SGSA)
797.       IF (LII.EQ.1 .AND. HP.GE.EFD(LII)) TCELE(1)=WSELE(1)
798.       IF (HP.LE.EFD(LII)) THEN
799.       ICONTR=1
800.       IF (LII.EQ.NUMCS .AND. HP.LT.EFD(LII))THEN
801.       HP=EFD(LII)
802.       HTC=EFD(LII)
803.       ENDIF
804.C      If the program finds the plunge point then the hydraulic parameters
805.C      for the rest of section will change due to turbidity current elevation.
806.C      This will be done in the TC subroutin.
807.       CALL TC(LII,EFD,EFW,VLCITY,WSELE,TCELE,QW,RLENGTH,ELETALN,
808.      &AMGS,SGCP,SGSP,SGSA,SGW,VK,ACG,VS,DIST,ELEVN,IPOINT,AREA,WPR,
```

```
809.      &WWS,MSO,ANMAN,COK,HRAD,CN,SMEAN,RLENTO,SC,FT,EO,HP,HTC)
810.       ENDIF
811.       ENDIF
812.400    CONTINUE
813.C      DMCLAY is accumulated clay passing the segment in kg.
814.       DMCLAY=DMCLAY+TCSP(1,1)*DUR*86400.
815.C      DCCLAY is accumlated clay passing the segment in cubic meters
816.       IF (IYEAR.GT.1)THEN
817.       DCCLAY=DMCLAY/(UWCP+CCCP*0.434*((IYEAR/(IYEAR-1))*LOG(IYEAR)-1))
818.       ELSE
819.       DCCLAY=DMCLAY/UWCP
820.       ENDIF
821.C      DMSILT is accumulated silt passing the segment in kg.
822.       DMSILT=DMSILT+(TCSP(2,1)+TCSP(3,1)+TCSP(4,1)
823.      &+TCSP(5,1))*DUR*86400.
824.C      DCSILT is accumlated silt passing the segment in cubic meters
825.       IF (IYEAR.GT.1)THEN
826.       DCSILT=DMSILT/(UWSP+CCSP*0.434*((IYEAR/(IYEAR-1))*LOG(IYEAR)-1))
827.       ELSE
828.       DCSILT=DMSILT/UWSP
829.       ENDIF
830.C      DMSAND is accumulated sand passing the segment in kg.
831.       DMSAND=DMSAND+(TCSP(6,1)+TCSP(7,1)+TCSP(8,1)
832.      &+TCSP(9,1)+TCSP(10,1)+TCSP(11,1)+TCSP(12,
833.      &1)+TCSP(13,1)+TCSP(14,1)+TCSP(15,1))*DUR*86400.
834.C      DCSAND is accumlated sand passing the segment in cubic meters
835.       DCSAND=DMSAND/UWSA
836.555    CONTINUE
837.       DAYS=DAYS-365.
838.C      CLAYTE is trap efficiency of clay
839.       IF (ACCLAY.EQ.0)THEN
840.       CLAYTE=100
841.       ELSE
842.       CLAYTE=(ACCLAY-DCCLAY)/ACCLAY
843.       ENDIF
844.C      SILTTE is trap efficiency of silt
845.       IF (ACSILT.EQ.0)THEN
846.       SILTTE=100
847.       ELSE
848.       SILTTE=(ACSILT-DCSILT)/ACSILT
849.       ENDIF
850.C      SANDTE is trap efficiency of sand
851.       IF (ACSAND.EQ.0)THEN
852.       SANDTE=100
853.       ELSE
854.       SANDTE=(ACSAND-DCSAND)/ACSAND
855.       ENDIF
856.C      TOTALTE is total trap efficiency of reservoir
```

```
      TOTALTE=(ACCLAY-DCCLAY+ACSILT-DCSILT+ACSAND-DCSAND)/(ACCLAY+
     &ACSILT+ACSAND)
      WRITE(2,*)'*************************************************
     &************'
      WRITE(2,*)'*          Final Results of Sedimentation Modelling
     &          *'
      WRITE(2,*)'*************************************************
     &************'
      WRITE(2,*)' '
      WRITE(2,*)' '
      DO 202 KG=1,NUMCS
      WRITE(2,*)'Cross section number  ',CSNUMBER(KG)
      WRITE(2,*) 'points DISTANCE,INITIAL ELEVATION AND FINAL ELEVATION'
  247 FORMAT(6X,F8.2,4X,F8.2,12X,F8.2)
      DO 201 KF=1,IPOINT(KG)
      WRITE(2,247)DIST(KG,KF),   ELEV(KG,KF),    ELEVN(KG,KF)
  201 CONTINUE
  202 CONTINUE
      WRITE(2,*)'*************************************************
     &************'
      WRITE(2,*)'*   Total Days   *             Total Sediment Inflow
     &          *'
      WRITE(2,*)'*                *  SAND & GRAVEL      SILT          CL
     &AY         *'
      WRITE(2,*)'*                *     (in m3)        (in m3)       (in
     &m3)        *'
  236 FORMAT('*',1X,F10.2,5X,'*',4X,D8.2,8X,D8.2,6X,D8.2,6X,'*')
      WRITE(2,236)DAYS,ACSAND, ACSILT, ACCLAY
      WRITE(2,*)'*************************************************
     &************'
      WRITE(2,*)'*                Total Sediment Outflow
     &          *'
      WRITE(2,*)'*           SAND & GRAVEL      SILT          CLAY
     &          *'
      WRITE(2,*)'*              (in m3)        (in m3)       (in m3)
     &          *'
  237 FORMAT('*',9X,D10.2,6X,D10.2,5X,D10.2,15X,'*')
      WRITE(2,237)DCSAND,DCSILT,DCCLAY
      WRITE(2,*)'*************************************************
     &************'
      WRITE(2,*)'*                Trap Efficiency of Reservoir
     &          *'
      WRITE(2,*)'*     SAND & GRAVEL      SILT       CLAY       TOTAL
     &          *'
  239 FORMAT('*',8X,F6.4,8X,F6.4,6X,F6.4,5X,F6.4,14X,'*')
      WRITE(2,239)SANDTE,SILTTE,CLAYTE,TOTALTE
      WRITE(2,*)'*************************************************
     &************'
```

```
905.C
906.       WRITE(2,*)'  '
907.       WRITE(2,*)'  SECTION  DISCHARGE   WS ELE   DISTANCE   INITIAL TALW
908.      &AGE  FINAL TALWAGE'
909.       WRITE(2,*)'    NO.      (m3/s)        (m)   FROM DAM(m)      ELE.(m)
910.      &         ELE.(m)'
911.       DO 980 NZZ=1,NUMCS
912.       NZ=NUMCS+1-NZZ
913.249    FORMAT(F8.2,2X,F8.2,3X,F8.2,3X,F8.2,5X,F8.2,8X,F8.2)
914.       WRITE(2,249)CSNUMBER(NZ),QW,WSELE(NZ),RLENTO(NZ), ELETAL(NZ),
915.      &  ELETALN(NZ)
916.980    CONTINUE
917.       WRITE (2,*)'PERCENTAGE OF EACH PARTICLE SIZE IN COVER LAYER'
918.       WRITE (2,*)'CROSS SECTION    RLENTO    CLAY(%)       SILT(%)
919.      & SAND(%)'
920.       DO 990 NZT=1,NUMCS
921.       PSILT=PCSP(2,NZT)+PCSP(3,NZT)+PCSP(4,NZT)+PCSP(5,NZT)
922.       PSAND=PCSP(6,NZT)+PCSP(7,NZT)+PCSP(8,NZT)+PCSP(9,NZT)+PCSP(10,NZT)
923.      &+PCSP(11,NZT)+PCSP(12,NZT)+PCSP(13,NZT)+PCSP(14,NZT)+PCSP(15,NZT)
924.       WRITE (2,*)CSNUMBER(NZT),RLENTO(NZT),PCSP(1,NZT),PSILT,PSAND
925.990    CONTINUE
926.       WRITE(*,*)'The program terminated succesfully, see "',output1,'"fi
927.      &le for the results'
928.299    STOP
929.       END
930.
931.
932.       SUBROUTINE GEO(RLENGTH1,PCSP,LII,DTT,TCSP,VS,EFDD,SGW,ACG,
933.      &NIS,QW,TCD,HRADD,S,IYEAR,EFWW,UWCP,CCCP,UWSP,CCSP,UWSA,DCL,DSSL
934.      &,DIAL,AMGS,PRSP,T0,TCS,AM1)
935.       DIMENSION CDBM(15),PCSP(15,100),TCSP(15,101),VS(15),
936.      &AMGS(15),PRSP(15,100),DYC(15),DYS(15)
937.       DOUBLE PRECISION CDBM,TCSP
938.       DO 5 NO=1,NIS
939.       DO 55 MW=1,15
940.       DYC(MW)=0
941.       DYS(MW)=0
942.55     CONTINUE
943.       DIALL=DIAL
944.       DCLL=DCL
945.       DSSLL=DSSL
946.C      T0 is the bed shear stress
947.       T0=SGW*1000.*ACG*HRADD*S
948.       PD=1.-T0/TCD
949.       IF (T0.LT.TCD)THEN
950.       DO 592 KP=1,5
951.C      IF (T0.LT.TCD)THEN
952.       CONCU=TCSP(KP,LII+1)/QW
```

```
953.C     The effect of flocculation on particle fall velocity has been considered,
954.C     from Migniot (1989) method
955.      IF(KP.LE.3)THEN
956.      CONCD=CONCU*2.718**(-VS(KP)*250.*(AMGS(KP)*1000.)**(-1.8)
957.     &*PD*DTT/(EFDD))
958.      ELSE
959.      CONCD=CONCU*2.718**(-VS(KP)
960.     &*PD*DTT/(EFDD))
961.      ENDIF
962.      TCSP(KP,LII)=CONCD*QW
963.      IF (TCSP(KP,LII).LT.1E-10) TCSP(KP,LII)=0
964.      QD=(CONCU-CONCD)*QW*DTT
965.       IF (KP.EQ.1)THEN
966.       UW=UWCP+CCCP*ALOG10(IYEAR)
967.       DYC(KP)=QD/(UW*EFWW*RLENGTH1)
968.       ELSE
969.       UW=UWSP+CCSP*ALOG10(IYEAR)
970.       DYC(KP)=QD/(UW*EFWW*RLENGTH1)
971.       DYS(KP)=0
972.       ENDIF
973.592   CONTINUE
974.      ELSEIF(T0.GT.TCS)THEN
975.C  DTCS is erosion rate in kg/s, AM1 in kg/m2/s and TCS is critical shear stress
976.C     CONCU in ppm
977.      CONCU=(TCSP(1,LII+1)+TCSP(2,LII+1)+TCSP(3,LII+1)+TCSP(4,LII+1)+
978.     &TCSP(5,LII+1))*1000/(QW*2.65)
979.      CONCD=CONCU+AM1*EFWW*RLENGTH1*(T0/TCS-1.0)/(QW*SGW*1000.)
980.C     PPM is concentration of sediment in ppm
981.C     The concentration of cohesive sediment should not axceed from 80000 ppm
982.      IF(CONCD.GT.80000.) CONCD=80000.
983.C     QS is amount of cohesive sediment scour from the control volume in kg
984.      QS=(CONCU*2.65/1000.-CONCD*2.65/1000.)*DTT*QW
985.c      QS=(CONCU-CONCD)/1.E6*QW*dtt
986.       IF (ABS(QS).LT.1.E-6)THEN
987.       QS=0
988.       DO 597 KPP=1,5
989.       DYC(KPP)=0
990.       DYS(KPP)=0
991.       TCSP(KPP,LII)=TCSP(KPP,LII+1)
992.597     CONTINUE
993.       GO TO 18
994.       ENDIF
995.      UWC=UWCP+CCCP*ALOG10(IYEAR)
996.      UWS=UWSP+CCSP*ALOG10(IYEAR)
997.C     CGSCL is the amount of cohesive sediment aviable in cover layer in kg
998.      CGSCL=(PCSP(1,LII)/100.*UWC+(PCSP(2,LII)+PCSP(3,LII)+
999.     &PCSP(4,LII)+PCSP(5,LII))/100.*UWS)*DCLL*RLENGTH1*EFWW
1000.      CGSSL=(PRSP(1,LII)/100.*UWC+(PRSP(2,LII)+PRSP(3,LII)+
```

```
1001.      &PRSP(4,LII)+PRSP(5,LII))/100.*UWS)*DSSLL*RLENGTH1*EFWW
1002.        IF((CGSCL+CGSSL).LT.0.002)THEN
1003.        DO 617 KPT=1,5
1004.        DYC(KPT)=0
1005.        DYS(KPT)=0
1006.        TCSP(KPT,LII)=TCSP(KPT,LII+1)
1007.617       CONTINUE
1008.        ELSEIF(CGSCL.LT.0.001)THEN
1009.           IF(CGSSL.GE.ABS(QS))THEN
1010.           QSS=ABS(QS)
1011.           COPC=QSS/CGSSL
1012.           DO 612 KPO=1,5
1013.           DYC(KPO)=0
1014.           DYS(KPO)=-PRSP(1,LII)/100.*COPC*DSSLL
1015.              IF(KPO.EQ.1)THEN
1016.              TCSP(KPO,LII)=TCSP(KPO,LII+1)-DYS(KPO)*RLENGTH1*EFWW*
1017.      &         UWC/dtt
1018.              ELSE
1019.              TCSP(KPO,LII)=TCSP(KPO,LII+1)-DYS(KPO)*RLENGTH1*EFWW*
1020.      &         UWS/dtt
1021.              ENDIF
1022.612         CONTINUE
1023.           ELSE
1024.           DO 613 KPR=1,5
1025.           DYC(KPR)=0
1026.           DYS(KPR)=-PRSP(1,LII)/100.*DSSLL
1027.              IF(KPR.EQ.1)THEN
1028.              TCSP(KPR,LII)=TCSP(KPR,LII+1)-DYS(KPR)*RLENGTH1*EFWW*
1029.      &         UWC/dtt
1030.              ELSE
1031.              TCSP(KPO,LII)=TCSP(KPR,LII+1)-DYS(KPO)*RLENGTH1*EFWW*
1032.      &         UWS/dtt
1033.              ENDIF
1034.613         CONTINUE
1035.           ENDIF
1036.        ELSEIF(CGSCL.GE.ABS(QS))THEN
1037.        COPC=ABS(QS)/CGSCL
1038.        DO 599 KPM=1,5
1039.        DYC(KPM)=-PCSP(1,LII)/100.*COPC*DCLL
1040.        DYS(KPM)=0
1041.           IF(KPM.EQ.1)THEN
1042.           TCSP(KPM,LII)=TCSP(KPM,LII+1)-DYC(KPM)*RLENGTH1*EFWW*UWC/dtt
1043.           ELSE
1044.           TCSP(KPM,LII)=TCSP(KPM,LII+1)-DYC(KPM)*RLENGTH1*EFWW*UWS/dtt
1045.           ENDIF
1046.599      CONTINUE
1047.        ELSEIF((CGSCL+CGSSL).GE.ABS(QS))THEN
1048.        QSS=ABS(QS)-CGSCL
```

```
1049.         COPC=QSS/CGSSL
1050.         DO 611 KPO=1,5
1051.         DYC(KPO)=-PCSP(1,LII)/100.*DCLL
1052.         COPC=QSS/CGSSL
1053.         DYS(KPO)=-PRSP(1,LII)/100.*COPC*DSSLL
1054.            IF(KPO.EQ.1)THEN
1055.            TCSP(KPO,LII)=TCSP(KPO,LII+1)-(DYC(KPO)+DYS(KPO))*RLENGTH1*
1056.      &       EFWW*UWC/DTT
1057.            ELSE
1058.            TCSP(KPO,LII)=TCSP(KPO,LII+1)-(DYC(KPO)+DYS(KPO))*RLENGTH1*
1059.      &       EFWW*UWS/DTT
1060.            ENDIF
1061.611       CONTINUE
1062.         ELSE
1063.         DO 615 KPR=1,5
1064.         DYC(KPR)=-PCSP(1,LII)/100.*DCLL
1065.         DYS(KPR)=-PRSP(1,LII)/100.*DSSLL
1066.            IF(KPR.EQ.1)THEN
1067.            TCSP(KPR,LII)=TCSP(KPR,LII+1)-(DYC(KPR)+DYS(KPR))*RLENGTH1*
1068.      &       EFWW*UWC/DTT
1069.            ELSE
1070.            TCSP(KPO,LII)=TCSP(KPR,LII+1)-(DYC(KPR)+DYS(KPO))*RLENGTH1*
1071.      &       EFWW*UWS/DTT
1072.            ENDIF
1073.615       CONTINUE
1074.         ENDIF
1075.       ELSE
1076.       DO 593 KPP=1,5
1077.       DYC(KPP)=0
1078.       DYS(KPP)=0
1079.       TCSP(KPP,LII)=TCSP(KPP,LII+1)
1080.593    CONTINUE
1081.       ENDIF
1082.c      592   CONTINUE
1083.18       DO 591 KO=6,15
1084.C      CDBM is the amount of sediment subject to deposition(+) or scour(-)in kg
1085.       CDBM(KO)=DTT*(TCSP(KO,LII+1)-TCSP(KO,LII))
1086.       IF (ABS(CDBM(KO)).LT.(1.E-10)) CDBM(KO)=0
1087.       IF (TCSP(KO,LII+1).LT.1.E-10) TCSP(KO,LII+1)=0
1088.C      DECAY is characteristic rate for deposition.
1089.       DECAY=VS(KO)*DTT/EFDD
1090.       IF (DECAY.GT.1) DECAY=1.0
1091.C      ENTRA is entraiment ratio.
1092.       ENTRA=RLENGTH1/(30.*EFDD)
1093.C      ENTCO is entrainment coefficient.
1094.       ENTCO=1.368-2.718**(-ENTRA)
1095.       IF (ENTCO.GT.1) ENTCO=1.0
1096.       IF (CDBM(KO).GE.0)THEN
```

```
1097.       CDBM(KO)=CDBM(KO)*DECAY
1098.       TCSP(KO,LII)=TCSP(KO,LII+1)-CDBM(KO)/DTT
1099.C      DYC( ) is the change in depth of cover bed, due to deposition
1100.C      or scour in meter.
1101.       DYC(KO)=CDBM(KO)/(UWSA*RLENGTH1*EFWW)
1102.       DYS(KO)=0
1103.       ELSEIF (PCSP(1,LII).LE.10.)THEN
1104.C      AGSCL is the weight particles of each grain size available in
1105.C      cover layer of bed.
1106.       AGSCL=DCLL*PCSP(KO,LII)*RLENGTH1*EFWW*UWSA/100.
1107.       CDBM(KO)=CDBM(KO)*ENTCO
1108.       TCSP(KO,LII)=TCSP(KO,LII+1)-CDBM(KO)/DTT
1109.       IF (AGSCL.LT.(-CDBM(KO)))THEN
1110.C        TPCSP is the percent of grain size greater than this size
1111.C        avilable in the cover layer.
1112.       TPCSP=0
1113.       DO 545 MX=KO+1,15
1114.       TPCSP=TPCSP+PCSP(MX,LII)
1115.545      CONTINUE
1116.       IF (TPCSP.LT.40) CFA=1
1117.C        When the bed cover is between 40 and 100,a linear constrain factor
1118.C        (CFA) is applied for scour from sub-surface layer.
1119.       IF (TPCSP.GE.40) CFA=TPCSP*(-1./60.)+5./3.
1120.C        AGSSL is the weight of particles of each grain size available
1121.C        in sub-surface layer of bed
1122.       AGSSL=CFA*DSSLL*PRSP(KO,LII)*RLENGTH1*EFWW*UWSA/100.
1123.C        TOTAGS is total weight of the particles of all grain sizes
1124.C        avilable in active layer of bed
1125.       TOTAGS=AGSCL+AGSSL
1126.         IF (TOTAGS.GT.(-CDBM(KO)))THEN
1127.         RESID=-CDBM(KO)-AGSCL
1128.C        DYS( ) is the change in depth of sub-surface bed, due to scour in meter
1129.         DYS(KO)=-RESID/(UWSA*RLENGTH1*EFWW)
1130.         DYC(KO)=-DCLL*PCSP(KO,LII)/100.
1131.         ELSE
1132.         CDBM(KO)=-TOTAGS
1133.         TCSP(KO,LII)=TCSP(KO,LII+1)-CDBM(KO)/DTT
1134.         DYS(KO)=-DSSLL*PRSP(KO,LII)*CFA/100.
1135.         DYC(KO)=-DCLL*PCSP(KO,LII)/100.
1136.         ENDIF
1137.       ELSE
1138.       PERC=-CDBM(KO)*100./(DCLL*PCSP(KO,LII)*RLENGTH1*EFWW*UWSA)
1139.       DYC(KO)=-DCLL*PCSP(KO,LII)*PERC/100.
1140.       DYS(KO)=0
1141.       ENDIF
1142.       ELSE
1143.       TCSP(KO,LII)=TCSP(KO,LII+1)
1144.       DYC(KO)=0
```

```
1145.       DYS(KO)=0
1146.       ENDIF
1147.591    CONTINUE
1148.       DYCT=DYC(1)+DYC(2)+DYC(3)+DYC(4)+DYC(5)+DYC(6)+DYC(7)+DYC(8)+
1149.      &DYC(9)+DYC(10)+DYC(11)+DYC(12)+DYC(13)+DYC(14)+DYC(15)
1150.       DYST=DYS(1)+DYS(2)+DYS(3)+DYS(4)+DYS(5)+DYS(6)+DYS(7)+DYS(8)+
1151.      &DYS(9)+DYS(10)+DYS(11)+DYS(12)+DYS(13)+DYS(14)+DYS(15)
1152.       DO 521 IR=1,15
1153.C      Calculation of each grain size percent in cover layer after time step
1154.       IF ((DCLL+DYCT).LE.1.E-5)THEN
1155.       PCSP(IR,LII)=0
1156.       ELSE
1157.       PCSP(IR,LII)=(PCSP(IR,LII)*DCLL+DYC(IR)*100.)/(DCLL+DYCT)
1158.       IF (PCSP(IR,LII).LT.1.E-6) PCSP(IR,LII)=0
1159.       ENDIF
1160.C      Calculation of each grain size percent in inactive layer after time step
1161.       IF ((DSSLL+DIALL+DYST).LE.1.E-5)THEN
1162.       PRSP(IR,LII)=0
1163.       ELSE
1164.       PRSP(IR,LII)=(PRSP(IR,LII)*(DSSLL+DIALL)+DYS(IR)*100.)/(DSSLL+
1165.      &DIALL+DYST)
1166.       IF (PRSP(IR,LII).LT.1.E-6) PRSP(IR,LII)=0
1167.       ENDIF
1168.521    CONTINUE
1169.       BGS=0
1170.       DO 557 JTD=1,15
1171.       IF (TCSP(JTD,LII).NE.0)THEN
1172.C      BGS is the largest grain size in transport.
1173.       BGS=AMGS(JTD)/1000.
1174.       ENDIF
1175.557    CONTINUE
1176.C      Checkpoint for depth of cover layer. If it is less than one grain size
1177.C      the new cover layer will be assigned combining the cover layer and
1178.C      sub-surface layer.
1179.       IF ((DCLL+DYCT).LE.BGS)THEN
1180.       DO 577 IP=1,15
1181.       PCSP(IP,LII)=(PCSP(IP,LII)*(DCLL+DYCT)+PRSP(IP,LII)*DSSLL)
1182.      &/(DCLL+DYCT+DSSLL)
1183.577    CONTINUE
1184.       DIALL=DIALL+DCLL+DYCT-0.06
1185.C      Depth of new cover layer
1186.       DCLL=0.06
1187.       ELSEIF ((DCLL+DYCT).GT.0.6)THEN
1188.       DO 589 IO=1,15
1189.       PRSP(IO,LII)=(PRSP(IO,LII)*(DSSLL+DIALL)+PCSP(IO,LII)*(DCLL+DYCT-
1190.      &0.06))/(DSSLL+DIALL+DCLL+DYCT-0.06)
1191.589    CONTINUE
1192.       DCLL=0.06
```

```
1193.       DIALL=DIALL+(DCLL+DYCT-0.06)
1194.       ELSE
1195.C      Depth of new cover layer
1196.       DCLL=DCLL+DYCT
1197.       ENDIF
1198.C      Calculation of each grain size percent in inactive layer after time step
1199.       IF ((DSSLL+DIALL+DYST).LE.0)THEN
1200.       DIALL=0
1201.       DSSLL=0
1202.       ELSE
1203.C      Depth of inactive layer after time step
1204.       DIALL=DIALL+DYST
1205.       ENDIF
1206.5      CONTINUE
1207.       DIAL=DIALL
1208.       DSSL=DSSLL
1209.       DCL=DCLL
1210.       RETURN
1211.       END
1212.C
1213.       SUBROUTINE APR(LM,DIST,ELEVN,IP,WSELL,AREAA,WPRR,EFDD,EFWW,WWSS,
1214.      &ELETALL)
1215.       DIMENSION DIST(100,100),ELEVN(100,100)
1216.       N=IP
1217.       AREAA=0.0
1218.       WPRR=0.0
1219.       DAD=0.0
1220.       AD=0.0
1221.       ELETALL=100000.
1222.       WWSS=0
1223.       DO 354 ICC=1,N
1224.       IF (ELETALL.LT.ELEVN(LM,ICC)) GO TO 354
1225.       ELETALL=ELEVN(LM,ICC)
1226.354    CONTINUE
1227.365    DO 310 ICC=2,N
1228.       IF (ELEVN(LM,ICC).GT.WSELL) GO TO 302
1229.       GO TO 303
1230.302    IF (ELEVN(LM,ICC-1).GE.WSELL) GO TO 310
1231.       GO TO 306
1232.303    IF (ELEVN(LM,ICC).EQ.WSELL) GO TO 308
1233.       GO TO 304
1234.308    IF (ELEVN(LM,ICC-1).GE.WSELL) GO TO 310
1235.       GO TO 312
1236.304    IF (ELEVN(LM,ICC-1).GT.WSELL) GO TO 306
1237.312    H2=WSELL-ELEVN(LM,ICC)
1238.       H1=WSELL-ELEVN(LM,ICC-1)
1239.       X1=DIST(LM,ICC)-DIST(LM,ICC-1)
1240.C      WIDTH OF WATER SURFACE
```

```
1241.       WWSS=WWSS+X1
1242.       A=(H1+H2)*X1/2.
1243.       AREAA=AREAA+A
1244.       HD=ABS(H2-H1)
1245.       P=SQRT(X1**2.+HD**2.)
1246.       WPRR=WPRR+P
1247.       DAD=DAD+A*((H1+H2)/2.)**(5./3.)
1248.       AD=AD+A*((H1+H2)/2.)**(2./3.)
1249.       GO TO 310
1250.306    IF ((DIST(LM,ICC)-DIST(LM,ICC-1)).LE.0.000001) GO TO 310
1251.       AA=(ELEVN(LM,ICC)-ELEVN(LM,ICC-1))/(DIST(LM,ICC)-DIST(LM,ICC-1))
1252.       B=ELEVN(LM,ICC)-AA*DIST(LM,ICC)
1253.       IF (ABS(AA).LE.0.0000001) GO TO 310
1254.       DIS=(WSELL-B)/AA
1255.       IF (ELEVN(LM,ICC).GT.WSELL)THEN
1256.       H1=WSELL-ELEVN(LM,ICC-1)
1257.       X1=DIS-DIST(LM,ICC-1)
1258.       ELSE
1259.       H1=WSELL-ELEVN(LM,ICC)
1260.       X1=DIST(LM,ICC)-DIS
1261.       ENDIF
1262.       A=H1*X1/2.
1263.       AREAA=AREAA+A
1264.       P=SQRT(H1**2.+X1**2.)
1265.       WPRR=WPRR+P
1266.       DAD=DAD+A*(H1/2.)**(5./3.)
1267.       AD=AD+A*(H1/2.)**(2./3.)
1268.       WWSS=WWSS+X1
1269.310    CONTINUE
1270.       EFDD=DAD/AD
1271.       EFWW=AD/((EFDD)**(5./3.))
1272.       RETURN
1273.       END
1274.C
1275.       SUBROUTINE SEDMETHOD(ITCM,SGSA,SGW,VLCITYY,EFDD,HRADD,ANMANN,
1276.      &AMGS,ACG,EFWW,VK,VS,TEM,QW,QSP)
1277.       DIMENSION AMGS(15),QSP(15),VS(15)
1278.       DOUBLE PRECISION VK,D50G,D50A,D90,D65,D35,S,F6I,F5I,F4I,PAM
1279.      &,SHV,B,HRADB
1280.C      Calculation of potential sediment transport
1281.       S=(VLCITYY*ANMANN)**2./HRADD**(4./3.)
1282.       DELTA=(SGSA/SGW)-1.0
1283.C      DELTA is the submerged specific gravity of the sediment, RP is the
1284.C      particle Reynolds number
1285.       DO 200 j=6,15
1286.C      D50G is geometric mean diameter of the particles and D50A is
1287.C      arithmetic mean diameter of the particles
1288.       D50G=AMGS(J)/1000.0
```

```
1289.       D50A=D50G*1.06
1290.       D90=D50G*1.343
1291.       D65=D50G*1.17
1292.       D35=D50G*0.95
1293.       DELTA=(SGSA/SGW)-1.0
1294.C      DELTA is the submerged specific gravity of the sediment, RP is the
1295.C      particle Reynolds number
1296.       IF (ITCM.EQ.1)GO TO 110
1297.       IF (ITCM.EQ.2)GO TO 120
1298.       IF (ITCM.EQ.3)GO TO 130
1299.       IF (ITCM.EQ.4)GO TO 140
1300.       IF (ITCM.EQ.5)GO TO 150
1301.       IF (ITCM.EQ.6)GO TO 160
1302.       IF (ITCM.EQ.7)GO TO 170
1303.C      Estimate potential sediment transport from MEYER-PETER AND MULLER
1304.C      METHOD(1948)-bed load.
1305.110    ANS=(D90)**(1./6.0)/26.0
1306.       HRADB=(VLCITYY*ANS)**(3./2.)/(S)**(3./4.0)
1307.C      SHST is dimensionless shear stress
1308.       SHST=HRADB*S/(DELTA*D50A)
1309.C      STP is dimensionless sediment transport parameter.
1310.       IF (SHST.LT.0.047)THEN
1311.       STP=0
1312.       ELSE
1313.       STP=8.*(SHST-0.047)**(3./2.)
1314.       END IF
1315.C      QSP is total bed load transport in kg/sec
1316.       QSPP=STP*(SGSA*1000.*ACG)*EFWW*(ACG*DELTA*(D50A)**3.)**0.5
1317.       QSP(J)=QSPP/ACG
1318.       GO TO 200
1319.C      Estimate potential sediment transport from BAGNOLD
1320.C      METHOD(1966)-bed load and suspended load.
1321.C      Hydraulic radius is used in BSHS0.
1322.120    BSHS0=SGW*1000.*ACG*HRADD*S
1323.C      BSHS0 is the bed shear stress for the wide channel.
1324.C      SHV is shear velocity.
1325.       SHV=(BSHS0/(SGW*1000.))**0.5
1326.       G=((SHV*D50A)/VK)*(SGSA*1000./(14.*SGW*1000.))**0.5
1327.       G2=G**2.
1328.       IF (G2.LE.150) THEN
1329.       TDSF=0.75
1330.C      TDSF is tan. of the angle of dynamic solid friction.
1331.       ELSE IF (G2.LT.6000)THEN
1332.       TDSF=-0.236*ALOG10(G2)+1.25
1333.       ELSE
1334.       TDSF=0.374
1335.       END IF
1336.       IF (D50A*1000.LT.0.06)THEN
```

```
1337.C      EB is estimateed bed load transport efficiency
1338.       EB=-0.012*ALOG10(3.28*VLCITYY)+0.15
1339.       ELSE IF (D50A*1000.0.LT.0.2)THEN
1340.       EB=-0.013*ALOG10(3.28*VLCITYY)+0.145
1341.       ELSE IF (D50A*1000.0.LT.0.7)THEN
1342.       EB=-0.016*ALOG10(3.28*VLCITYY)+0.139
1343.       ELSE
1344.       EB=-0.028*ALOG10(3.28*VLCITYY)+0.135
1345.       ENDIF
1346.C      QSB is estimated bed load transport rate and qss suspended load rate.
1347.       QSBW=(1./((SGSA-SGW)/SGSA))*BSHS0*VLCITYY*(EB/TDSF)
1348.       QSB=QSBW/ACG
1349.       QSSW=0.01*(BSHS0*VLCITYY**2./(VS(J)*(SGSA-SGW)/SGSA))
1350.       QSS=QSSW/ACG
1351.       QSP(J)=(QSB+QSS)*EFWW
1352.       GO TO 200
1353.C      Estimate potential sediment transport from ENGELUND AND HANSEN
1354.C      METHOD(1967)-total load.
1355.130    QSP(J)=0.05*EFWW*SGSA*1000.*VLCITYY**2.*(HRADD*S)**1.5*(ACG)**
1356.      &(-0.5)*DELTA**(-2.)*D50G**(-1.)
1357.       GO TO 200
1358.C      Estimate potential sediment transport from TOFFALETI
1359.C      METHOD(1967)-bed and suspended load.
1360.140    TDF=32.+(9./5.)*TEM
1361.       YA=EFDD*3.281/11.24
1362.       YB=EFDD*3.281/2.5
1363.       CZ=260.67-0.667*TDF
1364.       SI=S*EFDD*3.281*CZ
1365.       ZV=0.1198+0.00048*TDF
1366.       T=1.1*(0.051+0.00009*TDF)
1367.       HRADB=(VLCITYY*3.281)**1.5*(D65*3.281)**0.25/(117.57*S**0.75)
1368.       SHV=(ACG*3.281*HRADB*S)**0.5
1369.       PAM=(VK*10.76*100000.)**(1./3.)/(10.*SHV)
1370.       IF (PAM.LT.0.5)THEN
1371.       A=11.*PAM**(-1.408)
1372.       ELSE IF (PAM.LT.0.67)THEN
1373.       A=36.268*PAM**0.3127
1374.       ELSE IF (PAM.LT.0.73)THEN
1375.       A=246.944*PAM**5.1032
1376.       ELSE IF (PAM.LT.1.25)THEN
1377.       A=49.0
1378.       ELSE
1379.       A=26.432*PAM**2.7635
1380.       ENDIF
1381.       B=PAM*S*D65*3.281*100000.
1382.       IF (B.LT.0.25)THEN
1383.       AK4=1.0
1384.       ELSE IF (B.LT.0.35)THEN
```

```
1385.       AK4=5.3155*B**1.2051
1386.       ELSE
1387.       AK4=0.5*B**(-1.0465)
1388.       ENDIF
1389.       A=A*AK4
1390.       IF (A.LT.16)THEN
1391.       A=16
1392.       ENDIF
1393.       ZMI=VLCITYY*3.281*VS(J)*3.281/SI
1394.       IF (ZMI.LT.ZV*1.5)THEN
1395.       ZMI=1.5*ZV
1396.       ENDIF
1397.       ZLI=0.756*ZMI
1398.       ZUI=1.5*ZMI
1399.       F1I=ZLI-ZV
1400.       F2I=ZMI-ZV
1401.       F3I=ZUI-ZV
1402.       F4I=1.-F1I
1403.       IF (F4I.LT.1E-10) F4I=0
1404.       F5I=1.-F2I
1405.       F6I=1.-F3I
1406.       GFI=0.6*(T*A*D50G*3.281/(0.00058*(VLCITYY*3.281)**2.))**(-5./3.)
1407.       IF (F4I.EQ.0)THEN
1408.       XI=0
1409.       ELSE
1410.       XI=F4I*GFI/(YA**F4I-((2.*D50G*3.281)**F4I))
1411.       ENDIF
1412.       IF (XI.LT.1E-7) XI=0
1413.       CI=EFWW*3.281*XI
1414.C      Bed load transport in tonnes per day.
1415.       QSBI=10*CI*(2.*D50G*3.281)**F4I
1416.       QSB=QSBI/10.
1417.C      Checkpoint for evalution of bed load.
1418.       UDI=(1+ZV)*VLCITYY*(2*D50G/EFDD)**ZV
1419.       IF (XI.EQ.0)THEN
1420.       UBLI=0
1421.       ELSE
1422.       UBLI=XI/43.2*UDI*(2*D50G)**F1I
1423.       ENDIF
1424.       IF (UBLI.GT.100)THEN
1425.       QSB=(100./UBLI)*QSB
1426.       CI=QSB/(2*D50G)**F4I
1427.       ENDIF
1428.       IF (F4I.EQ.0)THEN
1429.       QSLI=0
1430.       ELSE
1431.       QSLI=10*(CI/F4I)*(YA**F4I-(2.*D50G*3.281)**F4I)
1432.       ENDIF
```

```
1433.       QSLI=QSLI/10.
1434.       IF (CI.EQ.0)THEN
1435.       QSMI=0
1436.       ELSE
1437.       QSMI=10*(CI/F5I)*YA**(F2I-F1I)*(YB**F5I-(YA**F5I))
1438.       ENDIF
1439.       QSMI=QSMI/10.
1440.       IF (CI.EQ.0)THEN
1441.       QSUI=0
1442.       ELSE
1443.       QSUI=10*(CI/F6I)*YA**(F2I-F1I)*YB**(F3I-F2I)*((EFDD*3.281)**F6I-
1444.      &(YB**F5I))
1445.       ENDIF
1446.       QSUI=QSUI/10.
1447.C      Suspended load transport in tonnes per day.
1448.       QSS=QSLI+QSMI+QSUI
1449.       IF (QSS.LT.0)THEN
1450.       QSS=0
1451.       ENDIF
1452.C      Total load transport in kg per second.
1453.       QSP(J)=(QSB+QSS)*1000./86400.
1454.       GO TO 200
1455.C      Estimate potential sediment transport from ACKERS AND WHITE
1456.C      METHOD(1973)-total load.
1457.150    DGR=D35*(DELTA*ACG/(VK**2.))**(1./3.)
1458.       AN=1-0.56*ALOG10(DGR)
1459.       AM=1.34+9.66/DGR
1460.       A=0.14+0.23/SQRT(DGR)
1461.       ALC=2.86*ALOG10(DGR)-((ALOG10(DGR))**2.)-3.53
1462.       C=10.**ALC
1463.       SHV=(ACG*EFDD*S)**0.5
1464.       FGR=(SHV**AN/SQRT(ACG*DELTA*D35))*(VLCITYY/(SQRT(32.0)*ALOG10(10.*
1465.      &EFDD/D35)))**(1.-AN)
1466.       FGRA=FGR/A-1.0
1467.       IF (FGRA.LT.0)THEN
1468.       FGRA=0.0
1469.       ENDIF
1470.       GGR=C*FGRA**AM
1471.       QSP(J)=VLCITYY*EFWW*D35*GGR*SGSA*1000.*(SHV/VLCITYY)**(-AN)
1472.       GO TO 200
1473.C      Estimate potential sediment transport from YANG
1474.C      METHOD(1973)-total load.
1475.160    SHV=SQRT(ACG*HRADD*S)
1476.       DSHV=SHV*D50G/VK
1477.       IF (DSHV.LT.70)THEN
1478.       VC=VS(J)*((2.5/(ALOG10(SHV*D50G/VK)-0.06))+0.66)
1479.       IF (VC.LT.1E-10) VC=0
1480.       ELSE
```

```
1481.       VC=2.05*VS(J)
1482.       ENDIF
1483.       REP=VS(J)*D50G/VK
1484.       IF (D50G.LT.0.002)THEN
1485.       AJ=272000.*REP**(-0.286)*(SHV/VS(J))**(-0.457)
1486.       AK=1.799-0.178*LOG(REP)-0.136*LOG(SHV/VS(J))
1487.       IF (AJ.LT.1E-10) AJ=0
1488.       IF (AK.LT.1E-10) AK=0
1489.       ELSE
1490.       AJ=4797334.*REP**(-0.633)*(SHV/VS(J))**(-4.816)
1491.       AK=2.784-0.132*LOG(REP)-0.122*LOG(SHV/VS(J))
1492.       IF (AJ.LT.1E-10) AJ=0
1493.       IF (AK.LT.1E-10) AK=0
1494.       ENDIF
1495.       ACHACK=VLCITYY-VC
1496.       IF (ACHACK.LT.0)THEN
1497.       CT=0
1498.       ELSE
1499.       CT=AJ*((VLCITYY*S/VS(J))-(VC*S/VS(J)))**AK
1500.       IF (CT.LT.1E-10) CT=0
1501.       ENDIF
1502.       QSP(J)=1E-3*SGW*QW*CT
1503.       GO TO 200
1504.C      Estimate potential sediment transport from HABIBI and SIVAKUMAR
1505.C      METHOD(1993),(1994)suspended load and bed load.
1506.170    RP90=(D90*(DELTA*ACG*D90)**0.5)/VK
1507.C      Estimation of sediment fall velocity, VS90, (Dietrich, 1984).
1508.       ARP90=RP90**2.
1509.       ADS90=ALOG10(ARP90)
1510.       AOW90=-3.7617+1.92944*ADS90-0.09815*ADS90**2.-0.00575*ADS90**3.+
1511.      &0.00056*ADS90**4.
1512.       W90=10.**AOW90
1513.       VS90=(ACG*DELTA*VK*W90)**(1./3.)
1514.       SHV=(ACG*HRADD*S)**0.5
1515.       QSS=(0.02*S*EFDD*VLCITYY**2.)*(1+(SHV/(0.4*VLCITYY))**2.)/(2.*
1516.      &DELTA*VS(J))
1517.       CL=SHV/VS(J)
1518.       IF(CL.LE.1.8)ALADA=1.32
1519.       IF(CL.GT.1.8)ALADA=0.4*VS(J)/SHV
1520.       QSB=ALADA*S*EFDD*SHV**2./(DELTA*0.4*VS90)
1521.       QSP(J)=(QSS+QSB)*EFWW*SGSA*1000.
1522.200    CONTINUE
1523.       RETURN
1524.       END
1525.C
1526.       SUBROUTINE BED(LII,DIST,EFWW,WSELLL,IP,DBCH,COM,ELEVN,ELEV,ELETALN
1527.      &)
1528.       DIMENSION DIST(100,100),ELE(100,100),ELEVN(100,100),ELETALN(100),
```

```
1529.      &ELEV(100,100)
1530.C     TOTA is the total area that should be reduced or increased in the
1531.C     cross section
1532.      TOTA=ABS(DBCH*EFWW)
1533.      DO 4 IB=1,IP
1534.      ELE(LII,IB)=ELEVN(LII,IB)
1535.4     CONTINUE
1536.      ELETALL=100000.
1537.      DO 359 ICC=1,IP
1538.      IF (ELETALL.LT.ELE(LII,ICC)) GO TO 359
1539.      ELETALL=ELE(LII,ICC)
1540.      HTALL=WSELLL-ELETALL
1541.359   CONTINUE
1542.      IF (COM.LE.1.AND.DBCH.LE.0)THEN
1543.      DO 356 IGH=1,100
1544.      AREAA=0.0
1545.      IF(ABS(DBCH).LT.0.000001) DBCH=0
1546.      DO 310 ICC=2,IP
1547.      IF (ELE(LII,ICC).GT.WSELLL) GO TO 302
1548.      GO TO 303
1549.302   IF (ELE(LII,ICC-1).GE.WSELLL) GO TO 310
1550.      GO TO 306
1551.303   IF (ELE(LII,ICC).EQ.WSELLL) GO TO 308
1552.      GO TO 304
1553.308   IF (ELE(LII,ICC-1).GE.WSELLL) GO TO 310
1554.      DH=0
1555.      GO TO 312
1556.304   IF (ELE(LII,ICC-1).GT.WSELLL) GO TO 306
1557.      H1=WSELLL-ELE(LII,ICC)
1558.      IF(ABS(DBCH).LT.0.000001)THEN
1559.      DH=0
1560.      ELSE
1561.      DH=DBCH/HTALL*H1*(H1/HTALL)**COM
1562.      ENDIF
1563.      IF (ABS(DH).LT.0.000001) DH=0
1564.312   X1=DIST(LII,ICC)-DIST(LII,ICC-1)
1565.      A=ABS(DH+DHP)*X1/2.
1566.      AREAA=AREAA+A
1567.      ELEVN(LII,ICC)=ELE(LII,ICC)+DH
1568.      DHP=DH
1569.      GO TO 310
1570.306   IF ((DIST(LII,ICC)-DIST(LII,ICC-1)).LE.0) GO TO 310
1571.      AA=(ELE(LII,ICC)-ELE(LII,ICC-1))/(DIST(LII,ICC)-DIST(LII,ICC-1))
1572.      B=ELE(LII,ICC)-AA*DIST(LII,ICC)
1573.      DIS=(WSELLL-B)/AA
1574.      IF (ELE(LII,ICC).GT.WSELLL)THEN
1575.      DH=0
1576.      X1=DIS-DIST(LII,ICC-1)
```

```
1577.       A=ABS(DHP)*X1/2
1578.       AREAA=AREAA+A
1579.       ELEVN(LII,ICC)=ELE(LII,ICC)+DH
1580.       DHP=0
1581.       ELSE
1582.       H1=WSELLL-ELE(LII,ICC)
1583.       IF(ABS(DBCH).LT.0.000001) THEN
1584.       DH=0
1585.       ELSE
1586.       DH=DBCH/HTALL*H1*(H1/HTALL)**COM
1587.       ENDIF
1588.       X1=DIST(LII,ICC)-DIS
1589.       IF (ABS(DH).LT.0.0001) DH=0
1590.       A=ABS(DH)*X1/2.
1591.       ELEVN(LII,ICC)=ELE(LII,ICC)+DH
1592.       AREAA=AREAA+A
1593.       DHP=DH
1594.       ENDIF
1595.310    CONTINUE
1596.       IF(ABS(AREAA).GT.TOTA-0.1 .AND.ABS(AREAA).LT.TOTA+0.1)GO TO 313
1597.       IF(DBCH.EQ.0) GO TO 313
1598.       IF (AREAA.EQ.0)GO TO 313
1599.       IF(IGH.GE.100)GO TO 356
1600.       DBCH=DBCH*TOTA/ABS(AREAA)
1601.356    CONTINUE
1602.313    ELETALN(LII)=ELETALL+DBCH
1603.       ELSEIF (COM.LE.1)THEN
1604.       DO 640 IPO=1,1000
1605.       SEDEL=ELETALL+DBCH
1606.       AREAA=0.0
1607.       DO 317 JCC=2,IP
1608.       IF(DBCH.LT.0.0000001) THEN
1609.       DBCH=0
1610.       ELEVN(LII,JCC)=ELE(LII,JCC)
1611.       ELSE
1612.       IF (ELE(LII,JCC).GT.SEDEL) GO TO 342
1613.       GO TO 343
1614.342    IF (ELE(LII,JCC-1).GE.SEDEL) GO TO 317
1615.       GO TO 346
1616.343    IF (ELE(LII,JCC).EQ.SEDEL) GO TO 348
1617.       GO TO 344
1618.348    IF (ELE(LII,JCC-1).GE.SEDEL) GO TO 317
1619.       GO TO 347
1620.344    IF (ELE(LII,JCC-1).GT.SEDEL) GO TO 346
1621.347    H2=SEDEL-ELE(LII,JCC)
1622.       H1=SEDEL-ELE(LII,JCC-1)
1623.       X1=DIST(LII,JCC)-DIST(LII,JCC-1)
1624.       A=(H1+H2)*X1/2.
```

```
1625.       AREAA=AREAA+A
1626.       ELEVN(LII,JCC)=SEDEL
1627.       IF(JCC.EQ.2)ELEVN(LII,1)=SEDEL
1628.       GO TO 317
1629.346    IF ((DIST(LII,JCC)-DIST(LII,JCC-1)).LE.0) GO TO 317
1630.       AA=(ELE(LII,JCC)-ELE(LII,JCC-1))/(DIST(LII,JCC)-DIST(LII,JCC-1))
1631.       B=ELE(LII,JCC)-AA*DIST(LII,JCC)
1632.       DIS=(SEDEL-B)/AA
1633.       IF (ELE(LII,JCC).GT.SEDEL)THEN
1634.       H1=SEDEL-ELE(LII,JCC-1)
1635.       X1=DIS-DIST(LII,JCC-1)
1636.       ELSE
1637.       H1=SEDEL-ELE(LII,JCC)
1638.       X1=DIST(LII,JCC)-DIS
1639.       ELEVN(LII,JCC)=SEDEL
1640.       ENDIF
1641.       A=H1*X1/2.
1642.       AREAA=AREAA+A
1643.       ENDIF
1644.317    CONTINUE
1645.       IF (AREAA.GT.TOTA-0.2 .AND. AREAA.LT.TOTA+0.2)GO TO 613
1646.       IF (DBCH.EQ.0) GO TO 613
1647.       IF (AREAA.EQ.0)GO TO 613
1648.       IF (IPO.EQ.1000)GO TO 613
1649.       IF ((TOTA/AREAA).GT.1.5)THEN
1650.       DBCH=1.5*DBCH
1651.       ELSEIF ((TOTA/AREAA).LT.0.7) THEN
1652.       DBCH=0.7*DBCH
1653.       ELSEIF(AREAA.GT.TOTA)THEN
1654.       DBCH=DBCH-0.05
1655.       ELSE
1656.       DBCH=DBCH+0.05
1657.       ENDIF
1658.640    CONTINUE
1659.613    ELETALN(LII)=SEDEL
1660.       ELSE
1661.       DO 50 IB=1,IP
1662.       ELE(LII,IB)=ELEV(LII,IB)
1663.50     CONTINUE
1664.       ELETALL=100000.
1665.       DO 314 ICC=1,IP
1666.       IF (ELETALL.LT.ELE(LII,ICC)) GO TO 314
1667.       ELETALL=ELE(LII,ICC)
1668.       HTALL=WSELLL-ELETALL
1669.314    CONTINUE
1670.       AREA1=0
1671.       SEDEL1=ELETALN(LII)
1672.       DO 327 JCC=2,IP
```

```
1673.       IF (ELE(LII,JCC).GT.SEDEL1) GO TO 372
1674.       GO TO 373
1675.372    IF (ELE(LII,JCC-1).GE.SEDEL1) GO TO 327
1676.       GO TO 376
1677.373    IF (ELE(LII,JCC).EQ.SEDEL1) GO TO 378
1678.       GO TO 394
1679.378    IF (ELE(LII,JCC-1).GE.SEDEL1) GO TO 327
1680.       GO TO 377
1681.394    IF (ELE(LII,JCC-1).GT.SEDEL1) GO TO 376
1682.377    H2=SEDEL1-ELE(LII,JCC)
1683.       H1=SEDEL1-ELE(LII,JCC-1)
1684.       X1=DIST(LII,JCC)-DIST(LII,JCC-1)
1685.       A=(H1+H2)*X1/2.
1686.       AREA1=AREA1+A
1687.       GO TO 327
1688.376    IF ((DIST(LII,JCC)-DIST(LII,JCC-1)).LE.0) GO TO 327
1689.       AA=(ELE(LII,JCC)-ELE(LII,JCC-1))/(DIST(LII,JCC)-DIST(LII,JCC-1))
1690.       B=ELE(LII,JCC)-AA*DIST(LII,JCC)
1691.       DIS=(SEDEL1-B)/AA
1692.       IF (ELE(LII,JCC).GT.SEDEL1)THEN
1693.       H1=SEDEL1-ELE(LII,JCC-1)
1694.       X1=DIS-DIST(LII,JCC-1)
1695.       ELSE
1696.       H1=SEDEL1-ELE(LII,JCC)
1697.       X1=DIST(LII,JCC)-DIS
1698.       ENDIF
1699.       A=H1*X1/2.
1700.       AREA1=AREA1+A
1701.327    CONTINUE
1702.       ITC=0
1703.       DO 644 ISD=1,1000
1704.       IF(ABS(DBCH).LT.0.000001) DBCH=0
1705.       SEDEL2=ELETALN(LII)+DBCH
1706.       IF(SEDEL2.LT.ELETALL)THEN
1707.       ITC=ITC+1
1708.       IF(ITC.GT.8)GO TO 682
1709.       SEDEL2=ELETALL
1710.       ENDIF
1711.       AREA2=0
1712.       DO 318 JCC=2,IP
1713.       IF (ELE(LII,JCC).GT.SEDEL2) GO TO 352
1714.       GO TO 353
1715.352    IF (ELE(LII,JCC-1).GE.SEDEL2)THEN
1716.       IF(JCC.EQ.2)ELEVN(LII,1)=ELE(LII,1)
1717.       ELEVN(LII,JCC)=ELE(LII,JCC)
1718.       GO TO 318
1719.       ELSE
1720.       GO TO 366
```

```
1721.       ENDIF
1722.353    IF (ELE(LII,JCC).EQ.SEDEL2) GO TO 358
1723.       GO TO 364
1724.358    IF (ELE(LII,JCC-1).GE.SEDEL2)THEN
1725.       ELEVN(LII,JCC-1)=ELE(LII,JCC-1)
1726.       ELEVN(LII,JCC)=ELE(LII,JCC)
1727.       GO TO 318
1728.       ELSE
1729.       GO TO 357
1730.       ENDIF
1731.364    IF (ELE(LII,JCC-1).GT.SEDEL2)THEN
1732.       ELEVN(LII,JCC-1)=ELE(LII,JCC-1)
1733.       GO TO 366
1734.       ENDIF
1735.357    H2=SEDEL2-ELE(LII,JCC)
1736.       H1=SEDEL2-ELE(LII,JCC-1)
1737.       X1=DIST(LII,JCC)-DIST(LII,JCC-1)
1738.       A=(H1+H2)*X1/2.
1739.       AREA2=AREA2+A
1740.       ELEVN(LII,JCC)=SEDEL2
1741.       IF(JCC.EQ.2)ELEVN(LII,1)=SEDEL2
1742.       GO TO 318
1743.366    IF ((DIST(LII,JCC)-DIST(LII,JCC-1)).LE.0 .AND.ELE(LII,JCC-1).GT.
1744.      &ELE(LII,JCC))THEN
1745.       ELEVN(LII,JCC)=SEDEL2
1746.       GO TO 318
1747.       ELSEIF((DIST(LII,JCC)-DIST(LII,JCC-1)).LE.0 .AND. ELE(LII,JCC-1)
1748.      &.LT.ELE(LII,JCC))THEN
1749.       ELEVN(LII,JCC)=ELE(LII,JCC)
1750.       GO TO 318
1751.       ENDIF
1752.       AA=(ELE(LII,JCC)-ELE(LII,JCC-1))/(DIST(LII,JCC)-DIST(LII,JCC-1))
1753.       B=ELE(LII,JCC)-AA*DIST(LII,JCC)
1754.       DIS=(SEDEL2-B)/AA
1755.       IF (ELE(LII,JCC).GT.SEDEL2)THEN
1756.       H1=SEDEL2-ELE(LII,JCC-1)
1757.       X1=DIS-DIST(LII,JCC-1)
1758.       ELSE
1759.       H1=SEDEL2-ELE(LII,JCC)
1760.       X1=DIST(LII,JCC)-DIS
1761.       ELEVN(LII,JCC)=SEDEL2
1762.       ENDIF
1763.       A=H1*X1/2.
1764.       AREA2=AREA2+A
1765.318    CONTINUE
1766.       AREAA=AREA1-AREA2
1767.       IF(ABS(AREAA).GT.TOTA-0.2 .AND. ABS(AREAA).LT.TOTA+0.2)GO TO 682
1768.       IF (DBCH.EQ.0) GO TO 682
```

```
1769.       IF (AREAA.EQ.0)GO TO 682
1770.       IF ((ABS(TOTA)/ABS(AREAA)).GT.1.5)THEN
1771.       DBCH=1.5*DBCH
1772.       ELSEIF ((ABS(TOTA)/ABS(AREAA)).LT.0.7) THEN
1773.       DBCH=0.7*DBCH
1774.       ELSEIF(ABS(AREAA).GT.ABS(TOTA))THEN
1775.       IF (DBCH.LT.0) DBCH=DBCH+0.05
1776.       IF (DBCH.GT.0) DBCH=DBCH-0.05
1777.       ELSE
1778.       IF (DBCH.LT.0) DBCH=DBCH-0.05
1779.       IF (DBCH.GT.0) DBCH=DBCH+0.05
1780.       ENDIF
1781.644    CONTINUE
1782.682    ELETALN(LII)=SEDEL2
1783.       ENDIF
1784.       RETURN
1785.       END
1786.
1787.       SUBROUTINE TC(LII,EFD,EFW,VLCITY,WSELE,TCELE,QW,RLENGTH,ELETALN,
1788.      &AMGS,SGCP,SGSP,SGSA,SGW,VK,ACG,VS,DIST,ELEVN,IPOINT,AREA,WPR,
1789.      &WWS,MSO,ANMAN,COK,HRAD,CN,SMEAN,RLENTO,SC,FT,E0,HP,HTC)
1790.       DIMENSION EFD(100),EFW(100),VLCITY(100),WSELE(100)
1791.      &,TCELE(100),RLENGTH(101),ELETALN(100),AMGS(15),VS(15),HRAD(100),
1792.      &DIST(100,100),ELEVN(100,100),IPOINT(100),AREA(100),COK(100),
1793.      &WPR(100),WWS(100),ANMAN(100),DETC(100),RLENTO(100)
1794.       DOUBLE PRECISION VK
1795.       LLI=LII
1796.C      The effect of flocculation on particle fall velocity has been
1797.C      considered, Migniot (1989).
1798.       VSM=VS(MSO)*250.*(AMGS(MSO)*1000.)**(-1.8)
1799.C      R is the submerged specific gravity of the sediment, RP is the
1800.C      particle Reynolds number
1801.       IF (MSO.EQ.1)SGP=SGCP
1802.       IF (MSO.GT.1 .AND. MSO.LE.5)SGP=SGSP
1803.       IF (MSO.GT.5)SGP=SGSA
1804.       R=(SGP/SGW)-1.
1805.       RP=(AMGS(MSO)/1000.*(R*ACG*AMGS(MSO)/1000.)**0.5)/VK
1806.C      R0 is concentration ratio (near-bed concentration over the
1807.C      layer-averaged concentration), it is almost a constant, equal
1808.C      to about 2.0 Parker et al. (1987). CD is a bed friction
1809.C      coefficient equal to 0.002 in reservoir (Garcia,1985)
1810.       R0=2.0
1811.       CD=0.002
1812.       ELETALL=ELETALN(1)
1813.       IF (TCELE(1).LT.(HTC+ELETALL)) TCELE(1)=HTC+ELETALL
1814.       WSEL=TCELE(1)
1815.       IP=IPOINT(1)
1816.       CALL APR(1,DIST,ELEVN,IP,WSEL,AREAA,WPRR,EFDD,EFWW,WWSS,ELETALL)
```

```
1817.       DETC(1)=EFDD
1818.C      HTC is the normal underflow depth
1819.       HTC=HT(1,DIST,ELEVN,IP,QW,EFWW,EFDD,SMEAN,SC,E0,ACG,FT)
1820.       IF(DETC(1).LT.HTC)THEN
1821.       DETC(1)=HTC
1822.       DO 77 KX=2,LLI-1
1823.       IP=IPOINT(KX)
1824.       EFDD=HP
1825.       HTC=HT(KX,DIST,ELEVN,IP,QW,EFWW,EFDD,SMEAN,SC,E0,ACG,FT)
1826.       DETC(KX)=HTC
1827.       IF(DETC(KX).GE.EFD(KX))THEN
1828.       TCELE(KX)=WSELE(KX)
1829.       LLII=KX
1830.       GO TO 60
1831.       ENDIF
1832.77     CONTINUE
1833.       GO TO 60
1834.       ENDIF
1835.       IF (DETC(1).GE.EFD(1)) GO TO 45
1836.       LOL=0
1837.       EFWT=0
1838.       DO 15 LTT=1,2
1839.       IF (LTT.EQ.1)THEN
1840.       LT=1
1841.       EFDD=DETC(1)
1842.       ELSE
1843.       LT=LLI
1844.       EFDD=HP
1845.       ENDIF
1846.       ELETALL=ELETALN(LT)
1847.       IP=IPOINT(LT)
1848.       CALL APT(LT,DIST,ELEVN,IP,WSEL,AREAA,WPRR,EFDD,EFWW,WWSS,ELETALL)
1849.       EFWT=EFWT+EFWW
1850.       LOL=LOL+1
1851.15     CONTINUE
1852.       EFWM=EFWT/LOL
1853.       AREA1=EFWM*DETC(1)
1854.       U0=QW/AREA1
1855.       Z0=RP**0.65*(U0*(CD**0.5)/VSM)
1856.C      ES is sediment entraiment function from the author's study formula,
1857.C      C is sediment concentration, U is turbidity current velocity,
1858.C      H is thickness of current, T is the volumetric sediment discharge
1859.C      per unit width and RI is Richardson number
1860.       ES0=0.00000033*Z0**4./(1.+0.0000011*Z0**4.)
1861.       C00=ES0/R0
1862.       U00=U0
1863.       H000=DETC(1)
1864.       DO 30 J=1,50
```

```
1865.       C0=C00
1866.       H0=H000
1867.       U0=U00
1868.       T0=C0*H0*U0
1869.C      EW is water entrainment coefficient, it is estimated from this
1870.C      study equation
1871.C      The Runge-Kutta numerical method is used for system of equations
1872.       DO 10 I=2,LLI-1
1873.       DX=RLENGTH(I)
1874.       F1=F(ACG,R,H0,VSM,SMEAN,U0,RP,T0)
1875.       G1=G(ACG,R,T0,U0,H0,F1)
1876.       E1=E(RP,U0,VSM,T0,H0)
1877.       F2=F(ACG,R,H0+DX*F1/2.,VSM,SMEAN,U0+DX*G1/2.,RP,T0+DX*E1/2.)
1878.       G2=G(ACG,R,T0+DX*E1/2.,U0+DX*G1/2.,H0+DX*F1/2.,F2)
1879.       E2=E(RP,U0+DX*G1/2.,VSM,T0+DX*E1/2.,H0+DX*F1/2.)
1880.       F3=F(ACG,R,H0+DX*F2/2.,VSM,SMEAN,U0+DX*G2/2.,RP,T0+DX*E2/2.)
1881.       G3=G(ACG,R,T0+DX*E2/2.,U0+DX*G2/2.,H0+DX*F2/2.,F3)
1882.       E3=E(RP,U0+DX*G2/2.,VSM,T0+DX*E2/2.,H0+DX*F2/2.)
1883.       F4=F(ACG,R,H0+DX*F3,VSM,SMEAN,U0+DX*G3,RP,T0+DX*E3)
1884.       G4=G(ACG,R,T0+DX*E3,U0+DX*G3,H0+DX*F3,F4)
1885.       E4=E(RP,U0+DX*G3,VSM,T0+DX*E3,H0+DX*F3)
1886.       H1=H0-DX*(F1+2.*F2+2.*F3+F4)/6.0
1887.       IP=IPOINT(I)
1888.       EFDD=HP
1889.       HTC=HT(I,DIST,ELEVN,IP,QW,EFWW,EFDD,SMEAN,SC,E0,ACG,FT)
1890.       IF (H1.LE.0.7*HTC)THEN
1891.       H1=HTC
1892.       DO 70 KY=I,LLI-1
1893.       IP=IPOINT(KY)
1894.       EFDD=HP
1895.       HTC=HT(KY,DIST,ELEVN,IP,QW,EFWW,EFDD,SMEAN,SC,E0,ACG,FT)
1896.       DETC(KY)=HTC
1897.       IF(DETC(KY).GE.EFD(KY))THEN
1898.       TCELE(KY)=WSELE(KY)
1899.       LLII=KY
1900.       CC=ABS(CN-C1)
1901.       IF (CC.LE.(CN/100.)) THEN
1902.       GO TO 60
1903.       ELSE
1904.       CC0=C00-(C1-CN)/2.
1905.       IF (CC0.LT.0)THEN
1906.       C00=C00/5.
1907.       ELSE
1908.       C00=CC0
1909.       ENDIF
1910.       ENDIF
1911.       IF(C00.LT.1.E-15)C00=1.E-15
1912.       IF (J.EQ.50)GO TO 60
```

```
1913.       GO TO 30
1914.       ENDIF
1915.70     CONTINUE
1916.       GO TO 62
1917.       ELSEIF(H1.LE.HTC)THEN
1918.       DETC(I)=HTC
1919.       U1=U0-DX*(G1+2.*G2+2.*G3+G4)/6.0
1920.       IF(U1.LT.1.E-4)U1=1.E-4
1921.       T1=T0-DX*(E1+2.*E2+2.*E3+E4)/6.0
1922.       IF (T1.LT.1.E-8)T1=1.E-8
1923.       C1=T1/(H1*U1)
1924.       DO 71 KQ=I+1,LLI-1
1925.       IP=IPOINT(KQ)
1926.       EFDD=HP
1927.       HTC=HT(KQ,DIST,ELEVN,IP,QW,EFWW,EFDD,SMEAN,SC,E0,ACG,FT)
1928.       DETC(KQ)=HTC
1929.       IF(DETC(KQ).GE.EFD(KQ))THEN
1930.       TCELE(KQ)=WSELE(KQ)
1931.       LLII=KQ
1932.       CC=ABS(CN-C1)
1933.       IF (CC.LE.(CN/100.))THEN
1934.       GO TO 60
1935.       ELSE
1936.       CC0=C00-(C1-CN)/2.
1937.       IF (CC0.LT.0)THEN
1938.       C00=C00/5.
1939.       ELSE
1940.       C00=CC0
1941.       ENDIF
1942.       ENDIF
1943.       IF(C00.LT.1.E-15)C00=1.E-15
1944.       IF (J.EQ.50)GO TO 60
1945.       GO TO 30
1946.       ENDIF
1947.71     CONTINUE
1948.       GO TO 62
1949.       ELSE
1950.       U1=U0-DX*(G1+2.*G2+2.*G3+G4)/6.0
1951.       IF(U1.LT.1.E-4)U1=1.E-4
1952.       T1=T0-DX*(E1+2.*E2+2.*E3+E4)/6.0
1953.       IF (T1.LT.1.E-8)T1=1.E-8
1954.       C1=T1/(H1*U1)
1955.       R0=2.0
1956.       CD=0.002
1957.       Z1=RP**0.65*(U1*(CD**0.5)/VSM)
1958.       IF(Z.GT.20) Z=20.
1959.       ES1=0.00000033*Z1**4/(1+0.0000011*Z1**4)
1960.C      TE is the equilibrium value of the sediment transport
```

```
1961.       CO=C1*R0-ES1
1962.       IF (CO.LT.0) ES1=C1*R0
1963.       DETC(I)=H1
1964.       IF (DETC(I).GE.EFD(I))THEN
1965.       TCELE(I)=WSELE(I)
1966.       LLII=I
1967.       GO TO 60
1968.       ENDIF
1969.       H0=H1
1970.       U0=U1
1971.       T0=T1
1972.       ENDIF
1973.10     CONTINUE
1974.62     CC=ABS(CN-C1)
1975.       IF (CC.LE.(CN/100.))THEN
1976.       LLII=I
1977.       GO TO 60
1978.       ELSE
1979.       CC0=C00-(C1-CN)/2.
1980.       IF (CC0.LT.0)THEN
1981.       C00=C00/5.
1982.       ELSE
1983.       C00=CC0
1984.       ENDIF
1985.       ENDIF
1986.       IF(C00.LT.1.E-15)C00=1.E-15
1987.30     CONTINUE
1988.       LLII=LLI
1989.60     DO 74 IG=1,LLII-1
1990.       ELETALL=ELETALN(IG)
1991.       EFDD=DETC(IG)
1992.       IP=IPOINT(IG)
1993.       CALL APT(IG,DIST,ELEVN,IP,WSEL,AREAA,WPRR,EFDD,EFWW,WWSS,ELETALL)
1994.       TCELE(IG)=WSEL
1995.       AREA(IG)=AREAA
1996.       WPR(IG)=WPRR
1997.       HRAD(IG)=AREAA/WPRR
1998.       COK(IG)=(1./ANMAN(IG))*AREA(IG)*HRAD(IG)**(2./3.)
1999.       VLCITY(IG)=QW/AREAA
2000.       EFD(IG)=EFDD
2001.       EFW(IG)=EFWW
2002.       ELETALN(IG)=ELETALL
2003.       WWS(IG)=WWSS
2004.74     CONTINUE
2005.45     RETURN
2006.       END
2007.
2008.       FUNCTION F(ACG,R,HH,VSM,SMEAN,UU,RP,TT)
```

```
2009.       double precision EW,RI
2010.       IF (UU.LT.1.E-4)UU=1.E-4
2011.       IF (TT.LT.1.E-8)TT=1.E-8
2012.       RI=(ACG*R*TT)/(UU**3.0)
2013.       EW=0.075/(1.+(976.*(RI**2.12)))**0.5
2014.       R0=2.0
2015.       CD=0.002
2016.       Z=RP**0.65*(UU*(CD**0.5)/VSM)
2017.       IF(Z.GT.20) Z=20.
2018.       ES=0.00000033*Z**4/(1+0.0000011*Z**4)
2019.       TE=ES*HH*UU/R0
2020.       IF (TE.GT.TT) TE=TT
2021.       S2=0.75
2022.       S1=0.25
2023.       F=(-RI*SMEAN*S2+CD+(2.-RI*S1/2.)*EW+RI*R0*(VSM/(2.*UU))*
2024.      &(TE/TT-1.))/(1.-RI)
2025.       RETURN
2026.       END
2027.       FUNCTION G(ACG,R,TT,UU,HH,FF)
2028.       double precision ew,ri
2029.       IF (UU.LT.1.E-4)UU=1.E-4
2030.       IF (TT.LT.1.E-8)TT=1.E-8
2031.       RI=(ACG*R*TT)/UU**3.
2032.       EW=0.075/(1.+(976.*(RI**2.12)))**0.5
2033.       G=(UU/HH)*(EW-FF)
2034.       RETURN
2035.       END
2036.       FUNCTION E(RP,UU,VSM,TT,HH)
2037.       IF (UU.LT.1.E-4)UU=1.E-4
2038.       IF (TT.LT.1.E-8)TT=1.E-8
2039.       R0=2.0
2040.       CD=0.002
2041.       Z=RP**0.65*(UU*(CD**0.5)/VSM)
2042.       IF(Z.GT.20) Z=20.
2043.       ES=0.00000033*Z**4/(1+0.0000011*Z**4)
2044.       TE=ES*HH*UU/R0
2045.       IF (TE.GT.TT) TE=TT
2046.       E=(TT*R0*VSM)*(TE/TT-1.0)/(HH*UU)
2047.       RETURN
2048.       END
2049.
2050.       FUNCTION HT(LM,DIST,ELEVN,IP,QW,EFWW,EFDD,SMEAN,SC,E0,ACG,FT)
2051.       DIMENSION DIST(100,100),ELEVN(100,100)
2052.       CALL APT(LM,DIST,ELEVN,IP,WSEL,AREAA,WPRR,EFDD,EFWW,WWSS,ELETALL)
2053.       Q0=QW/EFWW
2054.       S2=0.75
2055.       S1=0.25
2056.       DC=0
```

```
2057.       IF (SMEAN.LT.SC) THEN
2058.C      HT is the normal underflow depth
2059.       HT=(FT*Q0**2./(SMEAN*S2*E0*ACG))**(1./3.)*(1.+DC)
2060.       ELSE
2061.       HT=(Q0**2./(S1*E0*ACG))**(1./3.0)*(1.0+DC)
2062.       ENDIF
2063.       IF(ABS(HT-EFDD).GT.0.5)THEN
2064.       DO 78 KF=1,50
2065.       EFDD=(HT+EFDD)/2.
2066.       CALL APT(LM,DIST,ELEVN,IP,WSEL,AREAA,WPRR,EFDD,EFWW,WWSS,ELETALL)
2067.       Q0=QW/EFWW
2068.       S2=0.75
2069.       S1=0.25
2070.       DC=0
2071.       IF (SMEAN.LT.SC) THEN
2072.C      HT is the normal underflow depth
2073.       HT=(FT*Q0**2./(SMEAN*S2*E0*ACG))**(1./3.)*(1.+DC)
2074.       ELSE
2075.       HT=(Q0**2./(S1*E0*ACG))**(1./3.0)*(1.0+DC)
2076.       ENDIF
2077.       IF(ABS(HT-EFDD).LT.0.5)GO TO 79
2078.78     CONTINUE
2079.       ENDIF
2080.79     RETURN
2081.       END
2082.
2083.
2084.       SUBROUTINE APT(LM,DIST,ELEVN,IP,WSELL,AREAA,WPRR,EFDD,EFWW,WWSS,
2085.      &ELETALL)
2086.       DIMENSION DIST(100,100),ELEVN(100,100)
2087.       N=IP
2088.       ELETALL=100000.
2089.       DO 354 ICC=1,N
2090.       IF (ELETALL.LT.ELEVN(LM,ICC)) GO TO 354
2091.       ELETALL=ELEVN(LM,ICC)
2092.354    CONTINUE
2093.       WSELL=ELETALL+EFDD
2094.       DO 11 IE=1,50
2095.       WWSS=0
2096.       AREAA=0.0
2097.       WPRR=0.0
2098.       DAD=0.0
2099.       AD=0.0
2100.       DO 310 ICC=2,N
2101.       IF (ELEVN(LM,ICC).GT.WSELL) GO TO 302
2102.       GO TO 303
2103.302    IF (ELEVN(LM,ICC-1).GE.WSELL) GO TO 310
2104.       GO TO 306
```

```
2105.303   IF (ELEVN(LM,ICC).EQ.WSELL) GO TO 308
2106.      GO TO 304
2107.308   IF (ELEVN(LM,ICC-1).GE.WSELL) GO TO 310
2108.      GO TO 312
2109.304   IF (ELEVN(LM,ICC-1).GT.WSELL) GO TO 306
2110.312   H2=WSELL-ELEVN(LM,ICC)
2111.      H1=WSELL-ELEVN(LM,ICC-1)
2112.      X1=DIST(LM,ICC)-DIST(LM,ICC-1)
2113.      WWSS=WWSS+X1
2114.      A=(H1+H2)*X1/2.
2115.      AREAA=AREAA+A
2116.      HD=ABS(H2-H1)
2117.      P=SQRT(X1**2.+HD**2.)
2118.      WPRR=WPRR+P
2119.      DAD=DAD+A*((H1+H2)/2.)**(5./3.)
2120.      AD=AD+A*((H1+H2)/2.)**(2./3.)
2121.      GO TO 310
2122.306   IF ((DIST(LM,ICC)-DIST(LM,ICC-1)).LE.0.000001) GO TO 310
2123.      AA=(ELEVN(LM,ICC)-ELEVN(LM,ICC-1))/(DIST(LM,ICC)-DIST(LM,ICC-1))
2124.      B=ELEVN(LM,ICC)-AA*DIST(LM,ICC)
2125.      IF (ABS(AA).LE.0.0000001) GO TO 310
2126.      DIS=(WSELL-B)/AA
2127.      IF (ELEVN(LM,ICC).GT.WSELL)THEN
2128.      H1=WSELL-ELEVN(LM,ICC-1)
2129.      X1=DIS-DIST(LM,ICC-1)
2130.      ELSE
2131.      H1=WSELL-ELEVN(LM,ICC)
2132.      X1=DIST(LM,ICC)-DIS
2133.      ENDIF
2134.      A=H1*X1/2.
2135.      AREAA=AREAA+A
2136.      P=SQRT(H1**2.+X1**2.)
2137.      WPRR=WPRR+P
2138.      DAD=DAD+A*(H1/2.)**(5./3.)
2139.      AD=AD+A*(H1/2.)**(2./3.)
2140.      WWSS=WWSS+X1
2141.310   CONTINUE
2142.      EFDDD=DAD/AD
2143.      EFWW=AD/((EFDDD)**(5./3.))
2144.      IF (ABS(EFDD-EFDDD).LT.0.1)GO TO 17
2145.      WSELL=WSELL+(EFDD-EFDDD)/3.
2146.11    CONTINUE
2147.17    RETURN
2148.      END
```

APPENDIX E.

INPUT DATA GUIDE TO "DEPO" MODEL

Variable	Description
MA	Identification word (character), should be written in one line.
ANMAN	Manning's *n* value for the cross section. (The program uses Manning's *n* value same as the value in previous cross section, If 0 is used for ANMAN)
CONCO	Contraction coefficient. (The program uses CONCO value same as the value in previous cross section, If 0 is used for CONCO)
EXPANCO	Expansion coefficient. (The program uses EXPANCO value same as the value in previous cross section, If 0 is used for EXPANCO)
CS	Identification word (character), should be written in one line.
CSNUMBER	Cross section identification number
IPOINT	Number of coordinate points used in **GE** records. It should not more than 100 points. (If 0 is used for IPOINT the program will repeat last **GE** data for the present cross section. Therefore, no **GE** records will be needed if IPOINT= 0).
RLENGTH	Reach length between current cross section and the downstream cross section in meter (use 0 for the first cross section).
DBM	Depth of bed material of section in meter. (The program will assign 5m if 0 used for DBM)
GE	Identification word (character), should be written in one line.
DIST(1)	Distance of first point in the cross section (meter).
ELEV(1)	Elevation of first point in the cross section (meter). It should be written pair with DIST(1) in one line.
DIST(2)	Distance of second point in the cross section (meter).
ELEV(2)	Elevation of second point in the cross section (meter). It should be written pair with DIST(2) in one line.

Continue DIST(?), ELEV(?) values for up to 100.
Repeat the above record for the next upstream cross section and continue for up to 100 cross sections.

EC	Identification word (character), should be written in one line. It shows end of geometric input.
SPROPER	Identification Word (character), should be written in one line.

Variable	Description
SGW	Specific Gravity of Water. (Program uses SGW = 1.0, if 0 is entered in this part).
ASG	Acceleration Due to Gravity. (program uses ASG= 9.81 if 0 is entered in this part).
CLAY	Identification Word (character).
SGCP	Specific gravity of clay particles. (program uses SGCP = 2.65 if 0 enter in this part).
UWCP	The initial unit weight for clay deposits,(kg/m^3). (program uses UWCP= 481 if 0 is entered in this part).
CCCP	Compaction coefficient for clay deposits, (kg/m^3/year). (program uses CCCP= 256 if 0 is entered in this part).
TCD	The average bed shear stress in N/m^2 above which clay and silt grain will not be deposited. (program uses TCD=0.06 for concentration less than 300 mg/L and 0.078 for concentration more than 300 mg/L if 0 is entered in this part)
TCS	Critical bed shear stress above which clay and silt particles will be scoured from the bed (N/m^2).
AM1	Erosion rate for particle scour in kg/m^2/s.
SILT	Identification Word (character).
SGSP	Specific gravity of silt particles. (Program uses SGSP = 2.65 if 0 is entered in this part)
UWSP	The initial unit weight for silt deposits, (kg/m^3). (program uses UWSP=1041 if 0 is entered in this part).
CCSP	Compaction coefficient for silt deposits, (kg/m^3/year). (program uses CCSP= 91.3 if 0 is entered in this part).
SAND	Identification Word (character).
ITCM	Transport capacity method to be used to estimate sediment load . Put 1 for using Meyer-Peter and Muller (1948). Put 2 for using Bagnold's (1966). Put 3 for using Engelund and Hansen (1967). Put 4 for Toffaleti's (1966). Put 5 for using Ackers and White (1973). Put 6 for using Yang's (1973). Put 7 for using Habibi and Sivakumar (1993).
SGSA	Specific gravity of sand particles. (program uses SGSA= 2.65 if 0 is entered in this part).
UWSA	The unit weight of deposited sand particles, (kg/m^3). (program uses UWSA=1490 if 0 is entered in this part). This value does not change with time.
GSF	Grain shape factor. (program uses GSF= 0.667 if 0 is entered in this part).

BEDPART	Identification Word (character).
NUMBCS	Number of cross section mentioned below for bed gradation.
NIS	Iteration to calculate bed material gradation. (The program calculate a value if 0 is entered in this part.)
CSEC	Cross section identification number.
PRSP(1,S)	Percentage of clay particle in bed.
PRSP(2,S)	Percentage of very fine silt in bed.
...	
..	
PRSP(15,S)	Percentage of very coarse gravel.
CSEC	Cross section identification number.
PRSP(1,S)	Percentage of clay particle in bed.
PRSP(2,S)	Percentage of very fine silt in bed.
...	
..	
PRSP(15,S)	Percentage of very coarse gravel.

Continue for the other cross sections. It is not necessary to mention all the cross sections. The program will find the bed grain size for all cross sections by interpolation.

Table E.1 Sediment grain size classes.

Number	Classification	Grain Size (mm)	Mean Geometric size (mm)
1	Clay	>.004	
2	Very fine silt	.004-.008	.005
3	Fine silt	.008-.016	.011
4	Medium silt	.016-.031	.022
5	Coarse silt	.031-.0625	.044
6	Very fine sand	.062-.125	.088
7	Fine sand	.125-.250	.177
8	Medium sand	.25-.50	.354
9	Coarse sand	.50-1.0	.707
10	Very coarse sand	1-2	1.414
11	Very fine gravel	2-4	2.828
12	Fine gravel	4-8	5.657
13	Medium gravel	8-16	11.31
14	Coarse gravel	16-32	22.63
15	Very coarse gravel	32-64	45.26

Variable **Description**

TC	Turbidity Current Identification Word (character).
TUCU	Character defines user option about considering turbidity currents effects in processes. Write 'Y ' for considering or 'N' for ignoring. If the answer was 'Y' then enter the next value.
MSO	The mean size of outflow sediments (write a No.,1 to 15 from Table E.1)
OPERATION	Identification Word (character).
NUMQ	Number of water discharge mentioned below.
COM	Distribution option for sediment deposition and scour in cross sections. The value more than one for flat distribution and a value between 0 and 1 for ratio distribution.
QW	Water discharges in m^3/s. Outflow from downstream of reservoir.
WSEL	Downstream water surface elevation (m).
DUR	Flow duration in days for this step.
TEM	Water temperature in degrees Celsius, for this step

If TUCU is 'Y' then enter the next value

TCELEI	The approximate elevation of turbidity currents near dam wall (in meter) for the specific QW. (if this elevation was equal or greater than the downstream water surface elevation then the calculation of turbidity current will be ignored and if this value was less than the calculated normal depth of the turbidity current, then the normal depth will be applied automatically for this value).

APPENDIX F

AN EXAMPLE OF INPUT AND OUTPUT FILES OF "DEPO" MODEL

'nput Data File for Dez Reservoir - Considering Alternative ɔottom gate

Page 1

```
MA
0.021     .1     .3
CS
1        15       0.0   0
GE
0         350
5         330
30        310
45        282
55        240
65        220
68        200
85        180
100       200
105       228
115       245
125       284
150       310
169       340
182       350
MA
0.021     .1     .3
CS
7        11       290.0    0
GE
0         350
45        250
67        240
110       200
130       190
140       180
155       180
175       250
210       250
230       300
242       350
MA
0.021     .1     .3
CS
3        19       880.0    0
GE
```

Page 2

```
0         350
100       310
145       300
300       240
325       220
365       200
410       190
440       180
485       180
550       200
630       220
745       240
760       250
825       270
840       280
865       270
885       280
915       280
1000      350
MA
0.021     .1     .3
CS
18       19       320.0   0
GE
0         350
75        300
160       270
200       250
275       230
395       180
460       180
500       190
500       210
610       210
625       220
725       230
890       240
990       250
1010      260
1110      280
1140      290
```

Page 3

```
1165    310
1265    350
MA
0.021    .1    .3
CS
124      36     1650.0     0
GE
0       350
51      340
95      330
133     320
269     301
380     281
563     260
794     260
898     260
958     251
1071    241
1089    241
1125    212
1167    183
1210    183
1249    202
1281    222
1337    222
1439    213
1488    213
1541    223
1584    242
1658    242
1687    232
1772    232
1796    242
1818    252
1983    253
2020    272
2151    282
2196    292
2272    302
2394    312
2426    321
2445    342
2476    352
MA
0.021    .1    .3
CS
48      49    3450.0      0
GE
0       350
140     320
210     310
245     300
305     300
330     310
385     310
415     320
450     320
```

Page 4

```
535     300
715     290
770     280
780     270
800     270
815     280
870     290
940     330
950     340
1190    340
1200    350
1300    360
1400    350
1500    350
1590    320
1650    290
1740    260
1950    240
1990    230
2050    190
2075    186
2100    190
2160    230
2210    230
2240    220
2260    220
2290    240
2680    240
2760    250
2810    250
2900    260
2920    270
3020    280
3080    290
3190    290
3240    310
3360    310
3380    320
3440    320
3500    350
MA
0.021    .1    .3
CS
57      47     1161.6    0
GE
0       350
42      331
92      312
208     311
247     291
282     270
306     261
435     251
595     251
625     241
648     230
655     221
```

Page 5

```
686     201
706     191
726     187
746     191
770     200
774     211
779     221
809     240
849     281
921     281
945     301
1017    301
1078    290
1100    281
1118    271
1138    270
1149    277
1188    290
1201    301
1244    310
1311    311
1372    301
1409    290
1522    291
1548    300
1574    301
1610    290
1656    281
1735    281
1768    291
1819    301
1864    320
1896    330
1908    340
1964    350
MA
0.021    .1     .3
CS
93      32      1789.8    0
GE
0       350
37      330
44      310
55      300
75      290
93      280
104     270
109     260
124     250
140     240
152     230
184     200
199     190
218     190
237     190
269     220
295     240
```

Page 6

```
350     240
386     250
416     260
506     270
563     270
587     270
618     280
646     290
714     300
797     300
813     309
865     318
925     329
982     339
1012    349
MA
0.021    .1     .3
CS
100      26      720.2    0
GE
0       349
13      339
45      329
66      319
94      309
125     290
155     270
178     249
200     240
223     220
249     200
278     192
295     192
312     192
334     201
352     220
365     230
383     241
428     260
508     270
532     280
545     290
576     300
596     310
626     329
701     350
MA
0.021    .1     .3
CS
96      25      320.6     0
GE
0       349
37      330
58      310
74      300
125     280
135     270
```

```
                    Page 7
149      260
158      250
200      231
241      194
273      194
291      211
309      221
317      231
324      241
348      250
354      260
426      271
456      280
470      291
476      301
489      310
514      320
534      341
560      350
MA
0.021     .1     .3
CS
103       29    1230.3    0
GE
0        349
14       339
25       330
39       319
45       309
74       290
80       280
91       270
104      260
115      250
145      230
153      220
185      200
207      196
229      200
256      220
270      230
280      240
289      250
315      260
350      270
414      280
423      290
457      300
477      310
492      320
502      331
523      340
544      350
MA
0.021     .1     .3
CS
112       23     750.0    0
```

```
                    Page 8
GE
0        350
31       330
53       310
85       290
126      270
155      260
189      250
245      230
259      220
281      200
299      197
317      200
331      210
344      220
362      230
373      250
410      270
434      280
452      290
481      300
534      310
577      330
636      350
MA
0.021     .1     .3
CS
109       20      780.0    0
GE
0        350
72       330
131      320
185      310
243      290
318      280
345      260
380      240
397      230
430      200
448      198
467      200
495      230
503      250
524      260
561      270
652      280
697      300
740      330
765      350
MA
0.021     .1     .3
CS
126       28     810.0      0
GE
0        350
34       338
56       328
```

```
                    Page 9
100       318
136       308
161       298
216       288
244       278
322       269
354       259
359       249
376       239
392       229
430       209
443       202
458       202
473       202
479       209
496       219
516       240
531       250
558       259
616       270
652       290
716       320
763       330
779       340
792       350
MA
0.021     .1      .3
CS
113       24      660.0     0
GE
0         350
71        330
118       320
151       310
209       300
240       290
306       271
375       260
407       250
473       241
550       220
582       203
606       203
630       203
633       211
648       228
660       241
666       250
681       261
721       280
752       290
770       310
819       341
833       350
MA
0.021     .1      .3
CS
```



```
                    Page 10
118       22      870.0     0
GE
0         348
35        339
138       319
221       299
246       288
332       269
340       259
359       249
379       239
390       229
434       204
488       204
508       220
514       231
546       240
564       250
586       260
612       280
644       300
663       310
701       340
709       350
MA
0.021     .1      .3
CS
131       25      1010.0    0
GE
0         350
13        341
28        330
38        320
65        300
94        280
96        270
120       250
134       240
155       220
165       211
178       205
192       211
205       220
239       230
250       240
260       250
288       270
352       280
449       290
493       300
540       320
597       330
667       340
739       350
MA
0.021     .1      .3
CS
```

Page 11

```
159       23      600.0       0
GE
0         349
21        339
49        309
69        299
75        289
110       269
130       249
154       229
169       219
179       209
196       207
214       210
238       230
250       240
265       250
274       260
301       270
313       280
344       300
370       320
378       330
405       340
463       350
MA
0.021     .1      .3
CS
163       25      790.0       0
GE
0         350
41        330
48        320
72        310
89        300
187       280
214       270
231       260
263       250
276       230
292       220
305       210
321       208
337       210
361       220
376       240
424       270
478       280
561       290
617       310
680       320
745       320
766       329
788       340
799       350
MA
0.021     .1      .3
```

Page 12

```
CS
167       27      880.0       0
GE
0         350
15        339
72        320
98        310
129       300
191       290
259       290
382       280
443       280
505       270
542       260
564       240
587       230
608       210
626       210
643       210
673       230
701       250
720       260
769       280
793       290
879       290
916       310
924       320
947       330
977       340
997       350
MA
0.021     .1      .3
CS
179       20      1160.0      0
GE
0         350
37        330
130       310
165       300
185       290
450       290
632       280
803       280
845       260
873       241
924       212
955       212
987       212
1036      230
1068      251
1322      251
1371      281
1401      311
1441      331
1508      350
MA
0.021     .1      .3
```

Page 13

```
CS
188     29     1070.0         0
GE
0       348
21      338
68      328
107     309
151     279
164     270
168     260
176     250
220     240
230     230
261     220
284     213
300     213
317     213
335     220
403     240
455     250
473     250
502     240
532     240
562     250
607     260
633     270
688     300
742     310
770     320
780     330
800     340
807     350
MA
0.021     .1     .3
CS
192       25      690.0       0
GE
0       350
22      340
29      330
60      310
89      300
101     290
179     290
205     280
255     280
320     260
342     250
353     240
430     215
480     215
503     230
525     240
530     250
589     270
627     280
685     290
```

Page 14

```
747     300
848     310
861     320
992     340
1043    350
MA
0.021     .1     .3
CS
193       20      360.0       0
GE
0       350
26      330
45      320
94      300
104     290
125     280
156     270
200     250
210     240
246     220
270     217
295     220
330     240
377     260
397     270
420     280
532     300
543     310
562     320
623     350
MA
0.021     .1     .3
CS
198       18      970.0       0
GE
0       350
86      310
100     300
117     290
140     270
163     260
177     250
224     220
242     218
261     220
313     240
345     250
385     270
400     280
473     290
502     300
536     319
578     349
MA
0.021     .1     .3
CS
206       25      780.0       0
```

Page 15

```
GE
0       360
48      340
92      309
276     288
330     277
341     266
346     256
385     220
401     220
417     220
451     256
498     286
530     295
571     295
585     285
620     285
634     294
687     304
725     313
824     313
860     333
963     332
991     321
1068    341
1093    349
MA
0.021    .1    .3
CS
207      19    1170.0      0
GE
0       350
46      339
81      319
120     309
210     309
239     299
324     288
346     269
350     258
372     239
385     225
416     225
422     229
439     249
516     279
559     299
583     309
617     329
643     349
MA
0.021    .1    .3
CS
221     26    2350        0
GE
0       350
54      320
```

Page 16

```
83      310
133     300
165     280
180     270
226     260
242     251
265     251
290     260
304     270
342     280
401     281
464     271
487     261
523     250
620     231
660     226
701     232
805     252
847     262
901     282
918     293
951     303
970     312
1012    352
MA
0.021    .1    .3
CS
230     18    820.0       0
GE
0       349
109     310
119     300
139     290
166     270
187     260
194     250
211     240
213     230
230     227
248     230
269     240
278     250
303     270
349     290
391     300
412     310
548     350
MA
0.021    .1    .3
CS
235     16    370.0       0
GE
0       350
29      330
50      320
88      300
129     290
```

Page 17

```
181     260
206     250
232     230
251     228
271     230
301     250
320     259
343     279
402     309
453     330
493     349
MA
0.021    .1    .3
CS
234      18     320.0      0
GE
0       350
98      340
129     330
217     330
260     320
276     310
317     300
333     290
339     280
370     264
422     230
438     229
454     230
501     270
519     290
570     320
595     340
614     350
MA
0.021    .1    .3
CS
249     15     850.0      0
GE
0       350
32      330
78      330
131     310
214     290
248     270
312     230
328     230
344     230
354     240
362     250
436     299
475     309
519     329
543     349
MA
0.021    .1    .3
CS
```

Page 18

```
252     16     1030.0     0
GE
0       350
79      320
206     310
249     290
289     260
307     250
324     230
339     230
354     230
383     240
444     270
556     290
575     300
612     310
656     330
693     350
MA
0.021    .1    .3
CS
274     14     1690.5     0
GE
0       349
29      319
96      280
141     234
169     234
199     269
233     299
327     320
355     329
417     329
505     320
769     329
817     330
1124    350
MA
0.021    .1    .3
CS
297      17    2680.0    0
GE
0       350
20      330
80      300
181     290
211     270
222     260
235     250
259     241
270     241
280     241
290     250
334     280
356     290
389     310
398     320
```

```
                    Page 19
455     340
558     350
MA
0.021    .1    .3
CS
303      14     550.0    0
GE
0       350
44      330
62      320
170     310
213     300
235     280
286     244
316     244
351     259
404     309
445     329
572     329
614     339
639     349
MA
0.021    .1    .3
CS
311      20     1240.0     0
GE
0       350
37      340
65      320
122     310
176     310
188     300
231     289
454     279
466     269
478     259
509     250
524     247
540     250
563     259
590     279
635     300
648     310
678     320
742     329
794     350
MA
0.021    .1    .3
CS
335      16     1500.0    0
GE
0       350
37      340
65      330
122     320
176     319
188     299
```

```
                    Page 20
481     289
515     252
527     252
538     252
559     269
594     289
598     298
624     318
652     338
689     348
MA
0.021    .1    .3
CS
361      15     2940.0     0
GE
0       350
19      334
39      320
80      310
109     290
140     280
157     270
209     266
261     270
292     280
322     280
343     290
367     310
411     330
482     350
MA
0.021    .1    .3
CS
392      21     1759.9    0
GE
0     350
50.5     330
92.5     320
127.4     300
162.3     270
185.4     270
208.7     270
222.6     280
260.3     300
332.7     320
371.3     320
391.6    300
410.6    300
493.1     320
552.8     320
587.6     310
647.9     310
687.5     320
712.5     330
822.0     330
952.5    350
MA
```

```
                    Page 21
0.021     .1     .3
CS
420       19      2309.0    0
GE
0      350
24.5       340
34.3       330
63      310
101.1      290
130.3      274
162.9       274
196.2      290
231.6       300
250.6       310
275.7       320
295      329
346.3       329
411.9      300
424.2       290
441     300
484.3       329
510      340
524.7     350
MA
0.021     .1     .3
CS
500       12     880.0       0
GE
0     350
26.7       340
68.7       330
84.5       320
172      281
186.6       276
201.1       281
219.9       291
261.8      301
280.4       321
330.3       330
366.1       350
MA
0.021     .1     .3
CS
616       11     2430.0      0
GE
0          349
47         340
104        320
114        310
133        300
174        290
186        287
198        290
232        300
277        320
382        350
MA
```

```
                    Page 22
0.021     .1     .3
CS
629       12      800.0     0
GE
0          349
60         339
93         329
111        310
136        300
182        290
195        290
207        290
253        310
263        320
278        330
302        350
MA
0.021     .1     .3
CS
645       13      1070.0    0
GE
0      350
21.2       340
34.7      330
43.4       320
59.9      310
69.6       300
99.9       292
116.9       292
134     292
153.8       300
165.2      310
193.4       330
249.3      350
MA
0.021     .1     .3
CS
642       11      430.0     0
GE
0          350
19         330
39         320
69         300
80         293
100        293
120        293
174        300
192        320
215        330
245        350
MA
0.021     .1     .3
CS
684       10      1590.0    0
GE
0          350
31         340
```

```
                    Page 23
50          330
83          310
93          300
113         297
133         300
179         310
204         320
304         350
MA
0.021       .1      .3
CS
692         12      1040.0    0
GE
0           350
20          340
54          340
69          330
96          320
115         310
146         300
166         298
186         300
219         320
242         340
269         350
MA
0.021       .1      .3
CS
710         13      940.0   0
GE
0           351
16          341
29          330
60          321
70          311
98          300
122         300
145         300
194         310
235         311
250         320
289         340
304         350
MA
0.021       .1      .3
CS
720         12      640.0     0
GE
0           351
52          340
84          330
102         320
133         310
154         300
175         301
197         301
218         310
```

```
                    Page 24
241         320
276         340
287         350
MA
0.021       .1      .3
CS
738         10      1242.0    0
GE
0           350
21          330
101         320
138         310
149         302
183         302
217         302
264         330
285         340
310         350
MA
0.021       .1      .3
CS
755         9       1000.0      0
GE
0           350
24          330
50          320
94          310
149         305
205         310
222         320
246         330
282         350
MA
0.021       .1      .3
CS
770         11       960        0
GE
0           350
19          339
49          330
74          319
104         310
137         308
169         310
191         320
205         330
215         340
229         350
MA
0.021       .1      .3
CS
780         10      720.0   0
GE
0           350
44          340
59          330
84          320
```

Page 25

```
99      310
129     308
159     310
204     330
214     340
229     350
MA
0.021    .1    .3
CS
793      9     590.0     0
GE
0       350
29      340
39      330
85      310
118     309
150     310
170     330
175     340
190     350
```

Page 26

```
MA
0.021    .1    .3
CS
803      10     400.0      0
GE
0       350
15      340
23      330
40      320
52      310
104     309
139     320
169     330
195     340
210     350
EC
SPROPER
0  0
CLAY  0   0   0   0  0  0  9.17  0.4
SILT  0   0   0
SAND  6   0   0   0      30.0
```

Page 27

```
WDSLOAD  2
 44.  220.188  0.514 0.118 0.129 0.109 0.09 0.04 0 0 0 0 0 0 0 0 0 0
 2511. 2219593. 0.514 0.118 0.129 0.109 0.09 0.04 0 0 0 0 0 0 0 0 0 0
BEDPART  1  50
803   0   0  0  2  6  18  32  26  4  4  3  3  2 0 0
TC Y
2
OPERATION   396   1.5
    44      290   18.27 28  290
    79      312   36.5  18  312
    100     320   36.5  38  320
    170     289   36.5  10  289
    295     329   36.5  18  329
    405     350   36.5  30  350
    770     343.2 10.95 25  195
    1100    335   3.65  25  195
    2300    335   0.18  25  195
    2510    335   0.15  25  195
    2000    335   0.4   25  195
    1700    335   1.1   25  195
    1310    335   1.8   25  195
    570     343.2 18.25 25  195
    220     320   36.5  38  320
    128     321   36.5  10  321
    62      299   36.5  32  299
    52      290   18.25 28  290
    44      290   18.27 28  290
    79      312   36.5  18  312
    100     320   36.5  38  320
    170     289   36.5  10  289
    295     329   36.5  18  329
    405     350   36.5  30  350
    770     343.2 10.95 25  195
    1100    335   3.65  25  195
```

Page 28

2300	335	0.18	25	195
2510	335	0.15	25	195
2000	335	0.4	25	195
1700	335	1.1	25	195
1310	335	1.8	25	195
570	343.2	18.25	25	195
220	320	36.5	38	320
128	321	36.5	10	321
62	299	36.5	32	299
52	290	18.25	28	290
44	290	18.27	28	290
79	312	36.5	18	312
100	320	36.5	38	320
170	289	36.5	10	289
295	329	36.5	18	329
405	350	36.5	30	350
770	343.2	10.95	25	195
1100	335	3.65	25	195
2300	335	0.18	25	195
2510	335	0.15	25	195
2000	335	0.4	25	195
1700	335	1.1	25	195
1310	335	1.8	25	195
570	343.2	18.25	25	195
220	320	36.5	38	320
128	321	36.5	10	321
62	299	36.5	32	299
52	290	18.25	28	290
44	290	18.27	28	290
79	312	36.5	18	312
100	320	36.5	38	320
170	289	36.5	10	289
295	329	36.5	18	329
405	350	36.5	30	350
770	343.2	10.95	25	195
1100	335	3.65	25	195
2300	335	0.18	25	195
2510	335	0.15	25	195
2000	335	0.4	25	195
1700	335	1.1	25	195
1310	335	1.8	25	195
570	343.2	18.25	25	195
220	320	36.5	38	320
128	321	36.5	10	321
62	299	36.5	32	299
52	290	18.25	28	290
44	290	18.27	28	290
79	312	36.5	18	312
100	320	36.5	38	320
170	289	36.5	10	289
295	329	36.5	18	329
405	350	36.5	30	350
770	343.2	10.95	25	195
1100	335	3.65	25	195
2300	335	0.18	25	195
2510	335	0.15	25	195

Page 29

2000	335	0.4	25	195
1700	335	1.1	25	195
1310	335	1.8	25	195
570	343.2	18.25	25	195
220	320	36.5	38	320
128	321	36.5	10	321
62	299	36.5	32	299
52	290	18.25	28	290
44	290	18.27	28	290
79	312	36.5	18	312
100	320	36.5	38	320
170	289	36.5	10	289
295	329	36.5	18	329
405	350	36.5	30	350
770	343.2	10.95	25	195
1100	335	3.65	25	195
2300	335	0.18	25	195
2510	335	0.15	25	195
2000	335	0.4	25	195
1700	335	1.1	25	195
1310	335	1.8	25	195
570	343.2	18.25	25	195
220	320	36.5	38	320
128	321	36.5	10	321
62	299	36.5	32	299
52	290	18.25	28	290
44	290	18.27	28	290
79	312	36.5	18	312
100	320	36.5	38	320
170	289	36.5	10	289
295	329	36.5	18	329
405	350	36.5	30	350
770	343.2	10.95	25	195
1100	335	3.65	25	195
2300	335	0.18	25	195
2510	335	0.15	25	195
2000	335	0.4	25	195
1700	335	1.1	25	195
1310	335	1.8	25	195
570	343.2	18.25	25	195
220	320	36.5	38	320
128	321	36.5	10	321
62	299	36.5	32	299
52	290	18.25	28	290
44	290	18.27	28	290
79	312	36.5	18	312
100	320	36.5	38	320
170	289	36.5	10	289
295	329	36.5	18	329
405	350	36.5	30	350
770	343.2	10.95	25	195
1100	335	3.65	25	195
2300	335	0.18	25	195
2510	335	0.15	25	195
2000	335	0.4	25	195
1700	335	1.1	25	195

Page 30

1310	335	1.8	25	195
570	343.2	18.25	25	195
220	320	36.5	38	320
128	321	36.5	10	321
62	299	36.5	32	299
52	290	18.25	28	290
44	290	18.27	28	290
79	312	36.5	18	312
100	320	36.5	38	320
170	289	36.5	10	289
295	329	36.5	18	329
405	350	36.5	30	350
770	343.2	10.95	25	195
1100	335	3.65	25	195
2300	335	0.18	25	195
2510	335	0.15	25	195
2000	335	0.4	25	195
1700	335	1.1	25	195
1310	335	1.8	25	195
570	343.2	18.25	25	195
220	320	36.5	38	320
128	321	36.5	10	321
62	299	36.5	32	299
52	290	18.25	28	290
44	290	18.27	28	290
79	312	36.5	18	312
100	320	36.5	38	320
170	289	36.5	10	289
295	329	36.5	18	329
405	350	36.5	30	350
770	343.2	10.95	25	195
1100	335	3.65	25	195
2300	335	0.18	25	195
2510	335	0.15	25	195
2000	335	0.4	25	195
1700	335	1.1	25	195
1310	335	1.8	25	195
570	343.2	18.25	25	195
220	320	36.5	38	320
128	321	36.5	10	321
62	299	36.5	32	299
52	290	18.25	28	290
44	290	18.27	28	290
79	312	36.5	18	312
100	320	36.5	38	320
170	289	36.5	10	289
295	329	36.5	18	329
405	350	36.5	30	350
770	343.2	10.95	25	195
1100	335	3.65	25	195
2300	335	0.18	25	195
2510	335	0.15	25	195
2000	335	0.4	25	195
1700	335	1.1	25	195
1310	335	1.8	25	195
570	343.2	18.25	25	195
220	320	36.5	38	320

Page 31

128	321	36.5	10	321
62	299	36.5	32	299
52	290	18.25	28	290
44	290	18.27	28	290
79	312	36.5	18	312
100	320	36.5	38	320
170	289	36.5	10	289
295	329	36.5	18	329
405	350	36.5	30	350
770	343.2	10.95	25	195
1100	335	3.65	25	195
2300	335	0.18	25	195
2510	335	0.15	25	195
2000	335	0.4	25	195
1700	335	1.1	25	195
1310	335	1.8	25	195
570	343.2	18.25	25	195
220	320	36.5	38	320
128	321	36.5	10	321
62	299	36.5	32	299
52	290	18.25	28	290
44	290	18.27	28	290
79	312	36.5	18	312
100	320	36.5	38	320
170	289	36.5	10	289
295	329	36.5	18	329
405	350	36.5	30	350
770	343.2	10.95	25	195
1100	335	3.65	25	195
2300	335	0.18	25	195
2510	335	0.15	25	195
2000	335	0.4	25	195
1700	335	1.1	25	195
1310	335	1.8	25	195
570	343.2	18.25	25	195
220	320	36.5	38	320
128	321	36.5	10	321
62	299	36.5	32	299
52	290	18.25	28	290
44	290	18.27	28	290
79	312	36.5	18	312
100	320	36.5	38	320
170	289	36.5	10	289
295	329	36.5	18	329
405	350	36.5	30	350
770	343.2	10.95	25	195
1100	335	3.65	25	195
2300	335	0.18	25	195
2510	335	0.15	25	195
2000	335	0.4	25	195
1700	335	1.1	25	195
1310	335	1.8	25	195
570	343.2	18.25	25	195
220	320	36.5	38	320
128	321	36.5	10	321
62	299	36.5	32	299
52	290	18.25	28	290

Page 32

44	290	18.27	28	290
79	312	36.5	18	312
100	320	36.5	38	320
170	289	36.5	10	289
295	329	36.5	18	329
405	350	36.5	30	350
770	343.2	10.95	25	195
1100	335	3.65	25	195
2300	335	0.18	25	195
2510	335	0.15	25	195
2000	335	0.4	25	195
1700	335	1.1	25	195
1310	335	1.8	25	195
570	343.2	18.25	25	195
220	320	36.5	38	320
128	321	36.5	10	321
62	299	36.5	32	299
52	290	18.25	28	290
44	290	18.27	28	290
79	312	36.5	18	312
100	320	36.5	38	320
170	289	36.5	10	289
295	329	36.5	18	329
405	350	36.5	30	350
770	343.2	10.95	25	195
1100	335	3.65	25	195
2300	335	0.18	25	195
2510	335	0.15	25	195
2000	335	0.4	25	195
1700	335	1.1	25	195
1310	335	1.8	25	195
570	343.2	18.25	25	195
220	320	36.5	38	320
128	321	36.5	10	321
62	299	36.5	32	299
52	290	18.25	28	290
44	290	18.27	28	290
79	312	36.5	18	312
100	320	36.5	38	320
170	289	36.5	10	289
295	329	36.5	18	329
405	350	36.5	30	350
770	343.2	10.95	25	195
1100	335	3.65	25	195
2300	335	0.18	25	195
2510	335	0.15	25	195
2000	335	0.4	25	195
1700	335	1.1	25	195
1310	335	1.8	25	195
570	343.2	18.25	25	195
220	320	36.5	38	320
128	321	36.5	10	321
62	299	36.5	32	299
52	290	18.25	28	290
44	290	18.27	28	290
79	312	36.5	18	312
100	320	36.5	38	320

Page 33

170	289	36.5	10	289
295	329	36.5	18	329
405	350	36.5	30	350
770	343.2	10.95	25	195
1100	335	3.65	25	195
2300	335	0.18	25	195
2510	335	0.15	25	195
2000	335	0.4	25	195
1700	335	1.1	25	195
1310	335	1.8	25	195
570	343.2	18.25	25	195
220	320	36.5	38	320
128	321	36.5	10	321
62	299	36.5	32	299
52	290	18.25	28	290
44	290	9.125	28	290
79	312	18.25	18	312
100	320	18.25	38	320
170	289	18.25	10	289
295	329	18.25	18	329
405	350	18.25	30	350
770	343.2	5.475	25	195
1100	335	1.825	25	195
2300	335	0.09	25	195
2510	335	0.075	25	195
2000	335	0.2	25	195
1700	335	0.55	25	195
1310	335	0.9	25	195
570	343.2	9.125	25	195
220	320	18.25	38	320
128	321	18.25	10	321
62	299	18.25	32	299
52	290	9.125	28	290
44	290	9.125	28	290
79	312	18.25	18	312
100	320	18.25	38	320
170	289	18.25	10	289
295	329	18.25	18	329
405	350	18.25	30	350
770	343.2	5.475	25	195
1100	335	1.825	25	195
2300	335	0.09	25	195
2510	335	0.075	25	195
2000	335	0.2	25	195
1700	335	0.55	25	195
1310	335	0.9	25	195
570	343.2	9.125	25	195
220	320	18.25	38	320
128	321	18.25	10	321
62	299	18.25	32	299
52	290	9.125	28	290
44	290	9.125	28	290
79	312	18.25	18	312
100	320	18.25	38	320
170	289	18.25	10	289
295	329	18.25	18	329
405	350	18.25	30	350

Page 34				
770	343.2	5.475	25	195
1100	335	1.825	25	195
2300	335	0.09	25	195
2510	335	0.075	25	195
2000	335	0.2	25	195
1700	335	0.55	25	195
1310	335	0.9	25	195
570	343.2	9.125	25	195
220	320	18.25	38	320
128	321	18.25	10	321
62	299	18.25	32	299
52	290	9.125	28	290
44	290	9.125	28	290
79	312	18.25	18	312
100	320	18.25	38	320

Page 35				
170	289	18.25	10	289
295	329	18.25	18	329
405	350	18.25	30	350
770	343.2	5.475	25	195
1100	335	1.825	25	195
2300	335	0.09	25	195
2510	335	0.075	25	195
2000	335	0.2	25	195
1700	335	0.55	25	195
1310	335	0.9	25	195
570	343.2	9.125	25	195
220	320	18.25	38	320
128	321	18.25	10	321
62	299	18.25	32	299
52	290	9.125	28	290

Output File for Dez Reservoir - considering alternative bottom gate

Estimated bed elevation of Dez Reservoir after 30 year operation with considering alternative bottom gate using DEPO model. All distances and elevations are presented in meter.

```
**********************************************************************
*          Final Results of Sedimentation Modelling                  *
**********************************************************************


Cross section number      1.00000
points DISTANCE,INITIAL ELEVATION AND FINAL ELEVATION
          0.00       350.00              350.00
          5.00       330.00              330.00
         30.00       310.00              310.00
         45.00       282.00              282.00
         55.00       240.00              240.00
         65.00       220.00              220.00
         68.00       200.00              200.00
         85.00       180.00              192.77
        100.00       200.00              200.00
        105.00       228.00              228.00
        115.00       245.00              245.00
        125.00       284.00              284.00
        150.00       310.00              310.00
        169.00       340.00              340.00
        182.00       350.00              350.00
Cross section number      7.00000
points DISTANCE,INITIAL ELEVATION AND FINAL ELEVATION
          0.00       350.00              350.00
         45.00       250.00              250.00
         67.00       240.00              240.00
```

```
        110.00      200.00              200.00
        130.00      190.00              193.85
        140.00      180.00              193.85
        155.00      180.00              193.85
        175.00      250.00              250.00
        210.00      250.00              250.00
        230.00      300.00              300.00
        242.00      350.00              350.00
Cross section number      3.00000
points DISTANCE,INITIAL ELEVATION AND FINAL ELEVATION
          0.00      350.00              350.00
        100.00      310.00              310.00
        145.00      300.00              300.00
        300.00      240.00              240.00
        325.00      220.00              220.00
        365.00      200.00              200.00
        410.00      190.00              190.26
        440.00      180.00              190.26
        485.00      180.00              190.26
        550.00      200.00              200.00
        630.00      220.00              220.00
        745.00      240.00              240.00
        760.00      250.00              250.00
        825.00      270.00              270.00
        840.00      280.00              280.00
        865.00      270.00              270.00
        885.00      280.00              280.00
        915.00      280.00              280.00
       1000.00      350.00              350.00
Cross section number      18.0000
points DISTANCE,INITIAL ELEVATION AND FINAL ELEVATION
          0.00      350.00              350.00
         75.00      300.00              300.00
        160.00      270.00              270.00
        200.00      250.00              250.00
        275.00      230.00              230.00
        395.00      180.00              185.39
        460.00      180.00              185.39
        500.00      190.00              190.00
        500.00      210.00              210.00
        610.00      210.00              210.00
        625.00      220.00              220.00
        725.00      230.00              230.00
        890.00      240.00              240.00
        990.00      250.00              250.00
       1010.00      260.00              260.00
       1110.00      280.00              280.00
       1140.00      290.00              290.00
       1165.00      310.00              310.00
       1265.00      350.00              350.00
Cross section number      124.000
points DISTANCE,INITIAL ELEVATION AND FINAL ELEVATION
          0.00      350.00              350.00
         51.00      340.00              340.00
         95.00      330.00              330.00
        133.00      320.00              320.00
        269.00      301.00              301.00
        380.00      281.00              281.00
```

563.00	260.00	260.00
794.00	260.00	260.00
898.00	260.00	260.00
958.00	251.00	251.00
1071.00	241.00	241.00
1089.00	241.00	241.00
1125.00	212.00	212.00
1167.00	183.00	185.79
1210.00	183.00	185.79
1249.00	202.00	202.00
1281.00	222.00	222.00
1337.00	222.00	222.00
1439.00	213.00	213.00
1488.00	213.00	213.00
1541.00	223.00	223.00
1584.00	242.00	242.00
1658.00	242.00	242.00
1687.00	232.00	232.00
1772.00	232.00	232.00
1796.00	242.00	242.00
1818.00	252.00	252.00
1983.00	253.00	253.00
2020.00	272.00	272.00
2151.00	282.00	282.00
2196.00	292.00	292.00
2272.00	302.00	302.00
2394.00	312.00	312.00
2426.00	321.00	321.00
2445.00	342.00	342.00
2476.00	352.00	352.00

Cross section number 48.0000

points DISTANCE, INITIAL ELEVATION AND FINAL ELEVATION

0.00	350.00	350.00
140.00	320.00	320.00
210.00	310.00	310.00
245.00	300.00	300.00
305.00	300.00	300.00
330.00	310.00	310.00
385.00	310.00	310.00
415.00	320.00	320.00
450.00	320.00	320.00
535.00	300.00	300.00
715.00	290.00	290.00
770.00	280.00	280.00
780.00	270.00	270.00
800.00	270.00	270.00
815.00	280.00	280.00
870.00	290.00	290.00
940.00	330.00	330.00
950.00	340.00	340.00
1190.00	340.00	340.00
1200.00	350.00	350.00
1300.00	360.00	360.00
1400.00	350.00	350.00
1500.00	350.00	350.00
1590.00	320.00	320.00
1650.00	290.00	290.00
1740.00	260.00	260.00

1950.00	240.00	240.00
1990.00	230.00	230.00
2050.00	190.00	191.02
2075.00	186.00	191.02
2100.00	190.00	191.02
2160.00	230.00	230.00
2210.00	230.00	230.00
2240.00	220.00	220.00
2260.00	220.00	220.00
2290.00	240.00	240.00
2680.00	240.00	240.00
2760.00	250.00	250.00
2810.00	250.00	250.00
2900.00	260.00	260.00
2920.00	270.00	270.00
3020.00	280.00	280.00
3080.00	290.00	290.00
3190.00	290.00	290.00
3240.00	310.00	310.00
3360.00	310.00	310.00
3380.00	320.00	320.00
3440.00	320.00	320.00
3500.00	350.00	350.00

Cross section number 57.0000

points DISTANCE, INITIAL ELEVATION AND FINAL ELEVATION

0.00	350.00	350.00
42.00	331.00	331.00
92.00	312.00	312.00
208.00	311.00	311.00
247.00	291.00	291.00
282.00	270.00	270.00
306.00	261.00	261.00
435.00	251.00	251.00
595.00	251.00	251.00
625.00	241.00	241.00
648.00	230.00	230.00
655.00	221.00	221.00
686.00	201.00	201.00
706.00	191.00	196.05
726.00	187.00	196.05
746.00	191.00	196.05
770.00	200.00	200.00
774.00	211.00	211.00
779.00	221.00	221.00
809.00	240.00	240.00
849.00	281.00	281.00
921.00	281.00	281.00
945.00	301.00	301.00
1017.00	301.00	301.00
1078.00	290.00	290.00
1100.00	281.00	281.00
1118.00	271.00	271.00
1138.00	270.00	270.00
1149.00	277.00	277.00
1188.00	290.00	290.00
1201.00	301.00	301.00
1244.00	310.00	310.00
1311.00	311.00	311.00

```
      1372.00      301.00            301.00
      1409.00      290.00            290.00
      1522.00      291.00            291.00
      1548.00      300.00            300.00
      1574.00      301.00            301.00
      1610.00      290.00            290.00
      1656.00      281.00            281.00
      1735.00      281.00            281.00
      1768.00      291.00            291.00
      1819.00      301.00            301.00
      1864.00      320.00            320.00
      1896.00      330.00            330.00
      1908.00      340.00            340.00
      1964.00      350.00            350.00
Cross section number      93.0000
points DISTANCE,INITIAL ELEVATION AND FINAL ELEVATION
         0.00      350.00            350.00
        37.00      330.00            330.00
        44.00      310.00            310.00
        55.00      300.00            300.00
        75.00      290.00            290.00
        93.00      280.00            280.00
       104.00      270.00            270.00
       109.00      260.00            260.00
       124.00      250.00            250.00
       140.00      240.00            240.00
       152.00      230.00            230.00
       184.00      200.00            200.00
       199.00      190.00            195.17
       218.00      190.00            195.17
       237.00      190.00            195.17
       269.00      220.00            220.00
       295.00      240.00            240.00
       350.00      240.00            240.00
       386.00      250.00            250.00
       416.00      260.00            260.00
       506.00      270.00            270.00
       563.00      270.00            270.00
       587.00      270.00            270.00
       618.00      280.00            280.00
       646.00      290.00            290.00
       714.00      300.00            300.00
       797.00      300.00            300.00
       813.00      309.00            309.00
       865.00      318.00            318.00
       925.00      329.00            329.00
       982.00      339.00            339.00
      1012.00      349.00            349.00
Cross section number      100.000
points DISTANCE,INITIAL ELEVATION AND FINAL ELEVATION
         0.00      349.00            349.00
        13.00      339.00            339.00
        45.00      329.00            329.00
        66.00      319.00            319.00
        94.00      309.00            309.00
       125.00      290.00            290.00
       155.00      270.00            270.00
       178.00      249.00            249.00
```

200.00	240.00	240.00
223.00	220.00	220.00
249.00	200.00	200.00
278.00	192.00	195.92
295.00	192.00	195.92
312.00	192.00	195.92
334.00	201.00	201.00
352.00	220.00	220.00
365.00	230.00	230.00
383.00	241.00	241.00
428.00	260.00	260.00
508.00	270.00	270.00
532.00	280.00	280.00
545.00	290.00	290.00
576.00	300.00	300.00
596.00	310.00	310.00
626.00	329.00	329.00
701.00	350.00	350.00

Cross section number 96.0000

points DISTANCE,INITIAL ELEVATION AND FINAL ELEVATION

0.00	349.00	349.00
37.00	330.00	330.00
58.00	310.00	310.00
74.00	300.00	300.00
125.00	280.00	280.00
135.00	270.00	270.00
149.00	260.00	260.00
158.00	250.00	250.00
200.00	231.00	231.00
241.00	194.00	199.05
273.00	194.00	199.05
291.00	211.00	211.00
309.00	221.00	221.00
317.00	231.00	231.00
324.00	241.00	241.00
348.00	250.00	250.00
354.00	260.00	260.00
426.00	271.00	271.00
456.00	280.00	280.00
470.00	291.00	291.00
476.00	301.00	301.00
489.00	310.00	310.00
514.00	320.00	320.00
534.00	341.00	341.00
560.00	350.00	350.00

Cross section number 103.000

points DISTANCE,INITIAL ELEVATION AND FINAL ELEVATION

0.00	349.00	349.00
14.00	339.00	339.00
25.00	330.00	330.00
39.00	319.00	319.00
45.00	309.00	309.00
74.00	290.00	290.00
80.00	280.00	280.00
91.00	270.00	270.00
104.00	260.00	260.00
115.00	250.00	250.00
145.00	230.00	230.00

```
        153.00      220.00              220.00
        185.00      200.00              202.19
        207.00      196.00              202.19
        229.00      200.00              202.19
        256.00      220.00              220.00
        270.00      230.00              230.00
        280.00      240.00              240.00
        289.00      250.00              250.00
        315.00      260.00              260.00
        350.00      270.00              270.00
        414.00      280.00              280.00
        423.00      290.00              290.00
        457.00      300.00              300.00
        477.00      310.00              310.00
        492.00      320.00              320.00
        502.00      331.00              331.00
        523.00      340.00              340.00
        544.00      350.00              350.00
Cross section number      112.000
points DISTANCE,INITIAL ELEVATION AND FINAL ELEVATION
          0.00      350.00              350.00
         31.00      330.00              330.00
         53.00      310.00              310.00
         85.00      290.00              290.00
        126.00      270.00              270.00
        155.00      260.00              260.00
        189.00      250.00              250.00
        245.00      230.00              230.00
        259.00      220.00              220.00
        281.00      200.00              204.39
        299.00      197.00              204.39
        317.00      200.00              204.39
        331.00      210.00              210.00
        344.00      220.00              220.00
        362.00      230.00              230.00
        373.00      250.00              250.00
        410.00      270.00              270.00
        434.00      280.00              280.00
        452.00      290.00              290.00
        481.00      300.00              300.00
        534.00      310.00              310.00
        577.00      330.00              330.00
        636.00      350.00              350.00
Cross section number      109.000
points DISTANCE,INITIAL ELEVATION AND FINAL ELEVATION
          0.00      350.00              350.00
         72.00      330.00              330.00
        131.00      320.00              320.00
        185.00      310.00              310.00
        243.00      290.00              290.00
        318.00      280.00              280.00
        345.00      260.00              260.00
        380.00      240.00              240.00
        397.00      230.00              230.00
        430.00      200.00              203.73
        448.00      198.00              203.73
        467.00      200.00              203.73
        495.00      230.00              230.00
```

503.00	250.00	250.00
524.00	260.00	260.00
561.00	270.00	270.00
652.00	280.00	280.00
697.00	300.00	300.00
740.00	330.00	330.00
765.00	350.00	350.00

Cross section number 126.000

points DISTANCE, INITIAL ELEVATION AND FINAL ELEVATION

0.00	350.00	350.00
34.00	338.00	338.00
56.00	328.00	328.00
100.00	318.00	318.00
136.00	308.00	308.00
161.00	298.00	298.00
216.00	288.00	288.00
244.00	278.00	278.00
322.00	269.00	269.00
354.00	259.00	259.00
359.00	249.00	249.00
376.00	239.00	239.00
392.00	229.00	229.00
430.00	209.00	209.16
443.00	202.00	209.16
458.00	202.00	209.16
473.00	202.00	209.16
479.00	209.00	209.16
496.00	219.00	219.00
516.00	240.00	240.00
531.00	250.00	250.00
558.00	259.00	259.00
616.00	270.00	270.00
652.00	290.00	290.00
716.00	320.00	320.00
763.00	330.00	330.00
779.00	340.00	340.00
792.00	350.00	350.00

Cross section number 113.000

points DISTANCE, INITIAL ELEVATION AND FINAL ELEVATION

0.00	350.00	350.00
71.00	330.00	330.00
118.00	320.00	320.00
151.00	310.00	310.00
209.00	300.00	300.00
240.00	290.00	290.00
306.00	271.00	271.00
375.00	260.00	260.00
407.00	250.00	250.00
473.00	241.00	241.00
550.00	220.00	220.00
582.00	203.00	209.82
606.00	203.00	209.82
630.00	203.00	209.82
633.00	211.00	211.00
648.00	228.00	228.00
660.00	241.00	241.00
666.00	250.00	250.00
681.00	261.00	261.00

```
        721.00      280.00              280.00
        752.00      290.00              290.00
        770.00      310.00              310.00
        819.00      341.00              341.00
        833.00      350.00              350.00
Cross section number      118.000
points DISTANCE,INITIAL ELEVATION AND FINAL ELEVATION
          0.00      348.00              348.00
         35.00      339.00              339.00
        138.00      319.00              319.00
        221.00      299.00              299.00
        246.00      288.00              288.00
        332.00      269.00              269.00
        340.00      259.00              259.00
        359.00      249.00              249.00
        379.00      239.00              239.00
        390.00      229.00              229.00
        434.00      204.00              207.39
        488.00      204.00              207.39
        508.00      220.00              220.00
        514.00      231.00              231.00
        546.00      240.00              240.00
        564.00      250.00              250.00
        586.00      260.00              260.00
        612.00      280.00              280.00
        644.00      300.00              300.00
        663.00      310.00              310.00
        701.00      340.00              340.00
        709.00      350.00              350.00
Cross section number      131.000
points DISTANCE,INITIAL ELEVATION AND FINAL ELEVATION
          0.00      350.00              350.00
         13.00      341.00              341.00
         28.00      330.00              330.00
         38.00      320.00              320.00
         65.00      300.00              300.00
         94.00      280.00              280.00
         96.00      270.00              270.00
        120.00      250.00              250.00
        134.00      240.00              240.00
        155.00      220.00              220.00
        165.00      211.00              216.34
        178.00      205.00              216.34
        192.00      211.00              216.34
        205.00      220.00              220.00
        239.00      230.00              230.00
        250.00      240.00              240.00
        260.00      250.00              250.00
        288.00      270.00              270.00
        352.00      280.00              280.00
        449.00      290.00              290.00
        493.00      300.00              300.00
        540.00      320.00              320.00
        597.00      330.00              330.00
        667.00      340.00              340.00
        739.00      350.00              350.00
Cross section number      159.000
points DISTANCE,INITIAL ELEVATION AND FINAL ELEVATION
```

```
          0.00      349.00              349.00
         21.00      339.00              339.00
         49.00      309.00              309.00
         69.00      299.00              299.00
         75.00      289.00              289.00
        110.00      269.00              269.00
        130.00      249.00              249.00
        154.00      229.00              229.00
        169.00      219.00              219.00
        179.00      209.00              214.02
        196.00      207.00              214.02
        214.00      210.00              214.02
        238.00      230.00              230.00
        250.00      240.00              240.00
        265.00      250.00              250.00
        274.00      260.00              260.00
        301.00      270.00              270.00
        313.00      280.00              280.00
        344.00      300.00              300.00
        370.00      320.00              320.00
        378.00      330.00              330.00
        405.00      340.00              340.00
        463.00      350.00              350.00
Cross section number      163.000
points DISTANCE,INITIAL ELEVATION AND FINAL ELEVATION
          0.00      350.00              350.00
         41.00      330.00              330.00
         48.00      320.00              320.00
         72.00      310.00              310.00
         89.00      300.00              300.00
        187.00      280.00              280.00
        214.00      270.00              270.00
        231.00      260.00              260.00
        263.00      250.00              250.00
        276.00      230.00              230.00
        292.00      220.00              220.00
        305.00      210.00              215.54
        321.00      208.00              215.54
        337.00      210.00              215.54
        361.00      220.00              220.00
        376.00      240.00              240.00
        424.00      270.00              270.00
        478.00      280.00              280.00
        561.00      290.00              290.00
        617.00      310.00              310.00
        680.00      320.00              320.00
        745.00      320.00              320.00
        766.00      329.00              329.00
        788.00      340.00              340.00
        799.00      350.00              350.00
Cross section number      167.000
points DISTANCE,INITIAL ELEVATION AND FINAL ELEVATION
          0.00      350.00              350.00
         15.00      339.00              339.00
         72.00      320.00              320.00
         98.00      310.00              310.00
        129.00      300.00              300.00
        191.00      290.00              290.00
```

```
        259.00      290.00              290.00
        382.00      280.00              280.00
        443.00      280.00              280.00
        505.00      270.00              270.00
        542.00      260.00              260.00
        564.00      240.00              240.00
        587.00      230.00              230.00
        608.00      210.00              219.09
        626.00      210.00              219.09
        643.00      210.00              219.09
        673.00      230.00              230.00
        701.00      250.00              250.00
        720.00      260.00              260.00
        769.00      280.00              280.00
        793.00      290.00              290.00
        879.00      290.00              290.00
        916.00      310.00              310.00
        924.00      320.00              320.00
        947.00      330.00              330.00
        977.00      340.00              340.00
        997.00      350.00              350.00
Cross section number      179.000
points DISTANCE,INITIAL ELEVATION AND FINAL ELEVATION
          0.00      350.00              350.00
         37.00      330.00              330.00
        130.00      310.00              310.00
        165.00      300.00              300.00
        185.00      290.00              290.00
        450.00      290.00              290.00
        632.00      280.00              280.00
        803.00      280.00              280.00
        845.00      260.00              260.00
        873.00      241.00              241.00
        924.00      212.00              223.32
        955.00      212.00              223.32
        987.00      212.00              223.32
       1036.00      230.00              230.00
       1068.00      251.00              251.00
       1322.00      251.00              251.00
       1371.00      281.00              281.00
       1401.00      311.00              311.00
       1441.00      331.00              331.00
       1508.00      350.00              350.00
Cross section number      188.000
points DISTANCE,INITIAL ELEVATION AND FINAL ELEVATION
          0.00      348.00              348.00
         21.00      338.00              338.00
         68.00      328.00              328.00
        107.00      309.00              309.00
        151.00      279.00              279.00
        164.00      270.00              270.00
        168.00      260.00              260.00
        176.00      250.00              250.00
        220.00      240.00              240.00
        230.00      230.00              230.00
        261.00      220.00              225.06
        284.00      213.00              225.06
        300.00      213.00              225.06
```

```
        317.00      213.00              225.06
        335.00      220.00              225.06
        403.00      240.00              240.00
        455.00      250.00              250.00
        473.00      250.00              250.00
        502.00      240.00              240.00
        532.00      240.00              240.00
        562.00      250.00              250.00
        607.00      260.00              260.00
        633.00      270.00              270.00
        688.00      300.00              300.00
        742.00      310.00              310.00
        770.00      320.00              320.00
        780.00      330.00              330.00
        800.00      340.00              340.00
        807.00      350.00              350.00
Cross section number      192.000
points DISTANCE,INITIAL ELEVATION AND FINAL ELEVATION
          0.00      350.00              350.00
         22.00      340.00              340.00
         29.00      330.00              330.00
         60.00      310.00              310.00
         89.00      300.00              300.00
        101.00      290.00              290.00
        179.00      290.00              290.00
        205.00      280.00              280.00
        255.00      280.00              280.00
        320.00      260.00              260.00
        342.00      250.00              250.00
        353.00      240.00              240.00
        430.00      215.00              224.03
        480.00      215.00              224.03
        503.00      230.00              230.00
        525.00      240.00              240.00
        530.00      250.00              250.00
        589.00      270.00              270.00
        627.00      280.00              280.00
        685.00      290.00              290.00
        747.00      300.00              300.00
        848.00      310.00              310.00
        861.00      320.00              320.00
        992.00      340.00              340.00
       1043.00      350.00              350.00
Cross section number      193.000
points DISTANCE,INITIAL ELEVATION AND FINAL ELEVATION
          0.00      350.00              350.00
         26.00      330.00              330.00
         45.00      320.00              320.00
         94.00      300.00              300.00
        104.00      290.00              290.00
        125.00      280.00              280.00
        156.00      270.00              270.00
        200.00      250.00              250.00
        210.00      240.00              240.00
        246.00      220.00              226.48
        270.00      217.00              226.48
        295.00      220.00              226.48
        330.00      240.00              240.00
```

```
        377.00      260.00              260.00
        397.00      270.00              270.00
        420.00      280.00              280.00
        532.00      300.00              300.00
        543.00      310.00              310.00
        562.00      320.00              320.00
        623.00      350.00              350.00
Cross section number      198.000
points DISTANCE,INITIAL ELEVATION AND FINAL ELEVATION
          0.00      350.00              350.00
         86.00      310.00              310.00
        100.00      300.00              300.00
        117.00      290.00              290.00
        140.00      270.00              270.00
        163.00      260.00              260.00
        177.00      250.00              250.00
        224.00      220.00              229.46
        242.00      218.00              229.46
        261.00      220.00              229.46
        313.00      240.00              240.00
        345.00      250.00              250.00
        385.00      270.00              270.00
        400.00      280.00              280.00
        473.00      290.00              290.00
        502.00      300.00              300.00
        536.00      319.00              319.00
        578.00      349.00              349.00
Cross section number      206.000
points DISTANCE,INITIAL ELEVATION AND FINAL ELEVATION
          0.00      360.00              360.00
         48.00      340.00              340.00
         92.00      309.00              309.00
        276.00      288.00              288.00
        330.00      277.00              277.00
        341.00      266.00              266.00
        346.00      256.00              256.00
        385.00      220.00              240.84
        401.00      220.00              240.84
        417.00      220.00              240.84
        451.00      256.00              256.00
        498.00      286.00              286.00
        530.00      295.00              295.00
        571.00      295.00              295.00
        585.00      285.00              285.00
        620.00      285.00              285.00
        634.00      294.00              294.00
        687.00      304.00              304.00
        725.00      313.00              313.00
        824.00      313.00              313.00
        860.00      333.00              333.00
        963.00      332.00              332.00
        991.00      321.00              321.00
       1068.00      341.00              341.00
       1093.00      349.00              349.00
Cross section number      207.000
points DISTANCE,INITIAL ELEVATION AND FINAL ELEVATION
          0.00      350.00              350.00
         46.00      339.00              339.00
```

```
        81.00      319.00              319.00
       120.00      309.00              309.00
       210.00      309.00              309.00
       239.00      299.00              299.00
       324.00      288.00              288.00
       346.00      269.00              269.00
       350.00      258.00              258.00
       372.00      239.00              239.95
       385.00      225.00              239.95
       416.00      225.00              239.95
       422.00      229.00              239.95
       439.00      249.00              249.00
       516.00      279.00              279.00
       559.00      299.00              299.00
       583.00      309.00              309.00
       617.00      329.00              329.00
       643.00      349.00              349.00
Cross section number      221.000
points DISTANCE,INITIAL ELEVATION AND FINAL ELEVATION
         0.00      350.00              350.00
        54.00      320.00              320.00
        83.00      310.00              310.00
       133.00      300.00              300.00
       165.00      280.00              280.00
       180.00      270.00              270.00
       226.00      260.00              260.00
       242.00      251.00              251.00
       265.00      251.00              251.00
       290.00      260.00              260.00
       304.00      270.00              270.00
       342.00      280.00              280.00
       401.00      281.00              281.00
       464.00      271.00              271.00
       487.00      261.00              261.00
       523.00      250.00              250.00
       620.00      231.00              237.87
       660.00      226.00              237.87
       701.00      232.00              237.87
       805.00      252.00              252.00
       847.00      262.00              262.00
       901.00      282.00              282.00
       918.00      293.00              293.00
       951.00      303.00              303.00
       970.00      312.00              312.00
      1012.00      352.00              352.00
Cross section number      230.000
points DISTANCE,INITIAL ELEVATION AND FINAL ELEVATION
         0.00      349.00              349.00
       109.00      310.00              310.00
       119.00      300.00              300.00
       139.00      290.00              290.00
       166.00      270.00              270.00
       187.00      260.00              260.00
       194.00      250.00              250.00
       211.00      240.00              240.75
       213.00      230.00              240.75
       230.00      227.00              240.75
       248.00      230.00              240.75
```

```
        269.00      240.00              240.75
        278.00      250.00              250.00
        303.00      270.00              270.00
        349.00      290.00              290.00
        391.00      300.00              300.00
        412.00      310.00              310.00
        548.00      350.00              350.00
Cross section number      235.000
points DISTANCE,INITIAL ELEVATION AND FINAL ELEVATION
          0.00      350.00              350.00
         29.00      330.00              330.00
         50.00      320.00              320.00
         88.00      300.00              300.00
        129.00      290.00              290.00
        181.00      260.00              260.00
        206.00      250.00              250.00
        232.00      230.00              242.34
        251.00      228.00              242.34
        271.00      230.00              242.34
        301.00      250.00              250.00
        320.00      259.00              259.00
        343.00      279.00              279.00
        402.00      309.00              309.00
        453.00      330.00              330.00
        493.00      349.00              349.00
Cross section number      234.000
points DISTANCE,INITIAL ELEVATION AND FINAL ELEVATION
          0.00      350.00              350.00
         98.00      340.00              340.00
        129.00      330.00              330.00
        217.00      330.00              330.00
        260.00      320.00              320.00
        276.00      310.00              310.00
        317.00      300.00              300.00
        333.00      290.00              290.00
        339.00      280.00              280.00
        370.00      264.00              264.00
        422.00      230.00              242.49
        438.00      229.00              242.49
        454.00      230.00              242.49
        501.00      270.00              270.00
        519.00      290.00              290.00
        570.00      320.00              320.00
        595.00      340.00              340.00
        614.00      350.00              350.00
Cross section number      249.000
points DISTANCE,INITIAL ELEVATION AND FINAL ELEVATION
          0.00      350.00              350.00
         32.00      330.00              330.00
         78.00      330.00              330.00
        131.00      310.00              310.00
        214.00      290.00              290.00
        248.00      270.00              270.00
        312.00      230.00              250.67
        328.00      230.00              250.67
        344.00      230.00              250.67
        354.00      240.00              250.67
        362.00      250.00              250.67
```

```
        436.00      299.00              299.00
        475.00      309.00              309.00
        519.00      329.00              329.00
        543.00      349.00              349.00
Cross section number      252.000
points DISTANCE,INITIAL ELEVATION AND FINAL ELEVATION
          0.00      350.00              350.00
         79.00      320.00              320.00
        206.00      310.00              310.00
        249.00      290.00              290.00
        289.00      260.00              260.00
        307.00      250.00              251.40
        324.00      230.00              251.40
        339.00      230.00              251.40
        354.00      230.00              251.40
        383.00      240.00              251.40
        444.00      270.00              270.00
        556.00      290.00              290.00
        575.00      300.00              300.00
        612.00      310.00              310.00
        656.00      330.00              330.00
        693.00      350.00              350.00
Cross section number      274.000
points DISTANCE,INITIAL ELEVATION AND FINAL ELEVATION
          0.00      349.00              349.00
         29.00      319.00              319.00
         96.00      280.00              280.00
        141.00      234.00              256.41
        169.00      234.00              256.41
        199.00      269.00              269.00
        233.00      299.00              299.00
        327.00      320.00              320.00
        355.00      329.00              329.00
        417.00      329.00              329.00
        505.00      320.00              320.00
        769.00      329.00              329.00
        817.00      330.00              330.00
       1124.00      350.00              350.00
Cross section number      297.000
points DISTANCE,INITIAL ELEVATION AND FINAL ELEVATION
          0.00      350.00              350.00
         20.00      330.00              330.00
         80.00      300.00              300.00
        181.00      290.00              290.00
        211.00      270.00              270.00
        222.00      260.00              260.35
        235.00      250.00              260.35
        259.00      241.00              260.35
        270.00      241.00              260.35
        280.00      241.00              260.35
        290.00      250.00              260.35
        334.00      280.00              280.00
        356.00      290.00              290.00
        389.00      310.00              310.00
        398.00      320.00              320.00
        455.00      340.00              340.00
        558.00      350.00              350.00
Cross section number      303.000
```

```
points DISTANCE,INITIAL ELEVATION AND FINAL ELEVATION
          0.00      350.00              350.00
         44.00      330.00              330.00
         62.00      320.00              320.00
        170.00      310.00              310.00
        213.00      300.00              300.00
        235.00      280.00              280.00
        286.00      244.00              261.63
        316.00      244.00              261.63
        351.00      259.00              261.63
        404.00      309.00              309.00
        445.00      329.00              329.00
        572.00      329.00              329.00
        614.00      339.00              339.00
        639.00      349.00              349.00
Cross section number      311.000
points DISTANCE,INITIAL ELEVATION AND FINAL ELEVATION
          0.00      350.00              350.00
         37.00      340.00              340.00
         65.00      320.00              320.00
        122.00      310.00              310.00
        176.00      310.00              310.00
        188.00      300.00              300.00
        231.00      289.00              289.00
        454.00      279.00              288.11
        466.00      269.00              288.11
        478.00      259.00              288.11
        509.00      250.00              288.11
        524.00      247.00              288.11
        540.00      250.00              288.11
        563.00      259.00              288.11
        590.00      279.00              288.11
        635.00      300.00              300.00
        648.00      310.00              310.00
        678.00      320.00              320.00
        742.00      329.00              329.00
        794.00      350.00              350.00
Cross section number      335.000
points DISTANCE,INITIAL ELEVATION AND FINAL ELEVATION
          0.00      350.00              350.00
         37.00      340.00              340.00
         65.00      330.00              330.00
        122.00      320.00              320.00
        176.00      319.00              319.00
        188.00      299.00              300.64
        481.00      289.00              300.64
        515.00      252.00              300.64
        527.00      252.00              300.64
        538.00      252.00              300.64
        559.00      269.00              300.64
        594.00      289.00              300.64
        598.00      298.00              300.64
        624.00      318.00              318.00
        652.00      338.00              338.00
        689.00      348.00              348.00
Cross section number      361.000
points DISTANCE,INITIAL ELEVATION AND FINAL ELEVATION
          0.00      350.00              350.00
```

19.00	334.00	334.00
39.00	320.00	320.00
80.00	310.00	310.00
109.00	290.00	290.41
140.00	280.00	290.41
157.00	270.00	290.41
209.00	266.00	290.41
261.00	270.00	290.41
292.00	280.00	290.41
322.00	280.00	290.41
343.00	290.00	290.41
367.00	310.00	310.00
411.00	330.00	330.00
482.00	350.00	350.00

Cross section number 392.000

points DISTANCE, INITIAL ELEVATION AND FINAL ELEVATION

0.00	350.00	350.00
50.50	330.00	330.00
92.50	320.00	320.00
127.40	300.00	319.44
162.30	270.00	319.44
185.40	270.00	319.44
208.70	270.00	319.44
222.60	280.00	319.44
260.30	300.00	319.44
332.70	320.00	320.00
371.30	320.00	320.00
391.60	300.00	319.44
410.60	300.00	319.44
493.10	320.00	320.00
552.80	320.00	320.00
587.60	310.00	319.44
647.90	310.00	319.44
687.50	320.00	320.00
712.50	330.00	330.00
822.00	330.00	330.00
952.50	350.00	350.00

Cross section number 420.000

points DISTANCE, INITIAL ELEVATION AND FINAL ELEVATION

0.00	350.00	350.00
24.50	340.00	340.00
34.30	330.00	330.00
63.00	310.00	312.76
101.10	290.00	312.76
130.30	274.00	312.76
162.90	274.00	312.76
196.20	290.00	312.76
231.60	300.00	312.76
250.60	310.00	312.76
275.70	320.00	320.00
295.00	329.00	329.00
346.30	329.00	329.00
411.90	300.00	312.76
424.20	290.00	312.76
441.00	300.00	312.76
484.30	329.00	329.00
510.00	340.00	340.00
524.70	350.00	350.00

```
Cross section number      500.000
points DISTANCE,INITIAL ELEVATION AND FINAL ELEVATION
          0.00       350.00              350.00
         26.70       340.00              340.00
         68.70       330.00              330.00
         84.50       320.00              320.00
        172.00       281.00              312.45
        186.60       276.00              312.45
        201.10       281.00              312.45
        219.90       291.00              312.45
        261.80       301.00              312.45
        280.40       321.00              321.00
        330.30       330.00              330.00
        366.10       350.00              350.00
Cross section number      616.000
points DISTANCE,INITIAL ELEVATION AND FINAL ELEVATION
          0.00       349.00              349.00
         47.00       340.00              340.00
        104.00       320.00              320.67
        114.00       310.00              320.67
        133.00       300.00              320.67
        174.00       290.00              320.67
        186.00       287.00              320.67
        198.00       290.00              320.67
        232.00       300.00              320.67
        277.00       320.00              320.67
        382.00       350.00              350.00
Cross section number      629.000
points DISTANCE,INITIAL ELEVATION AND FINAL ELEVATION
          0.00       349.00              349.00
         60.00       339.00              339.00
         93.00       329.00              329.00
        111.00       310.00              318.67
        136.00       300.00              318.67
        182.00       290.00              318.67
        195.00       290.00              318.67
        207.00       290.00              318.67
        253.00       310.00              318.67
        263.00       320.00              320.00
        278.00       330.00              330.00
        302.00       350.00              350.00
Cross section number      645.000
points DISTANCE,INITIAL ELEVATION AND FINAL ELEVATION
          0.00       350.00              350.00
         21.20       340.00              340.00
         34.70       330.00              330.00
         43.40       320.00              320.00
         59.90       310.00              317.63
         69.60       300.00              317.63
         99.90       292.00              317.63
        116.90       292.00              317.63
        134.00       292.00              317.63
        153.80       300.00              317.63
        165.20       310.00              317.63
        193.40       330.00              330.00
        249.30       350.00              350.00
Cross section number      642.000
points DISTANCE,INITIAL ELEVATION AND FINAL ELEVATION
```

```
          0.00       350.00              350.00
         19.00       330.00              330.00
         39.00       320.00              320.56
         69.00       300.00              320.56
         80.00       293.00              320.56
        100.00       293.00              320.56
        120.00       293.00              320.56
        174.00       300.00              320.56
        192.00       320.00              320.56
        215.00       330.00              330.00
        245.00       350.00              350.00
Cross section number      684.000
points DISTANCE, INITIAL ELEVATION AND FINAL ELEVATION
          0.00       350.00              350.00
         31.00       340.00              340.00
         50.00       330.00              330.00
         83.00       310.00              323.67
         93.00       300.00              323.67
        113.00       297.00              323.67
        133.00       300.00              323.67
        179.00       310.00              323.67
        204.00       320.00              323.67
        304.00       350.00              350.00
Cross section number      692.000
points DISTANCE, INITIAL ELEVATION AND FINAL ELEVATION
          0.00       350.00              350.00
         20.00       340.00              340.00
         54.00       340.00              340.00
         69.00       330.00              330.00
         96.00       320.00              322.78
        115.00       310.00              322.78
        146.00       300.00              322.78
        166.00       298.00              322.78
        186.00       300.00              322.78
        219.00       320.00              322.78
        242.00       340.00              340.00
        269.00       350.00              350.00
Cross section number      710.000
points DISTANCE, INITIAL ELEVATION AND FINAL ELEVATION
          0.00       351.00              351.00
         16.00       341.00              341.00
         29.00       330.00              330.00
         60.00       321.00              327.38
         70.00       311.00              327.38
         98.00       300.00              327.38
        122.00       300.00              327.38
        145.00       300.00              327.38
        194.00       310.00              327.38
        235.00       311.00              327.38
        250.00       320.00              327.38
        289.00       340.00              340.00
        304.00       350.00              350.00
Cross section number      720.000
points DISTANCE, INITIAL ELEVATION AND FINAL ELEVATION
          0.00       351.00              351.00
         52.00       340.00              340.00
         84.00       330.00              330.00
        102.00       320.00              327.11
```

```
        133.00      310.00              327.11
        154.00      300.00              327.11
        175.00      301.00              327.11
        197.00      301.00              327.11
        218.00      310.00              327.11
        241.00      320.00              327.11
        276.00      340.00              340.00
        287.00      350.00              350.00
Cross section number      738.000
points DISTANCE,INITIAL ELEVATION AND FINAL ELEVATION
          0.00      350.00              350.00
         21.00      330.00              332.05
        101.00      320.00              332.05
        138.00      310.00              332.05
        149.00      302.00              332.05
        183.00      302.00              332.05
        217.00      302.00              332.05
        264.00      330.00              332.05
        285.00      340.00              340.00
        310.00      350.00              350.00
Cross section number      755.000
points DISTANCE,INITIAL ELEVATION AND FINAL ELEVATION
          0.00      350.00              350.00
         24.00      330.00              333.08
         50.00      320.00              333.08
         94.00      310.00              333.08
        149.00      305.00              333.08
        205.00      310.00              333.08
        222.00      320.00              333.08
        246.00      330.00              333.08
        282.00      350.00              350.00
Cross section number      770.000
points DISTANCE,INITIAL ELEVATION AND FINAL ELEVATION
          0.00      350.00              350.00
         19.00      339.00              339.00
         49.00      330.00              334.89
         74.00      319.00              334.89
        104.00      310.00              334.89
        137.00      308.00              334.89
        169.00      310.00              334.89
        191.00      320.00              334.89
        205.00      330.00              334.89
        215.00      340.00              340.00
        229.00      350.00              350.00
Cross section number      780.000
points DISTANCE,INITIAL ELEVATION AND FINAL ELEVATION
          0.00      350.00              350.00
         44.00      340.00              340.00
         59.00      330.00              335.36
         84.00      320.00              335.36
         99.00      310.00              335.36
        129.00      308.00              335.36
        159.00      310.00              335.36
        204.00      330.00              335.36
        214.00      340.00              340.00
        229.00      350.00              350.00
Cross section number      793.000
points DISTANCE,INITIAL ELEVATION AND FINAL ELEVATION
```

```
          0.00       350.00              350.00
         29.00       340.00              340.00
         39.00       330.00              335.61
         85.00       310.00              335.61
        118.00       309.00              335.61
        150.00       310.00              335.61
        170.00       330.00              335.61
        175.00       340.00              340.00
        190.00       350.00              350.00
Cross section number      803.000
points DISTANCE,INITIAL ELEVATION AND FINAL ELEVATION
          0.00       350.00              350.00
         15.00       340.00              340.00
         23.00       330.00              334.63
         40.00       320.00              334.63
         52.00       310.00              334.63
        104.00       309.00              334.63
        139.00       320.00              334.63
        169.00       330.00              334.63
        195.00       340.00              340.00
        210.00       350.00              350.00
**********************************************************************
*   Total Days   *              Total Sediment Inflow                 *
*                *  SAND & GRAVEL      SILT          CLAY             *
*                *     (in m3)        (in m3)       (in m3)          *
*    7299.96     *    0.53E+07        0.79E+08      0.15E+09         *
**********************************************************************
*                 Total Sediment Outflow                             *
*           SAND & GRAVEL      SILT          CLAY                    *
*              (in m3)        (in m3)       (in m3)                  *
*           0.14E-05        0.39E+08      0.86E+08                   *
**********************************************************************
*                 Trap Efficiency of Reservoir                       *
*     SAND & GRAVEL      SILT       CLAY       TOTAL                 *
*        1.0000         0.5101      0.4110     0.4588                *
**********************************************************************
```

SECTION NO.	DISCHARGE (m3/s)	WS ELE (m)	DISTANCE FROM DAM(m)	INITIAL TALWAGE ELE.(m)	FINAL TALWAGE ELE.(m)
803.00	52.00	336.07	60303.90	309.00	334.63
793.00	52.00	335.95	59903.90	309.00	335.61
780.00	52.00	335.61	59313.90	308.00	335.36
770.00	52.00	335.11	58593.90	308.00	334.89
755.00	52.00	333.26	57633.90	305.00	333.08
738.00	52.00	332.22	56633.90	302.00	332.05
720.00	52.00	327.97	55391.90	300.00	327.11
710.00	52.00	327.58	54751.90	300.00	327.38
692.00	52.00	324.23	53811.90	298.00	322.78
684.00	52.00	323.94	52771.90	297.00	323.67
642.00	52.00	321.01	51181.90	293.00	320.56
645.00	52.00	321.03	50751.90	292.00	317.63
629.00	52.00	321.02	49681.90	290.00	318.67
616.00	52.00	320.88	48881.90	287.00	320.67
500.00	52.00	319.77	46451.90	276.00	312.45
420.00	52.00	319.77	45571.90	274.00	312.76
392.00	52.00	319.62	43262.90	270.00	319.44
361.00	52.00	300.83	41503.00	266.00	290.41
335.00	52.00	300.76	38563.00	252.00	300.64

311.00	52.00	290.00	37063.00	247.00	288.11
303.00	52.00	290.00	35823.00	244.00	261.63
297.00	52.00	290.00	35273.00	241.00	260.35
274.00	52.00	290.00	32593.00	234.00	256.41
252.00	52.00	290.00	30902.50	230.00	251.40
249.00	52.00	290.00	29872.50	230.00	250.67
234.00	52.00	290.00	29022.50	229.00	242.49
235.00	52.00	290.00	28702.50	228.00	242.34
230.00	52.00	290.00	28332.50	227.00	240.75
221.00	52.00	290.00	27512.50	226.00	237.87
207.00	52.00	290.00	25162.50	225.00	239.95
206.00	52.00	290.00	23992.50	220.00	240.84
198.00	52.00	290.00	23212.50	218.00	229.46
193.00	52.00	290.00	22242.50	217.00	226.48
192.00	52.00	290.00	21882.50	215.00	224.03
188.00	52.00	290.00	21192.50	213.00	225.06
179.00	52.00	290.00	20122.50	212.00	223.32
167.00	52.00	290.00	18962.50	210.00	219.09
163.00	52.00	290.00	18082.50	208.00	215.54
159.00	52.00	290.00	17292.50	207.00	214.02
131.00	52.00	290.00	16692.50	205.00	216.34
118.00	52.00	290.00	15682.50	204.00	207.39
113.00	52.00	290.00	14812.50	203.00	209.82
126.00	52.00	290.00	14152.50	202.00	209.16
109.00	52.00	290.00	13342.50	198.00	203.73
112.00	52.00	290.00	12562.50	197.00	204.39
103.00	52.00	290.00	11812.50	196.00	202.19
96.00	52.00	290.00	10582.20	194.00	199.05
100.00	52.00	290.00	10261.60	192.00	195.92
93.00	52.00	290.00	9541.40	190.00	195.17
57.00	52.00	290.00	7751.60	187.00	196.05
48.00	52.00	290.00	6590.00	186.00	191.02
124.00	52.00	290.00	3140.00	183.00	185.79
18.00	52.00	290.00	1490.00	180.00	185.39
3.00	52.00	290.00	1170.00	180.00	190.26
7.00	52.00	290.00	290.00	180.00	193.85
1.00	52.00	290.00	0.00	180.00	192.77

PERCENTAGE OF EACH PARTICLE SIZE IN COVER LAYER

CROSS SECTION	RLENTO	CLAY(%)	SILT(%)	SAND(%)
1.00000	0.000000	89.0480	10.9513	0.605527E-03
7.00000	290.000	87.8824	12.1174	0.444835E-05
3.00000	1170.00	85.7781	14.2220	0.000000
18.0000	1490.00	79.3638	20.6362	0.000000
124.000	3140.00	59.3534	40.6466	0.000000
48.0000	6590.00	67.3800	32.6200	0.116764E-04
57.0000	7751.60	71.9224	28.0482	0.291286E-01
93.0000	9541.40	73.8672	26.0967	0.356065E-01
100.000	10261.6	75.8213	24.0581	0.120456
96.0000	10582.2	76.6970	23.2092	0.946985E-01
103.000	11812.5	73.9133	26.0626	0.246501E-01
112.000	12562.5	74.7980	25.1679	0.339729E-01
109.000	13342.5	78.9197	21.0103	0.705191E-01
126.000	14152.5	74.7187	25.2643	0.174461E-01
113.000	14812.5	71.4091	28.5876	0.285038E-02
118.000	15682.5	72.5798	27.4174	0.215732E-02
131.000	16692.5	75.2875	24.7059	0.601099E-02
159.000	17292.5	76.7335	23.2502	0.164532E-01
163.000	18082.5	77.3761	22.6170	0.672043E-02

167.000	18962.5	72.6678	27.3314	0.658113E-03
179.000	20122.5	71.6221	28.3774	0.862278E-04
188.000	21192.5	67.3081	32.6922	0.000000
192.000	21882.5	73.5407	26.4592	0.406790E-04
193.000	22242.5	73.1439	26.8560	0.103054E-04
198.000	23212.5	71.2821	28.7178	0.000000
206.000	23992.5	72.4362	27.5639	0.487784E-05
207.000	25162.5	69.7562	30.2441	0.000000
221.000	27512.5	64.9689	35.0310	0.000000
230.000	28332.5	70.5023	29.4976	0.000000
235.000	28702.5	69.6887	30.3113	0.109809E-04
234.000	29022.5	69.7866	30.2134	0.000000
249.000	29872.5	68.1835	31.8165	0.000000
252.000	30902.5	66.6569	33.3430	0.000000
274.000	32593.0	68.1460	31.8540	0.000000
297.000	35273.0	65.9007	34.0994	0.000000
303.000	35823.0	66.3759	33.6241	0.000000
311.000	37063.0	60.6663	39.3338	0.000000
335.000	38563.0	61.4820	38.5178	0.000000
361.000	41503.0	53.6650	46.3350	0.000000
392.000	43262.9	53.8927	46.1073	0.000000
420.000	45571.9	46.9507	53.0493	0.864254E-05
500.000	46451.9	45.0987	54.8755	0.256275E-01
616.000	48881.9	36.6819	40.6153	22.7026
629.000	49681.9	39.4081	49.3553	11.2363
645.000	50751.9	41.3915	47.3295	11.2793
642.000	51181.9	37.5198	48.7057	13.7746
684.000	52771.9	23.7475	28.0565	48.1960
692.000	53811.9	36.5714	39.6455	23.7830
710.000	54751.9	32.1144	40.9935	26.8913
720.000	55391.9	25.9105	26.9983	47.0914
738.000	56633.9	40.0449	47.7406	12.2148
755.000	57633.9	39.8620	57.7187	2.42023
770.000	58593.9	18.7250	31.0024	50.2725
780.000	59313.9	10.6230	19.3746	70.0028
793.000	59903.9	10.3941	18.6444	70.9613
803.000	60303.9	19.8111	37.9530	42.2368

APPENDIX G.

SUSPENDED SEDIMENT LOAD MEASURED AT TALE-ZANG MONITORING STATION

Q (m3/s)	Sediment Load (Tonnes/Day)	Q (m3/s)	Sediment Load (Tonnes/Day)	Q (m3/s)	Sediment Load (Tonnes/Day)
46	179.0	91	301.0	140	206.0
53	263.0	92	1094.0	141	4799.0
53	633.0	92	1741.0	142	2053.0
55	137.0	94	580.0	143	3724.0
55	166.0	94	309.0	146	85832.0
55	282.0	95	1023.0	151	13098.0
56	141.0	96	240.0	153	6279.0
56	381.0	99	618.0	157	1438.0
58	582.0	99	2524.0	160	3691.0
61	685.0	102	1057.0	161	3130.0
62	221.0	103	819.0	170	1586.0
62	394.0	105	1376.0	171	3915.0
63	332.0	107	998.0	172	8125.0
63	359.0	108	21938.0	172	2363.0
63	399.0	108	1782.0	174	2646.0
64	635.0	110	410.0	176	1385.0
64	1744.0	110	2245.0	176	2600.0
65	790.0	112	1172.0	176	4668.0
69	2808.0	112	1519.0	180	4821.0
70	193.0	115	2056.0	182	2749.0
72	442.0	117	2264.0	183	3953.0
72	2853.0	120	1559.0	184	2480.0
74	710.0	121	3596.0	185	6128.0
76	440.0	122	483.0	188	1040.0
76	5799.0	123	806.0	189	11839.0
77	356.0	125	791.0	190	2528.0
78	203.0	127	3555.0	193	3568.0
78	478.0	131	2366.0	199	1926.0
79	683.0	133	1023.0	201	1907.0
81	267.0	133	2078.0	201	3763.0
81	399.0	133	3735.0	203	6864.0
85	583.0	134	1135.0	204	4177.0
86	1146.0	134	1957.0	204	4124.0
86	1441.0	137	1385.0	205	3384.0
87	188.0	138	670.0	206	18315.0
87	502.0	139	1333.0	207	17205.0
89	461.0	140	4801.0	212	5733.0

Q (m3/s)	Sediment Load (Tonnes/Day)	Q (m3/s)	Sediment Load (Tonnes/Day)	Q (m3/s)	Sediment Load (Tonnes/Day)
213	7453.0	334	13607.0	581	108053.0
218	2788.0	335	23908.0	590	113880.0
218	9543.0	338	25086.0	590	54136.0
218	11037.0	345	6438.0	596	15038.0
220	7196.0	347	28901.0	599	46578.0
220	15947.0	355	29972.0	608	51533.0
224	21773.0	358	19934.0	635	58650.0
225	9428.0	360	13965.0	636	57258.0
227	4135.0	364	3554.0	644	100755.0
227	15180.0	364	36041.0	653	55178.0
230	7290.0	372	39698.0	677	113164.0
234	5095.0	373	8057.0	680	41009.0
238	5613.0	374	29050.0	684	150257.0
247	3244.0	376	25372.0	690	69870.0
249	7286.0	379	11025.0	697	68712.0
254	11189.0	379	20332.0	699	55139.0
255	4693.0	379	56816.0	702	131566.0
258	8961.0	379	8448.0	705	36608.0
258	94559.0	389	72529.0	727	108656.0
260	8154.0	391	23884.0	727	112744.0
260	8616.0	398	22627.0	741	505521.0
261	4984.0	402	13337.0	742	67442.0
261	5938.0	408	96771.0	743	97760.0
267	4523.0	428	17899.0	768	43750.0
270	8258.0	436	20380.0	787	96691.0
271	13393.0	437	25750.0	788	89650.0
281	11751.0	448	7858.0	791	42372.0
284	7778.0	453	18746.0	791	129785.0
286	3437.0	459	69270.0	822	115662.0
290	11801.0	462	29658.0	833	70028.0
291	2841.0	463	17121.0	835	149626.0
294	7122.0	465	65326.0	843	181117.0
298	30871.0	494	26046.0	845	147601.0
302	10802.0	508	45628.0	879	204352.0
305	13802.0	518	19110.0	882	100362.0
310	17918.0	537	46397.0	884	146193.0
312	31971.0	553	45534.0	905	215692.0
314	9143.0	560	70539.0	959	277324.0
316	10904.0	571	728916.0	964	135423.0
320	16368.0	572	78777.0	964	181470.0
329	18567.0	578	91624.0	1264	300982.0
330	11547.0	580	35680.0	2133	1302386.0

APPENDIX H

ACCURACY OF THE EQUIPMENT AND MEASURED PARAMETERS

Equipment	Parameter	Unit	Accuracy
Orifice flow meter	Discharge	L/s	±0.5 mm height of mercury (= ±0.005 L/s)
Thermometer	Temperature	°C	±0.5 Celsius degree
Two dimensional fibre optic Laser Doppler Velocimeter system from TSI Incorporated	Velocity	m/s	very high accurate with measurement of very slow flow and flow reversals
A fibre optic turbidity probe (Analite Portable Nephelometer from McVAN Instruments)	Sediment concentration and fractional density	NTU	in high sensitive range (range from 0.1 to 199.9) was ± 0.1 NTU and for the other range (range from 2 to 1999) was ± 1 NTU
Laser particle sizer (model 2600 of Malvern Company)	Particle size distribution curve (range from 0.5 μm to 564 μm)	μm	± 4% on volume median diameter
Scale	to weight the sampled particles	g	± 0.0005 g
	The error in determination of height of gravity current head, H_f	mm	probably ±5%.
	The error in determination of velocity of the head of gravity current, U_f	cm/s	probably less than ±2.5%.
	The error in determination of density differences, Δ		should be less than ±2.5%
	The error in determination of distance	mm	less than ±1 mm
	The error to get sample from deposited material	g/cm^2	probably less than ±2.5%

APPENDIX I

RAW DATA OF THE EXPERIMENTS

Experiment no.: 1 **Date: 14-11-94**

Concentration of particle in mixing tank: 6 g/L

Volume of water: 567 L

Temperature: 20°C **Starting time: 3.52 pm**

Inflow discharge: 0.14 L/s **Outflow: 0.307 L/s**

Height of turbidity current at station

	St. 0	St. 1	St. 2	St. 3	St. 4	St. 5	St. 6	St. 7
Height (cm)	4.0	4.0	3.5	3.0	3.5	4.5	4.3	4.5

Height of water in the flume: 50 cm **End time: 5:00 pm**

Inflow concentration at flume entrance: 4.25 g/L

Outflow concentration: 0.32 g/L

Sediment deposition at station (Sample area = 114.04 cm^2)

	St. 0+ 150 mm	St. 1	St. 2	St. 3	St. 4	St. 5	St. 6	St. 7
Weight of particles (g)	55.37	35.13	21.18	13.41	9.63	7.00	5.23	3.36
Deposition per unit area (g)	0.4855	0.3080	0.1857	0.1176	0.0844	0.0614	0.0459	0.0295

Experiment No. 1: Particle Size Analysis										
High Size	Inflow	St. 0	St. 1	St. 2	St. 3	St. 4	St. 5	St. 6	St. 7	Outflow
(μm)	Under %	Under %	Under %	Under %	Under %	Under %	Under %	Under %	Under %	Under %
188	100	100	100	100	100	100	100	100	100	100
175	100	99.3	100	100	100	100	100	99.8	100	100
163	100	98.6	100	100	100	99.9	100	99.7	100	100
151	100	97.7	99.9	100	100	99.9	100	99.7	100	100
141	99.9	96.5	99.8	100	100	99.9	100	99.7	100	100
131	99.8	94.9	99.6	100	100	99.9	100	99.7	100	100
122	99.6	93	99.2	99.9	100	99.9	100	99.6	100	100
113	99.2	90.4	98.3	99.8	99.9	99.9	100	99.6	100	100
105	98.2	87.3	96.4	99.8	99.9	99.9	99.9	99.6	100	100
97.8	96.3	83.5	92.8	99.7	99.8	99.9	99.8	99.6	100	100
90.9	93.5	78.8	87.9	99	99.5	99.9	99.7	99.6	100	100
84.5	90	73.3	82	96.7	98.7	99.9	99.3	99.6	100	100
78.6	85.8	67	75.4	93	97.5	99.9	98.7	99.6	100	100
73.1	81.2	60.3	68.1	88.6	95.7	99.9	97.8	99.6	99.9	100
68	76.1	53.3	60.5	83.5	93.4	99.5	96.4	99.5	99.9	100
63.2	70.8	46.5	52.9	77.8	90.3	98.3	94.6	99	99.9	99.9
58.8	65.4	40.2	45.8	71.6	86.2	95.8	92	97.6	99.5	99.7
54.7	60.1	34.7	39.6	64.8	80.9	91.7	88.5	95.1	98	99.2
50.8	55	30.2	34.5	57.7	74.4	86	84.2	91.3	95.4	98.3
47.3	50.1	26.6	30.5	50.4	67	79.1	79.1	86.5	91.9	97
44	45.5	23.8	27.3	43.4	59.2	71.5	73.4	81.1	87.5	95.2
40.9	41.4	21.4	24.5	36.9	51.5	63.9	67.4	75.1	82.5	92.8
38	37.1	19.2	21.9	31.5	44.6	56.7	61.4	68.9	77.1	89.8
35.4	33.4	16.9	19.1	27.3	38.9	50.6	55.6	62.8	71.3	86.1
32.9	30	14.6	16.3	24.3	34.3	45.5	50.2	57	65.3	81.6
30.6	27	12.4	13.7	22	30.7	41.2	45.1	51.6	59.3	76.5
28.4	24.2	10.5	11.4	20.2	27.7	37.4	40.4	46.7	53.3	70.9
26.4	21.8	9.1	9.7	18.5	25.2	34	36.1	42.4	47.5	64.8
24.6	19.6	8	8.5	16.7	22.8	30.8	32.2	38.5	42	58.5
22.9	17.6	7.1	7.6	14.8	20.6	27.6	28.6	34.8	37	52.4
21.3	15.8	6.4	6.9	12.8	18.3	24.4	25.2	30.9	32.6	46.7
19.8	13.9	5.8	6.3	10.7	15.9	21.1	22.1	26.7	28.8	41.6
18.4	12.2	5.1	5.6	8.7	13.5	17.9	19.2	22.5	25.4	37
17.1	10.5	4.5	4.9	7	11.3	15.1	16.6	18.8	22.1	32.6
15.9	9	3.9	4.2	5.7	9.5	12.8	14.1	15.9	18.8	28.3
14.8	7.6	3.3	3.5	4.9	8	10.9	11.9	13.7	15.5	24
13.7	6.3	2.7	2.8	4.4	6.8	9.5	9.9	12.1	12.4	19.9
12.8	5.3	2.3	2.3	4.1	5.9	8.3	8.2	10.8	9.8	16.2
11.9	4.5	1.9	1.9	3.7	5.1	7.2	6.8	9.5	7.8	12.9
11.1	3.8	1.6	1.6	3.3	4.5	6.3	5.6	8.4	6.3	10.2
10.3	3.3	1.4	1.5	3	3.9	5.4	4.7	7.3	5.3	8.1
9.56	2.9	1.2	1.3	2.5	3.4	4.7	4	6.4	4.6	6.6
8.89	2.6	1.1	1.2	2.1	3	4.2	3.5	5.6	4.2	5.6
8.27	2.3	1	1.1	1.7	2.7	3.7	3.1	4.9	3.8	5
7.69	2	0.8	1	1.4	2.4	3.3	2.7	4.3	3.5	4.5
7.15	1.8	0.7	0.8	1.2	2.1	2.9	2.4	3.8	3.1	4.1
6.65	1.6	0.6	0.7	1	1.9	2.6	2.1	3.4	2.7	3.7
6.18	1.4	0.5	0.7	0.9	1.7	2.3	1.9	3.1	2.4	3.3
5.75	1.3	0.5	0.6	0.9	1.6	2.2	1.7	2.8	2.1	3
5.35	1.2	0.4	0.6	0.8	1.4	2	1.5	2.6	1.9	2.7
4.97	1.1	0.4	0.5	0.7	1.3	1.8	1.4	2.4	1.6	2.4
4.62	1	0.3	0.5	0.6	1.2	1.6	1.2	2.2	1.4	2
4.3	0.8	0.3	0.4	0.5	1	1.4	1	1.9	1.1	1.6
4	0.7	0.2	0.4	0.4	0.9	1.2	0.8	1.6	0.9	1.3
3.72	0.6	0.2	0.3	0.3	0.8	1	0.6	1.3	0.7	1
3.46	0.5	0.2	0.3	0.2	0.7	0.8	0.5	1	0.5	0.7
3.21	0.4	0.1	0.2	0.2	0.6	0.7	0.4	0.8	0.4	0.6
2.99	0.4	0.1	0.2	0.1	0.5	0.6	0.3	0.6	0.4	0.5
2.78	0.3	0.1	0.2	0.1	0.5	0.5	0.3	0.5	0.3	0.4
2.59	0.3	0.1	0.2	0.1	0.4	0.5	0.2	0.4	0.3	0.4
2.4	0.3	0.1	0.2	0.1	0.4	0.5	0.2	0.4	0.3	0.3
2.24	0.3	0.1	0.2	0.1	0.3	0.4	0.2	0.3	0.3	0.3
2.08	0.2	0.1	0.1	0.1	0.3	0.4	0.1	0.3	0.2	0.2
1.93	0.2	0.1	0.1	0.1	0.3	0.3	0.1	0.2	0.2	0.2

Experiment no.: 2 **Date: 16-11-94**

Concentration of particle in mixing tank: 8 g/L

Volume of water = 433.35 L

Temperature: 19.5°C **Starting time: 2.23 pm**

Inflow discharge: 0.08 L/s **Outflow: 0.13 L/s**

Height of turbidity current at station

	St. 0	St. 1	St. 2	St. 3	St. 4	St. 5	St. 6	St. 7
Height (cm)	4.0	3.0	3.0	3.0	3.2	3.5	4.2	5.0

Height of water in the flume: 500 mm **End time: 3.55 pm**

Inflow concentration at flume entrance: 5.96 g/L

Outflow concentration: 0.23 g/L

Sediment deposition at station (Sample area = 38.046 cm^2)

	St. 0 +20 cm	St. 1	St. 2	St. 3	St. 4	St. 5	St. 6	St. 7
Weight of particles (g)	21.28	11.09	5.55	3.2	2.23	1.48	1.06	0.72
Deposition per unit area (g)	0.5593	0.2915	0.1459	0.0841	0.0586	0.0389	0.0279	0.0189

Experiment No. 2: Particle Size Analysis										
High Size	Inflow	St. 0	St. 1	St. 2	St. 3	St. 4	St. 5	St. 6	St. 7	Outflow
(μm)	Under %	Under %	Under %	Under %	Under %	Under %	Under %	Under %	Under %	Under %
188	100	100	100	100	100	100	100	100	100	100
175	100	100	100	100	100	100	100	100	100	100
163	100	100	100	100	100	100	100	100	100	100
151	100	100	100	100	100	100	100	100	100	100
141	99.9	100	100	100	100	100	100	100	100	100
131	99.9	99.9	99.9	100	100	100	100	100	100	100
122	99.7	99.8	99.9	100	100	100	100	100	100	100
113	99.5	99.6	99.7	99.9	100	100	100	100	100	100
105	98.8	99.1	99.5	99.9	100	100	100	100	100	100
97.8	97.4	97.9	98.9	99.8	100	100	100	100	100	100
90.9	95.1	95.9	97.3	99.7	100	100	100	100	100	100
84.5	91.9	92.8	94.3	99.5	100	100	100	100	100	100
78.6	88.1	88.8	89.9	99.2	99.9	99.9	100	100	100	100
73.1	83.7	84.2	84.8	98.5	99.9	99.9	100	100	100	100
68	78.9	79	79.1	97.1	99.9	99.9	100	100	100	100
63.2	73.7	73.4	73	94.9	99.8	99.9	100	100	100	100
58.8	68.3	67.4	66.5	91.4	99.5	99.9	99.9	100	100	100
54.7	62.8	61.1	59.7	86.4	97.3	99.1	99.2	99.7	99.9	99.9
50.8	57.4	54.6	52.8	79.8	92.9	96.9	97.9	99.2	99.7	99.8
47.3	52	48.1	46	72	86.9	93.2	95.8	98.2	99.1	99.5
44	46.9	41.7	39.5	63.5	79.7	88.3	93	96.6	98.2	99.1
40.9	42.2	35.9	33.7	55	72.2	82.8	89.4	94.2	96.5	98.4
38	37.8	30.8	28.7	47.2	64.9	76.9	84.9	90.9	93.9	97.3
35.4	33.9	26.5	24.9	40.7	58.3	70.8	79.6	86.4	90.2	95.7
32.9	30.5	23.1	22	35.5	52.4	64.6	73.6	81	85.4	93.6
30.6	27.5	20.5	19.8	31.4	47.1	58.5	67.2	74.9	79.8	90.8
28.4	24.8	18.3	18	27.9	42.2	52.4	60.6	68.3	73.4	87.2
26.4	22.4	16.6	16.4	24.9	37.6	46.7	54.2	61.5	66.6	82.8
24.6	20.1	15.1	14.8	22.2	33.2	41.2	48.1	54.8	59.6	77.7
22.9	18	13.6	13.1	19.6	29	36.3	42.5	48.6	53.1	72.3
21.3	15.9	12.1	11.3	17.2	25.2	31.9	37.6	43.1	47.3	66.8
19.8	13.9	10.4	9.5	14.8	21.7	28	33.4	38.3	42.4	61.5
18.4	12	8.6	7.8	12.5	18.5	24.6	29.6	34.1	38.1	56.3
17.1	10.2	7.1	6.3	10.4	15.6	21.1	25.8	29.9	33.6	50.8
15.9	8.6	5.8	5.2	8.6	13	17.6	21.9	25.5	28.8	44.9
14.8	7.2	4.9	4.4	7.1	10.6	14.1	17.9	20.9	23.6	38.9
13.7	6	4.2	3.9	5.8	8.6	10.9	14.2	16.5	18.4	32.8
12.8	5.1	3.7	3.6	4.8	7	8.4	11	12.7	14.1	27.1
11.9	4.3	3.2	3.2	4	5.8	6.7	8.9	9.8	10.7	22.1
11.1	3.7	2.9	2.9	3.4	4.9	5.6	6.9	7.6	8.2	17.8
10.3	3.2	2.6	2.6	3	4.3	5	5.7	6.2	6.6	14.3
9.56	2.8	2.3	2.2	2.6	3.8	4.6	5	5.2	5.6	11.8
8.89	2.4	2	1.9	2.3	3.4	4.2	4.4	4.7	5	10.2
8.27	2.1	1.7	1.6	2	3	3.8	4	4.3	4.6	9.1
7.69	1.8	1.5	1.3	1.8	2.6	3.4	3.6	3.9	4.3	8.2
7.15	1.6	1.3	1.2	1.6	2.3	2.9	3.3	3.6	3.9	7.4
6.65	1.4	1.1	1	1.4	2	2.4	2.9	3.1	3.4	6.7
6.18	1.3	1	1	1.3	1.7	2	2.5	2.8	3	6
5.75	1.2	0.9	0.9	1.2	1.5	1.7	2.2	2.4	2.6	5.4
5.35	1.1	0.9	0.9	1	1.4	1.5	2	2.1	2.3	4.9
4.97	1	0.8	0.8	0.9	1.3	1.4	1.8	1.8	1.9	4.4
4.62	0.9	0.7	0.7	0.8	1.1	1.2	1.5	1.6	1.6	3.8
4.3	0.8	0.6	0.6	0.7	0.9	1	1.2	1.3	1.3	3.1
4	0.7	0.5	0.5	0.6	0.7	0.8	1	1	1	2.5
3.72	0.6	0.5	0.4	0.5	0.6	0.7	0.8	0.8	0.8	1.9
3.46	0.5	0.4	0.4	0.4	0.4	0.5	0.6	0.6	0.6	1.5
3.21	0.4	0.3	0.3	0.3	0.4	0.4	0.5	0.5	0.5	1.2
2.99	0.4	0.3	0.3	0.3	0.3	0.3	0.4	0.4	0.4	1
2.78	0.3	0.3	0.3	0.3	0.3	0.2	0.4	0.4	0.4	0.9
2.59	0.3	0.2	0.3	0.2	0.2	0.2	0.3	0.3	0.4	0.8
2.4	0.3	0.2	0.2	0.2	0.2	0.2	0.3	0.3	0.3	0.7
2.24	0.3	0.2	0.2	0.2	0.2	0.2	0.3	0.3	0.3	0.6
2.08	0.2	0.2	0.2	0.2	0.2	0.2	0.2	0.2	0.2	0.5
1.93	0.2	0.2	0.2	0.1	0.1	0.1	0.2	0.2	0.2	0.4

Experiment no.: 4 **Date: 18.11.94**

Concentration of particle in mixing tank: 10 g/L

Temperature: 19°C **Starting time: 10:36 am**

Inflow discharge: 0.175 L/s **Outflow: 0.322 L/s**

Height of turbidity current at station

	St. 0	St. 1	St. 2	St. 3	St. 4	St. 5	St. 6	St. 7
Height (cm)	4.0	4.0	4.2	4.5	4.5	4.5	5.0	5.0

Height of water in the flume: 50 cm **End time: 11:13 am**

Inflow concentration at flume entrance: 8.24 g/L

Outflow concentration: 0.65 g/L

Sediment deposition (Sample area = 38.046 cm^2)

	St. 0 +20 cm	St. 1	St. 2	St. 3	St. 4	St. 5	St. 6	St. 7
Weight of particles (g)	15.62	12.33	9.05	6.26	4.19	3.15	2.54	2.09
Deposition per unit area (g)	0.41055	0.32408	0.2379	0.16454	0.1101	0.0828	0.06676	0.05493

Experiment No. 4: Particle Size Analysis										
High Size	Inflow	St. 0	St. 1	St. 2	St. 3	St. 4	St. 5	St. 6	St. 7	Outflow
(μm)	Under %	Under %	Under %	Under %	Under %	Under %	Under %	Under %	Under %	Under %
188	100	100	100	100	100	100	100	100	100	100
175	100	99.7	100	100	100	100	100	100	100	100
163	100	99.2	100	100	100	100	100	99.9	100	100
151	100	98.6	99.9	100	100	100	100	99.9	100	100
141	99.9	97.6	99.8	100	100	100	100	99.9	100	100
131	99.8	96.3	99.5	99.9	100	100	100	99.9	100	100
122	99.7	94.5	98.9	99.8	99.9	100	100	99.9	100	100
113	99.4	92.1	97.6	99.6	99.8	99.9	100	99.9	100	100
105	98.6	89	95.3	99.1	99.8	99.9	99.9	99.9	100	100
97.8	97	85.2	91.5	97.9	99.7	99.9	99.8	99.9	100	100
90.9	94.5	80.5	86.5	95.4	99	99.5	99.5	99.9	100	100
84.5	91.3	74.8	81	91	96.8	98.6	99.1	99.9	100	100
78.6	87.4	68.2	75	85.1	93.3	97.1	98.3	99.9	99.9	100
73.1	83	61.2	68.3	78.4	89.1	94.9	97.1	99.9	99.8	100
68	78.2	53.9	61.2	71.4	84.2	92.1	95.3	99.9	99.8	100
63.2	73.1	46.8	54.2	64.2	78.7	88.4	92.6	98.8	99.8	100
58.8	67.8	40.2	47.6	57	72.5	83.5	88.8	96.6	98.9	99.9
54.7	62.5	34.6	41.6	50.3	65.6	77.3	83.7	92.5	95.9	99.5
50.8	57.4	30	36.5	44.3	58.3	69.8	77.2	86.4	90.6	98.5
47.3	52.4	26.5	32.3	38.9	50.7	61.3	69.6	78.9	83.6	97
44	47.6	23.8	28.9	34.2	43.3	52.5	61.3	70.7	75.7	94.7
40.9	43.1	21.5	25.9	30.1	36.6	44.1	53.2	62.4	67.6	91.8
38	38.9	19.3	23	26.4	31	36.8	45.7	54.6	59.9	88
35.4	35	16.9	20.3	23	26.8	31.2	39.5	48.1	53.3	83.2
32.9	31.5	14.4	17.5	20.1	23.9	27.2	34.4	42.7	47.8	77.7
30.6	28.3	12	15	17.5	21.8	24.3	30.3	38.2	43	71.7
28.4	25.4	9.9	12.8	15.3	20.1	22	27	34.4	38.7	65.6
26.4	22.8	8.4	11.1	13.4	18.5	19.9	24.1	30.9	34.6	59.5
24.6	20.5	7.3	9.7	11.8	16.7	17.9	21.6	27.6	30.6	53.8
22.9	18.3	6.5	8.6	10.5	14.8	15.8	19.2	24.5	26.7	48.4
21.3	16.3	6	7.7	9.2	12.7	13.6	17	21.5	23.1	43.6
19.8	14.3	5.5	6.9	8	10.6	11.4	14.7	18.5	19.7	39.3
18.4	12.4	5	6.1	6.9	8.6	9.3	12.4	15.7	16.6	35.3
17.1	10.7	4.5	5.4	6	6.9	7.4	10.4	13.2	13.9	31.4
15.9	9.1	3.9	4.7	5.2	5.7	6	8.6	11	11.6	27.5
14.8	7.7	3.3	4.1	4.5	5	4.9	7.2	9.2	9.7	23.5
13.7	6.5	2.7	3.4	4	4.6	4.2	6	7.8	8.2	19.6
12.8	5.5	2.3	2.9	3.5	4.2	3.6	5	6.6	6.9	16.1
11.9	4.6	1.9	2.5	3	3.9	3.1	4.3	5.7	5.8	13
11.1	3.9	1.6	2.1	2.7	3.5	2.7	3.7	4.9	4.9	10.5
10.3	3.3	1.4	1.9	2.3	3.1	2.3	3.2	4.3	4.2	8.5
9.56	2.9	1.3	1.7	2	2.7	2	2.8	3.8	3.7	7.1
8.89	2.5	1.2	1.5	1.7	2.3	1.7	2.5	3.4	3.3	6.2
8.27	2.2	1.1	1.3	1.5	1.9	1.5	2.2	3	2.9	5.6
7.69	1.9	1	1.2	1.3	1.6	1.3	2	2.6	2.5	5
7.15	1.7	0.9	1.1	1.2	1.4	1.1	1.8	2.3	2.2	4.6
6.65	1.5	0.8	1	1.1	1.3	1	1.6	2	1.9	4.1
6.18	1.4	0.7	0.9	1	1.2	0.9	1.4	1.8	1.7	3.7
5.75	1.3	0.6	0.8	1	1.1	0.8	1.3	1.6	1.5	3.4
5.35	1.2	0.6	0.7	0.9	1.1	0.8	1.1	1.5	1.4	3
4.97	1.1	0.5	0.7	0.9	1	0.7	1	1.4	1.3	2.7
4.62	1	0.5	0.6	0.8	0.9	0.6	0.9	1.2	1.1	2.4
4.3	0.8	0.4	0.5	0.7	0.8	0.6	0.8	1	1	2
4	0.7	0.4	0.5	0.6	0.7	0.5	0.7	0.9	0.8	1.6
3.72	0.6	0.3	0.4	0.5	0.6	0.4	0.6	0.7	0.6	1.3
3.46	0.5	0.3	0.4	0.4	0.5	0.3	0.5	0.6	0.5	1
3.21	0.4	0.3	0.3	0.3	0.5	0.3	0.4	0.5	0.4	0.9
2.99	0.3	0.2	0.3	0.3	0.4	0.3	0.3	0.4	0.3	0.7
2.78	0.3	0.2	0.3	0.3	0.4	0.2	0.3	0.3	0.3	0.6
2.59	0.3	0.2	0.3	0.3	0.4	0.2	0.3	0.3	0.3	0.6
2.4	0.3	0.2	0.2	0.3	0.3	0.2	0.2	0.3	0.3	0.5
2.24	0.2	0.2	0.2	0.2	0.3	0.2	0.2	0.3	0.2	0.4
2.08	0.2	0.1	0.2	0.2	0.3	0.2	0.2	0.2	0.2	0.4
1.93	0.2	0.1	0.2	0.2	0.2	0.1	0.2	0.2	0.2	0.3

Experiment no.: 6 **Date: 20.11.94**

Concentration of particle in mixing tank: 11.41 g/L

Temperature: 1`9.2 **Starting time: 1:54 pm**

Inflow discharge: 0.19 L/s **Outflow: 0.345 L/s**

Height of turbidity current at station

	St. 0	St. 1	St. 2	St. 3	St. 4	St. 5	St. 6	St. 7
Height (cm)	4.0	4.5	4.5	5.0	5.0	5.0	5.0	5.0

Height of water in the flume: 50 cm **End time: 2:35 pm**

Inflow concentration at flume entrance: 9.42 g/L

Outflow concentration: 0.91 g/L

Sediment deposition (Sample area = 38.046 cm^2)

	St. 0 +25cm	St. 1	St. 2	St. 3	St. 4	St. 5	St. 6	St. 7
Weight of particles (g)	20.32	16.23	11.36	7.73	5.31	4.05	3.03	2.45
Deposition per unit area (g)	0.5141	0.4266	0.29858	0.20317	0.13483	0.10645	0.07964	0.06439

Experiment No. 6: Particle Size Analysis										
High Size	Inflow	St. 0	St. 1	St. 2	St. 3	St. 4	St. 5	St. 6	St. 7	Outflow
(μm)	Under %	Under %	Under %	Under %	Under %	Under %	Under %	Under %	Under %	Under %
188	100	100	100	100	100	100	100	100	100	100
175	100	98.4	100	100	100	100	99.9	100	100	100
163	100	96.7	100	100	100	100	99.9	100	100	100
151	100	94.9	99.9	100	100	100	99.9	100	100	100
141	99.9	92.9	99.7	99.9	100	100	99.9	100	100	100
131	99.9	90.6	99.4	99.9	99.9	100	99.9	100	100	100
122	99.7	88	98.7	99.8	99.9	100	99.9	100	100	100
113	99.5	85	97.1	99.6	99.8	99.9	99.9	100	100	100
105	98.9	81.6	94.5	99	99.6	99.8	99.9	100	100	100
97.8	97.5	77.7	90.5	97.7	99.1	99.7	99.9	100	100	100
90.9	95.3	73.2	85.5	95.3	97.9	99.2	99.9	100	100	100
84.5	92.3	68	80.1	91.4	95.8	98.1	99.9	100	100	100
78.6	88.6	62.3	74.2	86.4	92.7	96.4	99.9	99.9	99.9	100
73.1	84.4	56.3	67.8	80.7	89.1	94.2	99.8	99.8	99.9	100
68	79.8	50.2	61	74.4	84.9	91.3	99.4	99.8	99.9	100
63.2	74.9	44.2	54.1	67.8	80	87.7	98	99.8	99.8	100
58.8	69.8	38.5	47.7	61	74.4	83.1	95	99	99.5	99.9
54.7	64.7	33.5	41.9	54.2	67.9	77.3	90.1	96	97.1	99.5
50.8	59.6	29.3	36.9	47.5	60.8	70.5	83.5	90.8	92.4	98.7
47.3	54.7	25.8	32.7	41.2	53.3	62.8	75.6	83.8	85.6	97.4
44	50	22.9	29.2	35.4	45.7	54.8	66.9	75.8	77.5	95.5
40.9	45.5	20.5	26.1	30.2	38.7	47.1	58.3	67.7	69.3	93
38	41.2	18.2	23.1	25.8	32.7	40.3	50.2	60	61.5	89.7
35.4	37.3	15.9	20.3	22.4	28	34.7	43.5	53.3	54.8	85.5
32.9	33.7	13.8	17.4	19.7	24.5	30.5	38	47.7	49.1	80.5
30.6	30.3	11.8	14.9	17.6	22	27.1	33.6	42.8	44.2	75
28.4	27.2	10	12.7	15.9	19.9	24.4	29.9	38.4	39.9	69.1
26.4	24.4	8.6	11	14.3	18.1	22.1	26.8	34.2	35.9	63.1
24.6	21.8	7.5	9.7	12.8	16.2	19.9	23.9	30.2	32	57.1
22.9	19.4	6.7	8.7	11.2	14.4	17.8	21.3	26.3	28.3	51.4
21.3	17.3	6	7.9	9.7	12.6	15.7	18.6	22.8	24.6	46.1
19.8	15.3	5.4	7.2	8.2	10.7	13.6	16	19.6	21	41.4
18.4	13.6	4.8	6.5	6.8	8.9	11.5	13.4	16.7	17.5	37.2
17.1	11.9	4.2	5.7	5.7	7.4	9.6	11	14.1	14.5	33.1
15.9	10.3	3.7	4.9	4.8	6.2	8	8.9	11.7	11.9	29
14.8	8.7	3.2	4.1	4.2	5.3	6.7	7.2	9.7	9.8	25
13.7	7.2	2.7	3.4	3.7	4.6	5.7	5.8	8	8.2	21.1
12.8	6	2.3	2.8	3.4	4	4.9	4.8	6.6	6.9	17.4
11.9	4.9	1.9	2.4	3	3.5	4.3	4	5.6	6	14.2
11.1	4.1	1.7	2.1	2.6	3	3.7	3.5	4.8	5.2	11.4
10.3	3.5	1.4	1.9	2.3	2.6	3.3	3.1	4.2	4.6	9.2
9.56	3	1.3	1.7	2	2.3	2.9	2.8	3.8	4.2	7.6
8.89	2.7	1.1	1.5	1.7	2	2.6	2.5	3.5	3.7	6.6
8.27	2.5	1	1.4	1.4	1.7	2.3	2.2	3.1	3.3	5.9
7.69	2.2	0.9	1.3	1.2	1.5	2	1.9	2.8	2.9	5.4
7.15	2	0.9	1.1	1.1	1.4	1.8	1.7	2.4	2.4	4.9
6.65	1.8	0.8	1	1	1.2	1.6	1.5	2	2.1	4.4
6.18	1.6	0.7	0.9	0.9	1.1	1.4	1.3	1.7	1.7	4
5.75	1.5	0.6	0.8	0.9	1	1.3	1.1	1.5	1.6	3.6
5.35	1.4	0.6	0.7	0.8	1	1.2	1	1.3	1.4	3.3
4.97	1.3	0.6	0.7	0.8	0.9	1.1	0.9	1.2	1.3	2.9
4.62	1.1	0.5	0.6	0.7	0.8	1	0.8	1.1	1.2	2.6
4.3	0.9	0.5	0.6	0.6	0.7	0.8	0.7	1	1.1	2.1
4	0.7	0.4	0.5	0.5	0.6	0.7	0.6	0.8	0.9	1.7
3.72	0.6	0.4	0.4	0.5	0.5	0.6	0.5	0.7	0.7	1.4
3.46	0.5	0.4	0.4	0.4	0.4	0.5	0.4	0.5	0.6	1.1
3.21	0.4	0.3	0.3	0.4	0.4	0.4	0.3	0.4	0.5	0.9
2.99	0.4	0.3	0.3	0.3	0.3	0.4	0.3	0.4	0.4	0.8
2.78	0.4	0.3	0.3	0.3	0.3	0.3	0.3	0.3	0.3	0.7
2.59	0.4	0.3	0.3	0.3	0.3	0.3	0.2	0.3	0.3	0.6
2.4	0.3	0.3	0.3	0.3	0.3	0.3	0.2	0.3	0.3	0.5
2.24	0.3	0.2	0.2	0.3	0.2	0.3	0.2	0.2	0.2	0.5
2.08	0.3	0.2	0.2	0.2	0.2	0.2	0.2	0.2	0.2	0.4
1.93	0.3	0.2	0.2	0.2	0.2	0.2	0.2	0.2	0.2	0.3

Experiment no.: 8 **Date: 1.12.94**

Concentration of particle in mixing tank: 8 g/L

Temperature: 20° C **Starting time: 11:42 am**

Inflow discharge: 0.275 L/s **Outflow:-**

Head velocity

	St. 0	St. 1	St. 2	St. 3	St. 4	St. 5	St. 6	St. 7
Time (s)		0	28		70		110	
Height (cm)			14		14		15	
Velocity (cm/s)		1.786		2.381		2.5		

Height of turbidity current at station

	St. 0	St. 1	St. 2	St. 3	St. 4	St. 5	St. 6	St. 7
Height (cm)			4.0		4.0		5.0	

Height of water in the flume: 48 cm **End time: 11:50 am**

Inflow concentration at flume entrance: 6.37 g/L

Outflow concentration: 1.11 g/L

Head Concentration

Height from bed (mm)	St. 2 Turbidity (NTU)	Volumetric Concentration	St. 4 Turbidity (NTU)	Volumetric Concentration	St. 6 Turbidity (NTU)	Volumetric Concentration
10	75	0.000373	137	0.000677	148	0.000731
20	125	0.000619				
30	65	0.000323	78	0.000388	80	0.000397
40						
50			42	0.000209	85	0.000422
60						
70			18	0.0000899	32	0.00016
Average				0.000439		0.000461

Experiment No. 8: Particle Size Analysis							
High Size	Inflow	St. 2 head	St. 2 Body	St. 4 head	St. 4 Body	St. 6 head	St. 6 Body
(μm)	Under %	Under %	Under %	Under %	Under %	Under %	Under %
188	100	100	100	100	100	100	100
175	100	100	100	100	100	100	100
163	100	100	100	100	100	100	100
151	100	100	100	100	100	100	100
141	100	100	100	100	100	100	100
131	100	100	100	100	100	100	100
122	99.9	100	100	100	100	100	100
113	99.9	100	100	100	100	100	100
105	99.7	100	100	100	100	100	100
97.8	99.5	100	100	100	100	100	100
90.9	98.7	99.9	100	100	100	100	100
84.5	96.9	99.7	100	100	100	100	100
78.6	94.3	99.2	100	100	100	99.9	100
73.1	91.3	98.4	99.9	99.9	99.9	99.9	100
68	87.8	97.1	99.7	99.7	99.9	99.7	100
63.2	83.9	95.1	98.7	98.8	99.9	98.8	100
58.8	79.6	92.3	96.9	97.1	99.5	96.6	99.9
54.7	75	88.5	93.9	94.2	98	93.7	99.4
50.8	70.2	83.6	89.8	90.1	95.3	89.2	98.1
47.3	65.1	77.8	84.8	85.3	91.7	83.8	95.7
44	60	71.5	79.2	79.7	87.2	77.8	92.4
40.9	55	65.1	73.3	73.8	82.1	71.5	88.3
38	50.2	59.2	67.4	67.9	76.5	65.4	83.4
35.4	45.7	53.9	61.9	62.2	70.6	59.8	77.8
32.9	41.7	49.4	56.8	56.9	64.5	54.7	71.6
30.6	38	45.5	52.2	52	58.8	50.2	65.3
28.4	34.7	41.9	47.9	47.5	53.5	46	59.4
26.4	31.8	38.5	44.1	43.5	48.9	42.1	54.2
24.6	29.1	35.3	40.5	40	45.1	38.5	49.7
22.9	26.5	32.1	37.1	36.6	41.6	35	45.8
21.3	24	28.8	33.8	33.4	38.2	31.6	42.2
19.8	21.5	25.5	30.5	30.2	34.8	28.3	38.9
18.4	18.9	22.3	27.2	26.9	31.2	25	35.5
17.1	16.5	19.1	23.7	23.5	27.4	21.8	31.7
15.9	14.1	16.2	20.3	20.1	23.4	18.6	27.3
14.8	12	13.6	17	16.8	19.4	15.6	22.7
13.7	10.1	11.3	14	13.7	15.7	12.8	18.1
12.8	8.5	9.3	11.4	11.2	12.6	10.4	14.3
11.9	7.2	7.8	9.5	9.2	10.3	8.9	11.5
11.1	6.2	6.5	8	7.7	8.9	7.2	9.6
10.3	5.4	5.5	6.9	6.7	7.4	6.1	8.3
9.56	4.8	4.7	6.1	5.9	6.6	5.3	7.4
8.89	4.2	4.1	5.4	5.3	5.9	4.7	6.8
8.27	3.7	3.6	4.8	4.7	5.2	4.2	6.3
7.69	3.2	3.1	4.2	4.2	4.6	3.7	5.7
7.15	2.8	2.7	3.7	3.7	4	3.2	4.9
6.65	2.4	2.3	3.1	3.1	3.4	2.7	4.1
6.18	2.1	2	2.7	2.7	2.9	2.3	3.3
5.75	1.9	1.8	2.3	2.3	2.5	2	2.8
5.35	1.7	1.6	2.1	2.1	2.3	1.8	2.5
4.97	1.6	1.5	1.9	1.8	2	1.6	2.2
4.62	1.5	1.3	1.7	1.6	1.8	1.4	2
4.3	1.3	1.1	1.5	1.4	1.6	1.2	1.7
4	1.1	0.9	1.2	1.2	1.3	1	1.4
3.72	0.9	0.7	1	1	1	0.8	1.2
3.46	0.7	0.6	0.8	0.8	0.8	0.7	1
3.21	0.6	0.5	0.6	0.7	0.6	0.5	0.8
2.99	0.5	0.4	0.5	0.5	0.5	0.4	0.6
2.78	0.5	0.3	0.4	0.5	0.4	0.4	0.5
2.59	0.4	0.3	0.4	0.4	0.4	0.3	0.5
2.4	0.4	0.3	0.3	0.4	0.3	0.3	0.4
2.24	0.3	0.2	0.3	0.3	0.3	0.3	0.4
2.08	0.3	0.2	0.3	0.3	0.2	0.2	0.3
1.93	0.2	0.2	0.2	0.2	0.2	0.2	0.3

Experiment no.: 9 **Date: 1.12.94**

Concentration of particle in mixing tank: 8 g/L

Temperature: 21° C **Starting time: 12.33 pm**

Inflow discharge: 0.15 L/s **Outflow:**

Head velocity

	St. 0	St. 1	St. 2	St. 3	St. 4	St. 5	St. 6	St. 7
Time (s)		0	32	63	95	134	160	196
Height (cm)		10	11	11	11	11	11.5	11.5
Velocity (cm/s)			1.58		1.41		1.61	

Height of turbidity current at station (not collected)

	St. 0	St. 1	St. 2	St. 3	St. 4	St. 5	St. 6	St. 7
Height (cm)								

Height of water in the flume: 48 cm **End time:-**

Inflow concentration at flume entrance: 4.95 g/L

Outflow concentration: 0.53 g/L

Head Concentration

Height from bed (mm)	St. 2 Turbidity (NTU)	Volumetric Concentration	St. 4 Turbidity (NTU)	Volumetric Concentration	St. 6 Turbidity (NTU)	Volumetric Concentration
10	55	0.000274	65	0.000323	55	0.000274
20						
30	44	0.000219	41	0.000204	40	0.000199
40						
50	12	5.99E-05	17	8-49E-05	12	5.99E-05
60						
70	10	5E-05	6	3E-05	3	1.5E-05
80						
90					2	1E-05
Average		0.000203		0.000232		0.000211

Experiment No. 9: Particle Size Analysis							
High Size	Inflow	St. 2 head	St. 2 Body	St. 4 head	St. 4 Body	St. 6 head	St. 6 Body
(μm)	Under %	Under %	Under %	Under %	Under %	Under %	Under %
188	100	100	100	100	100	100	100
175	100	99.9	100	100	100	100	100
163	100	99.8	100	100	100	100	100
151	100	99.8	100	100	100	100	100
141	99.9	99.7	100	100	100	100	100
131	99.8	99.7	100	100	100	100	100
122	99.6	99.7	100	100	100	100	100
113	99.3	99.7	100	100	100	100	100
105	98.5	99.7	100	100	100	100	100
97.8	96.8	99.7	100	100	100	100	100
90.9	94.4	99.7	100	100	100	100	100
84.5	91.4	99.7	100	100	100	100	100
78.6	87.9	99.7	100	100	100	100	100
73.1	83.9	99.7	100	99.9	100	99.9	100
68	79.6	99.6	100	99.9	100	99.9	100
63.2	75	99	100	99.9	100	99.9	100
58.8	70.4	97.9	99.9	99.4	100	99.7	100
54.7	65.7	96	99.4	97.9	100	98.7	100
50.8	61.1	93.4	98	95.2	99.7	96.9	100
47.3	56.7	90.1	95.6	91.6	99.1	94.2	99.7
44	52.4	86.1	92.3	87.2	97.8	90.7	98.8
40.9	48.2	81.4	88.2	82.2	95.3	86.6	96.8
38	44.1	76.1	83.6	76.7	91.4	81.8	93.5
35.4	40.1	70.3	78.3	70.9	85.8	76.4	88.6
32.9	36.2	64.1	72.6	65	79	70.6	82.4
30.6	32.5	58.1	66.8	59.3	71.7	64.9	75.7
28.4	29.3	52.6	61.2	54.1	64.9	59.4	69
26.4	26.5	47.8	56.1	49.4	59.1	54.6	63.1
24.6	24.1	43.9	51.5	45.4	54.5	50.3	58
22.9	21.9	40.4	47.4	41.7	50.5	46.4	53.6
21.3	19.8	37.3	43.7	38.3	47	42.8	49.7
19.8	17.8	34.4	40.3	34.9	43.6	39.2	46.2
18.4	15.8	31.3	37	31.5	40	35.5	42.6
17.1	13.8	28	33.3	27.8	35.7	31.4	38.4
15.9	11.9	24.3	29	23.9	30.8	26.8	33.4
14.8	10.1	20.3	24.4	19.9	25.4	22.1	27.8
13.7	8.4	16.6	19.8	16.1	20	17.6	22.1
12.8	6.9	13.5	15.8	12.9	15.5	14	17.2
11.9	5.7	11.4	12.8	10.5	12.2	11.3	13.5
11.1	4.8	9.9	10.6	8.8	9.8	9.5	10.8
10.3	4	9	9.1	7.5	8.3	8.3	9
9.56	3.5	8.3	8.2	6.7	7.4	7.5	8
8.89	3	7.6	7.5	6	6.8	6.9	7.4
8.27	2.7	7	7	5.4	6.3	6.3	7
7.69	2.4	6.2	6.3	4.9	5.7	5.6	6.5
7.15	2.1	5.4	5.5	4.2	5	4.8	5.7
6.65	1.9	4.6	4.6	3.6	4.2	3.9	4.8
6.18	1.6	3.9	3.8	3	3.5	3.2	3.9
5.75	1.5	3.4	3.2	2.6	2.9	2.7	3.2
5.35	1.4	3.1	2.8	2.3	2.5	2.4	2.7
4.97	1.2	2.8	2.5	2.1	2.2	2.2	2.2
4.62	1.1	2.6	2.2	1.8	1.9	2	1.9
4.3	1	2.2	1.9	1.6	1.6	1.7	1.6
4	0.8	1.9	1.6	1.3	1.3	1.4	1.3
3.72	0.7	1.6	1.4	1.1	1.1	1.2	1.2
3.46	0.6	1.2	1.1	0.9	0.9	0.9	1
3.21	0.5	0.9	0.9	0.7	0.7	0.7	0.9
2.99	0.5	0.6	0.7	0.5	0.6	0.6	0.8
2.78	0.4	0.5	0.6	0.4	0.5	0.5	0.7
2.59	0.4	0.4	0.5	0.4	0.5	0.4	0.7
2.4	0.3	0.3	0.5	0.3	0.4	0.4	0.6
2.24	0.3	0.3	0.4	0.3	0.4	0.3	0.5
2.08	0.3	0.2	0.4	0.3	0.3	0.3	0.5
1.93	0.2	0.2	0.3	0.2	0.3	0.2	0.4

Experiment no.: 10 **Date: 1.12.94**

Concentration of particle in mixing tank: 8 g/L

Temperature: 21° C **Starting time: 5:45 pm**

Inflow discharge: 0.095 L/s **Outflow:**

Head velocity

	St. 0	St. 1	St. 2	St. 3	St. 4	St. 5	St. 6	St. 7
Time (s)		0	43	83	120	158	203	255
Height (cm)		9	10	10	10	9	9	9.5
Velocity (cm/s)			1.20		1.333		1.03	

Height of turbidity current at station (not collected)

	St. 0	St. 1	St. 2	St. 3	St. 4	St. 5	St. 6	St. 7
Height (cm)								

Height of water in the flume: 48 cm **End time: 5:55 pm**

Inflow concentration at flume entrance: 4.13 g/L

Outflow concentration: 0.3 g/L

Head Concentration

Height from bed (mm)	St. 2 Turbidity (NTU)	Volumetric Concentration	St. 4 Turbidity (NTU)	Volumetric Concentration	St. 6 Turbidity (NTU)	Volumetric Concentration
10	32	0.00016	43	0.000214	27	0.000135
20						
30	34	0.00017	23	0.000115	16	7.99E-05
40						
50	8	4E-05	6	3E-05	7	3.5E-05
60						
70	3	1.5E.05	4	2E-05	2	1E-05
80						
90	2	1E-05	1	5E-06	1	5E-06
Average		0.000143		0.000157		0.000098

Experiment No. 10: Particle Size Analysis							
High Size	Inflow	St. 2 head	St. 2 Body	St. 4 head	St. 4 Body	St. 6 head	St. 6 Body
(μm)	Under %	Under %	Under %	Under %	Under %	Under %	Under %
188	100	100	100	100	100	100	100
175	100	100	100	100	100	100	100
163	100	100	100	100	100	100	100
151	100	100	100	100	100	100	100
141	100	100	100	100	100	100	100
131	99.9	100	100	100	100	100	100
122	99.9	100	100	100	100	100	100
113	99.8	100	100	100	100	100	100
105	99.5	100	100	100	100	100	100
97.8	98.9	100	100	100	100	100	100
90.9	97.6	100	100	100	100	100	100
84.5	95.1	100	100	100	100	100	100
78.6	91.7	100	100	100	100	100	100
73.1	87.8	99.9	100	100	100	100	100
68	83.5	99.8	100	100	100	100	100
63.2	78.8	99.5	100	100	100	100	100
58.8	73.9	98.6	100	100	100	100	100
54.7	68.9	96.3	99.8	99.7	100	100	100
50.8	63.7	92.8	99.2	99.1	99.9	99.7	99.9
47.3	58.6	88.3	98	97.7	99.9	99.2	99.8
44	53.6	83	95.9	95.6	99.9	98.1	99.4
40.9	48.7	77.3	93.1	92.6	99.5	96.2	98.5
38	44	71.4	89.2	88.7	98.2	93.4	97
35.4	39.6	65.6	84.3	83.6	95.8	89.5	94.8
32.9	35.5	60	78.5	77.6	92.2	84.6	91.7
30.6	31.9	54.8	72.3	71.4	87.8	79.2	87.9
28.4	28.8	50.1	66.4	65.4	82.8	73.7	83.4
26.4	26.1	45.9	61	60	77.4	68.4	78.4
24.6	23.9	42.2	56.3	55.2	71.7	63.4	72.9
22.9	21.8	38.7	52.1	51.1	66	58.9	67.3
21.3	19.8	35.4	48.4	47.5	60.6	54.6	61.8
19.8	17.8	32	45	44.2	55.5	50.6	56.6
18.4	15.6	28.5	41.5	40.7	50.6	46.6	51.5
17.1	13.5	24.9	37.4	36.7	45.6	42.1	46.4
15.9	11.4	21.1	32.7	31.8	40.4	37	41.1
14.8	9.5	17.4	27.4	26.5	35.1	31.4	35.8
13.7	7.9	14	22.2	21.1	29.9	25.8	30.4
12.8	6.5	11.2	17.7	16.6	24.9	20.7	25.3
11.9	5.5	9	14.1	13.1	20.3	16.5	20.7
11.1	4.7	7.5	11.5	10.7	16.4	13.1	16.8
10.3	4.1	6.4	9.8	9.1	13.3	10.7	13.5
9.56	3.6	5.6	8.7	8.1	11	9	11.2
8.89	3.1	5	7.9	7.5	9.4	8	9.5
8.27	2.8	4.5	7.4	7	8.2	7.3	8.4
7.69	2.4	3.9	6.7	6.3	7.3	6.6	7.5
7.15	2.1	3.4	5.9	5.5	6.5	5.9	6.6
6.65	1.8	2.8	5	4.6	5.8	5.1	5.8
6.18	1.5	2.4	4.1	3.8	5.1	4.4	5.1
5.75	1.4	2	3.5	3.1	4.6	3.8	4.6
5.35	1.3	1.8	3	2.7	4.1	3.3	4.1
4.97	1.1	1.6	2.6	2.3	3.7	2.9	3.7
4.62	1	1.4	2.3	2	3.2	2.6	0.2
4.3	0.9	1.2	2	1.8	2.7	2.2	2.7
4	0.8	1	1.7	1.5	2.2	1.8	2.2
3.72	0.6	0.9	1.4	1.3	1.8	1.5	1.8
3.46	0.5	0.7	1.2	1.1	1.4	1.2	1.4
3.21	0.4	0.6	1	0.9	1.1	1	1.2
2.99	0.4	0.5	0.8	0.7	0.9	0.8	0.9
2.78	0.3	0.4	0.7	0.6	0.8	0.7	0.8
2.59	0.3	0.4	0.6	0.5	0.7	0.6	0.7
2.4	0.2	0.3	0.5	0.4	0.6	0.6	0.6
2.24	0.2	0.3	0.5	0.4	0.5	0.5	0.5
2.08	0.2	0.2	0.4	0.3	0.4	0.4	0.4
1.93	0.2	0.2	0.3	0.3	0.4	0.4	0.4

Experiment no.: 11 **Date: 1.12.94**

Concentration of particle in mixing tank: 8 g/L

Temperature: 21° C **Starting time: 6:30 pm**

Inflow discharge: 0.185 L/s **Outflow:**

Head velocity

	St. 0	St. 1	St. 2	St. 3	St. 4	St. 5	St. 6	St. 7
Time (s)		0	31	60	85	112	149	174
Height (cm)	4	11.5	11	11	11	11.5	11.5	11.5
Velocity (cm/s)		1.667		1.923		1.613		

Height of turbidity current at station

	St. 0	St. 1	St. 2	St. 3	St. 4	St. 5	St. 6	St. 7
Height (cm)	4.0	7.0	7.0	7.0	7.0	7.0	7.0	7.0

Height of water in the flume: 48 cm **End time: 6:45 pm**

Inflow concentration at flume entrance: 5.14 g/L

Outflow concentration: 0.64 g/L

Head Concentration

Height from bed (mm)	St. 2 Turbidity (NTU)	Volumetric Concentration	St. 4 Turbidity (NTU)	Volumetric Concentration	St. 6 Turbidity (NTU)	Volumetric Concentration
10	100	0.000496	120	0.000594	81	0.000402
20						
30	63	0.000313	40	0.000199	61	0.000304
40						
50	20	9.98E-05	20	0.00013	20	9.98E-05
60						
70	12	5.99E-05	12	5.99E-05	10	5E-05
80						
90	7	3.5E-05	10	5E-05	8	4E-05
Average		0.000357		0.000394		0.000294

Experiment No. 11: Particle Size Analysis							
High Size	Inflow	St. 2 head	St. 2 Body	St. 4 head	St. 4 Body	St. 6 head	St. 6 Body
(μm)	Under %	Under %	Under %	Under %	Under %	Under %	Under %
188	100	100	100	100	100	100	100
175	100	100	100	100	100	100	100
163	100	100	100	100	100	100	100
151	100	100	100	100	100	100	100
141	99.9	100	100	100	100	100	100
131	99.9	100	100	100	100	100	100
122	99.7	100	100	100	100	100	100
113	99.5	100	100	100	100	100	100
105	98.9	100	100	100	100	100	100
97.8	97.6	100	100	100	100	100	100
90.9	95.7	99.9	100	100	100	100	100
84.5	93.2	99.5	100	100	100	100	100
78.6	90.1	98.9	99.9	100	100	100	100
73.1	86.6	97.8	99.9	99.9	100	99.9	100
68	82.7	96.3	99.9	99.8	100	99.9	100
63.2	78.6	94.1	99.9	99.4	100	99.9	100
58.8	74.2	91.1	99.8	98.2	99.9	99.7	100
54.7	69.7	87.2	98.8	96	99.6	98.9	99.9
50.8	65.1	82.2	96.4	92.7	98.9	97.2	99.9
47.3	60.6	76.3	92.8	88.5	97.7	94.8	99.9
44	56	69.9	88.2	83.6	95.7	91.7	99.4
40.9	51.6	63.5	83	78.3	92.9	87.8	97.6
38	47.3	57.4	77.6	72.7	88.9	83.1	94.2
35.4	43.1	51.9	71.9	67	83.7	77.7	89.5
32.9	39.1	47.1	66.3	61.6	77.6	71.7	83.7
30.6	35.4	43	60.9	56.4	71.1	65.7	77.3
28.4	32.1	39.3	55.9	51.6	64.9	60	70.8
26.4	29.2	36.1	51.4	47.4	59.4	54.9	64.7
24.6	26.7	33.2	47.4	43.6	54.6	50.5	59.3
22.9	24.4	30.3	43.7	40.2	50.6	46.7	54.5
21.3	22.2	27.4	40.1	36.9	47	43.2	50.3
19.8	20	24.3	36.4	33.6	43.7	39.8	46.6
18.4	17.8	21.2	32.6	30.2	40.4	36.5	43
17.1	15.6	18.1	28.6	26.6	36.5	32.6	38.9
15.9	13.5	15.2	24.4	22.8	31.9	28.3	34.2
14.8	11.4	12.6	20.2	18.9	26.8	23.7	29
13.7	9.5	10.3	16.3	15.3	21.7	19.1	23.7
12.8	7.8	8.5	13	12.3	17.3	15.2	19
11.9	6.5	7.1	10.6	10.1	13.9	12.3	15.1
11.1	5.4	6.1	8.8	8.5	11.4	10.2	12.2
10.3	4.6	5.3	7.6	7.4	9.7	8.7	10.1
9.56	4	4.6	6.8	6.5	8.6	7.7	8.7
8.89	3.6	4.1	6.1	5.9	7.8	7	7.8
8.27	3.2	3.5	5.5	5.3	7.2	6.4	7.1
7.69	2.9	3.1	4.6	4.7	6.5	5.7	6.5
7.15	2.5	2.6	4.2	4.1	5.8	5	5.9
6.65	2.2	2.2	3.4	3.5	4.9	4.3	5.1
6.18	1.9	1.9	2.8	2.9	4.2	3.7	4.4
5.75	1.7	1.7	2.4	2.5	3.6	3.2	3.9
5.35	1.5	1.5	2.1	2.3	3.2	2.8	3.4
4.97	1.4	1.4	1.9	2	2.8	2.5	3
4.62	1.3	1.2	1.8	1.8	2.5	2.2	2.6
4.3	1.1	1.1	1.5	1.6	2.1	1.9	2.2
4	1	0.9	1.3	1.4	1.8	1.6	1.8
3.72	0.8	0.8	1.1	1.1	1.5	1.4	1.5
3.46	0.7	0.6	0.9	0.9	1.2	1.1	1.2
3.21	0.7	0.5	0.7	0.8	1	0.9	1
2.99	0.6	0.4	0.5	0.6	0.9	0.8	0.9
2.78	0.5	0.3	0.5	0.6	0.7	0.7	0.7
2.59	0.5	0.3	0.4	0.5	0.6	0.6	0.7
2.4	0.5	0.3	0.4	0.4	0.6	0.6	0.6
2.24	0.4	0.2	0.3	0.4	0.5	0.5	0.5
2.08	0.4	0.2	0.3	0.3	0.4	0.4	0.4
1.93	0.3	0.2	0.2	0.3	0.4	0.4	0.4

Experiment no.: 12 **Date: 2.12.94**

Concentration of particle in mixing tank: 4 g/L

Temperature: 19° C **Starting time: 9:55 am**

Inflow discharge: 0.175 L/s **Outflow:**

Head velocity

	St. 0	St. 1	St. 2	St. 3	St. 4	St. 5	St. 6	St. 7
Time (s)		0	37	85	120	160	205	250
Height (cm)			16	16	16	16	16	16
Velocity (cm/s)		1.176		1.333		1.111		

Height of turbidity current at station

	St. 0	St. 1	St. 2	St. 3	St. 4	St. 5	St. 6	St. 7
Height (cm)		8.0	8.0	8.0	8.0	8.0	8.0	8.0

Height of water in the flume: 48 cm **End time: 10:07 am**

Inflow concentration at flume entrance: 3.85 g/L

Outflow concentration: 0.43 g/L

Head Concentration

Height from bed (mm)	St. 2 Turbidity (NTU)	Volumetric Concentration	St. 4 Turbidity (NTU)	Volumetric Concentration	St. 6 Turbidity (NTU)	Volumetric Concentration
10	26	0.00013	44	0.000219	55	0.000274
20						
30	54	0.000294	61	0.000304	41	0.000204
40						
50	20	9.98E-05	21	0.000105	31	0.000155
60						
70	10	5E-05	11	5.5E-05	23	0.000115
80						
90			9	4-5E-05	11	5.5E-05
Average		0.000176		0.0002		0.000181

Experiment No. 12: Particle Size Analysis							
High Size	Inflow	St. 2 head	St. 2 Body	St. 4 head	St. 4 Body	St. 6 head	St. 6 Body
(μm)	Under %	Under %	Under %	Under %	Under %	Under %	Under %
188	100	100	100	100	100	100	100
175	98.7	100	100	100	100	100	100
163	97.4	100	100	100	100	100	100
151	96	100	100	100	100	100	100
141	94.4	100	100	100	100	100	100
131	92.7	99.9	100	100	100	100	100
122	90.6	99.9	100	100	100	100	100
113	88.3	99.8	100	100	100	100	100
105	85.5	99.4	100	100	100	99.9	100
97.8	82.4	98.7	100	100	100	99.8	100
90.9	78.8	97.4	100	99.9	100	99.5	100
84.5	74.7	95.6	100	99.8	100	99	100
78.6	70.1	93.3	99.9	99.6	100	98.3	100
73.1	65.2	90.5	99.9	99.1	100	97.4	100
68	60.2	87.4	99.8	98.2	100	96.1	99.9
63.2	55.1	83.8	99.3	96.8	100	94.5	99.9
58.8	50.2	79.8	97.9	94.8	99.9	92.2	99.6
54.7	45.7	75.4	95.2	91.9	99.4	89.4	99
50.8	41.6	70.6	91.1	88.2	98.2	85.9	98.1
47.3	38	65.5	86.1	83.7	96.1	81.9	96.7
44	34.7	60.2	80.5	78.4	93.2	77.2	94.8
40.9	31.6	55	74.6	72.8	89.3	72.2	92
38	28.7	49.9	68.9	67	84.5	66.9	88.3
35.4	25.8	45	63.6	61.2	78.5	61.4	83.6
32.9	22.9	40.6	58.8	55.6	71.9	56	78
30.6	20.3	36.6	54.4	50.3	65.1	50.8	71.9
28.4	17.9	33.1	50.3	45.7	58.8	46	65.7
26.4	16	30.1	46.3	41.7	53.3	41.8	59.6
24.6	14.4	27.6	42.5	38.4	48.9	38.2	53.9
22.9	13.1	25.3	38.9	35.5	45.1	34.9	48.6
21.3	11.9	23.1	35.3	32.6	41.7	31.7	43.7
19.8	10.8	20.8	31.7	29.8	38.5	28.7	39.2
18.4	9.6	18.4	28.2	26.7	35.2	25.6	35
17.1	8.4	16	24.7	23.4	31.4	22.4	31
15.9	7.3	13.5	21.2	19.8	27	19.2	27.1
14.8	6.2	11.1	17.7	16.2	22.3	16.1	23.3
13.7	5.1	9	14.5	12.8	17.6	13.2	19.7
12.8	4.2	7.2	11.9	10	13.7	10.7	16.3
11.9	3.5	5.9	9.8	8	10.9	8.8	13.3
11.1	2.9	5	8.3	6.7	8.9	7.3	10.6
10.3	2.5	4.4	7.2	5.9	7.6	6.1	8.5
9.56	2.2	3.9	6.4	5.2	6.7	5.3	6.9
8.89	1.9	3.5	5.7	4.7	6.1	4.6	5.8
8.27	1.8	3.1	5.1	4.2	5.5	4	4.9
7.69	1.6	2.7	4.5	3.7	5	3.5	4.3
7.15	1.4	2.4	3.9	3.2	4.4	3.1	3.8
6.65	1.2	2	3.2	2.7	3.8	2.7	3.3
6.18	1.1	1.7	2.7	2.3	3.2	2.4	2.9
5.75	0.9	1.5	2.3	2	2.7	2.1	2.6
5.35	0.9	1.3	2.1	1.8	2.4	1.9	2.3
4.97	0.8	1.2	1.9	1.6	2.1	1.7	2.1
4.62	0.7	1.1	1.7	1.4	1.8	1.5	1.8
4.3	0.6	0.9	1.5	1.2	1.6	1.3	1.6
4	0.5	0.8	1.3	1	1.3	1.1	1.4
3.72	0.5	0.7	1	0.9	1.1	0.9	1.1
3.46	0.4	0.5	0.8	0.7	0.9	0.8	0.9
3.21	0.4	0.5	0.7	0.6	0.7	0.6	0.8
2.99	0.3	0.4	0.5	0.5	0.6	0.5	0.7
2.78	0.3	0.3	0.5	0.4	0.5	0.5	0.6
2.59	0.3	0.3	0.4	0.4	0.5	0.4	0.5
2.4	0.2	0.3	0.4	0.3	0.4	0.4	0.4
2.24	0.2	0.2	0.3	0.3	0.4	0.3	0.4
2.08	0.2	0.2	0.3	0.3	0.3	0.3	0.3
1.93	0.2	0.2	0.2	0.2	0.3	0.2	0.3

Experiment no.: 13 **Date: 2.12.94**

Concentration of particle in mixing tank: 4 g/L

Temperature: 21° C **Starting time: 10:54**

Inflow discharge: 0.228 L/s **Outflow:**

Head velocity

	St. 0	St. 1	St. 2	St. 3	St. 4	St. 5	St. 6	St. 7
Time (s)		0	35	65	93	124	155	190
Height (cm)	4	15	14.5	15	15	15	15	16
Velocity (cm/s)			1.538		1.695		1.515	

Height of turbidity current at station

	St. 0	St. 1	St. 2	St. 3	St. 4	St. 5	St. 6	St. 7
Height (cm)	4.0	6.0	6.0	6.0	6.0	6.0	6.0	6.0

Height of water in the flume: 48 cm **End time:-**

Inflow concentration at flume entrance: 3.67 g/L

Outflow concentration: 0.5 g/L

Head Concentration

Height from bed (mm)	St. 2 Turbidity (NTU)	Volumetric Concentration	St. 4 Turbidity (NTU)	Volumetric Concentration	St. 6 Turbidity (NTU)	Volumetric Concentration
10	31	0.000155	58	0.000289	45	0.000224
20						
30	41	0.000204	41	0.000204	50	0.000249
40						
50	15	7.49E-05	15	7.49E-05	20	9.98E-05
60						
70					11	5.5E-05
Average		0.00013		0.000188		0.000178

Experiment No. 13: Particle Size Analysis							
High Size	Inflow	St. 2 head	St. 2 Body	St. 4 head	St. 4 Body	St. 6 head	St. 6 Body
(μm)	Under %	Under %	Under %	Under %	Under %	Under %	Under %
188	100	100	100	100	100	100	100
175	100	100	100	100	100	100	100
163	100	100	100	100	100	100	100
151	100	100	100	100	100	100	100
141	99.9	100	100	100	100	100	100
131	99.8	100	100	100	100	100	100
122	99.6	100	100	100	100	100	100
113	99.1	100	100	100	100	100	100
105	98.2	99.9	100	100	100	100	100
97.8	96.5	99.9	100	100	100	100	100
90.9	94.1	99.7	100	99.9	100	100	100
84.5	91.3	98.7	100	99.6	100	100	100
78.6	88.1	97.4	99.9	99.1	100	99.9	100
73.1	84.5	95.4	99.9	98.3	99.9	99.7	100
68	80.4	93	99.8	97.1	99.9	99	100
63.2	76.1	90	99.6	95.3	99.9	97.9	100
58.8	71.5	86.4	98.7	92.8	99.7	96	100
54.7	66.9	82.2	96.3	89.5	98.7	93.3	99.7
50.8	62.2	77.3	92.6	85.3	96.7	89.6	99
47.3	57.5	71	87.7	80.3	93.7	85	97.8
44	52.8	66	82.2	74.7	89.8	79.8	95.7
40.9	48.4	60.2	76.2	68.8	85.2	74.2	92.7
38	44.1	54.5	70.2	62.9	80	68.5	88.3
35.4	40.1	49.3	64.4	57.2	74.1	62.8	82.6
32.9	36.3	44.6	58.9	51.9	67.9	57.4	75.8
30.6	32.9	40.4	53.9	47	61.7	52.3	68.8
28.4	29.8	36.6	49.3	42.7	56	47.7	62.2
26.4	27.1	33.3	45.1	38.9	51	43.6	56.5
24.6	24.6	30.4	41.1	35.6	46.8	39.9	51.9
22.9	22.3	27.6	37.9	32.5	43	36.5	48
21.3	20.1	24.8	34.6	29.5	39.6	33.3	44.5
19.8	18	22.1	31.3	26.5	36.3	30.1	41.3
18.4	15.9	19.3	28	23.3	33	26.8	37.9
17.1	13.9	16.5	24.5	20.2	29.2	23.4	33.9
15.9	12	13.7	20.9	17	25.1	19.9	29.2
14.8	10.2	11.2	17.2	13.9	20.8	16.5	24.2
13.7	8.6	8.9	13.7	11.1	16.6	13.3	19.1
12.8	7.2	7	10.9	8.9	13	10.8	14.9
11.9	6	5.6	8.7	7.2	10.4	8.8	11.8
11.1	5	4.7	7.3	6	8.5	7.4	9.6
10.3	4.2	4	6.2	5.1	7.2	6.4	8.1
9.56	3.6	3.4	5.5	4.5	6.3	5.7	7.2
8.89	3.2	3	4.9	4	5.7	5.1	6.5
8.27	2.8	2.6	4.4	3.5	5.1	4.5	5.9
7.69	2.5	2.3	3.9	3.1	4.6	4	5.4
7.15	2.2	2	3.4	2.7	4.1	3.5	4.7
6.65	1.9	1.7	2.9	2.3	3.5	2.9	4
6.18	1.7	1.4	2.4	2	3	2.5	3.4
5.75	1.5	1.2	2.1	1.7	2.5	2.2	3
5.35	1.4	1.1	1.8	1.6	2.2	1.9	2.6
4.97	1.2	1	1.6	1.4	2	1.8	2.3
4.62	1.1	0.9	1.5	1.3	1.7	1.6	2
4.3	1	0.8	1.3	1.1	1.5	1.4	1.7
4	0.8	0.7	1.1	0.9	1.2	1.2	1.5
3.72	0.7	0.6	0.9	0.8	1	1	1.2
3.46	0.6	0.5	0.7	0.6	0.8	0.8	1
3.21	0.5	0.4	0.6	0.5	0.7	0.6	0.8
2.99	0.5	0.3	0.5	0.4	0.6	0.5	0.7
2.78	0.4	0.3	0.4	0.3	0.5	0.4	0.6
2.59	0.4	0.2	0.4	0.3	0.4	0.4	0.5
2.4	0.4	0.2	0.3	0.3	0.4	0.4	0.5
2.24	0.3	0.2	0.3	0.2	0.3	0.3	0.4
2.08	0.3	0.2	0.2	0.2	0.3	0.3	0.4
1.93	0.2	0.1	0.2	0.2	0.2	0.2	0.3

Experiment no.: 14 **Date: 5.12.94**

Concentration of particle in mixing tank: 4 g/L

Temperature: 21° C **Starting time: 9:45 am**

Inflow discharge: 0.146 L/s **Outflow:**

Head velocity

	St. 0	St. 1	St. 2	St. 3	St. 4	St. 5	St. 6	St. 7
Time (s)		0	40	80	115	157	203	250
Height (cm)	4	12	11	11.5	10.5	11.5	11	12
Velocity		1.25		1.299		1.075		

Height of turbidity current at station

	St. 0	St. 1	St. 2	St. 3	St. 4	St. 5	St. 6	St. 7
Height (cm)	4.0	3.5	3.5	3.7	3.9	4.0	4.2	4.5

Height of water in the flume: 50 cm **End time: 9:55 am**

Inflow concentration at flume entrance: 2.31 g/L

Outflow concentration: 0.38 g/L

Head Concentration

Height from bed (mm)	St. 2 Turbidity (NTU)	Volumetric Concentration	St. 4 Turbidity (NTU)	Volumetric Concentration	St. 6 Turbidity (NTU)	Volumetric Concentration
10	20	9.98E-05	46	0.000229	35	0.000175
20			41	0.000204	31	0.000155
30	44	0.000219	36	0.000179	31	0.000155
40			23	0.000115	20	9.98E-05
50	20	9.98E-05	20	9.98E-05	15	7.49E-05
60			15	7.49E-05	12	5.99E-05
70	10	5E-05	11	5.5E-05	13	6.49E-05
80			11	5.5E-05	8	4E-05
90	10	5E-05	8	4E-05	7	3.5E-05
100					4	2E-05
Average		0.000138		0.000162		0.000128

Experiment No. 14: Particle Size Analysis							
High Size	Inflow	St. 2 head	St. 2 Body	St. 4 head	St. 4 Body	St. 6 head	St. 6 Body
(μm)	Under %	Under %	Under %	Under %	Under %	Under %	Under %
188	100	100	100	100	100	100	100
175	100	100	100	100	100	100	100
163	100	100	100	100	100	100	100
151	100	100	100	100	100	100	100
141	99.9	100	100	100	100	100	100
131	99.8	100	100	100	100	100	100
122	99.5	100	100	100	100	100	100
113	99	100	100	100	100	100	100
105	98	100	100	100	100	100	100
97.8	96.1	100	100	100	100	100	100
90.9	93.5	99.9	100	100	100	100	100
84.5	90.5	99.5	100	100	100	100	100
78.6	87	99.8	100	100	100	100	100
73.1	83.1	97.8	99.9	99.9	100	99.9	100
68	78.8	96.3	99.9	99.8	100	99.9	100
63.2	74.3	94.3	99.9	99.5	100	99.9	99.9
58.8	69.6	91.4	99.7	98.5	100	99.7	99.9
54.7	65	87.7	98.5	96.3	99.7	98.8	99.9
50.8	60.4	82.9	96.4	93.1	99	97.1	99.8
47.3	55.9	77.4	93.4	88.9	97.6	94.7	99.5
44	51.6	71.3	89.6	84.1	95.3	91.4	98.7
40.9	47.3	65.1	85.1	78.7	92.1	87.4	97.2
38	43.1	59	79.9	73	87.7	82.7	94.5
35.4	39.1	53.3	74.1	67.2	82.1	77.3	90.7
32.9	35.2	48.1	68	61.5	75.6	71.3	85.7
30.6	31.6	43.6	62	56.1	68.8	65.3	80.1
28.4	28.3	39.6	56.5	51	62.3	59.6	74.1
26.4	25.5	36.1	51.6	46.4	56.7	54.4	68.2
24.6	23	33.2	47.5	42.4	52.1	49.8	62.5
22.9	20.9	30.4	43.9	38.7	48.1	45.8	57.1
21.3	18.9	27.6	40.5	35.3	44.7	42.1	52.2
19.8	16.9	24.7	37.2	32.1	41.4	38.6	47.6
18.4	15	21.6	33.7	28.9	38.1	35	43.2
17.1	13.1	18.5	30	25.4	34.1	31.1	38.8
15.9	11.3	15.4	25.8	21.6	29.4	26.7	34.1
14.8	9.5	12.5	21.4	17.8	24.2	22.1	29.3
13.7	7.8	9.9	17.2	14.1	19	17.6	24.5
12.8	6.4	7.9	13.6	11.1	14.7	13.8	20
11.9	5.3	6.4	10.9	8.9	11.6	10.9	16.1
11.1	4.3	5.4	8.9	7.4	9.5	8.9	12.9
10.3	3.6	4.8	7.5	6.3	8.2	7.5	10.4
9.56	3.1	4.2	6.6	5.6	7.4	6.6	8.5
8.89	2.7	3.8	5.9	5.1	6.8	5.9	7.3
8.27	2.4	3.3	5.3	4.6	6.3	5.4	6.5
7.69	2.1	2.9	4.8	4.1	5.7	4.8	5.8
7.15	1.8	2.4	4.2	3.5	4.9	4.2	5.2
6.65	1.6	2	3.6	3	4.1	3.6	4.6
6.18	1.4	1.7	3	2.5	3.3	3	4.1
5.75	1.3	1.4	2.6	2.1	2.8	2.6	3.7
5.35	1.2	1.3	2.3	1.9	2.4	2.3	3.3
4.97	1.1	1.2	2.1	1.7	2.1	2	2.9
4.62	1	1.1	1.8	1.5	1.9	1.8	2.6
4.3	0.8	0.9	1.6	1.3	1.6	1.6	2.2
4	0.7	0.8	1.3	1.1	1.4	1.3	1.8
3.72	0.6	0.6	1.1	0.9	1.2	1.1	1.5
3.46	0.5	0.5	0.9	0.8	1	0.9	1.2
3.21	0.5	0.4	0.7	0.6	0.8	0.8	1
2.99	0.4	0.3	0.6	0.5	0.7	0.6	0.8
2.78	0.4	0.2	0.5	0.4	0.6	0.6	0.7
2.59	0.3	0.2	0.5	0.4	0.5	0.5	0.6
2.4	0.3	0.2	0.4	0.3	0.5	0.4	0.5
2.24	0.3	0.2	0.4	0.3	0.4	0.4	0.5
2.08	0.2	0.1	0.3	0.3	0.3	0.3	0.4
1.93	0.2	0.1	0.3	0.2	0.3	0.3	0.3

Experiment no.: 15 **Date: 5.12.94**

Concentration of particle in mixing tank: 4 g/L

Temperature: 21° C **Starting time: 11:00 am**

Inflow discharge: 0.11 L/s **Outflow:**

Head velocity

	St. 0	St. 1	St. 2	St. 3	St. 4	St. 5	St. 6	St. 7
Time (s)		0	50	115	168	235	310	428
Height (cm)	4	12	10	12	12	11	8	7.5
Velocity			0.869		0.833		0.518	

Height of turbidity current at station

	St. 0	St. 1	St. 2	St. 3	St. 4	St. 5	St. 6	St. 7
Height (cm)	4.0	3.5	3.5	3.5	3.5	3.5	3.5	

Height of water in the flume: 50 cm **End time:**

Inflow concentration at flume entrance: 3.17 g/L

Outflow concentration: 0.24 g/L

Comment: mixing was high because the temperature difference between two layers

Head Concentration

Height from bed (mm)	St. 2 Turbidity (NTU)	Volumetric Concentration	St. 4 Turbidity (NTU)	Volumetric Concentration	St. 6 Turbidity (NTU)	Volumetric Concentration
10	26	0.00013	32	0.00016	36	0.000179
20	42	0.000209	29	0.000145	20	9.98E-05
30	30	0.00015	28	0.00014	23	0.000115
40	14	6.99E-05	24	0.00012	9	4.5E-05
50	12	5.99E-05	22	0.00011	7	3.5E-05
60	8	4E-05	18	8.99E-05	5	2.5E-05
70	7	3.5E-05	6	3E-05	7	3.5E-05
80	7	3.5E-05	9	4.5E-05	8	4E-05
90	7	3.5E-05	5	2.5E-05	5	2.5E-05
100			5	2.5E-05	4	2E-05
Average		0.000147		0.000127		0.000131

Experiment No. 15: Particle Size Analysis							
High Size	Inflow	St. 2 head	St. 2 Body	St. 4 head	St. 4 Body	St. 6 head	St. 6 Body
(μm)	Under %	Under %	Under %	Under %	Under %	Under %	Under %
188	100	100	100	100	100	100	100
175	100	100	100	100	100	100	100
163	100	100	100	100	100	100	100
151	100	100	100	100	100	100	100
141	99.9	100	100	100	100	100	100
131	99.8	100	100	100	100	100	100
122	99.7	100	100	100	100	100	100
113	99.4	100	100	100	100	100	100
105	98.6	100	100	100	100	100	100
97.8	97	100	100	100	100	100	100
90.9	94.9	100	100	100	100	100	100
84.5	91	100	100	100	100	100	100
78.6	86.9	100	100	100	100	100	100
73.1	82.3	99.9	100	100	100	100	100
68	77.2	99.7	100	100	100	100	100
63.2	72	98.6	100	99.9	100	100	100
58.8	66.6	96.6	100	99.8	99.9	100	100
54.7	61.4	93.4	99.6	99.1	99.7	99.7	100
50.8	56.4	89.1	98.7	97.5	99.4	99.2	100
47.3	51.7	83.9	97	95.3	98.8	98.2	100
44	47.2	78.1	94.4	92.2	97.8	96.5	100
40.9	42.9	71.9	91	88.4	96.3	94	99.9
38	38.8	65.8	86.7	83.7	94	90.3	99.7
35.4	34.8	59.9	81.5	78.3	90.8	85.4	98.8
32.9	31.1	54.6	75.5	72.2	86.7	79.5	97.2
30.6	27.6	49.7	69.3	66	82	73.3	94.7
28.4	24.6	45.3	63.3	60	76.7	67.1	91.2
26.4	22.1	41.1	57.8	54.5	70.9	61.4	86.7
24.6	20.1	37.9	53	49.6	65	56.4	81.2
22.9	18.3	34.6	48.9	45.2	59.1	51.9	75.3
21.3	16.6	31.5	45.2	41.1	53.4	47.9	69.2
19.8	15	28.6	41.8	37.4	48	44	63.1
18.4	13.3	25.6	38.5	33.7	43	40.2	57.2
17.1	11.6	22.3	34.6	29.9	38.1	35.9	51.2
15.9	9.9	18.9	30.1	25.9	33.4	31	45
14.8	8.3	15.4	25	21.9	28.9	25.8	38.8
13.7	6.8	12.1	20	17.9	24.6	20.6	32.7
12.8	5.6	9.5	15.6	14.4	20.6	16.2	26.9
11.9	4.6	7.7	12.3	11.4	17	12.8	21.7
11.1	3.9	6.4	9.9	9.1	13.8	10.3	17.1
10.3	3.3	5.6	8.2	7.3	11.2	8.5	13.5
9.56	2.9	5	7.2	6	9.1	7.4	10.8
8.89	2.5	4.6	6.5	5.2	7.6	6.6	9
8.27	2.2	4.1	5.9	4.6	6.4	5.9	7.8
7.69	1.9	3.6	5.4	4.1	5.5	5.3	6.9
7.15	1.7	3.1	4.8	3.6	4.8	4.7	6.1
6.65	1.5	2.5	4.1	3.2	4.2	4	5.4
6.18	1.3	2.1	3.4	2.8	3.7	3.4	4.7
5.75	1.2	1.8	2.9	2.5	3.3	2.9	4.2
5.35	1.1	1.5	2.5	2.2	3	2.6	3.8
4.97	1	1.4	2.2	2	2.7	2.3	3.4
4.62	0.9	1.2	1.9	1.7	2.4	2	2.9
4.3	0.7	1.1	1.6	1.5	2	1.7	2.4
4	0.6	0.9	1.3	1.2	1.7	1.4	1.9
3.72	0.5	0.7	1.1	1	1.4	1.1	1.5
3.46	0.4	0.6	0.9	0.8	1.2	0.9	1.2
3.21	0.4	0.4	0.7	0.7	1	0.7	0.9
2.99	0.3	0.3	0.6	0.6	0.8	0.6	0.7
2.78	0.3	0.3	0.5	0.5	0.7	0.5	0.6
2.59	0.2	0.2	0.5	0.4	0.6	0.4	0.5
2.4	0.2	0.2	0.4	0.4	0.5	0.4	0.5
2.24	0.2	0.2	0.4	0.3	0.4	0.3	0.4
2.08	0.2	0.2	0.3	0.3	0.4	0.3	0.3
1.93	0.1	0.1	0.3	0.3	0.3	0.2	0.3

Experiment no.: 16 **Date: 5.12.94**

Concentration of particle in mixing tank: 6 g/L

Temperature: 22° C **Starting time: 6:37 pm**

Inflow discharge: 0.11 L/s **Outflow:**

Head velocity

	St. 0	St. 1	St. 2	St. 3	St. 4	St. 5	St. 6	St. 7
Time (s)		0	54	98	145	187	240	300
Height (cm)	4	12	8	8	8	8.5	7.5	7.5
Velocity (cm/s)			1.020		1.123		0.885	

Height of turbidity current at station

	St. 0	St. 1	St. 2	St. 3	St. 4	St. 5	St. 6	St. 7
Height (cm)	4.0	2.5	2.5	2.5	3.0	3.3	3.5	3.5

Height of water in the flume: 50 cm **End time: 6:45 pm**

Inflow concentration at flume entrance: 4.55 g/L

Outflow concentration: 0.29 g/L

Head Concentration

Height from bed (mm)	St. 2 Turbidity (NTU)	Volumetric Concentration	St. 4 Turbidity (NTU)	Volumetric Concentration	St. 6 Turbidity (NTU)	Volumetric Concentration
10	54	0.000269	59	0.000294	36	0.000179
20						
30	25	0.000125	40	0.000199	30	0.00015
40						
50	14	6.99E-05	8	4E-05	10	5E-05
60						
70	8	4E-05	4	2E-05	3	1.5E-05
80						
90	3	1.5E-05	2	1E-05	2	1E-05
100	1	5E-06				
110			1	5E-06	1	5E-06
Average		0.000187		0.000232		0.000145

Experiment No. 16: Particle Size Analysis							
High Size	Inflow	St. 2 head	St. 2 Body	St. 4 head	St. 4 Body	St. 6 head	St. 6 Body
(μm)	Under %	Under %	Under %	Under %	Under %	Under %	Under %
188	100	100	100	100	100	100	100
175	99.2	100	100	100	100	100	100
163	98.4	100	100	100	100	100	100
151	97.5	100	100	100	100	100	100
141	96.5	100	100	100	100	100	100
131	95.2	100	100	100	100	100	100
122	93.7	100	100	100	100	100	100
113	91.9	100	100	100	100	100	100
105	89.7	100	100	100	100	100	100
97.8	87.1	100	100	100	100	100	100
90.9	84.1	100	100	99.9	100	100	100
84.5	80.5	100	100	99.6	100	99.7	100
78.6	76.5	100	100	99.2	100	99.3	100
73.1	72.2	99.9	100	98.5	100	98.7	100
68	67.5	99.7	100	97.6	100	97.8	100
63.2	62.8	98.7	100	96.3	100	96.6	100
58.8	58.1	96.8	100	94.6	100	95	100
54.7	53.5	93.8	99.8	92.3	99.9	92.9	100
50.8	49.1	89.7	99.5	89.3	99.9	90.3	100
47.3	45	84.8	98.8	85.8	99.9	87.2	99.9
44	41.2	79.2	97.4	81.8	99.8	83.6	99.9
40.9	37.5	73.3	95.2	77.3	98.9	79.5	99.6
38	34.1	67.4	91.9	72.5	97.1	75.1	98.7
35.4	30.7	61.7	87.3	67.4	94.3	70.4	97.2
32.9	27.6	56.4	81.6	62.2	90.5	65.5	94.7
30.6	24.7	51.5	75.5	57	85.8	60.6	91.4
28.4	22	47.1	69.2	52.2	80.6	55.8	87.2
26.4	19.7	43.2	63.3	47.7	74.9	51.2	82.1
24.6	17.7	39.7	58.1	43.7	69	47	76.3
22.9	15.9	36.4	53.6	40.1	63.3	43.2	70.4
21.3	14.2	33.2	49.9	36.8	58	39.8	64.8
19.8	12.7	30.1	46.8	33.8	53.1	36.7	59.6
18.4	11.2	26.9	43.9	30.7	48.5	33.6	54.8
17.1	9.8	23.6	40.2	27.4	43.8	30.1	49.7
15.9	8.5	20.2	35.5	23.7	38.9	26.1	44.3
14.8	7.3	16.9	29.9	19.7	33.7	21.9	38.5
13.7	6.2	13.8	24.1	15.9	28.5	17.6	32.7
12.8	5.2	11.3	19.1	12.6	23.7	14.1	27.1
11.9	4.3	9.3	15.3	10.3	19.3	11.4	22.1
11.1	3.6	7.9	12.5	8.6	15.6	9.6	17.8
10.3	3	6.9	10.7	7.5	12.7	8.3	14.4
9.56	2.6	6.1	9.5	6.8	10.5	7.5	11.9
8.89	2.2	5.5	8.7	6.3	9.1	6.9	10.2
8.27	1.9	5	8.1	5.8	8	6.4	9
7.69	1.7	4.5	7.3	5.2	7.1	5.7	8
7.15	1.5	3.9	6.5	4.5	6.4	5	7.1
6.65	1.3	3.3	5.5	3.7	5.6	4.1	6.3
6.18	1.2	2.8	4.6	3.1	5	3.4	5.5
5.75	1.1	2.5	4	2.6	4.4	2.8	4.9
5.35	1	2.2	3.4	2.2	4	2.4	4.4
4.97	0.9	1.9	3	2	3.6	2.2	3.9
4.62	0.8	1.7	2.6	1.8	3.1	1.9	3.4
4.3	0.7	1.5	2.2	1.5	2.7	1.7	2.9
4	0.6	1.3	1.9	1.3	2.2	1.4	2.4
3.72	0.6	1.1	1.6	1.1	1.8	1.2	2
3.46	0.5	0.9	1.3	0.9	1.5	1	1.6
3.21	0.4	0.7	1	0.8	1.2	0.8	1.3
2.99	0.4	0.6	0.8	0.7	1	0.7	1.1
2.78	0.4	0.6	0.7	0.6	0.9	0.6	0.9
2.59	0.3	0.5	0.6	0.5	0.8	0.5	0.8
2.4	0.3	0.4	0.5	0.5	0.7	0.5	0.7
2.24	0.3	0.4	0.4	0.4	0.6	0.4	0.6
2.08	0.2	0.3	0.4	0.4	0.5	0.4	0.5
1.93	0.2	0.3	0.3	0.3	0.4	0.3	0.4

Experiment no.: 17 **Date: 6.12.94**

Concentration of particle in mixing tank: 6 g/L

Temperature: 20° C **Starting time: 10:00 am**

Inflow discharge: 0.26 L/s **Outflow:**

Head velocity

	St. 0	St. 1	St. 2	St. 3	St. 4	St. 5	St. 6	St. 7
Time (s)		0	24	53	78	105	133	165
Height (cm)	4		12	12	12	12	12.5	13
Velocity (cm/s)			1.886		1.923		1.666	

Height of turbidity current at station

	St. 0	St. 1	St. 2	St. 3	St. 4	St. 5	St. 6	St. 7
Height (cm)	4.0	6.0	6.0	6.0	6.0	6.0	5.5	6.0

Height of water in the flume: 50 cm **End time:**

Inflow concentration at flume entrance: 3.11 g/L

Outflow concentration: 0.63 g/L

Head Concentration

Height from bed (mm)	St. 2 Turbidity (NTU)	Volumetric Concentration	St. 4 Turbidity (NTU)	Volumetric Concentration	St. 6 Turbidity (NTU)	Volumetric Concentration
10	110	0.000545	113	0.00056	78	0.000388
20						
30	40	0.000199	48	0.000239	63	0.000313
40						
50	14	6.99E-05	25	0.000125	45	0.000224
60						
70	8	4E-05	18	8.99E-05	13	6.49E-05
Average		0.000385		0.000361		0.000289

Experiment No. 17: Particle Size Analysis							
High Size	Inflow	St. 2 head	St. 2 Body	St. 4 head	St. 4 Body	St. 6 head	St. 6 Body
(μm)	Under %	Under %	Under %	Under %	Under %	Under %	Under %
188	100	100	100	100	100	100	100
175	100	100	100	100	100	100	100
163	100	100	100	100	100	100	100
151	100	100	100	100	100	100	100
141	100	100	100	100	100	100	100
131	99.9	100	100	100	100	100	100
122	99.9	100	100	100	100	100	100
113	99.8	99.9	100	100	100	100	100
105	99.5	99.8	100	100	100	100	100
97.8	98.9	99.7	100	100	100	100	100
90.9	97.8	99.2	100	100	100	100	100
84.5	96.1	97.9	100	99.9	100	100	100
78.6	93.8	95.9	99.9	99.7	99.9	100	100
73.1	91.2	93.4	99.9	99.3	99.9	99.9	100
68	88.2	90.5	99.8	98.4	99.9	99.8	100
63.2	84.8	87	99.4	97	99.9	99.5	100
58.8	81.1	82.9	98.4	94.6	99.8	98.5	99.9
54.7	77.1	78.3	96.2	91.3	98.8	96	99.5
50.8	72.8	73	92.8	86.9	96.4	92	98.5
47.3	68.2	67.3	88.5	81.5	92.7	87	96.8
44	63.5	61.3	83.6	75.5	87.8	81.3	94.3
40.9	58.8	55.5	78.3	69.3	82.4	75.2	90.9
38	54	50	72.8	63.3	76.8	69.2	86.4
35.4	49.4	45	67.2	57.7	71	63.6	80.7
32.9	44.9	40.7	61.9	52.8	65.2	58.4	74.2
30.6	40.8	36.9	56.9	48.2	59.8	53.7	67.4
28.4	37.1	33.5	52.3	44.1	54.8	49.4	61
26.4	33.8	30.6	48.1	40.3	50.4	45.4	55.4
24.6	30.9	27.9	44.4	36.8	46.5	41.6	50.7
22.9	28.3	25.4	40.9	33.5	42.9	38.1	46.7
21.3	25.8	22.9	37.5	30.3	39.5	34.7	43.3
19.8	23.4	20.3	34.1	27.2	36.1	31.3	40
18.4	20.9	17.7	30.6	24.1	32.6	27.8	36.8
17.1	18.4	15.2	26.9	21	28.8	24.3	33
15.9	15.7	12.7	23.2	17.9	24.6	20.8	28.6
14.8	13.1	10.5	19.4	14.8	20.3	17.3	23.8
13.7	10.7	8.6	15.9	12	16.3	14.1	19
12.8	8.6	7.1	12.9	9.7	13	11.5	14.9
11.9	7.1	6	10.6	7.9	10.7	9.5	11.8
11.1	5.9	5.2	8.8	6.6	9	8	9.5
10.3	5.1	4.6	7.5	5.7	8	7	8
9.56	4.5	4.1	6.6	5.1	7.2	6.3	7
8.89	4	3.7	5.9	4.5	6.6	5.7	6.3
8.27	3.6	3.2	5.3	4.1	6	5.1	5.8
7.69	3.2	2.8	4.7	3.6	5.4	4.5	5.3
7.15	2.8	2.4	4.1	3.1	4.6	3.9	4.7
6.65	2.4	2	3.5	2.6	3.7	3.2	4
6.18	2	1.7	3	2.2	3	2.7	3.4
5.75	1.8	1.5	2.6	1.9	2.6	2.3	3
5.35	1.6	1.3	2.3	1.7	2.3	2.1	2.6
4.97	1.4	1.2	2	1.6	2.1	1.9	2.3
4.62	1.3	1.1	1.8	1.4	1.9	1.7	2
4.3	1.1	1	1.6	1.2	1.7	1.5	1.7
4	1	0.8	1.3	1	1.4	1.3	1.4
3.72	0.8	0.7	1.1	0.9	1.2	1.1	1.2
3.46	0.7	0.6	0.9	0.7	1	0.9	1
3.21	0.5	0.5	0.8	0.6	0.8	0.8	0.8
2.99	0.4	0.4	0.6	0.5	0.7	0.7	0.7
2.78	0.4	0.3	0.6	0.4	0.6	0.6	0.6
2.59	0.3	0.3	0.5	0.4	0.5	0.5	0.6
2.4	0.3	0.3	0.4	0.3	0.4	0.5	0.5
2.24	0.3	0.2	0.4	0.3	0.4	0.4	0.4
2.08	0.2	0.2	0.3	0.3	0.3	0.4	0.4
1.93	0.2	0.2	0.3	0.2	0.3	0.3	0.3

Experiment no.: 18 **Date: 6.12.94**

Concentration of particle in mixing tank: 6 g/L

Volumetric Concentration = 0.002575

Temperature: 21° C **Starting time: 10:52 am**

Inflow discharge: 0.19 L/s **Outflow:**

Head velocity

	St. 0	St. 1	St. 2	St. 3	St. 4	St. 5	St. 6	St. 7
Time (s)		0	35	75	109	143	175	216
Height (cm)	4		13	13	13	13.5	13	13
Velocity(cm/s)		1.333		1.470		1.369		

Height of turbidity current at station

	St. 0	St. 1	St. 2	St. 3	St. 4	St. 5	St. 6	St. 7
Height (cm)	4.0	5.0	4.8	4.5	4.5	4.5	4.8	4.8

Height of water in the flume: 50 cm **End time: 11:02 am**

Inflow concentration at flume entrance: 2.73 g/L

Outflow concentration: 0.45 g/L

Head Concentration

Height from bed (mm)	St. 2 Turbidity (NTU)	Volumetric Concentration	St. 4 Turbidity (NTU)	Volumetric Concentration	St. 6 Turbidity (NTU)	Volumetric Concentration
10	34	0.00017	43	0.000214	55	0.000274
20						
30	66	0.000328	40	0.000199	44	0.000219
40						
50	38	0.000189	26	0.00013	29	0.000145
60						
70	14	6.99E-05	13	6.49E-05	14	6.99E-05
80						
90			6	3E-05	8	4E-05
Average		0.000213		0.000163		0.000194

Experiment No. 18: Particle Size Analysis							
High Size	Inflow	St. 2 head	St. 2 Body	St. 4 head	St. 4 Body	St. 6 head	St. 6 Body
(μm)	Under %	Under %	Under %	Under %	Under %	Under %	Under %
188	100	100	100	100	100	100	100
175	100	100	100	100	100	100	100
163	100	100	100	100	100	100	100
151	100	100	100	100	100	100	100
141	100	100	100	100	100	100	100
131	100	100	100	100	100	100	100
122	100	100	100	100	100	100	100
113	100	100	100	100	100	100	100
105	100	100	100	100	100	100	100
97.8	99.9	100	100	100	100	100	100
90.9	99.9	99.9	100	100	100	100	100
84.5	99.9	99.7	100	100	100	100	100
78.6	99.8	99.3	100	100	100	100	100
73.1	99.5	98.6	99.9	99.9	100	99.9	100
68	98.7	97.5	99.9	99.8	100	99.9	100
63.2	97.4	95.8	99.9	99.2	100	99.9	100
58.8	95.3	93.5	99.7	97.9	99.9	99.6	100
54.7	92.3	90.3	98.7	95.6	99.6	98.2	99.9
50.8	88.2	86.3	96.9	92.2	98.8	95.7	99.8
47.3	83.4	81.5	94.3	88	97.5	92.1	99.3
44	77.9	76.1	90.9	83.1	95.4	87.6	98.3
40.9	72.1	70.4	86.8	77.8	92.4	82.7	96.4
38	66.5	64.6	82	72.2	88.3	77.3	93.2
35.4	61.3	59	76.5	66.5	83.2	71.9	88.7
32.9	56.6	53.7	70.6	60.9	77.1	66.3	82.9
30.6	52.3	48.8	64.7	55.7	70.8	61	76.6
28.4	48.3	44.3	59.1	50.9	64.6	56	70.3
26.4	44.6	40.4	54.1	46.8	59	51.4	64.4
24.6	41.1	37	49.7	43.2	54.2	47.2	59.1
22.9	37.6	33.9	45.9	39.9	50.1	43.4	54.5
21.3	34.1	31	42.4	36.7	46.5	39.9	50.4
19.8	30.5	28.1	39.2	33.4	43.3	36.5	46.8
18.4	26.9	25.2	35.9	29.9	40	33	43.2
17.1	23.3	22	32.2	26.3	36.2	29.2	39.2
15.9	19.8	18.6	28	22.4	31.6	25	34.4
14.8	16.7	15.2	23.4	18.6	26.5	20.6	29
13.7	13.8	12	18.8	15.1	21.3	16.5	23.6
12.8	11.4	9.4	14.9	12.2	16.7	13.1	18.7
11.9	9.5	7.6	11.9	10	13.2	10.5	14.8
11.1	8	6.3	9.8	8.5	10.7	8.8	11.9
10.3	6.8	5.5	8.3	7.4	8.9	7.7	9.8
9.56	5.9	4.9	7.3	6.6	7.8	6.9	8.4
8.89	5.2	4.4	6.6	5.9	7.1	6.3	7.6
8.27	4.6	3.9	6	5.3	6.5	5.7	6.9
7.69	4	3.4	5.4	4.6	5.9	5.1	6.3
7.15	3.5	2.9	4.7	4	5.2	4.4	5.6
6.65	2.9	2.4	4	3.4	4.5	3.6	4.9
6.18	2.5	2	3.4	2.8	3.8	2.9	4.2
5.75	2.2	1.7	2.9	2.5	3.3	2.5	3.6
5.35	2	1.5	2.6	2.2	2.9	2.2	3.2
4.97	1.8	1.4	2.3	2	2.5	2	2.8
4.62	1.6	1.2	2	1.8	2.2	1.8	2.5
4.3	1.4	1.1	1.7	1.6	1.9	1.6	2.1
4	1.2	0.9	1.5	1.4	1.6	1.3	1.8
3.72	1	0.8	1.2	1.1	1.4	1.1	1.5
3.46	0.8	0.6	1	0.9	1.1	0.9	1.2
3.21	0.6	0.5	0.8	0.8	0.9	0.8	1
2.99	0.5	0.4	0.7	0.6	0.8	0.6	0.9
2.78	0.4	0.4	0.6	0.6	0.7	0.5	0.8
2.59	0.4	0.3	0.5	0.5	0.6	0.5	0.7
2.4	0.4	0.3	0.5	0.4	0.6	0.4	0.6
2.24	0.3	0.2	0.4	0.4	0.5	0.4	0.6
2.08	0.3	0.2	0.4	0.3	0.4	0.3	0.5
1.93	0.2	0.2	0.3	0.3	0.4	0.3	0.4

Experiment no.: 20 **Date: 8.12.94**

Concentration of particle in mixing tank: 10 g/L

Volumetric Concentration = 0.004292

Temperature: 22° C **Starting time: 10:42 am**

Inflow discharge: 0.225 L/s **Outflow:**

Head velocity

	St. 0	St. 1	St. 2	St. 3	St. 4	St. 5	St. 6	St. 7
Time (s)		0	22	50	70	92	118	146
Height (cm)		14	11	10	10	10	10.5	11
Velocity(cm/s)			2.000		2.380		1.851	

Height of turbidity current at station

	St. 0	St. 1	St. 2	St. 3	St. 4	St. 5	St. 6	St. 7
Height (cm)	4.0	4.0	4.0	4.0	4.0	4.5	5.0	5.5

Height of water in the flume: 50 cm **End time: 10:50 am**

Inflow concentration at flume entrance: 6.56 g/L

Outflow concentration: 1.05 g/L

Head Concentration

Height from bed (mm)	St. 2 Turbidity (NTU)	Volumetric Concentration	St. 4 Turbidity (NTU)	Volumetric Concentration	St. 6 Turbidity (NTU)	Volumetric Concentration
10	120	0.000594	110	0.000545	120	0.000594
20						
30	85	0.000422	105	0.000521	95	0.000471
40						
50	34	0.00017	23	0.000115	45	0.000224
60						
70	19	9.49E-05			15	7.49E-05
Average		0.000423		0.000453		0.000448

Experiment No. 20: Particle Size Analysis							
High Size	Inflow	St. 2 head	St. 2 Body	St. 4 head	St. 4 Body	St. 6 head	St. 6 Body
(μm)	Under %	Under %	Under %	Under %	Under %	Under %	Under %
188	100	100	100	100	100	100	100
175	100	100	100	100	100	100	100
163	100	100	100	100	100	100	100
151	100	100	100	100	100	100	100
141	100	100	100	100	100	100	100
131	99.9	100	100	100	100	100	100
122	99.8	100	100	100	100	100	100
113	99.7	100	100	100	100	100	100
105	99.3	100	100	100	100	100	100
97.8	98.4	100	100	100	100	100	100
90.9	96.9	99.9	100	100	100	100	100
84.5	94.9	99.5	100	100	100	100	100
78.6	92.3	98.7	100	99.9	100	99.9	100
73.1	89.3	97.4	99.9	99.9	100	99.9	100
68	86	95.6	99.8	99.8	100	99.9	100
63.2	82.3	93.2	99.6	99.8	100	99.9	100
58.8	78.2	90.1	98.7	99	99.9	99.8	100
54.7	73.9	86	96.5	96.8	99.5	98.5	99.8
50.8	69.3	80.9	93	92.9	98.2	95.5	99.1
47.3	64.5	75.2	88.5	87.8	96	91	97.9
44	59.7	69	83.3	82.1	92.9	85.4	95.8
40.9	55	63.1	77.7	76.2	88.9	79.5	93
38	50.3	57.7	72.1	70.7	84.1	73.8	89.1
35.4	45.9	53.2	66.7	65.9	78.5	68.6	84.1
32.9	41.8	49.5	61.7	61.9	72.3	63.9	78.3
30.6	37.9	46.2	56.9	57.7	65.9	59.3	72.1
28.4	34.4	42.9	52.5	53.5	59.9	54.7	65.9
26.4	31.3	39.3	48.2	48.9	54.5	49.9	60.1
24.6	28.4	35.4	44.2	44	49.8	44.9	54.9
22.9	25.7	31.3	40.4	39.2	45.7	40.1	50.3
21.3	23.2	27.9	36.8	34.7	42.1	35.7	46.4
19.8	20.7	24.5	33.3	30.7	38.9	31.3	42.9
18.4	18.2	21.9	29.9	27.3	35.7	28.1	39.7
17.1	15.9	19.3	26.3	24.1	32	24.7	35.9
15.9	13.6	16.3	22.7	21.1	27.7	21.3	31.4
14.8	11.5	14.5	19	18.1	23	17.9	26.4
13.7	9.6	12.3	15.6	15.2	18.3	14.7	21.4
12.8	7.9	10.4	12.7	12.5	14.3	11.9	16.9
11.9	6.6	8.7	10.4	10.1	11.4	9.4	13.4
11.1	5.4	7.4	8.7	8	9.4	7.5	10.8
10.3	4.6	6.2	7.4	6.4	8.1	6	9.1
9.56	3.9	5.4	6.6	5.3	7.3	5.1	8
8.89	3.4	4.7	5.9	4.7	6.8	4.5	7.3
8.27	3	4.2	5.4	4.4	6.3	4.1	6.9
7.69	2.7	3.7	4.8	4	5.7	3.7	6.3
7.15	2.4	3.2	4.1	3.6	5	3.2	5.6
6.65	2.1	2.7	3.5	3.1	4.1	2.7	4.8
6.18	1.8	2.3	2.9	2.6	3.4	2.3	4.1
5.75	1.7	2.1	2.5	2.2	2.8	2	3.5
5.35	1.5	2	2.2	1.9	2.4	1.8	3
4.97	1.4	1.9	2	1.7	2.1	1.6	2.6
4.62	1.3	1.8	1.8	1.4	1.9	1.4	2.3
4.3	1.1	1.6	1.5	1.2	1.7	1.2	2
4	1	1.4	1.3	1	1.4	1	1.7
3.72	0.8	1.1	1.1	0.9	1.2	0.9	1.4
3.46	0.7	0.9	1	0.8	1	0.8	1.2
3.21	0.6	0.7	0.8	0.7	0.9	0.7	1.1
2.99	0.6	0.5	0.7	0.7	0.7	0.6	1
2.78	0.5	0.5	0.6	0.6	0.7	0.6	0.9
2.59	0.5	0.4	0.6	0.6	0.6	0.6	0.8
2.4	0.5	0.4	0.5	0.6	0.5	0.5	0.7
2.24	0.4	0.4	0.5	0.5	0.5	0.5	0.7
2.08	0.4	0.3	0.4	0.5	0.4	0.4	0.6
1.93	0.3	0.3	0.4	0.4	0.3	0.4	0.5

Experiment no.: 21 **Date: 8.12.94**

Concentration of particle in mixing tank: 10 g/L

Volumetric Concentration = 0.004292

Temperature: 22° C **Starting time: 11:20 am**

Inflow discharge: 0.195 L/s **Outflow:**

Head velocity

	St. 0	St. 1	St. 2	St. 3	St. 4	St. 5	St. 6	St. 7
Time (s)		0	30	55	80	102	128	158
Height (cm)	4	12	11	10	11	11	11	11
Velocity (cm/s)		1.818		2.127		1.785		

Height of turbidity current at station

	St. 0	St. 1	St. 2	St. 3	St. 4	St. 5	St. 6	St. 7
Height (cm)	4.0	3.7	3.5	3.7	3.8	4.0	4.0	4.0

Height of water in the flume: 50 cm **End time: 11:28 am**

Inflow concentration at flume entrance: 5.81 g/L

Outflow concentration: 0.89 g/L

Head Concentration

Height from bed (mm)	St. 2 Turbidity (NTU)	Volumetric Concentration	St. 4 Turbidity (NTU)	Volumetric Concentration	St. 6 Turbidity (NTU)	Volumetric Concentration
10	108	0.000535	110	0.000545	110	0.000545
20						
30	54	0.000269	60	0.000299	50	0.000249
40						
50	29	0.000145	29	0.000145	25	0.000125
60						
70	21	0.000105			13	6.49E-05
Average		0.000349		0.000375		0.000369

Experiment No. 21: Particle Size Analysis							
High Size	Inflow	St. 2 head	St. 2 Body	St. 4 head	St. 4 Body	St. 6 head	St. 6 Body
(μm)	Under %	Under %	Under %	Under %	Under %	Under %	Under %
188	100	100	100	100	100	100	100
175	100	100	100	100	100	100	100
163	100	99.9	100	100	100	100	100
151	100	99.9	100	100	100	100	100
141	100	99.9	100	100	100	100	100
131	100	99.9	100	100	100	100	100
122	100	99.9	100	100	100	100	100
113	100	99.9	100	100	100	100	100
105	99.9	99.9	100	100	100	100	100
97.8	99.9	99.9	100	100	100	100	100
90.9	99.8	99.9	100	100	100	100	100
84.5	99	99.9	100	100	100	100	100
78.6	97.5	99.9	100	99.9	100	100	100
73.1	95.7	99.9	99.9	99.9	100	99.9	100
68	93.3	99.7	99.9	99.8	100	99.9	100
63.2	90.4	98.8	99.8	99.3	100	99.8	100
58.8	86.8	96.9	99.2	98	100	99.1	100
54.7	82.6	93.6	97.4	95.4	99.7	97.2	99.9
50.8	77.6	88.7	94.4	91.3	98.8	94	99.9
47.3	72.2	82.9	90.3	86.3	97	89.8	99.9
44	66.5	76.4	85.5	80.5	94.2	84.9	99.4
40.9	60.9	69.7	80.2	74.5	90.6	79.6	97.3
38	55.8	63.3	74.5	68.5	85.8	74.1	93.5
35.4	51.4	57.5	68.8	62.9	80	68.7	88
32.9	47.6	52.5	63.2	57.8	73.3	63.5	81.4
30.6	44.2	48.1	57.8	53.1	66.5	58.5	74.2
28.4	40.8	44.1	52.8	48.7	60.1	53.7	67.1
26.4	37.3	40.5	48.2	44.6	54.6	49.1	60.8
24.6	33.7	37.1	44	40.7	50	44.9	55.5
22.9	30.1	33.8	40.3	37.1	46.2	41	51.2
21.3	26.8	30.5	37	33.6	43	37.4	47.6
19.8	23.8	27.2	33.9	30.3	40.1	34	44.5
18.4	21	23.8	30.8	27	37.1	30.8	41.5
17.1	18.5	20.5	27.3	23.7	33.4	27.4	37.3
15.9	16.2	17.5	23.4	20.3	28.8	23.7	32.8
14.8	14	14.7	19.3	17	23.7	19.9	27.1
13.7	12	12.3	15.3	13.9	18.5	16.2	21.2
12.8	10.1	10.2	12	11.4	14.3	13.1	16.3
11.9	8.4	8.6	9.6	9.4	11.3	10.7	12.7
11.1	7	7.2	8	8	9.4	8.9	10.2
10.3	5.9	6.2	6.9	7	8.2	7.7	8.7
9.56	5	5.4	6.3	6.2	7.6	6.9	7.8
8.89	4.5	4.7	5.8	5.6	7.1	6.3	7.2
8.27	4	4.2	5.4	5.1	6.6	5.7	6.8
7.69	3.6	3.7	4.8	4.5	6	5.2	6.2
7.15	3.2	3.2	4.2	3.9	5.2	4.5	5.5
6.65	2.7	2.8	3.4	3.2	4.3	3.8	4.7
6.18	2.4	2.4	2.8	2.7	3.5	3.2	3.9
5.75	2.1	2.1	2.3	2.3	2.9	2.7	3.2
5.35	1.9	1.9	1.9	2	2.4	2.4	2.7
4.97	1.8	1.7	1.7	1.8	2.1	2.1	2.3
4.62	1.6	1.5	1.5	1.7	1.9	1.9	2
4.3	1.4	1.3	1.4	1.4	1.6	1.6	1.7
4	1.2	1.1	1.2	1.2	1.4	1.4	1.4
3.72	1	0.9	1	1	1.2	1.2	1.2
3.46	0.9	0.8	0.9	0.9	1	1	1
3.21	0.7	0.6	0.8	0.7	0.9	0.9	0.9
2.99	0.7	0.5	0.7	0.6	0.7	0.8	0.8
2.78	0.6	0.5	0.6	0.6	0.7	0.7	0.7
2.59	0.6	0.4	0.5	0.5	0.6	0.6	0.6
2.4	0.6	0.4	0.5	0.5	0.5	0.6	0.6
2.24	0.5	0.4	0.4	0.4	0.5	0.5	0.5
2.08	0.5	0.3	0.4	0.4	0.4	0.4	0.4
1.93	0.4	0.3	0.3	0.3	0.3	0.4	0.4

Experiment no.: 22 **Date: 8.12.94**

Concentration of particle in mixing tank: 10 g/L

Temperature: 22° C **Starting time: 3:30 pm**

Inflow discharge: 0.155 L/s **Outflow:**

Head velocity

	St. 0	St. 1	St. 2	St. 3	St. 4	St. 5	St. 6	St. 7
Time (s)		0	34	65	90	120	150	180
Height (cm)	4	9	9	9	9	9.5	9.5	9.5
Velocity (cm/s)		1.538		1.818		1.670		

Height of turbidity current at station

	St. 0	St. 1	St. 2	St. 3	St. 4	St. 5	St. 6	St. 7
Height (cm)	4.0	2.4	2.5	2.5	2.5	3.0	3.0	3.0

Height of water in the flume: 50 cm **End time: 3:38 pm**

Inflow concentration at flume entrance: 6.98 g/L

Outflow concentration: 0.63 g/L

Head Concentration

Height from bed (mm)	St. 2 Turbidity (NTU)	Volumetric Concentration	St. 4 Turbidity (NTU)	Volumetric Concentration	St. 6 Turbidity (NTU)	Volumetric Concentration
10	99	0.000491	68	0.000338	62	0.000309
20						
30	26	0.00013	50	0.000249	28	0.00014
40						
50	2	1E-05	4	2E-05	6	3E-05
60						
70	10	5E-05	6	3E-05	8	4E-05
80						
90			9	4.5E-05	9	4.5E-05
Average		0.000377		0.000271		0.000218

Experiment No. 22: Particle Size Analysis							
High Size	Inflow	St. 2 head	St. 2 Body	St. 4 head	St. 4 Body	St. 6 head	St. 6 Body
(μm)	Under %	Under %	Under %	Under %	Under %	Under %	Under %
188	100	100	100	100	100	100	100
175	100	100	100	100	100	100	100
163	100	100	100	100	100	100	100
151	100	100	100	100	100	100	100
141	99.9	100	100	100	100	100	100
131	99.8	100	100	100	100	100	100
122	99.6	100	100	100	100	100	100
113	99.3	100	100	100	100	100	100
105	98.5	100	100	100	100	100	100
97.8	96.7	100	100	100	100	100	100
90.9	94.2	100	100	100	100	100	100
84.5	91	100	100	100	100	100	100
78.6	87.2	99.9	100	100	100	100	100
73.1	83	99.9	100	99.9	100	99.9	100
68	78.4	99.8	100	99.9	100	99.9	100
63.2	73.6	99.8	100	99.9	100	99.9	100
58.8	68.7	99.3	99.9	99.7	100	99.8	100
54.7	64	97	99.5	98.2	99.9	98.9	100
50.8	59.4	92.6	98.4	95.4	99.7	97	99.9
47.3	55.1	86.6	96.5	91.3	99.1	94.3	99.7
44	51	79.8	93.6	86.3	97.9	90.8	99.1
40.9	47	72.7	89.9	80.7	95.7	89.5	97.8
38	43	66.2	85.3	74.9	92.2	81.6	95.5
35.4	39	60.6	79.6	69.1	87.3	76.2	92.1
32.9	35.1	56	73.2	63.3	81.2	70.3	87.7
30.6	31.4	51.9	66.8	57.8	74.6	64.4	82.5
28.4	28	48.1	60.7	52.8	68	58.8	76.7
26.4	25	44.3	55.4	48.1	62	53.8	70.8
24.6	22.4	40.3	51	44	56.7	49.4	64.8
22.9	20.2	36.3	47.2	40.1	52.1	45.4	59
21.3	18.1	32.3	43.8	36.5	47.9	41.7	53.7
19.8	16.3	20.3	40.6	32.9	44	38.1	48.9
18.4	14.6	24.4	37.2	29.3	40.3	34.5	44.4
17.1	13	20.8	33.2	25.6	36.1	30.5	40
15.9	11.3	17.5	28.5	21.7	31.5	26	35.3
14.8	9.7	14.6	23.5	17.8	26.5	21.4	30.5
13.7	8.1	12	18.5	14.3	21.5	16.9	25.8
12.8	6.7	9.9	14.4	11.3	17.1	13.2	21.3
11.9	5.5	8.1	11.5	9.1	13.5	10.6	17.3
11.1	4.5	6.7	9.4	7.6	10.8	8.8	13.9
10.3	3.7	5.6	8.1	6.5	8.8	7.7	11.2
9.56	3.1	4.7	7.2	5.7	7.5	6.9	9.2
8.89	2.7	4	6.5	5.1	6.6	6.3	7.8
8.27	2.4	3.4	5.8	4.6	6	5.7	6.9
7.69	2.2	2.9	5.2	4	5.4	5.1	6.1
7.15	1.9	2.5	4.5	3.4	4.8	4.3	5.5
6.65	1.8	2.1	3.8	2.8	4.2	3.6	4.9
6.18	1.6	1.8	3.3	2.4	3.6	2.9	4.3
5.75	1.5	1.6	2.9	2	3.2	2.5	3.9
5.35	1.3	1.5	2.6	1.8	2.9	2.2	3.6
4.97	1.2	1.4	2.3	1.7	2.6	2	3.2
4.62	1.1	1.3	2.1	1.5	2.3	1.8	2.9
4.3	1	1.1	1.8	1.3	1.9	1.6	2.4
4	0.9	0.9	1.6	1.1	1.6	1.4	2
3.72	0.8	0.8	1.3	1	1.3	1.2	1.7
3.46	0.7	0.6	1.1	0.8	1.1	1	1.4
3.21	0.7	0.5	0.9	0.7	0.9	0.8	1.2
2.99	0.6	0.5	0.7	0.6	0.8	0.7	1
2.78	0.6	0.4	0.6	0.5	0.7	0.6	0.9
2.59	0.6	0.4	0.5	0.5	0.7	0.5	0.8
2.4	0.5	0.4	0.5	0.4	0.6	0.5	0.7
2.24	0.5	0.3	0.4	0.4	0.5	0.4	0.6
2.08	0.4	0.3	0.4	0.3	0.5	0.4	0.5
1.93	0.4	0.3	0.3	0.3	0.4	0.3	0.5

Experiment no.: 23 **Date: 8.12.94**

Concentration of particle in mixing tank: 10 g/L

Temperature: 22° C **Starting time: 4:13 pm**

Inflow discharge: 0.1 L/s **Outflow:**

Head velocity

	St. 0	St. 1	St. 2	St. 3	St. 4	St. 5	St. 6	St. 7
Time (s)		0	37		103	140	175	220
Height (cm)	4	10	8		7.5	7.5	7.5	9
Velocity (cm/s)		1.351			1.351		1.25	

Height of turbidity current at station

	St. 0	St. 1	St. 2	St. 3	St. 4	St. 5	St. 6	St. 7
Height (cm)	4.0	2.3	2.1	2.2	2.2	2.5	2.8	2.9

Height of water in the flume: 50 cm **End time: 4:23 pm**

Inflow concentration at flume entrance: 5.37 g/L

Outflow concentration: 0.37 g/L

Head Concentration

Height from bed (mm)	St. 2 Turbidity (NTU)	Volumetric Concentration	St. 4 Turbidity (NTU)	Volumetric Concentration	St. 6 Turbidity (NTU)	Volumetric Concentration
10	68	0.000338	82	0.000407	55	0.000274
20						
30	15	7.49E-05	28	0.00014	24	0.00012
40						
50	5	2.5E-05	8	4E-05	12	5.99E-05
60						
70	2	1E-05	4	2E-05	3	1.5E-05
80						
90	4	2E-05	6	3E-05	4	2E-05
Average		0.000269		0.000308		0.000199

Experiment No. 23: Particle Size Analysis							
High Size	Inflow	St. 2 head	St. 2 Body	St. 4 head	St. 4 Body	St. 6 head	St. 6 Body
(μm)	Under %	Under %	Under %	Under %	Under %	Under %	Under %
188	100	100	100	100	100	100	100
175	100	100	100	100	100	100	100
163	100	100	100	100	100	100	100
151	100	100	100	100	100	100	100
141	100	100	100	100	100	100	100
131	99.9	100	100	100	100	100	100
122	99.8	100	100	100	100	100	100
113	99.7	100	100	100	100	100	100
105	99.4	100	100	100	100	100	100
97.8	98.6	100	100	100	100	100	100
90.9	97.1	100	100	100	100	100	100
84.5	94.5	100	100	100	100	100	100
78.6	91	99.9	100	100	100	100	100
73.1	87	99.9	100	100	100	99.9	100
68	82.7	99.9	100	100	100	99.9	100
63.2	78.1	99.9	100	100	100	99.9	100
58.8	73.4	99.7	100	99.9	99.9	99.8	100
54.7	68.6	98	99.7	99.5	99.9	98.9	100
50.8	63.9	94.6	99	98.5	99.8	96.9	99.9
47.3	59.3	89.7	97.7	96.7	99.5	93.8	99.9
44	54.8	83.6	95.7	94.1	98.9	89.9	99.9
40.9	50.4	77.1	92.7	90.7	97.8	85.4	99.8
38	46.1	70.7	88.8	86.4	95.9	80.7	99.1
35.4	41.8	64.7	83.7	81	93.2	75.8	97.5
32.9	37.7	59.1	77.6	74.9	89.5	70.9	94.8
30.6	33.8	54	71.2	68.5	85.1	65.9	91.1
28.4	30.2	49.3	64.8	62.2	79.8	61.1	86.6
26.4	27.1	44.9	58.8	56.5	73.9	56.4	81.2
24.6	24.3	40.9	53.4	51.3	67.6	51.8	75.2
22.9	21.9	37	48.6	46.6	61.2	47.4	69
21.3	19.6	33.4	44.3	42.3	55.2	43.3	63
19.8	17.6	29.9	40.4	38.3	49.7	39.3	57
18.4	15.6	26.4	36.7	34.3	44.6	35.3	52.2
17.1	13.6	22.8	32.9	30.3	39.7	31.2	46.9
15.9	11.8	19.3	28.7	26.1	35	26.8	41.4
14.8	10	15.8	24.3	21.9	30.2	22.3	35.8
13.7	8.3	12.7	20	17.9	25.7	18.1	30.3
12.8	6.9	10.2	16	14.4	21.5	14.5	25.1
11.9	5.7	8.3	12.8	11.5	17.7	11.8	20.5
11.1	4.8	7	10.1	9.3	14.5	9.8	16.6
10.3	4.1	6.2	8.1	7.5	11.8	8.3	13.4
9.56	3.5	5.5	6.7	6.2	9.6	7.3	11
8.89	3	4.9	5.8	5.3	8.1	6.4	9.2
8.27	2.6	4.4	5.1	4.6	6.8	5.7	8
7.69	2.3	3.8	4.5	4.1	5.9	5	6.9
7.15	2	3.2	4	3.6	5.1	4.2	6.1
6.65	1.8	2.6	3.5	3.1	4.4	3.5	5.3
6.18	1.6	2.1	3.1	2.7	3.9	2.9	4.7
5.75	1.4	1.8	2.8	2.4	3.5	2.6	4.3
5.35	1.3	1.6	2.5	2.2	3.1	2.3	3.9
4.97	1.2	1.5	2.2	2	2.8	2.1	3.5
4.62	1.1	1.4	2	1.8	2.5	2	3.1
4.3	1	1.2	1.7	1.5	2.2	1.7	2.7
4	0.9	1	1.4	1.3	1.9	1.4	2.2
3.72	0.8	0.8	1.1	1	1.6	1.2	1.8
3.46	0.7	0.7	0.9	0.8	1.3	0.9	1.4
3.21	0.6	0.5	0.7	0.7	1.1	0.7	1.1
2.99	0.5	0.4	0.6	0.6	0.9	0.6	0.9
2.78	0.5	0.3	0.5	0.5	0.8	0.5	0.7
2.59	0.5	0.3	0.5	0.4	0.7	0.4	0.6
2.4	0.4	0.2	0.4	0.4	0.6	0.4	0.5
2.24	0.4	0.2	0.4	0.3	0.5	0.3	0.5
2.08	0.3	0.2	0.3	0.3	0.4	0.3	0.4
1.93	0.3	0.1	0.3	0.2	0.4	0.2	0.3

Experiment no.: 24 **Date: 9.12.94**

Concentration of particle in mixing tank: 10 g/L

Temperature: 19° C **Starting time: 4:55 pm**

Inflow discharge: 0.145 L/s **Outflow:**

Head velocity

	St. 0	St. 1	St. 2	St. 3	St. 4	St. 5	St. 6	St. 7
Time (s)		0	31	62	90	117	145	178
Height (cm)	4	10.5	10.5	10.5	10.5	10.5	10.5	9.5
Velocity (cm/s)			1.612		1.818		1.639	

Height of turbidity current at station

	St. 0	St. 1	St. 2	St. 3	St. 4	St. 5	St. 6	St. 7
Height (cm)	4.0	2.5	2.5	2.8	3.0	3.5	4.0	4.2

Height of water in the flume: 50 cm **End time: 5:10 pm**

Inflow concentration at flume entrance: 8.03 g/L

Outflow concentration: 0.67 g/L

Head Concentration

Height from bed (mm)	St. 2 Turbidity (NTU)	Volumetric Concentration	St. 4 Turbidity (NTU)	Volumetric Concentration	St. 6 Turbidity (NTU)	Volumetric Concentration
10	119	0.000589	120	0.000594	115	0.00057
20						
30	28	0.00014	49	0.000244	41	0.000204
40						
50	19	9.49E-05	21	0.000105	17	8.49E-05
Average		0.000425		0.000412		0.000399

Experiment No. 24: Particle Size Analysis							
High Size	Inflow	St. 2 head	St. 2 Body	St. 4 head	St. 4 Body	St. 6 head	St. 6 Body
(μm)	Under %	Under %	Under %	Under %	Under %	Under %	Under %
188	100	100	100	100	100	100	100
175	100	100	100	100	100	100	100
163	100	100	100	100	100	100	100
151	100	100	100	100	100	100	100
141	100	100	100	100	100	100	100
131	100	100	100	100	100	100	100
122	99.9	100	100	100	100	100	100
113	99.9	100	100	100	100	100	100
105	99.7	100	100	100	100	100	100
97.8	99.5	100	100	100	100	100	100
90.9	98.8	100	100	100	100	100	100
84.5	96.9	100	100	100	100	100	100
78.6	94.2	99.9	100	100	100	100	100
73.1	91	99.9	100	99.9	100	100	100
68	87.3	99.8	100	99.9	100	100	100
63.2	83.3	99.4	99.9	99.8	100	100	100
58.8	79	98.1	99.8	99.2	99.8	99.9	99.9
54.7	74.4	95	99.4	97.4	99.2	99.2	99.8
50.8	69.7	90	98.7	94.3	97.8	97.9	99.6
47.3	64.8	83.8	97.6	90.3	95.4	95.8	99.2
44	59.8	76.8	96	85.4	92.6	93	98.4
40.9	54.9	69.6	93.7	80	88.7	89.4	97
38	50	62.8	90.5	74.1	83.9	85	94.9
35.4	45.2	56.8	86.3	68	78	79.8	91.8
32.9	40.7	51.8	81.1	61.9	71.5	74	87.7
30.6	36.5	47.4	75.4	56.1	64.8	68	82.9
28.4	32.8	43.6	69.3	50.7	58.6	62	77.4
26.4	29.6	40.1	63.3	46	53.1	56.3	71.4
24.6	26.8	36.8	57.1	41.9	48.5	51.1	65.2
22.9	24.4	33.4	51.4	38.2	44.6	46.3	59
21.3	22.1	29.9	46.2	34.8	41.1	42	53.2
19.8	19.9	26.1	41.5	31.5	38	38	47.8
18.4	17.6	22.3	37.3	28.2	34.9	34.3	42.9
17.1	15.3	18.7	33.2	24.8	31.3	30.5	38.1
15.9	13.1	15.5	29.3	21.1	27.1	26.5	33.5
14.8	11	12.8	25.2	17.4	22.5	22.5	29
13.7	9	10.6	21.4	14	18	18.6	24.7
12.8	7.4	8.9	17.9	11.1	14.2	15.1	20.7
11.9	6.2	7.6	14.7	9.1	11.3	12.2	17.1
11.1	5.2	6.6	11.9	7.6	9.3	9.9	14
10.3	4.5	5.9	9.7	6.6	7.9	8.1	11.4
9.56	3.9	5.1	7.9	5.8	6.9	6.8	9.3
8.89	3.5	4.4	6.6	5.2	6.2	5.8	7.7
8.27	3	3.7	5.6	4.6	5.5	5.1	6.6
7.69	2.6	3.1	4.9	4	5	4.5	5.6
7.15	2.3	2.5	4.2	3.5	4.3	4	4.9
6.65	2	2.1	3.7	2.9	3.7	3.5	4.3
6.18	1.7	1.7	3.3	2.5	3.2	3.1	3.8
5.75	1.5	1.6	2.9	2.1	2.8	2.8	3.3
5.35	1.4	1.5	2.6	1.9	2.5	2.5	3
4.97	1.3	1.4	2.4	1.8	2.2	2.3	2.7
4.62	1.2	1.3	2.1	1.6	2	2.1	2.4
4.3	1	1.2	1.8	1.4	1.7	1.8	2.1
4	0.9	1	1.6	1.2	1.5	1.5	1.8
3.72	0.8	0.8	1.3	1	1.2	1.3	1.5
3.46	0.7	0.6	1.1	0.8	1	1	1.3
3.21	0.6	0.4	0.9	0.7	0.8	0.9	1.1
2.99	0.5	0.3	0.8	0.6	0.7	0.7	0.9
2.78	0.4	0.3	0.7	0.5	0.6	0.7	0.8
2.59	0.4	0.2	0.6	0.5	0.5	0.6	0.7
2.4	0.4	0.2	0.5	0.4	0.5	0.5	0.6
2.24	0.3	0.2	0.4	0.4	0.4	0.5	0.5
2.08	0.3	0.2	0.4	0.3	0.3	0.4	0.5
1.93	0.3	0.1	0.3	0.3	0.3	0.3	0.4

Experiment no.: 27 **Date: 23.12.94**

Density fractional in mixing tank, Δ = 0.01404

Temperature: 23 ° C **Starting time: 11:00 am**

Inflow discharge: 0.12 L/s **Outflow:**

Head velocity

	St. 0	St. 1	St. 2	St. 3	St. 4	St. 5	St. 6	St. 7
Time (s)		0	26	0	19	40	60	83
Height (cm)			6	7	7	7	7	7
Velocity (cm/s)			1.923		2.380		2.320	

Height of turbidity current at station

	St. 0	St. 1	St. 2	St. 3	St. 4	St. 5	St. 6	St. 7
Height (cm)	4.0	1.3	1.3	1.3	1.5	1.5	1.5	2.0

Height of water in the flume: 50 cm **End time:**

Head Concentration

Height from bed (mm)	St. 2 Turbidity (NTU)	Density Fraction, Δ	St. 4 Turbidity (NTU)	Density Fraction, Δ	St. 6 Turbidity (NTU)	Density Fraction, Δ
10	6	0.002789	1.4	0.000686	6.5	0.003003
20						
30	2	0.000974	2.3	0.001116	1.6	0.000782
40						
50	0.2	0.0000993			0.2	0.000099
60						
Average		0.002262		0.000827		0.002466

Experiment no.: 28 **Date: 23.12.94**

Density fractional in mixing tank, Δ = 0.01404

Temperature: 23.5 ° C **Starting time: 11:35 am**

Inflow discharge: 0.215 L/s **Outflow:**

Head velocity

	St. 0	St. 1	St. 2	St. 3	St. 4	St. 5	St. 6	St. 7
Time (s)		0	19	40	57	73	90	106
Height (cm)		8.5	9	9	9	9	9	9
Velocity (cm/s)			2.500		3.030		3.030	

Height of turbidity current at station

	St. 0	St. 1	St. 2	St. 3	St. 4	St. 5	St. 6	St. 7
Height (cm)	4.0	1.6	1.6	1.6	1.8	2.0	2.2	3.5

Height of water in the flume: 50 cm **End time:**

Head Concentration

Height from bed (mm)	St. 2 Turbidity (NTU)	Density Fraction, Δ	St. 4 Turbidity (NTU)	Density Fraction, Δ	St. 6 Turbidity (NTU)	Density Fraction, Δ
10	6.6	0.003046	6.8	0.003131	9.1	0.004075
20						
30	3.1	0.00149	8.4	0.003793	2.8	0.001351
40						
50	0.3	0.000149			0.4	0.000198.
60						
70					0.1	4.97E-05
80						
Average		0.002403		0.002844		0.003249

Experiment no.: 29 **Date: 23.12.94**

Density fractional in mixing tank, Δ = 0.01404

Temperature: 23 ° C **Starting time: 12:10 pm**

Inflow discharge: 0.265 L/s **Outflow:**

Head velocity

	St. 0	St. 1	St. 2	St. 3	St. 4	St. 5	St. 6	St. 7
Time (s)		0	18	35	50	64	78	93
Height (cm)			7.5	9	9.5	10	9.5	9.5
Velocity (cm/s)		2.857		3.448		3.448		

Height of turbidity current at station

	St. 0	St. 1	St. 2	St. 3	St. 4	St. 5	St. 6	St. 7
Height (cm)	4.0	2.0	2.0	2.0	2.0	2.5	2.5	3.0

Height of water in the flume: 50 cm **End time:**

Head Concentration

Height from bed (mm)	St. 2 Turbidity (NTU)	Density Fraction, Δ	St. 4 Turbidity (NTU)	Density Fraction, Δ	St. 6 Turbidity (NTU)	Density Fraction, Δ
10	6.5	0.003003	8.9	0.003995	9.5	0.004233
20						
30	3.5	0.001675	3.5	0.001675	3.7	0.001766
40						
50	0.4	0.000198	0.3	0.000149	0.5	0.000248
60						
Average		0.002398		0.00316		0.003268

Experiment no.: 30 **Date: 26.12.94**

Density fractional in mixing tank, Δ = 0.01184

Temperature: 22 ° C **Starting time: 12.06 pm**

Inflow discharge: 0.14 L/s **Outflow:**

Head velocity

	St. 0	St. 1	St. 2	St. 3	St. 4	St. 5	St. 6	St. 7
Time (s)		0	32	48	60	81	99	
Height (cm)		7	7	8.5	8.5	8.5	8.5	
Velocity (cm/s)			2.083		3.030		2.780	

Height of turbidity current at station

	St. 0	St. 1	St. 2	St. 3	St. 4	St. 5	St. 6	St. 7
Height (cm)	4.0	2.2	2.5	2.5	3.0	4.0	4.5	

Height of water in the flume: 50 cm **End time: 12:12 pm**

Head Concentration

Height from bed (mm)	St. 2 Turbidity (NTU)	Density Fraction, Δ	St. 4 Turbidity (NTU)	Density Fraction, Δ	St. 6 Turbidity (NTU)	Density Fraction, Δ
10	8.4	0.003463			8.4	0.003463
20						
30	4.8	0.001979			5	0.002061
40						
50	1	0.000412			2.3	0.000948
60						
70	1	0.000412			1.5	0.000618
80						
90	0.3	0.000131			0.8	0.00033
Average		0.002667				0.002432

Experiment no.: 31 **Date: 26.12.94**

Density fractional in mixing tank, Δ = 0.01184

Temperature: 22 ° C **Starting time: 3:45 pm**

Inflow discharge: 0.195 L/s **Outflow:**

Head velocity

	St. 0	St. 1	St. 2	St. 3	St. 4	St. 5	St. 6	St. 7
Time (s)			0	14	28	40	53	67
Height (cm)			9.5	9.5	9.5	9.5	9.5	9.5
Velocity (cm/s)		7.142		3.846		3.703		

Height of turbidity current at station

	St. 0	St. 1	St. 2	St. 3	St. 4	St. 5	St. 6	St. 7
Height (cm)	4.0	3.5	3.5	3.5	3.5	5.5	6.0	6.0

Height of water in the flume: 50 cm **End time:**

Head Concentration

Height from bed (mm)	St. 2 Turbidity (NTU)	Density Fraction, Δ	St. 4 Turbidity (NTU)	Density Fraction, Δ	St. 6 Turbidity (NTU)	Density Fraction, Δ
10	10	0.004123			11.4	0.0047
20						
30	5.6	0.002309			5.5	0.002267
40						
50	0.6	0.000247			3.6	0.001484
60						
70	1.8	0.000742			2	0.000825
80						
90	0.9	0.000371			1.6	0.00066
140						
Average		0.002992				0.003115

Experiment no.: 32 **Date: 26.12.94**

Density fractional in mixing tank, Δ = 0.01184

Temperature: 22 ° C **Starting time: 4:25 pm**

Inflow discharge: 0.255 L/s **Outflow:**

Head velocity

	St. 0	St. 1	St. 2	St. 3	St. 4	St. 5	St. 6	St. 7
Time (s)		0	15	29	41	54	67	80
Height (cm)		10.5	11	12	12	12.5	12	12.5
Velocity (cm/s)			3.448		4.000		3.846	

Height of turbidity current at station

	St. 0	St. 1	St. 2	St. 3	St. 4	St. 5	St. 6	St. 7
Height (cm)	4.0	4.3	4.3	4.3	4.5	4.5	4.5	4.5

Height of water in the flume: 50 cm **End time:**

Head Concentration

Height from bed (mm)	St. 2 Turbidity (NTU)	Density Fraction, Δ	St. 4 Turbidity (NTU)	Density Fraction, Δ	St. 6 Turbidity (NTU)	Density Fraction, Δ
10	9	0.00371			10.5	0.004741
20						
30	6	0.002474			5	0.002061
40						
50	1.5	0.000618			2	0.000825
60						
70	0.1	4.12E-05			1.1	0.000453
80						
90	0.4	0.000165			0.6	0.000247
100						
Average		0.00288				0.002979

Experiment no.: 33 **Date: 27.12.94**

Density fractional in mixing tank, Δ = 0.008

Temperature: 21° C **Starting time: 10:50 am**

Inflow discharge: 0.13 L/s **Outflow:**

Head velocity

	St. 0	St. 1	St. 2	St. 3	St. 4	St. 5	St. 6	St. 7
Time (s)		0	18	41	60	78	99	120
Height (cm)		14	12	10.5	10.5	10.5	10.5	11
Velocity (cm/s)			2.439		2.702		2.380	

Height of turbidity current at station

	St. 0	St. 1	St. 2	St. 3	St. 4	St. 5	St. 6	St. 7
Height (cm)	4.0	4.0	3.5	4.0	4.0	4.0	4.0	4.0

Height of water in the flume: 50 cm **End time:**

Head Concentration

Height from bed (mm)	St. 2 Turbidity (NTU)	Density Fraction, Δ	St. 4 Turbidity (NTU)	Density Fraction, Δ	St. 6 Turbidity (NTU)	Density Fraction, Δ
10	6.5	0.00273	4.8	0.002016	4.6	0.001932
20						
30	4.2	0.001767				
40						
50	3.3	0.001386				
60						
70	1.1	0.000462				
80						
Average		0.001883				

Experiment no.: 34 **Date: 27.12.94**

Density fractional in mixing tank, Δ = 0.008

Temperature: 22° C **Starting time: 11:30 am**

Inflow discharge: 0.21 L/s **Outflow:**

Head velocity

	St. 0	St. 1	St. 2	St. 3	St. 4	St. 5	St. 6	St. 7
Time (s)		0	22	40	55	70	86	103
Height (cm)		11	12	12	12	12	11.5	12
Velocity (cm/s)			2.500		3.333		3.030	

Height of turbidity current at station

	St. 0	St. 1	St. 2	St. 3	St. 4	St. 5	St. 6	St. 7
Height (cm)	4.0	4.5	4.5	4.5	4.5	4.5	4.5	4.5

Height of water in the flume: 50 cm **End time:**

Head Concentration

Height from bed (mm)	St. 2 Turbidity (NTU)	Density Fraction, Δ	St. 4 Turbidity (NTU)	Density Fraction, Δ	St. 6 Turbidity (NTU)	Density Fraction, Δ
10	4	0.00168	5.2	0.002184	5.2	0.002184
20						
30	3.4	0.001428	4	0.00168	4.1	0.001722
40						
50	2.1	0.000882			2	0.00084
60						
70	1.3	0.000546			1.1	0.000462
80						
90					0.1	4.2E-05
100						
Average		0.001198		0.001442		0.001644

Experiment no.: 35 **Date: 27.12.94**

Density fractional in mixing tank, Δ = 0.008

Temperature: 22° C **Starting time: 11:54 am**

Inflow discharge: 0.255 L/s **Outflow:**

Head velocity

	St. 0	St. 1	St. 2	St. 3	St. 4	St. 5	St. 6	St. 7
Time (s)		0	19	36	51	67	82	98
Height (cm)		14	13.5	13.5	13.5	13.5	13.5	13.5
Velocity (cm/s)			2.777		3.225		3.225	

Height of water in the flume: 50 cm **End time:**

Head Concentration

Height from bed (mm)	St. 2 Turbidity (NTU)	Density Fraction, Δ	St. 4 Turbidity (NTU)	Density Fraction, Δ	St. 6 Turbidity (NTU)	Density Fraction, Δ
10	3.6	0.001512			5.4	0.002268
20						
30	4.8	0.002016			4.3	0.001806
40						
50	5.4	0.002268			3.2	0.001344
60						
70	3.1	0.001302			2.1	0.000882
80						
90					1.5	0.00063
100						
Average		0.001615				0.001542

Experiment no.: 36 **Date: 27.12.94**

Density fractional in mixing tank, Δ = 0.008

Temperature: 25° C **Starting time: 4:30 pm**

Inflow discharge: 0.11 L/s **Outflow:**

Head velocity

	St. 0	St. 1	St. 2	St. 3	St. 4	St. 5	St. 6	St. 7
Time (s)		0	18	40	60	76	92	115
Height (cm)		10.5	8.5	8.5	8.5	8.5	8.5	10
Velocity (cm/s)			2.500		2.777		2.564	

Height of turbidity current at station

	St. 0	St. 1	St. 2	St. 3	St. 4	St. 5	St. 6	St. 7
Height (cm)	4.0	4.0	3.0	3.0	3.0	3.5	4.0	5.0

Height of water in the flume: 50 cm **End time: 4:35 pm**

Head Concentration

Height from bed (mm)	St. 2 Turbidity (NTU)	Density Fraction, Δ	St. 4 Turbidity (NTU)	Density Fraction, Δ	St. 6 Turbidity (NTU)	Density Fraction, Δ
10	2.7	0.001134	5.9	0.002478	5.4	0.002268
20						
30	1.1	0.000462	3.1	0.001302	3.1	0.001302
40						
50	0		1.6	0.000672	2	0.00084
60						
70					1	0.00042
80						
90					0.6	0.000252
100						
Average		0.000765		0.00173		0.001581

Experiment no.: 37 **Date: 27.12.94**

Density fractional in mixing tank, Δ = 0.00744

Temperature: 22° C **Starting time: 5:00 pm**

Inflow discharge: 0.19 L/s **Outflow:**

Head velocity

	St. 0	St. 1	St. 2	St. 3	St. 4	St. 5	St. 6	St. 7
Time (s)		0	20	39	58	74	92	111
Height (cm)		12	13	13	13	12.5	12.5	12.5
Velocity (cm/s)			2.564		2.857		2.702	

Height of turbidity current at station

	St. 0	St. 1	St. 2	St. 3	St. 4	St. 5	St. 6	St. 7
Height (cm)	4.0	4.5	4.5	4.5	4.5	4.8	4.8	4.5

Height of water in the flume: 50 cm **End time:**

Head Concentration

Height from bed (mm)	St. 2 Turbidity (NTU)	Density Fraction, Δ	St. 4 Turbidity (NTU)	Density Fraction, Δ	St. 6 Turbidity (NTU)	Density Fraction, Δ
10	5.1	0.001444	5.2	0.001472	5.6	0.001585
20						
30	4.5	0.001274	4.3	0.001217	4.1	0.001161
40						
50	2.5	0.000708	1.6	0.000453	2.1	0.000595
60						
70					1	0.000283
80						
90					0.5	0.000142
100						
Average						

Experiment no.: 38 **Date: 27.12.94**

Density fractional in mixing tank, Δ = 0.00744

Temperature: 22° C **Starting time: 6:20 pm**

Inflow discharge: 0.24 L/s **Outflow:**

Head velocity

	St. 0	St. 1	St. 2	St. 3	St. 4	St. 5	St. 6	St. 7
Time (s)		0	20	40	54	69	86	
Height (cm)		16	14	14	14	14	14	14.5
Velocity(cm/sec)			2.50		3.45		2.94	

Height of turbidity current at station

	St. 0	St. 1	St. 2	St. 3	St. 4	St. 5	St. 6	St. 7
Height (cm)	4.0	5.0	5.5	5.5	5.5	5.5	6.0	6.0

Height of water in the flume: 50 cm **End time:**

Head Concentration

Height from bed (mm)	St. 2 Turbidity (NTU)	Density Fraction, Δ	St. 4 Turbidity (NTU)	Density Fraction, Δ	St. 6 Turbidity (NTU)	Density Fraction, Δ
10	4.5	0.001274	3.5	0.000991	4.9	0.001387
20						
30	4.5	0.001274	2.1	0.000595	4.1	0.001161
40						
50	2.1	0.000595			2.5	0.000708
60						
70					0.8	0.000226
80						
Average		0.000913		0.000579		0.001011

Experiment no.: 39 **Date: 27.12.94**

Density fractional in mixing tank, Δ = 0.00744

Temperature: 22° C **Starting time: 7:25 pm**

Inflow discharge: 0.29 L/s **Outflow:**

Head velocity

	St. 0	St. 1	St. 2	St. 3	St. 4	St. 5	St. 6	St. 7
Time (sec)		0	20	37	54	68	84	99
Height (cm)		13	15	15	15.5	15	15	15
Velocity (cm/s)			2.702		3.225		3.225	

Height of turbidity current at station

	St. 0	St. 1	St. 2	St. 3	St. 4	St. 5	St. 6	St. 7
Height (cm)	4.0	3.5	4.5	5.2	5.5	5.5	5.5	5.5

Height of water in the flume: 50 cm **End time:**

Head Concentration

Height from bed (mm)	St. 2 Turbidity (NTU)	Density Fraction, Δ	St. 4 Turbidity (NTU)	Density Fraction, Δ	St. 6 Turbidity (NTU)	Density Fraction, Δ
10	7.8	0.002208			8.5	0.002406
20						
30	6.5	0.00184			7.5	0.002123
40						
50	5.4	0.001529			5.1	0.001444
60						
70	2.5	0.000708			2.6	0.000736
80						
Average		0.001534				0.001675

Experiment no.: 40 **Date: 28.12.94**

Density fractional in mixing tank, Δ = 0.005

Temperature: 22° C **Starting time: 11:15 am**

Inflow discharge: 0.15 L/s **Outflow:**

Head velocity

	St. 0	St. 1	St. 2	St. 3	St. 4	St. 5	St. 6	St. 7
Time (s)		0	25	52	73	94	116	139
Height (cm)		14.5	13	13.5	14	13.5	13.5	14
Velocity (cm/s)			1.923		2.380		2.222	

Height of turbidity current at station

	St. 0	St. 1	St. 2	St. 3	St. 4	St. 5	St. 6	St. 7
Height (cm)	4.0	5.0	5.5	6.0	6.0	6.0	6.0	6.0

Height of water in the flume: 50 cm **End time:**

Head Concentration

Height from bed (mm)	St. 2 Turbidity (NTU)	Density Fraction, Δ	St. 4 Turbidity (NTU)	Density Fraction, Δ	St. 6 Turbidity (NTU)	Density Fraction, Δ
10	5.4	0.003141	4.2	0.002443	2.6	0.001513
20						
30	4.2	0.002443	3.8	0.002211	0.6	0.000349
40						
50	3.6	0.002094	3.2	0.001862	0.2	0.000116
60						
70	3.1	0.001803	2.6	0.001513	0	
80						
Average		0.002149		0.00178		0.00111

Experiment no.: 41 **Date: 28.12.94**

Density fractional in mixing tank, Δ = 0.005

Temperature: 22° C **Starting time: 11:43 am**

Inflow discharge: 0.233 L/s **Outflow:**

Head velocity

	St. 0	St. 1	St. 2	St. 3	St. 4	St. 5	St. 6	St. 7
Time (s)		0	25	43	61	78	96	115
Height (cm)		15	14.5	14.5	14.5	15	15	15
Velocity (cm/s)			2.325		2.857		2.702	

Height of turbidity current at station

	St. 0	St. 1	St. 2	St. 3	St. 4	St. 5	St. 6	St. 7
Height (cm)	4.0	8.0	7.0	7.0	7.0	7.0	7.0	7.0

Height of water in the flume: 50 cm **End time:**

Head Concentration

Height from bed (mm)	St. 2 Turbidity (NTU)	Density Fraction, Δ	St. 4 Turbidity (NTU)	Density Fraction, Δ	St. 6 Turbidity (NTU)	Density Fraction, Δ
10	1.2	0.000698	3.6	0.002094	4.1	0.002385
20						
30	0.9	0.000524	3.5	0.002036	3.4	0.001978
40						
50	0.5	0.000291	2.9	0.001687	3.1	0.001803
60						
70					2.2	0.00128
80						
90					1.5	0.000873
Average		0.000439		0.001532		0.001671

Experiment no.: 42 **Date: 28.12.94**

Density fractional in mixing tank, Δ = 0.00144

Temperature: 22° C **Starting time: 2:30 pm**

Inflow discharge: 0.29 L/s **Outflow:**

Head velocity

	St. 0	St. 1	St. 2	St. 3	St. 4	St. 5	St. 6	St. 7
Time (s)		0	26	53	80	105	130	159
Height (cm)		18	24	21	21	21	21	21
Velocity (cm/s)			1.886		1.923		1.851	

Height of turbidity current at station

	St. 0	St. 1	St. 2	St. 3	St. 4	St. 5	St. 6	St. 7
Height (cm)	4.0	10.0	10.5	11.0	11.0	11.0	11.0	11.0

Height of water in the flume: 50 cm **End time:**

Head Concentration

Height from bed (mm)	St. 2 Turbidity (NTU)	Density Fraction, Δ	St. 4 Turbidity (NTU)	Density Fraction, Δ	St. 6 Turbidity (NTU)	Density Fraction, Δ
10	2.1	0.001019	1.5	0.000728	2	0.00097
20					1.5	0.000728
30	2.3	0.000146	1.6	0.000776	1.4	0.000679
40					1.1	0.000534
50	1.1	0.000534	1.5	0.000728		
60						
70	1.8	0.000873				
80						
Average		0.000599		0.000535		0.000577

Experiment no.: 43 **Date: 28.12.94**

Density fractional in mixing tank, Δ = 0.00144

Temperature: 23° C **Starting time: 3:00 pm**

Inflow discharge: 0.238 L/s **Outflow:**

Head velocity

	St. 0	St. 1	St. 2	St. 3	St. 4	St. 5	St. 6	St. 7
Time (s)		0	23	48	71	92	114	139
Height (cm)		19	21	20	20	18	18	18
Velocity (cm/s)			2.083		2.272		2.127	

Height of turbidity current at station

	St. 0	St. 1	St. 2	St. 3	St. 4	St. 5	St. 6	St. 7
Height (cm)	4.0	11.0	10.0	10.0	10.0	10.5	10.5	10.5

Height of water in the flume: 50 cm **End time:**

Head Concentration

Height from bed (mm)	St. 2 Turbidity (NTU)	Density Fraction, Δ	St. 4 Turbidity (NTU)	Density Fraction, Δ	St. 6 Turbidity (NTU)	Density Fraction, Δ
10	0.8	0.000388	2.2	0.001067	2.3	0.001116
20						
30	0.5	0.000243	2	0.00097	2	0.00097
40						
50	0.2	9.7E-05	2.2	0.001067	1.8	0.000873
60						
70	0		1.9	0.000922	1.6	0.000776
80						
90			0		1.5	
Average		0.000217		0.000787		0.000779

Experiment no.: 44 **Date: 28.12.94**

Density fractional in mixing tank, Δ = 0.00144

Temperature: 22° C **Starting time: 3:25 pm**

Inflow discharge: 0.175 L/s **Outflow:**

Head velocity

	St. 0	St. 1	St. 2	St. 3	St. 4	St. 5	St. 6	St. 7
Time (s)		0	35	68	101	135	168	202
Height (cm)		19	19	19	19	19	19	19
Velocity (cm/s)			1.470		1.492		1.492	

Height of turbidity current at station

	St. 0	St. 1	St. 2	St. 3	St. 4	St. 5	St. 6	St. 7
Height (cm)	4.0	11.0	10.0	10.5	10.5	10.5	10.5	10.5

Height of water in the flume: 50 cm **End time:**

Head Concentration

Height from bed (mm)	St. 2 Turbidity (NTU)	Density Fraction, Δ	St. 4 Turbidity (NTU)	Density Fraction, Δ	St. 6 Turbidity (NTU)	Density Fraction, Δ
10	1.5	0.000728	2.1	0.001019	2	0.00097
20						
30	0.9	0.000437	1.9	0.000922	1.8	0.000873
40						
50	0.9	0.000437	1.8	0.000873	1.6	0.000776
60						
70	0.6	0.000291	1.6	0.000776	1.5	0.000728
80						
90	0.5	0.000243	1.5	0.000728	1.2	0.000582
100						
Average		0.000418		0.000735		0.000679

Experiment no.: 47 **Date: 2.1.95**

Density fractional in mixing tank, Δ = 0.00774

Temperature: 23° C **Starting time:**

Inflow discharge: 0.147 L/s **Outflow:**

Height of water in the flume: 50 cm **End time:**

Body Concentration

Height from bed (mm)	St. 2 Turbidity (NTU)	Density Fraction, Δ	St. 4 Turbidity (NTU)	Density Fraction, Δ	St. 6 Turbidity (NTU)	Density Fraction, Δ
10	4.5	0.002242			5.5	0.00275
20	2.1	0.001046			3.3	0.001644
30	0	0			1.1	0.000548
40					0	0
50						
Average		0.001862				0.002138

Experiment no.: 48 **Date: 2.1.95**

Density fractional in mixing tank, Δ = 0.00774

Temperature: 23° C **Starting time:**

Inflow discharge: 0.215 L/s **Outflow:**

Height of water in the flume: 50 cm **End time:**

Body Concentration

Height from bed (mm)	St. 2 Turbidity (NTU)	Density Fraction, Δ	St. 4 Turbidity (NTU)	Density Fraction, Δ	St. 6 Turbidity (NTU)	Density Fraction, Δ
10	10	0.004048			9.7	0.003927
20	6.8	0.002753			8.3	0.00336
30	0.9	0.000364			6.4	0.002591
40	0	0			3.2	0.001295
50					0	0
60						
Average		0.003363				0.003142

Experiment no.: 49 **Date: 2.1.95**

Density fractional in mixing tank, Δ = 0.00574

Temperature:° C **Starting time: 7 pm**

Inflow discharge: 0.11 L/s **Outflow:**

Height of water in the flume: 50 cm **End time:**

Body Concentration

Height from bed (mm)	St. 2 Turbidity (NTU)	Density Fraction, Δ	St. 4 Turbidity (NTU)	Density Fraction, Δ	St. 6 Turbidity (NTU)	Density Fraction, Δ
10	3.5	0.001277			3.2	0.001167
20	0.5	0.000182			1.2	0.000438
30	0	0			0	0
40						
Average		0.00114				0.000968

Experiment no.: 50 **Date: 4.1.95**

Density fractional in mixing tank, Δ = 0.00349

Temperature: 22° C **Starting time: 11:30 am**

Inflow discharge: 0.17 L/s **Outflow:**

Height of water in the flume: 50 cm **End time:**

Comment: volume of water in mixing tank = 567 L

salt added = 3 kg

turbidity in mixing tank =9 NTU

Body Concentration

Height from bed (mm)	St. 2 Turbidity (NTU)	Density Fraction, Δ	St. 4 Turbidity (NTU)	Density Fraction, Δ	St. 6 Turbidity (NTU)	Density Fraction, Δ
10	5.2	0.002025			4.7	0.00183
20	4.0	0.001558			3.8	0.00148
30	2.0	0.000779			3.1	0.001207
40	0.5	0.000195			1	0.000389
50	0	0			0	0
60						
Average		0.001574				0.001457

Experiment no.: 51 **Date: 4.1.95**

Density fractional in mixing tank, Δ =0.00349

Temperature: 22° C **Starting time:**

Inflow discharge: 0.23 L/s **Outflow:**

Height of water in the flume: 50 cm **End time:**

Comment: as same as experiment 50

volume of water in mixing tank = 567 L

salt added = 3 kg

turbidity in mixing tank =9 NTU

Body Concentration

Height from bed (mm)	St. 2 Turbidity (NTU)	Density Fraction, Δ	St. 4 Turbidity (NTU)	Density Fraction, Δ	St. 6 Turbidity (NTU)	Density Fraction, Δ
10	4.5	0.001752			4.7	0.00183
20	4	0.001558			4.1	0.001597
30	3.8	0.00148			3.7	0.001441
40	3	0.001168			3.3	0.001285
50	1	0.000389			2.8	0.00109
60	0	0			0.6	0.000234
70					0	0
80						
Average		0.00145				0.001454

Experiment no.: 52 **Date: 5.1.95**

Density fractional in mixing tank, Δ = 0.00894

Temperature: 22.5° C **Starting time: 4:50 pm**

Inflow discharge: 0.145 L/s **Outflow:**

Height of water in the flume: cm **End time:**

Comment: Volume of water = 595 L

salt = 6 kg

Turbidity in mixing tank = 24 NTU

Body Concentration

Height from bed (mm)	St. 2 Turbidity (NTU)	Density Fraction, Δ	St. 4 Turbidity (NTU)	Density Fraction, Δ	St. 6 Turbidity (NTU)	Density Fraction, Δ
10	11.9	0.004451			11.5	0.004302
20	5	0.00187			7.5	0.002805
30	0.8	0.000299			4	0.001496
40	0	0			0.5	0.000187
50					0	0
60						
Average		0.003534				0.003259

Experiment no.: 53 **Date: 5.1.95**

Density fractional in mixing tank, Δ = 0.00894

Temperature:° C **Starting time: 5:20 pm**

Inflow discharge: 0.250 L/s Outflow:

Height of water in the flume: 50 cm **End time:**

Comment: as same as 52

Volume of water = 595 L

salt = 6 kg

Turbidity in mixing tank = 24 NTU

Body Concentration

Height from bed (mm)	St. 2 Turbidity (NTU)	Density Fraction, Δ	St. 4 Turbidity (NTU)	Density Fraction, Δ	St. 6 Turbidity (NTU)	Density Fraction, Δ
10	13.5	0.00505			13	0.004863
20	10	0.003741			Turbidity meter stoped	
30	5.5	0.002057				
40	2	0.000748				
50	0.6	0.000224				
60	0	0				
70						
Average		0.003751				0.004863

Experiment no.: 54 **Date: 6.1.95**

Density fractional in mixing tank, Δ = 0.01119

Temperature: 22.5° C **Starting time: 4:15 pm**

Inflow discharge: 0.19 L/s **Outflow:**

Height of water in the flume: 50 cm **End time:**

Comment:

Turbidity in mixing tank = 28.3 NTU

Volume of water = 615.6 L

Salt = 10 kg

Body Concentration

Height from bed (mm)	St. 2 Turbidity (NTU)	Density Fraction, Δ	St. 4 Turbidity (NTU)	Density Fraction, Δ	St. 6 Turbidity (NTU)	Density Fraction, Δ
10	15	0.005956			14	0.005559
20	7	0.002779			11.5	0.004566
30	1.5	0.000596			7.1	0.002819
40	0.2	0.0000794			3.8	0.001509
50	0	0			0.5	0.000199
60					0	0
70						
Average		0.004629				0.004232

Experiment no.: 55 **Date: 6.1.95**

Density fractional in mixing tank, Δ = 0.01119

Temperature: 22.5° C **Starting time:**

Inflow discharge: 0.265 L/s **Outflow:**

Height of water in the flume: 50 cm **End time:**

Comment: same as 54

Turbidity in mixing tank = 28.3 NTU

Volume of water = 615.6 L

Salt = 10 kg

Body Concentration

Height from bed (mm)	St. 2 Turbidity (NTU)	Density Fraction, Δ	St. 4 Turbidity (NTU)	Density Fraction, Δ	St. 6 Turbidity (NTU)	Density Fraction, Δ
10	17	0.00675			16.4	0.006512
20	16	0.006353			14.5	0.005757
30	14.5	0.005757			13.5	0.00536
40	11	0.004368			11.5	0.004566
50	3	0.001191			8.5	0.003375
60	0.3	0.000119			4	0.001588
70	0	0			0.8	0.000318
80					0	0
90						
Average		0.005688				0.005064

Experiment no.: 56 Date: 9.1.95

Concentration of particle in mixing tank: 3.382 g/L

Volumetric concentration: 0.001452 **Temperature: 22° C**

Starting time: 6:15 pm **Inflow discharge: 0.23 L/s**

Outflow: 0.422 L/s **Height of water in the flume: 50 cm**

End time:

Inflow concentration at flume entrance: 2.15 g/L

Outflow concentration: 0.41 g/L

Command: Turbidity meter did not work.

Experiment No. 56: Particle Size Analysis					
High Size	Inflow	St. 2	St. 4	St. 6	Outflow
(μm)	Under %	Under %	Under %	Under %	Under %
188	100	100	100	100	100
175	100	100	100	100	100
163	100	100	100	100	100
151	100	100	100	100	100
141	100	100	100	100	100
131	100	100	99.9	100	100
122	100	100	99.8	100	100
113	100	100	99.7	99.9	100
105	100	100	99.3	99.9	100
97.8	100	100	98.4	99.9	100
90.9	100	100	96.8	99.5	100
84.5	99.7	100	94.4	98.3	100
78.6	99.2	100	91.5	96.5	100
73.1	98.3	100	88.2	94.2	99.9
68	97	100	84.7	91.7	99.9
63.2	95.2	100	81	89	99.9
58.8	92.5	99.9	77.4	86	99.9
54.7	89	99.3	73.9	82.9	99.9
50.8	84.6	97.9	70.7	79.7	99.9
47.3	79.4	95.6	67.6	76.5	99.9
44	73.7	92.4	64.6	73.1	99.6
40.9	69.7	88.4	61.4	69.6	98.5
38	62.3	83.5	58	65.9	96.4
35.4	57.1	77.7	54.1	62.1	93.3
32.9	52.5	71.3	49.8	58.3	89.2
30.6	48.4	64.8	45.4	54.4	84.3
28.4	44.5	58.8	41.2	50.5	78.8
26.4	40.9	53.6	37.1	46.8	72.8
24.6	37.5	49.2	33.5	43.1	66.8
22.9	34.1	45.5	30.2	39.6	60.8
21.3	30.9	42.2	27.2	36.2	55.2
19.8	27.7	39.2	24.6	32.8	50
18.4	24.6	36.1	22.1	29.4	45.3
17.1	21.4	32.4	19.7	26	40.7
15.9	18.3	28.2	17.2	22.4	36.2
14.8	15.4	23.6	14.7	18.9	31.7
13.7	12.8	19	12.3	15.5	27.4
12.8	10.6	15.2	10.1	12.7	23.4
11.9	8.9	12.3	8.4	10.4	19.6
11.1	7.6	10.3	6.9	8.7	16.3
10.3	6.7	8.9	5.8	7.4	13.6
9.56	5.9	7.9	4.9	6.4	11.3
8.89	5.3	7.2	4.3	5.6	9.6
8.27	4.7	6.6	3.8	5.9	8.3
7.69	4.1	5.9	3.4	4.3	7.2
7.15	3.5	5.1	3	3.7	6.3
6.65	2.9	4.4	2.6	3.2	5.6
6.18	2.5	3.7	2.4	2.8	4.9
5.75	2.2	3.2	2.2	2.5	4.4
5.35	2	2.8	2	2.2	4
4.97	1.9	2.6	1.9	2	3.6
4.62	1.8	2.3	1.7	1.8	3.2
4.3	1.6	2	1.5	1.6	2.8
4	1.4	1.7	1.3	1.4	2.4
3.72	1.2	1.5	1.1	1.2	2.1
3.46	1	1.2	1	1	1.7
3.21	0.8	1	0.9	0.8	1.5
2.99	0.7	0.9	0.8	0.7	1.2
2.78	0.6	0.8	0.7	0.6	1.1
2.59	0.5	0.7	0.6	0.5	0.9
2.4	0.5	0.6	0.6	0.5	0.8
2.24	0.4	0.5	0.5	0.4	0.7
2.08	0.4	0.5	0.5	0.4	0.6
1.93	0.3	0.4	0.4	0.3	0.5

Experiment no.: 57 **Date: 10.1.95**

Concentration of particle in mixing tank: 1.703 g/L

olumetric concentration: 0.000731

Temperature: 22.5° C **Starting time: 5:00 pm**

Inflow discharge: 0.145 L/s **Outflow: 0.422 L/s**

Height of water in the flume: 50 cm **End time:**

Inflow concentration at flume entrance: 1.701 g/L

Outflow concentration: 0.153 g/L

Command: The current mixed with the clear water.

Body Concentration

Height from bed (mm)	St. 2 Turbidity (NTU)	Volumetric Concentration	St. 4 Turbidity (NTU)	Volumetric Concentration	St. 6 Turbidity (NTU)	Volumetric Concentration
10	42	0.000209			23	0.000115
20	35	0.000175			19	0.0000949
30	29	0.000145			16	0.0000799
40	25	0.000125			11	0.000055
50	28	0.00014			10	0.00005
60	20	0.0000998			8	0.00004
70	6	0.00003			7	0.000035
80	0	0			5	0.000025
90	0	0			5	0.000025
100	0	0			0	0
Average		0.000153				0.0000735

Experiment No. 57: Particle Size Analysis					
High Size	Inflow	St. 2	St. 4	St. 6	Outflow
(μm)	Under %	Under %	Under %	Under %	Under %
188	100	100	100	100	100
175	100	100	100	100	100
163	100	100	100	100	100
151	100	100	100	100	100
141	100	100	100	100	100
131	100	100	100	100	100
122	100	100	100	100	100
113	99.9	100	100	100	100
105	99.8	100	100	100	100
97.8	99.7	100	100	100	100
90.9	99.1	100	100	100	100
84.5	97.6	100	100	100	100
78.6	95.3	100	100	100	100
73.1	92.6	99.9	100	100	100
68	89.4	99.9	100	100	100
63.2	85.9	99.9	100	100	99.9
58.8	82	99.8	100	100	99.9
54.7	77.8	99	99.9	99.9	99.9
50.8	73.2	97	99.7	99.7	99.9
47.3	68.4	93.8	99.2	99.4	99.7
44	63.5	89.6	98.3	98.6	99.2
40.9	58.5	84.8	96.7	97.4	98.1
38	53.5	79.3	94.1	95.3	96.2
35.4	48.7	73.3	90.3	92.4	93.3
32.9	44	67.1	85.5	88.6	89.5
30.6	39.8	61	80	84	84.8
28.4	36	55.4	74	78.5	79.4
26.4	32.7	50.5	67.7	72.5	73.4
24.6	29.9	46.4	61.5	66	67.1
22.9	27.3	42.8	55.5	59.6	60.9
21.3	24.9	39.7	49.9	53.6	54.9
19.8	22.5	36.7	44.9	48	49.4
18.4	20	33.6	40.4	43	44.3
17.1	17.5	29.9	36	38.3	39.4
15.9	15	25.6	31.7	33.7	34.6
14.8	12.5	21	27.4	29.2	29.8
13.7	10.3	16.5	23.3	25	25.3
12.8	8.4	12.9	19.4	21	21.2
11.9	7.1	10.4	16	17.4	17.6
11.1	6.1	8.8	13	14.3	14.5
10.3	5.4	7.8	10.5	11.7	12
9.56	4.8	7.1	8.6	9.7	10
8.89	4.2	6.5	7.2	8.2	8.4
8.27	3.7	5.9	6.1	7	7.2
7.69	3.2	5.2	5.3	6.1	6.2
7.15	2.8	4.5	4.6	5.4	5.4
6.65	2.4	3.7	4	4.7	4.7
6.18	2.1	3	3.5	4.2	4.1
5.75	1.9	2.5	3.1	3.7	3.6
5.35	1.7	2.2	2.8	3.3	3.2
4.97	1.6	2.1	2.5	3	2.9
4.62	1.5	1.9	2.2	2.6	2.5
4.3	1.3	1.7	1.9	2.3	2.2
4	1.1	1.5	1.6	1.9	1.8
3.72	0.9	1.3	1.4	1.6	1.5
3.46	0.8	1	1.2	1.4	1.3
3.21	0.7	0.8	1	1.1	1
2.99	0.6	0.6	0.8	1	0.9
2.78	0.5	0.5	0.7	0.8	0.7
2.59	0.4	0.4	0.6	0.7	0.6
2.4	0.4	0.4	0.5	0.6	0.5
2.24	0.4	0.3	0.4	0.5	0.5
2.08	0.3	0.3	0.4	0.5	0.4
1.93	0.3	0.2	0.3	0.4	0.3

Experiment no.: 58 **Date: 10.1.95**

Concentration of particle in mixing tank: 3.373 g/L

Volumetric concentration: 0.001448

Temperature: 22.5° C **Starting time: 7:00 pm**

Inflow discharge: 0.152 L/s **Outflow: 0.422 L/s**

Height of water in the flume: 50 cm **End time:**

Inflow concentration at flume entrance: 2.91 g/L

Outflow concentration: 0.294 g/L

Body Concentration

Height from bed (mm)	St. 2 Turbidity (NTU)	Volumetric Concentration	St. 4 Turbidity (NTU)	Volumetric Concentration	St. 6 Turbidity (NTU)	Volumetric Concentration
10	70	0.000348			42	0.000209
20	65	0.000323			35	0.000175
30	50	0.000249			29	0.000145
40	41	0.000204			15	0.0000749
50	39	0.000194			9	0.000045
60	35	0.000175			9	0.000045
70	18	0.0000899			7	0.000035
80	15	0.0000749			6	0.00003
90	11	0.000055			6	0.00003
100	0	0			5	0.000025
110	0	0			4	0.00002
120	0	0			4	0.00002
Average		0.000242			0.000128	

Experiment No. 58: Particle Size Analysis					
High Size	Inflow	St. 2	St. 4	St. 6	Outflow
(μm)	Under %	Under %	Under %	Under %	Under %
188	100	100	100	100	100
175	100	100	100	100	100
163	100	100	100	100	100
151	100	100	100	100	100
141	99.9	100	100	100	100
131	99.7	100	100	100	100
122	99.4	100	100	100	100
113	98.7	100	100	100	100
105	97.3	100	100	100	100
97.8	95.1	100	100	100	100
90.9	92.1	100	100	100	100
84.5	88.8	100	100	100	100
78.6	85.1	100	100	100	100
73.1	80.9	99.9	100	100	100
68	76.4	99.9	100	100	100
63.2	71.7	99.6	99.9	100	100
58.8	67	98.7	99.8	100	100
54.7	62.4	96.9	99.4	100	99.9
50.8	58	94	98.8	99.9	99.8
47.3	53.9	90.2	97.8	99.9	99.8
44	49.9	85.7	96.2	99.9	99.8
40.9	46	80.6	93.9	99.5	99.8
38	42.2	75	90.5	98.4	99.1
35.4	38.3	69	86.1	96.2	96.3
32.9	34.5	63	80.8	92.9	91.4
30.6	30.9	57.2	74.9	88.6	85.4
28.4	27.7	51.9	68.7	83.3	78.7
26.4	24.8	47.3	62.5	77.2	71.7
24.6	22.4	43.6	56.5	70.5	64.6
22.9	20.3	40.3	51	63.7	57.9
21.3	18.5	37.2	46	57.2	52
19.8	16.8	34.2	41.5	51.2	47.1
18.4	15.1	31.1	37.5	45.7	42.8
17.1	13.5	27.6	33.6	40.5	38.4
15.9	11.7	23.7	29.7	35.5	33.7
14.8	10	19.6	25.8	30.7	28.7
13.7	8.4	15.7	22	26	23.7
12.8	6.9	12.5	18.4	21.6	19.1
11.9	5.8	10.2	15.1	17.7	15.1
11.1	4.9	8.7	12.3	14.2	11.9
10.3	4.1	7.7	9.9	11.3	9.5
9.56	3.6	6.9	8.1	9.1	7.7
8.89	3.2	6.3	6.8	7.4	6.6
8.27	2.9	5.8	5.9	6.2	5.8
7.69	2.6	5.1	5.1	5.3	5.2
7.15	2.3	4.4	4.5	4.5	4.6
6.65	2	3.7	4	3.9	4
6.18	1.8	3	3.5	3.4	3.5
5.75	1.6	2.6	3.1	3	3.1
5.35	1.4	2.3	2.8	2.7	2.8
4.97	1.3	2.1	2.5	2.4	2.5
4.62	1.2	1.9	2.2	2.2	2.2
4.3	1.1	1.7	1.9	1.9	1.9
4	0.9	1.5	1.7	1.6	1.6
3.72	0.8	1.3	1.5	1.3	1.3
3.46	0.7	1.1	1.2	1.1	1.1
3.21	0.6	0.9	1.1	0.9	0.9
2.99	0.5	0.7	0.9	0.8	0.8
2.78	0.5	0.6	0.8	0.7	0.7
2.59	0.4	0.5	0.7	0.6	0.6
2.4	0.4	0.5	0.7	0.5	0.5
2.24	0.4	0.4	0.6	0.5	0.5
2.08	0.3	0.4	0.5	0.4	0.4
1.93	0.3	0.3	0.4	0.3	0.3

Experiment no.: 59 **Date: 10 .1.95**

Concentration of particle in mixing tank: 3.373 g/L

Volumetric concentration: 0.001448

Temperature: 22.5° C **Starting time:**

Inflow discharge: 0.265 L/s **Outflow: 0.422 L/s**

Height of water in the flume: 50 cm **End time:**

Inflow concentration at flume entrance: 2.763 g/L

Outflow concentration: 0.377 g/L

Body Concentration

Height from bed (mm)	St. 2 Turbidity (NTU)	Volumetric Concentration	St. 4 Turbidity (NTU)	Volumetric Concentration	St. 6 Turbidity (NTU)	Volumetric Concentration
10	111	0.00055			55	0.000274
20	110	0.000545			53	0.000264
30	72	0.000358			45	0.000224
40	70	0.000348			40	0.000199
50	65	0.000323			30	0.000150
60	50	0.000249			22	0.00011
70	40	0.000199			16	0.0000799
80	35	0.000175			15	0.0000749
90	12	0.0000599			12	0.0000599
100						
Average		0.000388				0.000198

Experiment No. 59: Particle Size Analysis					
High Size	Inflow	St. 2	St. 4	St. 6	Outflow
(μm)	Under %	Under %	Under %	Under %	Under %
188	100	100	100	100	100
175	100	100	100	100	100
163	100	100	100	100	100
151	100	100	100	100	100
141	100	100	100	100	100
131	100	100	100	100	100
122	100	100	100	100	100
113	100	100	100	100	100
105	100	100	100	100	100
97.8	100	100	100	100	100
90.9	100	100	100	100	100
84.5	99.7	100	100	100	100
78.6	99	100	100	100	100
73.1	97.8	99.9	100	99.9	100
68	96.1	99.9	100	99.9	100
63.2	93.7	99.8	100	99.9	100
58.8	90.4	99.2	99.9	99.8	99.9
54.7	86.1	97.6	99.5	99.8	99.8
50.8	80.7	95.1	98.6	99.8	99.5
47.3	74.4	91.7	97.3	99.5	98.8
44	67.7	87.4	95.4	98.7	97.7
40.9	61	82.4	92.7	97.2	95.8
38	54.9	76.5	89.1	94.7	92.8
35.4	49.8	69.9	84.5	90.9	88.8
32.9	45.6	62.9	79.1	85.9	83.6
30.6	42	56.2	73.1	80.2	77.9
28.4	38.9	50.2	67	73.9	71.8
26.4	35.9	45.4	61	67.4	65.6
24.6	33	41.7	55.3	60.9	59.7
22.9	30	38.5	50	54.8	54
21.3	26.9	35.6	45	49.2	48.7
19.8	23.7	32.5	40.5	44.3	43.9
18.4	20.5	29.3	36.3	39.8	39.4
17.1	17.5	25.7	32.3	35.5	35
15.9	14.8	21.9	28.3	31.2	30.7
14.8	12.4	18	24.3	26.9	26.5
13.7	10.5	14.3	20.6	22.7	22.5
12.8	8.8	11.2	17.1	18.7	18.8
11.9	7.5	8.9	13.9	15.2	15.5
11.1	6.5	7.3	11.3	12.2	12.7
10.3	5.6	6.1	9.1	9.7	10.4
9.56	4.9	5.3	7.5	7.9	8.6
8.89	4.3	4.7	6.3	6.5	7.2
8.27	3.7	4.2	5.4	5.6	6.1
7.69	3.2	3.7	4.7	4.8	5.3
7.15	2.8	3.2	4.1	4.2	4.6
6.65	2.4	2.8	3.7	3.7	4
6.18	2.1	2.4	3.2	3.3	3.5
5.75	1.8	2.1	2.9	2.9	3.2
5.35	1.7	1.9	2.6	2.6	2.9
4.97	1.5	1.7	2.3	2.4	2.6
4.62	1.4	1.5	2.1	2.1	2.3
4.3	1.2	1.4	1.8	1.9	2
4	1.1	1.2	1.5	1.6	1.8
3.72	0.9	1	1.3	1.4	1.5
3.46	0.8	0.9	1.1	1.1	1.3
3.21	0.7	0.7	0.9	1	1.1
2.99	0.6	0.6	0.8	0.8	0.9
2.78	0.5	0.6	0.7	0.7	0.8
2.59	0.5	0.5	0.6	0.6	0.7
2.4	0.4	0.5	0.5	0.6	0.6
2.24	0.4	0.4	0.5	0.5	0.5
2.08	0.3	0.4	0.4	0.4	0.5
1.93	0.3	0.3	0.3	0.4	0.4

Experiment no.: 60 **Date: 11.1.95**

Concentration of particle in mixing tank: 5.005 g/L

Volumetric concentration: 0.002148

Temperature: 22° C **Starting time: 11:15 am**

Inflow discharge: 0.26 L/s **Outflow: 0.422 L/s**

Height of water in the flume: 50 cm **End time:**

Inflow concentration at flume entrance: 3.785 g/L

Outflow concentration: 0.587 g/L

Body Concentration

Height from bed (mm)	St. 2 Turbidity (NTU)	Volumetric Concentration	St. 4 Turbidity (NTU)	Volumetric Concentration	St. 6 Turbidity (NTU)	Volumetric Concentration
10	-	-	-	-	92	0.000457
20	-	-	-	-	75	0.000373
30	-	-	-	-	64	0.000318
40	-	-	-	-	49	0.000244
50	-	-	-	-	19	0.0000949
60					17	0.0000849
70					8	0.00004
80					5	0.000025
90					0	0
100					0	0
110					0	0
120						
130						
140						
Average						0.000322

Experiment No. 60: Particle Size Analysis					
High Size	Inflow	St. 2	St. 4	St. 6	Outflow
(μm)	Under %	Under %	Under %	Under %	Under %
188	100	100	100	100	100
175	100	100	100	100	100
163	100	100	100	100	100
151	100	100	100	100	100
141	100	100	100	100	100
131	100	100	100	100	100
122	99.9	100	100	100	100
113	99.8	100	100	100	100
105	99.7	100	100	100	100
97.8	99.2	100	100	100	100
90.9	98.3	100	100	100	100
84.5	96.5	100	100	100	100
78.6	93.9	100	100	100	100
73.1	90.9	99.9	100	100	100
68	87.6	99.9	100	100	100
63.2	83.9	99.8	100	100	100
58.8	79.9	99.4	99.9	100	100
54.7	75.6	97.9	99.4	100	100
50.8	71.2	95.4	98.4	99.8	99.9
47.3	66.6	92.1	96.8	99.3	99.9
44	61.9	88	94.4	98.2	99.4
40.9	57.1	83.2	91.1	96	97.4
38	52.3	78	86.6	92.4	93.7
35.4	47.6	72.3	80.9	87.1	88.5
32.9	43.1	66.5	74.2	80.6	82.2
30.6	38.8	60.9	67.4	73.5	75.2
28.4	34.9	55.6	60.9	66.5	68.3
26.4	31.5	51	55.2	60.2	62
24.6	28.6	47	50.4	54.8	56.6
22.9	26	43.5	46.5	50.3	52.1
21.3	23.7	40.2	43.1	46.6	48.4
19.8	21.5	37.1	40.1	43.4	45.3
18.4	19.4	33.7	37.1	40.4	42.3
17.1	17.2	30	33.6	36.8	38.7
15.9	14.9	25.9	29.3	32.3	34.2
14.8	12.5	21.6	24.4	27.1	28.9
13.7	10.3	17.4	19.6	21.8	23.5
12.8	8.4	13.9	15.4	17.1	18.6
11.9	6.9	11.4	12.2	13.5	14.9
11.1	5.7	9.7	9.9	10.8	12.1
10.3	4.9	8.5	8.4	9	10.1
9.56	4.2	7.6	7.4	7.8	8.9
8.89	3.8	6.9	6.8	7.1	8.1
8.27	3.4	6.3	6.2	6.6	7.5
7.69	3	5.5	5.7	6	6.8
7.15	2.6	4.8	5	5.3	6
6.65	2.3	4	4.2	4.6	5.2
6.18	2	3.3	3.5	3.9	4.4
5.75	1.8	2.8	3	3.3	3.8
5.35	1.6	2.5	2.6	2.9	3.3
4.97	1.5	2.3	2.4	2.5	2.9
4.62	1.3	2.1	2.1	2.2	2.6
4.3	1.2	1.9	1.9	1.9	2.3
4	1.1	1.7	1.6	1.7	2.1
3.72	1	1.5	1.4	1.4	1.8
3.46	0.8	1.2	1.2	1.2	1.5
3.21	0.7	1	1	1	1.3
2.99	0.7	0.8	0.8	0.9	1.1
2.78	0.6	0.7	0.7	0.8	1
2.59	0.5	0.6	0.6	0.7	0.9
2.4	0.5	0.5	0.6	0.6	0.8
2.24	0.4	0.5	0.5	0.6	0.7
2.08	0.4	0.4	0.4	0.5	0.6
1.93	0.3	0.3	0.4	0.4	0.5

Experiment no.: 61 **Date: 11.1.95**

Concentration of particle in mixing tank: 5.005 g/L

Volumetric concentration: 0.002148

Temperature: 23° C **Starting time: 3:15 pm**

Inflow discharge: 0.14 L/s **Outflow: 0.422 L/s**

Height of water in the flume: 50 cm **End time:**

Inflow concentration at flume entrance: 3.282 g/L

Outflow concentration: 0.294 g/L

Body Concentration

Height from bed (mm)	St. 2 Turbidity (NTU)	Volumetric Concentration	St. 4 Turbidity (NTU)	Volumetric Concentration	St. 6 Turbidity (NTU)	Volumetric Concentration
10	100	0.000496	-	-	45	0.000224
20	75	0.000373	-	-	45	0.000224
30	35	0.000175	-	-	20	0.0000998
40	5	0.000025	-	-	12	0.0000599
50	5	0.000025	-	-	7	0.000035
60	4	0.00002			5	0.000025
70	0	0			3	0.000015
80	0	0			0	0
Average		0.000374				0.00017

Experiment No. 61: Particle Size Analysis					
High Size	Inflow	St. 2	St. 4	St. 6	Outflow
(μm)	Under %	Under %	Under %	Under %	Under %
188	100	100	100	100	100
175	100	100	100	100	100
163	100	100	100	100	100
151	100	100	100	100	100
141	100	100	100	100	100
131	99.9	100	100	100	100
122	99.9	100	100	100	100
113	99.8	100	100	100	100
105	99.5	100	100	100	100
97.8	98.8	100	100	100	100
90.9	97.6	100	100	100	100
84.5	95.5	100	100	100	100
78.6	92.8	100	100	100	100
73.1	89.7	100	100	100	100
68	86.2	100	100	100	100
63.2	82.4	100	100	100	100
58.8	78.2	99.9	99.9	99.9	100
54.7	73.8	99.3	99.9	99.8	100
50.8	69.2	97.8	99.8	99.6	99.9
47.3	64.5	95.2	99.4	99.2	99.9
44	59.7	91.7	98.4	98.3	99.9
40.9	54.9	87.3	96.5	96.7	99.3
38	50.2	82.1	93.1	94.3	98.1
35.4	45.6	76.1	88.2	90.7	96
32.9	41.2	69.6	81.9	86.2	92.9
30.6	37.1	63.1	75.1	81	88.9
28.4	33.5	57.2	68.2	75.4	83.9
26.4	30.2	52.2	61.9	69.6	78.1
24.6	27.4	48	56.3	63.7	71.6
22.9	24.9	44.6	51.5	58.1	64.9
21.3	22.5	41.4	47.3	52.8	58.4
19.8	20.3	38.5	43.6	47.9	52.4
18.4	18.1	35.3	40.1	43.3	46.9
17.1	15.9	31.7	36.3	38.7	41.7
15.9	13.7	27.4	32	34.1	36.6
14.8	11.5	22.7	27.3	29.5	31.8
13.7	9.6	18.1	22.5	25.1	27.1
12.8	7.8	14.3	18.2	21	22.8
11.9	6.5	11.6	14.6	17.3	18.9
11.1	5.4	9.7	11.7	14.2	15.5
10.3	4.5	8.5	9.5	11.7	12.6
9.56	3.9	7.7	8	9.7	10.4
8.89	3.4	7	7	8.2	8.7
8.27	3	6.4	6.3	7	7.4
7.69	2.7	5.7	5.7	6.1	6.4
7.15	2.3	4.9	5	5.3	5.6
6.65	2	4.1	4.4	4.6	4.9
6.18	1.8	3.4	3.8	4.1	4.3
5.75	1.6	2.9	3.4	3.6	3.8
5.35	1.4	2.5	3	3.2	3.4
4.97	1.3	2.3	2.7	2.9	3
4.62	1.2	2.1	2.4	2.6	2.7
4.3	1.1	1.8	2.1	2.3	2.3
4	1	1.6	1.8	2	2
3.72	0.9	1.4	1.5	1.7	1.7
3.46	0.8	1.2	1.3	1.4	1.4
3.21	0.7	1	1.1	1.2	1.2
2.99	0.6	0.8	0.9	1	1
2.78	0.6	0.7	0.8	0.8	0.9
2.59	0.5	0.6	0.7	0.7	0.8
2.4	0.5	0.5	0.6	0.6	0.7
2.24	0.4	0.5	0.6	0.6	0.6
2.08	0.4	0.4	0.5	0.5	0.5
1.93	0.3	0.3	0.4	0.4	0.4

Experiment no.: 62 **Date: 11 .1.95**

Concentration of particle in mixing tank: 5.005 g/L

Volumetric concentration: 0.002148

Temperature: 23.5° C **Starting time: 5:00 pm**

Inflow discharge: 0.21 L/s **Outflow: 0.422 L/s**

Height of water in the flume: 50 cm **End time:**

Inflow concentration at flume entrance: 3.952 g/L

Outflow concentration: 0.447 g/L

Body Concentration

Height from bed (mm)	St. 2 Turbidity (NTU)	Volumetric Concentration	St. 4 Turbidity (NTU)	Volumetric Concentration	St. 6 Turbidity (NTU)	Volumetric Concentration
10	120	0.000594	-	-	80	0.000397
20	100	0.000496	-	-	70	0.000348
30	85	0.000422	-	-	50	0.000249
40	60	0.000299	-	-	30	0.00015
50	50	0.000249	-	-	25	0.000125
60	20	0.0000998			20	0.0000998
70	15	0.0000749			15	0.0000749
80	12	0.0000599			12	0.0000599
90	8	0.00004			11	0.000055
100	0	0			0	0
Average		0.000407				0.000257

Experiment No. 62: Particle Size Analysis					
High Size	Inflow	St. 2	St. 4	St. 6	Outflow
(μm)	Under %	Under %	Under %	Under %	Under %
188	100	100	100	100	100
175	100	100	100	100	100
163	100	100	100	100	100
151	100	100	100	100	100
141	99.9	100	100	100	100
131	99.8	100	100	100	100
122	99.6	100	100	100	100
113	99.1	100	100	100	100
105	98.1	100	100	100	100
97.8	96.2	100	100	100	100
90.9	93.4	100	100	100	100
84.5	90.1	100	100	100	100
78.6	86.2	100	100	100	100
73.1	81.9	99.9	100	99.9	100
68	77.2	99.7	99.9	99.9	100
63.2	72.4	98.9	99.7	99.9	100
58.8	67.6	97.3	99.2	99.9	99.9
54.7	63	94.7	98.2	99.9	99.8
50.8	58.7	91.2	96.7	99.8	99.6
47.3	54.8	86.9	94.7	99.6	99.1
44	51	81.9	92	99	98.1
40.9	47.3	76.6	88.6	97.7	96.4
38	43.4	70.9	84.3	95.6	93.8
35.4	39.5	65.3	79.2	92.5	90
32.9	35.4	59.8	73.3	88.3	85.3
30.6	31.6	54.5	67.2	83.2	79.7
28.4	28.1	49.7	61.1	77.6	73.7
26.4	25.1	45.4	55.4	71.5	67.5
24.6	22.7	41.6	50.1	65.2	61.3
22.9	20.6	38.3	45.4	59	55.3
21.3	18.8	35.1	41.1	53.3	49.9
19.8	17.1	32.2	37.2	48.1	44.9
18.4	15.5	29.2	33.6	43.4	40.4
17.1	13.8	26	30.1	38.8	36.1
15.9	12	22.4	26.5	34.2	31.8
14.8	10.1	18.6	22.9	29.7	27.6
13.7	8.3	14.9	19.3	25.2	23.5
12.8	6.8	12	16.1	21.1	19.7
11.9	5.6	9.8	13.2	17.4	16.3
11.1	4.7	8.3	10.8	14.2	13.4
10.3	4	7.3	8.8	11.6	10.9
9.56	3.5	6.6	7.3	9.6	9
8.89	3.1	6	6.2	8.1	7.6
8.27	2.8	5.5	5.4	7	6.5
7.69	2.5	4.9	4.8	6.1	5.7
7.15	2.2	4.3	4.2	5.3	5
6.65	1.9	3.6	3.7	4.7	4.4
6.18	1.7	3	3.3	4.1	3.8
5.75	1.5	2.6	2.9	3.7	3.4
5.35	1.4	2.3	2.6	3.3	3.1
4.97	1.3	2.1	2.4	2.9	2.8
4.62	1.2	1.9	2.1	2.6	2.5
4.3	1.1	1.7	1.9	2.3	2.2
4	1	1.5	1.6	2	1.9
3.72	0.9	1.3	1.4	1.7	1.6
3.46	0.8	1.1	1.2	1.4	1.4
3.21	0.7	0.9	1	1.2	1.2
2.99	0.6	0.7	0.9	1	1
2.78	0.5	0.6	0.8	0.8	0.9
2.59	0.5	0.5	0.7	0.7	0.7
2.4	0.4	0.5	0.6	0.6	0.7
2.24	0.4	0.4	0.5	0.6	0.6
2.08	0.4	0.4	0.5	0.5	0.5
1.93	0.3	0.3	0.4	0.4	0.4

Experiment no.: 63 **Date: 12 .1.95**

Concentration of particle in mixing tank: 6.584 g/L

Volumetric concentration: 0.002826

Temperature: 23.2° C **Starting time: 6:00 pm**

Inflow discharge: 0.145 L/s **Outflow: 0.422 L/s**

Height of water in the flume: 50 cm **End time:**

Inflow concentration at flume entrance: 5.216 g/L

Outflow concentration: 0.318 g/L

Body Concentration

Height from bed (mm)	St. 2 Turbidity (NTU)	Volumetric Concentration	St. 4 Turbidity (NTU)	Volumetric Concentration	St. 6 Turbidity (NTU)	Volumetric Concentration
10	140	0.000692	-	-	84	0.000417
20	80	0.000397	-	-	55	0.000274
30	47	0.000234	-	-	20	0.0000998
40	28	0.00014	-	-	12	0.0000599
50	24	0.00012	-	-	9	0.000045
60	15	0.0000749			8	0.00004
70	11	0.000055			6	0.00003
80	0	0			0	0
Average		0.000428				0.000277

Experiment No. 63: Particle Size Analysis					
High Size	Inflow	St. 2	St. 4	St. 6	Outflow
(μm)	Under %	Under %	Under %	Under %	Under %
188	100	100	100	100	100
175	100	100	100	100	100
163	99.9	100	100	100	100
151	99.8	100	100	100	100
141	99.4	100	100	100	100
131	98.8	100	100	100	100
122	98	100	100	100	100
113	96.8	100	100	100	100
105	95.2	100	100	100	100
97.8	93.1	100	100	100	100
90.9	90.5	100	100	100	100
84.5	87.4	100	100	100	100
78.6	83.7	100	100	100	100
73.1	79.6	100	100	100	99.9
68	75.2	100	100	100	99.9
63.2	70.7	100	100	100	99.9
58.8	66.2	99.8	99.9	99.9	99.9
54.7	61.8	99.3	99.7	99.8	99.9
50.8	57.6	98.3	99.3	99.7	99.9
47.3	53.7	96.6	98.7	99.4	99.9
44	49.9	94.2	97.6	98.7	99.8
40.9	46.2	90.8	95.9	97.4	99.1
38	42.5	86.3	93.2	95.4	97.6
35.4	38.6	80.6	89.5	92.5	95.3
32.9	34.7	74	84.8	88.6	92.2
30.6	31	67.1	79.5	83.9	88.1
28.4	27.7	60.5	73.6	78.6	83.1
26.4	24.7	54.5	67.4	72.7	77.2
24.6	22.2	49.3	61.2	66.6	70.7
22.9	20	44.9	55.2	60.4	64.1
21.3	18.1	41.1	49.6	54.6	57.6
19.8	16.3	37.7	44.6	49.2	51.4
18.4	14.6	34.4	40	44.1	45.8
17.1	12.8	30.8	35.5	39.2	40.3
15.9	11	26.8	31.2	34.3	35
14.8	9.3	22.4	26.9	29.5	29.9
13.7	7.6	18.1	22.8	24.9	25.1
12.8	6.2	14.3	19	20.6	20.8
11.9	5	11.3	15.5	16.8	16.9
11.1	4.2	9	12.6	13.6	13.7
10.3	3.6	7.4	10.2	11	11
9.56	3.1	6.3	8.3	9.1	9
8.89	2.7	5.5	7	7.6	7.5
8.27	2.4	5	6	6.6	6.4
7.69	2.1	4.5	5.3	5.7	5.6
7.15	1.9	4.1	4.6	5	4.9
6.65	1.7	3.6	4.1	4.4	4.3
6.18	1.5	3.2	3.7	3.9	3.8
5.75	1.4	2.9	3.3	3.5	3.4
5.35	1.3	2.6	3	3.2	3.1
4.97	1.2	2.3	2.7	2.9	2.8
4.62	1.1	2.1	2.4	2.6	2.5
4.3	1	1.8	2.1	2.3	2.1
4	0.9	1.5	1.8	2	1.8
3.72	0.8	1.3	1.6	1.7	1.5
3.46	0.7	1.1	1.3	1.4	1.3
3.21	0.6	0.9	1.1	1.2	1.1
2.99	0.5	0.8	1	1.1	0.9
2.78	0.5	0.7	0.9	0.9	0.8
2.59	0.4	0.6	0.8	0.8	0.7
2.4	0.4	0.6	0.7	0.7	0.6
2.24	0.4	0.5	0.6	0.6	0.5
2.08	0.3	0.4	0.5	0.5	0.4
1.93	0.3	0.4	0.4	0.5	0.4

Experiment no.: 64 **Date: 13 .1.95**

Concentration of particle in mixing tank: 6.584 g/L

Volumetric concentration: 0.002826

Temperature: 24° C **Starting time: 5:45 pm**

Inflow discharge: 0.25 L/s **Outflow: 0.422 L/s**

Height of water in the flume: 50 cm **End time:**

Inflow concentration at flume entrance: 4.67 g/L

Outflow concentration: 0.271 g/L

Body Concentration

Height from bed (mm)	St. 2 Turbidity (NTU)	Volumetric Concentration	St. 4 Turbidity (NTU)	Volumetric Concentration	St. 6 Turbidity (NTU)	Volumetric Concentration
10	175	0.000863	-	-	165	0.000814
20	150	0.000741	-	-	92	0.000457
30	100	0.000496	-	-	55	0.000274
40	90	0.000447	-	-	35	0.000175
50	50	0.000249	-	-	15	0.0000749
60	41	0.000204			13	0.0000649
70	27	0.000135			10	0.00005
80	23	0.000115			8	0.00004
90	17	0.0000849			8	0.00004
100	14	0.0000699			6	0.00003
Average		0.000554				0.000492

Experiment No. 64: Particle Size Analysis					
High Size	Inflow	St. 2	St. 4	St. 6	Outflow
(μm)	Under %	Under %	Under %	Under %	Under %
188	100	100	100	100	100
175	100	100	100	100	100
163	100	100	100	100	100
151	100	100	100	100	100
141	100	100	100	100	100
131	100	100	100	100	100
122	100	100	100	100	100
113	99.9	100	100	100	100
105	99.8	100	100	100	100
97.8	99.7	100	100	100	100
90.9	99.1	100	100	100	100
84.5	97.6	100	100	100	100
78.6	95.4	100	100	100	100
73.1	92.6	99.9	100	100	100
68	89.6	99.9	99.9	100	99.9
63.2	86.1	99.9	99.8	100	99.8
58.8	82.3	99.4	99.4	99.8	99.4
54.7	78.2	98	98.6	99.5	98.2
50.8	73.8	95.5	97.3	99	96.3
47.3	69.2	92.1	95.6	98.1	93.7
44	64.4	87.9	93.2	96.6	90.4
40.9	59.6	83.1	90.1	94.4	86.5
38	54.8	77.7	86.1	91.1	81.9
35.4	50	71.8	81.2	86.7	76.7
32.9	45.4	65.8	75.6	81.3	71.1
30.6	41	60	69.6	75.3	65.3
28.4	37	54.5	63.5	69.1	59.8
26.4	33.5	49.7	57.7	62.9	54.7
24.6	30.4	45.5	52.3	56.9	50.2
22.9	27.6	41.8	47.3	51.4	46
21.3	25	38.4	42.7	46.3	42.3
19.8	22.5	35.2	38.6	41.6	38.7
18.4	20.1	32	34.8	37.3	35.2
17.1	17.7	28.3	31	33.2	31.3
15.9	15.1	24.3	27.3	29	27
14.8	12.6	20	23.6	25	22.5
13.7	10.3	15.8	20	21.1	18.1
12.8	8.4	12.5	16.7	17.4	14.4
11.9	6.9	10	13.8	14.2	11.7
11.1	5.8	8.4	11.3	11.5	9.8
10.3	5.1	7.3	9.3	9.3	8.4
9.56	4.5	6.6	7.7	7.6	7.5
8.89	4	5.9	6.6	6.4	6.8
8.27	3.5	5.4	5.7	5.6	6.1
7.69	3.1	4.8	5	4.9	5.5
7.15	2.7	4.2	4.5	4.3	4.8
6.65	2.4	3.6	4	3.9	4.1
6.18	2.1	3.1	3.6	3.5	3.6
5.75	1.9	2.7	3.2	3.2	3.2
5.35	1.8	2.5	3	2.9	2.9
4.97	1.6	2.2	2.7	2.6	2.6
4.62	1.5	2	2.4	2.4	2.4
4.3	1.4	1.8	2.1	2.1	2.1
4	1.2	1.6	1.8	1.8	1.8
3.72	1	1.3	1.6	1.6	1.5
3.46	0.9	1.1	1.3	1.3	1.3
3.21	0.8	0.9	1.1	1.1	1.1
2.99	0.7	0.8	1	1	0.9
2.78	0.6	0.7	0.9	0.9	0.8
2.59	0.6	0.6	0.8	0.8	0.7
2.4	0.5	0.6	0.7	0.7	0.6
2.24	0.5	0.5	0.6	0.6	0.6
2.08	0.4	0.4	0.5	0.5	0.5
1.93	0.4	0.4	0.4	0.4	0.4

Experiment no.: 65 **Date: 17.1.95**

Concentration of particle in mixing tank: 8.398 g/L

Volumetric concentration: 0.003604

Temperature: 23° C **Starting time: 10:50**

Inflow discharge: 0.16 L/s **Outflow: 0.422 L/s**

Height of water in the flume: 50 cm **End time:**

Inflow concentration at flume entrance: 6.826 g/L

Outflow concentration: 0.517 g/L

Body Concentration

Height from bed (mm)	St. 2 Turbidity (NTU)	Volumetric Concentration	St. 4 Turbidity (NTU)	Volumetric Concentration	St. 6 Turbidity (NTU)	Volumetric Concentration
10	155	0.000765	-	-	105	0.000521
20	100	0.000496	-	-	80	0.000397
30	38	0.000189	-	-	35	0.000175
40	27	0.000135	-	-	20	0.0000998
50	23	0.000115	-	-	17	0.0000849
60	21	0.000105			16	0.0000799
70	15	0.0000749			14	0.0000699
80	14	0.0000699			10	0.00005
90	14	0.0000699			12	0.0000599
100	13	0.0000649			9	0.000045
110						
Average		0.000446				0.000314

Experiment No. 65: Particle Size Analysis					
High Size	Inflow	St. 2	St. 4	St. 6	Outflow
(µm)	Under %	Under %	Under %	Under %	Under %
188	100	100	100	100	100
175	100	100	100	100	100
163	100	100	100	100	100
151	100	100	100	100	100
141	100	100	100	100	100
131	99.9	100	100	100	100
122	99.8	100	100	100	100
113	99.7	100	100	100	100
105	99.2	100	100	100	100
97.8	98.2	100	100	100	100
90.9	96.5	100	100	100	100
84.5	94.1	100	100	100	100
78.6	91	100	100	100	100
73.1	87.5	100	100	100	100
68	83.7	99.9	100	100	100
63.2	79.6	99.9	100	100	100
58.8	75.3	99.7	99.9	100	100
54.7	71	98.9	99.8	100	100
50.8	66.6	97.3	99.6	100	100
47.3	62.3	94.9	99	100	100
44	57.9	91.8	97.9	100	100
40.9	53.6	87.9	95.7	99.9	100
38	49.3	83.1	92.2	99.7	99.9
35.4	44.9	77.5	87.2	98.9	99.6
32.9	40.6	71.1	80.9	97.3	98.6
30.6	36.5	64.6	74	94.5	96.4
28.4	32.8	58.3	66.9	90.4	92.6
26.4	29.5	52.5	60.2	84.8	86.8
24.6	26.7	47.4	54.2	78	79.5
22.9	24.1	42.8	48.8	70.9	71.8
21.3	21.8	38.8	44.2	64.2	64.5
19.8	19.7	35.2	40.3	58.3	58
18.4	17.6	31.8	36.7	53.1	52.4
17.1	15.4	28.2	32.8	47.9	47.1
15.9	13.3	24.3	28.6	42.3	41.8
14.8	11.1	20.3	24.1	36.6	36.4
13.7	9.1	16.4	19.6	30.9	31.1
12.8	7.4	12.9	15.6	25.5	26
11.9	6.1	10.2	12.4	20.8	21.2
11.1	5.1	8.2	9.9	16.7	17.1
10.3	4.3	6.7	8	13.5	13.7
9.56	3.8	5.7	6.8	11.1	11.2
8.89	3.3	5	5.9	9.5	9.5
8.27	3	4.5	5.3	8.3	8.3
7.69	2.6	4	4.8	7.4	7.3
7.15	2.3	3.6	4.3	6.6	6.5
6.65	2.1	3.2	3.8	5.8	5.8
6.18	1.9	2.8	3.4	5.2	5.2
5.75	1.7	2.5	3.1	4.7	4.7
5.35	1.6	2.3	2.8	4.3	4.3
4.97	1.4	2.1	2.5	3.9	3.9
4.62	1.3	1.8	2.3	3.5	3.5
4.3	1.2	1.6	2	3	3
4	1.1	1.4	1.7	2.5	2.6
3.72	1	1.2	1.4	2.1	2.1
3.46	0.8	1	1.2	1.7	1.8
3.21	0.7	0.9	1	1.4	1.5
2.99	0.7	0.7	0.9	1.2	1.3
2.78	0.6	0.7	0.8	1	1.1
2.59	0.6	0.6	0.7	0.69	1
2.4	0.5	0.5	0.6	0.8	0.9
2.24	0.5	0.5	0.6	0.7	0.8
2.08	0.4	0.4	0.5	0.6	0.7
1.93	0.4	0.4	0.4	0.5	0.6

Experiment no.: 66 **Date: 17.1.95**

Concentration of particle in mixing tank: 8.398 g/L

Volumetric concentration: 0.003604

Temperature: 23.5° C **Starting time: 11:45**

Inflow discharge: 0.25 L/s Outflow: 0.422 L/s

Height of water in the flume: 50 cm **End time:**

Inflow concentration at flume entrance: 6.88 g/L

Outflow concentration: 0.693 g/L

Body Concentration

Height from bed (mm)	St. 2 Turbidity (NTU)	Volumetric Concentration	St. 4 Turbidity (NTU)	Volumetric Concentration	St. 6 Turbidity (NTU)	Volumetric Concentration
10	275	0.001345	-	-	150	0.000741
20	180	0.000887	-	-	120	0.000594
30	120	0.000594	-	-	80	0.000397
40	125	0.000619	-	-	50	0.000249
50	113	0.00056	-	-	45	0.000224
60	58	0.000289			35	0.000175
70	43	0.000214			29	0.000145
80	26	0.00013			27	0.000135
90	20	0.0000998			27	0.000135
100	14	0.0000699			20	0.0000998
110					18	0.0000899
Average		0.000792				0.000428

Experiment No. 66: Particle Size Analysis					
High Size	Inflow	St. 2	St. 4	St. 6	Outflow
(μm)	Under %	Under %	Under %	Under %	Under %
188	100	100	100	100	100
175	100	100	100	100	100
163	100	100	100	100	100
151	100	100	100	100	100
141	100	100	100	100	100
131	100	100	100	100	100
122	99.9	100	100	100	100
113	99.8	100	100	100	100
105	99.7	100	100	100	100
97.8	99.4	100	100	100	100
90.9	98.5	100	100	100	100
84.5	96.5	100	100	100	100
78.6	93.5	100	100	100	100
73.1	90	99.9	100	100	100
68	86.2	99.9	99.9	100	100
63.2	82	99.9	99.9	99.9	100
58.8	77.6	99.7	99.7	99.9	100
54.7	73.1	98.6	98.8	99.7	99.9
50.8	68.6	96.5	97.2	99.3	99.6
47.3	64	93.6	94.9	98.7	98.9
44	59.5	89.7	91.7	97.6	97.8
40.9	54.9	85.2	87.8	95.8	95.8
38	50.4	79.9	82.9	93.1	92.7
35.4	45.9	74	77.1	89.3	88.4
32.9	41.5	67.7	70.7	84.5	83
30.6	37.4	61.5	64.2	79	76.3
28.4	33.6	55.7	57.8	73.1	70.3
26.4	30.2	50.5	52.1	67	63.8
24.6	27.3	46.1	47.2	61	57.5
22.9	24.7	42.4	42.8	55.1	51.7
21.3	22.3	39	39.1	49.7	46.7
19.8	20.1	35.9	35.7	44.8	42.4
18.4	18	32.7	32.4	40.2	38.5
17.1	15.8	29.2	28.9	35.8	34.6
15.9	13.5	25.1	25.1	31.4	30.4
14.8	11.2	20.7	21	27.1	25.9
13.7	9	16.4	17	22.9	20.4
12.8	7.3	12.9	13.5	19	17.3
11.9	5.9	10.2	10.7	15.6	13.8
11.1	5	8.5	8.6	12.7	11
10.3	4.3	7.3	7.1	10.4	8.8
9.56	3.8	6.5	6	8.6	7.3
8.89	3.4	5.9	5.3	7.3	6.3
8.27	3	5.5	4.8	6.3	5.7
7.69	2.7	4.9	4.4	5.5	5.1
7.15	2.4	4.4	3.9	4.8	4.6
6.65	2.1	3.8	3.5	4.3	4.1
6.18	1.8	3.2	3.1	3.8	3.7
5.75	1.6	2.8	2.8	3.5	3.4
5.35	1.5	2.5	2.5	3.1	3.1
4.97	1.4	2.2	2.3	2.9	2.8
4.62	1.3	2	2.1	2.6	2.5
4.3	1.2	1.8	1.8	2.3	2.2
4	1.1	1.6	1.6	2	1.9
3.72	0.9	1.4	1.4	1.7	1.6
3.46	0.8	1.2	1.2	1.5	1.4
3.21	0.7	1	1	1.2	1.2
2.99	0.7	0.9	0.9	1.1	1.1
2.78	0.6	0.8	0.8	0.9	1
2.59	0.6	0.7	0.7	0.8	0.9
2.4	0.5	0.6	0.6	0.7	0.8
2.24	0.5	0.6	0.6	0.6	0.7
2.08	0.4	0.5	0.5	0.6	0.6
1.93	0.4	0.4	0.4	0.5	0.5